

SUBSTANTIATING DATA FOR  
**ARROW-WING SUPERSONIC CRUISE AIRCRAFT**  
**STRUCTURAL DESIGN CONCEPTS EVALUATION**

**Volume 4, Sections 15 through 21**

(NASA-CR-132575-4) ARROW-WING SUPERSONIC  
CRUISE AIRCRAFT STRUCTURAL DESIGN CONCEPTS  
EVALUATION. VOLUME 4: SECTIONS 15 THROUGH  
21 (Lockheed-California Co.) 430 p HC  
\$11.75

N76-28222  
Unclas  
CSCL 01C G3/05 46765

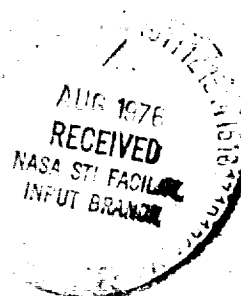
by

I. F. Sakata and G. W. Davis

Prepared under Contract No. NAS1-12288

Lockheed-California Company  
Burbank, California

for Langley Research Center



NATIONAL AERONAUTICS AND SPACE ADMINISTRATION



## TABLE OF CONTENTS

<u>Section</u>		<u>Page</u>
	Volume 1	
1	Summary	iii
2	Introduction	v
3	Acknowledgement	xi
4	Structural Design Concepts	1-1
5	Baseline Configuration	2-1
6	Aerodynamics	3-1
7	Structural Design Criteria	4-1
8	Structural Design Loads	5-1
9	Structural Temperatures	6-1
	Volume 2	
10	Materials and Producibility	7-1
11	Basic Design Parameters	8-1
12	Structural Analysis Models	9-1
13	Vibration and Flutter	10-1
14	Point Design Environment	11-1
	Volume 3	
15	Structural Concept Analysis	12-1
16	Fatigue and Fail-Safe Analysis	13-1
17	Acoustics	14-1
	Volume 4	
18	Mass Analysis	15-1
19	Production Costs	16-1
20	Concept Evaluation and Selection	17-1
21	Design	18-1
22	Propulsion-Airframe Integration	19-1
23	Advanced Technology Assessment	20-1
24	Design Methodology	21-1



SUMMARY

An analytical study was performed to determine the structural approach best suited for the design of a Mach 2.7 arrow-wing supersonic cruise aircraft.

Results, procedures, and principal justification of results are presented in Reference 1. Detailed substantiation data are given herein. In general, each major analysis is presented sequentially in separate sections to provide continuity in the flow of the design concepts analysis effort. In addition to the design concepts evaluation and the detailed engineering design analyses, supporting tasks encompassing: (1) the controls system development (2) the propulsion-airframe integration study, and (3) the advanced technology assessment are presented.

---

Reference 1 Sakata, I. F. and Davis, G. W.: Evaluation of Structural Design Concepts for an Arrow-Wing Supersonic Cruise Aircraft NASA CR- 1976

PRECEDING PAGE BLANK NOT FILMED



## INTRODUCTION

The design of an economically viable supersonic cruise aircraft requires reduced structural mass fractions attainable through application of new materials, advanced concepts and design tools. Configurations, such as the arrow-wing, show promise from the aerodynamic standpoint; however, detailed structural design studies are needed to determine the feasibility of constructing this type of aircraft with sufficiently low structural mass fraction.

For the past several years, the NASA Langley Research Center has been pursuing a supersonic cruise aircraft research program (1) to provide an expanded technology base for future supersonic aircraft, (2) to provide the data needed to assess the environmental and economic impacts on the United States of present and especially future foreign supersonic cruise aircraft, and (3) to provide a sound technical basis for any future consideration that may be given by the United States to the development of an environmentally acceptable and economically viable commercial supersonic cruise aircraft.

The analytical study, reported herein, was performed to provide data to support the selection of the best structural concept for the design of a supersonic cruise aircraft wing and fuselage primary structure considering near-term start-of-design technology. A spectrum of structural approaches for primary structure design that has found application or had been proposed for supersonic aircraft design; such as the Anglo-French Concorde supersonic transport, the Mach 3.0-plus Lockheed F-12 and the proposed Lockheed L-2000 and Boeing B-2707 supersonic transports were systematically evaluated for the given configuration and environmental criteria.

The study objectives were achieved through a systematic program involving the interactions between the various disciplines as shown in Figures A through C. These figures present an overview of the study effort and provides a summary statement of work, as follows:

- (1) Task I - Analytical Design Studies (Figure A).- This initial task involved a study wherein a large number of candidate structure

concepts were investigated and subjected to a systematic evaluation process to determine the most promising concepts. An airplane configuration refinement investigation, including propulsion-airframe integration study were concurrently performed.

- (2) Task II - Engineering Design/Analyses (Figure B).- The most promising concepts were analyzed assuming near-term start-of-design technology, critical design conditions and requirements identified, and construction details and mass estimates determined for the Final Design airplane. Concurrently, the impact of advanced technology on supersonic cruise aircraft design was explored.
- (3) Task III - Mass Sensitivity Studies (Figure C).- Starting with the Final Design airplane numerous sensitivity studies were performed. The results of these investigations and the design studies (Task I and Task II) identified opportunities for structural mass reduction and needed research and technology to achieve the objectives of reduced structural mass.

Displayed on the figures are the time-sequence and flow of data between disciplines and the reason for the make-up of the series of sections presented in this report. The various sections are independent of each other, except as specifically noted. Results of this structural evaluation are reported in Reference 1. This reference also includes the procedures and principal justification of results, whereas this report gives detailed substantiation of the results in Reference 1. This report is bound as four separate volumes.

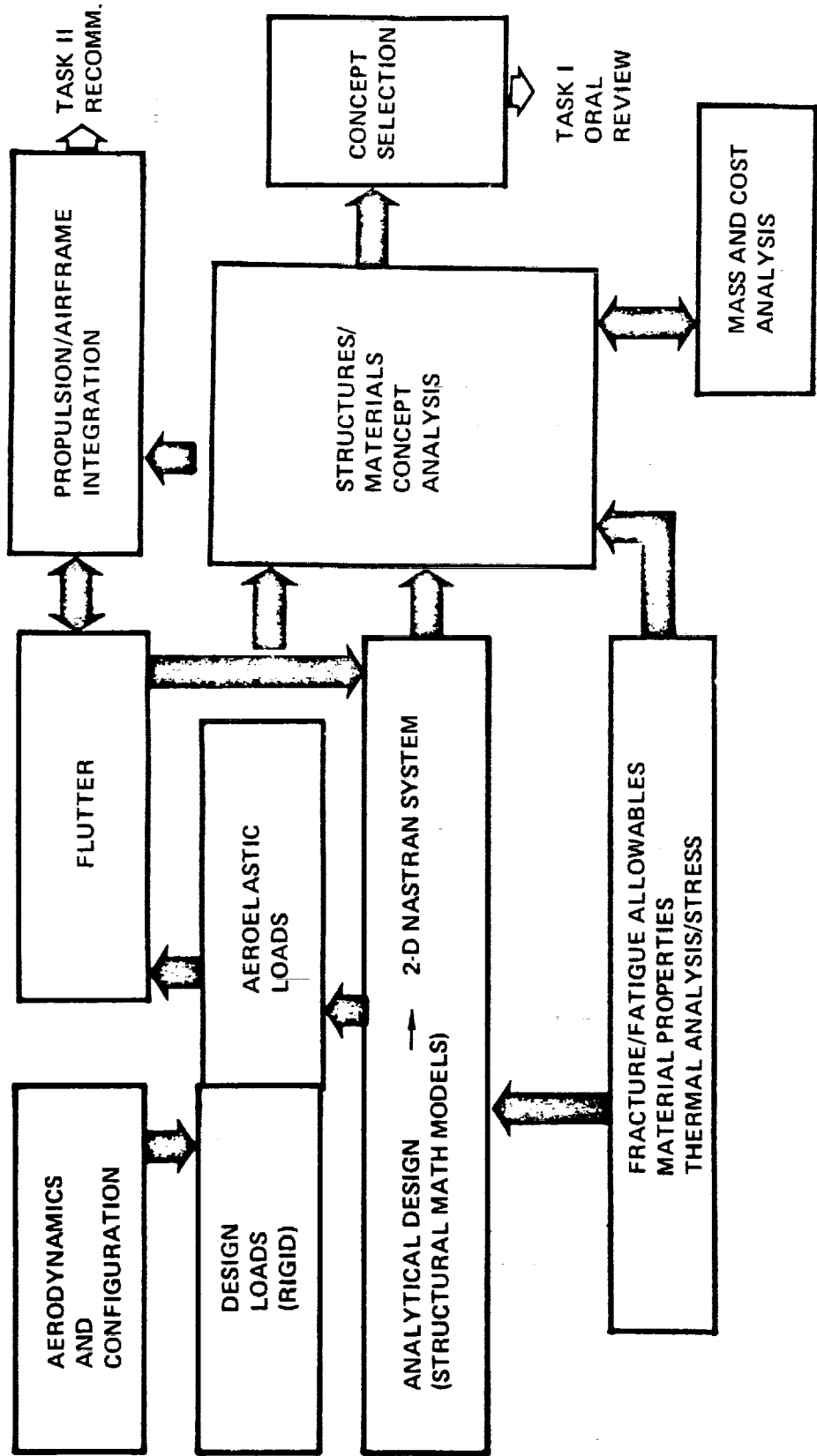


Figure A. Analytical Design Studies - Task I

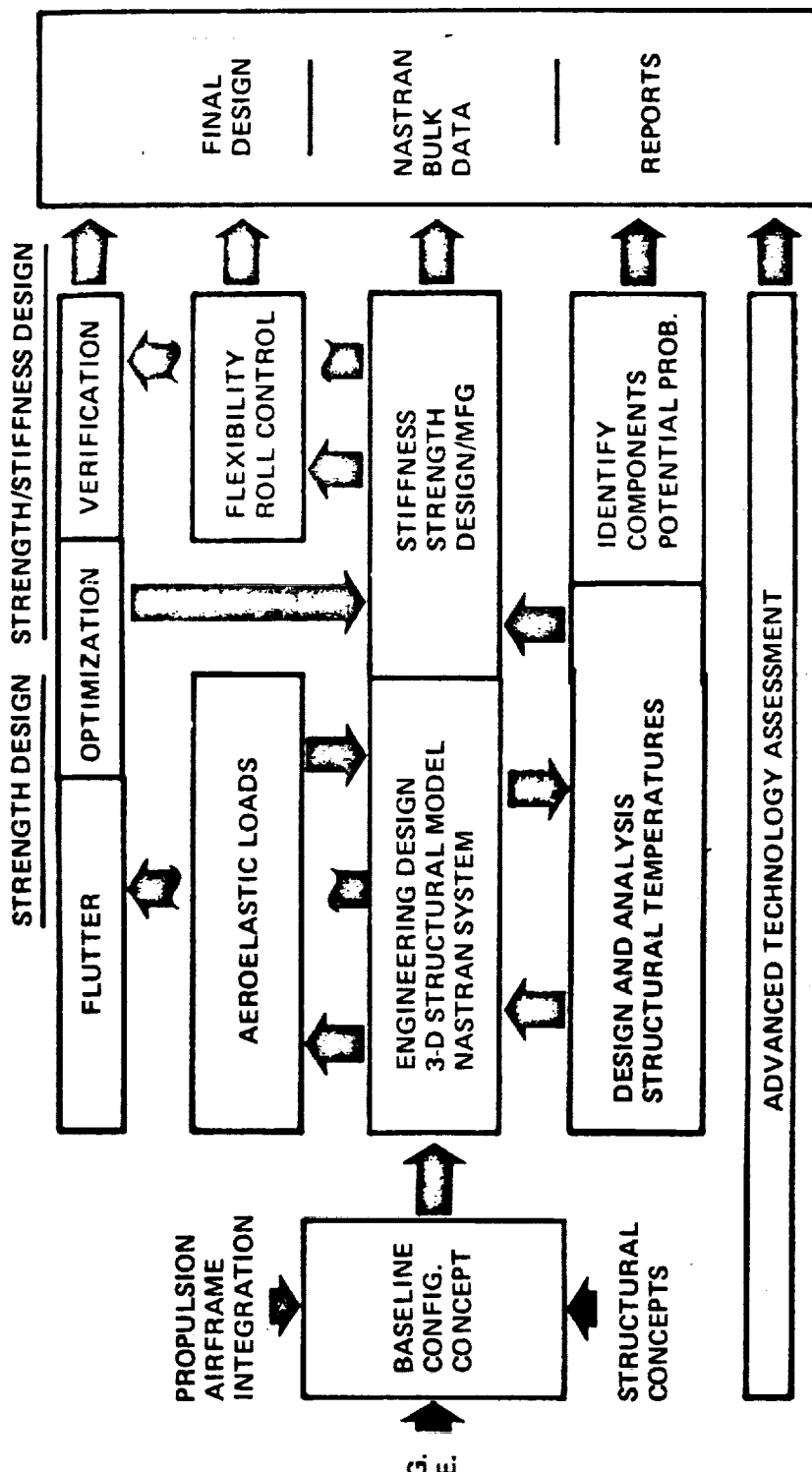


Figure B. Engineering Design and Analyses

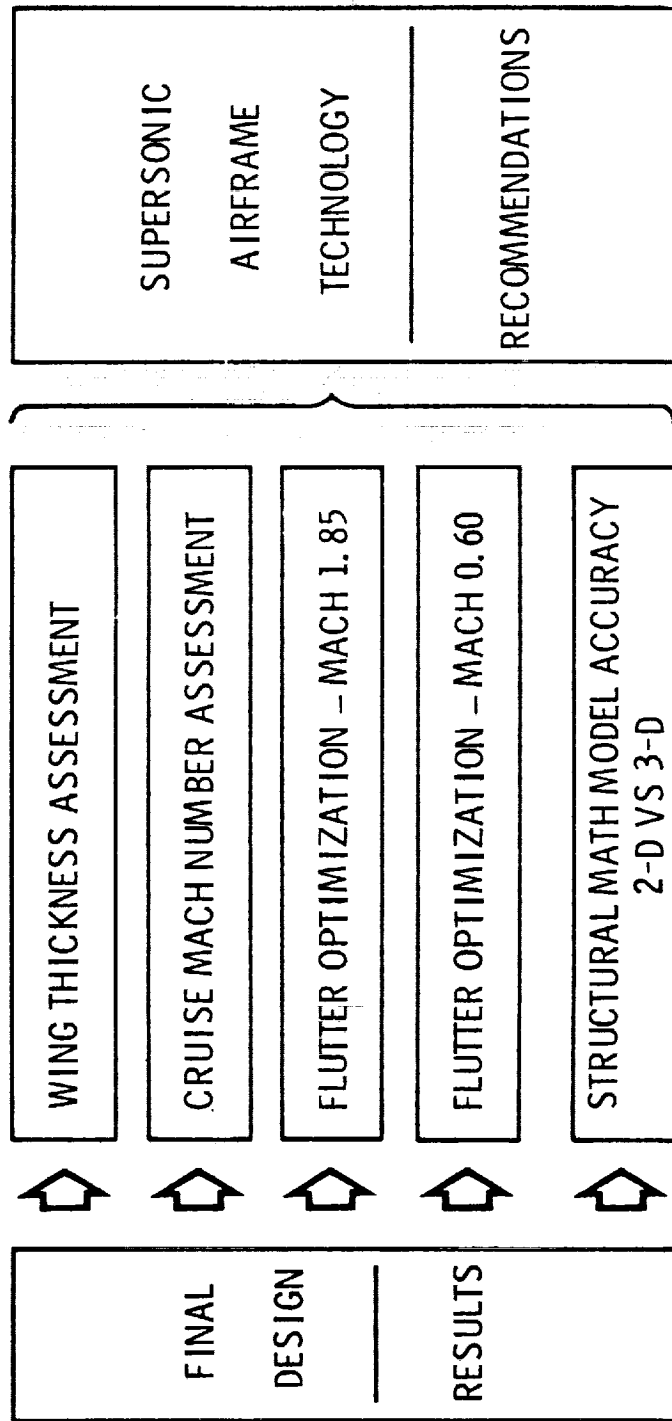


Figure C. Mass Sensitivity Studies



ACKNOWLEDGEMENT

This investigation was conducted under NASA Contract No. NAS1-12288, Study of Structural Design Concepts for an Arrow-Wing Supersonic Transport Configuration. The study was performed within the Science and Engineering Branch of the Lockheed-California Company, Burbank, California, with the participation of the Lockheed-Georgia Company in a composite design subcontract effort. I. F. Sakata was the Project Engineer, and G.W. Davis was the Lead Engineer. The other contributors to the program are acknowledged at each section.

Mr. J. C. Robinson of the Design Concepts Section, Thermal Structures Branch, and Dr. E. C. Yates, Jr., Computer Aided Methods Branch, Structures and Dynamics Division, NASA Langley Research Center, Hampton, Virginia, were the Technical Representative of the Contracting Officer (TRCO), and Alternate TRCO, respectively for the project.

**PRECEDING PAGE BLANK NOT FILMED**



SECTION 15

MASS ANALYSIS

by

R.N. Jensen and R.D. Mijares



## CONTENTS

<u>Section</u>		<u>Page</u>
INTRODUCTION		15-1
BASELINE CONFIGURATION MASS DATA		15-1
Airplane Mass Properties - Task I		15-1
Airplane Mass Properties - Task II		15-10
Weight Comparison Data		15-14
Detail Wing and Body Weights		15-14
STRUCTURAL MODEL MASS DATA		15-17
Grid Point Distribution - Task I		15-17
Grid Point Distribution - Task IIA		15-17
Grid Point Distribution - Task IIB (Strength/Stiffness)		15-27
STRUCTURAL CONCEPT MASS ANALYSIS		15-39
Method		15-39
WING STRUCTURE MASS - INITIAL SCREENING		15-39
Chordwise Stiffened Design Concepts		15-44
Spanwise Stiffened Design Concepts		15-48
Monocoque Design Concepts		15-50
WING STRUCTURE MASS - DETAILED CONCEPT ANALYSIS		15-50
Chordwise Stiffened Wing Design		15-52
Spanwise Stiffened Wing Design		15-58
Monocoque Wing Design		15-62
Composite Reinforced - Chordwise Stiffened Wing Design		15-75
Wing Tip Mass for Structural Arrangements		15-57
Wing Tip Mass Distribution Comparison		15-85

CONTENTS (Continued)

<u>Section</u>	<u>Page</u>
FUSELAGE STRUCTURE MASS - INITIAL SCREENING	15-85
FUSELAGE STRUCTURE DETAILED ANALYSIS	15-91
ASSET PROGRAM RESULTS - TASK I	15-96
FINAL DESIGN AIRPLANE MASS ESTIMATES	15-96
WING STRUCTURE MASS	15-100
Fuselage Structure Mass Estimates	15-101
REFERENCES	15-111

LIST OF FIGURES

<u>Figure</u>	<u>Page</u>
15-1      Interior Arrangement - Task I	15-3
15-2      Interior Arrangement - Task II	15-5
15-3      Center of Gravity Diagram - Task I	15-9
15-4      Aircraft Moment of Inertia - Task II	15-12
15-5      Center of Gravity Diagram - Task II	15-13
15-6      Configuration Comparison - Task I and Task II	15-25
15-7      Surface Panel Thickness - Strength Design	15-25
15-8      Surface Panel Thickness - Final Design	15-37
15-9      Wing Mass Estimation Methodology	15-40
15-10     Fuselage Mass Estimation Methodology	15-41
15-11     Wing Box Areas - Task I	15-43
15-12     Optimum Panel Weights - Chordwise Stiffened Design	15-54
15-13     Component Weight Penalties for a Damaged Spar Cap Chordwise Arrangement	15-56
15-14     Flutter Weight Increment Required Over Strength Design	15-57
15-15     Wing Structure Mass Estimate for Chordwise Stiff- ened Design	15-59
15-16     Optimum Panel Weights - Spanwise Stiffened Design	15-61
15-17     Wing Structure Mass Estimate for Spanwise Stiffened Design	15-63
15-18     Concept Weight Comparison - Monocoque Arrangement	15-64
15-19     Optimum Panel Weights - Monocoque Design (Welded Closures)	15-67
15-20     Fail-Safe Critical Areas of Wing Structure	15-72

LIST OF FIGURES (Cont.)

<u>Figure</u>		<u>Page</u>
15-21	Comparison of Optimum Panel Unit Weights - Composite Reinforced Versus All-Metallic Chordwise Stiffened Designs	15-79
15-22	Shear Thickness of Wing Tip Structure - Chordwise Stiffened	15-82
15-23	Shear Thickness of Wing Tip Structure - Spanwise Stiffened	15-83
15-24	Shear Thickness of Wing Tip Structure - Monocoque	15-84
15-25	Wing Tip Structure Planform Geometry - Task I	15-86
15-26	Comparison of SIC Mass Distribution - Task I and Task II	15-87
15-27	Wing Tip Mass Distributions - Task I and Task II	15-88
15-28	Wing Tip Box Geometry - Task I and Task II	15-89
15-29	Body Geometry - Task I	15-90
15-30	Skin and Stiffener Unit Weights - Initial Screening	15-93
15-31	Unit Weight for Closed Hat Stringer Design - Detailed Concept Analysis	15-94
15-32	Final Design Airplane - Wing Structure Mass at SIC Grid Point	15-103
15-33	Comparison of Inboard Wing Mass - Task II	15-105
15-34	Final Design Airplane - Fuselage Shell Structure Mass	15-106
15-35	Impact of Composite Reinforcements on Fuselage Shell Structure Mass	15-109

LIST OF TABLES

<u>Table</u>		<u>Page</u>
15-1	Estimated Group Weight and Balance Statement - Task I	15-7
15-2	Airplane Mass Moment of Inertia - Task I	15-8
15-3	Estimated Group Weight and Balance Statement - Task II	15-11
15-4	Preliminary Group Weight Comparison	15-15
15-5	Estimated Weights for Wing and Body - Task I	15-16
15-6	Operating Weight Empty Distribution - Task I	15-18
15-7	Payload Distribution - Task I	15-20
15-8	Fuel Distribution - Task I	15-21
15-9	Individual Component Weight Distribution - Task I	15-23
15-10	Moment of Inertia of Engine, Nacelle, and Propulsion System - Task I	15-24
15-11	Moment of Inertia of Wing Structure and Fuel - Task I	15-24
15-12	Airplane Geometric Parameters - Task I and Task II	15-26
15-13	Operating Weight Empty Distribution - Task IIB Strength/Stiffness Design	15-28
15-14	Payload and Fuel Distribution - Task II Strength/Stiffness Design (Lb/Side)	15-32
15-15	Individual Component Weight Distribution - Task IIB Strength/Stiffness Design	15-34
15-16	Mass Data for Flutter Analysis - Task IIB	15-35
15-17	Final Mass Distribution - Strength vs Strength/Stiffness Design	15-36
15-18	Fuel Distribution for Tank No. 16 - Strength vs Strength/Stiffness Design	15-38
15-19	Moment of Inertia - Wing, Payload and Fuel - Task II	15-38
15-20	Moment of Inertia - Aileron and Outboard Flaperon	15-38

LIST OF TABLES-(Cont.)

<u>Table</u>		<u>Page</u>
15-21	Summary of Wing Mass - Initial Screening	15-45
15-22	Estimated Wing Mass - Chordwise Stiffened Concept - Initial Screening	15-46
15-23	Estimated Wing Mass - Spanwise Stiffened Concept - Initial Screening	15-49
15-24	Summary of Wing Mass - Detailed Concept Analysis	15-51
15-25	Panel Load and Unit Weight - Chordwise Stiffened Design	15-53
15-26	Component Weight Derivation - Chordwise Stiffened Design - Detailed Concept Analysis	15-55
15-27	Panel Load and Unit Weight - Spanwise Stiffened Design	15-60
15-28	Estimated Wing Mass - Monocoque Design Concept	15-65
15-29	Panel Load and Unit Weight - Monocoque Welded Design	15-66
15-30	Component Unit Weight Derivation - Monocoque Welded Design	15-69
15-31	Estimated Wing Structure Mass - Monocoque (Welded) Concept	15-70
15-32	Basic Unit Weight Data for Monocoque Concepts	15-71
15-33	Fail-Safe Weight Increment - Aft Box	15-73
15-34	Fail-Safe Weight Increment - Tip Box	15-74
15-35	Comparison of Composite Reinforced Designs	15-76
15-36	Detailed Weights for Composite Reinforced Designs - Surface and Spar Caps	15-77
15-37	Detailed Weights for Composite Reinforced Designs - Spar Caps Only	15-78
15-38	Component Weight Derivation - Composite Reinforced Spar Caps Only	15-80
15-39	Component Weight Derivation - Composite Reinforced Spar Caps and Surface	15-81

LIST OF TABLES (Cont.)

<u>Table</u>		<u>Page</u>
15-40	Fuselage Concept Weights - Detailed Concept Analysis	15-92
15-41	Fuselage Shell Weights - Closed Hat-Stiffened Panel Concept - Task I	15-95
15-42	Aircraft Weight and Cost Summary	15-97
15-43	Final Design Airplane - Wing Mass Estimate	15-98
15-44	Final Design Airplane - Fuselage Mass Estimate	15-99
15-45	Wing Structure Fail-Safe Penalty	15-108
15-46	Final Design Airplane - Fuselage Unit Weights	15-108



## SECTION 15

### MASS ANALYSIS

#### INTRODUCTION

The analyses performed to provide structural mass estimates for the arrow-wing supersonic cruise aircraft described in Section 2, are presented in this section.

To realize the full potential for structural mass reduction, a spectrum of approaches for wing and fuselage primary structure design were investigated through analyses, design studies, and detailed design: (1) to assess the relative merits of various structural arrangements, concepts and materials (2) to select the structural approach best suited for the Mach 2.7 environment and (3) to provide construction details and structural mass estimates based on in-depth structural design studies.

#### BASELINE CONFIGURATION MASS DATA

The interior arrangement of the baseline configuration concepts adopted for the Task I and Task II studies are presented in Figures 15-1 and 15-2, respectively. The dimensional and mass characteristics for the configurations are fully described in Section 2. For completeness, however, the airplane mass property data are presented in the following sections along with a group weight comparison with the study of Reference 1.

#### Airplane Mass Properties - Task I

Estimated Group Weight and Balance Statement. - An Estimated Group Weight and Balance Statement is presented on Table 15-1 for the Baseline Configuration - Task I. The airplane has a taxi mass of 340,000 kilograms (750,000 pounds), and a range of 7800 kilometers (4200 n. miles) with a payload of 22,000 kilograms (49,000 pounds). This primarily titanium wing has a total planform area of 1,005 sq. meters and an aspect ratio of 1.62. Its mass includes the center section carry-through structure

under the floor, aerodynamic control surfaces and secondary structure. The horizontal stabilizer, and body mounted fin are all-movable. There are also fixed fins outboard on the wing. The body is 90.5 meters long, and will accommodate 23<sup>4</sup> passengers in five (5) abreast seating. The under floor baggage compartment is located between the nose landing gear and the wing carry-through structure.

The wing mounted main landing gear retracts into a well just outboard of the body. The axisymmetric inlets and duct-burning turbofan engines are under the wing with the thrust reversers just aft of the wing trailing edge. The engines are sized to provide a takeoff thrust to weight ratio of .36.

The mass estimates for the system and equipment reflect composite material application. Standard and operating equipment includes the crew, unusable fuel, and passenger service items.

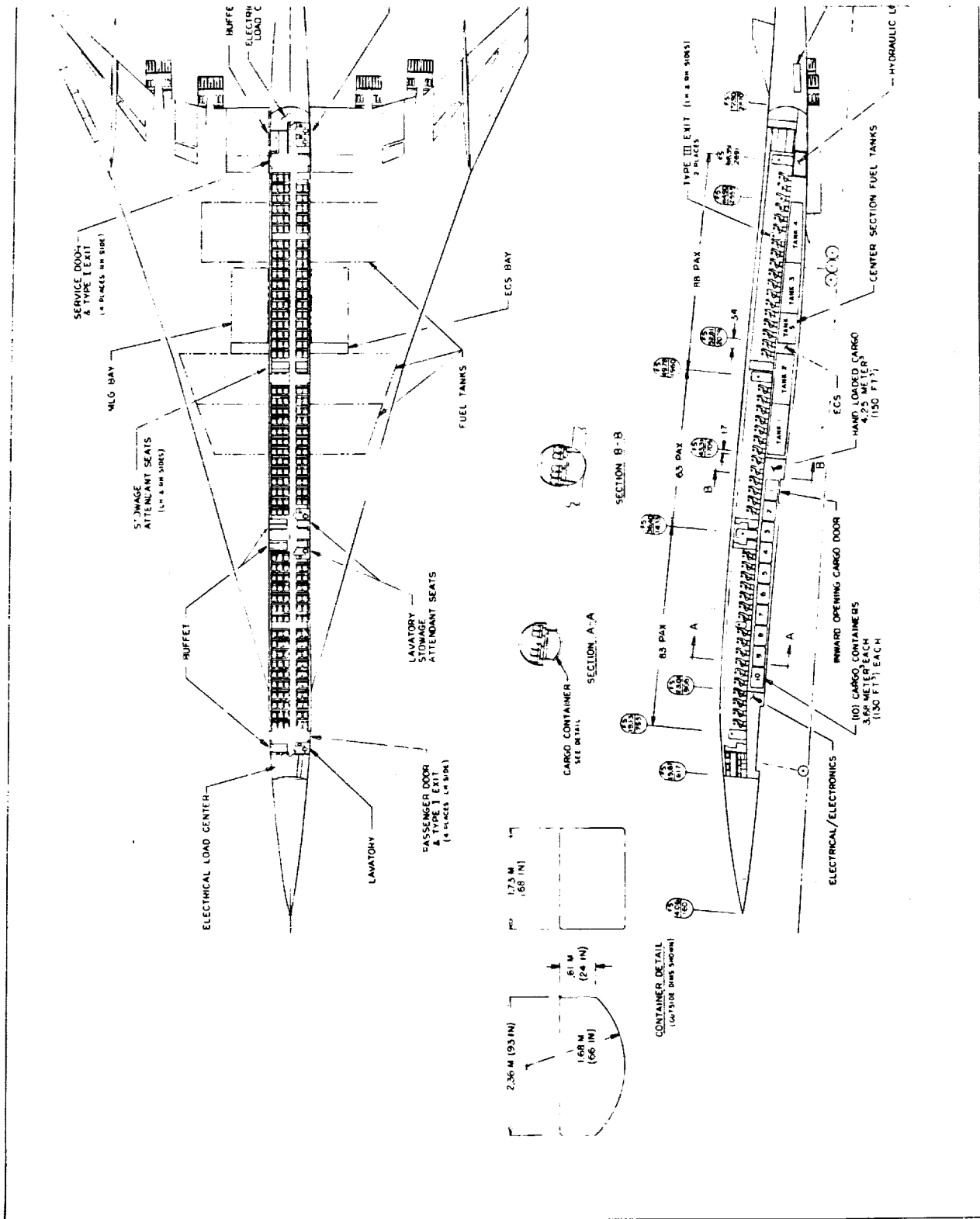
Mass Moment of Inertia. - Airplane mass moments of inertia were determined for the aeroelastic studies. The data for takeoff gross weight, operational weight empty and two intermediate flight conditions are summarized in Table 15-2.

Center of Gravity Travel. - The center of gravity travel is tailored to permit the airplane to cruise with a minimum trim drag penalty. This is accomplished by sequencing the fuel tanks. The forward body and forward wing tanks are used for climbing and accelerating to cruise Mach number. The remaining wing tanks and mid-body tanks are used during cruise. The last two body tanks contain the landing and reserve fuel.

The interior is configured for 23<sup>4</sup> passengers in five (5) abreast seating with a seat pitch of .86 meters. The baggage is loaded aft of the nose landing gear. Loadability studies indicate unrestricted passenger seating and small curve deviation from the straight payload line. This is primarily due to the low passenger mass to taxi mass fraction.

The fuel tank center of gravities are based on a fuel density of .803 kilogram/liter. The usable fuel volumes are calculated on the basis of 90-percent of the gross contour cross sectional area to allow for structure, systems and usable fuel.

The center of gravity travel shown in Figure 15-3 is used for the Task I Analytical Design Studies. The results of the design, stability and control, and weight and balance studies during Task I are reflected in a new travel diagram for the Engineering Design Study of Task II.



ORIGINAL PAGE  
POOR QUALITY  
FOLDOOUT FRAME 1



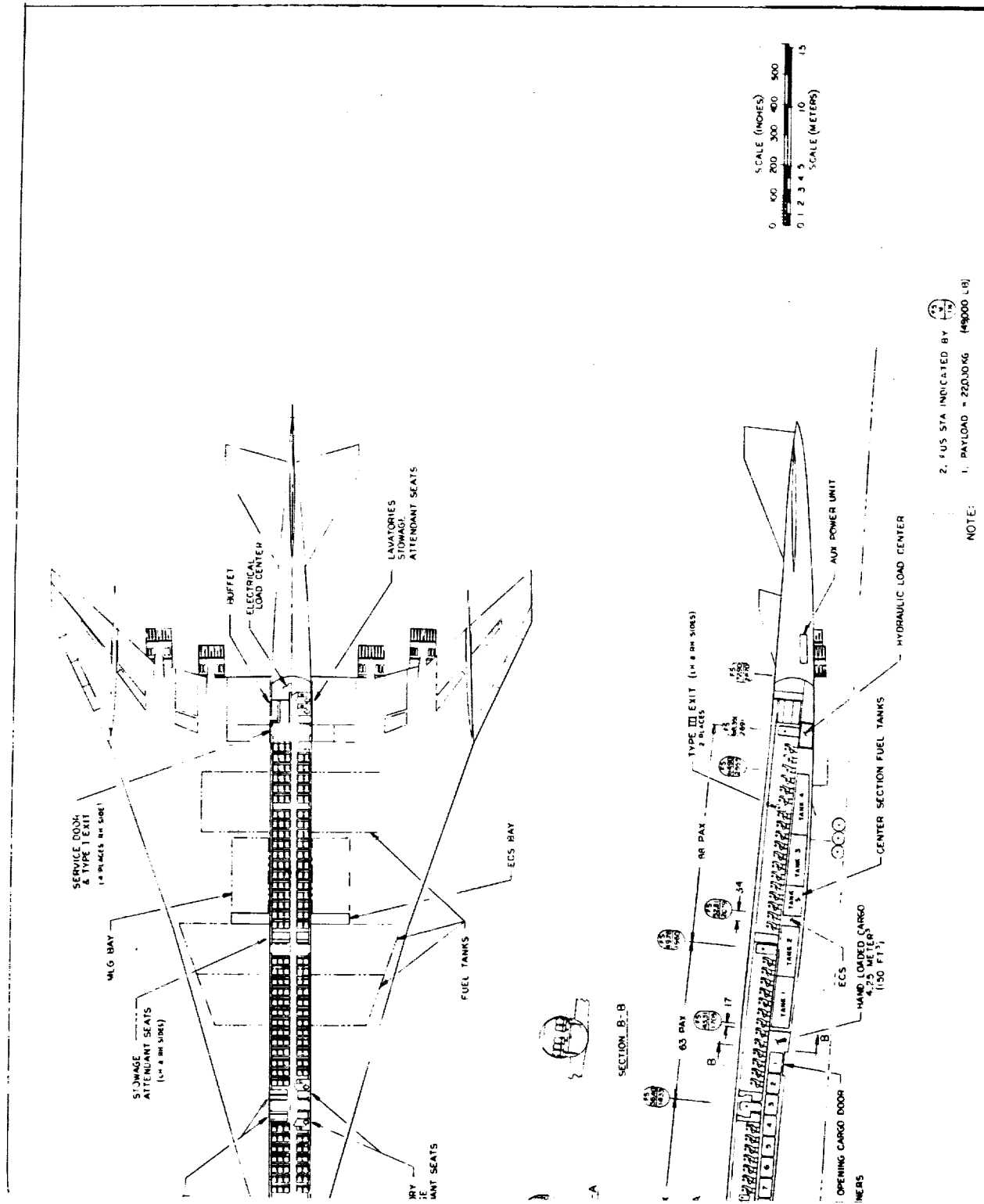
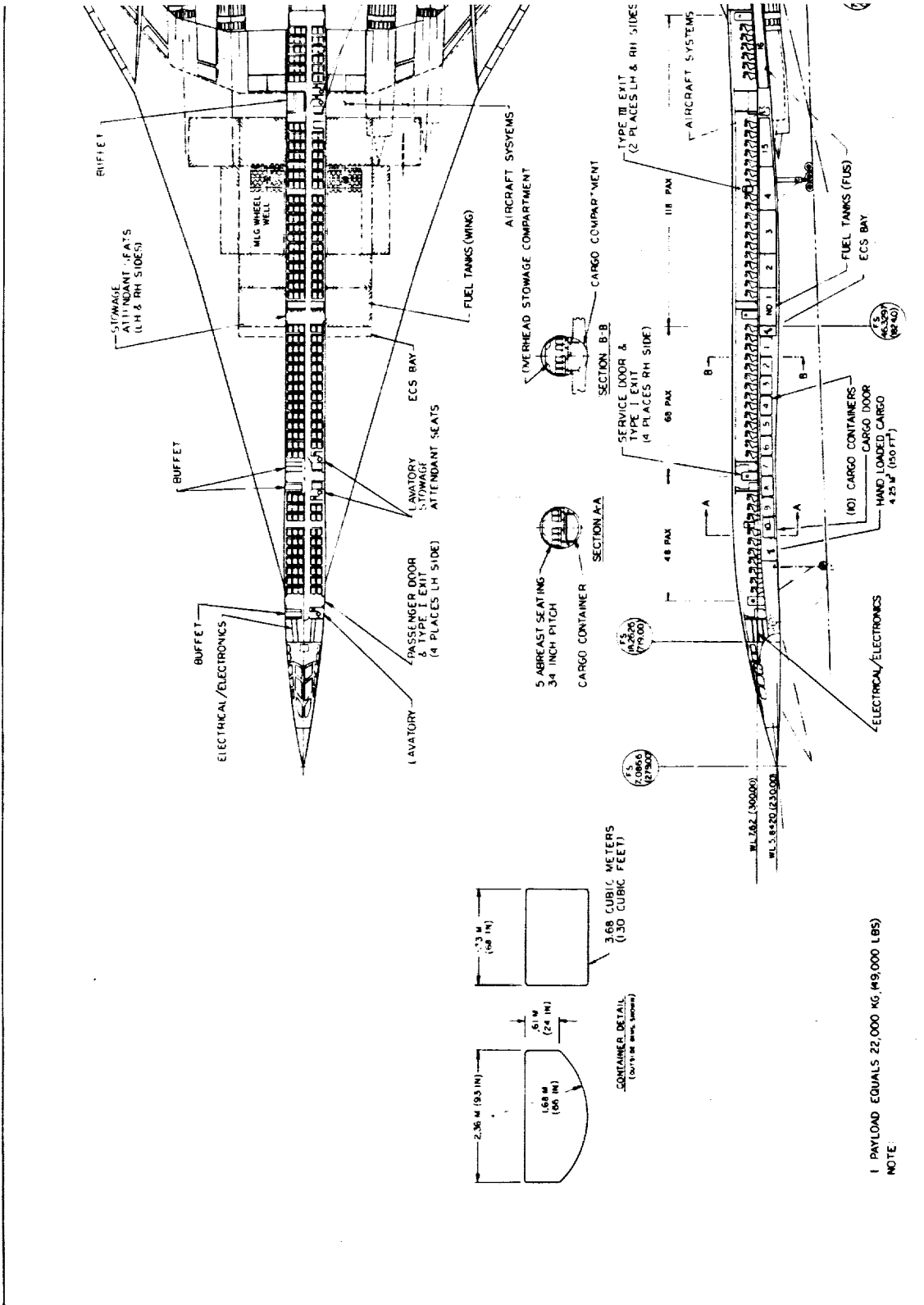


Figure 15-1. Interior Arrangement - Task I

153





PRECEDING PAGE BLANK NOT FILMED

FOLDOUT FRAME 1

ORIGINAL PAGE IS  
POOR QUALITY



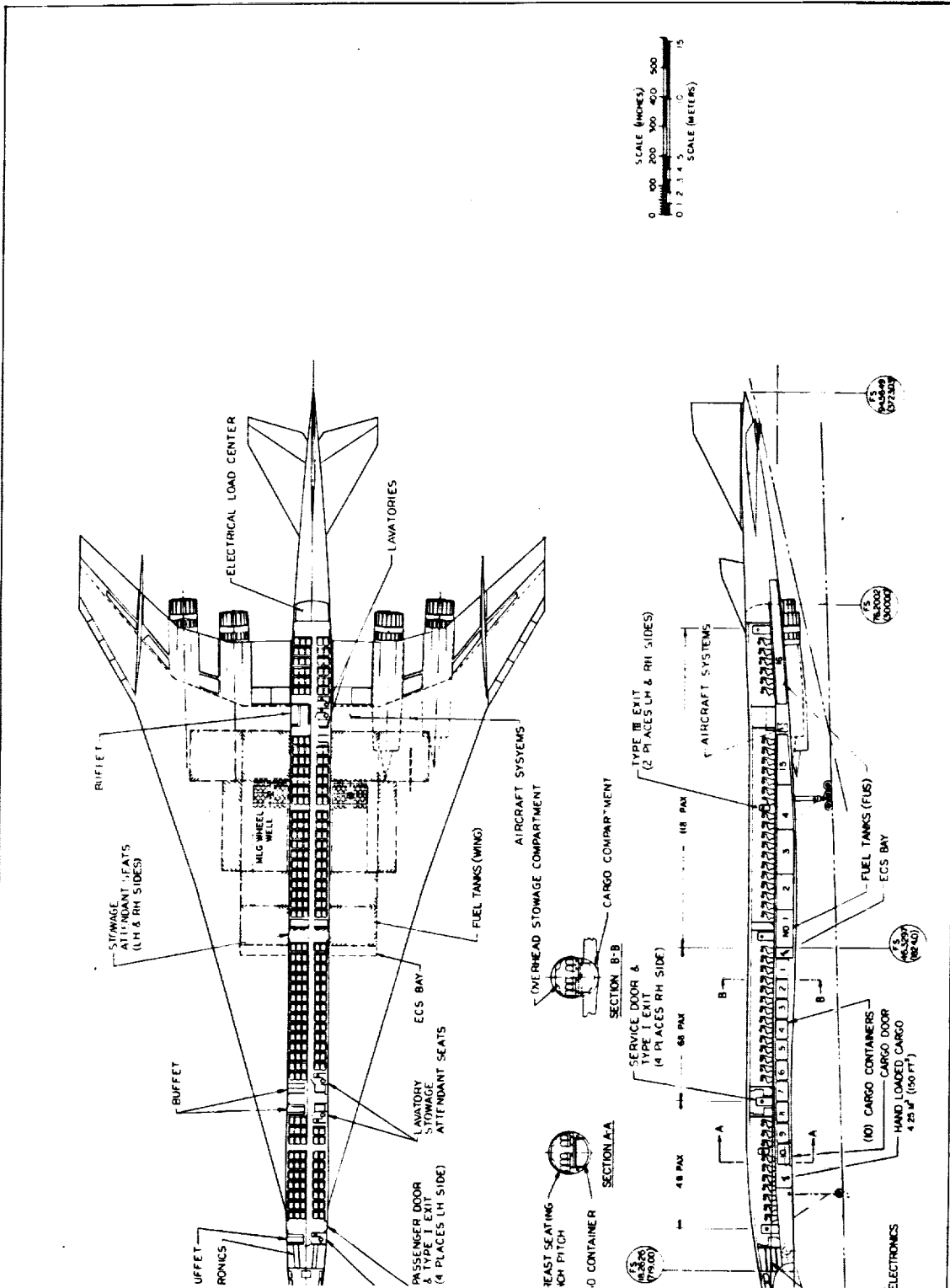


Figure 15-2. Interior Arrangement - Task II



TABLE 15-1. ESTIMATED GROUP WEIGHT AND BALANCE STATEMENT - TASK I

ITEM	% MAC	MASS (kg)	HORIZONTAL X-ARM	
			(lb)	(in)
WING	49.713	109,600	58.42	2,300
TAIL - FINS ON WING	1.270	2,800	75.69	2,980
TAIL - FIN ON BODY	1.043	2,300	89.66	3,580
TAIL - HORIZONTAL	2,830	6,240	87.63	3,450
BODY	18.597	41,000	47.55	1,872
LANDING GEAR - NOSE (UP)	1.361	3,000	17.53	690
LANDING GEAR - MAIN (UP)	12,428	27,400	58.32	2,296
AIR INDUCTION	8,074	17,800	67.56	2,660
NACELLES	2,223	4,900	71.55	2,817
PROPELLION - T/F ENGINE INBD.	10,115	22,300	70.87	2,790
PROPELLION - T/F ENGINE OUTBD.	10,115	22,300	72.31	2,847
PROPELLION - SYSTEMS	3,175	7,000	58.42	2,300
SURFACE CONTROLS	3,856	8,500	60.76	2,392
INSTRUMENTS	558	1,230	36.14	1,423
HYDRAULICS	2,585	5,700	58.65	2,309
ELECTRICAL	2,064	4,550	52.10	2,051
AVIONICS	862	1,900	24.64	970
FURNISHINGS & EQUIPMENT	5,216	11,500	43.36	1,707
ECS	3,765	8,300	47.98	1,889
TOLERANCE & OPTIONS	898	1,980	50.80	2,000
MEW	57.7	140,748	310,300	58.98
STD. & OPER. EQ.		4,887	10,700	43.18
OEW	56.1	145,635	321,000	58.45
PAY LOAD		22,000	49,000	42.11
ZFW	49.9	167,635	370,000	56.29
FUEL		172,355	380,000	53.01
TAXI MASS	45.1	340,000	750,000	54.64
NOSE	= 4.064m (160 in.)			2,151
MAC	= 34,4881 m. (11357.7964 in.)			
				LEMAC X = 39,0855 m. (1538.7961 in.)

PRECEDING PAGE BLANK NOT FILMED

ORIGINAL PAGE IS  
OF POOR QUALITY

TABLE 15-2. AIRPLANE MASS MOMENT OF INERTIA - TASK I

WEIGHT CONDITION	WEIGHT (LB)	X (IN)	Z (IN)	PITCH	ROLL	YAW
				$10^6$ SLUG-FT $^2$		
TAKE OFF GROSS	750,000	2151	—	40.8	6.51	47.3
OPER. EMPTY WT.	321,000	2301	—	27.7	4.68	32.2
INTERMEDIATE 1 • ZERO FUEL • FUEL (A)	699,300 370,000 329,300	2177 2216 2133	-141 -128 -155	39.9	6.36	46.2
INTERMEDIATE 2 • ZERO FUEL • FUEL (B)	455,950 370,000 85,950	2212 2216 2196	-133 -128 -157	35.2	4.75	39.9

NOTES: (A) TANKS NOS. 2-5, 8-11 PLUS: 50 PERCENT OF NOS. 1, 6 &amp; 7.

(B) TANKS NOS. 2 &amp; 4 PLUS 50 PERCENT OF NOS. 3 &amp; 5.

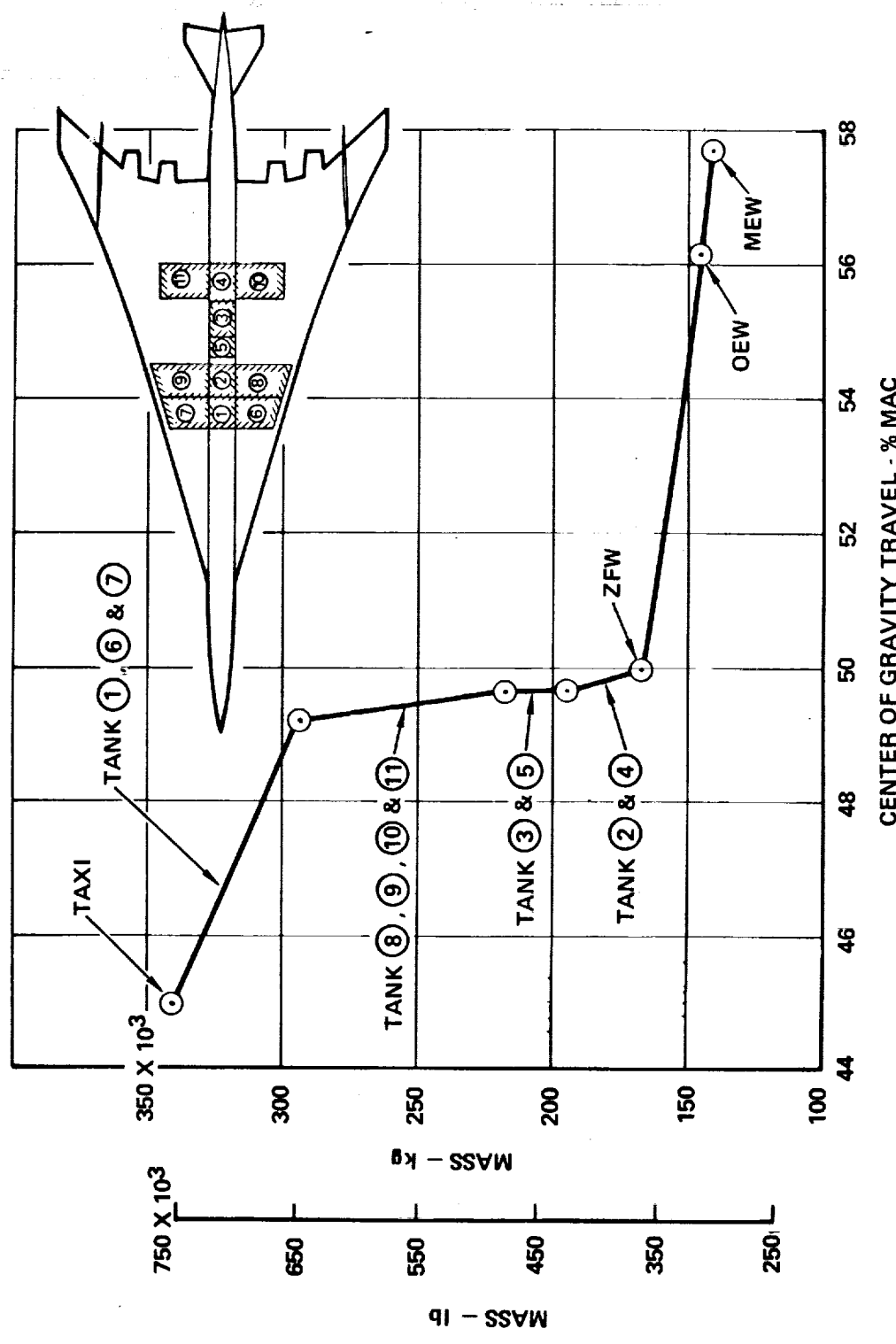


Figure 15-3. Center of Gravity Diagram - Task I

## Airplane Mass Properties - Task II

Estimated Group Weight and Balance Statement. - The airplane weight and balance data of Table 15-3 represent the various configurations evaluated during the Task II effort. The data reflect the configuration refinements adopted to the NASA 15F concept. All data are for a fixed sized aircraft with a takeoff gross mass of 340,000 kilograms (750,000 pounds) and payload of 22,000 kilograms (49,000 pounds).

- Task IIA Configuration Data - The Task I weight data (Table 15-1) were adjusted aft to reflect the effect of the configuration changes. The mass of each item was assumed invariant. The taxi mass is at the 52-percent MAC and the zero fuel weight (ZFW) is at the 53.9-percent MAC.
- Task IIB Baseline Data - The data is representative of the configuration changes adopted and the minimum mass wing and fuselage structural approach selected for the Task II effort. The engines have been resized to reflect an uninstalled sea level static thrust of 89,466 pounds per engine and appropriate mass changes for the larger air induction system and nacelles are indicated. The initial mass data does not include allowance for flutter suppression. The taxi mass is 340,000 kilograms (750,000 pounds) with the center of gravity located at the 52.5-percent MAC.
- Task IIB Final Data - The primary mass change is reflected by the increase in wing mass to include the requirements to suppress flutter. A trade off with fuel (Tank No. 16) is made to achieve the same center of gravity location as for the baseline data.

Mass Moment of Inertia. - Airplane mass moment of inertia were computed and plotted in Figure 15-4. The data is similar to that shown in Table 15-2 for the Task I airplane. The pitch moment of inertia is slightly less due to the shortened fuselage while the roll moment of inertia is greater due to the heavier propulsion packages. These data are used for the aeroelastic studies reported in Section 5 and 10.

Center of Gravity Travel. - The fuel management scheduling for airplane center of gravity control is shown in Figure 15-5. The sequencing of fuel is planned (1) to permit the airplane to cruise with a minimum of trim drag penalty and (2) to maximize the heat sink capability of the fuel by emptying the outboard wing tanks as early as possible in the mission.

TABLE 15-3 . ESTIMATED GROUP WEIGHT AND BALANCE STATEMENT - TASK II

ITEM	TASK IIA			TASK IIB				
	% MAC REFINE. DESIGN (LBS)	FUS. STA. (IN.)	% MAC DESIGN (LBS)	BASELINE DESIGN (LBS)	STRENGTH DESIGN (LBS)	FUS. STA. (IN.)	FINAL DESIGN (LBS)	FUS. STA. (IN.)
WING	109,600	2,370	89,770	87,660	2,393	90,584	2,409	
TAIL - FINS ON WING	2,800	2,991	2,800	2,800	2,991	2,800	2,991	
TAIL - FIN ON BODY	2,300	3,522	2,600	2,600	3,522	2,600	3,522	
TAIL - HORIZONTAL	6,240	3,449	7,950	7,950	3,449	7,950	3,449	
BODY	41,000	1,923	42,100	42,122	1,923	42,122	1,923	
LANDING GEAR - NOSE (UP)	3,000	915	3,000	3,000	915	3,000	915	
LANDING GEAR - MAIN (UP)	27,400	2,273	27,400	27,400	2,273	27,400	2,273	
AIR INDUCTION	17,800	2,667	19,760	19,760	2,626	19,760	2,626	
NACELLES	4,900	2,824	5,140	5,137	2,733	5,137	2,783	
PROPELLION - T/F ENGINE INBD.	22,300	2,813	25,560	25,562	2,790	25,562	2,790	
PROPELLION - T/F ENGINE OUTBD.	22,300	2,870	25,560	25,562	2,834	25,562	2,834	
PROPELLION - SYSTEMS	7,000	2,347	7,000	7,007	2,347	7,007	2,347	
SURFACE CONTROLS	8,500	2,445	8,500	8,500	2,445	8,500	2,445	
INSTRUMENTS	1,230	1,433	1,230	1,230	1,433	1,230	1,483	
HYDRAULICS	5,700	2,433	5,700	5,700	2,433	5,700	2,433	
ELECTRICAL	4,550	2,132	4,550	4,550	2,132	4,550	2,132	
AVIONICS	1,900	1,085	1,900	1,900	1,085	1,900	1,085	
FURNISHING & EQUIPMENT	11,500	1,842	11,500	11,500	1,342	11,500	1,842	
ECS	8,300	2,009	8,300	8,300	2,009	8,300	2,009	
TOLERANCE & OPTIONS	1,980	2,000	1,980	1,980	2,000	1,980	2,000	
MEW	STD & OPER. EQ.	2,372	62.2	302,300	300,220	2,389	303,144	2,394
OEW	PAYOUT	10,700	1,819	10,700	10,700	1,819	10,700	1,819
ZFW	FUEL	321,000	2,353	60.8	313,000	310,920	2,369	313,844
		49,000	1,776	49,000	49,000	1,771	49,000	1,771
		370,000	2,277	54.8	362,000	359,920	2,288	362,844
		380,000	2,226	388,000	390,080	2,228	387,156	2,223
	TAXI MASS	52.0	750,000	2,251	52.5	750,000	2,257	750,000
								2,257

LEMAC = FS 1548.2 MAC = 1351.06  
 X ARM = DISTANCE FROM FUSELAGE  
 STATION (F.S.) 0  
 FUS. NOSE AT F.S. 279

ORIGINAL PAGE IS  
OF POOR QUALITY

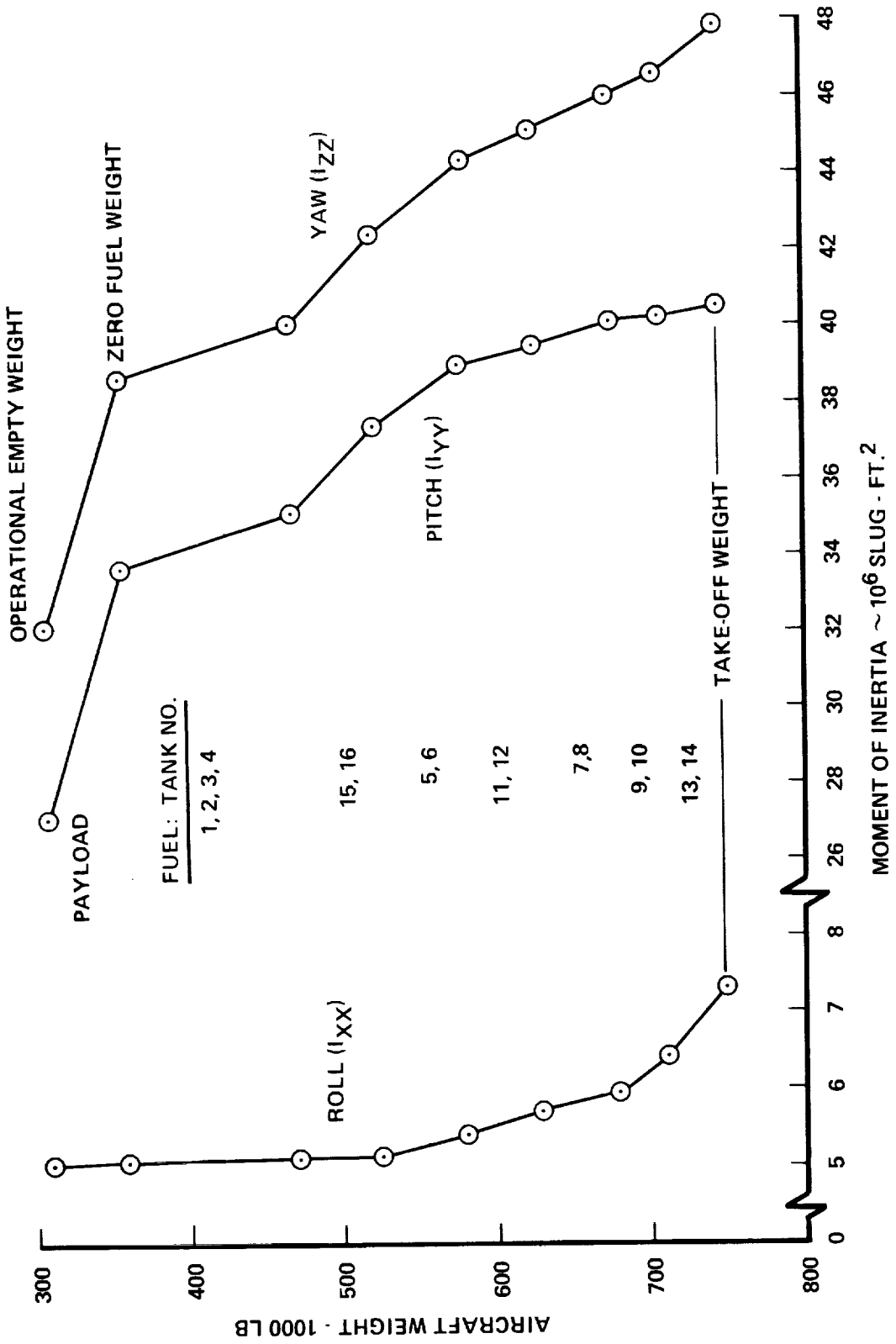


Figure 15-4. Aircraft Moment of Inertia - Task II

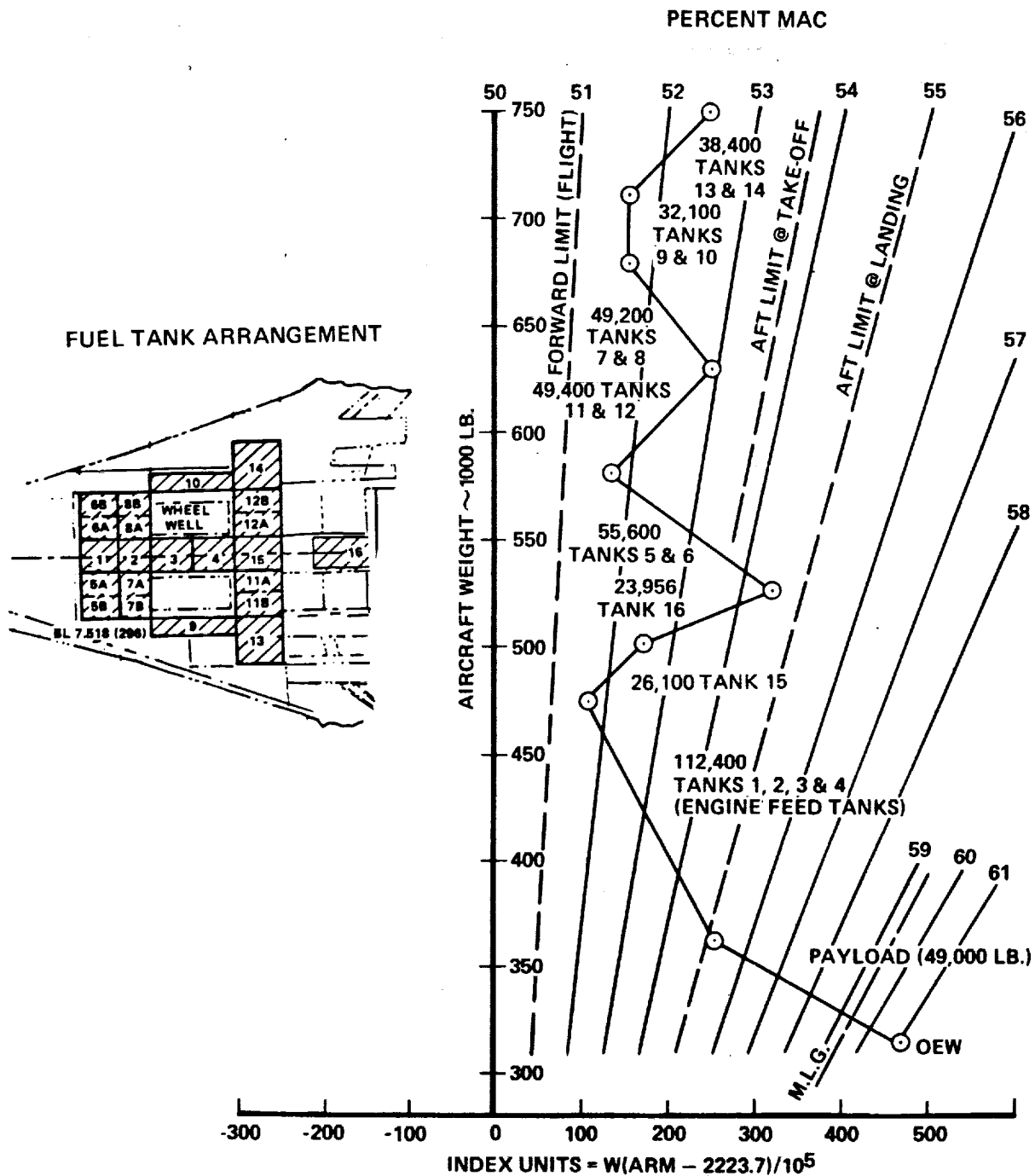


Figure 15-5. Center of Gravity Diagram - Task II

Tanks 1 through 4 are engine feed tanks and are kept full until all other tanks are empty. The usable fuel mass is based on a fuel density of 0.803 kilogram/liter (6.7 pound/gallon) and 90 percent of the gross volume to allow for structure, systems and unusable fuel. The forward limit for flight (51-percent MAC) and the aft limit for takeoff and landing are indicated at 53.5-percent MAC and 55-percent MAC, respectively.

#### Weight Comparison Data

To compare with previously established weight trends for supersonic cruise aircraft, a group weight comparison was made. The data, presented in Table 15-4, compares a preliminary weight estimate for the arrow-wing supersonic cruise aircraft derived from parametric relationship of the various items (i.e. wing, body) and data of Reference 1. The referenced data is for the Boeing 969-336C production configuration which was obtained by scaling-up-the group weights of the prototype aircraft. As noted on the table, the heavier wing weight used for the starting point of this study is offset by the lighter body structure weight which considers composite application in the cooled interior (i.e. floor beams, post, trim). The larger diameter turbofan engines result in an increase in inlet weights. The equipment and system weight reductions over the referenced data are achieved by utilizing composite materials.

#### Detail Wing and Body Weights

The scope of the study is to determine the structural approaches best suited for the wing and fuselage design of a Mach 2.7 supersonic cruise aircraft. To identify the relative weights of those components which make up the wing and body structure, these groups were further broken-down into more detailed components as presented in Table 15-5. This procedure isolates different types of structural elements and their relative weights. As the analyses of different elements are completed, the results are compared to the initial estimated values. The relative proportion between the primary structural elements is determined by typical percentages from previous studies and analyses. Other items, such as control surfaces, utilize representative unit weights and their respective areas. Door and windows are based on the size, type, and quantity.

TABLE 15-4. PRELIMINARY GROUP WEIGHT COMPARISON

REFERENCE	LOCKHEED ARROW-WING INITIAL DATA	BOEING 969-336C PRODUCTION
	PARAMETRIC DATA	REFERENCE 1
ITEM	WEIGHT (lbs)	WEIGHT (lbs)
WING	109,600	92,700
TAIL - HORIZONTAL	4,400	2,370
- VERTICAL	3,800	3,270
- CANARD	-	2,950
BODY	41,000	51,570
LAND. GEAR - NOSE	3,000	3,030
MAIN	27,400	27,910
AIR INDUCTION	17,200	} 15,650
NACELLE	6,800	
TOTAL STRUCTURE	(213,200)	(199,450)
PROPELLION - ENGINES	46,000	45,020
- SYSTEMS	7,000	6,310
SURFACE CONTROLS	8,500	12,450
INSTRUMENTS	1,230	3,400
HYDRAULICS	5,700	5,600
ELECTRICAL	4,550	5,050
AVIONICS	1,900	2,690
FURN. AND EQUIPMENT	11,500	21,290
ECS	8,300	8,100
OPTIONS AND TOLERANCES	2,420	5,480
MANUF. EMPTY WT. (MEW) STD AND OPER EQ.	310,300 10,700	314,840 11,810
OPER. EMPTY WT. (OEW) PAYLOAD	321,000 49,000	326,650 48,906
ZERO FUEL WEIGHT (ZFW) FUEL	370,000 380,000	375,556 374,444
TAXI WEIGHT	750,000	750,000

TABLE 15-5. ESTIMATED WEIGHTS FOR WING AND BODY - TASK I

ITEM	WEIGHT (lbs)	
	COMPONENT	GROUP
<b>WING GROUP:</b>		
CENTER SECTION	17,000	109,600
SURFACE MATERIAL	12,750 lb.	
SHEAR MATERIAL	3,400	
RIBS	850	
OUTER PANEL	66,620	
SURFACE MATERIAL	49,960	
SHEAR MATERIAL	7,330	
RIBS	9,330	
LEADING EDGE	5,470	
TRAILING EDGE	5,520	
MLG DOORS	3,600	
BODY FAIRING	1,600	
AILERONS	1,440	
T.E. FLAPS	6,880	
L.E. FLAPS	1,220	
SPOILERS	250	
<b>BODY GROUP:</b>		41,000
BULKHEADS AND FRAMES	4,940	
SKINS	10,510	
LONGERONS AND STIFFENERS	6,010	
NOSE AND FLIGHT STATION	2,500	
NLG WELL	900	
WINDSHIELD AND WINDOWS	1,680	
FLOORING AND SUPPORTS	3,820	
DOORS AND MECHANISM	4,170	
UNDERWING FAIRING	1,870	
CARGO COMPARTMENT PROVISIONS	1,060	
WING-BODY FITTINGS	1,500	
TAIL-BODY FITTINGS	600	
PROVISIONS FOR SYSTEMS	740	
FINISH AND SEALING	700	

## STRUCTURAL MODEL MASS DATA

### Grid Point Distribution - Task I

The data from the Estimated Group Weight and Balance Statement of Table 15-1 are distributed to the structural model grid points (SIC) for use in the static loads and flutter analysis programs. For the initial effort, a single mass distribution which is representative of the three structural arrangements is used.

Table 15-6 presents the Operating Weight Empty (OWE), Table 15-7 the payload, and Table 15-8 the fuel distribution by tank. Several individual components lumped in the SIC distribution are listed separately in Table 15-9.

The negative sense of weight values at some points are the result of applying a couple to obtain the correct center of gravity for the overhanging vertical fins. The mass moment of inertia for the propulsion system, wing, and fuel are presented in Tables 15-10 and 15-11. These data are based on the weight distribution at the SIC grid points. The grid point locations are defined in Section 9, Structural Analysis Models.

### Grid Point Distribution - Task IIA

For the Task IIA investigation, the Task I weight data (Table 15-1) were adjusted aft to reflect the configuration changes adopted. The configuration refinements are shown in Figure 15-6. The major configuration differences are delineated below:

- (1) Added wing area (50 sq. ft./side) outboard of BL 470 by reducing angle of the leading edge from 64.64-degrees to 60-degrees.
- (2) Increased number of fuel tanks and changed the tank arrangement to achieve an aft shift in center-of-gravity.
- (3) Reduced length of fuselage forebody by 119 inches, payload moved aft.
- (4) Increased fuselage-mounted vertical tail area from 290 sq. feet to 325 sq. feet.

The geometric parameters for these changes are defined in Table 15-12.

The appropriate changes to reflect the aforementioned refinements were made (data not included) including changes to the wing tip surface panel distribution to reflect strength-designed thicknesses (Figure 15-7). These data were then input to the static loads and flutter analysis programs.

TABLE 15-6. OPERATING WEIGHT EMPTY DISTRIBUTION - TASK I

SIC PT.	GP NO.	X IN.	Y IN.	W *	SIC PT.	GP NO.	X IN.	Y IN.	W *	SIC PT.	GP NO.	X IN.	Y IN.	W *
1 2 3 4 5 6 26	0102 0104 0106 0108 0110 3151 0212	200 400 600 800 1000 1210 1210	0 1284 2300 3157 3789 2614 450	280 32 48 63 77 90 101	12 3751 0224 0324 0424 0524 0724 0824	1955 62 125 196 232 296 335	0 485 625 520 478 655 70	2222 625 520 67 81	16 4151 36 0332	2330 125 196 0432 0532	0 62 125 105 114	0 2247 5373 594 5406 439 646 406 367	0 62 125 105 1032 1232 2330	
7	3251	1382	0	2807	13	3851	2045	0	2346	122	1232	2330	470	537
27	0214	1382	62	496	33	0226	62	2394	125	196	2432	17	4251	2405
43	0314	1382	125	793	49	0326	125	659	125	53	0334	37	0234	62
8	3351	1580	0	2561	64	0426	196	461	659	68	0434	125	125	445
28	0216	1580	62	495	91	0726	2045	365	403	82	0534	196	196	542
44	0316	1580	125	1043	102	0926	102	232	196	95	0734	232	196	481
59	0416	1580	196	500	14	3951	2145	0	2368	95	2405	296	296	428
29	0218	1680	0	1778	34	0228	62	454	106	0934	2405	296	1520	604
45	0318	1680	62	485	50	0328	125	659	115	1034	2415	406	406	445
60	0418	1680	125	672	65	0428	196	500	123	123	1234	2420	470	536
74	0518	1680	196	544	79	0528	232	457	18	4351	2485	0	0	1520
9	3451	1680	232	454	92	0728	296	653	38	0236	62	62	62	604
29	0218	1772	0	1994	103	0928	365	400	54	0336	125	560	560	536
45	0318	1772	62	491	112	1028	406	368	69	0436	196	480	480	470
60	0418	1772	125	647	15	4051	2235	0	2294	83	0536	232	232	1185
74	0518	1772	196	531	35	0230	62	450	96	0736	2485	296	296	1354
10	3551	2020	0	1994	51	0330	125	647	107	0936	2500	365	365	360
30	0320	2020	62	450	66	0430	196	490	116	1036	2508	406	406	1032
46	0420	2020	125	647	15	4051	2235	439	124	1236	2520	470	470	1110
61	0520	232	0	1984	80	0530	232	655	19	4451	2565	0	0	2887
75	0620	232	62	485	93	0730	296	400	39	0238	62	62	62	604
88	0722	232	125	640	104	0930	365	368	55	0338	125	542	542	536
11	3651	1865	0	1984	70	1030	406	406	70	0438	196	196	196	194
31	0222	1865	62	486	113	1030	435	435	84	0538	232	232	232	232
47	0322	1865	125	520	121	1130	2235	435	97	0738	2565	296	296	1122

ORIGINAL PAGE IS  
OF POOR QUALITY

TABLE 15-6. OPERATING WEIGHT EMPTY DISTRIBUTION - TASK I (Continued)

SIC PT.	GP NO.	X IN.	Y IN.	W *	SIC PT.	GP NO.	X IN.	Y IN.	W *	SIC PT.	GP NO.	X IN.	Y IN.	W *
108	0938	2590	365	360	129	1300	2400	496	162	1628	3032	701	52	
117	1038	2603	406	848	130	1304	2478	524	164	1630	3046	682	52	
125	1238	2625	470	1027	131	1310	2562	554	162	1634	3067	650	52	
20	4551	2640	0	876	133	1312	2595	510	124	165	1662	3047	771	
40	0240	62	420	125	132	1320	2645	585	143	166	1664	3055	761	
56	0340	508	135	196	134	1322	2670	552	124	167	1666	3064	750	
71	0440	469	135	1324	2698	515	121	168	1668	1668	3075	750	75	
85	0540	232	896	136	1326	2696	603	172	169	1670	3088	718	25	
98	0740	2640	296	1084	137	1328	2717	576	170	170	1674	3105	695	
109	0940	2678	365	360	138	1330	2742	543	171	171	1702	3098	794.4	
118	1040	2700	406	810	139	1332	2774	502	143	172	1704	3104	787	
126	1240	2730	470	952	140	1346	2772	640	205	173	1706	3111	779	
41	0242	2710	62	424	141	1348	2790	616	-284	174	1708	3119	769	
57	0342	125	750	143	142	1350	2812	588	-284	175	1710	3131	754	
72	0442	196	456	144	144	1352	2839	552	127	176	1714	3145	737	
86	0542	2710	232	845	145	1522	2860	523	328	177	1724	3116	794.4	
99	0742	2713	296	1035	146	1524	2863	656	156	179	1768	3152	794.4	
110	0942	2743	365	363	147	1526	2882	634	140	180	1790	3177	794.4	
119	1042	2763	406	761	148	1528	2904	603	2802	182	1794	3183	780	
127	1242	2798	470	903	149	1530	2924	578	163	181	1798	3197	794.4	
21	0143	2800	0	4114	150	1534	2959	534	218	218	218	3197	794.4	
42	0246	2855	62	107	151	1540	3001	578	109	183	0660	2660	264	
58	0346	125	215	196	152	1562	2922	711	116	184	0662	2800	264	
73	0446	215	215	107	153	1564	2934	695	117	185	1160	2720	438	
87	0546	232	155	154	156	2949	676	116	117	186	1162	2855	438	
100	0746	2855	296	75	155	1568	2968	652	117	117	117	116	9382	
111	0946	2868	365	150	156	1570	2986	630	116	116	116	720	3795	
120	1046	2880	406	75	158	1610	3024	664	42	128	1246	2900	50	
128	1246	2900	470	109	157	1614	3050	632	50	22	0145	3000	115	
23	0146	3200	0	2172	159	1622	2996	746	115	1624	3006	734	115	
24	0147	3360	0	1020	160	1624	3017	734	115	1626	3017	720	116	
25	0148	3470	0	1822	161	1626	3017	720	116	116	116	116	9382	

ORIGINAL PAGE IS  
OF POOR QUALITY

\* Pounds/side

TABLE 15-7. PAYLOAD DISTRIBUTION - TASK I

SIC PT.	GP NO.	X (y=0)	W Lbs/Side
4	0108	800	1240
5	0110	1000	2847
6	3151	1210	3680
7	3251	1382	2440
8	3351	1580	2440
9	3451	1680	1440
10	3551	1772	1240
11	3651	1865	1240
12	3751	1955	620
13	3851	2045	620
14	3951	2145	1240
15	4051	2235	1240
16	4151	2330	1240
17	4251	2405	1000
18	4351	2485	1000
19	4451	2565	973

TABLE 15-8. FUEL DISTRIBUTION - TASK I

SIC PT.	GP NO.	X IN.	Y IN.	FUEL TANK No.					TOTAL (LB/SIDE)
				1	2	3	4	5	
9 29 45 60 74	3451 0218 0318 0418 0518	1630 1680 1772 1772 1772	0 62 125 196 232	1050 1050 4200 4200 4200	- 800 1500 1500 200	- 1500 200 200 200	- 3600 6600 5000 2400	- 7800 6600 5000 2400	1050 1850 1500 200 4200
10 30 46 61 75	0220 0320 0420 0520 0620	1865 1865 1865 1865 1865	0 62 125 196 232	2600 2600 4000 2800 1900	2200 4000 2800 1900 1300	1650 3000 2100 1400 900	1650 3000 2100 1400 900	1600 3000 2100 1400 900	7800 6600 5000 2400 1200
11 31 47 62 76	0222 0322 0422 0522 0722	1865 1865 1865 1865 1865	0 62 125 196 232	4250 4250 4000 3800 3500	3900 6900 4500 4200 3100	3900 6900 4500 4200 3100	3900 6900 4500 4200 3100	3900 6900 4500 4200 3100	4250 8050 7000 4900 3300
12 32 48 63 77	0224 0324 0424 0524 0724	1955 1955 1955 1955 1955	0 62 125 196 232	4250 4250 4000 3800 3500	3900 6900 4500 4200 3100	3900 6900 4500 4200 3100	3900 6900 4500 4200 3100	3900 6900 4500 4200 3100	4250 8150 6900 4500 3100
89 90 91 92 101	0824 0824 0824 0824 101	1955 1955 1955 1955 1955	0 62 125 196 232	4250 4250 4000 3800 3500	3900 6900 4500 4200 3100	3900 6900 4500 4200 3100	3900 6900 4500 4200 3100	3900 6900 4500 4200 3100	4250 8150 6900 4500 3100
13 33 49 64 78	3851 0226 0326 0426 0526	2045 2045 2045 2045 2045	0 62 125 196 232	2175 2175 2175 2175 2175	1900 3300 2300 2200 1800	1900 3300 2300 2200 1800	1900 3300 2300 2200 1800	1900 3300 2300 2200 1800	2900 4800 3300 2300 2200
91 92 93 94 102	0726 0926 0926 0926 102	2145 2145 2145 2145 2145	0 62 125 196 232	4100 4100 4100 4100 4100	700 1000 1000 1000 1000	700 1000 1000 1000 1000	700 1000 1000 1000 1000	700 1000 1000 1000 1000	4800 4800 4800 4800 4800
14 34	0228 0228	15700 15700	16150 16150	45000 45000	9650 9650	1400 1400	1400 1400	1400 1400	122900 (Partial)
TOTAL (LB/SIDE)									

TABLE 15-8. FUEL DISTRIBUTION - TASK I (Continued)

SIC PR.	GP NO.	X IN.	Y IN.	FUEL TANK NO.	TOTAL (LB/SIDE)
15	4051	2235	0	4000	4000
35	0230	2235	62	4000	4000
16	4151	2330	0	2800	3800
36	0232	2330	62	2800	3800
17	4251	2405	0	-	2600
37	0234	0334	62	2600	5500
53	0334	125	125	2900	5400
68	0434	196	196	5400	3800
82	0534	232	232	3800	2700
95	0734	2405	296	2700	2600
18	4351	2485	0	2600	2600
38	0236	0336	62	2650	3000
54	0336	0436	125	-	5500
69	0436	196	196	4200	4200
83	0536	0736	232	2800	2800
96	0736	2485	296	2700	2700
19	4451	4451	0	1000	1000
39	0238	0238	62	-	560
55	0338	0338	125	1010	1010
70	0438	0438	196	780	780
84	0538	0538	232	530	530
97	0738	0738	296	520	520
TOTAL (LB/SIDE)				13600	39000
(Partial)				14500	67100

TABLE 15-9. INDIVIDUAL COMPONENT WEIGHT DISTRIBUTION - TASK I

SIC POINT	GRID POINT NO.	X (in.)	Y (in.)	WEIGHT lb/SIDE	ITEM
24	0147	3360	0	567	HORIZONTAL TAIL
25	0148	3470	0	2553	HORIZONTAL TAIL
24	0147	3360	0	-469	VERTICAL TAIL (MOVABLE)
25	0148	3470	0	+469 +860}	VERTICAL TAIL (MOVABLE)
33	0226	2045	62	1923	MLG (UP)
36	0232	2330	62	4928	MLG (UP)
64	0426	2045	196	1922	MLG (UP)
67	0432	2330	196	4927	MLG (UP)
3	0106	600	0	525	NLG (UP)
4	0108	800	0	975	NLG (UP)
141	1348	2790	616	-510	VERTICAL TAIL - WING
142	1350	2812	588	-510	VERTICAL TAIL - WING
148	1528	2904	603	+1020 +1400}	VERTICAL TAIL - WING
183	0660	2660	264	3795	ENGINES, NAC. AND PROP. SYS.
184	0662	2800	264	9795	ENGINES, NAC. AND PROP. SYS.
185	1160	2720	438	3684	ENGINES, NAC. AND PROP. SYS.
186	1162	2855	438	9382	ENGINES, NAC. AND PROP. SYS.

ORIGINAL PAGE IS  
OF POOR QUALITY

TABLE 15-10. MOMENT OF INERTIA OF ENGINE, NACELLE, AND PROPULSION SYSTEM - TASK I

SIC POINT	GRID PT. NO.	WEIGHT (lbs/SIDE)	$\bar{X}$ (in.)	$\bar{Y}$ (in.)	$\bar{Z}$ (in.)	1000 SLUG · ft <sup>2</sup>	
						$I_{oX}$	$I_{oY} = I_{oZ}$
183	0660	13,590	2761	264	-215	3.39	21.70
184	0662						
185	1160	13,066	2817	438	-207	3.23	20.83
186	1162						

TABLE 15-11. MOMENT OF INERTIA OF WING STRUCTURE AND FUEL - TASK I

ITEM		WEIGHT (lbs/SIDE)	$\bar{X}$ (in.)	$\bar{Y}$ (in.)	10 <sup>6</sup> SLUG · ft <sup>2</sup>	
					$I_{oZ}$	
WING STRUCTURE		75,737	2322	252	2.69	
FUEL		154,500	2082	145	2.71	
$\Sigma$	TOTAL	230,237	2161	181	6.15	

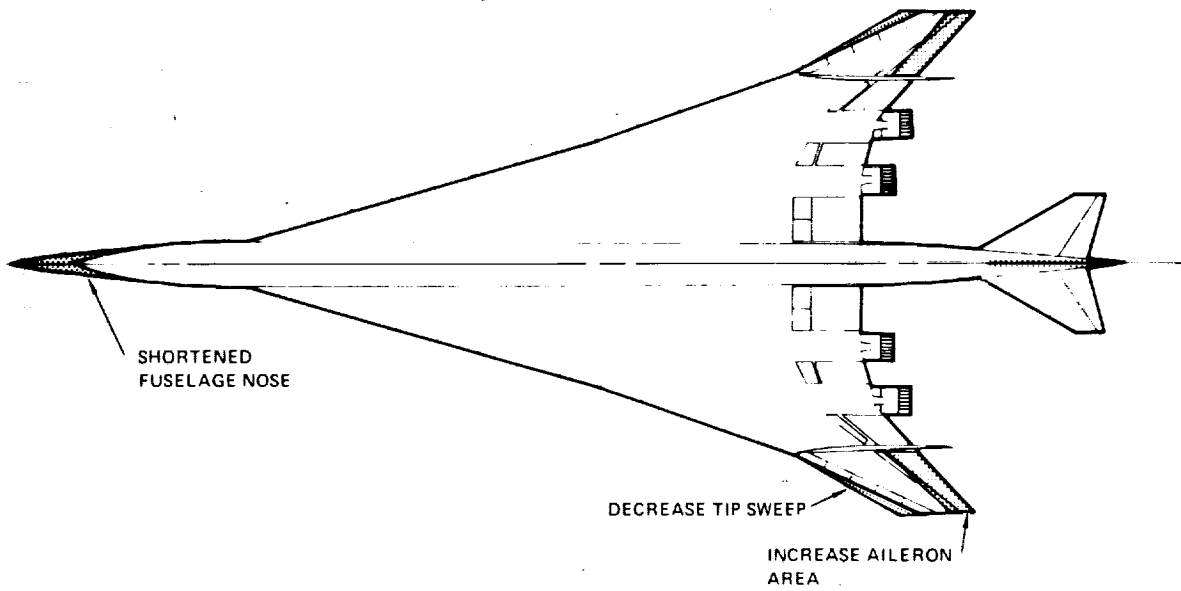
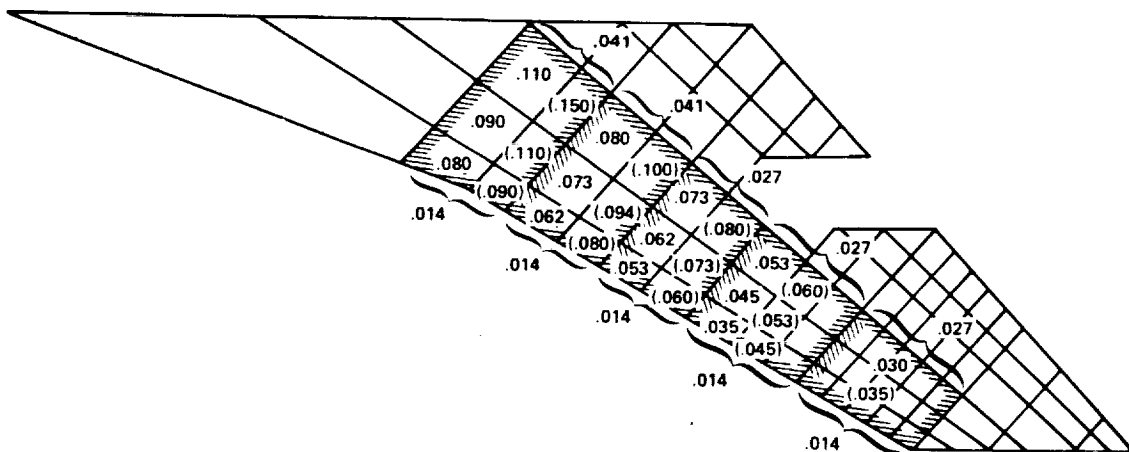


Figure 15-6. Configuration Comparison - Task I and Task II



**NOTE:**

- XXX = UPPER SURFACE EFFECTIVE THICKNESS (IN)
- (XXX) = LOWER SURFACE EFFECTIVE THICKNESS (IN)
- = BEAM WEB THICKNESS (IN)

Figure 15-7. Surface Panel Thickness - Strength Design

TABLE 15-12. AIRPLANE GEOMETRIC PARAMETERS - TASK I AND TASK II

			TASK I	TASK II
<u>WING:</u>	AREA (PARALLEL TO $Z_0$ PLANE)	ft <sup>2</sup>	10,822	10,923
	AR		1.62	1.607
	$\lambda$		0.08	0.113
	b	in.	1590	1590
	Cr	in.	2195.5	2195.5
	C <sub>t</sub>	in.	175.6	249.2
	MAC	in.	1357.8	1351.3
	L.E. SWEEP to BL 392	(degree)	74	74
	to BL 602	(degree)	70.84	70.84
	to BL 795	(degree)	64.64	60.00
<u>CONTROL SURFACES:</u>	L.E. FLAP AREA	(ft <sup>2</sup> )	159	133
	SPOILERS - PLAIN	(ft <sup>2</sup> )	120	110
	SPOILER - SLOT - DEFLECTORS	(ft <sup>2</sup> )	120	115
	FLAPS - INBOARD	(ft <sup>2</sup> )	316	306
	- FLAPERONS/AILERONS	(ft <sup>2</sup> )	310/180	247/250
<u>HORIZONTAL TAIL:</u>	AREA (WL PLANE)	(ft <sup>2</sup> )	795	795
	AR		1.607	1.607
	$\lambda$		0.225	0.225
	b	(in.)	441.6	441.6
	ELEVATOR AREA (2)	(ft <sup>2</sup> )	174	174
<u>FUSELAGE VERTICAL TAIL:</u>	AREA (MOVEABLE)	(ft <sup>2</sup> )	290	325
	AR		0.517	0.517
	$\lambda$		0.23	0.23
	b	(in.)	146.4	155.5
<u>WING VERTICAL TAIL:</u>	AREA (FIXED - 2)	(ft <sup>2</sup> )	466	466
	AR		0.495	0.495
	$\lambda$		0.136	0.136
	b	(in.)	129.0	129.0
<u>FUSELAGE:</u>	LENGTH	(in.)	3564.0	3444.0
	WIDTH	(in.)	135.0	135.0
	DEPTH	(in.)	166.0	166.0

### Grid Point Distribution - Task IIB (Strength/Stiffness)

The configuration refinements identified in Section 2 and summarized in the Grid Point Distribution discussions were adopted for the Task IIB strength and strength/stiffness design effort. The structural approach selected for these analyses is a Hybrid structural arrangement consisting of the chordwise stiffened design for the wing structure inboard of BL 406 and the monocoque design for the wing tip structure.

As shown in Table 15-3 the Task IIIA weight distribution was updated to include the engine size and weight increases to properly reflect the uninstalled sea level static thrust level of 89,466 pounds per engine instead of the 77,957 pounds per engine. Appropriate nacelle and air induction system weights were also included.

Table 15-13 presents the Operating Empty Weight (OEW) distribution for the strength/stiffness design; the payload and fuel (tanks 1 through 16) distributions are detailed in Table 15-14. The concentrated weight items which are included in the OEW distribution of Table 15-13 are identified separately in Table 15-15. The weight, center of gravity and moment of inertia data for tail surfaces and engines are contained in Table 15-16. These data were applied to the flutter analysis effort reported in Section 10.

The final strength/stiffness distribution resulting from the flutter optimization analysis is shown in Table 15-17 and pictorially displayed on Figure 15-8. To provide adequate torsional stiffness, a total weight increment of 1462 pounds per side is added to the wing tip box structure. To maintain constant aircraft gross weight, an equal weight is removed from Tank 16 fuel, as shown in Table 15-18.

The mass moment of inertia for the wing and contents is presented in Table 15-19. The data includes the wing fuel (BL 62 - BL 406) and payload distribution to BL 62.0. These data are based on the weight distribution at the SIC grid points. The moment of inertia data for the aileron and outboard flaperon are shown in Table 15-20. These data are based on an expression for calculation of the mass moment of inertia derived from the L-1011 wide body transport.

TABLE 15-13. OPERATING WEIGHT EMPTY DISTRIBUTION - TASK IIB  
STRENGTH/STIFFNESS DESIGN

MODEL GRID ID	WEIGHT (lb/SIDE)	COORDINATES		MODEL GRID ID	WEIGHT (lb/SIDE)	COORDINATES	
		X (in.)	Y (in.)			X (in.)	Y (in.)
3150	785	400.00	00.00	0212	2,923	1,210.00	62.00
3250	2,235	600.00	00.00	0214	3,036	1,382.00	62.00
3350	2,967	800.00	00.00	0216	1,654	1,580.00	62.00
3450	2,893	1,000.00	00.00	0218	1,154	1,680.00	62.00
3550	1,282	1,100.00	00.00	0220	1,330	1,772.00	62.00
0112	1,040	1,210.00	00.00	0222	1,309	1,865.00	62.00
0114	1,395	1,382.00	00.00	0224	1,136	1,955.00	62.00
0116	733	1,580.00	00.00	0226	1,186	2,045.00	62.00
0118	509	1,680.00	00.00	0228	1,815	2,145.00	62.00
0120	508	1,772.00	0.000	0230	1,785	2,235.00	62.00
0122	517	1,865.00	00.00	0232	1,686	2,330.00	62.00
0124	432	1,955.00	00.00	0234	1,164	2,405.00	62.00
0126	453	2,045.00	00.00	0236	1,163	2,485.00	62.00
0128	462	2,145.00	00.00	0238	2,586	2,565.00	62.00
0130	450	2,235.00	00.00	0240	2,637	2,640.00	62.00
0132	454	2,330.00	00.00	0242	288	2,710.00	62.00
0134	411	2,405.00	00.00	0246	100	2,855.00	62.00
0136	427	2,485.00	00.00	SUBTOTAL		(26,952)	(1,999.50)
0138	1,092	2,565.00	00.00				
0140	1,143	2,640.00	00.00	0416	480	1,580.00	196.00
5150	2,512	2,800.00	00.00	0418	175	1,680.00	196.00
5250	2,702	3,000.00	00.00	0420	220	1,772.00	196.00
5350	952	3,200.00	00.00	0422	287	1,865.00	196.00
5450	1,027	3,360.00	00.00	0424	282	1,955.00	196.00
5550	5,902	3,470.00	00.00	0426	392	2,045.00	196.00
SUBTOTAL		(33,283)	(2,109.40)	0428		310	2,145.00
				0430		1,614	2,235.00
0314	710	1,382.00	125.00	0432	1,126	2,330.00	196.00
0316	345	1,580.00	125.00	0434	370	2,405.00	196.00
0318	225	1,680.00	125.00	0436	335	2,485.00	196.00
0320	265	1,772.00	125.00	0438	430	2,565.00	196.00
0322	336	1,865.00	125.00	0440	600	2,640.00	196.00
0324	331	1,955.00	125.00	0442	768	2,710.00	196.00
0326	442	2,045.00	125.00	0446	155	2,855.00	196.00
0328	1,114	2,145.00	125.00	SUBTOTAL		(7,544)	(2,274.60)
0330	8,068	2,235.00	125.00				

REFER TO SECTION 9 STRUCTURAL ANALYSIS MODELS FOR GRID POINT LOCATIONS  
ON AIRCRAFT PLANFORM

TABLE 15-13. OPERATING WEIGHT EMPTY DISTRIBUTION - TASK IIB  
STRENGTH/STIFFNESS DESIGN (Continued)

MODEL GRID ID	WEIGHT (lb/SIDE)	COORDINATES		MODEL GRID ID	WEIGHT (lb/SIDE)	COORDINATES	
		X (in.)	Y (in.)			X (in.)	Y (in.)
0332	6,180	2,330.00	125.00	0620	215	1,772.00	266.00
0334	420	2,405.00	125.00	0722	275	1,865.00	299.50
0336	400	2,485.00	125.00	0724	182	1,955.00	296.00
0338	510	2,565.00	125.00	0726	242	2,045.00	296.00
0340	700	2,640.00	125.00	0728	342	2,145.00	296.00
0342	900	2,710.00	125.00	0730	336	2,235.00	296.00
0346	200	2,855.00	125.00	0732	340	2,330.00	296.00
SUBTOTAL	(21,146)	(2,248.30)		0734	400	2,405.00	296.00
0518	255	1,680.00	232.00	0736	400	2,485.00	296.00
0520	115	1,772.00	232.00	0738	1,745	2,565.00	296.00
0522	176	1,865.00	232.00	0740	1,695	2,640.00	296.00
0524	170	1,955.00	232.00	0742	1,100	2,713.00	296.00
0526	232	2,045.00	232.00	0746	200	2,855.00	296.00
0528	282	2,145.00	232.00	0824	187	1,955.00	332.50
0530	276	2,235.00	232.00	SUBTOTAL	(7,659)	(2,461.00)	
0532	280	2,330.00	232.00	1130	149	2,235.00	435.00
0534	355	2,405.00	232.00	1232	192	2,330.00	470.00
0536	325	2,485.00	232.00	1234	230	2,420.00	470.00
0538	1,655	2,565.00	232.00	1236	405	2,520.00	470.00
0540	1,610	2,640.00	232.00	1238	2,355	2,625.00	470.00
0542	1,035	2,710.00	232.00	1240	1,060	2,730.00	470.00
0546	140	2,855.00	232.00	1242	1,010	2,798.00	470.00
SUBTOTAL	(6,906)	(2,462.00)		1246	140	2,900.00	470.00
0926	242	2,045.00	365.00	SUBTOTAL	(5,541)	(2,646.70)	
0928	198	2,145.00	365.00	1522	230	2,818.00	676.00
0930	187	2,235.00	365.00	1524	154	2,831.50	660.00
0932	192	2,330.00	365.00	1526	202	2,854.00	633.00
0934	390	2,410.00	365.00	1528	2,569	2,882.00	600.00
0936	365	2,500.00	365.00	1530	450	2,905.50	573.00
0938	330	2,590.00	365.00	1534	125	2,949.00	521.50
0940	560	2,678.00	365.00				
0942	756	2,743.00	365.00				
0946	145	2,868.00	365.00				
SUBTOTAL	(3,365)	(2,520.40)					

REFER TO SECTION 9 STRUCTURAL ANALYSIS MODELS FOR GRID POINT LOCATIONS  
ON AIRCRAFT PLANFORM

15-29

ORIGINAL PAGE IS  
OF POOR QUALITY

15-29

TABLE 15-13. OPERATING WEIGHT EMPTY DISTRIBUTION - TASK IIB  
STRENGTH/STIFFNESS DESIGN (Continued)

MODEL GRID ID	WEIGHT (lb/SIDE)	COORDINATES		MODEL GRID ID	WEIGHT (lb/SIDE)	COORDINATES	
		X (in.)	Y (in.)			X (in.)	Y (in.)
1028	160	2,145.00	402.00	1540	180	2,998.00	573.00
1030	121	2,235.00	406.00	1562	245	2,882.00	712.00
1032	186	2,330.00	406.00	1564	165	2,894.00	698.00
1034	245	2,415.00	406.00	1566	222	2,914.00	675.30
1036	280	2,508.00	406.00	1568	304	2,937.70	647.00
1038	1,585	2,603.00	406.00	1570	340	2,958.50	623.00
1040	1,605	2,700.00	406.00	1610	250	3,007.00	668.00
1042	1,020	2,763.00	406.00	1614	75	3,046.00	623.00
SUBTOTAL	(5,332)	(2,624.30)		SUBTOTAL	(5,511)	(2,901.50)	
1300	132	2,399.00	495.00	1724	13	3,054.10	795.00
1304	181	2,475.50	523.00	1746	20	3,082.90	795.00
1310	168	2,555.50	552.00	1768	26	3,111.30	795.00
1312	275	2,589.50	511.70	1790	104	3,141.30	795.00
1320	131	2,636.50	581.30	1794	95	3,174.50	756.00
1322	180	2,659.20	554.30	1798	25	3,211.00	795.00
1324	263	2,691.00	516.80	SUBTOTAL	(283)	(3,147.30)	
1326	-488	2,686.80	600.00				
1328	173	2,703.00	581.00				
1330	238	2,732.80	546.50				
1332	477	2,769.00	503.30				
1346	254	2,755.70	639.50				
1348	197	2,770.00	622.00				
1350	318	2,796.00	592.00				
1352	426	2,828.50	554.00				
1354	536	2,854.00	524.00				
SUBTOTAL	(3,461)	(2,726.00)					
1622	192	2,961.00	758.00				
1624	106	2,971.80	745.20				
1626	129	2,987.00	727.20				
1628	214	3,005.50	705.50				

REFER TO SECTION 9 STRUCTURAL ANALYSIS  
MODELS FOR GRID POINT LOCATIONS ON  
AIRCRAFT PLANFORM

TABLE 15-13. OPERATING WEIGHT EMPTY DISTRIBUTION - TASK IIB  
STRENGTH/STIFFNESS DESIGN (Continued)

MODEL GRID ID	WEIGHT	COORDINATES		MODEL GRID ID	WEIGHT	COORDINATES	
	(lb/SIDE)	X (in.)	Y (in.)		(lb/SIDE)	X (in.)	Y (in.)
1630	122	3,023.80	684.00	ENGINE & <u>NACELLE:</u>			
1634	45	3,062.00	639.00	0660	1,306	2,660.00	264.00
1662	69	2,993.00	777.00	0662	12,759	2,800.00	264.00
1664	53	3,003.00	764.20	SUBTOTAL	(14,065)	(2,787.00)	
1666	78	3,017.00	748.30	ENGINE & <u>NACELLE:</u>			
1668	92	3,033.50	729.00	1160	2,500	2,720.00	438.00
1670	140	3,050.30	709.00	1162	11,565	2,855.00	438.00
1674	55	3,087.50	665.50	SUBTOTAL	(14,065)	(2,831.00)	
1702	26	3,025.10	795.00	WING FIN: <u>(REFERENCE)</u>			
1704	39	3,035.00	783.00	1326	-781		
1706	65	3,046.50	769.00	1528	2,181		
1708	104	3,061.00	752.00	SUBTOTAL	(1,400)	(2,990.90)	
1710	190	3,077.00	734.00	TOTAL O.E.W.	156,922	2,374.40	—
1714	90	3,113.00	691.50				
SUBTOTAL	(1,809)	(3,025.80)					

## **REFER TO SECTION 9 STRUCTURAL ANALYSIS MODELS FOR GRID POINT LOCATIONS ON AIRCRAFT PLANFORM**

TABLE 15-14. PAYLOAD AND FUEL DISTRIBUTION - TASK II STRENGTH/STIFFNESS DESIGN  
(LB/SIDE)

MODEL GRID	X (in.)	PAYLOAD	TANK NUMBER												$\rho$ FUEL = 6.7 lb/gal
			1	2	3	4	5	15	16	5	7	9	11	13	
$y = 0$															
3450	1000	2,084													
3550	1100	2,068													
0112	1210	914													
0114	1382	1,380													
0116	1580	1,489													
0118	1680	974													
0120	1772	342													
0122	1865	62													
0124	1955	557													
0126	2045	588													
0128	2145	587													
0130	2235	569													
0132	2330	526													
0134	2405	482													
0136	2485	464													
0138	2565	-													
0140	2640	218													
5150	2800	2,038													
5250	3000	-													
		(15,342)													
$y = 62.0$ in.															
0212	1210	914													
0214	1382	1,380													
0216	1580	1,490													
0218	1680	975													
0220	1772	343													
0222	1865	62													
0224	1955	557													
0226	2045	588													
0228	2145	588													
0230	2235	569													
0232	2330	526													
0234	2405	483													
0236	2485	464													
0238	2565	-													
0240	2640	219													
		(9,158)													

REFER TO SECTION 9 STRUCTURAL ANALYSIS MODELS FOR GRID POINT LOCATIONS  
ON AIRCRAFT PLANFORM

TABLE 15-14. PAYLOAD AND FUEL DISTRIBUTION - TASK II STRENGTH/STIFFNESS DESIGN  
(LB/SIDE) (Continued)

MODEL GRID	X (in.)	PAY. LOAD	TANK NUMBER												$\rho$ FUEL = 6.7 lb/gal
			1	2	3	4	15	16	5	7	9	11	13		
$Y = 135.0$ in.															
0322	1865														
0324	1955														
0326	2045														
0334	2405														
0336	2485														
0338	2565														
$Y = 196.0$ in.															
0422	1865														
0424	1955														
0426	2045														
0434	2405														
0436	2485														
0438	2565														
$Y = 232.0$ in.															
0522	1865														
0524	1955														
0526	2045														
0528	2145														
0530	2235														
0532	2330														
0534	2405														
0536	2485														
0538	2565														
$Y = 295.0$ in.															
0728	2145														
0730	2235														
0732	2330														
0734	2405														
0736	2485														
0738	2565														
$Y = 365.0$ in.															
0934	2410														
0936	2500														
0933	2590														
$Y = 406.0$ in.															
1034	2415														
1036	2508														
$TOTALS/SIDE$	24,500		14,800	12,800	14,400	14,400	13,050	15,200	27,800	24,600	16,050	24,700	955	1,160	
$X =$	1771.3		1892.0	2020.0	2155.0	2308.0	2469.6	2839.5	1892.0	2020.0	2232.0	2470.0	19,200	2465.5	

REFER TO SECTION 9 STRUCTURAL ANALYSIS MODELS FOR GRID POINT LOCATIONS  
ON AIRCRAFT PLANFORM

ORIGINAL PAGE IS  
OF POOR QUALITY

TABLE 15-15. INDIVIDUAL COMPONENT WEIGHT DISTRIBUTION - TASK IIB STRENGTH/STIFFNESS DESIGN

ITEM	GRID I.D.	WEIGHT (lb/SIDE)	$\bar{X}$ (in.)	$\bar{Y}$ (in.)	$\bar{Z}$ (in.)
NOSE LANDING GEAR (UP)		1,500	914.7	0	269.10
	3350	640	800.0	0	262.64
	3450	860	1000.0	0	273.97
MAIN LANDING GEAR (UP)		13,700	2273.0	137.2	297.80
	0330	6,810	2235.0	125.0	296.00
	0430	1,410	2235.0	196.0	304.00
	0332	4,540	2330.0	125.0	297.00
	0432	940	2330.0	196.0	306.00
VERTICAL TAIL - FUS. (MOVABLE)		1,300	3522.0	0	377.30
	5450	-615	3360.0	0	358.30
	5550	+1,915	3470.0	0	371.20
HORIZONTAL TAIL - FUS. (MOVABLE)		3,975	3449.0	0	368.70
	5450	760	3360.0	0	358.30
	5550	3,215	3470.0	0	371.20
AIR INDUCTION - INBOARD		4,940	2602.5	264.0	316.20
	0538	1,235	2565.0	232.0	313.00
	0738	1,235	2565.0	296.0	319.00
	0540	1,235	2640.0	232.0	313.00
	0740	1,235	2640.0	296.0	320.00
AIR INDUCTION - OUTBOARD		4,940	2649.7	488.0	322.10
	1033	1,235	2603.0	406.0	321.00
	1238	1,930	2625.0	470.0	319.50
	1040	1,235	2700.0	406.0	326.00
	1240	540	2730.0	470.0	325.20
ENGINES AND NACELLES - INBOARD		14,065	2787.0	264.0	305.00
	0660	1,306	2660.0	264.0	305.00
	0662	12,759	2800.0	264.0	305.00
ENGINES AND NACELLES - OUTBOARD		14,065	2831.0	438.0	311.00
	1160	2,500	2720.0	438.0	311.00
	1162	11,565	2855.0	438.0	311.00
WING FIN		1,400	2990.9	600.0	338.20
	1326	-781	2686.3	600.0	307.80
	1528	+2,181	2882.0	600.0	327.30

REFER TO SECTION 9 STRUCTURAL ANALYSIS MODELS FOR GRID POINT LOCATIONS  
ON AIRCRAFT PLANFORM

TABLE 15-16. MASS DATA FOR FLUTTER ANALYSIS - TASK IIB

ITEM	WEIGHT (lb/SIDE)	CENTER OF GRAVITY inch			MOM. OF INERTIA - ~ Slug-ft <sup>2</sup>		
		$\bar{X}$	$\bar{Y}$	$\bar{Z}$	$I_{X_0}$	$I_{Y_0}$	$I_{Z_0}$
VERTICAL TAIL ~ FUS.	1,300	3522.0	0	482.0	455	3,158	2,703
HORIZONTAL TAIL ~ FUS.	3,975	3449.0	75.3	375.0	2,091	6,159	8,250
ENGINES AND NACELLES:							
INBOARD:	14,065	2787.0	264.0	258.0	3,795	17,709	17,709
OUTBOARD:	14,065	2831.0	438.0	272.5	3,795	17,709	17,709
FIN ~ WING	1,400	2990.9	600.0	383.0	542	3,134	2,592
<u>SECT.</u>	<u>W.L.</u>						
1	312-340	240	2920	600	330	1.7	293.5
2	340-370	374	2952	600	354	6.1	611.5
3	370-400	332	2993	600	384	5.4	507.6
4	400-430	229	3034	600	414	3.7	203.1
5	430-455	125	3067	600	441	1.4	59.0
6	455-475	63	3096	600	464	0.5	14.2
7	475-TIP	37	3122	600	484	0.2	3.9

## NOTES:

REFER TO SECTION 9 STRUCTURAL ANALYSIS MODELS FOR GRID POINT LOCATIONS  
OF AIRCRAFT PLANFORM.

CENTER OF GRAVITY DIFFERENCES BETWEEN TABLE 15-16 AND TABLE 15-15  
ARE DUE TO 2-D GRID POINT LOCATIONS IN TABLE 15-15 NOT COINCIDENT WITH  
ACTUAL CENTER OF GRAVITY.

TABLE 15-17. FINAL MASS DISTRIBUTION - STRENGTH VS STRENGTH/STIFFNESS DESIGN

MODEL GRID ID	WEIGHT (lbs)		MODEL GRID ID	WEIGHT (lbs)	
	STRENGTH ONLY	STRENGTH/ STIFFNESS		STRENGTH ONLY	STRENGTH/ STIFFNESS
1300	132	132	1610	250	250
1304	168	181	1614	75	75
1310	156	168	1622	164	192
1312	270	275	1624	50	106
1320	150	131	1626	60	129
1322	180	180	1628	146	214
1324	240	263	1630	122	122
1326	-504	-488	1634	45	45
1328	144	173	1662	54	69
1330	190	238	1664	22	53
1332	410	477	1666	33	78
1346	234	254	1668	46	92
1348	138	197	1670	140	140
1350	257	318	1674	55	55
1352	364	426			
1354	536	536	1702	16	26
			1704	19	39
1522	210	230	1706	25	65
1524	103	154	1708	44	104
1526	131	202	1710	190	190
1528	2493	2569	1714	90	90
1530	450	450	1724	8	13
1534	125	125	1746	15	20
1540	180	180	1768	22	26
1562	208	245	1790	104	104
1564	84	165	1794	95	95
1566	108	222	1798	25	25
1568	190	304			
1570	340	340	TOTALS	9,602	11,064

REFER TO SECTION 9 STRUCTURAL ANALYSIS MODELS (FIGURE 9-5)

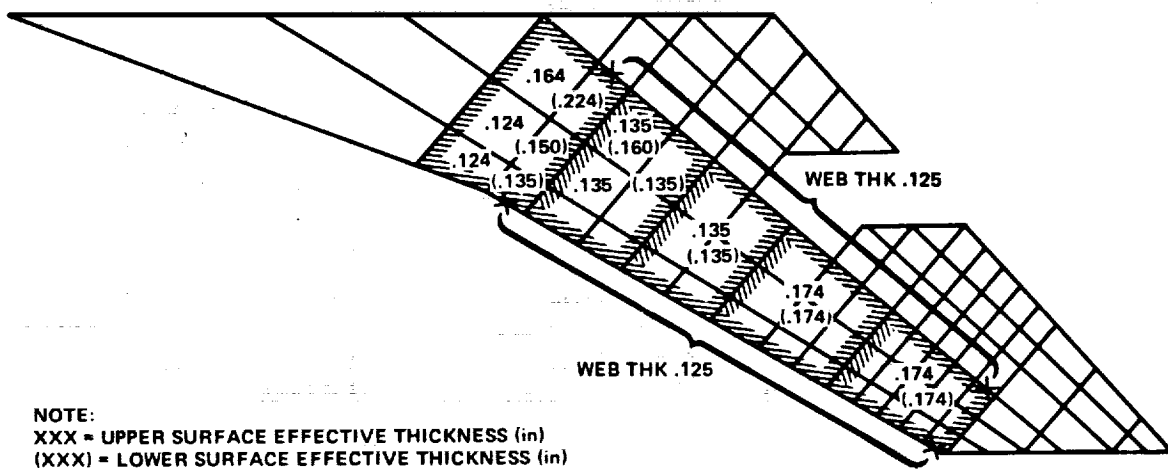


Figure 15-8. Surface Panel Thickness - Final Design

TABLE 15-18. FUEL DISTRIBUTION FOR TANK NO. 16 - STRENGTH VS STRENGTH/STIFFNESS DESIGN

MODEL GRID ID	TANK 16 FUEL (lb/side)	
	STRENGTH ONLY	STRENGTH/ STIFFNESS
0140	1,326	1,182
5150	6,013	5,359
5250	4,775	4,255
0240	1,326	1,182
TOTALS	13,440	11,978
REF. TANK 16 FUEL CAPACITY = 15,200 lb/SIDE		

TABLE 15-19. MOMENT OF INERTIA - WING, PAYLOAD AND FUEL - TASK II

ITEM	WEIGHT (lb/SIDE)	$\bar{X}$ (F.S.)	$\bar{Y}$ (B.L.)	$\bar{Z}$ (W.L.)	$I_{ZZ,c.g.}$ $10^6$ Slug - ft $^2$
WING AND CONTENTS @ OEW (A) (BL 62 TO TIP)	92,647	2320.1	223.1	275	4.32
PAYOUT (BL.62)	9,158	1820.4	62.0	310	0.34
FUEL (BL 62 to BL 406)	148,303	2191.0	160.8	270	2.18
WING AND CONTENTS @ TOW	250,108	2225.3	180.3	273.3	7.46

(A) DOES NOT INCLUDE WING FIN AND ENGINES

TABLE 15-20. MOMENT OF INERTIA - AILERON AND OUTBOARD FLAPERON

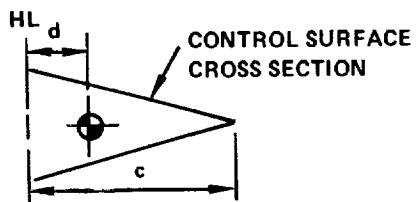
CONTROL SURFACE	AVERAGE (A) CHORD, C (in.)	WEIGHT, W (lb)	I <sub>HL</sub> (B)	
			(lb-in. $^2$ )	(lb-in.-sec $^2$ )
AILERON	65	625	$0.602 \times 10^6$	1560
OUTBOARD FLAPERON	76	504	$0.662 \times 10^6$	1720

(A) MEASURED NORMAL TO HINGE LINE

$$(B) I_{HL} = \left[ \frac{(Wc^2)}{12} + (Wd^2) \right]$$

$$I_{HL} = 0.228 Wc^2 \text{ (lb-in.}^2\text{)} \quad \text{WITH } d = 0.38c$$

$$I_{HL} = .00059 Wc^2 \text{ (lb-in.-sec}^2\text{)}$$



## STRUCTURAL CONCEPT MASS ANALYSIS

### Method

The Structural Concept Analysis section presents sized elements for selected wing and fuselage locations for each structural arrangement. The data reflects variable spar or rib spacing for each panel concept at the point design region specified. To determine the unit weights between analysis areas, the load/temperature map is utilized. This permits unit weights to be increased or decreased with corresponding changes in the load and temperature environment. Consideration is also given to the lightly loaded minimum gage regions.

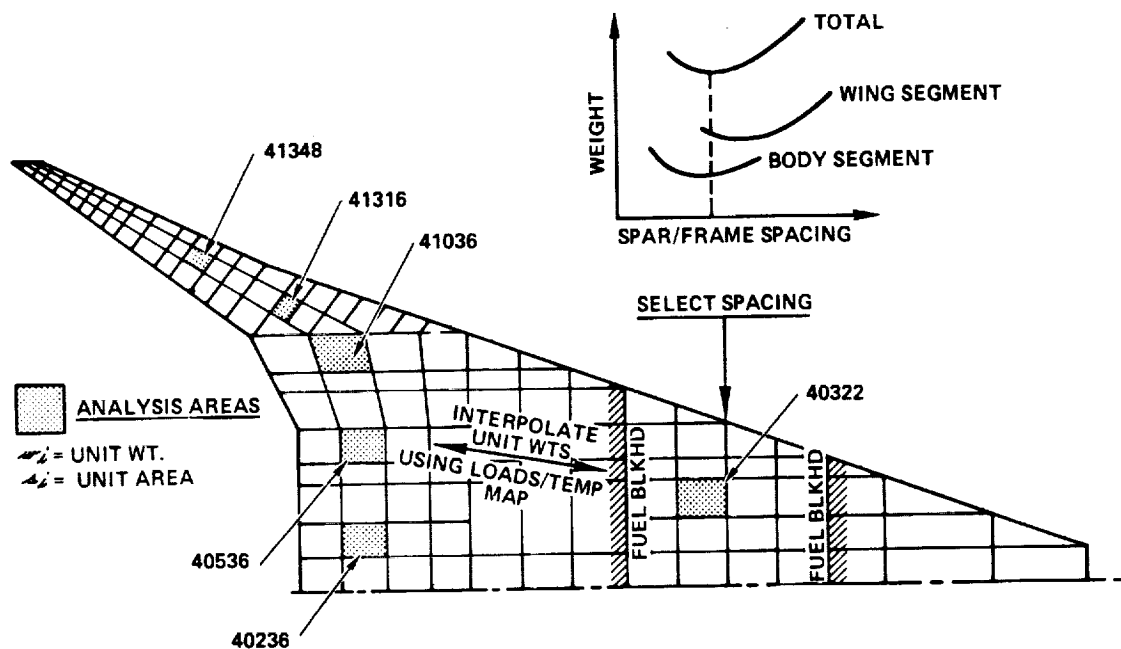
In the locations where wing spars mate to the body frames, the spacing is selected by the minimum weight combination of the wing and body segments.

Wing. - To obtain the basic wing box structure weight, the unit weights are integrated over the entire wing box areas as pictorially displayed in Figure 15-9. Assessment is also made of special structural items, access doors, systems provisions and other non-optimum items. The summation of the basic box structure, control surfaces, leading and trailing edges, result in the total wing group weight.

Fuselage. - In a similar manner to that described for the wing, four body analysis areas were selected to investigate the three candidate structural concepts of Task I. Interpolation between these areas provide sufficient information to derive a total basic shell structural weight. Special structural features are added to the basic shell structure to derive the total body weight. The procedure employed is outlined in Figure 15-10.

## WING STRUCTURE MASS-INITIAL SCREENING

Analysis regions for the initial screening of the candidate structural concepts are indicated in Figure 15-9. They are described as follows:



$$\sum_i w_i s_i = \text{BASIC BOX STRUCTURE MASS}$$

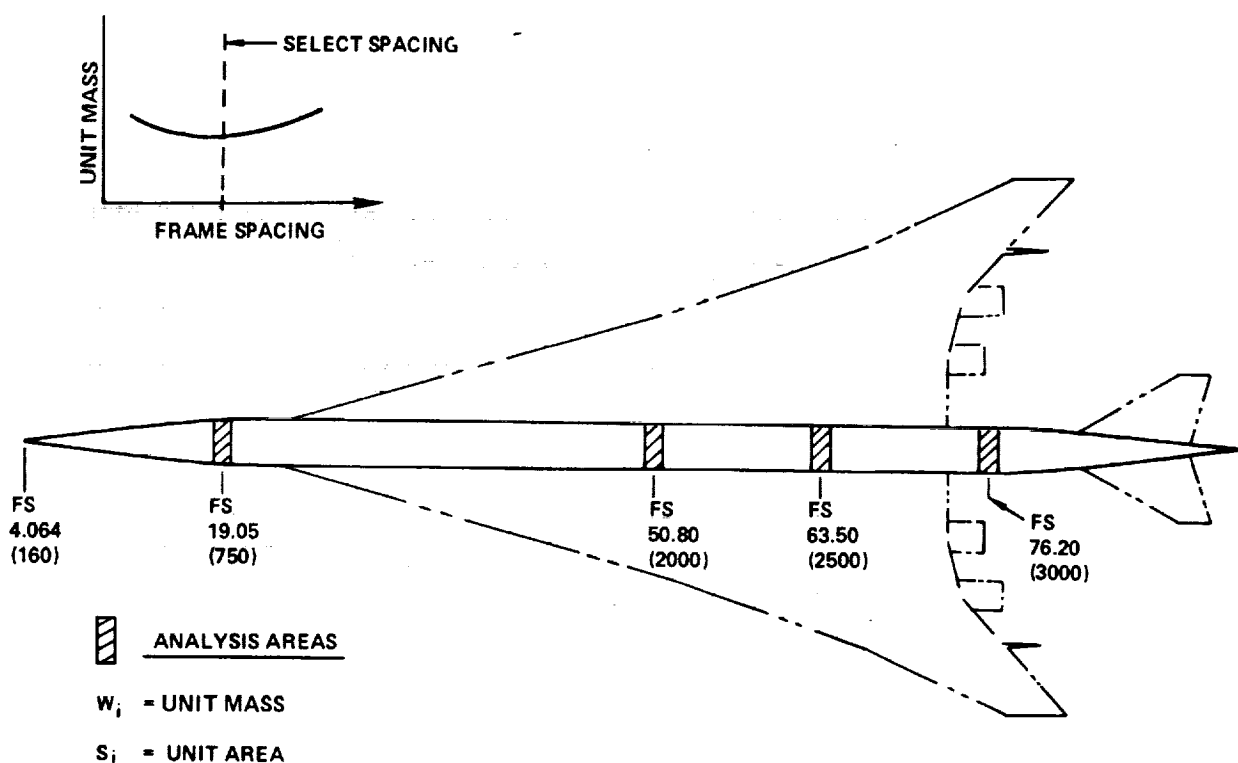
PLUS: BODY & OUTB'D JOINT RIBS, MLG WELL STR, ENG. & V. FIN RIB  
 FLAP, AILERON, SPOILER SUPT. STR.  
 FUEL BULKHEADS, ACCESS DOORS  
 JACK FTG'S, FAIRINGS, FILLETS, SEAL. & FINISH  
 LOCAL REINF., FASTENERS, SHIMS & CLIPS  
 PROVISIONS FOR SYSTEMS

**TOTAL = BOX STRUCTURE MASS**

PLUS: L.E. & FLAPS  
 T.E. & FLAPS, SPOILERS, AILERONS  
 BODY FAIRING  
 MLG DOORS

**TOTAL = WING MASS**

Figure 15-9. Wing Mass Estimation Methodology



$$\sum_i^n w_i s_i = \text{BASIC SHELL STRUCTURE MASS}$$

PLUS: NOSE AND FLIGHT STATION  
 NOSE LANDING GEAR WELL  
 WINDSHIELD AND WINDOWS  
 FLOORING AND SUPPORTS  
 DOORS AND MECHANISM  
 UNDER WING FAIRING  
 CARGO PROVISIONS  
 WING/BODY FRAMES AND FITTINGS  
 TAIL/BODY FRAMES AND FITTINGS  
 PROV. FOR SYSTEMS  
 FINISH AND SEALANT

---

**TOTAL = FUSELAGE MASS**

Figure 15-10. Fuselage Mass Estimation Methodology

<u>Point Design Region</u>	<u>Location</u>	<u>Area (Sq. Ft.)</u>
40322	Forward Box	44.4
40536	Aft Box	35.6
41348	Tip Box	10.3

By interpolation from the analysis point design regions, unit weights for each concept are applied to the panel areas shown in Figure 15-11 to derive the total box structural weight.

The initial screening data includes a non-optimum allowance for surface-to-cap joints of approximately 4-percent. Additional non-optimum allowances are applied to the box weight to arrive at a typical estimate of the "as-constructed" weight. These non-optimum allowances are itemized as:

	<u>Non optimum Factor (NOF)</u>
Joints and splices to surface panels	7-percent
Margins of safety (average)	3-percent
Sheet tolerances	2-percent
System provisions (Electrical, Fuel Controls)	5-percent
Access provisions (one surface only)	6-percent
Finish, sealant, misc.	3-percent
Total NOF	26-percent

Use of these allowances, for example, means that a stress analysis which indicates a five pound-per-square-foot panel yields an estimated fabricated weight of  $(1.26 \times 5.0) = 6.3$  pounds per square foot.

For comparison purposes, the wing weight was divided into two major categories:

- Variable weight
- Fixed weight

The variable weight consists of that portion of the box structure which is influenced by the structural concept being considered, such as the upper and lower surfaces and intermediate ribs and spars.

The fixed weight consists of those items which are unaffected by box structural concept, such as main landing gear provisions, surface controls, engine support structure, leading and trailing edge structure.

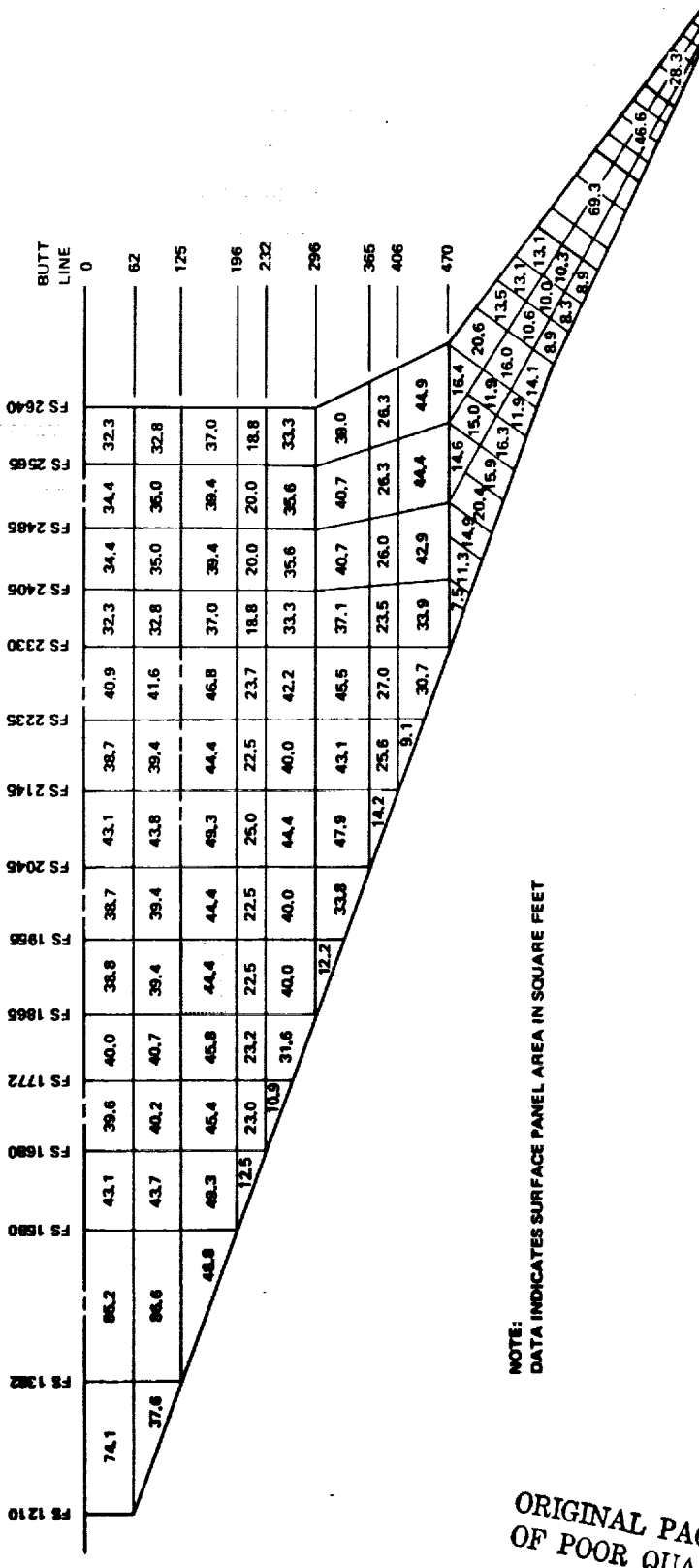


Figure 15-11. Wing Box Areas - Task I

The least weight concept for each stiffening arrangement is listed in Table 15-21. From this table, it appears that the convex beaded, chordwise stiffened arrangement with composite reinforced spar cap is preferred throughout the wing box. Subsequent flutter optimization resulted in the monocoque arrangement to be preferred for the tip structure from the least weight viewpoint.

#### Chordwise Stiffened Design Concepts

The chordwise stiffened designs employ surface panel concepts that have stiffening elements oriented in the chordwise direction. The substructure arrangement is essentially a multispar structure with widely spaced ribs. Submerged caps are provided except at panel closeouts and at fuel tank bulkheads. Four surface panel concepts were considered (see Section 1 Structural Design Concepts):

- Circular-arc concave beaded skin
- Circular-arc convex beaded skin
- Trapezoidal corrugation-concave beaded skin
- Beaded corrugation - concave beaded skin

The resulting wing weights are summarized in Table 15-22. The convex beaded concept was found to be significantly lighter than the others evaluated. In all cases, the spar weights are relatively heavy since the surface panels are ineffective in transmitting the wing span bending loads.

A general expression for deriving box panel unit weights, using the three analysis point design regions as a starting point, is based on the following parameters:

- Inplane loads:  $N_x$ ,  $N_y$ ,  $N_{xy}$
- Pressure loads:  $\Delta p$

The expression for the convex beaded optimum panel weight is:

$$w(\text{lb}/\text{ft}^2) = \left[ \left( |N_x| + |N_y| + |2 N_{xy}| + 350 |\Delta p| \right) \div (2190) \right]$$

Where,

$N_x$  = axial chordwise load (lb/in)

$N_y$  = axial spanwise load (lb/in)

$N_{xy}$  = panel shear flow (lb/in)

TABLE 15-21. SUMMARY OF WING MASS - INITIAL SCREENING

PLAN AREA (ft <sup>2</sup> )	ITEM	CHORDWISE CONVEX BEADED	SPANWISE HAT STIFFENED	MONOCOQUE H/C SAND. WELDED	CHORDWISE COMPOSITE REINFORCED
1231	VARIABLE WEIGHT (A)	56,655	62,176	50,796	43,624
	CENTER SECTION (BL 0-62)	(8,722)	(9,380)	(8,274)	(6,716)
	UPPER SURFACE	1,570	3,377	2,482	1,570
	LOWER SURFACE	1,570	3,518	2,532	1,570
	SPARS	4,884	1,041	2,325	2,878
5038	RIBS	693	1,444	935	698
	INTERM. PANEL (BL 62-470)	(39,296)	(43,478)	(35,514)	(30,258)
	UPPER	7,073	15,652	10,654	7,073
	LOWER	7,073	16,304	10,867	7,073
	SPARS	22,006	4,826	9,980	12,963
896	RIBS	3,144	6,696	4,013	3,144
	OUTER PANEL (BL 470-TIP)	(8,637)	(9,318)	(7,008)	(6,650)
	UPPER	1,555	3,355	2,102	1,555
	LOWER	1,555	3,494	2,145	1,555
	SPARS	4,837	1,034	1,969	2,850
1047	RIBS	690	1,435	792	690
	FIXED WEIGHT	(41,352)			(41,352)
	LEADING EDGE	5,235			5,235
	TRAILING EDGE	4,888			4,888
	BL 62 RIBS	1,430			1,430
1955	BL 470 RIBS	700			700
	FIN ATTACH RIBS	435			435
	REAR SPAR	3,400			3,400
	ENG. SUP'T STRUCTURE	3,580			3,580
	484				
484	MLG DOORS	2,904			2,904
	- WHEEL WELL AND ATTACH.	3,750			3,750
800	800				
	WING/BODY FAIRING	1,600			1,600
133	133				
	LE FLAPS	1,130			1,130
553	553				
	TE FLAPS	5,890			5,890
250	250				
	AILERONS	1,250			1,250
225	225				
	SPOILERS	1,360			1,360
	FUEL BULKHEADS	3,800			3,800
	TOTAL (STRENGTH DESIGN ONLY)	98,007	103,528	92,148	84,976

(A) BASED ON 20-INCH SPAR OR RIB SPACING

TABLE 15-22. ESTIMATED WING MASS - CHORDWISE STIFFENED CONCEPT - INITIAL SCREENING

ITEM	CONCAVE BEADED	CONVEX BEADED	TRAPEZOID NO BEAD	TRAPEZOID BEADED
VARIABLE WEIGHT:	(58,660)	(56,655)	(60,236)	(61,743)
CENTER SECTION	(9,030)	(8,722)	(9,273)	(9,505)
UPPER SURFACE	1,716	1,570	1,762	1,901
LOWER SURFACE	1,716	1,570	1,762	1,901
SPAR CAPS AND WEBS	4,876	4,884	5,007	5,038
RIBS	722	698	742	665
INTERM. PANEL (BL. 62 → 470)	(40,687)	(39,296)	(41,780)	(42,825)
UPPER SURFACE	7,730	7,073	7,938	8,565
LOWER SURFACE	7,730	7,073	7,938	8,565
SPARS	21,970	22,006	22,561	22,697
RIBS	3,257	3,144	3,343	2,998
OUTER PANEL (BL. 470 → TIP)	(8,943)	(8,637)	(9,183)	(9,413)
UPPER SURFACE	1,699	1,555	1,745	1,883
LOWER SURFACE	1,699	1,555	1,745	1,883
SPARS	4,829	4,837	4,959	4,989
RIBS	716	690	734	658
FIXED WEIGHT:	(41,352)			(41,352)
LEADING EDGE	5,235			5,235
TRAILING EDGE	4,888			4,888
B.L. 62 RIBS	1,430			1,430
B.L. 470 RIBS	700			700
FIN ATTACH RIBS	435			435
REAR SPAR	3,400			3,400
ENG. SUP'T. STRUCTURE	3,580			3,580
MLG DOORS	2,904			2,904
WHEEL WELL AND ATTACH.	3,750			3,750
WING/BODY FAIRING	1,600			1,600
LE FLAPS	1,130			1,130
TE FLAPS	5,890			5,890
AILERONS	1,250			1,250
SPOILERS	1,360			1,360
FUEL BULKHEADS	3,800			3,800
TOTAL (STRENGTH DESIGN ONLY)	100,012	98,007	101,588	103,095

$$\Delta p = \left( |\Delta p_u| + |\Delta p_l| \right), \text{ pressure load for combined upper and lower surfaces}$$

(lb/in<sup>2</sup>)

The total variable weight, then, after interpolating to determine each box panel unit weight is:

$$w_v = \left( \sum_1^n w_i s_i \right) (1.26) \quad (\text{Reference Figure 15-9})$$

For the convex beaded concept:

$$w_v = 56,655 \text{ pounds}; w_{ave} = \frac{w_v}{S_{box}} = \frac{56,655 \text{ (lb)}}{7,165 \text{ (ft}^2\text{)}} = 7.91 \text{ psf}$$

This result is based on the unit weights for the three analysis regions as tabulated below:

PANEL CONCEPT	Point Design Regions (A)			w <sub>ave</sub> (incl. 1.26 NOF)
	40322	40536	41348	
	Unit Weights ~ Pound per square foot			
Concave-Beaded	4.10	11.45	9.85	8.19
Convex-Beaded	3.80	11.30	9.75	7.91
Trapezoidal Corrugation	4.35	11.55	9.90	8.41
Beaded Corrugation	4.60	11.60	10.00	8.62

(A) Unit Weights do not include non optimum factor (NOF)

The total variable weight for the other concepts was facilitated by deriving a general expression, where:

$$w_v = \left( \frac{S_{box}}{5.17} \right) \left[ 3(w_{40322}) + (w_{40536}) + (w_{41348}) \right] 1.26$$

Temperature variation between panels is small and has negligible effect on the process of weight interpolation, since the structural concept for each point design already accounts for the effects of thermal stresses. For this reason, weight interpolation has been performed as a function of inplane loads and normal pressure loads.

## Spanwise Stiffened Design Concepts

The spanwise stiffened wing concept is a multirib design with closely spaced ribs and widely spaced spars. The surface panel configurations have effective load carrying capability in their stiffened (span) direction. Smooth skins are required for aerodynamic performance. The four spanwise stiffened designs investigated are as follows:

- Zee stiffened
- Integral zee stiffened
- Hat stiffened
- Integral stiffened

Their comparative weights are summarized in Table 15-23. As indicated on the table, the hat stiffener concept is the least weight. In all cases, the spar weights are relatively light, compared to the chordwise stiffened designs due to the ability of the surfaces to carry spanwise inplane loads.

A general expression for deriving box panel unit weight is:

$$w(\text{lb}/\text{ft}^2) = \left[ (|N_x| + |N_y| + |2N_{xy}| + 350|\Delta p|) \div (2190) \right]$$

where:

$N_x$  = axial chordwise load ( $\text{lb}/\text{in}$ )

$N_y$  = axial spanwise load ( $\text{lb}/\text{in}$ )

$N_{xy}$  = panel shear flow ( $\text{lb}/\text{in}$ )

$\Delta p$  = pressure load ( $\text{lb}/\text{in}^2$ )

Unit weights for each analysis panel of the four structural concepts are from Section 12 and are summarized below:

Panel Concept	Point Design Region (A)			$w_{ave}$ (incl. 1.26 NOF)
	40322	40536	41348	
	Unit Weight ~ Pound Per Square Foot (psf)			
Zee stiffened	4.95	13.30	8.55	8.77
Integral zee	4.70	13.80	8.50	8.69
Hat stiffened	4.70	13.75	8.50	8.68
Integral stiffened	5.40	14.25	9.65	9.58

(A) Unit weights do not include non optimum factor (NOF)

TABLE 15-23. ESTIMATED WING MASS - SPANWISE STIFFENED CONCEPT - INITIAL SCREENING

ITEM	ZEE STIFFENED	INTEGRAL ZEE	HAT STIFFENED	INTEGRAL STIFFENED
VARIABLE WEIGHT	(62,827)	(62,248)	(62,176)	(68,601)
CENTER SECTION	(9,479)	(9,393)	(9,380)	(10,353)
UPPER SURFACE	3,659	3,428	3,377	4,286
LOWER SURFACE	3,327	3,475	3,518	3,572
SPAR CAPS AND WEBS	1,043	1,043	1,041	1,046
RIBS	1,450	1,447	1,444	1,449
INTERM. PANEL (BL 62 → 470)	(43,931)	(43,528)	(43,478)	(47,962)
UPPER SURFACE	16,957	15,888	15,652	19,856
LOWER SURFACE	15,420	16,105	16,304	16,547
SPARS	4,832	4,832	4,826	4,844
RIBS	6,722	6,703	6,696	6,715
OUTER PANEL (BL 470 → TIP)	(9,417)	(9,327)	(9,318)	(10,286)
UPPER SURFACE	3,635	3,404	3,355	4,258
LOWER SURFACE	3,305	3,451	3,494	3,549
SPARS	1,036	1,036	1,034	1,039
RIBS	1,441	1,436	1,435	1,440
FIXED WEIGHT	(41,352)	← → (41,352)		
LEADING EDGE	5,235			5,235
TRAILING EDGE	4,883			4,883
B.L. 62 RIBS	1,430			1,430
B.L. 470 RIBS	700			700
FIN ATTACH RIBS	435			435
REAR SPAR	3,400			3,400
ENG. SUP'T. STRUCTURE	3,580			3,580
MLG DOORS	2,904			2,904
MLG WHEEL WELL AND ATTACH.	3,750			3,750
WING/BODY FAIRING	1,600			1,600
LE FLAPS	1,130			1,130
TE FLAPS	5,890			5,890
AILERONS	1,250			1,250
SPOILERS	1,360			1,360
FUEL BULKHEADS	3,800			3,800
TOTAL (STRENGTH DESIGN ONLY)	104,179	103,600	103,528	109,953

Total variable weight after interpolating to determine each box panel weight is:

$$w_v = \left( \sum_1^n w_i s_i \right) (1.26)$$

- For the hat stiffener concept, total variable weight is 62,176 pounds. This results in an average box unit weight of 8.68 pounds per square foot:

$$w_{ave} (\text{lb}/\text{ft}^2) = \left[ (62,176) \div (7165) \right] = 8.68$$

Total variable weight for the other structural concepts was facilitated by deriving a general expression where:

$$w_v = \left( \frac{s_{box}}{5.275} \right) \left[ \left( 3 w_{40322} + w_{40536} + w_{41348} \right)^{1.26} \right]$$

The weight distribution between center, intermediate and tip box structure was taken to be proportional to that found in the hat stiffened concept. Weight distribution between surfaces, ribs and spar is based on the structural analysis data of Section 12.

#### Monocoque Design Concepts

The monocoque construction consists of biaxially stiffened panels which support the principal load in both the span and chord direction. For the substructure arrangement, both multirib and multispar designs were evaluated. The initial screening and detailed analysis mass estimation of these concepts were performed concurrently and are reported in Monocoque Wing Design section.

#### WING STRUCTURE MASS-DETAILED CONCEPT ANALYSIS

As a result of the initial screening process, each of the most promising concepts were investigated further through the analysis of three additional point design regions. The results of this analysis effort is summarized in Table 15-24.

TABLE 15-24. SUMMARY OF WING MASS - DETAILED CONCEPT ANALYSIS

ARRANGEMENT	CHORDWISE		SPANWISE	MONOCOQUE		HYBRID	
SURFACE PANEL	CONVEX-BEADED	HAT	HAT	HONEYCOMB SAND.		BEST COMBINATION	
MATERIAL SYSTEM	TI-6A1-4V	COMPOSITE REINF.	TI-6A1-4V	TI-6A1-4V			
CONCEPT NO. (ASSET)	(1)	(5)	(6)	(2)	(3)	(4)	
VARIABLE WEIGHT	64,658	48,082	53,487	63,482	50,978	53,794	47,268
FORWARD BOX	22,090	20,580	24,184	25,364	21,982	24,057	20,580
SURFACES	9,545	9,452	14,655	15,842	14,656	14,386	
SPARS	9,975	8,558	6,959	3,913	4,616	5,965	
RIBS	2,570	2,570	2,570	5,609	2,710	3,706	
AFT BOX (FS 2330 TO 2640)	29,016	17,384	18,592	25,242	19,692	20,153	17,384
SURFACES	7,622	7,302	9,225	20,947	13,984	13,824	
SPARS	19,880	8,568	7,853	2,243	4,060	4,416	
RIBS	1,514	1,514	1,514	2,052	1,648	1,913	
TIP BOX (BL 470 TO TIP)	13,552	10,118	10,711	12,876	9,304	9,584	9,304
SURFACES	6,464	6,397	7,166	10,965	8,059	8,059	
SPARS	6,405	3,038	2,862	914	928	1,044	
RIBS	683	683	683	997	317	481	
TOTAL REINF. COMPOSITE		(5,480)	(10,668)				
FIXED WEIGHT	(41,352)						(41,352)
LEADING EDGE	5,235						5,235
TRAILING EDGE	4,888						4,888
B.L. 62 RIBS	1,430						1,430
B.L. 470 RIBS	700						700
FIN ATTACH RIBS	435						435
REAR SPAR	3,400						3,400
ENG. SUPT. STRUCT.	3,580						3,580
MLG ~ DOORS	2,904						2,904
~SUP'T. STRUCT	3,750						3,750
WING/BODY FAIRING	1,600						1,600
LE FLAPS	1,130						1,130
TE FLAPS	5,890						5,890
AILERONS	1,250						1,250
SPOILERS	1,360						1,360
FUEL BULKHEADS	3,800						3,800
TOTAL WING WEIGHT	106,010	89,434	94,839	104,834	92,330	95,146	88,620

NOTES:

1. ASSEMBLY JOINING FOR ALL CONCEPTS (EXCEPT CONCEPT (4)) IS MECHANICALLY FASTENED. CONCEPT (4) IS WELDED.
2. CONCEPT (5) - COMPOSITE REINFORCED (B/PI) SPAR CAPS ONLY
3. CONCEPT (6) - COMPOSITE REINFORCED SPAR CAPS AND SURFACE PANELS

For all-metallic construction, the mechanically fastened monocoque concept is least weight. However, the application of composite reinforcing (boron-polyimide) to the spar caps of the chordwise stiffened concept makes its variable weight lowest by almost 3000 pounds per aircraft. Furthermore, the best combination from a weight standpoint is an all-metallic, mechanically fastened-monocoque design for the wing tip structure with the forward and aft boxes constructed of convex beaded, chordwise stiffened surface panels with composite reinforced spar caps.

#### Chordwise Stiffened Wing Design

Analysis results of the 3 additional point design regions plus the three point design regions used in the initial screening are used to provide a better basis for evaluation of the variable weights of the wing box weight. The additional regions are described as follows:

<u>Point Design Region</u>	<u>Location</u>	<u>Area (Ft<sup>2</sup>)</u>
40236	Aft box	35.0
41036	Aft box	44.4
41316	Tip	11.9

The loads and unit weights for all six point design regions are compared in Table 15-25. The optimum unit weight from stress analysis is compared to the estimated unit weight derived from the modified loading parameter equation. This equation was used to calculate unit weights for the remaining box panels and re-evaluate the total variable weight.

Panel weights resulting from the detailed concept analysis are shown in Figure 15-12. These are optimum weights based on strength requirements only.

Fail-safe requirements for each point region are shown in Table 15-26. This data was converted to an average fail-safe penalty for each of the three point designs. Figure 15-13 indicates that the fail-safe increment is primarily applied to the spar web and clips (85-percent) with the remainder (15-percent) applied to the surface panels.

Flutter suppression requires the addition of the increment shown in Figure 15-14. For the chordwise stiffened design 2938 pounds per aircraft is required.

TABLE 15-25. PANEL LOAD AND UNIT WEIGHT - CHORDWISE STIFFENED DESIGN

POINT DESIGN REGION	INPLANE LOADS $N_X$ $N_Y$ $N_{XY}$	(lb/in.)	PRESSURE LOADS UPR. LWR. $\sum$	PANEL UNIT WEIGHTS				PANEL ESTIMATED WEIGHTS $W_{PANEL}$ (A) (lb/ft <sup>2</sup> )
				TOTAL	UPR	LWR	SPARS RIBS	
40322	488 -1,063 -120		-8.33 -9.47 17.80	3.80 0.83 0.94 1.53 (B) 0.50				3.82
40236	658 -16,387 -1,316		-8.96 -10.14 19.10	12.08 1.03 1.25 9.15 (B) 0.65				12.55
40536	-1,305 -14,379 -2,354		-7.47 -8.29 15.76	11.30 1.61 1.34 7.75 (B) 0.60				12.33
41036	-1,442 -9,156 -2,237		-1.27 0.11 1.38	8.25 1.35 1.45 4.95 0.50 (B)				7.40
41316	571 -16,982 +4,807		4.98 -0.26 5.24	15.38 2.60 2.05 10.13 0.60 (B)				13.81
41348	-1,433 -10,800 2,483		-5.07 1.0 6.07	9.75 1.63 1.32 6.20 0.60 (B)				9.20

(A)  $W_{PANEL} = [ |N_X| + |N_Y| + |2N_{XY}| + 350|\Delta \rho| ] \div 2100$ 

(B) INCLUDES STRESS NON OPTIMUM FACTOR

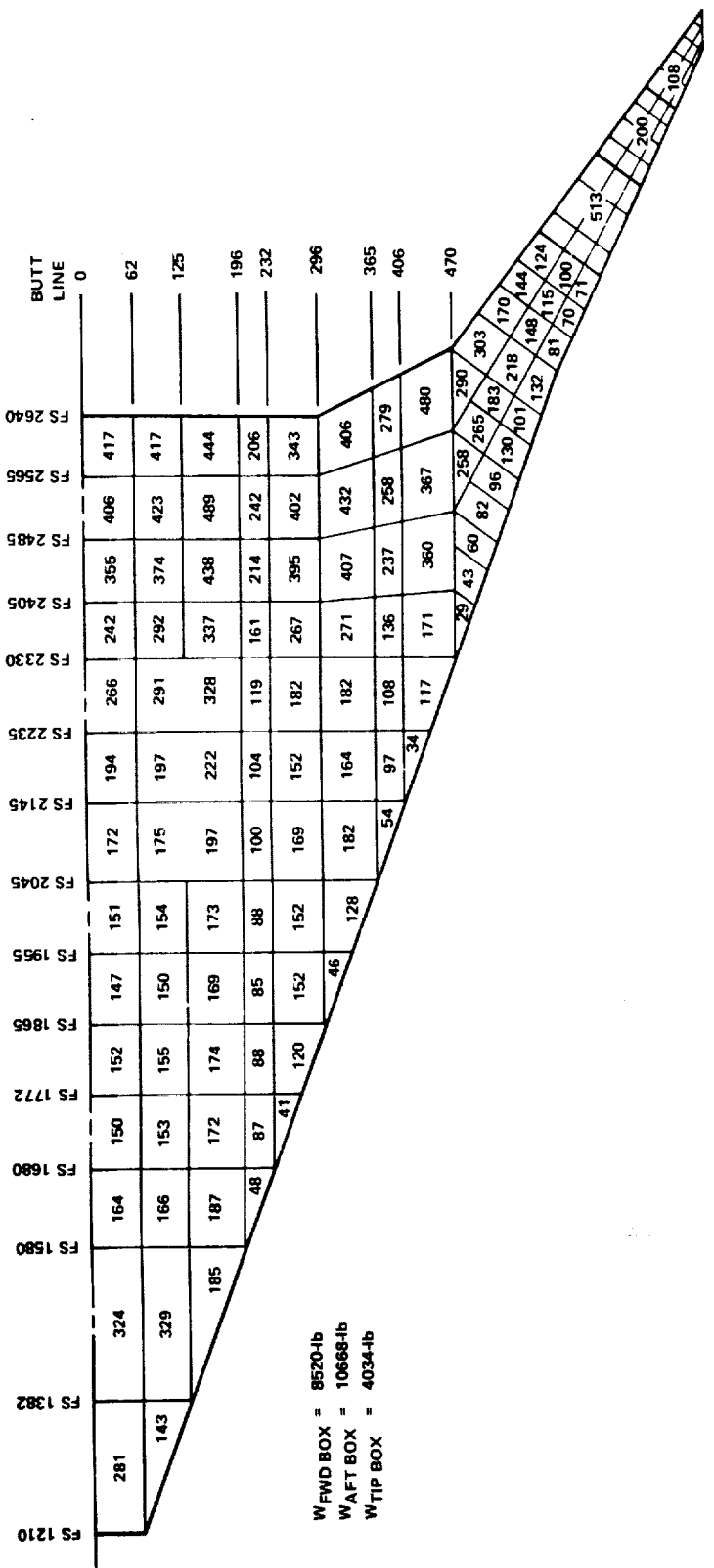


TABLE 15-26. COMPONENT WEIGHT DERIVATION - CHORDWISE STIFFENED DESIGN -  
DETAILED CONCEPT ANALYSIS

PANEL NO.	UNIT WEIGHTS (psf)				
	SURFACES	SPARS	FAIL-SAFE (B)	RIBS	TOTAL
40322	1.77	1.53	(0.10)	0.50	3.80
40236	2.28	9.15	(1.75)	0.65	12.08
40536	2.95	7.75	(0.93)	0.60	11.30
41036	2.80	4.95	(0.56)	0.50	8.25
41316	4.65	10.13	(1.00)	0.60	15.38
41348	2.95	6.20	(0.41)	0.60	9.75
<u>FWD. BOX (AREA = 4136.6 ft<sup>2</sup>/AIRCRAFT)</u>		<u>TOTAL</u> =	<u>5.340</u>	<u>UNIT WT. (psf)</u>	<u>BOX WT. (lb)</u>
SURFACES 0.122 (1.77 X 9 + 2.80) +		<u>FAIL-SAFE</u> 0.0225	2.3075		9,545
SPARS	0.122 (1.53 X 9 + 4.95) +	0.1275	2.4113		9,975
RIBS	0.122 (0.5 X 9 + 0.5) +	0.0112	0.6212		2,570
<u>AFT BOX (AREA = 2132.4 ft<sup>2</sup>/AIRCRAFT)</u>		<u>TOTAL</u> =	<u>13.067</u>	<u>UNIT WT. (psf)</u>	<u>BOX WT. (lb)</u>
SURFACES 0.3162 (2.28 + 2.95 + 2 X 2.80) +		<u>FAIL-SAFE</u> 0.150	3.574		7,622
SPARS	0.3162 (9.15 + 7.75 + 2 X 4.95) +	0.850	9.323		19,880
RIBS	0.3162 (0.65 + 0.60 + 2 X 0.50) +	0	0.710		1,514
<u>TIP BOX (AREA = 896 ft<sup>2</sup>/AIRCRAFT)</u>		<u>TOTAL</u> =	<u>15.125</u>	<u>UNIT WT. (psf)</u>	<u>BOX WT. (lb)</u>
SURFACES 0.3465 (4.65 + 2.95 + 2 X 1.77) +		<u>FAIL-SAFE</u> 0.075	3.935		3,526
FLUTTER INCREMENT		=	3.279		+2,938
SPARS	0.3465 (10.13 + 6.20 + 2 X 1.53) +	0.430	7.149		6,405
RIBS	0.3465 (0.6 + 0.6 + 2 X 0.5) +		0.762		683

(A) 20-INCH SPAR SPACING

(B) WEIGHT INCLUDED IN SURFACES, SPARS, AND RIBS

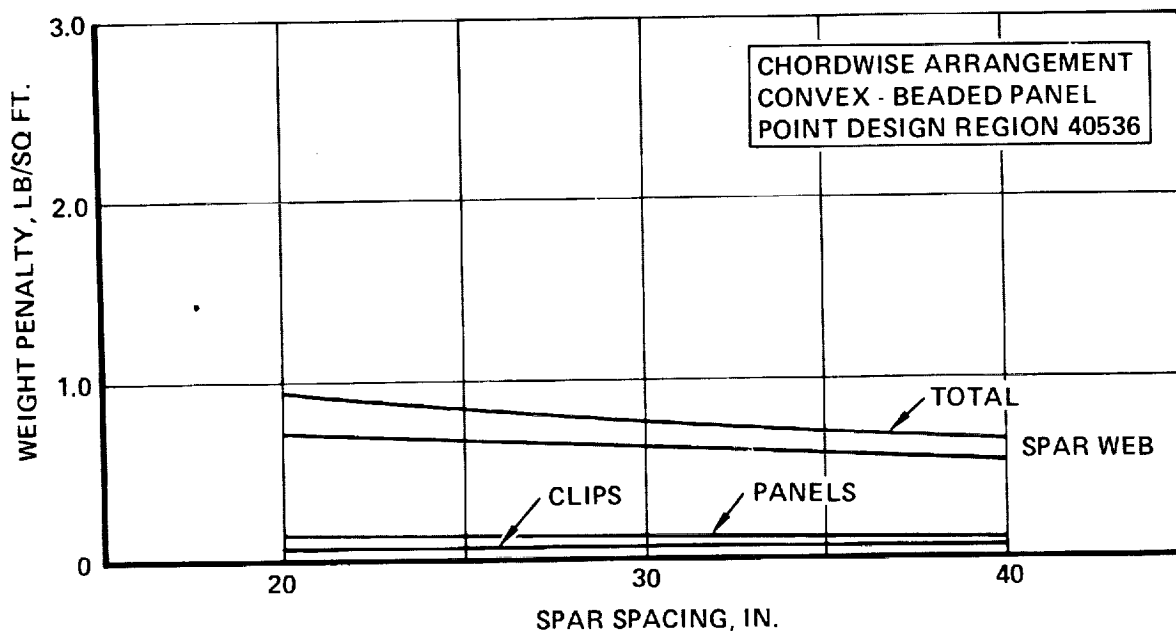


Figure 15-13. Component Weight Penalties for a Damaged Spar Cap Chordwise Arrangement

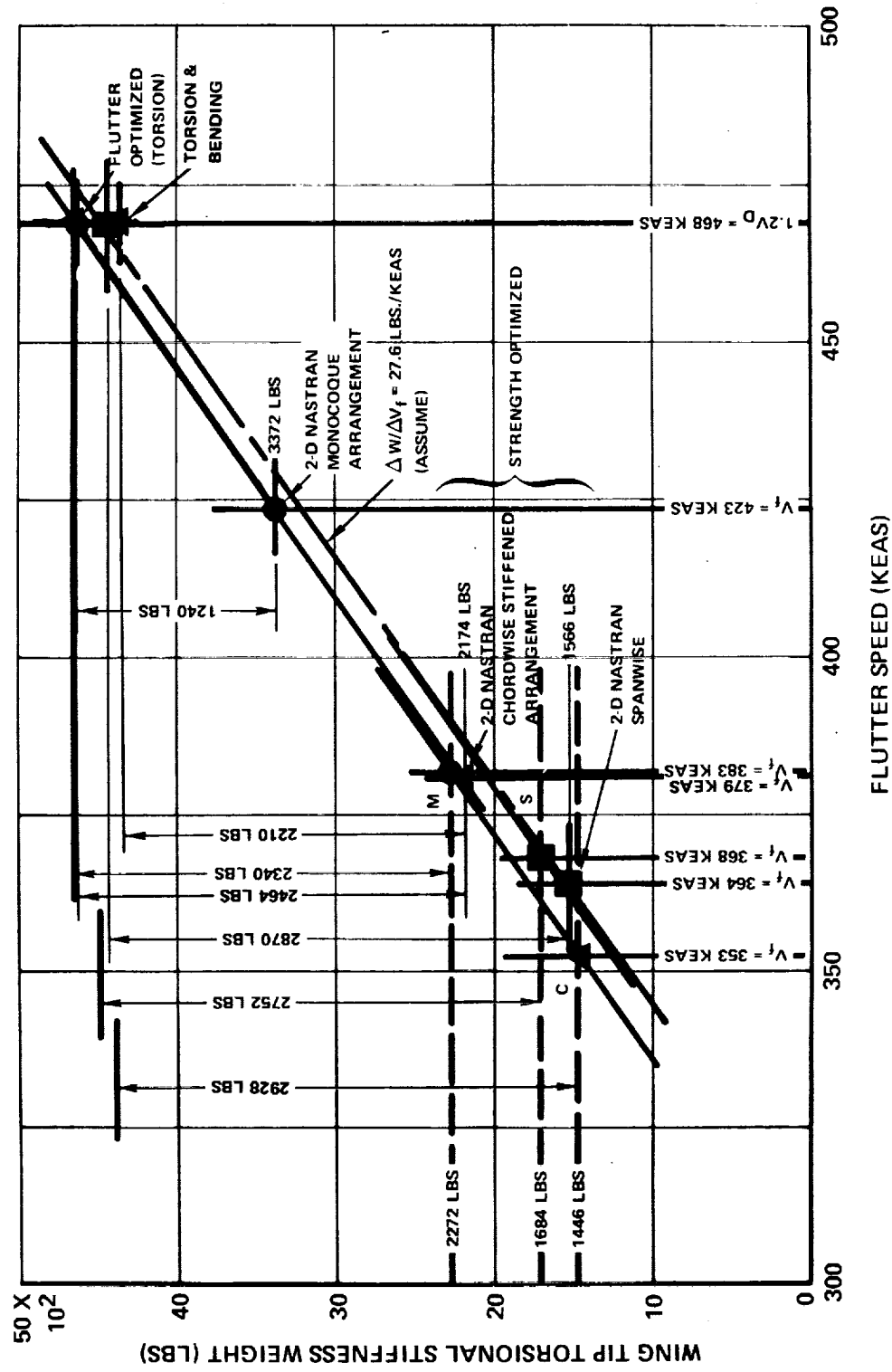


Figure 15-14. Flutter Weight Increment Required Over Strength Design

A build-up to total box weight, including the above increments is tabulated in Figure 15-15. Cumulative plots of the "strength" weight versus span are also shown.

From the total box weight of Figure 15-15, equations were developed to express the average box unit weight in terms of the detailed stress analysis point design region unit weight:

$$w_{\text{fwd box}} \left( \frac{\text{lb}}{\text{ft}^2} \right) = 0.1220 (9w_{40322} + w_{41036})$$

$$w_{\text{aft box}} \left( \frac{\text{lb}}{\text{ft}^2} \right) = 0.3162 (w_{40236} + w_{40536} + 2w_{41036})$$

$$w_{\text{tip box}} \left( \frac{\text{lb}}{\text{ft}^2} \right) = 0.3465 (w_{41316} + w_{41348} + 2w_{40322})$$

These equations are used in Table 15-26 to derive the component weight breakdown shown in Table 15-24.

#### Spanwise Stiffened Wing Design

The detailed concept analysis weights for the hat stiffened concept are obtained by incorporating into the estimation procedure, the results of the 3 additional point design regions (40236, 41036 and 41316).

The loads and unit weights for all 6 point design regions are compared in Table 15-27. The optimum unit weight from stress analysis are compared to the estimated unit weight derived from the modified loading parameter equation. This equation (Table 15-27) was used to calculate the unit weights for the remaining box panels and to reevaluate the total variable weight.

Panel weights resulting from this analysis are shown in Figure 15-16. These are optimum weights based on strength requirements only. No fail-safe increments are required for the spanwise stiffened design.

Flutter suppression requires the addition of the increment shown in Figure 15-14 to the wing tip structure. For the spanwise stiffened design 2928 pounds per aircraft is required to achieve the required flutter margin.

CHORDWISE STIFFENED - CONVEX BEADED

	WEIGHT/SIDE (LB.)		
	FWD. BOX	AFT BOX	TIP BOX
STRENGTH ONLY	8,520	10,668	4,034
NON-OPTIMUM	+2,215	+2,774	+1,049
FAIL-SAFE	+310	+1,066	+224
FLUTTER	-	-	+1,469
<b>TOTAL</b>	<b>11,045</b>	<b>14,508</b>	<b>6,776</b>

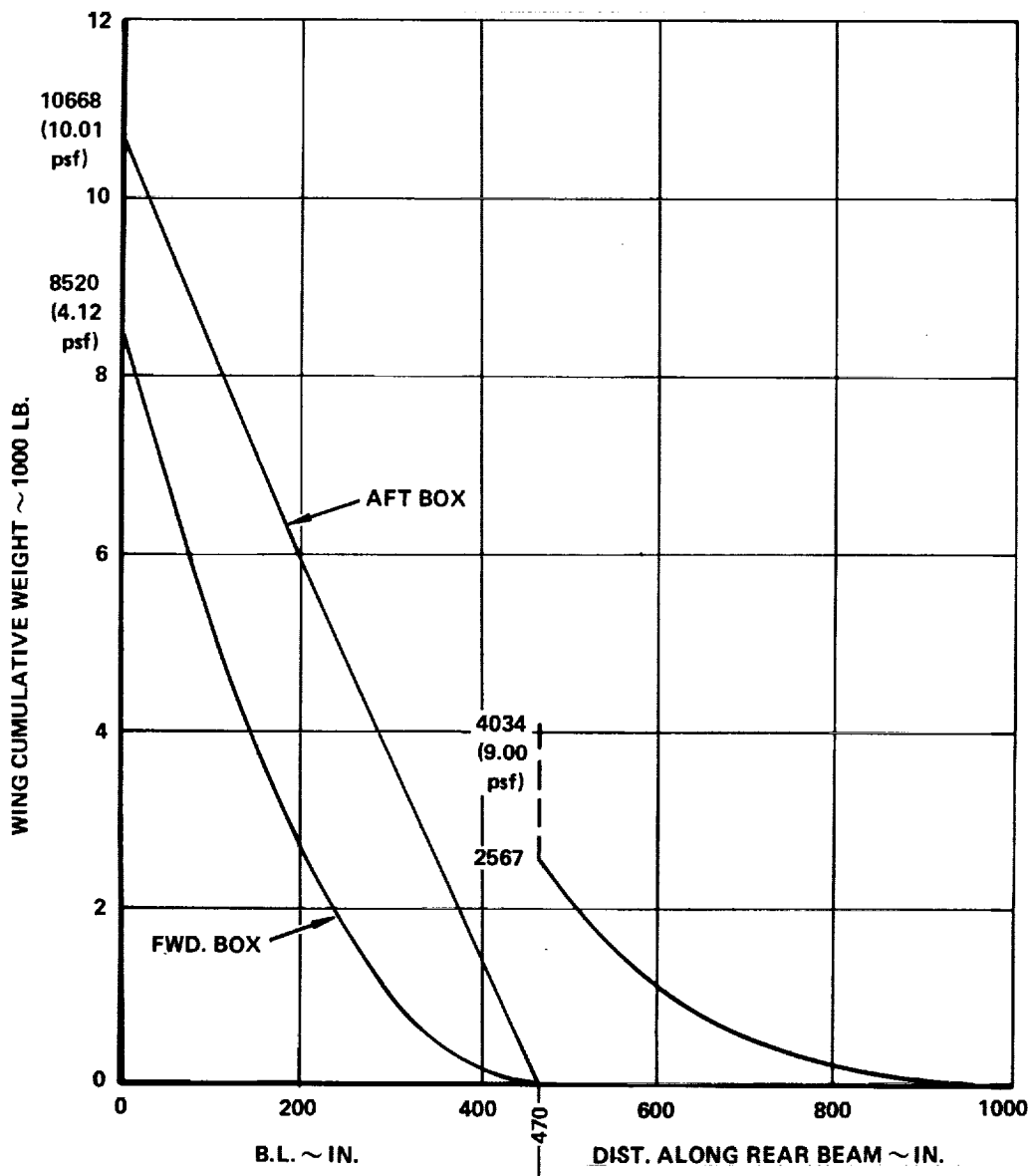


Figure 15-15. Wing Structure Mass Estimate for Chordwise Stiffened Design

TABLE 15-27. PANEL LOAD AND UNIT WEIGHT - SPANWISE STIFFENED DESIGN

PANEL NO.	INPLANE LOADS $N_X$ $N_Y$ $N_{XY}$	(lb/in.)	PRESSURE LOADS UPR. <u>LWR.</u> $\sum$	PANEL UNIT WEIGHTS				PANEL ESTIMATED WEIGHTS $W_{PANEL}^{(A)}$
				TOTAL	UPR.	LWR.	SPARS RIBS	
40322	11 -1,185 -290		-8.33 <u>-9.47</u> 17.80	<u>4.70</u>	1.50	1.20	0.80	3.81
40236	306 -16,986 -2,542		-8.96 <u>-10.14</u> 19.10	<u>12.75</u>	4.80	5.20	1.40	13.84
40536	518 -16,409 -4,174		-7.47 <u>-8.29</u> 15.76	<u>13.75</u>	5.20	6.35	1.10	14.66
41036	-450 -9,499 -3,227		1.27 <u>0.11</u> 1.33	<u>9.25</u>	3.70	4.20	0.75	8.04
41316	163 -17,949 4,292		4.98 <u>0.26</u> 5.24	<u>13.78</u>	5.70	6.35	1.13	13.53
41348	-1,028 -9,412 -2,750		5.07 <u>1.0</u> 6.07	<u>8.50</u>	3.40	3.65	0.55	8.60

$$(A) \quad W_{PANEL} = [ |N_X| + |N_Y| + |2N_{XY}| + 350|\Delta p| ] \div 2100$$

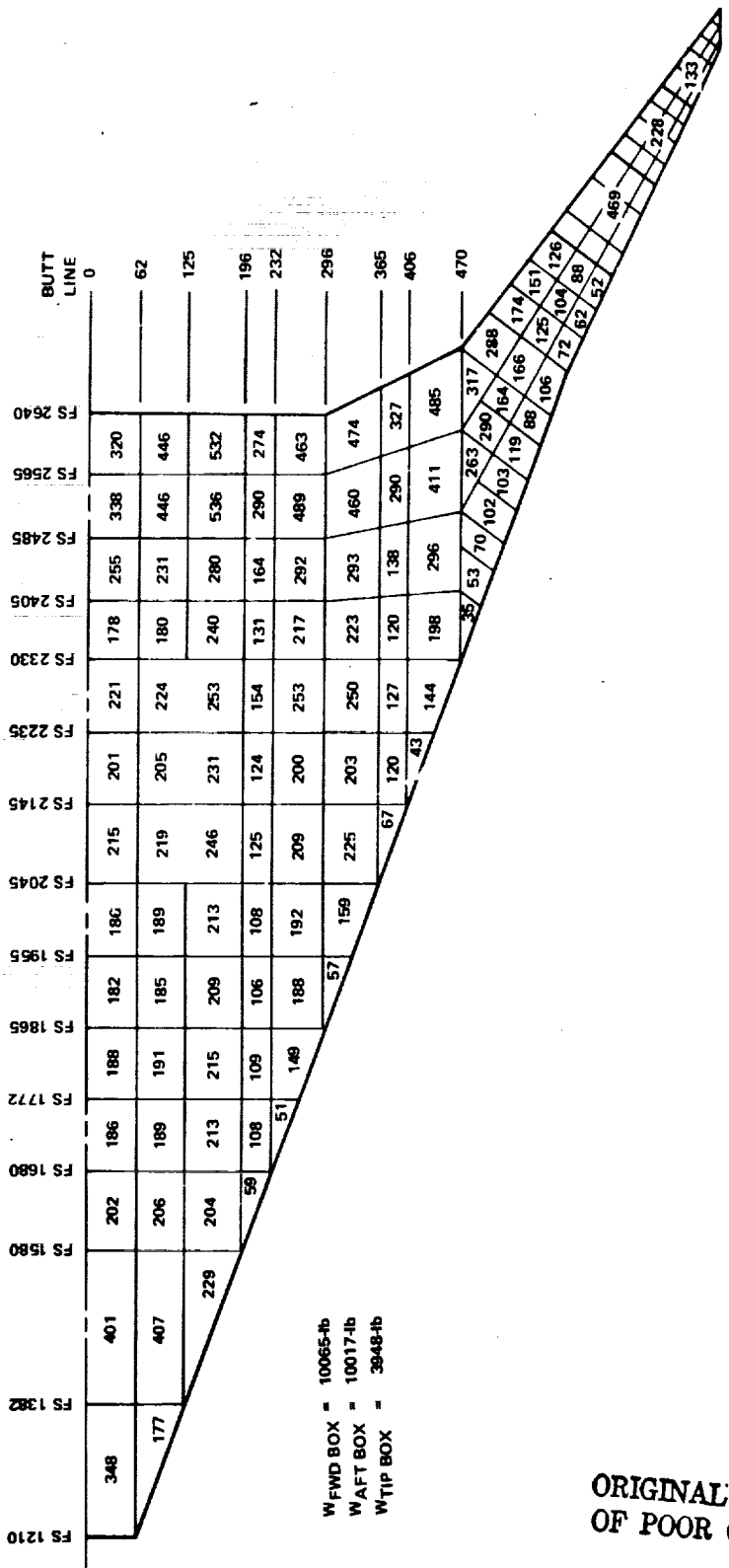


Figure 15-16. Optimum Panel Weights (lb./side) - Spanwise Stiffened Design

A build-up of the total weight for each box segment is tabulated on Figure 15-17. Cumulative plots of the strength-design weights versus span are also shown.

#### Monocoque Wing Design

This section presents the initial screening and detailed concept analysis mass estimation results for the monocoque designs. The three surface panel concepts investigated are as follows:

- Honeycomb sandwich - aluminum brazed - welded closures
- Honeycomb sandwich - aluminum brazed - mechanical fasteners
- Truss-core sandwich - mechanical fasteners

The relative weights for these 3 concepts are shown in Figure 15-18. These initial weights are for a 20-inch spar spacing and do not include allowance for weight increments for fail-safe design or flutter suppression. The data shown on Table 15-28 includes allowance for fail-safe and flutter suppression requirements. Appropriate spar spacing, as shown on the structural arrangement drawings of Section 18, are also considered in determining the detailed weights presented.

The basic unit weight data resulting from the detailed concept analysis are presented in Section 12 for the monocoque designs. These data identify unit weight of the surface panels, substructure, and combined surface panels and substructure at each point design region for strength requirements.

The scaling equation used for weight interpolation between the design analysis panels is shown in Table 15-29 for the welded closure concept:

$$w \text{ (lb/ft}^2) = \left[ (|N_x| + |N_y| + |2N_{xy}| + 350|\Delta P|) \div (3000) \right]$$

with the notation as described earlier for the Chordwise Stiffened Design Concepts. Panel weights resulting from this interpolation process are shown in Figure 15-19 for the welded closure design.

Weight equations were developed for the wing forward, aft and tip box areas which depend upon the detail stress analysis at each point design region:

SPANWISE STIFFENED - HAT SECTION

	WEIGHT/SIDE (LB.)		
	FWD. BOX	AFT BOX	TIP BOX
STRENGTH ONLY	10,065	10,017	3,948
NON-OPTIMUM	2,617	2,604	1,026
FAIL-SAFE	-	-	-
FLUTTER			1,464
(9.395 PSF)			
(A) 10,017			
(F) 10,065			
<b>TOTAL</b>	<b>12,682</b>	<b>12,621</b>	<b>6,438</b>

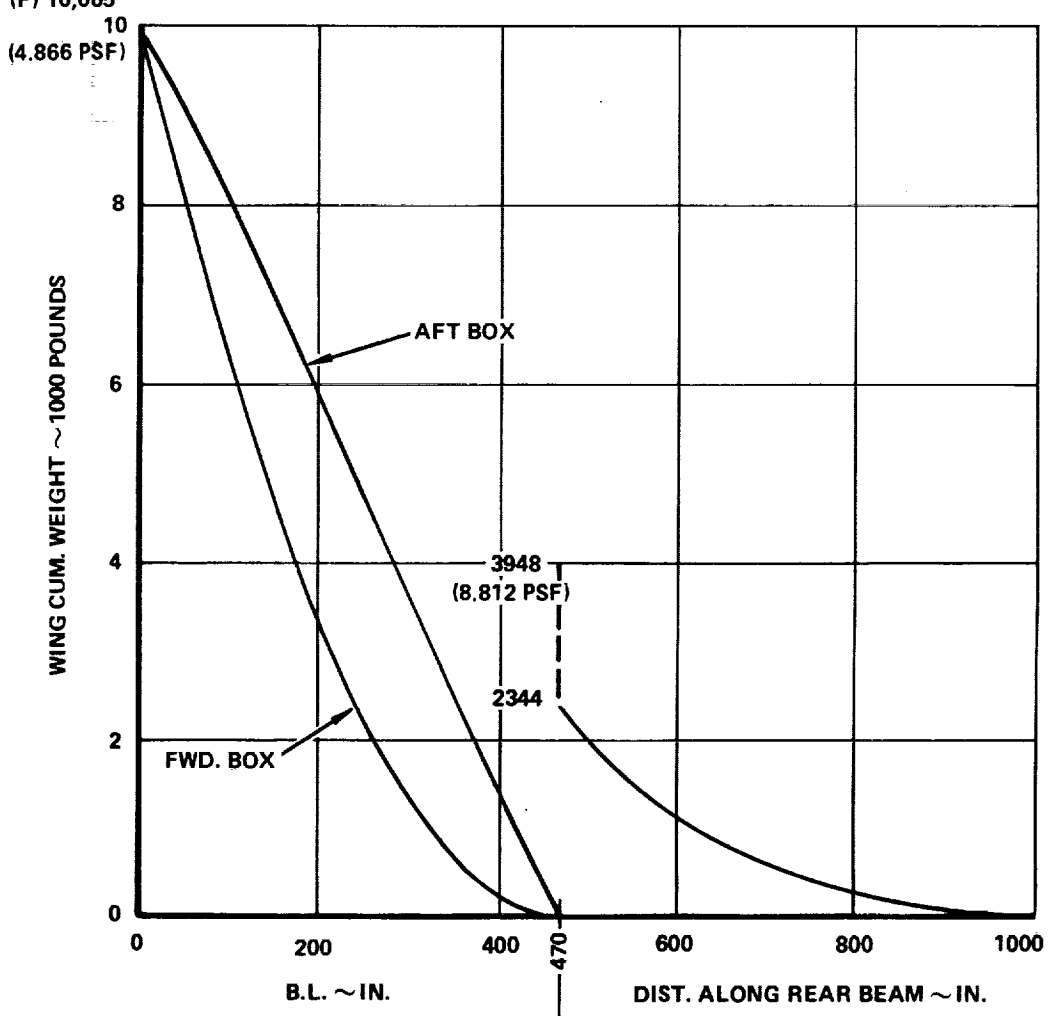


Figure 15-17. Wing Structure Mass Estimate for Spanwise Stiffened Design

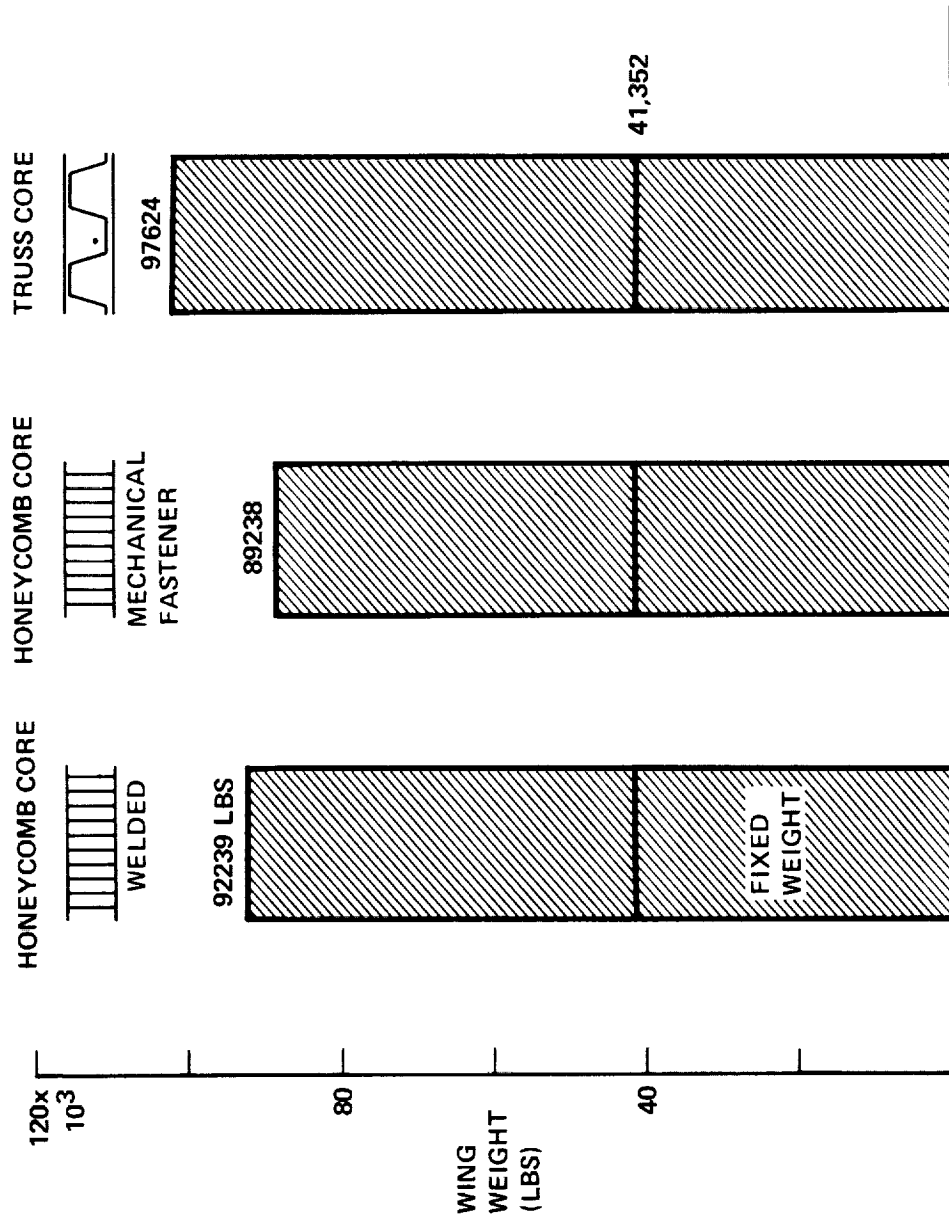


Figure 15-18. Concept Weight Comparison - Monocoque Arrangement

TABLE 15-28. ESTIMATED WING MASS - MONOCOQUE DESIGN CONCEPT

ITEM	HONEYCOMB MECH. FAST.	HONEYCOMB WELDED	TRUSSCORE
VARIABLE WEIGHT (lb)	50,978	53,794	59,066
FORWARD BOX (lb)	(21,982)	(24,057)	(28,667)
SURFACES	14,656	14,386	20,104
SPARS	4,616	5,965	5,502
RIBS	2,710	3,706	3,061
AFT BOX (lb)	(19,692)	(20,153)	(20,748)
SURFACES	13,984	13,717	14,948
SPARS	4,060	4,523	3,945
RIBS	1,648	1,913	1,855
TIP BOX (lb)	(9,304)	(9,584)	(9,651)
SURFACES	8,059	8,059	8,424
SPARS	928	1,044	806
RIBS	317	481	421
FIXED WEIGHT (lb)	41,352	41,352	41,352
TOTAL WING WEIGHT (lb)	92,330(A)(D)	95,146(B)(D)	100,418(C)(D)

(A) INCLUDES A FAIL-SAFE WEIGHT INCREMENT OF 752 LBS.

(B) INCLUDES A FAIL-SAFE WEIGHT INCREMENT OF 567 LBS.

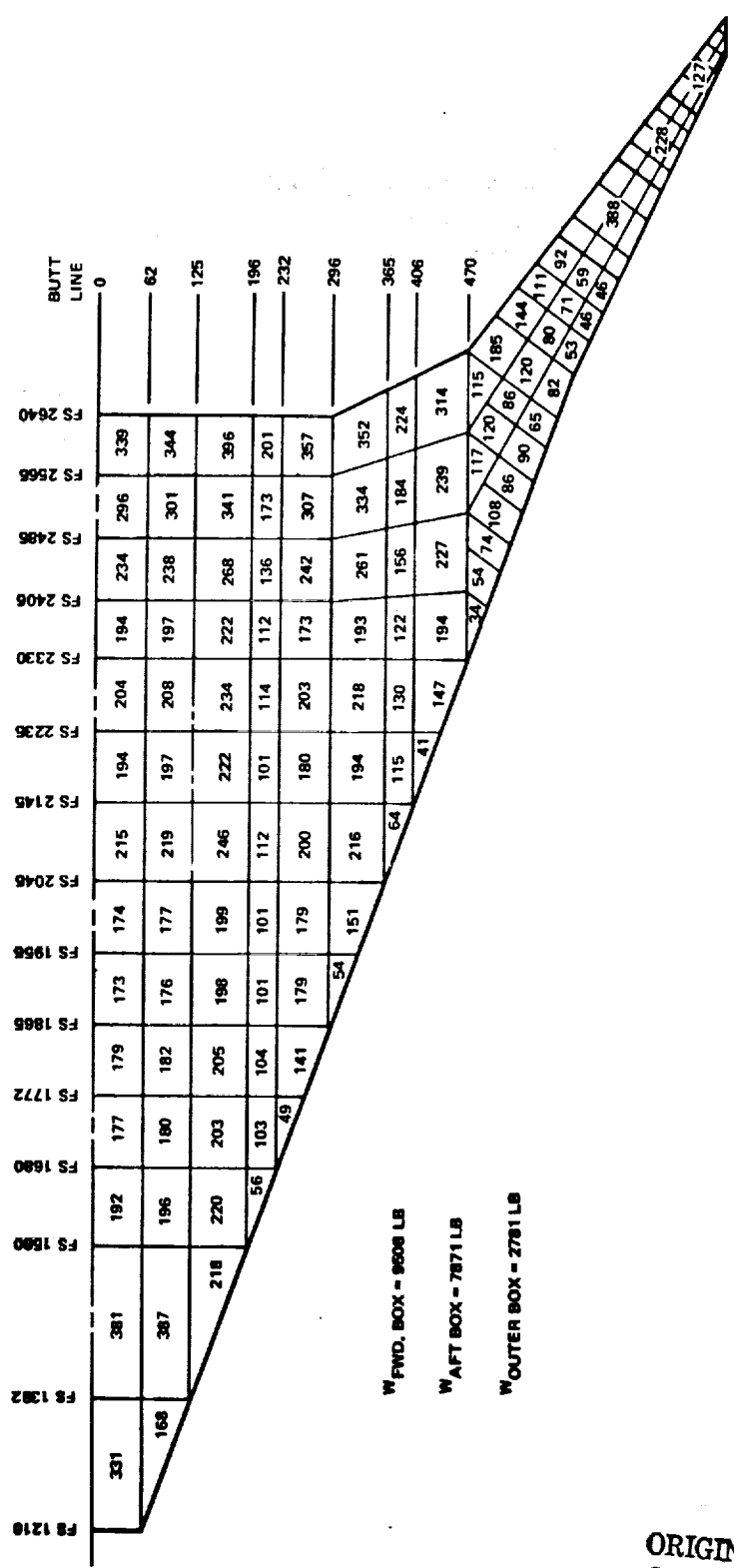
(C) INCLUDES A FAIL-SAFE WEIGHT INCREMENT OF 454 LBS.

(D) INCLUDES A FLUTTER WEIGHT INCREMENT OF 2,340 LBS.

TABLE 15-29. PANEL LOAD AND UNIT WEIGHT - MONOCOQUE WELDED DESIGN

PANEL NO.	INPLANE LOADS $N_X$ $N_Y$ $N_{XY}$	(lb/in.)	PRESSURE LOADS UPR. LWR. $\sum$	(lb/in. <sup>2</sup> )	PANEL UNIT WEIGHTS TOTAL UPR LWR SPARS RIBS	(lb/ft <sup>2</sup> )	PANEL ESTIMATED WEIGHT $W_{PANEL}$ (A) (lb/ft <sup>2</sup> )
40322	51 -529 -191		-8.33 -9.47 17.80		4.47 1.14 0.98 1.65 0.70		2.40
40236	-1,193 -11,638 -2,099		-8.96 -10.14 19.10		8.60 2.51 2.91 2.22 0.96		7.91
40536	-3,272 -11,787 -4,795		-7.47 -8.29 15.76		8.64 2.92 3.30 1.72 0.70		10.05
41036	-2,219 -6,423 -3,209		1.27 0.11 1.33		5.37 1.87 1.94 1.09 0.47		5.18
41316	-1,587 -12,183 +3,310		4.98 0.26 5.24		7.25 2.71 3.14 1.01 0.39		7.40
41348	-1,190 -7,263 +3,285		5.07 1.0 6.07		5.70 2.02 2.24 1.12 0.33		5.72

$$(A) \quad W_{PANEL} = [ |N_X| + |N_Y| + |2N_{XY}| + 350|\Delta p| ] \div 3000$$



$$w_{fb} = k_{fb} (6w_{40322} + w_{41036})$$

$$w_{ab} = k_{ab} (w_{40236} + w_{40536} + w_{41036})$$

$$w_{tb} = k_{tb} (w_{41316} + 2w_{41348})$$

Using the welded closure configuration as an example, Table 15-30 presents the method used to derive component weights shown in Table 15-31 and summarized in Table 15-28. The basic data used for the analyses are presented in Table 15-32.

The damage tolerance and flutter suppression weight increments are superimposed on the above results. A flutter penalty of 2340 pounds is identified in Figure 15-14 for the monocoque design. This value is an estimated amount over the strength-design requirements to be applied to the stiffness critical wing tip structure. Fail-safe critical areas are identified for both the wing tip (inboard) and the aft box in Figure 15-20. The weight increment is based on fail-safe analysis of the 2 point design regions indicated. The results of these analyses, as shown in Section 13, indicates that sizable penalties are required to meet the fail-safe requirements. However, the use of the fail-safe reinforcement provides additional cross sectional area which reduces the spanwise ( $N_y \div 1.5 T$ ) limit stress level from 52 ksi to 35 ksi or approximately 33 percent. This permits further reduction of the surface panel thickness and fail-safe reinforcement. This load redistribution process results in a surface panel thickness and fail-safe reinforcement combination shown on Table 15-33 and 15-34 for point design regions 40536 and 41348, respectively. As indicated on the tables, these results are applied to establish the mass increment to satisfy the fail-safe requirements for the wing aft box and tip box structure. The applicable areas (Figure 15-20) were obtained by reviewing the critical inplane loads and surface panel thicknesses and comparing the resulting limit stresses to the stress levels at the respective point design regions. The tables further define the weight increment for the various insert/closures used with the honeycomb panel design. It is noted that the welded closure method requires a smaller fail-safe increment than the mechanically fastened approach. Also, the welded method results in 540 pound reduction in fuel tank sealant in the forward and aft boxes. Unfortunately, the panel edges required for sufficient weld thickness and module-approach of assembly results in the welded design to be three-percent heavier than the mechanically fastened design.

TABLE 15-30. COMPONENT UNIT WEIGHT DERVIATION - MONOCOQUE WELDED DESIGN

OPTIMUM BOX WEIGHT (lb/side)		PLANFORM AREA (ft <sup>2</sup> /side)	=	OPTIMUM UNIT WT. (psf)	NON OPT FACTOR	=	UNIT WT. (INCL N.O.F.) (psf)
FWD	9508	2068.3		4.597	1.26		5.792
AFT	7871	1066.2		7.382	1.26		9.302
TIP	2781	448.0		6.207	1.26		7.821

UNIT WEIGHT EQUATION (20-inch SPAR SPACING):

$$w_{fb} = 0.180 (6 \times 4.47 + 5.37) = 5.792 \text{ psf}$$

$$w_{ab} = 0.4114 (8.6 + 8.64 + 5.37) = 9.302$$

$$w_{ob} = 0.4194 (7.25 + 2 \times 5.70) = 7.821$$

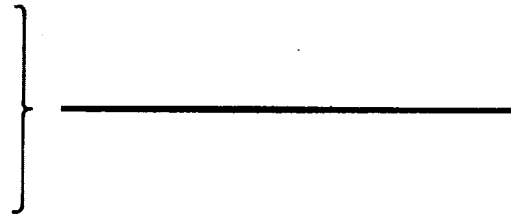


TABLE 15-31. ESTIMATED WING STRUCTURE MASS - MONOCOQUE (WELDED) CONCEPT

ITEM		UNIT WEIGHT (psf)	BOX WEIGHT (lb)
<u>FWD. BOX (AREA = 4136.6 ft<sup>2</sup>/AIRCRAFT)</u>	<u>TOTAL =</u>	<u>5.816</u>	<u>24,057</u>
SURFACES { w = 0.180 (6 X 2.63 + 3.9) REDUCED TANK SEALANT REQUIREMENT	=	3.543	14,656
SPARS w = 0.180 (6 X 1.16 + 1.05)	=	1.442	5,965
RIBS w = 0.180 (6 X 0.75 + 0.48)	=	0.896	3,706
<u>AFT BOX (AREA = 2132.4 ft<sup>2</sup>/AIRCRAFT)</u>	<u>TOTAL =</u>	<u>9.451</u>	<u>20,153</u>
SURFACES { REDUCED TANK SEALANT REQUIREMENT = w = 0.4114 (5.54 + 6.5 + 3.9) =	-0.125 6.558	-267 13,984	
SPARS { w = 0.4114 (2.08 + 1.54 + 1.05) FAIL-SAFE PROVISIONS =	1.921 0.20	4,523	
RIBS w = 0.4114 (1.00 + 0.70 + 0.48)	=	0.897	1,913
<u>OUTER BOX (AREA = 896 ft<sup>2</sup>/AIRCRAFT)</u>	<u>TOTAL =</u>	<u>10.697</u>	<u>9,584</u>
SURFACES { w = 0.4194 (6.22 + 2 X 4.50) FLUTTER PREVENTION =	6.383 2.612	5,719 +2,340	
SPARS { w = 0.4194 (0.72 + 2 X 0.85) FAIL-SAFE PROVISIONS =	1.015 0.150	1,044	
RIBS w = 0.4194 (0.48 + 2 X 0.40)	=	0.537	481

TABLE 15-32. BASIC UNIT WEIGHT DATA FOR MONOCOQUE CONCEPTS

DESIGN CONCEPT	POINT DESIGN	SPAR SPAC. (in.)	UNIT WEIGHTS (psf)			
			SURFACES	SPARS	RIBS	TOTAL
HONEYCOMB SANDWICH BRAZED-WELDED	40322	34.0	2.63	1.16	0.75	4.54
	40236	23.4	5.54	2.08	1.00	8.62
	40536	23.4	6.50	1.54	0.70	8.74
	41036	23.4	3.90	1.05	0.48	5.43
	41316	35.0	6.22	0.72	0.48	7.42
	41348	30.0	4.50	0.85	0.40	5.75
HONEYCOMB SANDWICH BRAZED-MECH. FASTENERS	40322	34.0	2.63	0.86	0.54	4.03
	40236	23.4	5.54	1.85	0.88	8.27
	40536	23.4	6.50	1.35	0.60	8.45
	41036	23.4	3.90	0.82	0.40	5.12
	41316	35.0	6.22	0.56	0.34	7.12
	41348	30.0	4.50	0.74	0.26	5.50
TRUSSCORE SANDWICH MECH. FASTENERS	40322	34.0	3.75	1.10	0.60	5.45
	40236	23.4	5.85	1.90	0.90	8.65
	40536	23.4	6.70	1.35	0.70	8.75
	41036	23.4	4.50	0.80	0.50	5.80
	41316	35.0	6.50	0.50	0.50	7.50
	41348	30.0	4.85	0.60	0.30	5.75

REFER TO SECTION 12 STRUCTURAL CONCEPT ANALYSIS

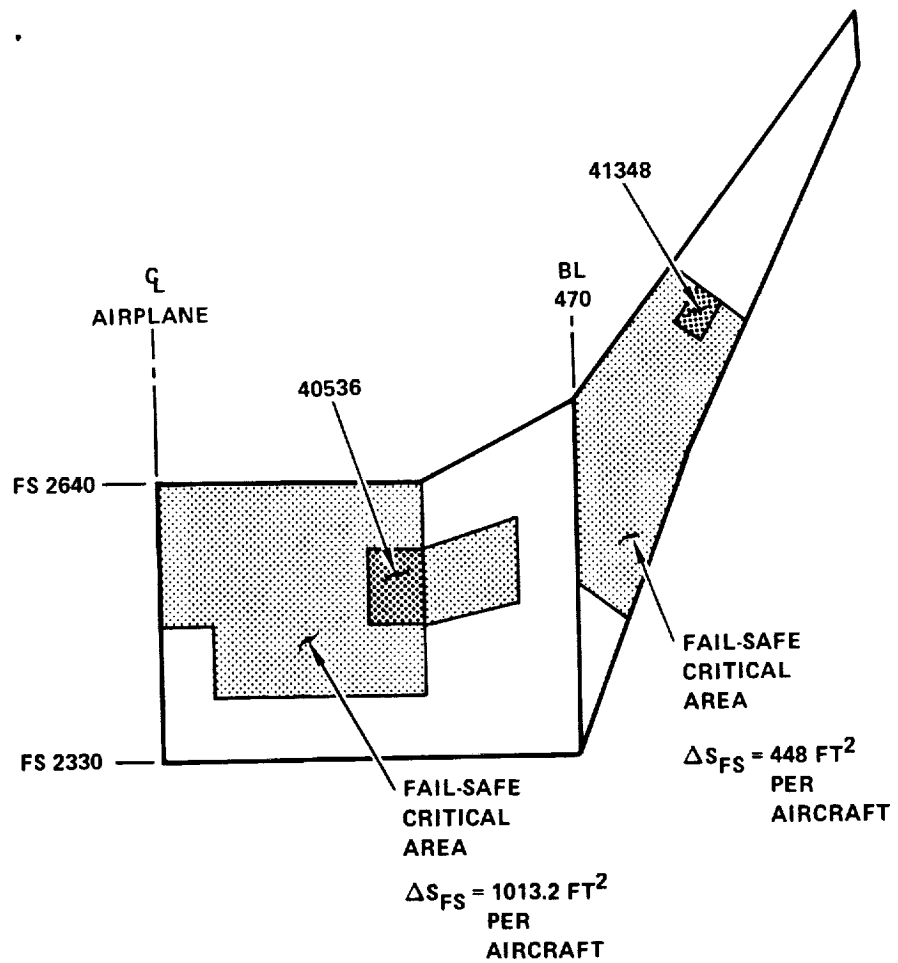


Figure 15-20. Fail-Safe Critical Areas of Wing Structure

TABLE 15-33. FAIL-SAFE WEIGHT INCREMENT - AFT BOX

HONEYCOMB SANDWICH PANEL DESIGN CONCEPT		SPAR SPAC. (in.)	MIN. DESIGN ASPAR (in <sup>2</sup> )	SKIN THICK. $\bar{t}_s$ (in.)	MFG. JOINT AWELD (in <sup>2</sup> )	FAIL-SAFE REQUIREMENT ASPAR (in <sup>2</sup> )	FAIL-SAFE STRAP ASTRAP (in <sup>2</sup> )	NO. STRAP n	UNIT WEIGHT (lb/ft <sup>2</sup> )	DELTA WEIGHT (lb/ft <sup>2</sup> )	EFF. PLAN. AREA (ft <sup>2</sup> )	DELTA WEIGHT (lb)
<b>POINT DESIGN 40536</b>		b										
<b>METALLIC INSERT - FASTENERS</b>												
STRENGTH - DESIGN	20	0.181	0.137	-	-	-	-	-	3.36	-	1031	-
FAIL-SAFE - NO REDISTRIBUTION	20	-	0.137	-	0.862	0.733	1	4.49	1.63	1031	1680	
FAIL-SAFE - REDISTRIBUTION	20	-	0.115	-	0.583	0.496	1	3.89	0.53	1031	546	
<b>METALLIC INSERT - WELDED</b>												
STRENGTH - DESIGN	20	0.181	0.137	0.181	-	-	-	-	3.57	-	1031	-
FAIL-SAFE - NO REDISTRIBUTION	20	-	0.137	0.862	0.862	-	-	-	5.14	1.57	1031	1619
FAIL-SAFE - REDISTRIBUTION	20	-	0.115	0.583	0.583	-	-	-	3.99	0.42	1031	433
<b>DENSIFIED CORE - FASTENERS</b>												
STRENGTH - DESIGN	20	0.088	0.137	-	-	-	-	-	3.26	-	1031	-
FAIL-SAFE - NO REDISTRIBUTION	20	-	0.137	-	0.733	0.733	1	4.84	1.58	1031	1628	
FAIL-SAFE - REDISTRIBUTION	20	-	0.115	-	0.496	0.496	1	3.79	0.53	1031	546	

ORIGINAL PAGE IS  
OF POOR QUALITY

TABLE 15-34. FAIL-SAFE WEIGHT INCREMENT - TIP BOX

HONEYCOMB SANDWICH PANEL DESIGN CONCEPT		SPAR SPAC.	MIN. DESIGN	SKIN THICK.	MFG. JOINT	FAIL-SAFE REQUIREMENT	NO. STRAP	UNIT WEIGHT	DELTA WEIGHT	EFF.PLAN. AREA	DELTA WEIGHT
b	A <sub>SPAR</sub> (in.)	A <sub>s</sub> (in.)	A <sub>WELD</sub> (in. <sup>2</sup> )	A <sub>SPAR</sub> (in. <sup>2</sup> )	A <sub>STRAP</sub> (in. <sup>2</sup> )	n	w	(lb/ft <sup>2</sup> )	Δ <sub>w</sub> (lb/ft <sup>2</sup> )	ΔS (ft <sup>2</sup> )	ΔW (lb)
POINT DESIGN 41348											
<u>METALLIC INSERT - FASTENERS</u>											
STRENGTH - DESIGN	20	0.181	0.091	-	-	-	-	2.30	-	-	-
FAIL-SAFE - NO REDISTRIBUTION	20	-	0.091	-	0.68	1	3.54	1.24	448	555	
FAIL-SAFE - REDISTRIBUTION	20	-	0.076	-	0.46	0.39	1	2.73	0.43	448	193
<u>METALLIC INSERT - WELDED</u>											
STRENGTH - DESIGN	20	0.181	0.091	0.181	-	-	-	2.51	-	-	-
FAIL-SAFE - NO REDISTRIBUTION	20	-	0.091	0.68	0.68	-	-	3.66	1.15	448	515
FAIL-SAFE - REDISTRIBUTION	20	-	0.076	0.46	0.46	-	-	2.81	0.30	448	134
<u>DENSIFIED CORE - FASTENERS</u>											
STRENGTH - DESIGN	20	0.088	0.091	-	-	-	-	2.19	-	-	-
FAIL-SAFE - NO REDISTRIBUTION	20	-	0.091	-	0.58	1	3.42	1.23	448	551	
FAIL-SAFE - REDISTRIBUTION	20	-	0.076	-	0.39	0.39	1	2.65	0.46	448	206

## Composite Reinforced-Chordwise Stiffened Wing Design

The chordwise stiffened arrangement described earlier, provides the basic approach offering the maximum mass savings potential for application of composites to the design. The two composite reinforced designs investigated are as follows:

- Composite reinforced spar caps with metallic beaded surface panels
- Composite reinforced spar caps and surface panels

A comparison of these two reinforcing methods are presented in Table 15-35 with their all-metallic counterpart. The results show an 11-percent to 13-percent reduction in total wing weight. Initial screening data used to derive this comparison is reported in Section 12.

Since the aforementioned results indicated that both concept weights were very close to each other, further detailed analyses were conducted. The results of the latter is presented in Tables 15-36 and 15-37. An interesting conclusion, when comparing the reinforced spar caps only with the all metallic design, is a one pound reduction in structure weight for each 0.40-pound of B/PI composite reinforcing material used.

Using the same equations as described earlier in the Chordwise Stiffened Design section, the box component weights are derived in Tables 15-38 and 15-39. Figure 15-21 shows the relationship between the all-metallic and composite reinforced spar cap optimum panel unit weights. For a minimum-gage all-metallic design (3.8 psf) there is no weight reduction possible by reinforcing the spar caps, since no further reduction in gages is possible. However, for a highly loaded all-metallic panel weighing 15 pounds per square foot, the addition of 2.4 pounds per square foot of composite reinforcement to the spar caps will reduce the overall panel weight to 9 pounds per square foot.

### Wing Tip Mass for Structural Arrangements

Surface panel shear thickness is a critical parameter for evaluation of outer wing torsional stiffness and flutter speed. Therefore, the estimated thicknesses used in the NASTRAN 2-D model were compared with those derived from the detailed stress analysis (strength design only) as shown in Figures 15-22 through 15-24. This data

TABLE 15-35. COMPARISON OF COMPOSITE REINFORCED DESIGNS

ARRANGEMENT	CHORDWISE STIFFENED		
PANEL CONCEPT	CONVEX BEADED		
MATERIAL APPLICATION	ALL METALLIC	COMPOSITE REINFORCED	
		SURFACE AND SPAR CAPS	SPAR CAPS
(SEE NOTES)	(A)	(B)	(A)
<u>VARIABLE WEIGHT</u>	(56,655)	(44,474)	(43,624)
CENTER SECTION	(8,722)	(6,847)	(6,716)
UPPER SURFACE	1,570	1,689	1,570
LOWER SURFACE	1,570	1,680	1,570
SPAR CAPS AND WEBS	4,884	2,780	2,878
RIBS	698	698	698
INTERM PANEL	(39,296)	(30,847)	(30,258)
UPPER SURFACE	7,073	7,610	7,073
LOWER SURFACE	7,073	7,593	7,073
SPAR CAPS AND WEBS	22,006	12,500	12,963
RIBS	3,144	3,144	3,144
OUTER PANEL	(8,637)	(6,780)	(6,650)
UPPER SURFACE	1,555	1,680	1,555
LOWER SURFACE	1,555	1,660	1,555
SPAR CAPS AND WEBS	4,837	2,750	2,850
RIBS	690	690	690
<u>FIXED WEIGHT</u>	(41,352)	(41,352)	(41,352)
TOTAL (STRENGTH DESIGN ONLY)	98,007	85,826 <sup>(C)</sup>	84,976

## NOTES:

- (A) 20-inch SPAR SPACING, 60-inch RIB SPACING
- (B) 40-inch SPAR SPACING IN HIGHLY LOADED AREAS ONLY
- (C) FORWARD BOX (FWD OF F.S. 2330) IS ALL METALLIC.  
TOTAL WEIGHT IS 89,494 lbs FOR 40-inch SPAR SPACING AND  
REINFORCED SURFACE AND CAPS THROUGHOUT.

TABLE 15-36. DETAILED WEIGHTS FOR COMPOSITE REINFORCED DESIGNS - SURFACE AND SPAR CAP

A. COMPOSITE REINFORCED (B/P) SURFACE AND SPAR CAPS - 40 inch SPAR SPACING

POINT DESIGN REGION	COMPOSITE REINFORCED DESIGN		ALL METAL-CHORDWISE STIFFENED DESIGN		TOTAL COMPOSITE REINFORCED DESIGN	ALL METAL DESIGN	RATIO OF: COMPOSITE TO METAL percent
	SURFACE	SPAR CAP	SURFACE	SPAR CAP			
	psf ~ pounds per square foot						
40322 (U)	1.341	0.177	1.62	0.60	4.46	4.87	91.6
(L)	1.497	0.203	1.41	—	(0.47)	—	
(C)	(0.37)	(0.10)	—	—			
40236 (U)	1.464	1.071	1.63	8.30	7.73	13.48	57.3
(L)	1.829	1.695	1.38	—	(2.83)		
(C)	(0.58)	(2.25)	—	—			
40536 (U)	1.958	0.98	2.241	7.07	7.55	12.85	58.8
(L)	1.536	1.48	1.943	—	(2.47)		
(C)	(0.53)	(1.94)	—	—			
41036 (U)	1.900	0.751	1.45	5.10	6.14	9.45	65.0
(L)	1.549	1.074	2.03	—	(1.79)		
(C)	(0.49)	(1.30)	—	—			
41316 (U)	2.305	1.381	2.80	11.05	8.95	17.16	53.2
(L)	2.120	2.201	2.37	—	(3.52)		
(C)	(0.44)	(3.08)	—	—			
41348 (U)	1.978	0.936	2.20	6.86	6.56	11.38	57.6
(L)	1.539	1.407	1.62	—	(2.36)		
(C)	(0.53)	(1.83)	—	—			

NOTES: (U) = UPPER; (L) = LOWER; (C) = COMPOSITE WEIGHT INCLUDED IN UNIT WEIGHT CALCULATIONS

TABLE 15-37. DETAILED WEIGHTS FOR COMPOSITE REINFORCED DESIGNS - SPAR CAPS ONLY

B. COMPOSITE REINFORCED (B/P) SPAR CAPS ONLY - 20 inch SPAR SPACING

POINT DESIGN REGION	SPAR CAPS			TOTAL	RATIO OF: COMPOSITE METAL		
	COMPOSITE REINFORCED		ALL-METAL DESIGN				
	COMP. ONLY	TOTAL					
	psf ~ pounds per square foot				percent		
40322 (U)	-	-	0.60	3.80	3.80		
(L)	-	-			100		
40236 (U)	0.720	1.239	7.92	7.14	12.08		
(L)	1.224	1.740			59.1		
40536 (U)	0.626	1.142	6.70	7.27	11.3		
(L)	1.012	1.531			64.3		
41036 (U)	0.384	0.902	4.60	5.68	8.25		
(L)	0.604	1.123			68.8		
41316 (U)	0.921	1.440	9.65	9.22	15.38		
(L)	1.531	2.047			59.9		
41348 (U)	0.543	1.061	5.90	6.29	9.75		
(L)	0.861	1.380			64.5		

(U) = UPPER; (L) = LOWER

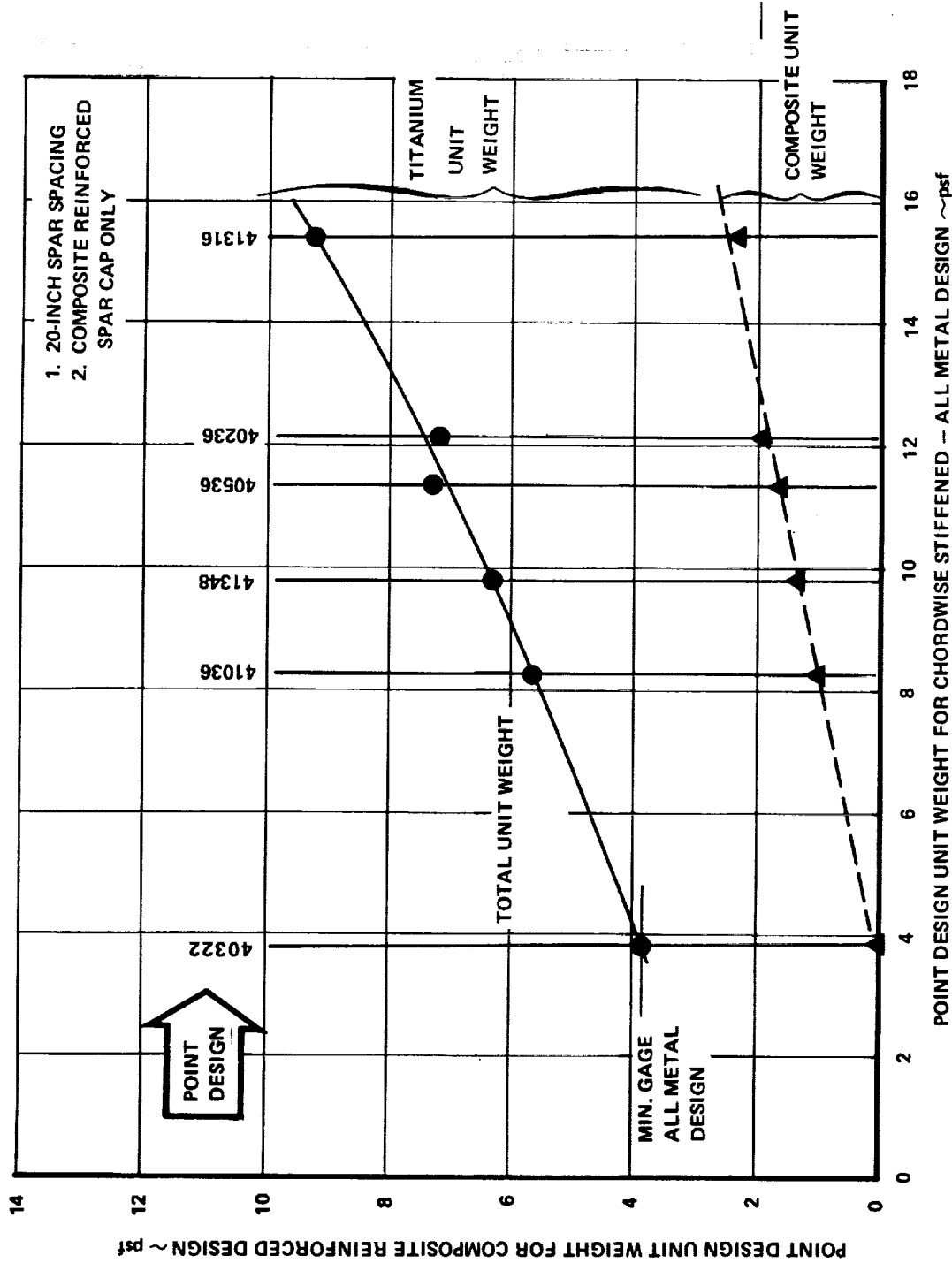


Figure 15-21 Comparison of Optimum Panel Unit Weights - Composite Reinforced Versus All-Metallic Chordwise Stiffened Designs

TABLE 15-38. COMPONENT WEIGHT DERIVATION - COMPOSITE REINFORCED SPAR CAPS ONLY

A. COMPOSITE REINFORCED SPARS ONLY (20-inch SPAR SPACING)	UNIT WEIGHT (lb/ft <sup>2</sup> )	BOX WEIGHT (lb)
<u>FORWARD BOX:</u> (AREA = 4136.6 ft <sup>2</sup> /AIRPLANE)	4.975	20,580
<ul style="list-style-type: none"> <li>● SURFACES } SAME AS ALL-METALLIC (LESS FAIL-SAFE)</li> <li>● RIBS }</li> <li>● SPARS = 0.122 (1.53 X 9 + 2.375) + 0.090      <u>FAIL-SAFE</u></li> </ul> <p>(COMPOSITES: 522 lb)</p>		(9,452) (2,570) (8,558)
<u>AFT BOX:</u> (AREA = 2132.4 ft <sup>2</sup> /AIRPLANE)	8.152	17,384
<ul style="list-style-type: none"> <li>● SURFACES } SAME AS ALL-METALLIC LESS FAIL-SAFE)</li> <li>● RIBS }</li> <li>● SPARS = 0.3162 (4.21 + 3.72 + 2 X 2.375) + 0.009</li> </ul> <p>(COMPOSITES: 3,762 lb)</p>	4.018	(7,302) (1,514) (8,568)
<u>TIP BOX:</u> (AREA = 896.0 ft <sup>2</sup> /AIRPLANE)	11.292	10,118
<ul style="list-style-type: none"> <li>● SURFACES } SAME AS ALL-METALLIC LESS FAIL-SAFE)</li> <li>● RIBS }</li> <li>● SPARS = 0.3465 (3.97 + 2.74 + 2 X 1.53) + 0.005      =</li> </ul> <p>(COMPOSITES: 1,196 lb)</p>	3.390	(3,459) (683) (3,038)
● FLUTTER INCREMENT	3.279	(2,938)

TOTAL COMPOSITE MATERIAL WEIGHT: 5,480 lb

TABLE 15-39. COMPONENT WEIGHT DERIVATION - COMPOSITE REINFORCED SPAR CAPS AND SURFACES

B. COMPOSITE REINFORCED SPARS AND SURFACES (40-INCH SPAR SPACING)	UNIT WEIGHT (lb/ft <sup>2</sup> )	BOX WEIGHT (lb)
<u>FORWARD BOX:</u> (AREA = 4136.6 ft <sup>2</sup> /AIRPLANE) <ul style="list-style-type: none"> <li>● SURFACES = 0.122 (9 X 2.838 + 3.449) + (0.006) (COMPOSITES: 1,635 lb)</li> <li>● RIBS           (SAME AS METALLIC)</li> <li>● SPARS       = 0.122 (9 X 1.31 + 2.175) - (0.022) (COMPOSITES: 919 lb)</li> </ul>	5.846 (3.543) (0.621) (1.682)	24,184 (14,655) (2,570) (6,959)
<u>AFT BOX:</u> (AREA = 2132.4 ft <sup>2</sup> /AIRPLANE) <ul style="list-style-type: none"> <li>● SURFACES = 0.3162 (3.293 + 3.49 + 2 X 3.449) = (COMPOSITES: 1,414 lb)</li> <li>● RIBS           (SAME AS METALLIC)</li> <li>● SPARS       = 0.3162 (3.996 + 3.51 + 2 X 2.175) - (0.066) = (COMPOSITES: 4,578 lb)</li> </ul>	8.719 (4.326) (0.710) (3.683)	18,592 (9,225) (1,514) (7,853)
<u>TIP BOX:</u> (AREA = 896.0 ft <sup>2</sup> /AIRPLANE) <ul style="list-style-type: none"> <li>● SURFACES = 0.3465 (4.425 + 3.517 + 2 X 2.838) = (COMPOSITES: 536 lb)</li> <li>● RIBS           (SAME AS METALLIC)</li> <li>● SPARS       = 0.3465 (4.062 + 2.643 + 2 X 1.31) - (0.037) (COMPOSITES: 1,586 lb)</li> <li>● FLUTTER INCREMENT</li> </ul>	11.954 (4.719) (0.762) (3.194) (3.279)	10,711 (4,228) (683) (2,862) (2,938)

TOTAL COMPOSITE MATERIAL WEIGHT: 10,668 lb.

NOTE: SHEAR THICKNESS, ( $t_s$ ) =  $0.78 \bar{t}$   
 WHERE  $\bar{t}$  = EQUIVALENT WEIGHT THICKNESS

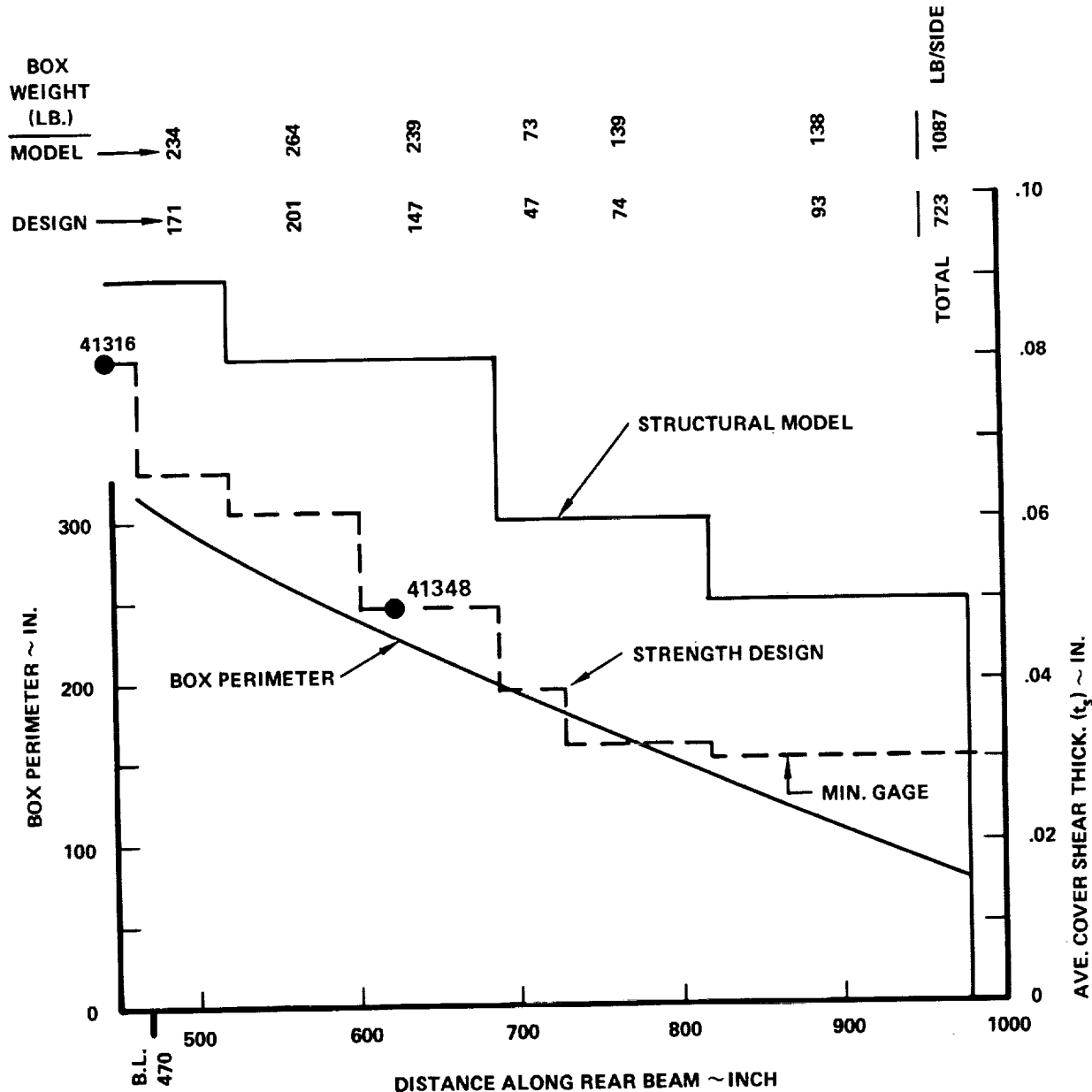


Figure 15-22. Shear Thickness of Wing Tip Structure - Chordwise Stiffened

NOTE: SHEAR THICKNESS ( $t_s$ ) =  $0.40t$   
WHERE  $t$  = EQUIVALENT WEIGHT THICKNESS

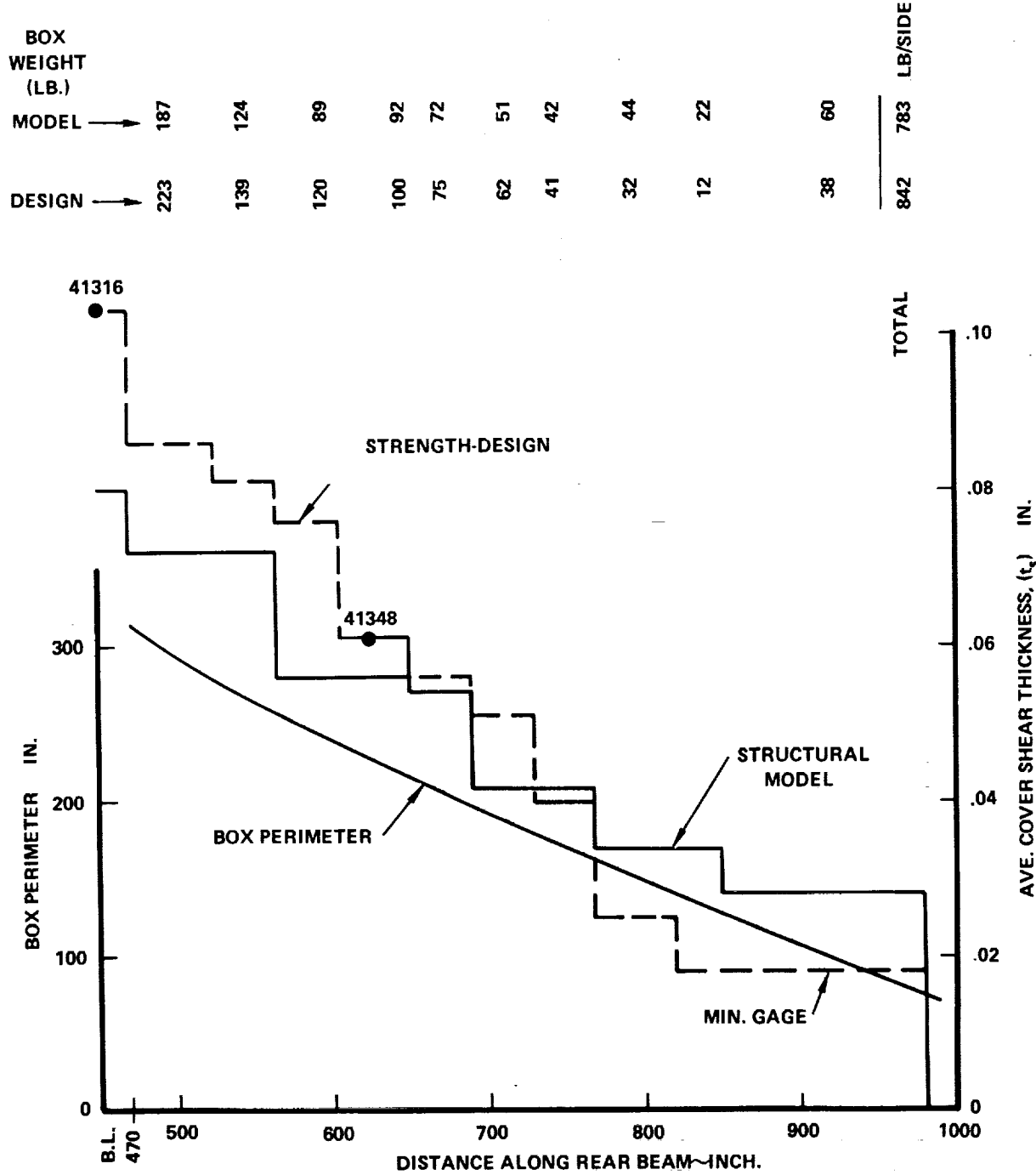


Figure 15-23. Shear Thickness of Wing Tip Structure - Spanwise Stiffened

NOTE: SHEAR THICKNESS ( $t_s$ ) =  $0.97\bar{t}$   
 WHERE  $\bar{t}$  = EQUIVALENT WEIGHT THICKNESS

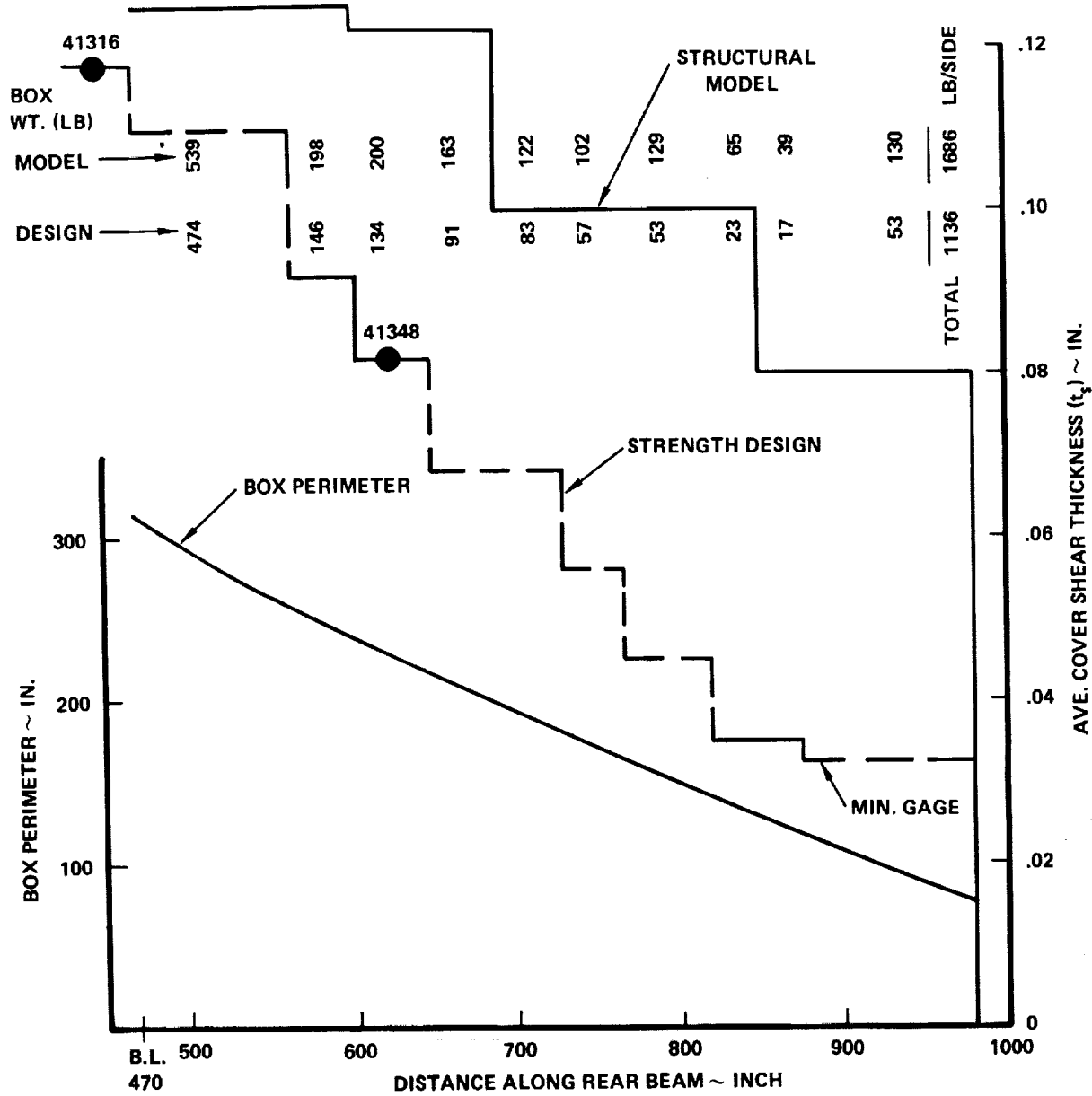


Figure 15-24. Shear Thickness of Wing Tip Structure - Monocoque

was used as the basis for evaluation of the flutter increment required for each structural concept (Reference Figure 15-14).

These mass data comparisons included only that portion of the outer box which lies perpendicular to the rear beam and outboard of butt line 470 as pictorially displayed on Figure 15-25.

From a weight efficiency standpoint, the monocoque arrangement is preferred, since 97-percent of the surface panel weight is effective in providing torsional stiffness. By comparison, the effective shear thicknesses for the chordwise and spanwise stiffened arrangements are only 78-percent and 40-percent, respectively.

#### Wing Tip Mass Distribution Comparison

The aeroelastic analysis of Task I used a single mass distribution for the 3 wing structural arrangements. Since wing tip mass distribution has a significant effect on flutter speed, several comparisons were made between the Task I and Task II distributions. Figure 15-26 compares the dead weight shear measured spanwise along the rear beam. The wing tip structure center of gravity at a percent of chord and wing weight distribution (pounds per inch) in the spanwise direction is compared in Figure 15-27. The wing tip box geometry is displayed in Figure 15-28 and shows that the Task II planform and wetted areas are slightly larger than Task I, while the effective span is decreased about 10 percent.

#### FUSELAGE STRUCTURE MASS-INITIAL SCREENING

The basic structural arrangement for the fuselage design is a uniaxial stiffened structure of skin and stringers with supporting frames. The panel structural concepts investigated are as follows:

- Zee stiffened
- Closed-hat stiffened
- Open-hat stiffened

Figure 15-29 presents the body perimeter, width, height and cross sectional areas of the fuselage. The perimeter was used to calculate the wetted areas for 200 inch

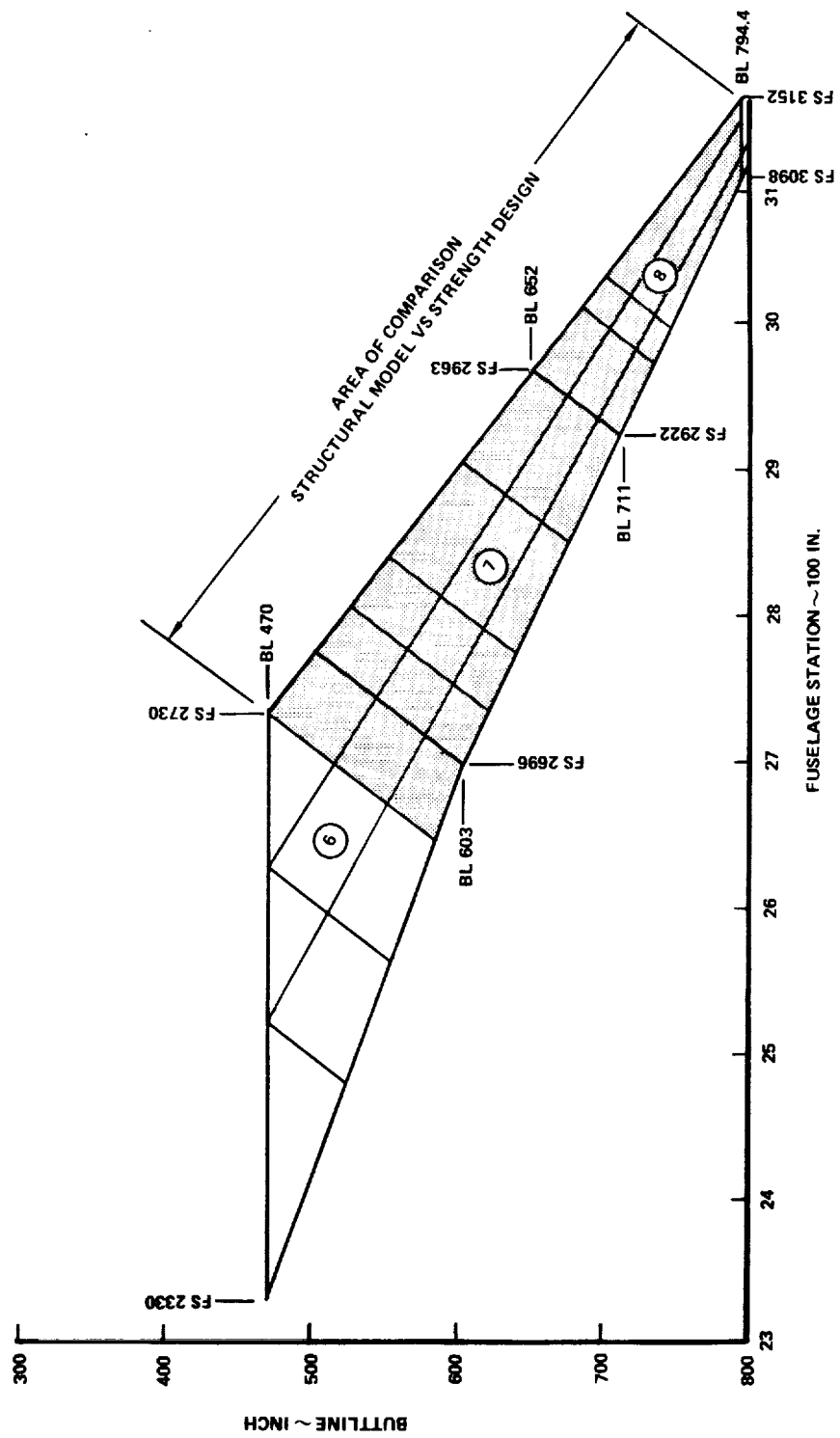


Figure 15-25. Wing Tip Structure Plansform Geometry - Task I

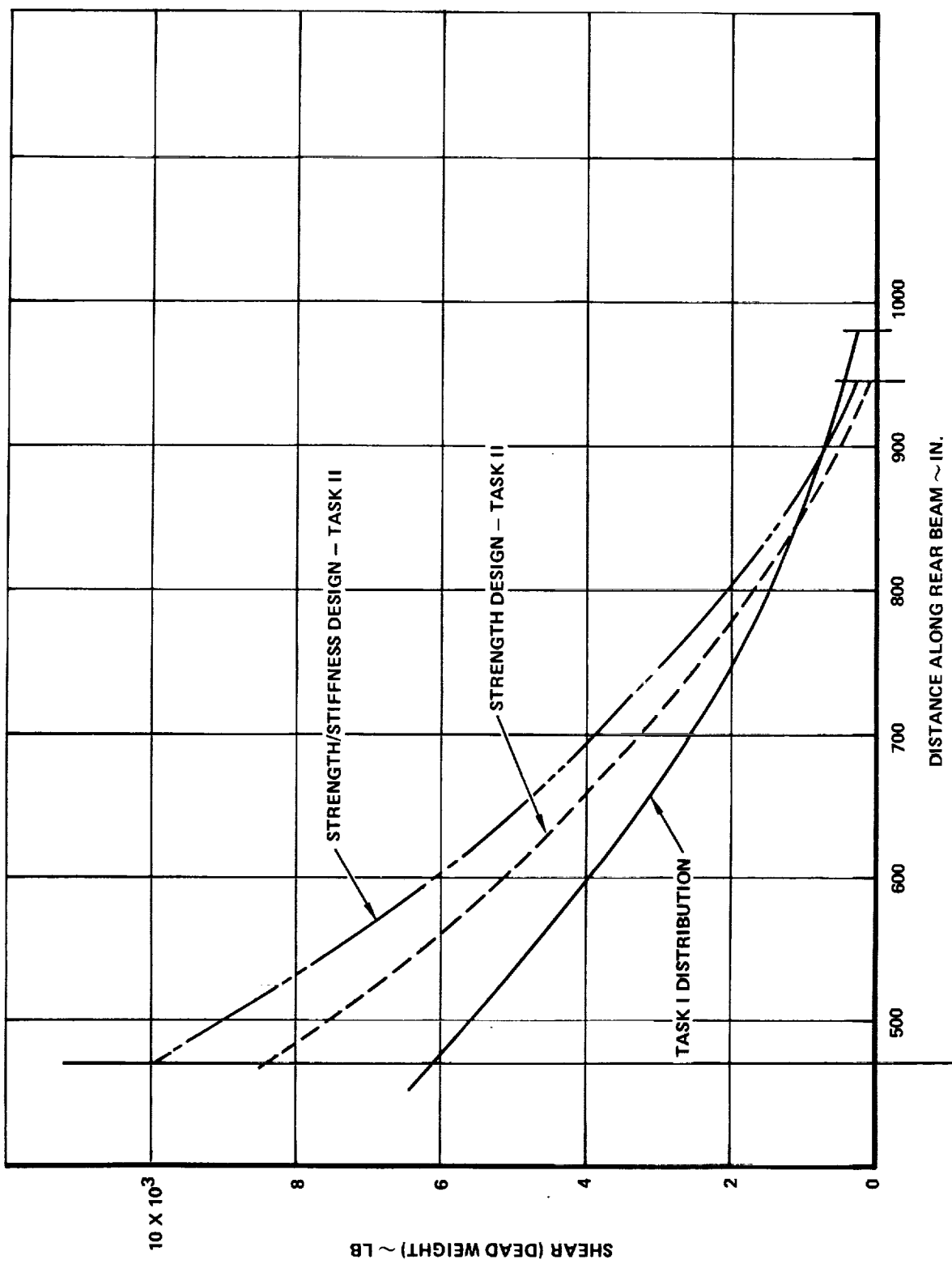


Figure 15-26 Comparison of SIC Mass Distribution - Task I and Task II

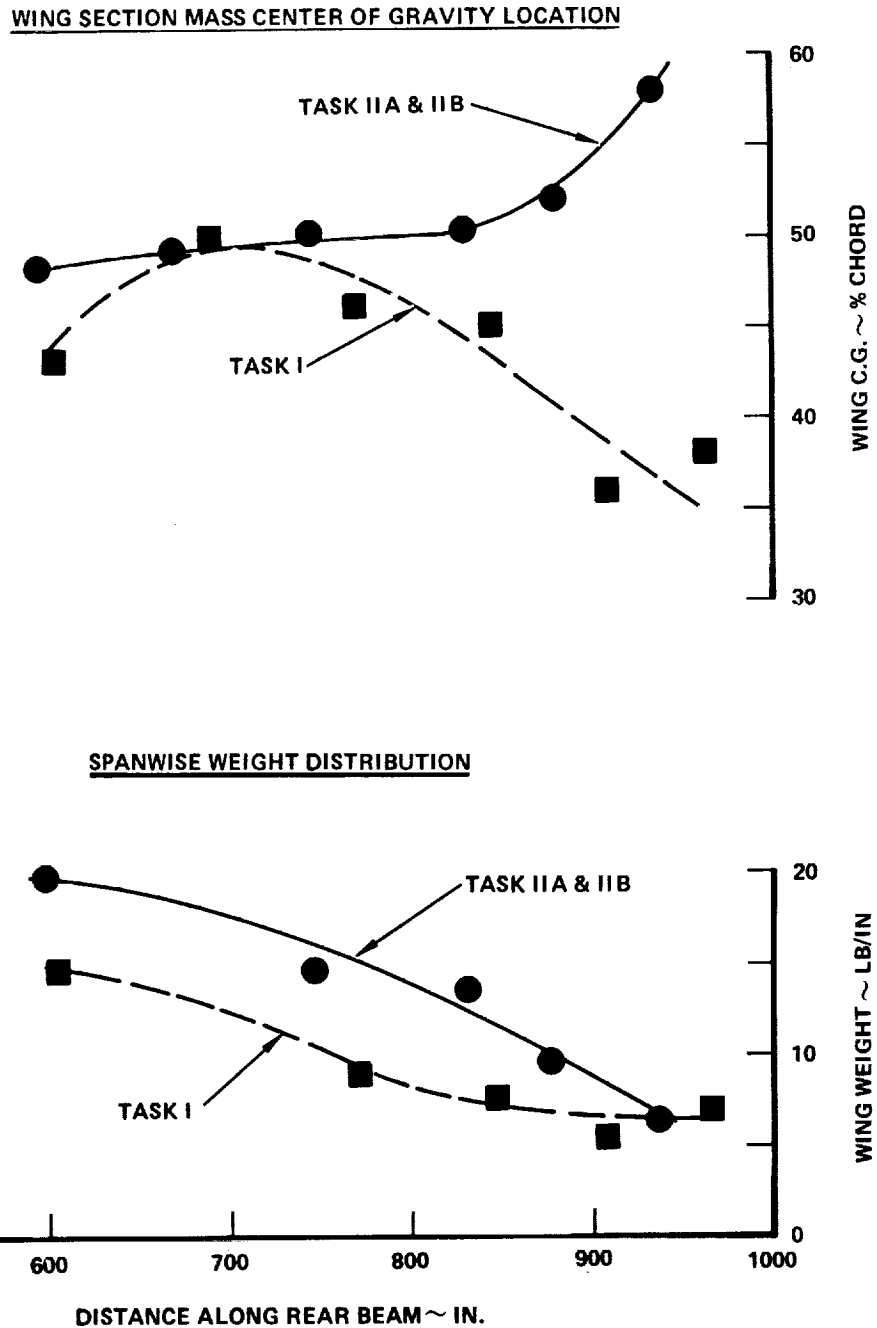


Figure 15-27. Wing Tip Mass Distributions - Task I and Task II

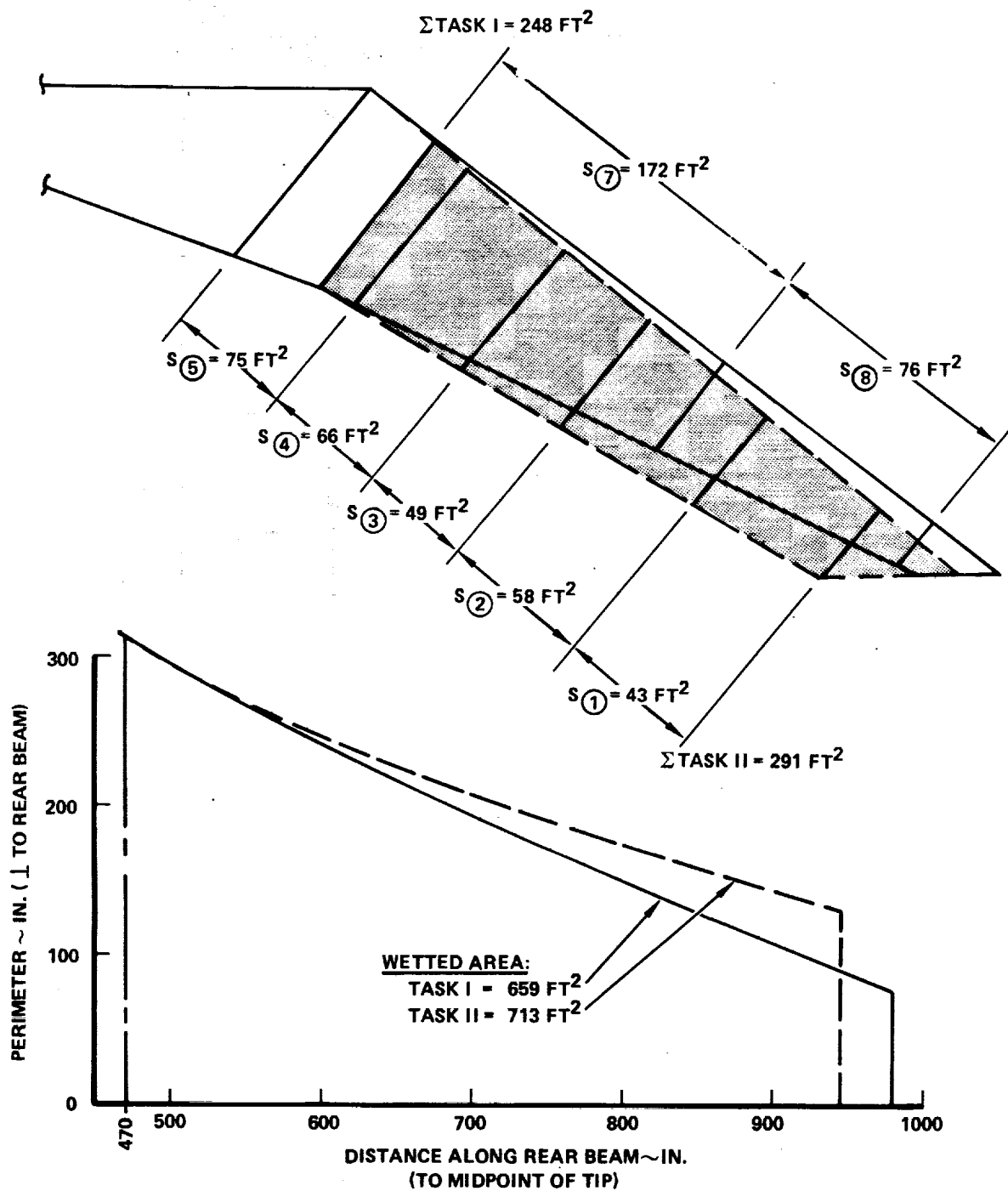


Figure 15-28. Wing Tip Box Geometry - Task I and Task II

$A_{SECT}$  = CROSS SECTIONAL AREA (IN<sup>2</sup>)  
 $H$  = FUSELAGE DEPTH (IN)  
 $W$  = FUSELAGE WIDTH (IN)  
 $P_{TOTAL}$  = TOTAL PERIMETER OF SHELL (IN)  
 $P_{UPR}$  = SHELL PERIMETER ABOVE THE FLOOR (IN)

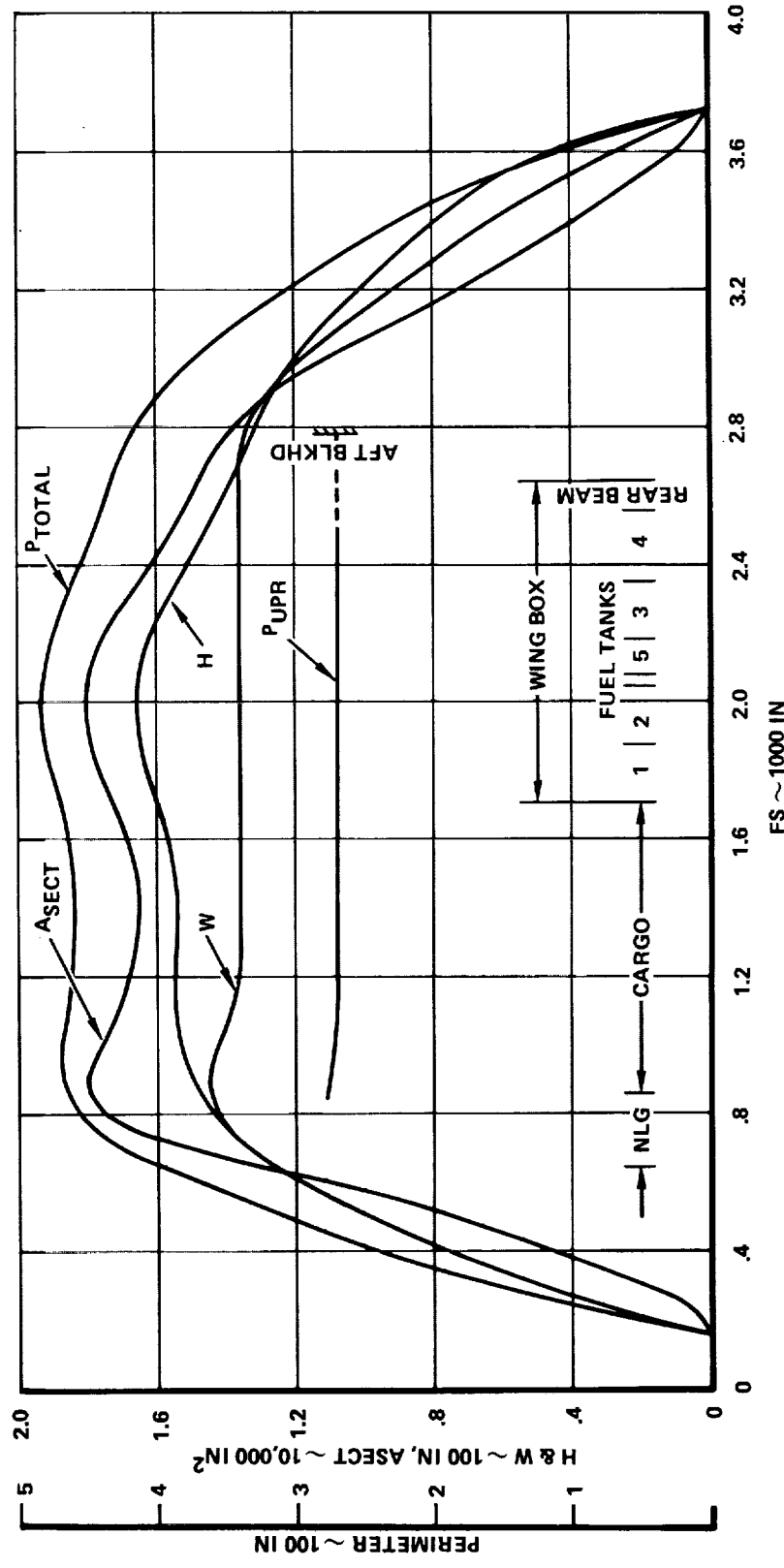


Figure 15-29. Body Geometry - Task I

segments. In the region of the wing box carry-through structure the body area is the circular arc segment above the upper wing surface. The segment areas and skin and stiffener unit weights are illustrated in Figure 15-30. The zee, open-hat and closed-hat stiffened concepts were analyzed at Fuselage Stations 2000, 2500 and 3000. As indicated on the figure, the closed-hat is 5- to 10-percent lighter and is selected for the weight calculation. The forward cabin utilizes zee stiffening and the transition assumes straight line extrapolation between the analysis points.

#### FUSELAGE STRUCTURE DETAILED ANALYSIS

For the detailed concept analysis, complete frame data and revised data for the closed-hat panel design were determined. The results of the analysis are identified on Table 15-40 in the shaded-column. The total fuselage weight for the zee- and open-hat stiffened shell are also shown. These data reflect the initial screening panel weights combined with the newly determined frame data for the closed-hat design. The weight trends, as indicated for the initial screening data for the panel concepts in Figure 15-30, are 5- to 6-percent lighter for the selected design concept. A minimum skin gage of .050-inch was used for the aft fuselage to meet the preliminary sonic fatigue requirements. Figure 15-31 and Table 15-41 illustrate the method used to derive the detailed fuselage shell weight for the closed-hat design. The mass data includes a non-optimum factor (NOF) applied to the shell structure unit weight to arrive at a typical estimate of the "as-constructed" weight. These non-optimum allowances are itemized as:

	<u>Non-Optimum Factor (NOF)</u>
Joints and splices	4-percent
Margins of safety (average)	3-percent
Sheet tolerances	2-percent
Access provisions	2-percent
Finish, sealant, misc.	<u>3-percent</u>
Total NOF	<u>14-percent</u>

Use of these allowances, as described earlier in the Wing Structure Mass-Initial Screening section, means that a stress analysis which indicates a 3-pounds-per-square-foot panel yields an estimated fabricated weight,  $(1.14 \times 3.0) = 3.52$  pounds per square foot.

TABLE 15-40. FUSELAGE CONCEPT WEIGHTS - DETAILED CONCEPT ANALYSIS

$$\text{AVERAGE SHELL MASS} = 0.232(w_{750} + w_{2000} + w_{2500} + w_{3000} + w_{3723})$$

OPTIMUM UNIT MASS (psf) AT STATION:	750 2000 2500 3000 3723	1.56 3.54 4.03 3.54 2.15	1.56 3.51 3.86 3.51 2.15
AVERAGE SHELL MASS (INCL. NOF), $w_{\text{SHELL}}$ (lb/ft <sup>2</sup> ) (kg/m <sup>2</sup> )		3.44 (16.80)	3.39 (16.55)
SHELL AREA (FS 690 TO 3723) = 7,167 ft <sup>2</sup> (666 m <sup>2</sup> )			<b>3.23 (15.77)</b>
SHELL MASS = (lb) (kg)		24,654 (11,183)	24,296 (11,020)
<b>FIXED MASS</b>			<b>23,148 (10,500)</b>
NOSE AND FLIGHT STATION	2,500		
NLG WELL	900		
WINDSHIELD AND WINDOWS	1,680		
FLOORING AND SUPTS.	3,820		
DOORS AND MECHANISM	4,170		
UNDERWING FAIRING	1,870		
CARGO COMPARTMENT PROV.	1,060		
WING/BODY FITTINGS	1,500		
TAIL/BODY FITTINGS	600		
PROV. FOR SYSTEMS	740		
FINISH AND SEALING	700		
<b>TOTAL FUSELAGE MASS (lb)</b> (kg)		44,194 (20,046)	43,836 (19,884)

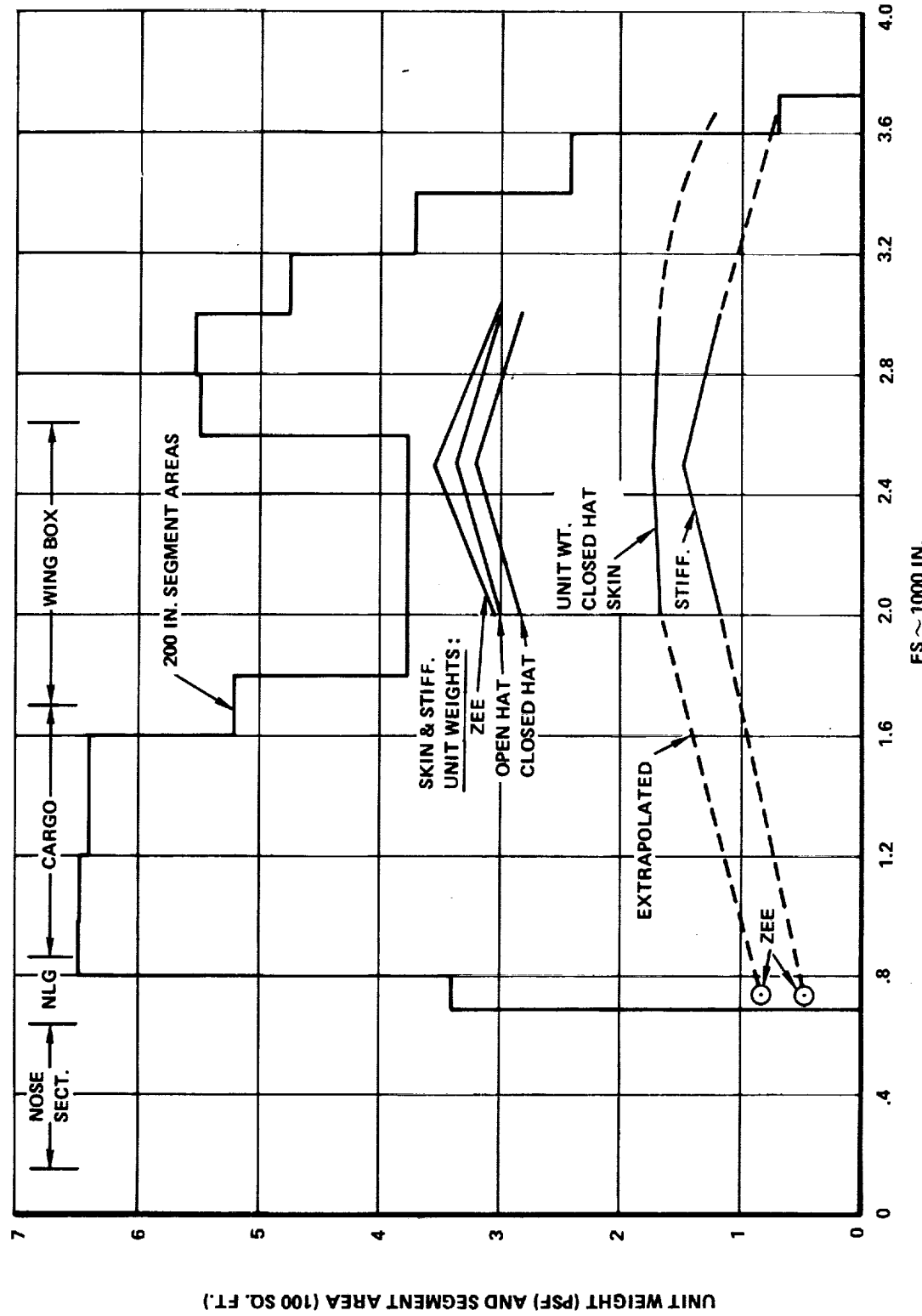


Figure 15-30. Skin and Stiffener Unit Weights - Initial Screening

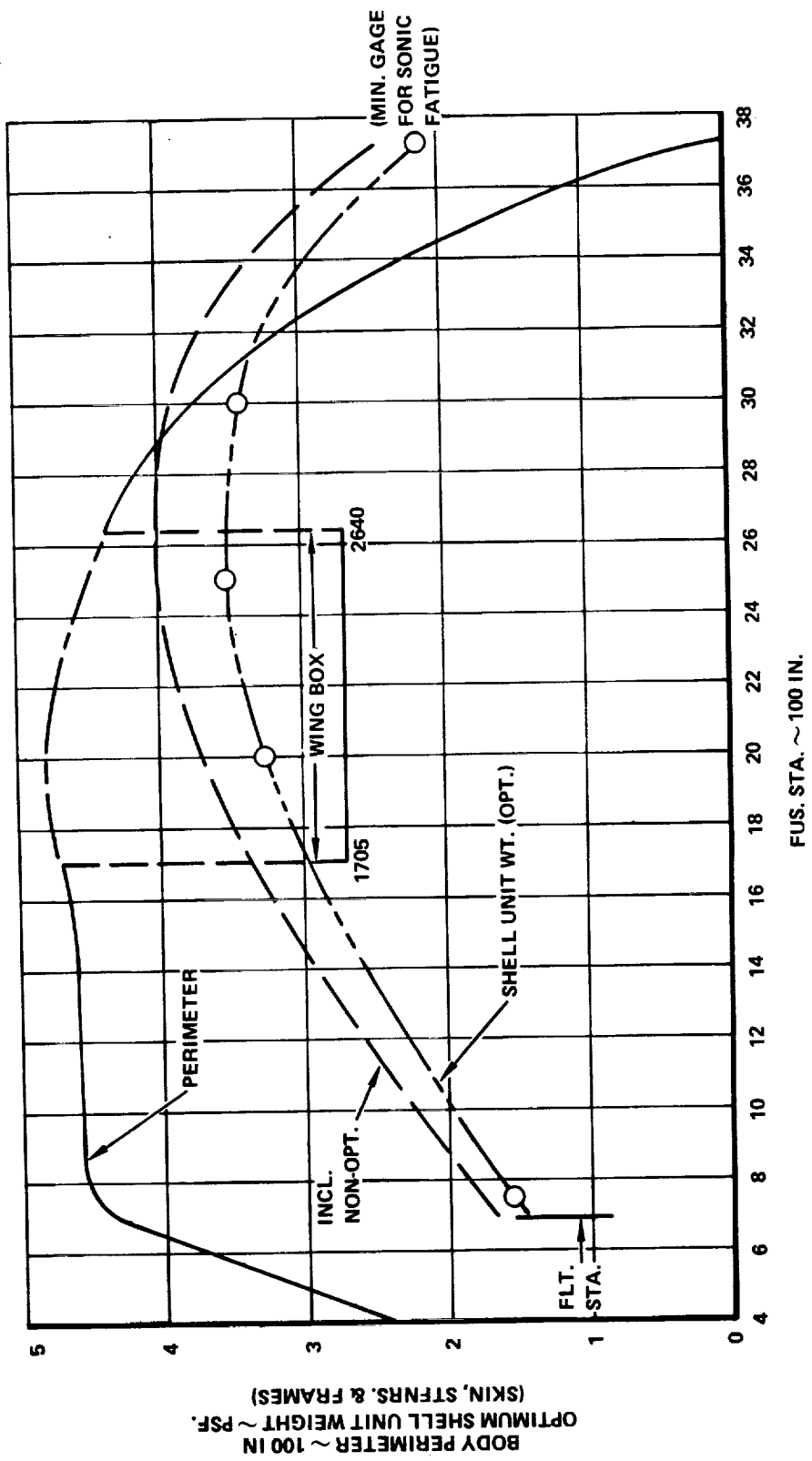


Figure 15-31. Unit Weight for Closed Hat Stringer Design - Detailed Concept Analysis

TABLE 15-41. FUSELAGE SHELL WEIGHTS - CLOSED HAT-STIFFENED PANEL CONCEPT - TASK I

SECT. F.S.	PERIMETER <sup>(A)</sup> (in.)	$\Delta S$ (ft <sup>2</sup> )	SHELL UNIT WT. (psf)	$\Delta W_{OPT}$ (lb)	C.G. (in.)
690 - 800	445	340	1.55	527	745
800 - 1000	457	635	1.80	1143	900
- 1200	457	635	2.12	1346	1100
- 1400	460	639	2.42	1546	1300
- 1600	462	642	2.70	1733	1500
- 1705	467	340	2.90	986	1653
1705 - 2640	270	1753	3.35	5873	2175
2640 - 2800	425	472	3.50	1652	2720
- 3000	397	551	3.45	1901	2900
- 3200	347	482	3.35	1615	3100
- 3400	272	378	3.13	1183	3300
- 3600	173	240	2.75	660	3500
- 3723	70	60	2.33	140	3660
<b>TOTALS</b>		<b>7167<sup>(B)</sup></b>		<b>20,305<sup>(C)</sup></b>	<b>2150</b>

(A) AVERAGE DATA FOR SHELL

(B) CUTOUT FOR WING EXCLUDED

(C) OPTIMUM WEIGHT; "AS-FABRICATED" WEIGHT = 1.14 X 20,305 = 23,148 lb  
(SKINS = 11,423 lb; STIFFENERS = 8,120 lb; FRAMES = 3,605 lb)

## ASSET PROGRAM RESULTS - TASK I

The ASSET Program synthesizes the vehicle so that it may be scaled up and down in size. The selected wing concepts are reflected by input coefficients to the wing group equation. The coefficients also consider those lightly loaded areas which are minimum gage, in addition to the primary load carrying structure.

Wing and fuselage weights resulting from the detailed concept analysis effort of Task I are reflected in the ASSET Program printouts. Data are presented for: (1) the aircraft scaled up to meet the range objective of 4200 nautical miles (7778 kilometers) and (2) the aircraft which has a takeoff weight of 750,000 pounds (340,000 kilograms) with variable range as dictated by the available fuel.

Table 15-42 summarizes the results of the ASSET runs for easy reference.

The wing concepts are described below:

1. Chordwise stiffened, Ti-6Al-4V Convex-beaded - mechanical fasteners
2. Spanwise stiffened, Ti-6Al-4V Hat - mechanical fasteners
3. Monocoque, Aluminum brazed honeycomb sandwich - mechanical fasteners
4. Monocoque, Aluminum brazed honeycomb sandwich - welded
5. Chordwise Stiffened, Convex-beaded, B/PI, composite reinforced spars
6. Best Combination:
  - Concept 5 for forward and aft box structure
  - Concept 3 for outer box structure

In all cases, the wing loading at takeoff ( $W_{TO}/S$ ) is 69.3 pounds per square foot and the thrust loading ( $T/W_{TO}$ ) is 0.477 pounds of thrust per pound of takeoff weight. This is an uninstalled S.L.S. thrust of 89,466 pounds per engine, increasing engine, nacelle and air induction weights over those carried for Task I.

## FINAL DESIGN AIRPLANE MASS ESTIMATES

Detailed weight descriptions of the wing and fuselage for the Final Design airplane are given in Tables 15-43 and 15-44, respectively.

TABLE 15-42. AIRCRAFT WEIGHT AND COST SUMMARY

WING CONCEPT	1	2	3	4	5	6								
RANGE, n.mi.	4,200	3,830	4,200	3,870	4,200	4,123								
WEIGHTS (lb)														
TAKEOFF FUEL AVAIL.	884,847	750,000	867,126	750,000	772,641	750,000								
ZERO FUEL PAYLOAD	454,156	371,525	444,772	372,685	389,532	382,241								
OPERATING OP. AND STD. ITEMS	430,691	378,475	422,353	377,315	373,109	364,982								
EMPTY WING TAIL BODY LANDING GEAR SURF. CONTR. NACELLES PROPULSION ENGINES AIR INDUCT. FUEL SYST. ENG. CONTR. INSTRUMENTS HYDRAULIC ELECTRICAL AVIONICS FURNISHINGS E.C.S. AUX. GEAR A.M.P.R.	49,000	383,681	329,475	373,353	328,315	324,109	315,982	333,338	318,759	316,481	313,125	313,963	312,322	49,000
11,448	10,653	11,357	10,564	10,915	10,776	10,995	10,751	10,751	10,861	10,802	10,839	10,809		
370,243	318,821	361,997	317,651	313,194	306,206	322,343	308,008	305,620	302,323	303,125	301,513			
128,895	106,010	125,254	104,834	95,682	92,330	101,296	95,146	90,785	89,434	89,276	88,620			
14,404	11,339	13,986	11,339	11,834	11,339	12,220	11,339	11,545	11,339	11,440	11,339			
46,109	42,688	45,675	42,688	43,283	42,688	43,733	42,688	42,939	42,688	42,812	42,688			
34,700	30,401	34,143	30,401	31,133	30,401	31,691	30,401	30,708	30,401	30,552	30,401			
8,726	8,500	8,697	8,500	8,539	8,500	8,569	8,500	8,517	8,500	8,508	8,500			
6,626	5,616	6,494	5,616	5,786	5,616	5,916	5,616	5,688	5,616	5,661	5,616			
60,316	51,124	59,108	51,124	52,667	51,124	53,850	51,124	51,772	51,124	51,442	51,124			
24,977	20,755	24,418	20,755	21,458	20,755	21,998	20,755	21,050	20,755	20,900	20,755			
6,326	5,598	6,239	5,603	5,789	5,662	5,872	5,649	5,729	5,676	5,706	5,679			
1,744	1,631	1,729	1,631	1,650	1,631	1,664	1,631	1,639	1,631	1,635	1,631			
1,365	1,230	1,347	1,230	1,253	1,230	1,270	1,230	1,239	1,230	1,235	1,230			
6,725	5,700	6,590	5,700	5,872	5,700	6,004	5,700	5,772	5,700	5,735	5,700			
4,650	4,550	4,637	4,550	4,567	4,550	4,581	4,550	4,557	4,550	4,554	4,550			
1,900														
11,500														
8,300														
1,980														
291,099	250,440	284,264	249,269	243,002	236,824	250,764	239,627	236,479	233,942	234,370	233,131			
103.2	90.6	99.8	89.2	107.5	104.9	109.4	104.8	94.7	93.8	94.0	93.6			
FLYAWAY COST (MIL. \$)														

ORIGINAL PAGE IS  
OF POOR QUALITY

TABLE 15-43. FINAL DESIGN AIRPLANE - WING MASS ESTIMATE

ITEM	WEIGHT (lb)
<u>VARIABLE WEIGHT</u>	49,232(A)(B)
FORWARD BOX (PLANFORM AREA = 4136.6 ft <sup>2</sup> )	(20,580)
● SURFACES ~ CONVEX BEADED, CHORDWISE STIFFENED	9,452
● SPARS ~ INCLUDING 522 lb COMPOSITES	8,558
● RIBS	2,570
AFT BOX (PLANFORM AREA = 2132.4 ft <sup>2</sup> )	(17,384)
● SURFACES ~ CONVEX BEADED, CHORDWISE STIFFENED	7,302
● SPARS ~ INCLUDING 3,762 lb COMPOSITES	8,568
● RIBS	1,514
TRANSITION ~ AFT BOX TO TIP BOX	(1,380)
TIP BOX (PLANFORM AREA = 947 ft <sup>2</sup> )	(9,888)
● SURFACES ~ BRAZED HONEYCOMB SAND., MECH. FAST.	8,235
● SPARS	1,336
● RIBS	317
<u>FIXED WEIGHT</u>	41,352
LEADING EDGE	1,047
TRAILING EDGE	1,941
WING/BODY FAIRING	800
LEADING EDGE FLAPS/SLATS	133
TRAILING EDGE FLAPS/FLAPERONS	553
AILERONS	250
SPOILERS	225
MAIN LANDING GEAR ~ DOORS	484
SUP'T. STRUCTURE	3,750
B.L. 62 RIBS	1,430
B.L. 470 RIBS	700
FIN ATTACH RIBS (B.L. 602)	435
REAR SPAR	3,400
ENGINE SUPPORT STRUCTURE	3,580
FUEL BULKHEADS	3,800
<b>TOTAL WING WEIGHT</b>	<b>90,584</b>

(A) INCLUDES FAIL-SAFE PENALTY OF 822 lb

(B) INCLUDES COMPOSITE MATERIAL WEIGHT OF 4,284 lb

TABLE 15-44. FINAL DESIGN AIRPLANE - FUSELAGE MASS ESTIMATE

ITEM	WEIGHT (lb)
<b>SHELL STRUCTURE</b>	22,582(A)
SKIN	11,144
STIFFENERS	7,921
FRAMES	3,517
<b>FIXED WEIGHT</b>	19,540
NOSE AND FLIGHT STATION	2,500
NOSE LANDING GEAR WELL	900
WINDSHIELD AND WINDOWS	1,680
FLOORING AND SUPPORTS	3,820
DOORS AND MECHANISM	4,170
UNDERWING FAIRING	1,870
CARGO COMPARTMENT PROV.	1,060
WING TO BODY FRAMES AND FITTINGS	1,500
TAIL TO BODY FRAMES AND FITTINGS	600
PROV. FOR SYSTEMS	740
FINISH AND SEALANT	700
<b>TOTAL FUSELAGE WEIGHT</b>	<b>42,122</b>

(A) INCLUDES FAIL-SAFE PENALTY OF 1,432 lb

The wing box (variable weight) represents the best combination of structural concepts, that is:

- Forward and aft box: convex beaded, chordwise stiffened surfaces with composite reinforced spar caps.
- Outer box: brazed honeycomb sandwich surfaces, mechanically fastened closures.

The weight description includes fail-safe provisions, allowances for flutter prevention, and panel thickness changes for manufacturing/design constraints. The fixed weight consists of those items which are unaffected by box structural concept, such as surface controls, engine rails, leading and trailing edge structure. Items in this category are weighed by comparison with previous supersonic cruise aircraft and contemporary aircraft.

The fuselage weight is also divided into two major categories, shell weight and fixed weight. Here again the shell weight is dependent upon structural concept, while the fixed weight such as doors, windows, flight station and fairing are unaffected. Fixed weight items are evaluated by comparison with L-2000 and contemporary aircraft.

#### WING STRUCTURE MASS

The wing structure mass for the Final Design Airplane is based on the NASTRAN strength-stiffness bulk data (Reference Section 9, Structural Analysis Models). Appropriate non-optimum factors are applied to the integrated mass data to obtain the "as-constructed" wing weights.

The effect of the various design parameters on the sizing of the structural elements are included in the determination of the bulk data flexibilities. The parameters include:

- Strength
- Fatigue Life
- Temperature
- Thermal Stress
- Flutter
- Aeroelastic Loads
- Jig-shape Effects on Loads
- Design & Manufacturing
- Material Selection (Including Composites)
- Minimum Gage

ORIGINAL PAGE IS  
OF POOR QUALITY

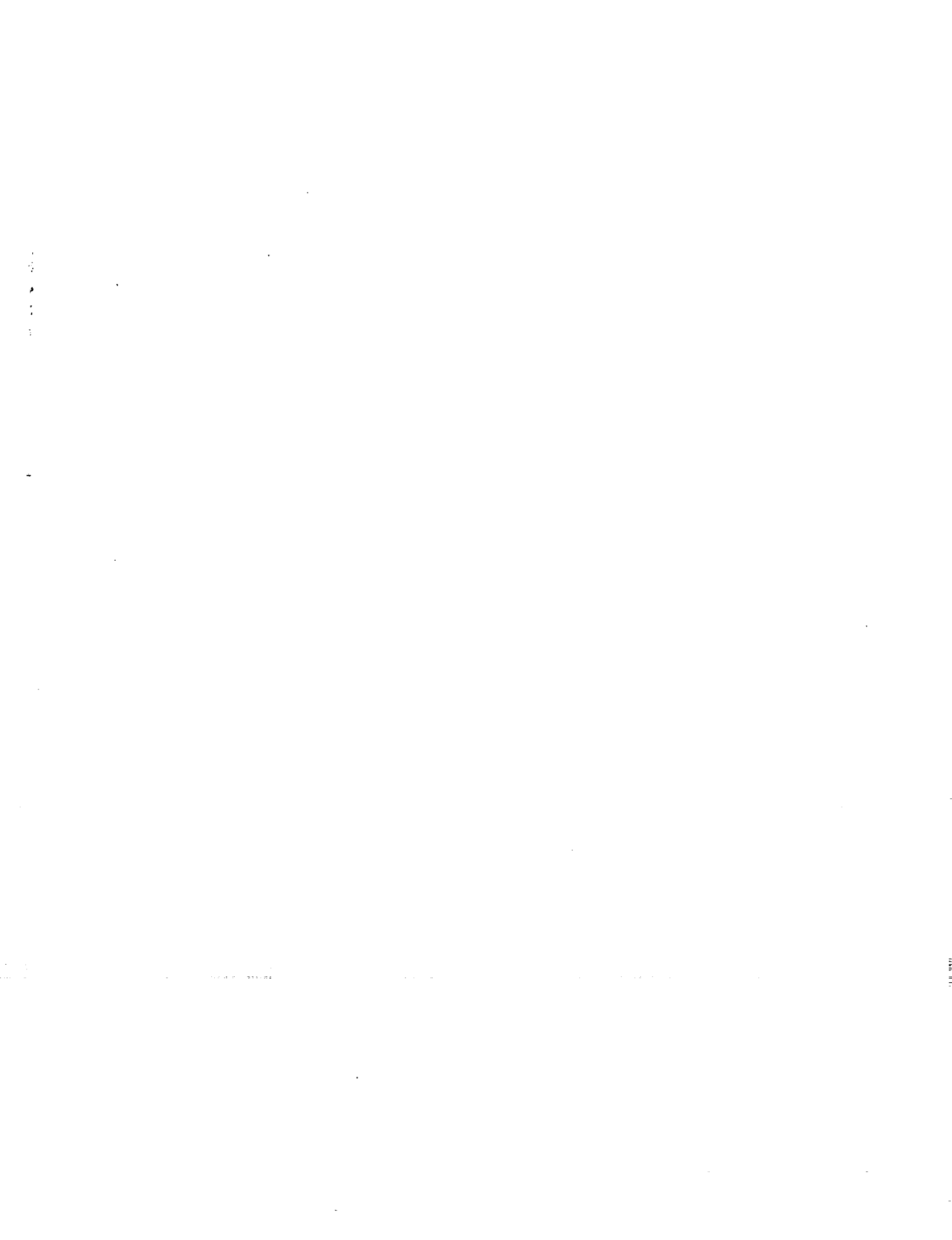
The integrated mass for the wing surface panel, substructure and non-optimum factor are shown at each grid point of the wing planform of Figure 15-32. Mass summations for the forward, aft, and tip boxes and transition are shown. Appropriate allowance for fail-safe requirements at the transition of the monocoque tip design to the chordwise stiffened aft box are included.

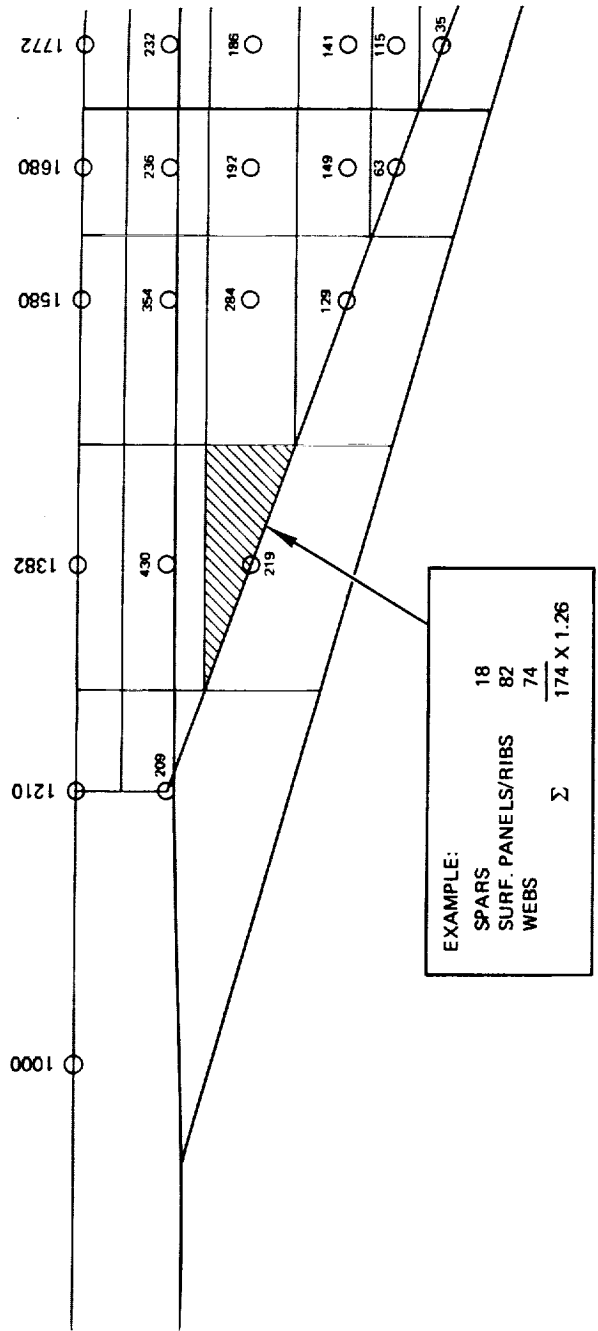
Figure 15-33 presents a comparison of the forward and aft box weights for the strength and strength-stiffness design. The cumulative weights for the wing inboard of BL470 are presented. The data generated indicated that except for small deviation in the aft box region, the strength-design and the strength/stiffness design are essentially unchanged. The change in aft box weight is partially attributed to load increases from jig shape effects on aeroelastic loads. These aft box mass increases as well as the wing fixed weight items are reflected in the SIC distribution.

Table 15-45 presents the mass increments required to meet the specified fail-safe criteria. The unit weight data are as calculated in Section 13 and distributed to the aft box and wing tip structure according to the associated stress levels. The data indicates the aft box penalties appear to be localized in the region of the propulsion system installations. The wing tip penalties are associated with spanwise fail-safe straps required to stop propagation of a chordwise crack in both skins of the honeycomb sandwich panels. It appears that this penalty can be further minimized if the tip structure were specifically designed to meet the stiffness requirement to suppress flutter in light of the fail-safe design requirements. Application of boron-aluminum surface panels in lieu of titanium honeycomb sandwich and considering a multispar design to minimize chordwise crack growth offer significant potential mass reduction for the wing tip structure design.

#### Fuselage Structure Mass Estimates

The fuselage mass estimates for the Final Design airplane are based on the verification of the results of the Detailed Concept Analysis of Task I (refer to Figure 15-31). The "as-constructed" fuselage weights were established by application of a non-optimum factor to the shell (i.e., skin-stringer and frame) unit weight determined for the five selected fuselage stations. This data is again presented on Figure 15-34, as corrected for the shortened nose and slightly altered wing carry through structure. Superimposed on the figure are (1) the verified unit





WFWD BOX = 10,290 LB/SIDE

WAFT BOX = 8,692 LB/SIDE

WTRANSITION = 690 LB/SIDE (WEIGHTS IN PARENTHESES)

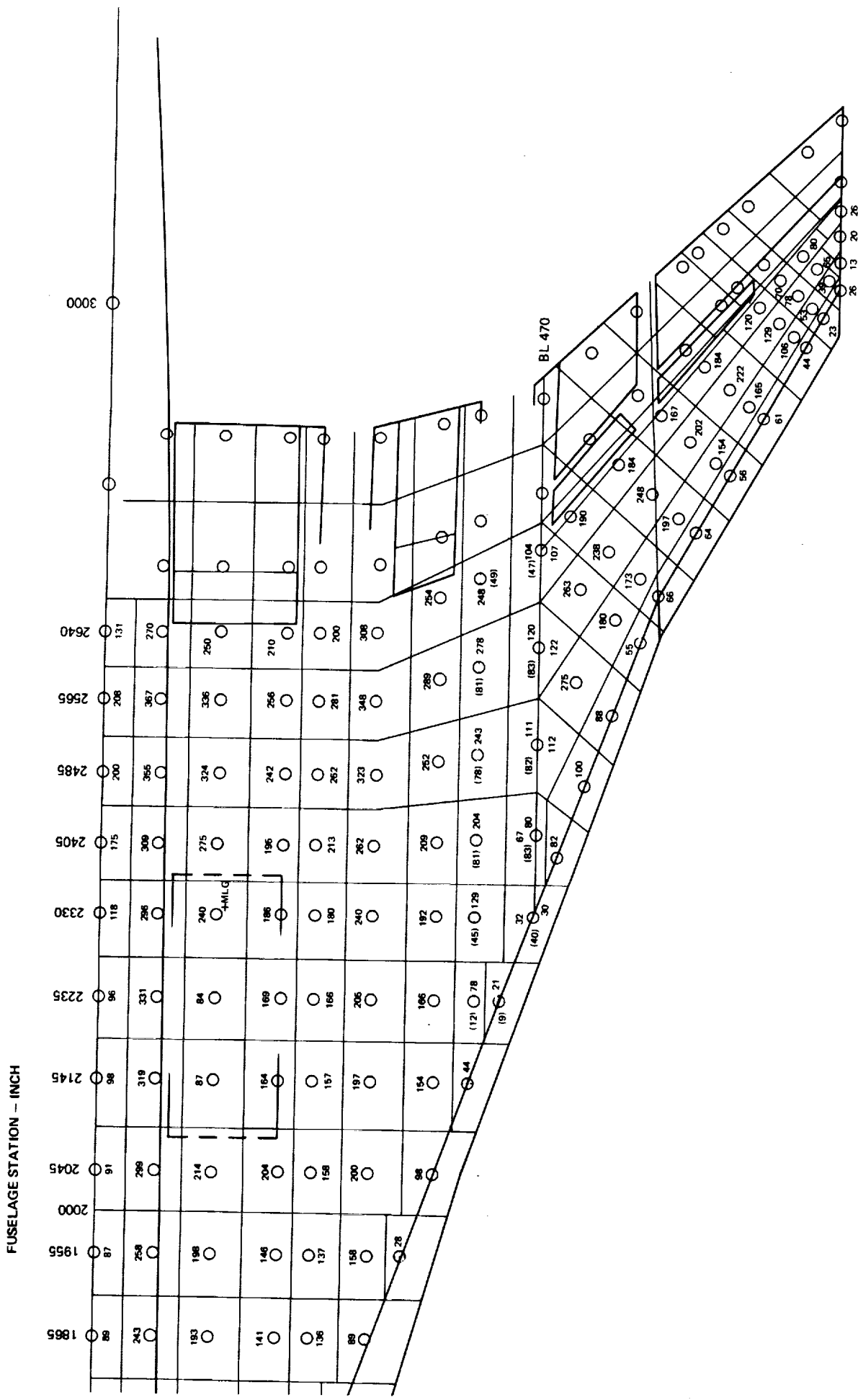
WTIP BOX = 4944

FOLDING FACE BLANK NOT FOLDED

FOLDOUT FRAME 1

FOLDOUT FRAME 2







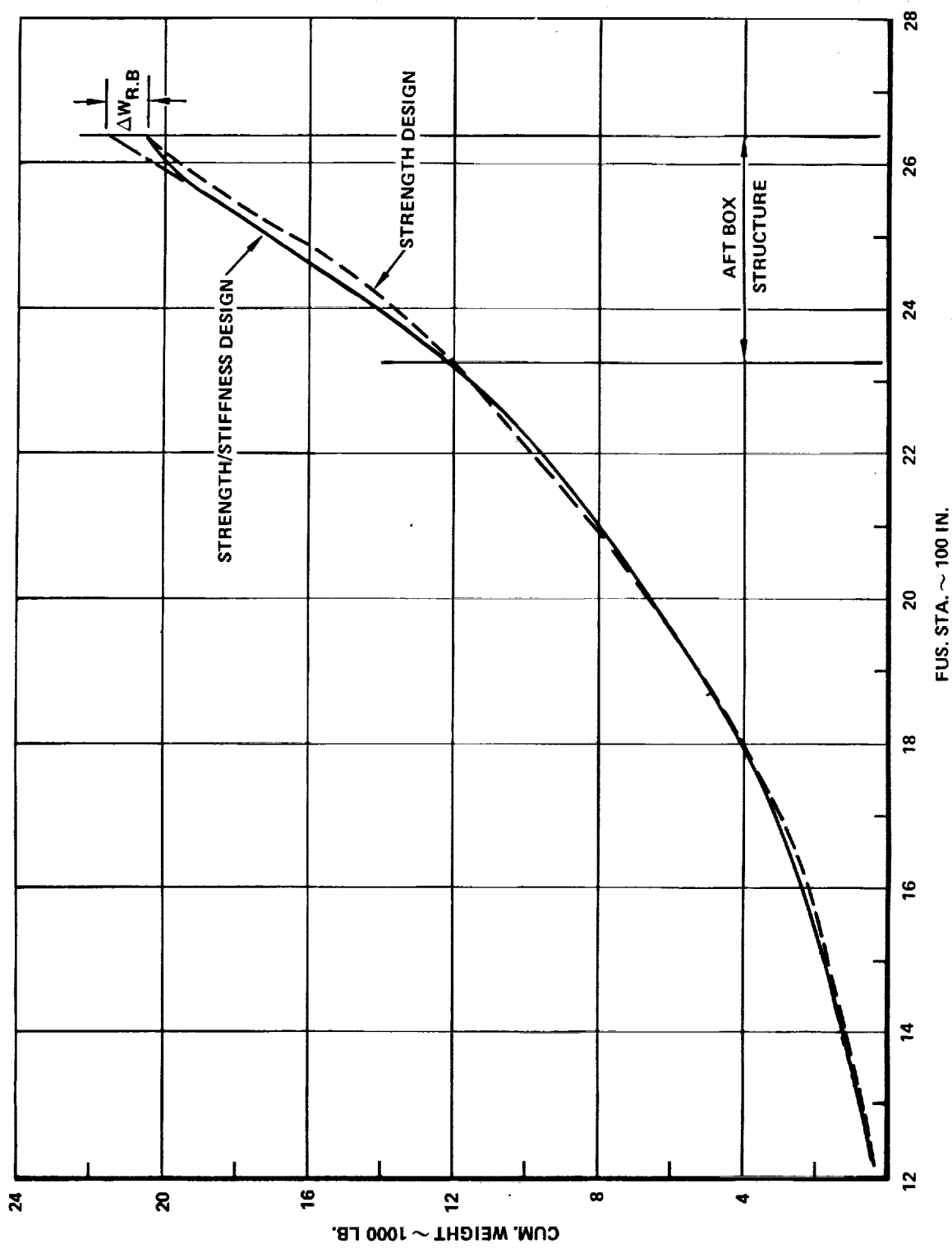


Figure 15-33. Comparison of Inboard Wing Masses - Task II

PRECEDING PAGE BLANK NOT FILMED

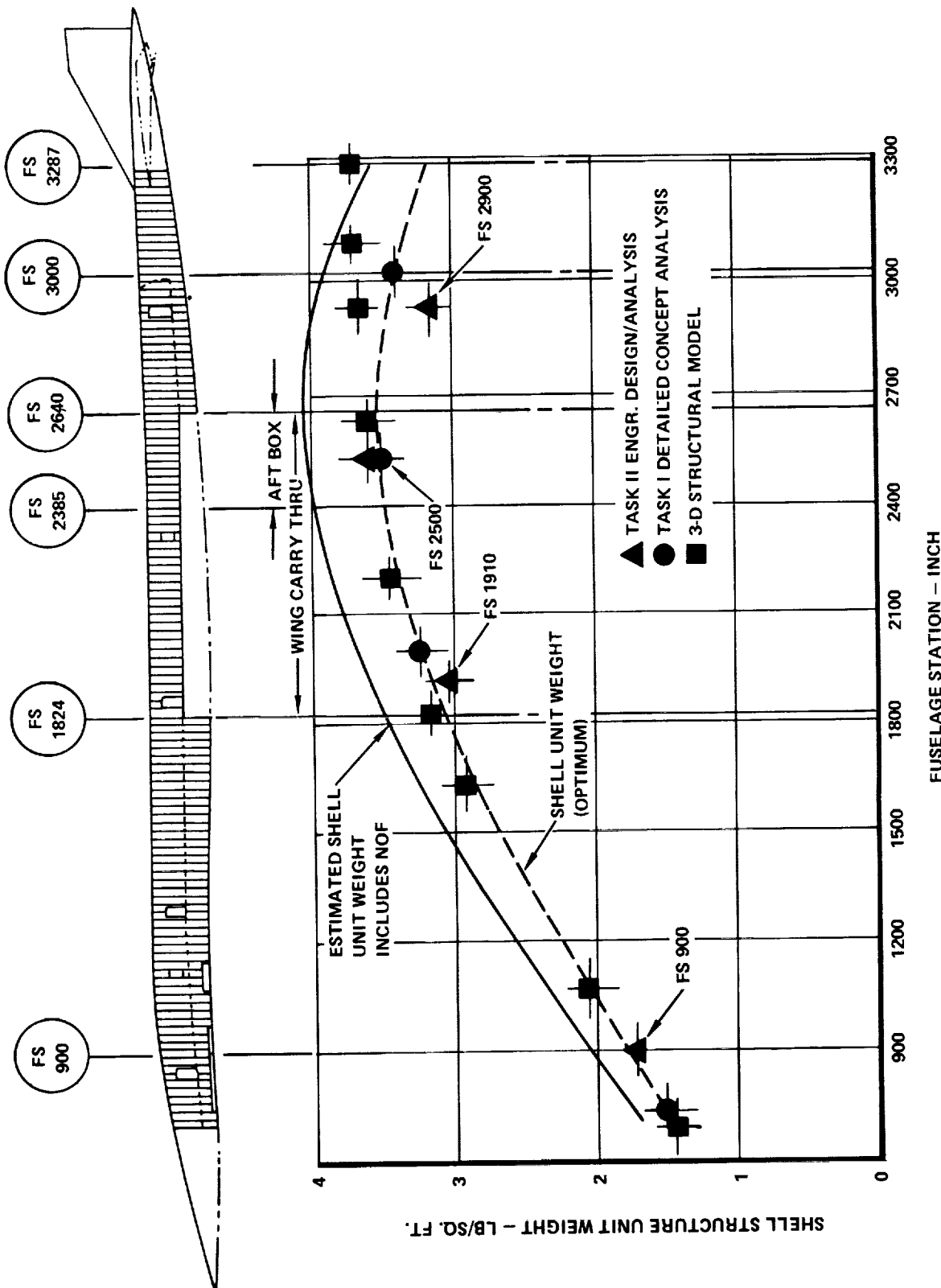


Figure 15-34. Final Design Airplane - Fuselage Shell Structure Mass

weights from the 3-D finite element structural model and (2) the unit weight calculations from detailed analysis of Task II which includes the strength and fail-safe requirements. The results of the detailed analysis (including strength and fail-safe design) are presented in Table 15-46 for F.S. 900, F.S. 1910, F.S. 2500 and F.S. 2900. The mass trends are very near the optimum shell weights calculated for Task I. In the aftbody, the results indicate values less than previously used. Rather than reduce the mass trends in the aftbody, the originally determined trends were maintained to provide adequate structural integrity for asymmetric conditions which were not fully investigated for the fuselage design.

Figure 15-35 presents the impact of composite reinforcement of the titanium hat section stringers with boron-aluminum and boron-polyimide. The results were constrained by frame and stringer spacing. Although approximately 5-percent reduction in shell structure unit weight is indicated on Figure 15-35, the effect on the total body weight is only slightly greater than 1-percent. The application of boron-polyimide shows slightly increased benefits over boron-aluminum. The Final Design airplane retains the basic skin-stringer-frame construction using titanium alloy 6Al-4V (annealed), although in the interior region (i.e., floors, floor beams, trim) epoxy resin composites are employed in selected areas.

**ORIGINAL PAGE IS  
OF POOR QUALITY**

TABLE 15-45. WING STRUCTURE FAIL-SAFE PENALTY

WING STRUCTURE	POINT DESIGN	EFFECTIVE AREA (ft <sup>2</sup> )	MASS INCREMENT	
			(lb/ft <sup>2</sup> )	(lb)
AFT BOX	41036	264.4	1.39	368
	40536	209.0	1.63	340
	$\Sigma$			(708)
TIP BOX	41316	115.8	0.81	94
	41348	214.4	0.09	20
	$\Sigma$			(114)
<b>TOTAL FAIL-SAFE PENALTY</b>				<b>(822)</b>

TABLE 15-46. FINAL DESIGN AIRPLANE - FUSELAGE UNIT WEIGHTS

POINT DESIGN REGION	(1) FUSELAGE UNIT WEIGHTS (lb/ft <sup>2</sup> )			
	PANEL	FRAME	FAIL-SAFE PENALTY	$\Sigma$ TOTAL
FS 800 - 1000	1.29	0.22	0.25	1.76
FS 1865 - 1955	2.40	0.46	0.22	3.08
FS 2485 - 2565	2.53	0.51	0.46	3.50
FS 2800 - 3000	2.56	0.20	0.10	2.86

(1) EXPRESSED AS EQUIVALENT SURFACE PANEL WEIGHT

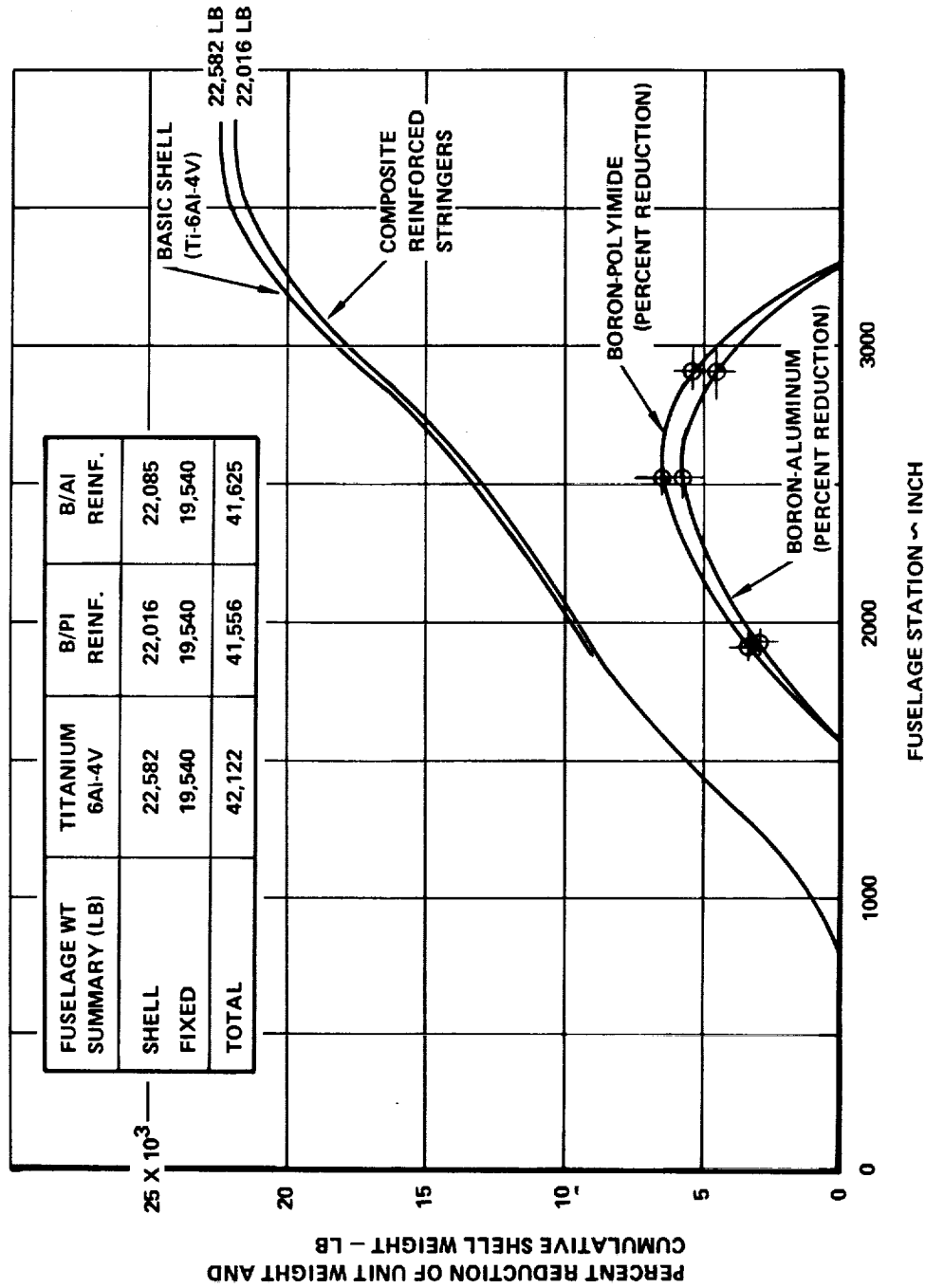


Figure 15-35. Impact of Composite Reinforcements on Fuselage Shell Structure Mass



- REFERENCES

1. Mach 2.7 Fixed Wing SST Model 969-336C (SCAT-15F) D6A11666-1 and D6A11666-2,  
The Boeing Company, July 1969

PRECEDING PAGE BLANK NOT FILMED



SECTION 16

PRODUCTION COSTS

BY

W. NEWCOMB



TABLE OF CONTENTS

<u>Section</u>	<u>Page</u>
INTRODUCTION	16-1
COST METHODOLOGY	16-1
DETAIL COSTING	16-2
COST RESULTS	16-7



LIST OF FIGURES

<u>Figures</u>		<u>Page</u>
16-1	Cost Analysis Methodology	16-3
16-2	Wing Point Design Regions	16-3
16-3	Wing Forward Area - Cost Analysis Region	16-4
16-4	Structural Details - Chordwise Stiffened Wing Design	16-4
16-5	Structural Details - Spanwise Stiffened Wing Design	16-5
16-6	Structural Details - Monocoque Wing Design	16-5
16-7	Structural Details - Monocoque (Welded) Wing Design	16-6
16-8	Structural Details - Composite Reinforced Wing Design	16-6

PRECEDING PAGE BLANK NOT FILMED



LIST OF TABLES

<u>Table</u>		<u>Page</u>
16-1	Total Manhour, Material & Tooling Costs	16-8
16-2	Production Costs - Chordwise Stiffened Wing Design	16-9
16-3	Production Costs - Spanwise Stiffened Wing Design	16-10
16-4	Production Costs - Monocoque Stiffened Wing Design	16-11
16-5	Production Costs - Monocoque (Welded) Wing Design	16-12
16-6	Production Costs - Composite Reinforced Wing Design	16-13
16-7	Summary of Production Costs	16-14

PRECEDING PAGE BLANK NOT FILMED



SECTION 16  
PRODUCTION COSTS

INTRODUCTION

The results of the analyses performed to develop production costs of the five wing structural arrangements are presented in this section.

The design concepts are identified as follows:

- (1) Chordwise stiffened wing design (Mechanically fastened)
- (2) Spanwise stiffened wing design (Mechanically fastened)
- (3) Monocoque wing design (Mechanically fastened)
- (4) Monocoque wing design (Jointed by welding)
- (5) Composite reinforced wing design (Mechanically fastened)

Each of the wing designs were analyzed in sufficient depth to establish credible production costs estimates to be used for conducting simplified cost benefit trade studies for the evaluation and selection of the best structural approach for a Mach 2.7 arrow-wing supersonic cruise aircraft. These estimates included production manhours, material costs, and fabrication and assembly tool-make time. The production costs for each wing design were translated into "value per pound" inputs to the ASSET (Advanced Synthesis and Evaluation Technique) computer program to determine fly-away and total system costs. The ASSET computer program and its usage is described in Section 17, Concept Evaluation and Selection.

COST METHODOLOGY

To achieve useable cost inputs for each of the wing designs, it proved necessary to evaluate the fabrication and assembly operation for each of the details in the surface panels and substructure of various areas of the airframe as generalized in Figure 16-1. This type of analysis was essential since each wing design, having the same planform and basically the same material usage, differed in many ways.

These differences included part count, methods used to produce the surface panels and internal structure, plus design difference resulting from constraints imposed by the location on the wing planform.

Analyses to the required detail were achieved by conducting the costing effort from the component level to the major assembly level. Areas of the wing, coincident with the point design regions used for the structural analysis, were adopted as shown in Figure 16-2. Three regions were selected for cost analysis: 40322, 40536, and 41348. The sizing data (i.e. skin thickness, cap size, etc.) in these regions were considered as representative for the wing forward area, wing aft box area and the wing tip, respectively. The major assembly costs for the three areas of the wing were then used to estimate average costs for the total wing structure.

Production wing panel sizes were determined for each of the five wing designs and the panels surrounding the "point design regions" were selected for analyses. Figure 16-3 shows details associated with forward wing area of wing design (2). Note that the panel structure is divided into six elements: upper and lower skin assemblies and two different spar and rib designs. This structural breakdown is typical in each panel, with each wing area, (forward, aft, outer), for each wing design.

#### DETAIL COSTING

Cost analyses were performed for the variety of structural details shown on Figures 16-4 through 16-8. Production costs were estimated for (1) the weld bonded beaded panel design, (2) the weld bonded hat stiffened panel design and (3) the aluminum brazed honeycomb core sandwich design, using appropriate advanced producibility techniques (see Section 7, Materials and Producibility). The variety of spar and rib configuration costs were determined for each wing design considering such factors as metal removal and welding requirements. Production manhours were developed using the joint designs shown in the figures, consistent with each design.

Fabrication data for the upper and lower skin assemblies were estimated by the man-hours and material weight per square foot of each panel. The fabrication data for the linear structure, such as caps, webs, etc., were determined by the lineal foot. All assembly data were based on type of joint design, such as number of fasteners, inches of weld, etc., and were also estimated by the lineal foot.

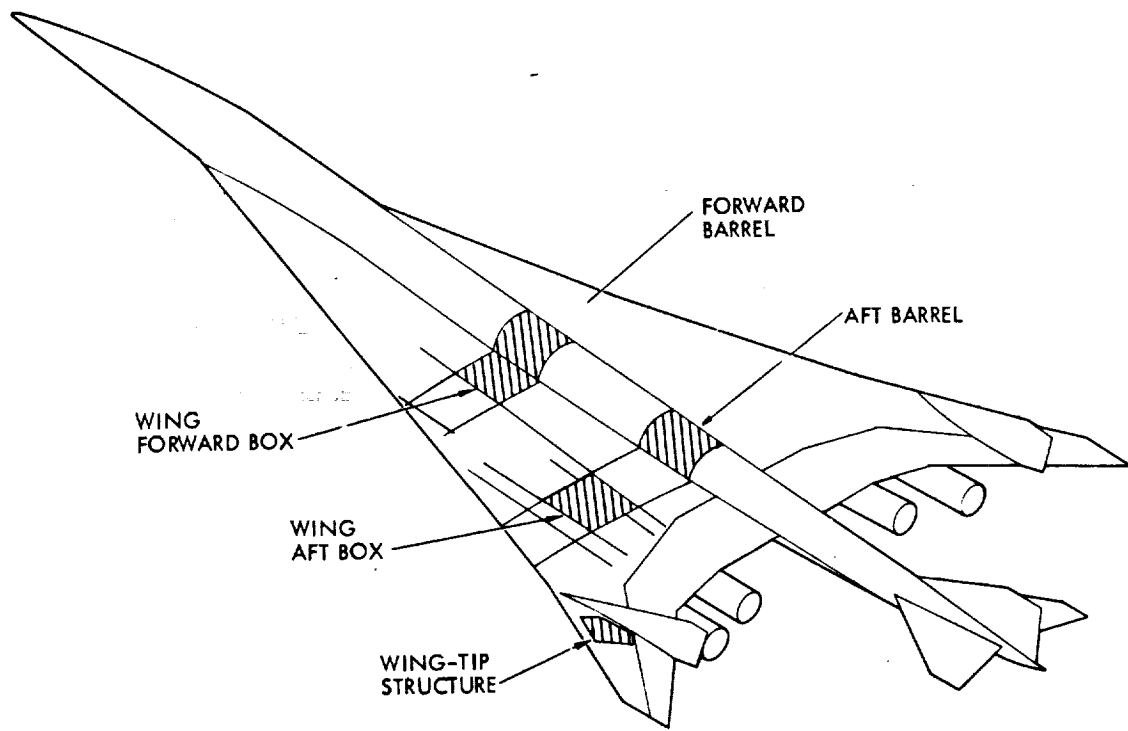


Figure 16-1. Cost Analysis Methodology

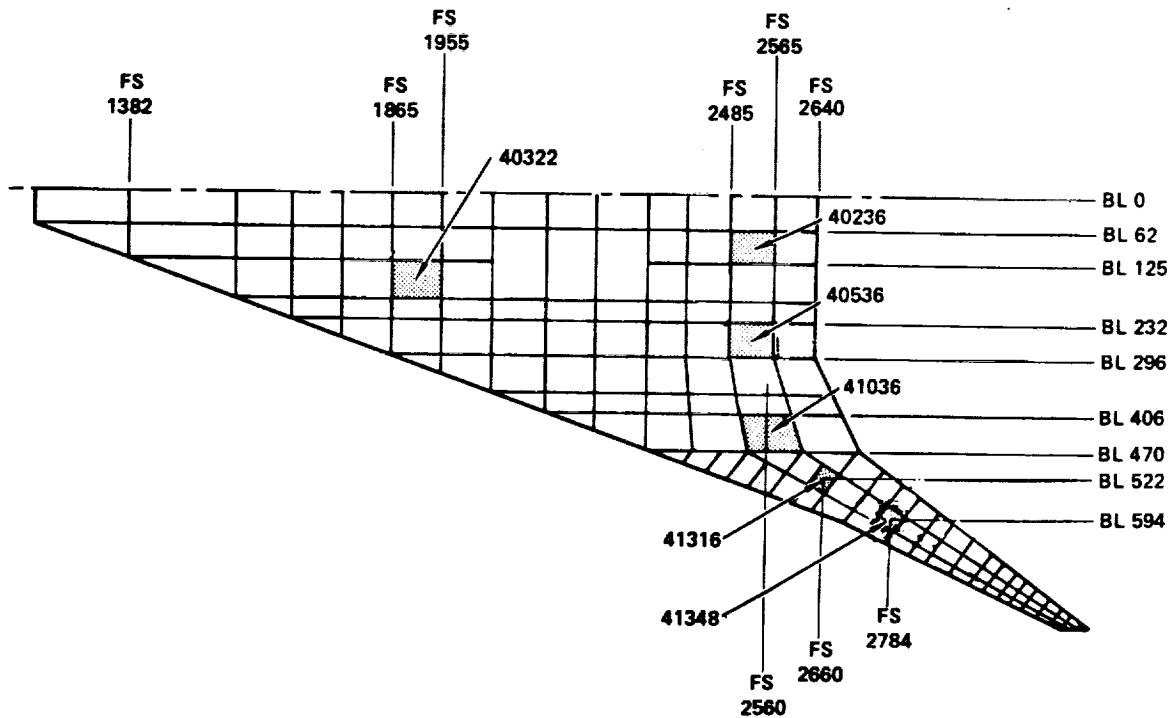


Figure 16-2. Wing Point Design Regions

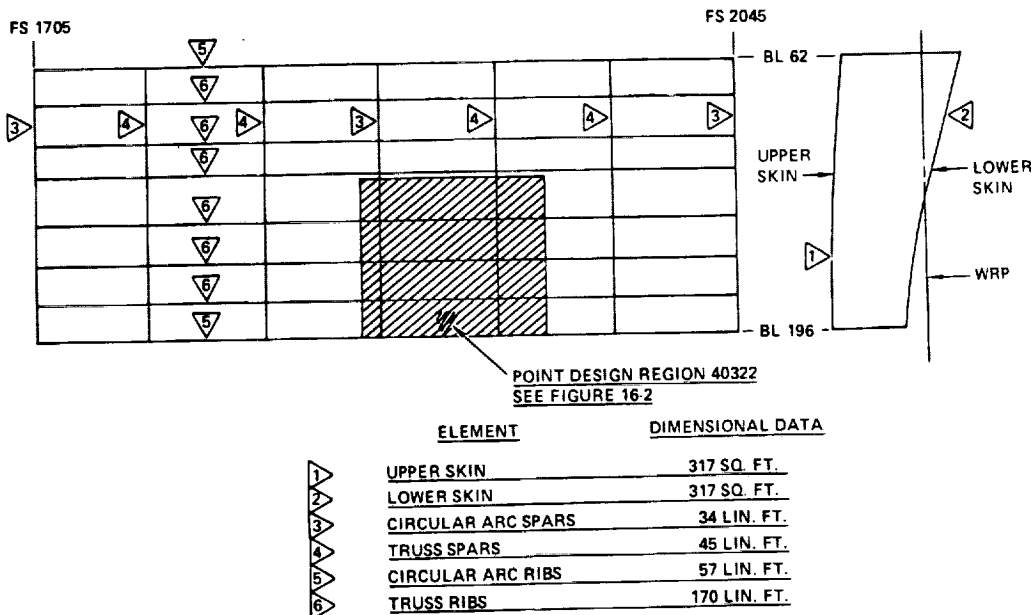


Figure 16-3. Wing Forward Area - Cost Analysis Region

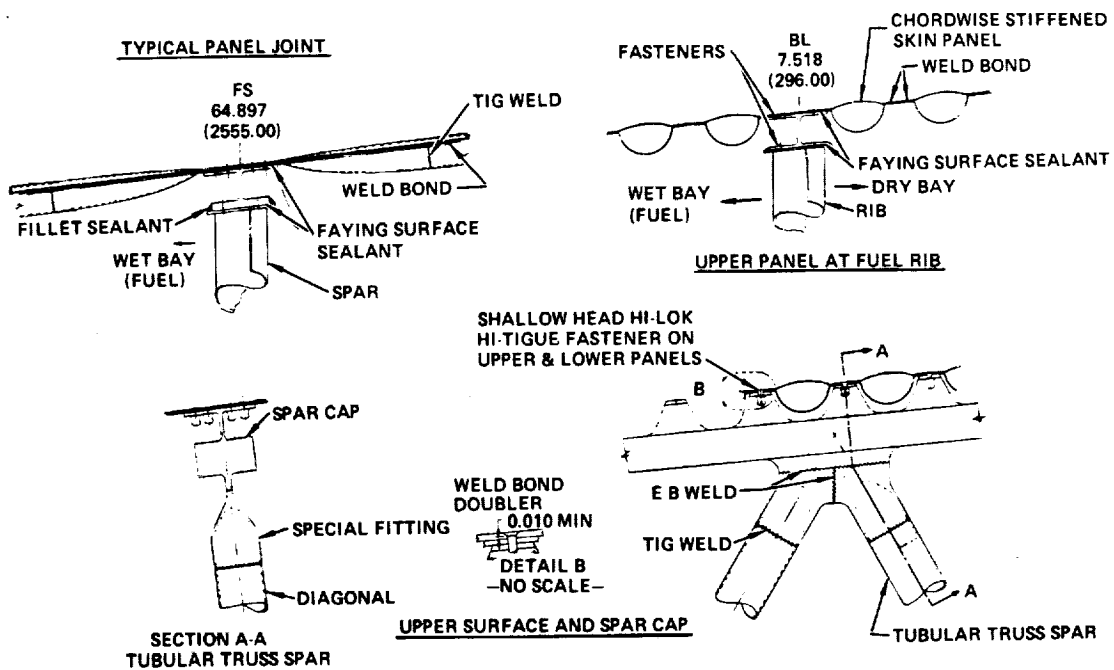


Figure 16-4. Structural Details - Chordwise Stiffened Wing Design

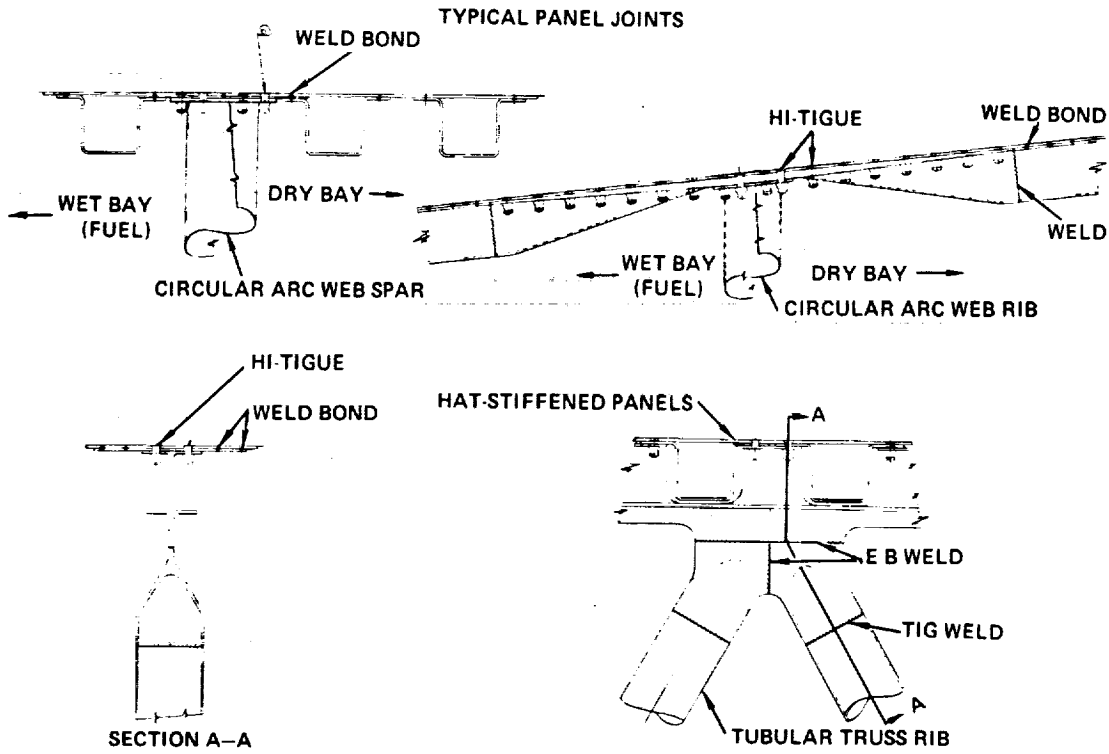


Figure 16-5. Structural Details - Spanwise Stiffened Wing Design

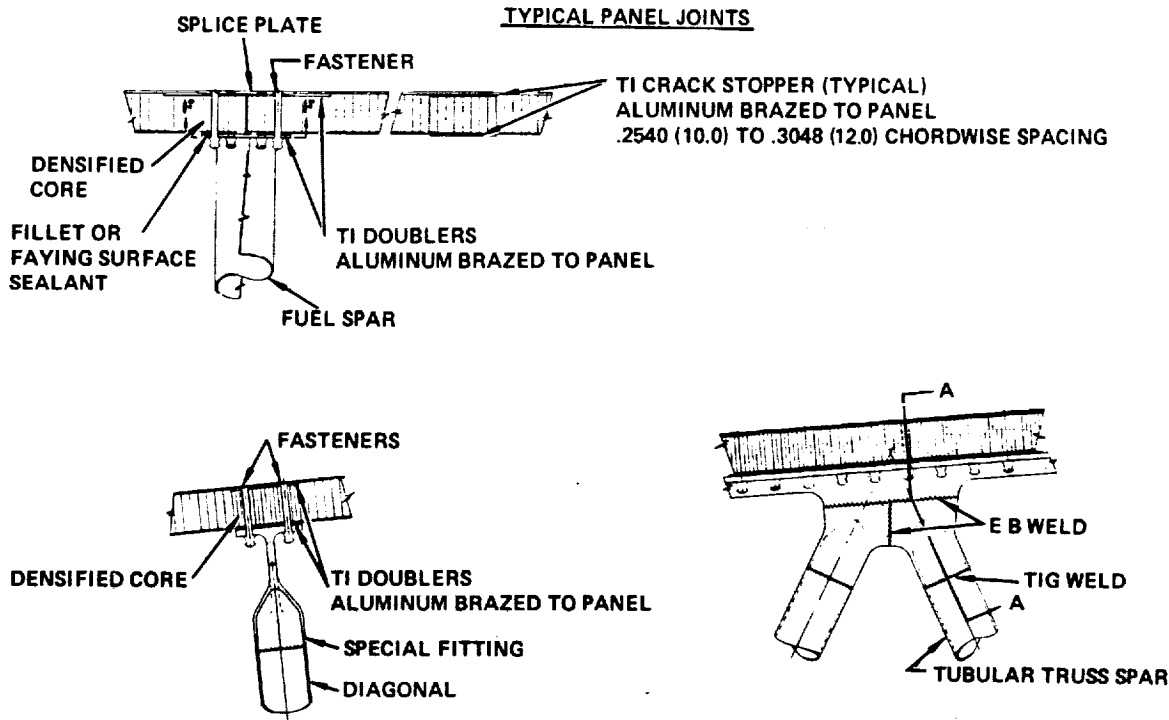


Figure 16-6. Structural Details - Monocoque Wing Design

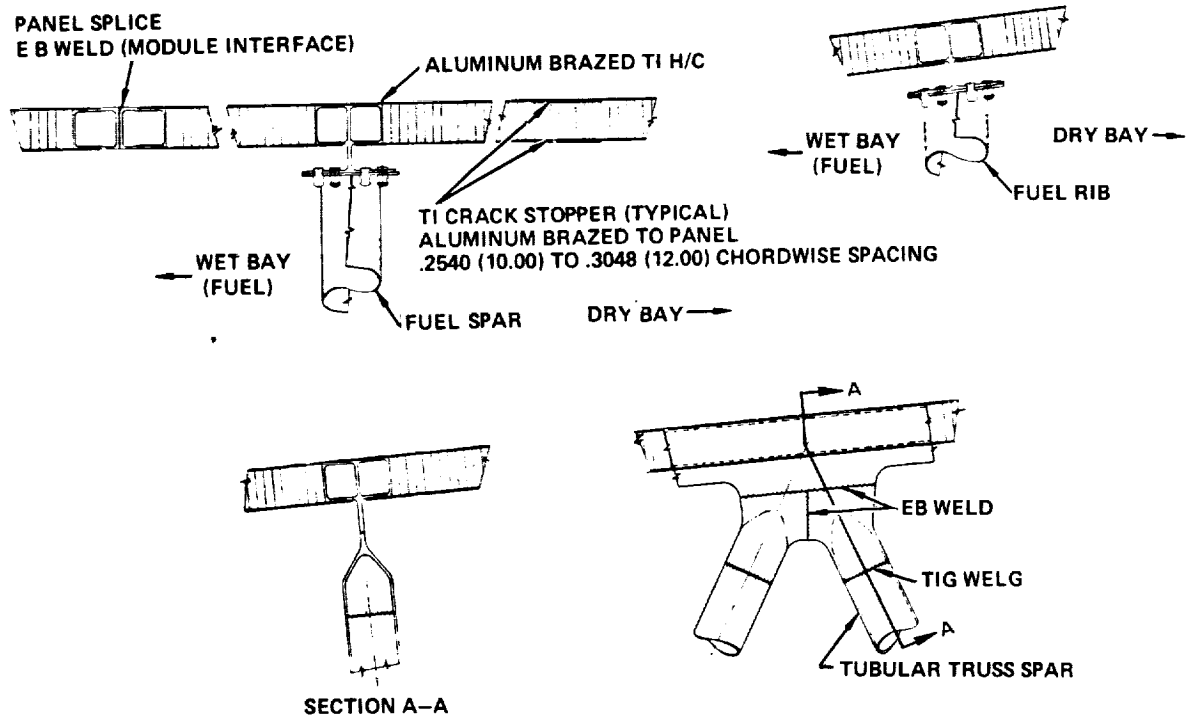


Figure 16-7. Structural Details - Monocoque (Welded) Wing Design

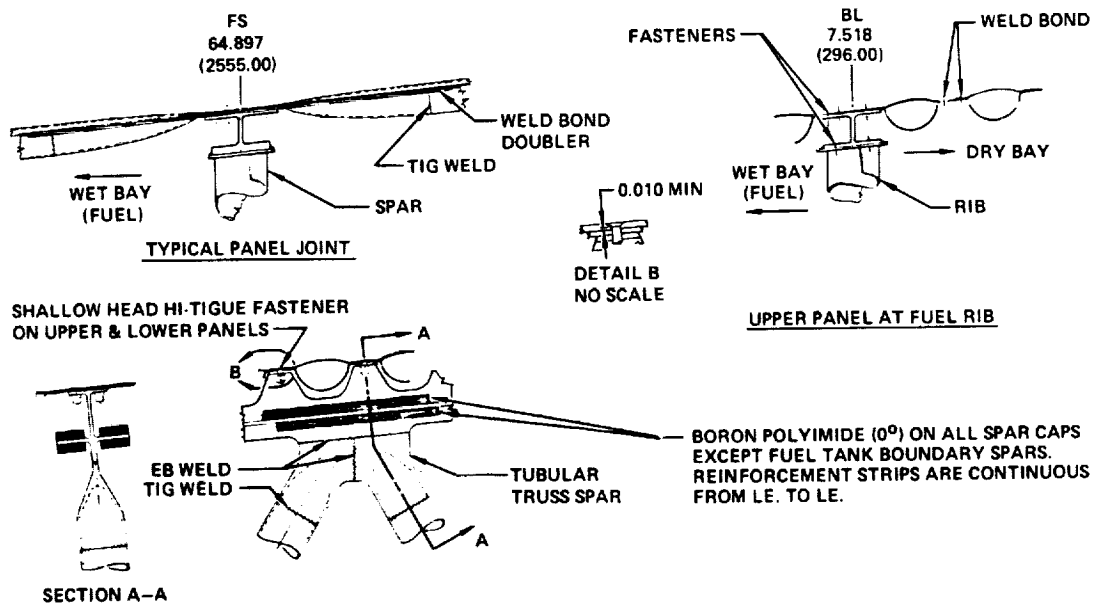


Figure 16-8. Structural Details - Composite Reinforced Wing Design

## COST RESULTS

Table 16-1 summarizes the total manhours, material costs and tool-make manhours for the forward, aft and outer wing areas to manufacture the first production aircraft. The cost for the honeycomb core surface panels are included as Material Dollars since they are considered as a purchased item.

Tables 16-2 through 16-6 presents the production costs for each wing design. The details of the forward wing area are provided for each design. The methodology used to adapt the total production manhours, tool-make manhours and material costs to "value per pound" increments for input into the ASSET computer program is also presented. The summary of production costs in terms of "value per pound" are tabulated in Table 16-7.

TABLE 16-1. TOTAL MANHOUR, MATERIAL AND TOOLING COSTS

ITEM	UNITS	DESIGN CONCEPTS				
		1	2	3	4	5
FABRICATION AND SUB ASSEMBLY MANHOURS	MANHOUR $\times 10^3$	456	394	701	717	439
JOINT ASSEMBLY AND TANK SEAL MANHOURS	MANHOUR $\times 10^3$	308	716	1623	90	354
TOTAL MANHOURS	MANHOUR $\times 10^3$	764	1140	2324	807	793
MATERIAL COST	\$ $\times 10^3$	1566	1881	3982	4033	2432
TOOL-MAKE MANHOURS	MANHOUR $\times 10^3$	8024	5127	6249	6117	8058
WEIGHT	LB $\times 10^3$	71	69	57	60	54

TABLE 16-2. PRODUCTION COSTS - CHORDWISE STIFFENED WING DESIGN

FORWARD WING AREA	OPERA. ITEM	VALUE PER FOOT	WEIGHT PER FOOT	VALUE PER LB.	TOTAL WEIGHT	TOTAL FAB. MANHRS.	TOTAL MATERIAL = DOLLARS	TOTAL TOOLING MANHRS.
UPPER SKIN	LABOR MATERIAL TOOLING	1.013	0.825	1.228	4,726	5,804	—	—
		—	0.825	25,000	4,726	—	118,150	—
		142.871	0.825	173,177	4,726	—	—	818,435
LOWER SKIN	LABOR MATERIAL TOOLING	1.242	0.942	1,319	4,726	6,234	—	—
		—	0.942	25,000	4,726	—	118,150	—
		142.871	0.942	151,668	4,726	—	—	716,783
TRUSS SPARS	LABOR MATERIAL TOOLING	45.349	2.597	17,462	7,954	138,893	—	—
		69.936	2.597	26,930	7,954	—	214,201	—
		273.801	2.597	105,430	7,954	—	—	838,590
CIRCULAR - ARC SPARS	LABOR MATERIAL TOOLING	40.760	3.886	10,489	2,114	22,174	—	—
		98.281	3.886	25,291	2,114	—	53,465	—
		400,000	3.886	102,934	2,114	—	—	217,603
TRUSS RIBS	LABOR MATERIAL TOOLING	53.220	1.368	38,904	2,570	99,983	—	—
		43.840	1.368	32,047	2,570	—	82,361	—
		182.615	1.368	133,490	2,570	—	—	343,069
$\Sigma$	FORWARD WING AREA					273,088	586,327	2,934,480
$\Sigma$	AFT AREA WING					136,768	651,933	1,494,318
$\Sigma$	OUTER WING AREA					45,825	247,470	968,517
$\Sigma$	ADDITIVES							
$\Sigma$	FABRICATION AND SUBASSEMBLY					455,681	1,485,730	5,397,315
$\Sigma$	ASSEMBLY AND TANK SEAL					308,403	80,230	2,627,000
$\Sigma$	TOTAL PER AIRCRAFT					70,589	764,084	1,565,960
$\Sigma$	VALUE PER POUND						10.824 M/H	\$ 22,184 M/H
								113,677 M/H

TABLE 16-3. PRODUCTION COSTS - SPANWISE STIFFENED WING DESIGN

FORWARD WING AREA	OPERA. ITEM	VALUE PER FOOT	WEIGHT PER FOOT	VALUE PER LB.	TOTAL WEIGHT	TOTAL FAB. MANHRS	TOTAL MATERIAL DOLLARS	TOTAL TOOLING MANHRS.
UPPER SKIN	LABOR MATERIAL TOOLING	2,822 37,850 44,480	1.514 1.514 1.514	1,864 25,000 29,379	7,921 7,921 7,921	14,765	198,025	232,711
LOWER SKIN	LABOR MATERIAL TOOLING	3,412 29,525 43,722	1.181 1.181 1.181	2,890 25,000 37,021	7,921 7,921 7,921	22,884	198,025	293,243
TRUSS SPARS	LABOR MATERIAL TOOLING	31,885 36,200 222,321	1,238 1,238 1,238	25,755 29,240 179,581	2,387 2,387 2,387	61,477	69,796	4,28,660
CIRCULAR ARC SPARS	LABOR MATERIAL TOOLING	30,569 114,870 369,643	4,974 4,974 4,974	6,146 23,090 74,315	1,526 1,526 1,526	9,379	35,235	113,405
TRUSS RIBS	LABOR MATERIAL TOOLING	34,328 45,520 89,399	1,250 1,250 1,250	27,462 36,420 71,519	4,880 4,880 4,880	134,015	177,681	349,013
CIRCULAR- ARC RIBS	LABOR MATERIAL TOOLING	7,665 86,800 56,820	2,783 2,783 2,783	2,754 31,190 20,417	729 729 729	2,008	22,738	14,884
$\Sigma$	FORWARD WING AREA					244,528	701,500	1,431,916
$\Sigma$	AFT WING AREA					73,971	631,398	443,033
$\Sigma$	OUTER WING AREA	CALCULATED AS ABOVE				27,845	315,018	335,402
$\Sigma$	ADITIVES					47,977	154,119	361,102
$\Sigma$	FABRICATION AND SUBASSEMBLY					394,321	1,802,035	2,571,453
$\Sigma$	ASSEMBLY AND TANK SEAL					716,000	78,866	2,556,000
$\Sigma$	TOTAL PER AIRCRAFT					69,412	1,110,321	1,880,901
$\Sigma$	VALUE PER POUND					15,996 M/H	\$27.097	73,869 M/H

TABLE 16-4. PRODUCTION COSTS - MONOCOQUE WING DESIGN

FORWARD WING AREA	OPERA. ITEM	VALUE PER FOOT	WEIGHT PER FOOT	VALUE PER LB.	TOTAL WEIGHT	TOTAL FAB. MANHRS.	TOTAL MATERIAL DOLLARS	TOTAL TOOLING MANHRS.
UPPER SKIN	LABOR MATERIAL TOOLING	24,248 124,803 9,414	1.764 1.764 1.764	13,746 70,750 5,337	7,255 7,255 7,255	99,735	513,291	38,720
LOWER SKIN	LABOR MATERIAL TOOLING	24,248 113,895 9,414	1.799 1.799 1.799	13,479 63,310 5,233	7,401 7,401 7,401	99,758	468,557	38,729
TRUSS SPARS	LABOR MATERIAL TOOLING	31,268 28,508 279,545	0.876 0.876 0.876	35,694 32,543 319,115	4,616 4,616 4,616	164,764	150,219	1,473,035
CIRCULAR - ARC RIBS	LABOR MATERIAL TOOLING	9,176 47,744 75,891	2,163 2,163 2,163	4,242 22,073 35,085	2,710 2,710 2,710	11,496	61,444	95,080
$\Sigma$	FORWARD WING AREA					375,753	1,193,511	1,645,564
$\Sigma$	AFT WING AREA					222,845	1,544,077	1,394,018
$\Sigma$	OUTER WING AREA	CALCULATED AS ABOVE				51,610	1,042,782	123,880
$\Sigma$	ADDITIVES					50,412	137,170	530,048
$\Sigma$	FABRICATION AND SUBASSEMBLY					700,620	3,917,540	3,693,510
$\Sigma$	ASSEMBLY AND TANK SEAL	CALCULATED AS ABOVE				1,622,959	64,661	2,600,000
$\Sigma$	TOTAL PER AIRCRAFT				56,908	2,323,579	3,982,201	6,293,510
$\Sigma$	VALUE PER POUND					40,830	69,976	110,591

TABLE 16-5. PRODUCTION COSTS - MONOCOQUE (WELDED) WING DESIGN

FORWARD WING AREA	OPERA. ITEM	VALUE PER FOOT	WEIGHT PER FOOT	VALUE PER LB	x TOTAL WEIGHT	TOTAL FAB. MANHRS.	TOTAL MATERIAL DOLLARS	TOTAL TOOLING MANHRS.
UPPER SKIN	LABOR MATERIAL TOOLING	32,330 124,803 27,426	1.764 1.764 1.764	18,327 70,750 15,548	7,255 7,255 7,255	132,962 513,291		112,801
LOWER SKIN	LABOR MATERIAL TOOLING	34,126 113,895 27,426	1.799 1.799 1.799	18,969 63,310 15,245	7,401 7,401 7,401	140,390 468,557		112,828
TRUSS SPARS	LABOR MATERIAL TOOLING	17,773 28,508 52,272	0.876 0.876 0.876	20,288 32,543 59,671	5,965 5,965 5,965	121,018 194,119		112,828
CIRCULAR - ARC RIBS	LABOR MATERIAL TOOLING	9,176 49,042 75,891	2,163 2,163 2,163	4,242 22,673 35,085	3,706 3,706 3,706	15,721 84,026	194,119 355,938	
$\Sigma$	FORWARD WING AREA					410,091	1,259,993	711,592
$\Sigma$	AFT WING AREA					171,652	1,586,825	391,810
$\Sigma$	OUTER WING AREA			CALCULATED AS ABOVE		84,715	1,048,537	583,724
$\Sigma$	ADITIVES					50,412	137,170	530,048
$\Sigma$	FABRICATION AND SUBASSEMBLY					716,870	4,032,525	2,217,174
$\Sigma$	ASSEMBLY AND TANK SEAL			CALCULATED AS ABOVE	90,336	—	3,900,000	
$\Sigma$	TOTAL PER AIRCRAFT				60,104	807,206	4,032,525	6,117,174
$\Sigma$	VALUE PER POUND					13,430 M/H	67,092 \$	101,776 M/H

TABLE 16-6. PRODUCTION COSTS - COMPOSITE REINFORCED WING DESIGN

FORWARD WING AREA	OPERA. ITEM	VALUE PER FOOT	WEIGHT PER FOOT	VALUE PER LB	TOTAL WEIGHT	TOTAL FAB. MANHRS.	MATERIAL DOLLARS	TOTAL TOOLING MANHRS.
UPPER SKIN	LABOR MATERIAL TOOLING	1,013 40,225 142,871	1,609 1,609 1,609	0.629 25,000 88,795	3,651 3,651 3,651	2,297	91,275	324,191
LOWER SKIN	LABOR MATERIAL TOOLING	1,242 33,375 142,871	1,335 1,335 1,335	0.930 25,000 107,020	3,651 3,651 3,651	3,395	91,275	390,730
TRUSS SPARS	LABOR MATERIAL TOOLING	48,967 591,900 342,251	6,380 6,380 6,380	7,675 92,770 53,644	7,883 7,883 7,883	60,502	731,306	422,876
CIRCULAR- ARC SPARS	LABOR MATERIAL TOOLING	44,378 578,290 500,000	7,574 7,574 7,574	5,859 76,350 66,015	4,485 4,485 4,485	26,278	342,430	296,077
TRUSS RIBS	LABOR MATERIAL TOOLING	53,220 163,000 182,615	3,597 3,597 3,597	14,796 45,316 50,769	2,214 2,214 2,214	32,758	100,330	112,403
CIRCULAR- ARC RIBS	LABOR MATERIAL TOOLING	36,863 74,485 249,293	2,865 2,865 2,865	12,867 25,999 87,013	1,430 1,430 1,430	18,400	37,179	124,429
$\Sigma$	FORWARD WING AREA					143,630	1,393,795	1,670,706
$\Sigma$	AFT WING AREA					248,931	546,183	2,776,071
$\Sigma$	OUTER WING AREA					46,454	430,149	1,011,601
$\Sigma$	ADITIVES							
$\Sigma$	FABRICATION AND SUBASSEMBLY					439,015	2,370,127	5,458,378
$\Sigma$	ASSEMBLY AND TANK SEAL					354,001	61,366	2,627,000
$\Sigma$	TOTAL PER AIRCRAFT					54,013	793,016	2,431,493
$\Sigma$	VALUE PER POUND					14,682 M/H	45,017 \$	149,693 M/H

ORIGINAL PAGE IS  
OF POOR QUALITY

TABLE 16-7. SUMMARY OF PRODUCTION COSTS

	DESIGN CONCEPTS			
	1	2	3	4
VALUE PER POUND				5
PRODUCTION MANHOURS/LB	10.8	16.0	40.8	13.4
				14.7
MATERIAL \$/LB	22.2	27.1	70.0	67.1
				45.0
TOOLMAKE MANHOURS/LB	114.0	73.9	109.6	101.8
				149.7

SECTION 17

CONCEPT EVALUATION AND SELECTION

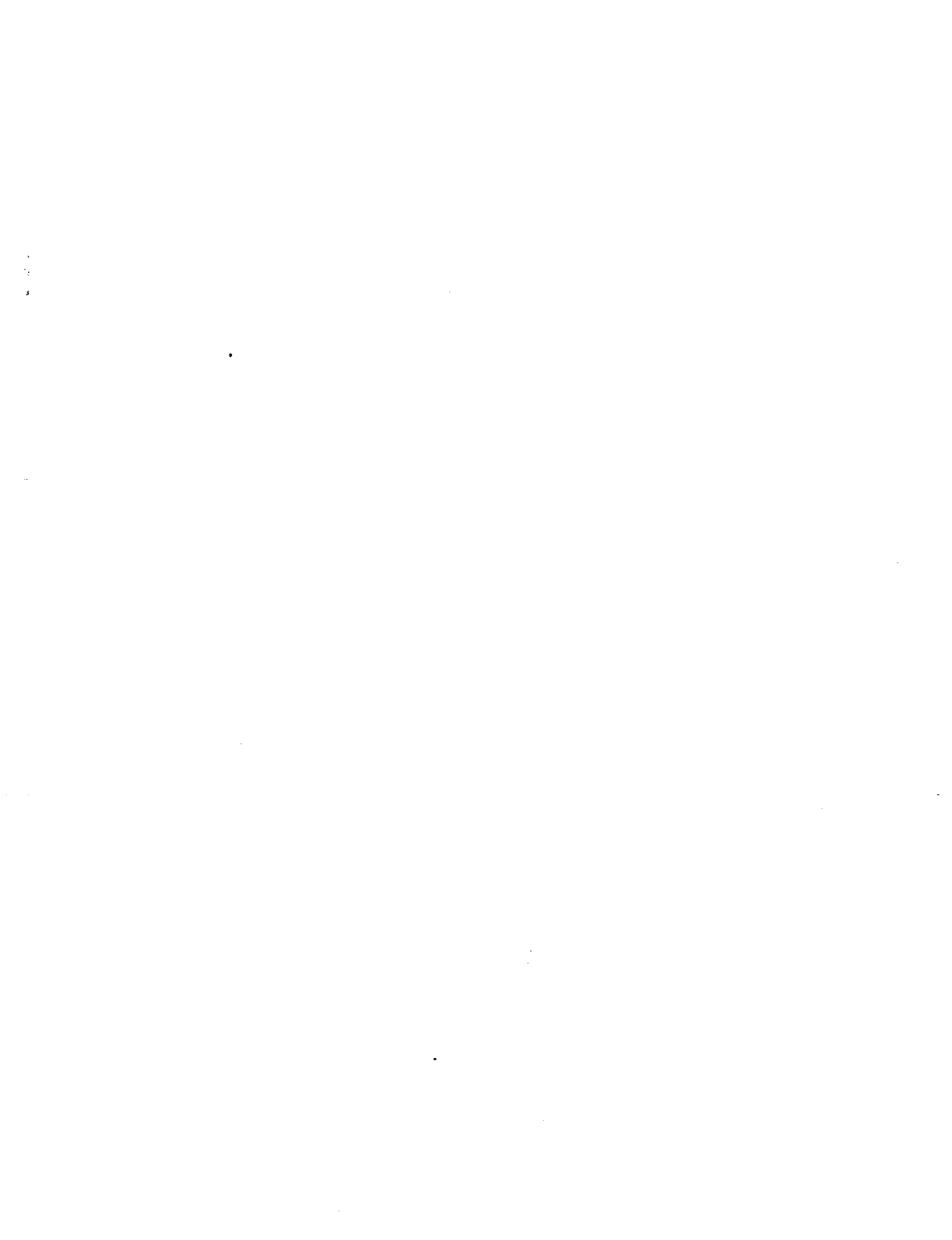
BY

I. F. SAKATA



CONTENTS

<u>Section</u>	<u>Page</u>
INTRODUCTION	17-1
EVALUATION CRITERIA	17-1
EVALUATION PROCEDURE	17-2
The ASSET Vehicle Synthesis Model	17-3
Cost Model Description	17-9
EVALUATION RESULTS	17-27
Constant Weight Aircraft	17-27
Constant Payload-Range Aircraft	17-29
CONCEPT SELECTION	17-36
REFERENCES	17-45
APPENDIX A. COMPUTER PRINTOUT ASSET PARAMETRIC ANALYSIS COMPOSITE REINFORCED WING DESIGN (WC5)	17-47



LIST OF FIGURES

<u>Figure</u>		<u>Page</u>
17-1	Concept Evaluation	17-4
17-2	The ASSET Synthesis Cycle	17-5
17-3	ASSET Program Schematic	17-5
17-4	Aircraft Flyaway Cost Model	17-15
17-5	Aircraft Sizing Results	17-30
17-6	Structural Mass Versus Cost	17-31
17-7	Technology Improvement Versus Cost	17-33
17-8	Technical Risk Versus Cost	17-34
17-9	Investment Versus Cost	17-35
17-10	Composite Reinforced Wing Design - Fasteners	17-39
17-11	Structural Approach for Task II	17-43

PRECEDING PAGE BLANK NOT FILMED



## LIST OF TABLES

<u>Table</u>		<u>Page</u>
17-1	ASSET Cost Input	17-13
17-2	Evaluation Data for Structural Arrangements	17-28
17-3	Concept Evaluation Summary - Constant Weight Aircraft	17-37
17-4	Concept Evaluation Summary - Constant Payload-Range Aircraft	17-37
17-5	Wing Weights for Structural Arrangements	17-42
17-6	Evaluation Data for Hybrid Structural Arrangement	17-44

*PRECEDING PAGE BLANK NOT FILMED*



## SECTION 17

### CONCEPTS EVALUATION AND SELECTION

#### INTRODUCTION

Analytical Design Studies (Task I) were performed to assess the relative merits of the various structural arrangements, concepts and materials applicable to the arrow-wing supersonic transport configuration defined in Section 2, Baseline Configuration Concept.

A spectrum of structural approaches for wing and fuselage applications that fully exploit the practically attainable advantages of near-term structures and materials technology were evaluated. Both smooth-skin and beaded-skin designs were explored considering advanced producibility techniques available for design of a near-term supersonic cruise aircraft.

The results of the detailed structural analysis were used to develop preliminary design drawings for mass and cost estimation. These data were then used for simplified cost benefit studies to evaluate the relative merits of each structural approach and identify those concepts which would merit further detailed engineering design and analysis (Task II).

#### EVALUATION CRITERIA

The criteria for evaluation of the structural design concepts include measures of: structural mass; mission capability; airplane size; development, production (material and fabrication), operational costs; and technology risk.

## EVALUATION PROCEDURE

The evaluation process is performed in two steps:

1. The structural mass of the aircraft is estimated for each of the candidate structural approaches based on the premise of a fixed vehicle size and taxi mass (340,000 kilograms). This permits the determination of the allowable fuel for the aircraft and hence its range capability. RDT&E, production and maintenance costs, for each of the candidate structural approaches are then determined. A direct comparison of the structural mass, range and cost is made on the basis of constant airplane configuration and gross mass. The main shortcoming of this approach is that, since all three factors of structural mass, range performance and cost are variables, one cannot establish a single criterion for the selection of the optimum concept. Thus, the purpose of this step is to establish the basis for the evaluation methodology that follows.
2. The airplane configuration and gross mass are resized to meet the payload (22,000 kg) and range (7,800 km) requirements. The purpose of the resizing is not to suggest that the airplane configuration (size) be changed, but rather to provide a tool for assessing the impact of the candidate structural concepts and materials evaluated on a common basis, i.e., constant payload/range performance. Once this is done, the concept evaluation and selection may be performed on the basis of minimum-total-system-cost (as tempered by technology availability and risk considerations).

In this context, total-system-cost includes the effects of:

- Structural efficiency/material properties
- Design considerations such as fuel tank sealing and ease of fabrication and assembly
- Varying thrust, engine size, and engine mass requirements as airplane size changes
- Impact of the structural/material concept, airplane size, and mass on fuel consumption; development, manufacturing and operating (maintenance) costs.

DOC (Direct Operating Cost) is a measure of total-system-cost that includes all the parameters noted and is chosen as the evaluation criterion in this study.

In order to assess the relative importance of the characteristics of each structural approach on the major component of DOC and provide a comparison between the cost and risk factors, the results of the aforementioned evaluation procedure are presented in the form of cost-benefit tradeoffs. Typical tradeoffs shown on Figure 17-1 are:

- Structural mass versus cost
- Technology improvement versus cost
- Technical risk versus cost
- Investment versus cost

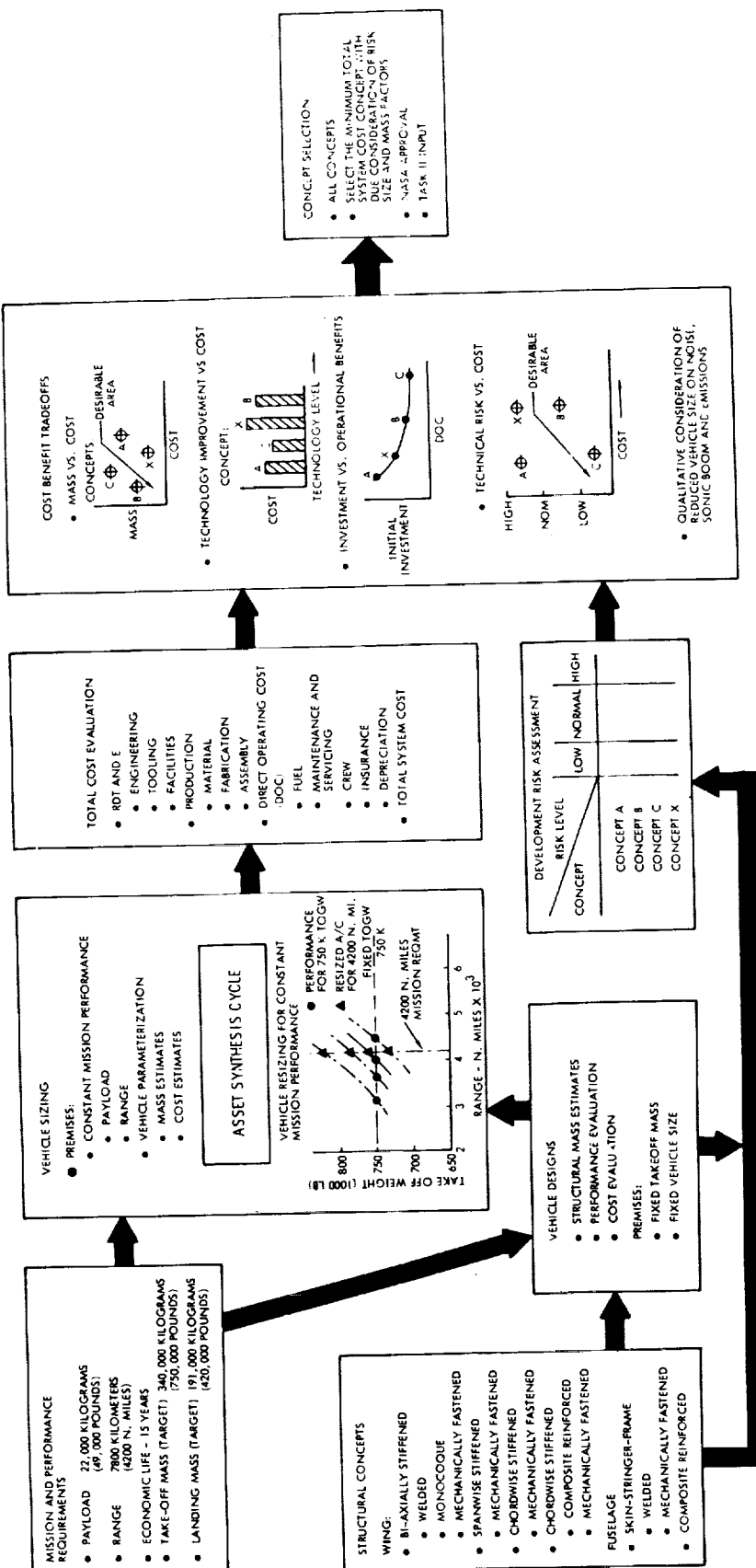
As noted above, the selection of the best concept is performed on the basis of minimum-total-system-cost to satisfy the given payload/range requirement at acceptable program technology risk levels.

#### The ASSET Vehicle Synthesis Model

The parametric sizing, and performance evaluation of the structural design concepts are performed through the use of the Lockheed developed ASSET (Advanced System Synthesis and Evaluation Technique) vehicle synthesis model. A schematic presentation of the primary input and output data involved in the ASSET Synthesis Cycle, is shown on Figure 17-2. The ASSET Program integrates input data describing vehicle geometry, aerodynamics, propulsion, structures/materials, weights, and subsystems, and determines candidate vehicles which satisfy given mission and payload requirements. It provides the means to assess the effects of design options (thrust/weight, wing loading, engine cycle, advanced materials usage, etc.) on the vehicle weight, size, and performance. The key elements and the flow of information through ASSET are depicted in Figure 17-3.

FIGURE 17-1. CONCEPT EVALUATION

ORIGINAL PAGE IS  
OF POOR QUALITY



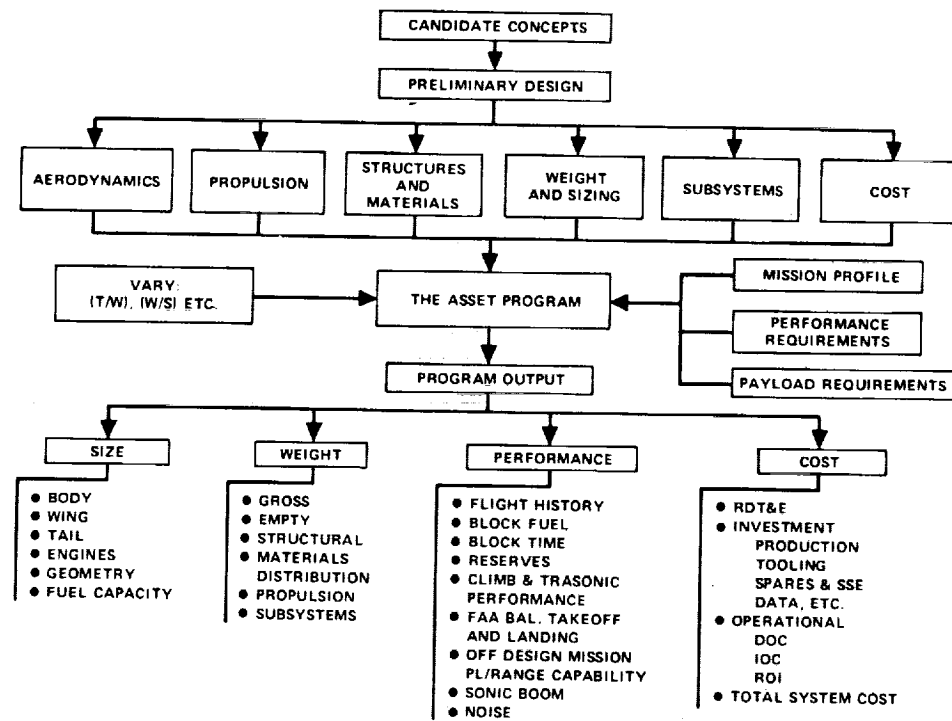


FIGURE 17-2. THE ASSET SYNTHESIS CYCLE

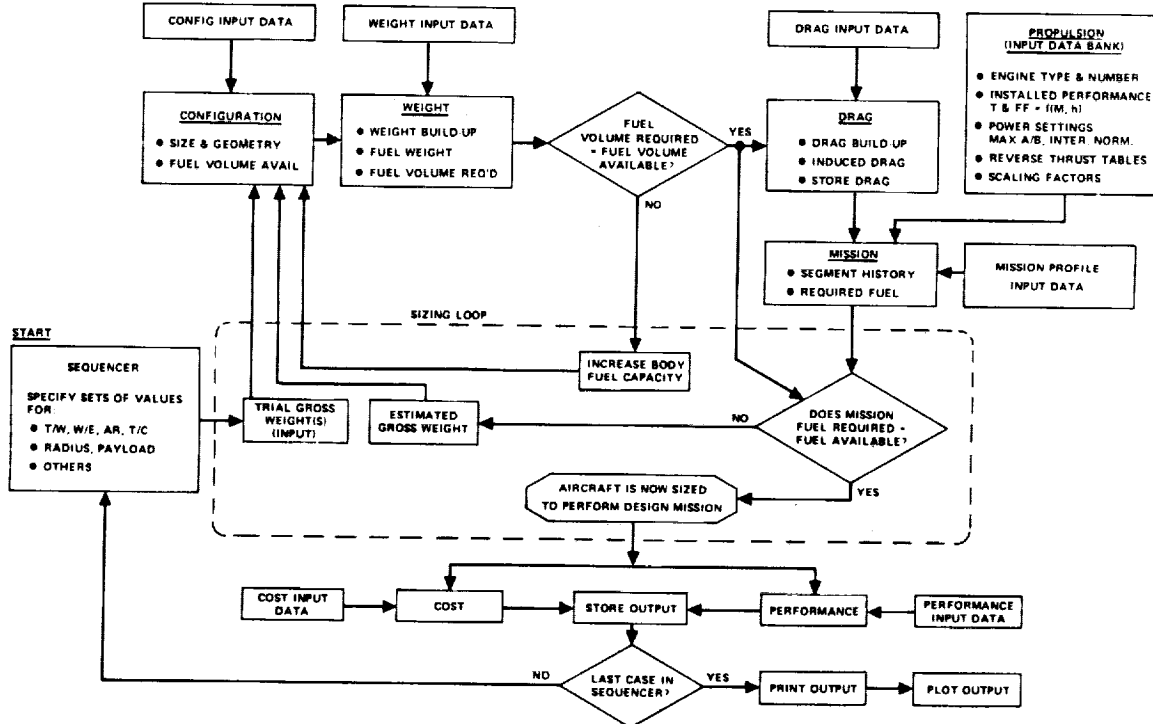


FIGURE 17-3. ASSET PROGRAM SCHEMATIC

ORIGINAL PAGE IS  
OF POOR QUALITY

The three major subprograms of ASSET are sizing, performance, and costing. The sizing subprogram sizes each parametric aircraft to a design mission. The design characteristics and component weights of the sized aircraft are then transferred to (1) the costing subprogram, which computes aircraft cost on the basis of component weights and materials, engine cycle and size, avionics packages, payload, production and operational schedules, and input cost factors, and (2) the performance subprogram which computes maximum speed, ceiling, landing and take-off distances and other performance parameters.

ASSET program output consists of a group weight statement, vehicle geometry description, mission profile summary, a summary of the vehicle's performance evaluation, and RDT&E, production and operational cost breakdowns (reference Appendix A).

Vehicle Sizing. - The sizing subprogram is composed of five routines: sequence, configuration, weight, drag, and mission. In addition, the sizing subprogram uses propulsion data input in the form of thrust and fuel flow tables and an independent atmosphere subroutine.

The sequence routine groups the sets of independent variables (design options and mission requirements) that are to be varied parametrically. Examples of these variables include (but are not limited to) thrust/weight, wing loading, aspect ratio, wing thickness ratio, wing sweep angle, design load factor, payload, equipment, avionics weights and volumes, materials usage factors, and design mission requirements (range, radius, endurance, speed, etc.).

The configuration routine computes the geometric data for the vehicle components (planform areas, wetted areas, frontal areas, lengths, diameters, chords, reference lengths, volumes, shapes, etc.) required by the weight and drag routines. The weight routine determines the component weight build-up, materials usage for the major airframe elements based on an input percentage distribution matrix and the fuel available. These data are utilized in the configuration routine. The configuration and weight routines, operating together, determine the geometric and weight characteristics for an airplane having an assumed trial takeoff gross weight. The

trial vehicle is geometrically sized to contain the crew, equipment, payload, propulsion system and fuel. The tails are sized to provide specified (input) tail volume coefficients.

The drag routine constructs a drag build-up composed of friction drag, zero-lift pressure drag, and induced drag. Friction drag is determined for each vehicle component over a range of Mach numbers and altitudes using the component wetted areas, reference lengths, and roughness and from drag factors. The zero-lift pressure drag for the wing is computed over the Mach number range by the drag subroutine using the wing geometry characteristics (sweep, thickness, aspect ratio, leading edge radius). The zero-lift pressure drags for other vehicle components are based on the component areas, determined by the configuration routine, and the input values of the component zero-lift pressure drag coefficients. Induced drag (including the effects of compressibility) of the trial aircraft, based on the wing geometry, is determined as a function of Mach number and lift coefficient by the drag routine. The computed drag build-up for the aircraft and propulsion data for the engine under study are input to the program. Applicable power setting (take-off, maximum, intermediate, maximum continuous, etc.) thrust and fuel flow data are provided as functions of Mach number and altitude. Partial power tables are used to simulate operation at thrust levels required during cruise or loiter.

The mission subroutine determines the fuel required to perform the design mission profile. The mission profile is assembled from specified flight segments, such as takeoff, climb, acceleration, cruise, loiter, etc. Simplified two dimensional point mass flight equations are used in determining the time history of the mission. Climbs follow predetermined speed-altitude schedules. Cruise and loiter segments may be performed at specified altitude and speed flight conditions, or the speed and/or the altitude can be optimized for maximum cruise range or maximum loiter endurance. Allowances are made for taxi, warmup and takeoff, landing, and fuel reserves.

An iterative convergence technique completes the sizing subprograms. The fuel available from the weight routine and the fuel required determined by the mission routine are compared. The iteration computes and passes new trial aircraft through the sizing cycle until acceptable agreement is reached between the

available and required fuel. At this point the vehicle is properly sized to perform the specified design mission.

Performance Evaluation. - Any or all of the following vehicle performance capabilities can be evaluated: Climb, maximum speed, maneuverability, airport performance, and alternate mission capability. The climb characteristics are assessed at specified vehicle weights for given thrust settings. The maximum rate of climb at sea level is determined at the takeoff weight for a zero-acceleration climb schedule. Ceiling altitudes are determined for specified rate of climb requirements for a series of aircraft weights ranging from the takeoff weight to the zero fuel weight. Service and cruise ceilings may be determined by specification of the appropriate thrust settings, and rate of climb requirements.

Speed characteristics are assessed for specified aircraft weights and thrust settings. The maximum speed at sea level, the maximum speed at the optimum altitude, and the corresponding optimum altitude are determined.

Airport performance is evaluated for standard or non-standard days. Aerodynamic data representing the maximum lift coefficient and drag polars for the aircraft in the takeoff and landing configurations are provided by input. The distance required to take off over a 50 foot obstacle is determined for defined thrust settings. Takeoff and transition speeds are specified as percentages of the stall speed. Landing distances over a 50-foot obstacle may be determined for both flared and unflared approaches. Approach and touchdown speed are specified as percentages of the stall speed. Sinking speeds at the 50-foot height and at touchdown are constrained below defined limits. Thrust reversal may be employed during the braking phase. Go-around rate of climb during the landing approach is computed for specified thrust settings. Any number of engines may be inoperative.

Alternate mission off-design performance for the synthesized aircraft is determined by the mission routine. The basic difference between the mission routine of sizing subprograms and the alternate mission performance evaluation is that the former determines the fuel required to perform the design mission, whereas the latter determines the mission capabilities (range, radius, endurance, etc.) with the

fuel available in the sized aircraft. The alternate mission profiles are assembled from specified flight segments (takeoff, climb, acceleration, cruise, loiter, etc.) in the same manner that the design (sizing) mission is constructed. However, one of the mission segments of the profile is a variable segment. Through an iterative convergence technique, the duration of the variable segment (distance, time, etc.) is adjusted so that the fuel required to perform the mission is equal to the onboard fuel. Payload and equipment weights, and fuel loads for the alternate missions are specified and may be different from those corresponding to the design mission.

Costing. - The costing program computes RDT&E, investment, and operational costs. Both the RDT&E and production (flyaway) aircraft costs are broken down by airframe, engines, avionics, and armament. Airframe costs are further broken down into engineering, tooling, manufacturing, quality control, and material costs. The various cost elements are computed on the basis of cost estimating relationships (CER) which are established by analysis of historical data of applicable aircraft programs, Lockheed's R&D and production experience, and subcontractor/supplier quotations. Cost input consists of dollars-per-hour (labor cost) and dollars-per-pound (material cost) factors by aircraft structural element and material, labor rates, production rates and schedule, learning curves, subsystem, engine and avionics cost factors, and operational (fuel, attrition, etc.) considerations. The model permits parametric costing as function of thrust, inert weight element and advanced material usage.

#### Cost Model Description

The cost models used in the evaluation of the arrow-wing configuration supersonic transport consists of subroutines to the ASSET program.

Development Cost Model. - The cost estimates for the primary elements of development cost are determined by cost estimating relationships (CER's) which are determined by statistical analysis of historical data from military programs. The basic equations used to estimate the development cost for the airframe and engine are modified versions of the CER's developed by the RAND Corporation (references 1

ORIGINAL PAGE IS  
OF POOR QUALITY

and 2). The RAND equations are modified to reflect airframe and engine manufacturer's experience. The airframe engineering hour estimates by the RAND CER's are modified to reflect a Lockheed in-house estimate. The Lockheed estimate is provided by a methodology that has been developed through a detailed analysis of Lockheed programs. The modifications to the RAND equations are provided by the application of K factors to the basic equations.

The development cost model includes the following elements:

Prototype Aircraft	Development Tooling
Design Engineering	Special Support Equipment
Development Test Articles	Development Spares
Flight Test	Technical Data
Engine Development	Avionics Development

The equations for determining the cost for each of the above elements are shown in the Development Cost Model that follows.

The cost for the prototype aircraft is determined from the flyaway cost model and input to the development model. The prototype aircraft are costed on the basis of the first few vehicles produced.

#### Development Cost Model

##### Prototype Aircraft

$$TPROT = TFLCO * XNYO$$

##### Design Engineering

$$RFDE = 0.0396 * WAMPR ** 0.791 * SS ** 1.526 * CXNYO ** 0.183$$

$$DIH = RFDE * XKE - SELHO = (\text{Design Engineering hours less sustaining})$$

$$DIEC = DIH (DER + OER) * (1 + APRFF) = (\text{design engineering cost})$$

### Tooling

DTHB = 4.0127 \* WAMPR \*\* 0.764 \* SS \*\* 0.899 \* CXNYO \*\* 0.178 \* DRT \* 0.066

IHT = DTHB \* XKT - PTLHO = (Design tooling hours less sustaining)

DTC = DTH (DTR + OTR) \* (1 + APRFF) = (Design tooling cost)

### Development Test Articles

DSTA = (TAFCO/CXNYO) \* XNSTA = (Cost for static test article)

DFTA = (TAFCO/CXNYO) \* XNFTA = (Cost for fatigue test article)

DMTS = (TAFCO/CXNYO) \* XMTSF = (Cost for systems test articles)

DART = (DSTA + DFTA + DMTS) \* (1 + APRFF)

### Flight Test

RFFT = 0.001244 \* WAMPR \*\* 1.16 \* SS \*\* 1.371 \* CXNYO \*\* 1.281

DFT = RFFT (1 + APRFF) \* XKFT = (Flight test cost including profit)

### Engine Development

CEDCM = XMMAX \*\* 0.62 [(CXNY10 + CXNYO) \* XNENG] \*\* 0.10

DCENG = CEDCF \* [(TCE/1000)/XNENG] \*\* CEDCE \* CEDCM

### Avionics

DAV = DPAVD \* WAVUN + FAVDC

### Spares

DSPAR = ADSF \* TAFCO + EDSF \* TENCO + AVDSF \* TAVCO

### Special Support Equipment

DSSE = DSSEF \* TFLCO

### Technical Data

```
DDATA = DTDF (TFLCO + DIEC + DTC + DART + DFT + DCENG + DLENG + DAV + DSPAR  
+ DSSE + DOT + DMT)
```

The description of the inputs and the factors for the development model are included along with the description of the inputs for the production model that follows.

Investment Cost Model. - The Investment Cost Models includes subroutines to provide the cost for the aircraft, the aircraft spares, and the special support equipment. The primary element of investment is the aircraft and it is given the most attention in terms of detail and consideration of the labor and material cost factors. The spares and special support equipment cost are treated as percentages of the fly-away cost of the aircraft. The production cost estimate is made to the same general level of detail as the airplane group weight statement. The production cost input format includes the following elements:

Material Cost Factors	Engineering Change Orders
Labor Cost Factors	Quality Assurance.
Labor Rates	Miscellaneous Costs
Sizing and Learning Curve Factors	Warranty
Sustaining Engineering	Insurance and Taxes
Sustaining Tooling	Profit

An illustrative example of the elements of the airframe and their representative cost factors is shown in Table 17-1. How these factors are applied is illustrated in the schematic of the flyaway cost model shown in Figure 17-4.

Airframe Material Cost - As shown by Table 17-1, the material cost factors include representative cost factors for various types of material for the structural elements of the airframe. The airframe production cost model has space for material cost factor inputs for aluminum, titanium, steel, composites, and other. The various types of materials are listed across the top of the input sheet (Table 17-1). A material cost factor is assigned to each type

**TABLE 17-1**  
**ASSET COST INPUT**  
**COMPOSITE REINFORCED WING DESIGN**

Flags and Misc Inputs	CEPENT 0 XMAX 2.7 XENC1 0	FAST 1.0 XMIN 0.25 TMATE 0	XAVG 1.0 XMIN 0.25 XMAX 0.75	PMR 1.73 XMIN 3.0 XMAX 3.0	SWF 36 XMIN 36 XMAX 36	SWH 4 XMIN 40 XMAX 40	SWL 36 XMIN 36 XMAX 36
Production Schedule (300 A/C)	XNY1 15 XNYT 36	XNYC 18 XNYQ 36	XNY3 24 XNY6 36	XNY5 30 XNYD 36	XNY5 36 XNYD 36	XNY5 36 XNYD 36	XNY5 36 XNYD 36
Material Type	AL	T1	Steel	Composite	Other		
Material Cost Factors ~ \$/lb	DPEAL 12.72 DPFAAL 12.72 DPFAL 12.72 DPFLAL 12.72 DPNAL 12.72 DPVAL 12.72 DPFAL 12.72	DPEATI 49.82 DPFATI 36.40 DPFTI 25.55 DPFTI 107.73 DPNTI 21.35 DPNTI 60.62 DPNTI 1.33, 30	DPEAST 15.90 DPFEST 15.90 DPFEST 15.90 DPFEST 16.41 DPNEST 20.88 DPNEST 46.45 DPNEST 1.33, 30	DPEACG 114.48 DPFACG 114.48 DPFACG 114.48 DPFACG 114.48 DPNACG 114.48 DPNACG 114.48 DPNACG 114.48	DPAET 12.72 DPFAT 12.72 DPFAT 12.72 DPFAT 12.72 DPNEAT 12.72 DPNEAT 12.72 DPNEAT 12.72	DPAET 12.72 DPFAT 12.72 DPFAT 12.72 DPFAT 12.72 DPNEAT 12.72 DPNEAT 12.72 DPNEAT 12.72	DPAET 12.72 DPFAT 12.72 DPFAT 12.72 DPFAT 12.72 DPNEAT 12.72 DPNEAT 12.72 DPNEAT 12.72
Labor Cost Factors ~ hr/1b	HPEAL 4.80 HPEAL 4.80 HPEAL 6.00 HPEAL 6.00 HPEAL 4.30 HPEAL 4.30 HPEAL 5.40 HPEAL 5.40 HSEAL 4.80	HPEATI 7.981 HPEATI 35.20 HPEATI 9.00 HPEATI 0.12 HPEATI 10.40 HPEATI 11.70 HPEATI 11.50	HPEAST 7.20 HPEAST 7.50 HPEAST 7.20 HPEAST 0.12 HPEAST 8.00 HPEAST 9.00 HPEAST 7.50	HPEACG 7.50 HPEACG 10.60 HPEACG 9.00 HPEACG 0.12 HPEACG 10.00 HPEACG 11.50 HPEACG 11.50	HPEAT 4.80 HPEAT 4.80 HPEAT 6.00 HPEAT 0.12 HPEAT 4.80 HPEAT 4.80 HPEAT 5.40 HPEAT 4.80	HPEAT 4.80 HPEAT 4.80 HPEAT 6.00 HPEAT 0.12 HPEAT 4.80 HPEAT 4.80 HPEAT 5.40 HPEAT 4.80	HPEAT 4.80 HPEAT 4.80 HPEAT 6.00 HPEAT 0.12 HPEAT 4.80 HPEAT 4.80 HPEAT 5.40 HPEAT 4.80
Non-Structural Element Cost Factors	DPEC 175.00 DPER 0 DPEI 51.60 DPAI 171.08 DPIY 161.63 DPEL 95.43 DPESS 15.90 DPEI 10.46 DPAI 0 DPAI 14.54 DPAI 0 DPAV 13.88 DPSI 0.50 DPSI 0 DPSI 126.61	PEFCMC 102.00 PEFCMC 0 PEFCMC 51.60 PEFCMC 171.08 PEFCMC 161.63 PEFCMC 95.43 PEFCMC 15.90 PEFCMC 10.46 PEFCMC 0 PEFCMC 14.54 PEFCMC 0 PEFCMC 13.88 PEFCMC 0.50 PEFCMC 0 PEFCMC 126.61	PEFCMC 102.00 PEFCMC 0 PEFCMC 51.60 PEFCMC 171.08 PEFCMC 161.63 PEFCMC 95.43 PEFCMC 15.90 PEFCMC 10.46 PEFCMC 0 PEFCMC 14.54 PEFCMC 0 PEFCMC 13.88 PEFCMC 0.50 PEFCMC 0 PEFCMC 126.61	PEFCMC 102.00 PEFCMC 0 PEFCMC 51.60 PEFCMC 171.08 PEFCMC 161.63 PEFCMC 95.43 PEFCMC 15.90 PEFCMC 10.46 PEFCMC 0 PEFCMC 14.54 PEFCMC 0 PEFCMC 13.88 PEFCMC 0.50 PEFCMC 0 PEFCMC 126.61	PEFCMC 102.00 PEFCMC 0 PEFCMC 51.60 PEFCMC 171.08 PEFCMC 161.63 PEFCMC 95.43 PEFCMC 15.90 PEFCMC 10.46 PEFCMC 0 PEFCMC 14.54 PEFCMC 0 PEFCMC 13.88 PEFCMC 0.50 PEFCMC 0 PEFCMC 126.61	PEFCMC 102.00 PEFCMC 0 PEFCMC 51.60 PEFCMC 171.08 PEFCMC 161.63 PEFCMC 95.43 PEFCMC 15.90 PEFCMC 10.46 PEFCMC 0 PEFCMC 14.54 PEFCMC 0 PEFCMC 13.88 PEFCMC 0.50 PEFCMC 0 PEFCMC 126.61	PEFCMC 102.00 PEFCMC 0 PEFCMC 51.60 PEFCMC 171.08 PEFCMC 161.63 PEFCMC 95.43 PEFCMC 15.90 PEFCMC 10.46 PEFCMC 0 PEFCMC 14.54 PEFCMC 0 PEFCMC 13.88 PEFCMC 0.50 PEFCMC 0 PEFCMC 126.61
Manufacturing Support Factors	UAPD 0.20 QAP 0.20	EPPO 0 ECP 0	-PMRO 0.15 TEMP 0.12	SEPO 0.15 SEP 0.12	RMRD 0.35 RMR 0.35	MUSCO 0.04 MUSC 0.04	
Eng & Avionics Prod Cost Factors	CEPFF 548,666	CERCE 0.60	*LEPCF 0	XLEPCF 1.0	DAVTP 0	FIVRC 500,000	
Tax Insurance, Warranty, and Profit Cost Factors	XTAIF 0.10 ATAPP 0.15	ETAPP 0 AVPF 0	XATAIF 0 XAVPF 0	XASAF 0.05	EMAF 0	ATMAP 0	
Sizing and Learning Curve Factors	WEMTM 227,064 WEMBL 227,064 XMB 100 XMB 100 XNEB 1.0 XNEB 1.0 XNAB 1.0	ZMCS 0.99 XUCG 0.96 XULCG 0.95 XULCS 0.90 XLEUCS 0.90 XLEUCS 0.90 XALCS 1.00					

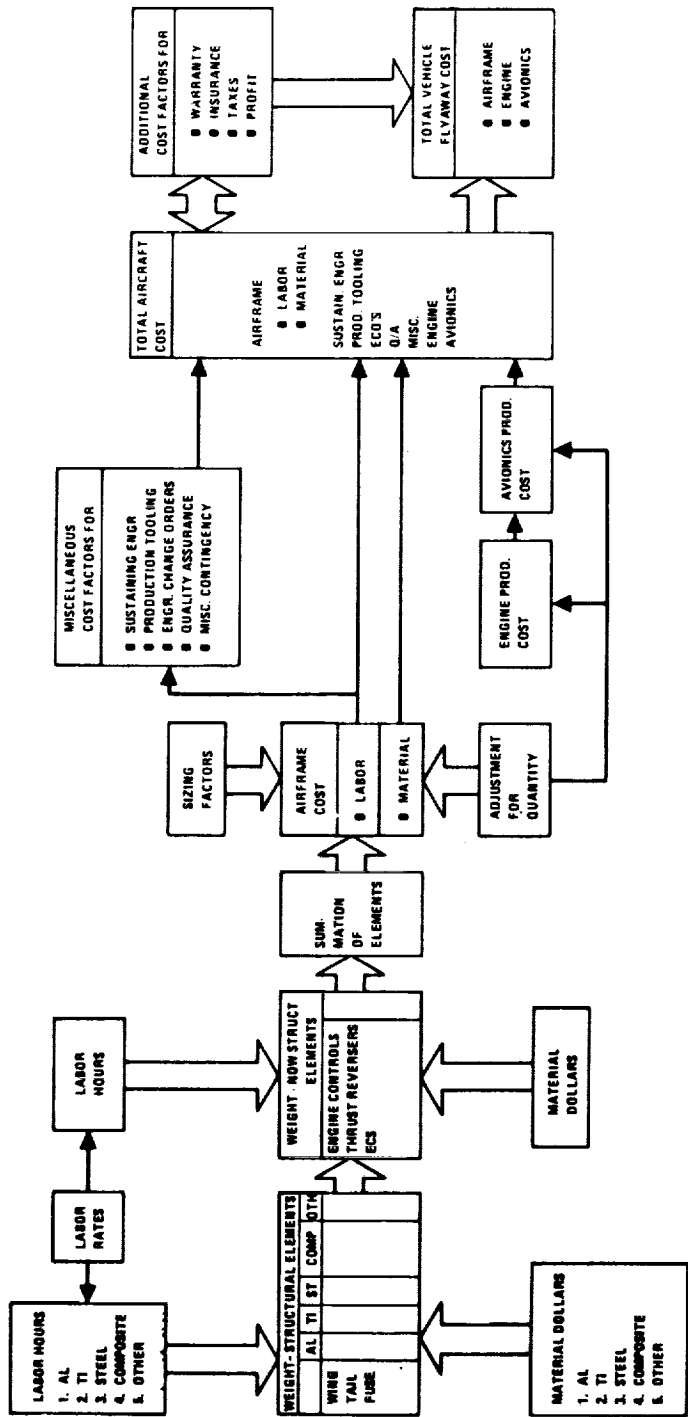
ORIGINAL PAGE IS  
OF POOR QUALITY

TABLE 17-1  
ASSET COST INPUT (Continued)

Material Type	AL	TI	Steel	Composite	Other
Labor Rates	DER 8.17	UTR 6.09	XNAR 5.10	XNAR 6.29	MISC 5.12
	QSR 9.20	DTR 12.36	QMR 10.77	QAR 10.77	MISC 10.77
	DEGR 0	DTR 0	XMR 0	QAGR 0	MISC 0
	QGCR 0	QGCR 0	XGCR 0	QGCR 0	MISC 0
Rate Cost Factors	XKE 0.72	XKT 0.86	XKPT 0.34	XTSNR 0	FAVDC 0
	XNSIA 1.0	XNFTA 1.0	XMSF 0.30	DEAVD 0	FAVDC 0
	CEDCF 71.346	CEDFC 0.55	XLEDFC 0	AVIDP 0	FAVDC 0
	DRT 1.0	ADSF 0.15	XDFC 0.50	AVDSP 0.30	FAVDC 0
Investment Cost Factors	TSEEF 0.06	TDIF 0.005	WT 0	WT 0	WT 0
	PRT 3.0	PCF 0	PTCF 1.0	PTCF 0.15	AVSF 0.30
	PSSEF 0.041	PTDF 0.005	PTC 0	PTC 0	SCFL 1.05
Operational (Military) Cost Factors					
Direct Operating Cost (DOC) Factors	XNRITE 13.0	YEAR 1973	XNPASS 3.0	XNATT 3.0	XLF 0.55
	SSPB 15.0	TFB 20.0	XNPASS 0.7	XNATT 0.95	WbF 0.5
	U 3600	IRA 0.0777	NTLTK 14.0	NTLTK 0.02	WbF 1.90
			CPT 0.02		
Indirect Operating Cost (IOC) Factors	REVPS 1.8E+06	AWCARC 7000	XKCB 58.0	XKAT 77.0	XKPB 0.58
	XKSR .0000	XKOE 2.87	XKOP .0001	XKOC .0005	XKPA 0.004
Return on Investment (ROI) Factor	XKPH .0000	XKPH 9.0	XKACC 0	TAVR 0.48	CARGF 0.30
	CPARE .0406				TCF 0.30

ORIGINAL PAGE IS  
OF POOR QUALITY

FIGURE 17-4. AIRCRAFT FLYAWAY COST MODEL



ORIGINAL PAGE IS  
OF POOR QUALITY

type of material as determined from the sizing program. The ASSET program determines the total weight of each element from the performance and configuration input data. After the total weight of the component is determined, the amount of each type of material is obtained by applying percentage factors to the total. The percentage factors for each type of material are established through previous analysis and input to the program.

Airframe Labor Cost - The same procedure as used in the materials is used in the labor subroutine, except that the labor is in hours. After the total number of hours are determined the labor rate is applied to arrive at the total labor cost.

The labor rates shown in Table 17-1 include the rates for design engineering, tooling, manufacturing, quality assurance, and miscellaneous. Only the labor rates for manufacturing and quality assurance are used for development engineering and tooling.

Non-Structural Elements Cost Factors - The cost factors for these elements includes both labor and material. This category includes the installation cost for the systems and equipment noted as well as their manufacturing cost with the exception of the engine and avionics. The installation costs for the engine and avionics are included here but the purchase costs for these items are shown separately.

After the labor hours, labor rates and material cost factors are applied to each material type, the elements are summed to arrive at a total airframe labor and material cost. These sums are then adjusted for quantity and size.

Sizing and Learning Curve Factors. - The sizing factors are included to account for scaling of the labor and material cost due to aircraft size. The learning curve factor accounts for cost change due to quantity produced. The labor and material cost factors shown in Table 17-1 are normalized to a particular vehicle weight and production quantity. The scaling factors modify the labor and material cost according to the size of the vehicle being analyzed and the number of aircraft in the production program. The sizing and learning curve factors include:

Material Sizing Factor	Labor Learning Curve
Labor Sizing Factor	Engine Learning Curve
Material Learning Curve	Avionics Learning Curve

As noted by Figure 17-4 the adjustment factors for quantity are applied to the engine and avionics as well as the labor and material.

Miscellaneous Factors - There are cost items which must be included in the production cost of the aircraft that are not part of the labor and material costs directly associated with the manufacturing of the vehicle. These are such items as quality assurance engineering changes, tool maintenance, sustaining engineering, warranty, taxes, insurance and miscellaneous costs. The costs for these items are added to the cost for the structural and non-structural elements to arrive at a total airframe cost. These factors are applied against the total airframe labor cost to arrive at the cost of each item. Costs are summed to obtain a total airframe cost.

Engine Cost - The engine cost estimate is provided by a production cost equation, or supplied by engine manufacturers, and input to the model. The equation is taken from the latest RAND revision (Reference 2) of their analysis of turbojet and turbofan production cost. The RAND equation has been modified by estimates provided by P&W and GE for the AST. The production cost equation for the duct burning turbofan is of the form:

$$\text{Engine Production Cost} = 631,000 \left( \frac{\text{TCE}}{1000} \right)^{0.6} \left( \text{XNENG} \right)^{-0.152}$$

where

TCE = maximum sea level static thrust

XNENG = number of engines in the production program.

The constant in the equation is changed to 546,000 for costing the turbojet engine.

Avionics - The avionics estimates are provided by vendors or in-house analysis and input to the model.

Additional Factors - The total summation of cost elements up to this point produces the flyaway cost of the aircraft without profit and costs for warranty, taxes, and insurance. The cost for these items is obtained by applying factors for each to the total aircraft cost. These costs are incorporated into the total aircraft production cost to arrive at the total vehicle flyaway cost except for the amortized R&D.

Development and Production Model Symbol Definitions

TFLCO	= Cost of prototype
CSTRT	= Print Indicator (1 = detail, 0 = summary)
FAST	= Indicator if AST or other
XMAXX	= Maximum Mach number
XMTN	= Minimum Mach Number - Stall Speed
XENGL	= Number of lift engines
TMAXLE	= Maximum thrust of lift engines
XNAVS	= Number of avionics suites
TMR	= Tooling material rate
XNY1-XNY	= Number of aircraft delivered per year
XNYO	= Number of aircraft in the development program
QAPO/QAP	= Quality assurance factor for development/and production
ECPO/ECP	= Engineering change order factor for development/and production
PTMPO/PTMP	= Tool maintenance factor for development/and production
SEPO/SEP	= Sustaining engineering factor for development/and production
RMRO/RMR	= Raw material rate for development and production
XMISCO/XMISC	= Miscellaneous cost factor for development/and production

CEPCF = Constant value for engine production cost formula - cruise engine  
CEPCE = Value of coefficient in engine production cost formula - cruise engine  
XLEPCF = Constant value for engine production cost formula - lift engines  
XLEPCE = Value of coefficient in engine production cost formula - lift engine  
DPAVP = Avionics production cost factor  
FAVPC = Production cost for avionics  
ATAIF = Airframe insurance factor  
ESTAIF = Engine insurance factor  
AVTAIF = Avionics insurance factor  
AWAF = Airframe warranty factor  
EWAF = Engine warranty factor  
AVWAF = Avionics warranty factor  
APRFF = Airframe profit factor  
EPRFF = Engine profit factor  
AVPRFF = Avionics profit factor  
WEMTBM = Weight empty of aircraft being evaluated  
WEMTBL = Weight empty of base line vehicle from which the cost factors were developed  
XNMB = Quantity at which the material factors were developed  
XNHB = Quantity at which the labor factors were developed  
XNCEB = Base quantity for cruise engines  
XNLEB = Base quantity for lift engines  
XNAB = Base quantity for avionics  
XMCS = Material cost sizing coefficient  
XHCS = Labor cost sizing coefficient.

XMLCS	= Material learning curve slope
XHLCS	= Labor learning curve slope
XCELCS	= Cruise engine learning curve slope
XLELCS	= Lift engine learning curve slope
DER	= Engineering labor rate (direct)
OER	= Engineering overhead rate (indirect)
DEGR	= } OEGR      = } Growth rates - not used XMGR      = }
DTR	= Tooling labor rate (direct)
OTR	= Tooling overhead (indirect)
DTGR	= } OTGR      = } Growth rates - not used XAGR      = }
DMR	= Manufacturing labor rate (direct)
OMR	= Manufacturing overhead rate (indirect)
DMGR	= } OMGR      = } Growth rates - not used XEGR      = }
DQAR	= Quality assurance labor rate (direct)
OQAR	= Quality assurance overhead rate (indirect)
DQAGR	= } OQAGR      = } Growth rates - not used
DMISC	= Labor rate for miscellaneous items
OMISC	= Overhead rate for miscellaneous items
XKE	= Complexity factor for engineering

XKT = Complexity factor for tooling  
XKFT = Complexity factor for flight test  
XNSTA = Number of test articles for structural tests  
XNFTA = Number of test articles for fatigue tests  
XMTSF = Number of test articles for systems test  
ETSMR = Engineering test material rate  
EFTMR = Flight material rate  
CEDCF = Constant value for cruise engine development cost equation  
CEDCE = Value of coefficient for development cost formula for cruise engines  
XLEDCE = Constant value for lift engine development equation  
XLEDCE = Value of coefficient for development cost formula for lift engines  
DPAVD = Development cost factor for avionics  
FAVDC = Development cost for avionics  
DRT = Production rate for development  
ADSF = Airframe spares factor for development  
EDSF = Engine spares factor for development  
AVDSF = Avionics spares factor development  
DSSEF = Special support cost factor for development  
DTDF = Technical data cost factor for development  
DOT = Operator trainer cost factor for development  
DMT = Maintenance trainer cost factor for development  
PRT = Maximum monthly production rate  
PECF = Constant term for production engineering cost formula  
PECE = Value of coefficient for production engineering cost formula  
APSF = Spares factor for production airframes

ORIGINAL PAGE IS  
OF POOR QUALITY

EPSF	= Spares factor for production engines
AVPSF	= Spares factor for production avionics
PSSEF	= Special support equipment cost factor for production
PTDF	= Technical data cost factor for production
POT	= Cost for operator trainers
PMT	= Cost for maintenance trainers
SCFM	= Material cost factor for maintenance
SCFL	= Labor cost factor for maintenance

Operating Cost Models. - The operating cost includes the standard elements normally found in the direct and indirect operating cost (DOC/IOC) as reported by the airlines. The DOC model is a modified version of the 1967 ATA method (Reference 3). The modifications to the DOC equations in the ATA method consists of: 1) combining the crew cost equations into a general expression for any number of crew members and 2) expanding the maintenance equations into greater detail. The more detailed maintenance equations are obtained from (Reference 4). The IOC model consists of set of expression derived through the combined efforts of Lockheed and Boeing (Reference 5). The indirect expense factors are those experienced by the international carriers (Reference 6).

#### DOC Model

<u>Flight Crew</u>	$[3.0 * (45 + SSFB) + 35 (XNCREW - 3) + IFB] * (1.0 + FCSIR)^{XNYR} * U$
<u>Fuel and Oil</u>	$1.02 * U * (FB/TB * CFT + XNENG * COT * 0.135)$
<u>Insurance</u>	$IRA * TUACC$
<u>Depreciation</u>	$(TUACC + SPARES)/PERIOD$
<u>Maintenance</u>	Equipment and Furnishings
Labor	$= [0.5TF + 1.0 + (4.5TF + 18) * WAF/10^6] * U/TB * MNTLR$
Material	$= [0.4TF + 1.20 + (14TF + 42) * WAF/10^6] * U/TB$

### Landing Gear

$$\text{Labor} = (1.0 + 10 * \text{WAF}/10^6) * \text{U/TB} * \text{MNTLR}$$

$$\text{Material} = (2.4 + 1.50 * \text{TUAFC}/10^6) * \text{U/TB}$$

### Tires and Brakes

$$\text{Material} = (1.2 + 7.0 * \text{WAF}/10^6) * \text{U/TB}$$

### Other Systems

$$\text{Labor} = (15\text{TF} + 3.3) * (\text{WAF}/10^6)^{0.5} * \text{XMMAX}^{0.5} * \text{U/TB} * \text{MNTLR}$$

$$\text{Material} = (1.4\text{TF} + 0.8) + 2.3\text{TF} + 0.7) * (\text{TUAFC}/10^6) * \text{XMMAX}^{0.5} * \text{U/TB}$$

### Structures

$$\text{Labor} = (1.0 + 50 * \text{WAF}/10^6) * \text{XMMAX}^{0.5} * \text{U/TB} * \text{MNTLR}$$

$$\text{Material} = (0.3 + 0.8\text{TUAFC}/10^6) * \text{XMMAX}^{0.5} * \text{U/TB}$$

### Other Power Plant

$$\text{Labor} = (19.0\text{TF} + 0.8) * (\text{WAF}/10^6)^{0.5} * \text{XMMAX}^{0.5} * \text{U/TB} * \text{MNTLR}$$

$$\text{Material} = 0.3\text{TF} + 0.1 + (0.8\text{TF} + 0.1) * (\text{TUAFC}/10^6) * \text{XMMAX}^{0.5}$$

Engine

$$\text{Labor} = [0.4TF + 0.2 + (0.018TF + 0.012) * TCE/XNENG/10^3] U/TB * MTLR * XNENG$$

$$\text{Material} = (3.8TF + 2.40) (ENG/10^5) U/TB * XNENG$$

The above formulas calculate the DOC in terms of dollars per aircraft year. This is converted to cents per seat mile by converting the dollars to cents and dividing each element by the seat miles flown per year.

IOC Model

Item I System Expense

$$\text{System Expense} = XKSE \times \text{direct maintenance labor dollar}$$

Item II Local Expense

$$\text{Local Expense} = XKLOE \times \frac{\text{maximum takeoff weight}}{1000} \times \text{departures}$$

Item III Aircraft Control

$$\text{Aircraft Control Expense} = XKCO \times \text{departures}$$

Item IV Cabin Attendant Expense

$$\text{Cabin Attendant Expense} = XKAT \times \text{Cabin attendant block hours}$$

ITEM V Food and Beverage Expense

$$\begin{aligned} \text{Food and Beverage Expense} &= XKFB \\ &\quad \times \text{weighted revenue passenger block hours} \end{aligned}$$

Item VI Passenger Handling Expense

$$\text{Passenger Handling Expense} = XKPH \times \text{Passengers enplaned}$$

Item VII Cargo Handling Expense

$$\text{Cargo Handling Expense} = XKCH \times \text{Total tons carried}$$

Item VIII Other Passenger Expense -

Other Passenger Expense = XKOP x Revenue Passenger miles

Item IX Other Cargo Expense

Other Cargo Expense = XKOC x Revenue Freight ton miles

Item X General and Administrative Expense

G&A Expense = XKGA x Direct plus indirect Operating expense  
less depreciation and insurance

#### DOC and IOC Model Symbol Definitions

XNRITE = Symbol for selecting the range

YEAR = Year input for calculating costs in the proper year's dollars

XNCREW = Number of personnel in the flight crew

XNPASS = Passenger capacity of the aircraft

XNATT = Number of cabin crew

XLF = Load factor

SSFB = Flight crew supersonic flight bonus

IFB = Flight crew international flight bonus

FCSIR = Flight crew salary inflation rate

ENGC = Engine cost per engine

MNTLIR = Maintenance labor inflation rate

TG = Ground time in minutes

U = Utilization

IRA = Insurance rate

PERIOD = Depreciation period

CFT = Cost of fuel (\$/LB)

COT = Cost of oil (\$/LB)

ORIGINAL PAGE IS  
OF POOR QUALITY

MBF = Maintenance burden factor  
REVPAS = Number of revenue passengers per year  
AVCARG = Average pounds of cargo per flight  
XKSE = System expense IOC factor  
XKLOE = Local IOC factor  
XKCO = Aircraft control IOC factor  
XKAT = Cabin attendant IOC factor  
XKFB = Food and beverage IOC factor  
XKPH = Passenger handling IOC factor  
XKCH = Cargo handling IOC factor  
XKOP = Other passenger expense IOC factor  
XKOC = Other cargo expense IOC factor  
XKGA = G&A expense IOC factor  
CFARE = Fare cost factor - (function of distance)  
XKFARE = Constant portion of the fare - (function of number of revenue passengers)  
XFACC = Facilities cost (dollar input)  
TAXR = Income tax rate (decimal)  
CARGF = Revenue per cargo ton mile  
FB = Block fuel  
TB = Block time  
WAF = Weight of airframe (weight empty - engines)  
TU AFC = Total airframe cost  
TF = Flight time  
TU ACC = Total aircraft flyaway cost including R&D

### Return on Investment (ROI) Model

The return on investment (ROI) for the AST is calculated by a simplified method in the ASSET program for comparative analysis.

### EVALUATION RESULTS

Five structural approaches were evaluated and compared using the results of the ASSET computer program. The wing design approaches included:

- (1) Chordwise stiffened wing arrangement, beaded skin panels, mechanical fasteners (WC1)
- (2) Spanwise stiffened wing arrangement, hat stiffened skin panels, mechanical fasteners (WC2)
- (3) Monocoque wing arrangement, aluminum brazed honeycomb sandwich skin panels, mechanical fasteners (WC3)
- (4) Monocoque wing arrangement, aluminum brazed honeycomb sandwich skin panels, welded (WC4)
- (5) Composite reinforced-chordwise stiffened wing arrangement, beaded skin panels, mechanical fasteners (WC5)

In evaluating each of the above wing designs, a skin stringer and frame construction was assumed for the fuselage.

A summary of the ASSET program results are presented in Table 17-2. The results include weight, geometry and cost data for both the constant-size and constant payload-range aircraft.

### CONSTANT WEIGHT AIRCRAFT

A comparison of the various parameter (i.e., structural mass, range, cost) for the constant size/weight aircraft indicates a variation in these parameters and the minimum does not necessarily identify the best concepts. The least weight wing

TABLE 17-2. EVALUATION DATA FOR STRUCTURAL ARRANGEMENTS

STRUCTURAL ARRANGEMENT	CHORDWISE (MECHANICAL) WC1	SPANWISE (MECHANICAL) WC2	MONOCOQUE (MECHANICAL) WC3	MONOCOQUE (WELDED) WC4	CHORDWISE (COMP. REINF.) WC5
<b>CONSTANT GTOW:</b>					
TOGW OWE	(LB) 329474	750000 328315	750000 315982	750000 318759	750000 313125
WING WEIGHT	(LB)	104834	92330	95146	89434
WING AREA	(FT <sup>2</sup> )	10822	10822	10822	10822
WING UNIT WT	(LB.FT-2)	9.80	9.69	8.53	8.26
RANGE	(N·Mi)	3830	3870	4123	4166
FLYAWAY COST	(MIL DOL)	90.65	89.19	104.93	93.81
DOC	(C/SM)	1.94	1.92	2.03	1.92
IOC	(C/SM)	0.94	0.93	0.91	0.90
ROI A.T.	(%)	1.12	1.48	0.30	1.74
<b>CONSTANT PAYLOAD-RANGE:</b>					
TOGW OWE	(LB) 381691	867126 373353	772641 324109	789992 333338	759498 316481
WING WEIGHT	(LB)	129895	125254	95682	90785
WING AREA	(FT <sup>2</sup> )	12768	12512	11149	10959
WING UNIT WT	(LB.FT-2)	10.20	10.00	8.58	8.28
RANGE	(N·Mi)	4200	4200	4200	4200
FLYAWAY COST	(MIL DOL)	103.19	99.83	107.52	94.73
DOC	(C/SM)	2.14	2.09	2.06	1.93
IOC	(C/SM)	0.94	0.94	0.91	0.90
ROI A.T.	(%)	-1.37	-0.74	-0.11	-0.64

concept is the composite reinforced design (WC5); the spanwise design (WC2) is, however, the least initial cost concepts as typified by the flyaway cost. It can be seen from the tabulated data that the weight savings realized by the application of composites to the spar caps permits approximately 16,600 pounds of additional fuel to be carried. Hence, the range capability of the structurally efficient composite reinforced design (WC5) is approximately 340 nautical miles greater than the chordwise wing design (WC1). All concepts, however, do not meet the range criteria of 4200 nautical miles. A reduction in structural mass of 1700 pounds is required to the composite reinforced design to satisfy the payload-range requirement.

#### CONSTANT PAYLOAD-RANGE AIRCRAFT

The constant payload-range data of Table 17-2 indicates that the takeoff gross weight of the resized aircraft varies from a maximum of 885,000 pounds to a minimum of 760,000 pounds. The data presents the minimum structural weight, size and cost to be the composite reinforced design (WC5).

Growth Factor. - Figure 17-5 visually displays the takeoff gross weight variation with the range capability of the constant-weight and constant payload-range aircraft. The trends presented indicates that the growth factor of this class of aircraft, which is represented by approximately 50-percent fuel, is 6 (i.e., a 1-pound increase in structural weight results in a 6-pound increase in the aircraft takeoff gross weight). Thus, the importance of minimizing structural mass is emphasized by these trends.

Structural Mass Versus Cost. - The wing mass variation with relative cost is presented in Figure 17-6. The data relates the structural efficiency of the design concepts with the direct operating cost, normalized to the least cost approach. DOC is a measure of total-system-cost that includes such parameters as: structural efficiency; engine requirement variation as the airplane size changes; the impact of airplane size, concept selection, and mass on fuel consumption; and development, manufacturing and operating (maintenance) costs. The desirable area, as visually displayed by the arrow, is the least weight and least cost region. The composite reinforced design (WC5) is the least weight and cost concept evaluated.

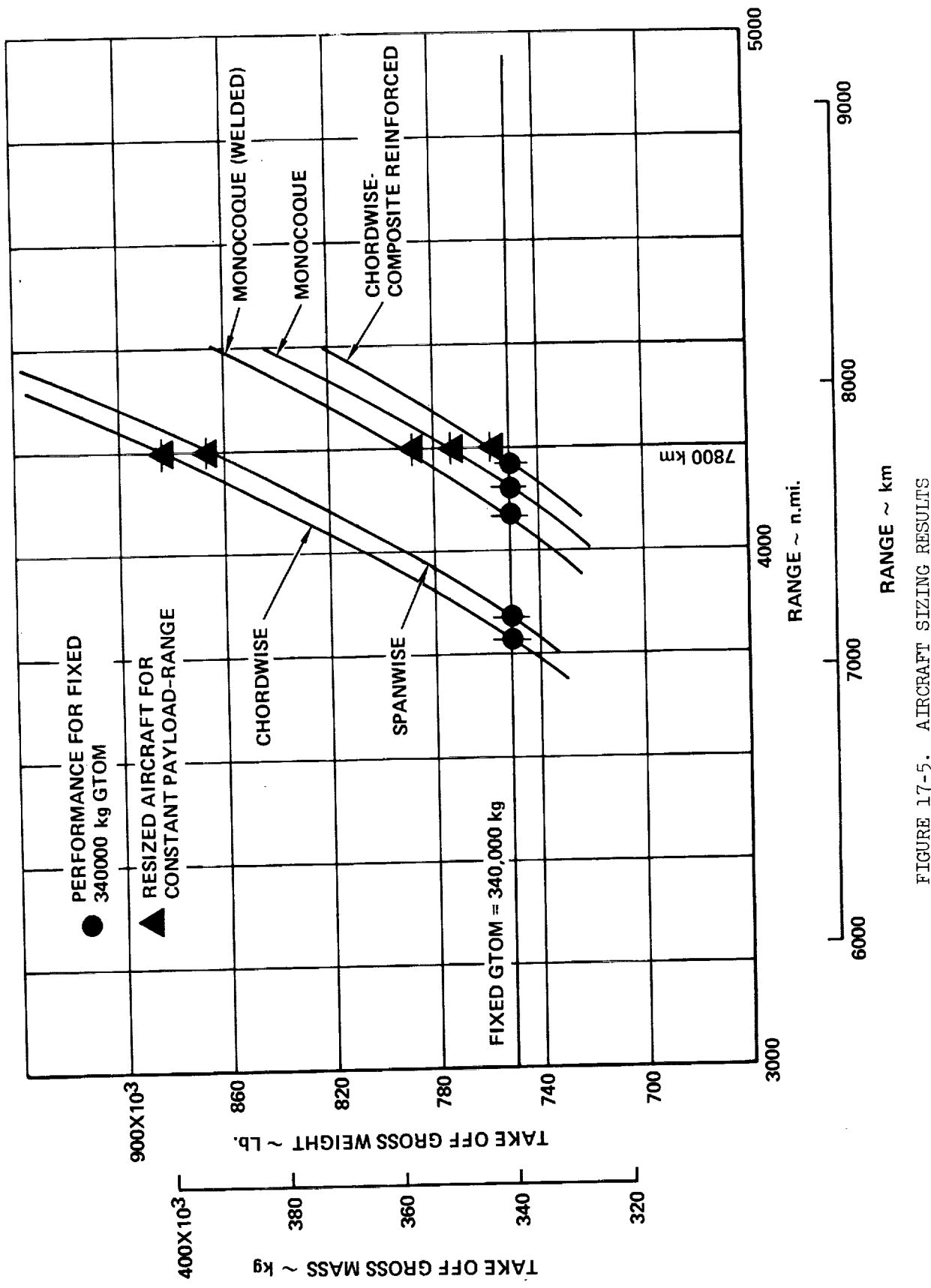


FIGURE 17-5. AIRCRAFT SIZING RESULTS

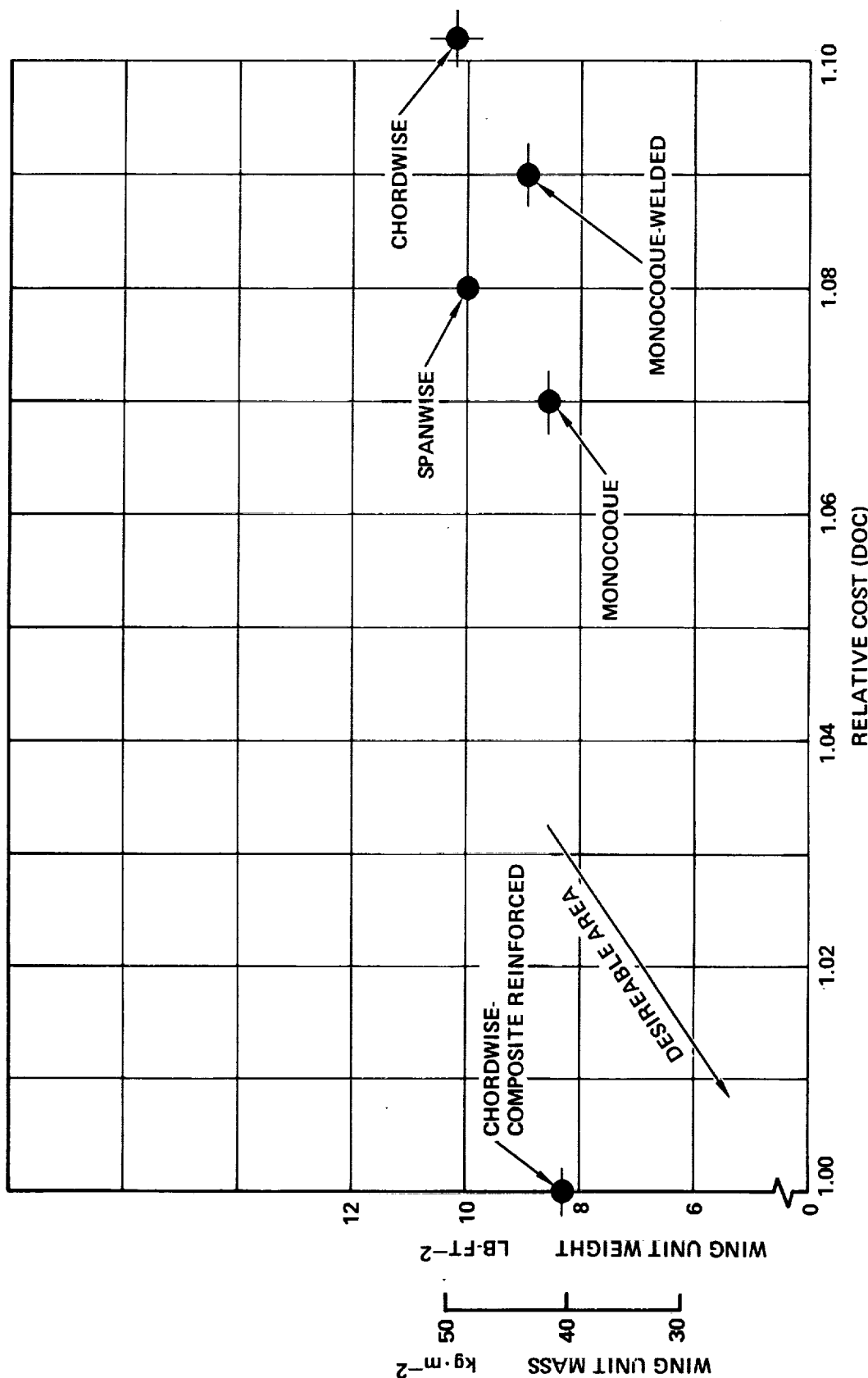


FIGURE 17-6. STRUCTURAL MASS VERSUS COST

Technology Improvement Versus Cost. - Figure 17-7 presents a bar chart relating the technology level of each design concept with the initial cost. The metallic stiffened skin approaches are displayed on the left hand side with the more advanced technology concepts on the right hand side. The initial cost is measured by the flyaway cost of the vehicles, normalized to the least cost system. The composite reinforced design (WC5) is the least cost with the monocoque approaches being approximately 15-percent greater.

Technology Risk Versus Cost. - Technology risk, as presented herein, is a quantitative factor related to the damage tolerance characteristics of the design concepts, tempered with an assessment of development risk. As shown in Figure 17-8 the spanwise and chordwise designs are considered as the least risk concepts; with the welded monocoque design representing the highest risk. Since the composite reinforced design is essentially a chordwise stiffened design with only the spar caps reinforced with Boron Polyimide (B/PI) composites, it is displayed above the chordwise design. The monocoque design is represented as nominal. The cost parameters are normalized (to the least cost concept) direct operating costs. The composite reinforced design is the most desirable of the five design concepts evaluated.

Investment Versus Cost. - Figure 17-9 presents the investment cost variation for each design concept with direct operating costs. Both cost values are normalized to the least cost approach.

Investment cost includes the cost for the aircraft, the aircraft spares and the special support equipment. The cost of the production aircraft is the primary element of investment. The spares and support equipment are treated as percentages of the flyaway cost of the aircraft.

As shown by the normalized values, the composite reinforced design is the least cost approach.

ORIGINAL PAGE IS  
OF POOR QUALITY

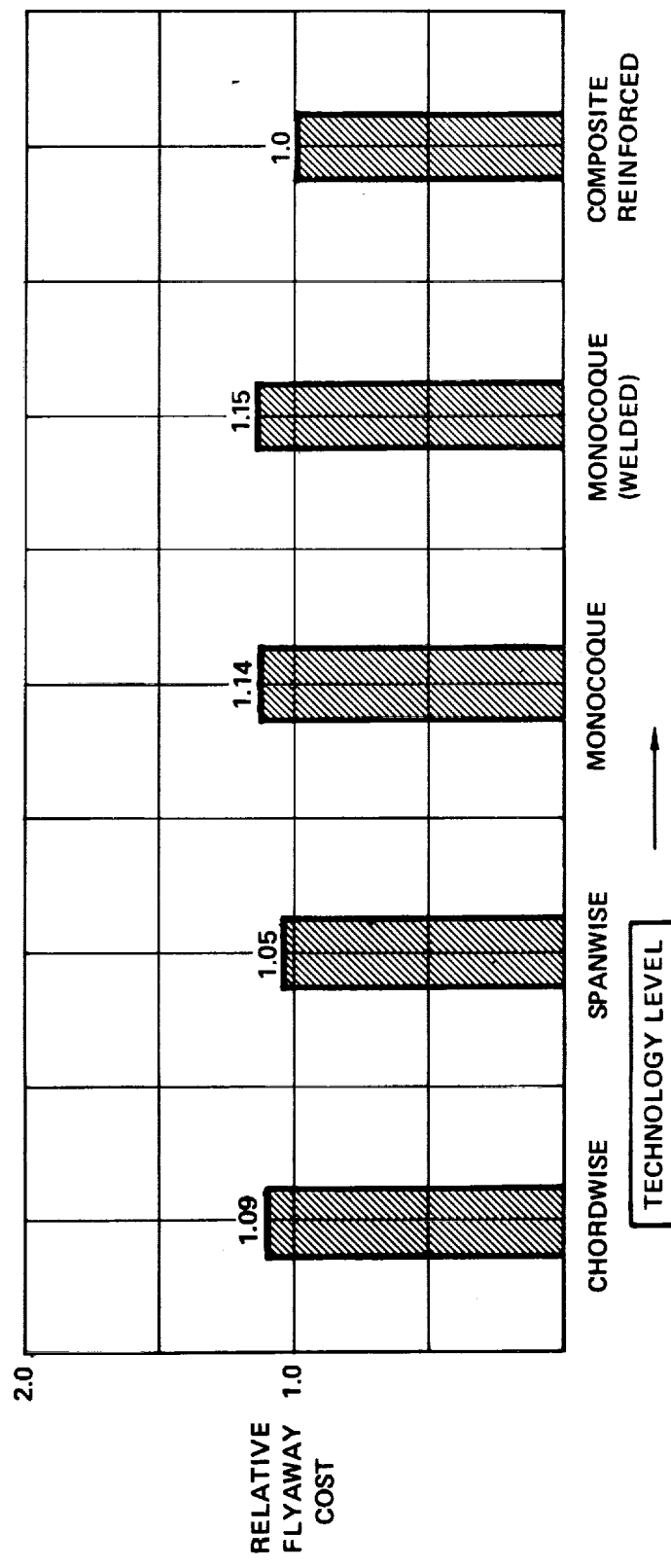


FIGURE 17-7. TECHNOLOGY IMPROVEMENT VERSUS COST

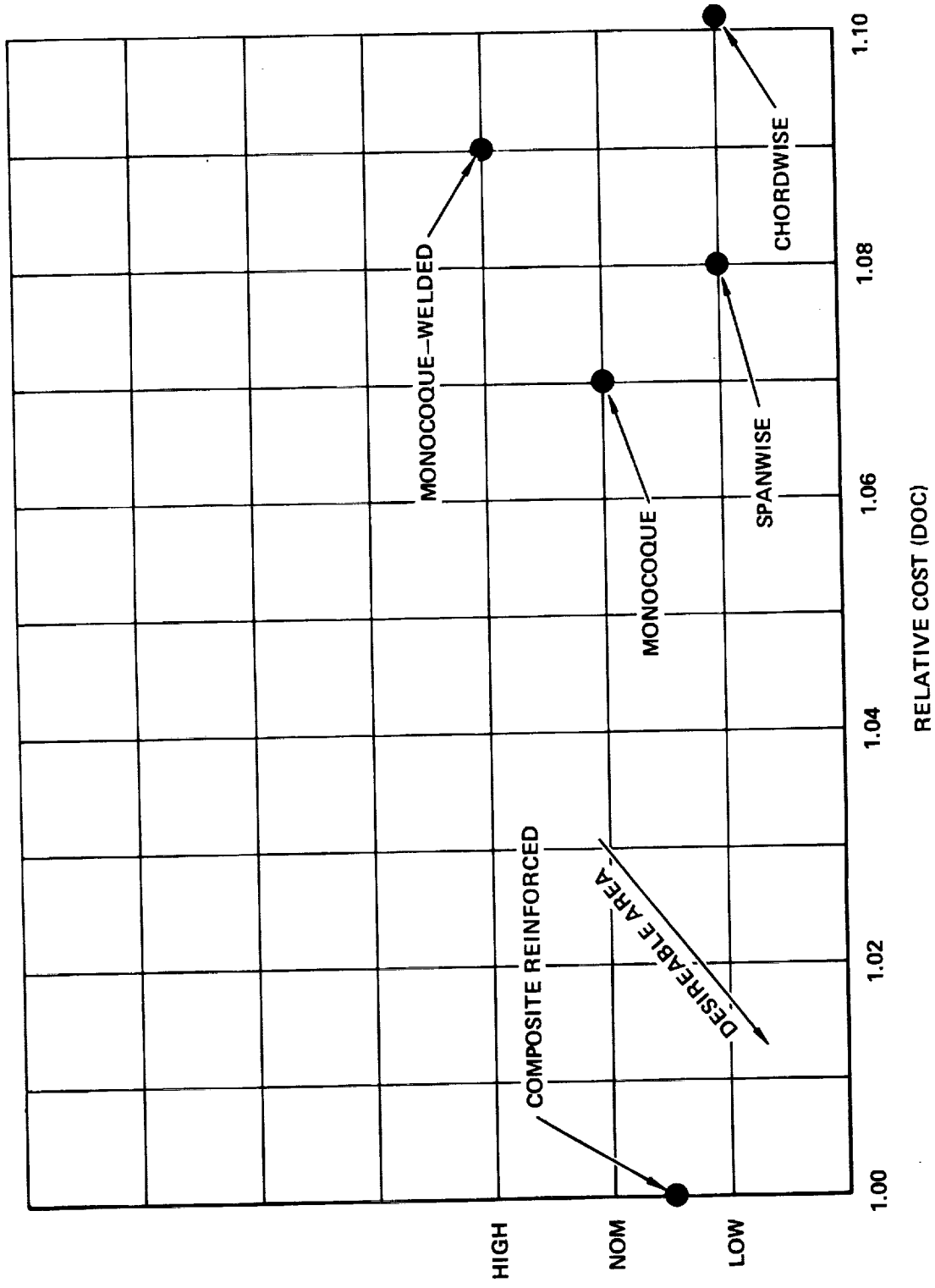


FIGURE 17-8. TECHNICAL RISK VERSUS COST

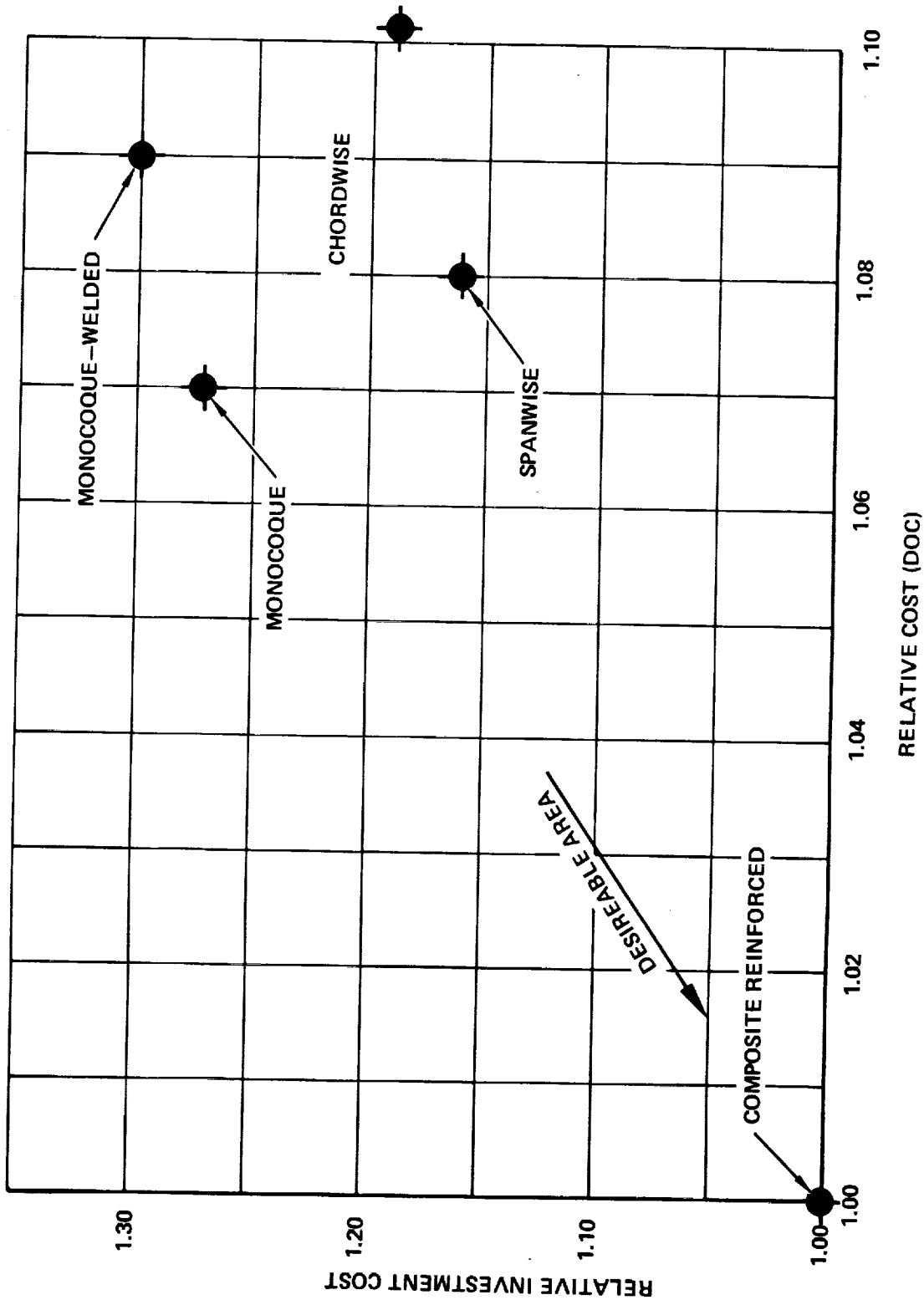


FIGURE 17-9. INVESTMENT VERSUS COST

## CONCEPT SELECTION

The various wing design concepts, each with a skin-stringer fuselage design, were evaluated with respect to structural mass, performance and cost. These factors were interrelated to yield a relative comparison, based on minimum-total-system-cost for a constant payload-range aircraft.

Based on a constant-weight airplane the ranking of the design concepts shown in Table 17-3 was obtained. When these design concepts were applied to a minimum total-system-cost airplane the ranking of the concepts was unchanged (Table 17-4). A comparison of the relative costs of the various wing design concepts is also presented in Table 17-4, and shows that the composite reinforced design is 7 to 11 percent less costly than the other design concepts.

The best homogeneous (single concept applied to total wing) structural approach for design of Mach 2.7 supersonic cruise aircraft is the least cost and weight chord-wise stiffened design with metallic surface panels and composite reinforced spars. The structural arrangement for this design concept is presented in Figure 17-10. Approximately 6000 pounds of composite material is used and results in a 16,600 pound weight saving of wing structural mass. Structurally efficient circular arc-convex beaded surface panels of titanium alloy (Ti-6Al-4V annealed) are used. The surface panel design is directed towards alleviating thermal stresses while utilizing both skins in resisting shear. With the beaded inner and outer skins, the surfaces do not participate in resisting wing bending and all the bending material is concentrated in the spar caps. The titanium spar caps are reinforced with boron/polyimide as shown in the figure. The reinforcement strips are continuous from BL 470L to BL 470R.

The importance of minimum mass structural concepts was emphasized by the increasing cost trends with an increase in wing structural mass as shown in Table 17-4. Weight inefficiencies evaluated under the payload-range constraints can and do raise costs appreciably. Furthermore, with the apparent high growth factor ( $GF \approx 6$ ) of this class of aircraft, it appears that considerable effort is warranted to remove unnecessary weight to minimize the cascading effect on aircraft size and takeoff gross weight.

ORIGINAL PAGE IS  
OF POOR QUALITY

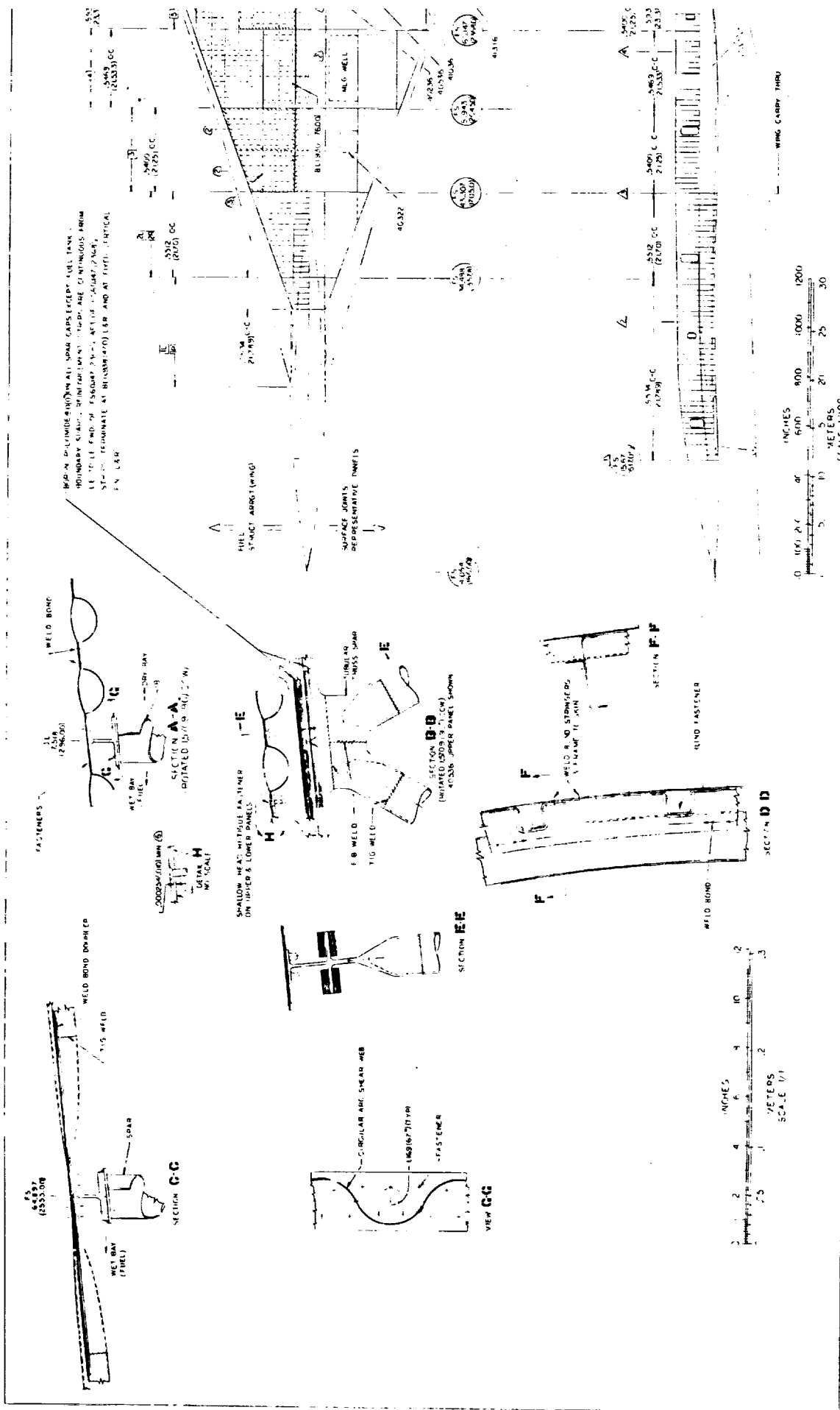
TABLE 17-3. CONCEPT EVALUATION SUMMARY - CONSTANT WEIGHT AIRCRAFT

CONCEPT	WING WEIGHT LBS/FT <sup>2</sup>	RELATIVE WEIGHT
(1) CHORDWISE STIFFENED – CONVEX-BEADED PANELS	9.80	1.19
(2) SPANWISE STIFFENED – HAT-STIFFENED PANELS	9.68	1.17
(3) MONOCOQUE – ALUMINUM BRAZED HONEYCOMB CORE PANELS	8.54	1.03
(4) MONOCOQUE – ALUMINUM BRAZED HONEYCOMB CORE PANELS (WELDED)	8.85	1.07
(5) CHORDWISE STIFFENED – CONVEX-BEADED PANELS; B/PI REINFORCED SPARS	8.25	1.00

TABLE 17-4. CONCEPT EVALUATION SUMMARY - CONSTANT PAYLOAD-RANGE AIRCRAFT

STRUCTURAL ARRANGEMENT AND CONCEPT	WING MASS			COST	
	kg • m <sup>-2</sup>	LB • FT <sup>-2</sup>	RELATIVE MASS	DOC (C/SM)	RELATIVE COST
(1) CHORDWISE STIFFENED – CONVEX-BEADED PANELS	49.80	10.20	1.23	2.14	1.11
(2) SPANWISE STIFFENED – HAT-STIFFENED PANELS	48.82	10.00	1.21	2.09	1.08
(3) MONOCOQUE – ALUMINUM BRAZED HONEYCOMB CORE PANELS	41.89	8.58	1.04	2.06	1.07
(4) MONOCOQUE – ALUMINUM BRAZED HONEYCOMB CORE PANELS (WELDED)	43.40	8.89	1.07	2.11	1.09
(5) CHORDWISE STIFFENED – CONVEX-BEADED PANELS; B/PI REINFORCED SPARS	40.43	8.28	1.00	1.93	1.00





PRECEDING PAGE BLANK NOT FILMED

ORIGINAL PAGE IS  
OF POOR QUALITY  
RELDOUT FRAME



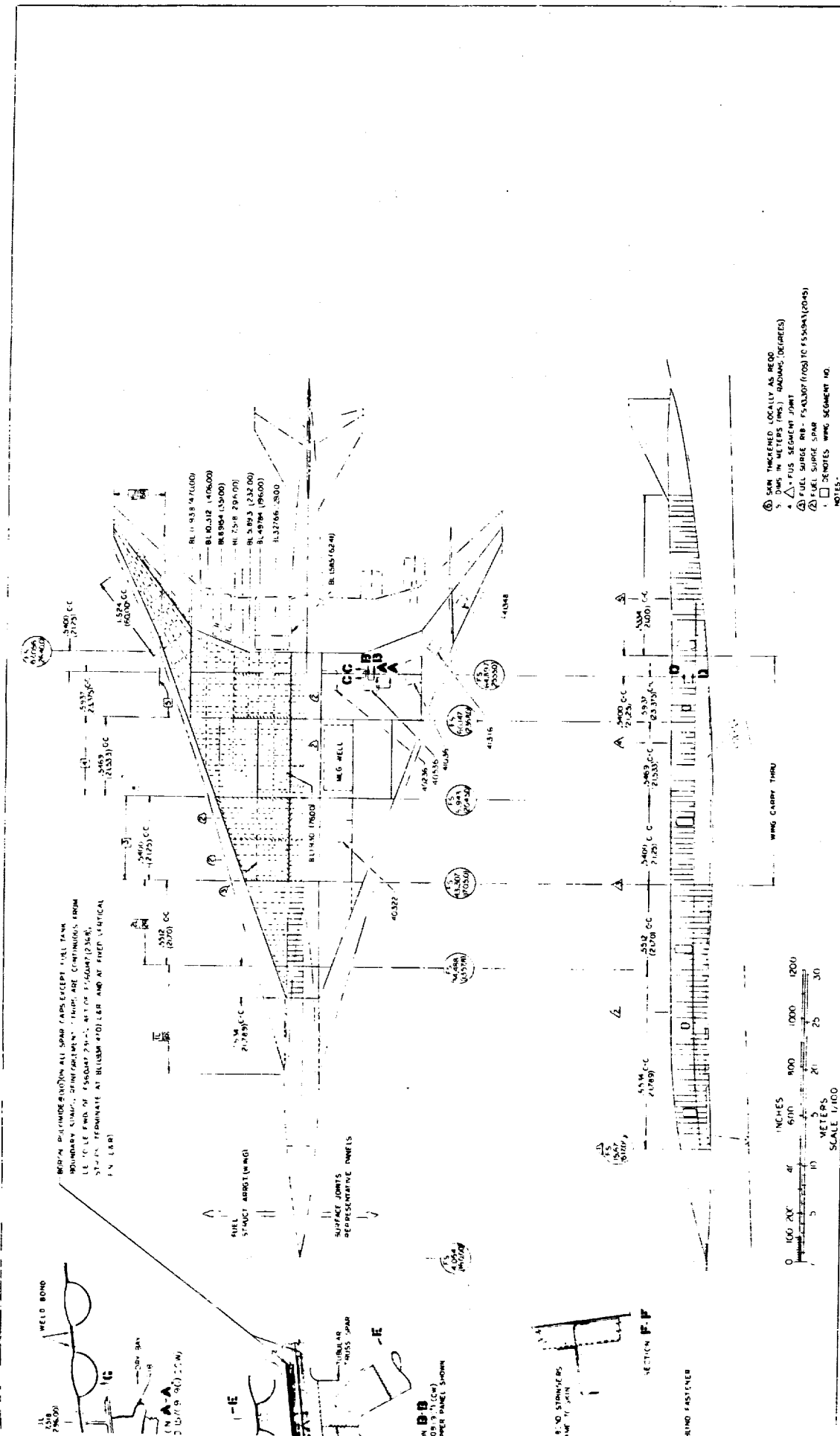


FIGURE 17-10. COMPOSITE REINFORCED WING DESIGN - FASTENERS



The structural weight for the various regions of the wing structure are shown in Table 17-5 for the five structural approaches. It appears that incorporating the minimum weight regions into the wing design would result in the best approach for a Mach 2.7 design.

Thus, the recommended structural approach for the Task II Detailed Engineering Design and Analysis is a hybrid structural approach consisting of the monocoque and chordwise stiffened structural arrangement as shown in Figure 17-11. A minimum structural mass airplane (near-term) is obtained by combining the minimum mass components (i.e., wing forward box, aft box and tip) as determined by the detailed structural analysis. Table 17-6 shows the airplane weight and cost parameters for this hybrid design, for both constant-weight and constant payload-range criteria. The hybrid design very nearly satisfies the payload-range requirement specified for the 750,000 pound baseline configuration concept.

PRECEDING PAGE BLANK NOT FILMED

TABLE 17-5. WING WEIGHTS FOR STRUCTURAL ARRANGEMENTS

WING WEIGHT AND SEGMENT	STRUCTURAL ARRANGEMENT				
	CHORDWISE	SPANWISE	MONOCOQUE	MONOCOQUE	CHORDWISE
WELD BOND	WELD BOND	WELD BOND	ALUM BRAZED	ALUM BRAZED	COMP. REINF.
MECH. FASTEN.	MECH. FASTEN.	MECH. FASTEN.	WELDED	WELDED	SPARS ONLY
<u>VARIABLE WEIGHT</u>					
● FWD. BOX	64,658 (22,090)	63,482 (25,364)	50,978 (21,982)	53,794 (24,057)	48,082 <u>(20,580)</u>
● AFT BOX		(25,242)	(19,692)	(20,153)	(17,384)
● TIP	(13,552)	(12,876)	(9,304)	(9,584)	(10,118)
<u>FIXED WEIGHT</u>	41,352	41,352	41,352	41,352	41,352
$\Sigma$ TOTAL~LB	106,010	104,834	92,330	95,146	89,434

NEAR-TERM 1980-81 START-OF-DESIGN

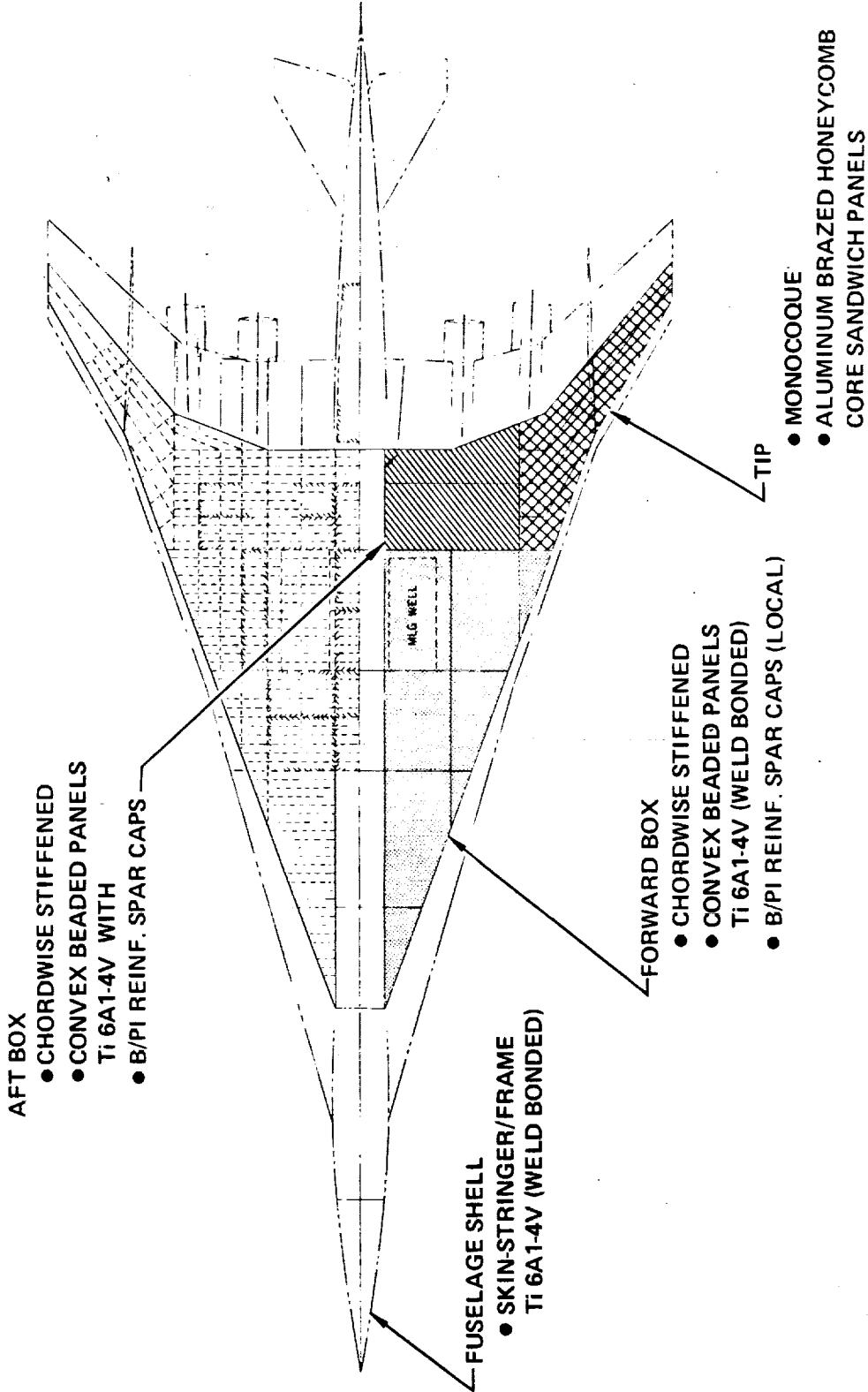


FIGURE 17-11. STRUCTURAL APPROACH FOR TASK II

TABLE 17-6. EVALUATION DATA FOR HYBRID STRUCTURAL ARRANGEMENT

STRUCTURAL ARRANGEMENT		HYBRID (MECHANICAL) WC7
<b>CONSTANT GTOW:</b>		
TOGW	(LB)	750000
OWE	(LB)	312322
WING WEIGHT	(LB)	88620
WING AREA	(FT <sup>2</sup> )	10822
WING UNIT WT	(LB.FT <sup>-2</sup> )	8.19
RANGE	(N.Mi)	4183
FLYAWAY COST	(MIL DOL)	93.57
DOC	(C/SM)	1.91
IOC	(C/SM)	0.90
ROI A.T.	(%)	1.82
<b>CONSTANT PAYLOAD-RANGE:</b>		
TOGW	(LB)	754665
OWE	(LB)	313963
WING WEIGHT	(LB)	89216
WING AREA	(FT <sup>2</sup> )	10889
WING UNIT WT	(LB.FT <sup>-2</sup> )	8.20
RANGE	(N.Mi)	4200
FLYAWAY COST	(MIL DOL)	94.02
DOC	(C/SM)	1.92
IOC	(C/SM)	0.90
ROI A.T.	(%)	1.73

## REFERENCES

- 1 Levenson, G.S.; Boren, H.E.; Tihansky, D.P.; Timson, F.S., "Cost-Estimating Relationships for Aircraft Airframes" R-761-PR (abridged), Rand, Santa Monica, February 1972.
- 2 Large, J.P., "Estimating Aircraft Turbine Engine Costs" RM-6384/l-PR, Rand, Santa Monica, September 1970.
- 3 Standard Method of Estimating Comparative Direct Operating Costs of Turbine Powered Transport Airplanes, Air Transport Association, December 1967.
- 4 "More Realism in a Standard Method for Estimating Airline Operating Expense," Lockheed California Company, Report OEA/SST/179, March 1966.
- 5 "Revisions to 1964 Lockheed/Boeing Indirect Operating Expense Method," Lockheed California Company, Report COA2061, December 1969.
- 6 Indirect Operating Expense Coefficients years 1963 through 1972, Lockheed California Company, COA/1277, June 1973.



APPENDIX A

COMPUTER PRINTOUT  
ASSET PARAMETRIC ANALYSIS

**PRECEDING PAGE BLANK NOT FILMED**

## INTERNATIONAL MISSION SUD LAY • 1404

T/A	AR	W/S	T/W
2.65	1.62	09.3	0.477

## WEIGHT STATEMENT

	WEIGHT (POUNDS)	WEIGHT FRACTION	(PERCENT)	
TAKE-OFF WEIGHT	1 7594.96.)	FUEL	51.88	
FUEL AVAILABLE	1 3940.17.)	FUEL		
ZERO FUEL WEIGHT	1 2654.81.)	PAYOUT	6.45	
PAYOUT	1 4900.)	OPERATING ITEMS		
OPERATING WEIGHT	1 3164.11.)	STANDARD ITEMS	1.43	
OPERATING ITEMS	1 5476.)	EMPTY WEIGHT		
STANDARD ITEMS	1 558.)	WING		
EMPTY WEIGHT	1 2050.20.)	TAIL	90785.	
		BODY	11545.	
		LANDING GEAR	42939.	
		SURFACE CONTROLS	30705.	
		NAZELLE AND ENGINE SECTION	8517.	
PROPULSION	1 5626.)	STRUCTURE		
WEIGHT OF LIFT ENGINES	1 0.)	FUEL SYSTEM		
VISITON CONTROL SYSTEM	1 0.)	ENGINE CERTIFICATES		
ENGINES	1 5172.)	INSTRUMENTS		
THRUST REVERSAL	1 0.)	HYDRAULIC		
EIK INSULATION SYSTEM	1 21059.)	ELECTRICAL		
FUEL SYSTEM	1 5727.)	AVIONICS		
INDIGNE CERTIFICATES	1 1639.)	ROKASPINGS AND EQUIPMENT		
INSTRUMENTS	1 1234.)	ENVIRONMENTAL CONTROL SYSTEM		
HYDRAULIC	1 5772.)	AUXILIARY GEAR		
ELECTRICAL	1 4557.)	Aux. Motor		
AVIONICS	1 1900.)	1 2364.74.)	1 TOTAL	100.00)
ROKASPINGS AND EQUIPMENT	1 11500.)			
ENVIRONMENTAL CONTROL SYSTEM	1 8300.)			
AUXILIARY GEAR	1 1950.)			
Aux. Motor	1 0.)			
		EXCESS FUEL CAPACITY = EXCESS FUEL CAPACITY = WING EXCESS FUEL CAPACITY = F		
		STRUCTURE ALUMINUM		
		0.6		

ORIGINAL PAGE IS  
OF POOR QUALITY

## W H I T E S M A R K I X

## ELEMENTS / MATERIAL

	AL	STEEL	CMP.	WHTR	TOTAL
BLT	4176.	77712.	1616.	5629.	1453.
TALL	52L.	10726.	115.	0.	185.
FUSL	1975.	34093.	773.	1073.	5024.
L. to L.	31.	7677.	11792.	0.	11209.
MULLIT	10t.	145.	1891.	0.	0.
PLT. INCL	968.	16050.	210.	0.	1221.
SL. GLS	2044.	383.	1789.	126.	4173.
TALL	9622.	150086.	16389.	2830.	23264.
					206388.

## CONFIGURATION GEOMETRY

BASIC WALL	ARIA(SLFT)	SPAN(SLFT)	APER(MALL)	L/4 SWTR	L/4 SWTR	UNLT(L)	MAC(LT)
INTUAKC. WIND --	ARIA(SLFT)	LXW. ARIA(L)	LXW. ARIA(L)	C.0	C.0	72.500	164.38
	10955.	9457.2	72.50	101.81	101.81		109.59
L/4SWTR. INCL - ANGLE(SLFT)	Y. DIA(SLFT)	L/4 SWTR	NCF(LFT)	SFL(LFT)	SFL(LFT)	Avg T/C	
10955.	0.0	72.50	101.81	0.0	0.0	2.65	
L/4 SWTR	ARIA(SLFT)	EFF. AR	Avg T/C	L(LFT)	L(LFT)	(B/2)/LW	P
	10955.	1.62	2.65	104.38	0.0	0.315	0.389
WIND BANK --	GEAR(LT)	CBAR(SLFT)	L(LFT)	RYING(CUH)	RYING(CUH)		
	150.41	.0.0	1.60	4576.30	2601.82		
ROOF LANT --	LTNG(LFT)	S. MELL(SLFT)	LTNG(LFT)	LTNG(DFT)	LTNG(DFT)		
	247.60	7876.0	9.47	13.22	137.30		
LANT --	LTNG(LFT)	SHD(LFT)	SHD(LFT)	FV(LC) F	FV(LC) F	V1 REF L(F)	
	116.33	11.50	9177.00	20000.00			
	SHD(LFT)	SHD(LFT)	L(LFT)	SVT(SLFT)	SVT(SLFT)	V1 REF L(F)	
	116.33	934.04	23.04	471.90	471.90	26.02	
PERF. LANT --	LT(LFT)	LT(LFT)	PUL(LFT)	PUL(LFT)	PUL(SWT)	NO. PDS	INLET(LFT)
	22.34	7.13	39.34	8.06	4601.53	4.	0.0

ORIGINAL PAGE IS  
OF POOR QUALITY

## MISSION SUMMARY

INTERNATIONAL MISSION SIL LAY + 14.4

SEGMENT	INITIAL ALTITUDE (FT)	INITIAL WEIGHT (LB)	INITIAL FUEL (LB)	SEGMENT DISTANCE (IN MIL)	TOTAL DISTANCE (IN MIL)	SEGMENT TIME (MIN)	TOTAL TIME (MIN)	SEGMENT STATE	TOTAL STATE	EXTRN THRUST TAB 1U	EXTRN THRUST TAB 1D	AVG L/D RATIO	AVG SFC (FF/T)	MAX OVER PRES		
<b>TAKOFF</b>																
POWER 1	0.	6.0	7594.05	3614.	3614.	0.	10.0	0.	-97101.	0.	0.0	0.571	0.0			
POWER 2	0.	6.314	7558.85	6112.	9725.	0.	0.5	10.5	0.	-97201.	0.	5.18	1.388	0.0		
CLIMB	0.	0.500	7447.75	1262.	16567.	4.	1.1	11.5	0.	-97201.	0.	7.45	1.446	0.0		
CRUISE	5000.	0.413	7445.11	4352.	21339.	0.	4.0	15.5	0.	-97101.	0.	8.24	0.727	0.0		
ACCEL	5100.	0.413	7381.94	1792.	23132.	1.	0.	15.8	0.	-97201.	0.	9.96	1.472	0.0		
CLIMB	5000.	0.524	7383.60	22784.	45416.	36.	4.7	20.5	0.	-97201.	0.	11.26	1.508	0.0		
CLIMB	34000.	0.984	7125.02	4915.24	95764.	254.	296.	14.2	34.7	0.	-97201.	0.	8.34	1.533	0.0	
CLIMB	33000.	1.003	6637.29	6.	95764.	0.	288.	0.0	34.7	0.	-97201.	0.	8.74	1.563	0.0	
CRUISE	33000.	1.020	6637.29	227210.	322974.	36494.	39490.	144.7	179.5	0.	-97201.	0.	8.63	1.498	0.0	
DESCEND	73000.	2.020	4225.14	97.	323076.	25.	401.5	0.9	180.4	0.	-97501.	0.	0.44	-0.769	0.0	
DESCEND	73000.	2.039	4204.22	1300.	324375.	157.	107.	1.1	193.5	0.	-97501.	0.	9.17	-0.386	0.0	
CRUISE	73000.	2.050	4351.63	1679.	326654.	33.	4200.	1.3	194.8	0.	-97201.	0.	8.50	1.511	0.0	
CRUISE	5000.	0.413	4356.44	767.	328721.	0.	4200.	5.0	164.6	0.	-97101.	0.	11.18	0.830	0.0	
RESET	0.	0.0	4207.77	0.	326721.	0.	4200.	0.0	192.1	0.	0.	0.	0.0	0.0	0.0	
RESET	0.	0.0	4307.77	0.	347721.	0.	4200.	0.0	192.1	0.	0.	0.	0.0	0.0	0.0	
RESERV	0.	0.0	4307.77	23070.	3517.71.	0.	0.	0.0	0.0	0.	0.	0.0	0.0	0.0	0.0	
CLIMB	0.	0.200	4077.07	2774.	35450.	2.	2.	0.4	0.4	0.	-97201.	0.	9.73	1.444	0.0	
CLIMB	1500.	0.500	4044.53	13428.	367933.	22.	23.	2.0	3.0	0.	-97201.	0.	9.84	1.503	0.0	
CRUISE	49000.	0.970	3915.53	10500.	37660.	167.	190.	19.0	22.0	0.	-97101.	0.	10.94	0.937	0.0	
DESENT	43000.	0.970	379215.	783.	379215.	55.	248.	7.9	30.3	0.	-97501.	0.	9.89	-0.491	0.0	
CRUISE	43000.	0.970	36212.	769.	379950.	12.	260.	1.1	31.7	0.	-97101.	0.	10.93	0.938	0.0	
ROUTE	1500.	0.519	379512.	14031.	394415.	0.	260.	36.0	31.7	0.	-97101.	0.	11.30	0.851	0.0	

TICKET = 756490.0 TGT L = 394017.0 UTIL K = 354014.0

PRODUCTION											
	PRODUCTION YEARS						6	7	8	9	TOTAL
	1	2	3	4	5	6	7	8	9	10	
ALUMINUM	1,272.12	1,102.03	1,020.96	1,000.62	1,527.96	1,417.44	1,334.03	1,266.41	1,232.97	1,193.80	13,065.29
ENGINEERING											
MURKS	44.34	36.64	40.25	4276.	4521.	4097.	3861.	3577.	3399.	3252.	39171.
LABOUR RATE	6.07	6.17	6.17	c.17	c.17	6.17	6.17	6.17	6.17	6.17	6.17
OVERHEAD RATE	5.00	5.00	5.00	9.20	9.20	9.20	9.20	9.20	9.20	9.20	9.20
TOTAL	62.41	62.81	62.81	74.30	74.30	71.17	68.03	62.13	69.04	68.49	680.40
TOOLING											
MURKS	53.66	47.76	4836.	5133.	5425.	4917.	4561.	4294.	4079.	3903.	47005.
LABOUR RATE	6.09	6.09	6.09	6.09	6.09	6.09	6.09	6.09	6.09	6.09	6.09
OVERHEAD RATE	12.20	12.36	12.36	12.36	12.36	12.36	12.36	12.36	12.36	12.36	12.36
TOTAL	97.71	98.62	99.12	98.71	100.09	98.71	98.71	98.71	98.71	98.71	867.25
MANUFACTURING											
PLUNGS	4913.	3614.	4656.	42776.	45209.	40975.	36011.	35770.	33969.	32524.	391711.
LABOUR RATE	5.12	5.12	5.12	5.12	5.12	5.12	5.12	5.12	5.12	5.12	5.12
OVERHEAD RATE	10.72	10.72	10.72	10.72	10.72	10.72	10.72	10.72	10.72	10.72	10.72
TOTAL	16.84	16.84	16.84	17.07	17.07	16.84	16.84	16.84	16.84	16.84	6204.70
QUALITY CONTROL											
MURKS	7.02	7.02	7.02	6555.	9442.	8195.	7602.	7154.	6798.	6505.	76342.
LABOUR RATE	6.29	6.29	6.29	6.29	6.29	6.29	6.29	6.29	6.29	6.29	6.29
OVERHEAD RATE	10.72	10.72	10.72	10.72	10.72	10.72	10.72	10.72	10.72	10.72	10.72
TOTAL	14.62	14.62	14.62	14.62	14.62	14.62	14.62	14.62	14.62	14.62	1332.60
MATERIALS											
IRON AND PURCHASE	19.86	18.65	18.65	135.67	128.12	151.59	151.95	149.85	146.10	146.61	1313.25
PURCHASE EQUIP	123.79	125.46	127.40	51.95	53.05	267.10	282.40	276.29	275.04	272.27	2438.90
TOTAL	140.45	126.97	126.97	387.61	451.72	441.70	434.15	428.13	423.14	418.87	3752.15
MISCELLANEOUS											
MURKS	11.67	10.62	10.62	1711.	1107.	1629.	1520.	1431.	1360.	1301.	15668.
LABOUR RATE	5.12	5.12	5.12	5.12	5.12	5.12	5.12	5.12	5.12	5.12	5.12
OVERHEAD RATE	10.72	10.72	10.72	10.72	10.72	10.72	10.72	10.72	10.72	10.72	10.72
TOTAL	27.95	26.56	25.56	27.10	28.64	25.96	24.08	22.66	21.54	20.61	243.19
ENGINES											
AERONAUTICS	9.06	12.06	12.06	15.00	16.00	16.00	16.00	16.00	16.00	16.00	150.00
MURKS	116.12	142.14	142.14	140.66	152.84	141.80	133.94	128.04	123.30	119.38	1308.53
INSURANCE	114.04	116.08	116.08	114.05	116.05	116.05	116.05	116.05	116.05	116.05	1347.66
MATERIALS	67.34	58.04	58.04	58.04	58.04	58.04	58.04	58.04	58.04	58.04	554.26
TOTAL MATERIAT	102.92	116.14	116.21	2144.00	2401.26	2444.54	2129.96	2042.24	1972.01	1919.74	20514.41

ORIGINAL PAGE IS  
OF POOR QUALITY

LDCI SUMMARY					
	TOTAL*	INVESTMENT	TOTAL#	PER PKWU	DIRECT OPERATIONAL COST (DOC)
			A/C**		C/S*** PERCENT
PROTOTYPE MANUFACTURE	\$16,000	PRODUCTION AIRCRAFT	20514.41	68361.31	FLIGHT CREW 0.0 FUEL AND OIL
DESIGN & ENGINEERING	962.62	PRODUCTION ENGINEERING	0.0	0.0	0.08861 4.00115
DEVELOPMENT TEST ARTICLES	421.17				0.16495 9.58196
FLIGHT TEST	116.33				0.59507 30.83002
ENGINE DEVELOPMENT CRUISE	456.61				0.47713 24.71965
ENGINE DEVELOPMENT LIFT	0.0				TOTAL DOC 1.93016 100.000
AVIONICS DEVELOPMENT	0.0				INDIRECT OPERATIONAL COST (IOC)
MAINTENANCE TRAINERS	0.0	MAINTENANCE TRAINERS	0.0	0.0	C/S*** PERCENT
OPERATOR TRAINERS	0.0	OPERATOR TRAINERS	0.0	0.0	0.00363 0.42532
DEVELOPMENT BUILDING	642.97	MANUFACTURE FACILITY	433.61	1445.36	SYSTEM
SPECIAL SUPPORT EQUIPMENT	16.32	SPECIAL SUPPORT EQUIPMENT	0.1.09	2803.63	LOCAL
DEVELOPMENT SPARES	159.14	MANUFACTURE SPARES	3012.04	10040.40	AIRCRAFT CONTROL
TECHNICAL DATA	21.57	TECHNICAL DATA	124.01	413.33	LADIN ATTENDANT
TOTAL KULT	4336.61	TOTAL INVESTMENT	24925.14	63063.94	FOOD AND BEVERAGE
MISU. LATA		RETURN ON INVESTMENT (ROI)			PASSENGER HANDLING
KANCE (ST. MILLS)	483.11	TOTAL REVENUE PER YEAR *	469.74	OTHER PASSENGER EXPENSE	0.33550 37.26233
BLUCK SPEEDO MILEAGE	1249.03	TOTAL EXPENSE PER YEAR *	449.40	OTHER CARGO EXPENSE	0.00278 0.30851
FATK (S)	248.73	TOTAL INVESTMENT *	1301.05	GENERAL + ADMINISTR.	0.12334 13.69668
FLEET SIZE	13.54	FATI BEFORE TAXES	2.99	TOTAL IOC	0.90037 100.000
PRODUCTION DATA		200.00	1.55		
KEY-PASSENGERS (MIL. PKW YR)	1.01				* = MILLIONS OF DOLLARS
AVER. CARB. PKW FLIGHT	2.00				** = 1000 OF DOLLARS PER PRODUCTION A/C
FLIGHTS PER A/C PER YEAR	1000.41				*** = UENTS PER SEAT MILE

## KITSARAH DEVELOPMENT TEST AND EVALUATION (ROUTE)

	DEVELOPMENT AND TEST	CONTRACTOR TEST AND EVALUATION	DEVELOPMENT AIRCRAFT	TOTAL ROUT AND E
AIRCRAFT	1517.41	467.40	636.94	2622.24
ENGINEERING				
MURKS	5510.0	10146.0	3162.0	5847.0
LABUK RATE	1.017	6.17	6.17	8.17
OVERHEAD RATE	5.420	9.20	9.20	9.20
TOTAL	784.00	174.24	54.63	1015.76
BUILDING				
FURKS	3644.0	2021.0	5242.0	44187.0
LABUK RATE	1.000	6.09	6.09	6.09
OVERHEAD RATE	1.000	12.36	12.36	12.36
TOTAL	125.00	45.36	96.71	178.08
MANUFACTURING				
MURKS	10489.0	10489.0	20567.0	31451.0
LABUK RATE	5.12	5.12	5.12	5.12
OVERHEAD RATE	10.72	10.72	10.72	10.72
TOTAL	166.06	166.06	332.12	498.16
QUALITY CONTROL				
MURKS	2097.0	4193.0	4193.0	6290.0
LABUK RATE	6.29	6.29	6.29	6.29
OVERHEAD RATE	10.72	10.72	10.72	10.72
TOTAL	35.07	71.32	71.32	107.00
MATERIAL				
KAW AND PACHAU	12.05	24.10	24.10	36.15
PUCHASU EQUIP	22.36	34.43	44.76	67.14
TOTAL	34.43	65.56	65.56	103.29
MISCELLANEOUS				
MURKS	419.0	839.0	839.0	1254.0
LABUK RATE	5.12	5.12	5.12	5.12
OVERHEAD RATE	10.72	10.72	10.72	10.72
TOTAL	0.64	13.28	13.28	19.93
ENGINES	45.01	80.04	80.04	1042.65
AVIONICS	0.00	2.00	2.00	2.00
PROFILATE (PERMATE)	22.74	70.11	95.54	393.34
INSURANCE FEES				
MARRANTY				
SUBTOTAL	2762.20	537.51	916.06	4155.76
OTHER ITEMS				179.05
TOTAL (ROUTE)				4334.81

17-53

ORIGINAL PAGE IS  
OF POOR QUALITY



## INITIAL MISSION SID DAY + 14.4 hr

	V/C	Air	W/S	F/W
	2.65	1.62	69.2	0.477

## WEIGHT SITUATION

	WEIGHT (POUNDS)	WEIGHT FRACTION (PERCENT)
TOTAL WEIGHT	1 750000.0	
FUEL AVAILABLE	277676.	FUEL
ZERO FUEL WEIGHT	362125.0	
PAYOUT	49000.	PAYOUT
OPERATING WEIGHT	313125.0	
OPERATING ITEMS	5473.	OPERATING ITEMS
STANDARD ITEMS	5329.	
EMPTY WEIGHT	302323.0	
WING	6436.	
TAIL	11339.	
BODY	4268.	STRUCTURE
LANDING GEAR	30+01.	
SURFACE CLOTHES	5500.	
NACELLE AND ENGINE SECTION	2616.	
PROPELLER	79165.0	PROPELLER
WINGLET/LIFT DEVICES	0.	
VEHICLE CONTROL SYSTEM	0.	
ENGINES	5112.	
TRANSI REVERSAL	0.	
FAIRING INJECTION SYSTEM	20752.	
FUEL SYSTEM	5676.	
ENGINE CONTROLS + SHIMM	1651.	
TRANSISTORS	1246.	
MATERIALS	5700.	
ELECTRICAL	4536.	
AVIONICS	1900.	
FURNISHINGS AND EQUIPMENT	11500.	EQUIPMENT
ENVIRONMENTAL CONTROL SYSTEM	1300.	
AUXILIARY POWER	1960.	
A.M.R.H.	43342.0	TOTAL
	100.00	
EXCESS FUEL CAPACITY - TALLY	36211.	
EXCESS FUEL CAPACITY - MIN	0.	
EXCESS LOAD LENGTH - PI	6.0	
STRUCTURE ALUMINUM		

17-55

ORIGINAL PAGE IS  
OF POOR QUALITY

## WEIGHTS MATRIX

ELEMENT / MATERIAL	AL	III.	STEEL	CMP.	OTHER	TOTAL
WING	4114.	76555.	1789.	5545.	1431.	89434.
TAIL	510.	10524.	113.	0.	181.	11339.
FUSEL	1964.	33895.	768.	1067.	4995.	42666.
L.O. b.	30.	7600.	11674.	0.	11096.	30601.
NACELL	107.	834.	1667.	0.	0.	2608.
AIR INDUC	955.	18389.	208.	0.	1204.	26755.
S. LIDS	2040.	363.	1765.	126.	4165.	8500.
Total:	9720.	146189.	18204.	6740.	23072.	205425.

## CONFIGURATION GEOMETRY

BASIC WING—	AREA(SQ.FT)	SPAN(FT)	TAKE OFF	C/4 SWEEP	L.E. SWEEP	CR(FT)	MAG(FT)
INDIVIDUAL WING—	AREA(SQ.FT)	EXP. AREA L.E. SWEEP	REF LIFT	SF(LSQ.FT)	Avg 1/C		
INDIVIDUAL WING—	AREA(SQ.FT)	9330.0	72.50	101.12	0.0	2.05	
INDIVIDUAL WING— AREA(SQ.FT)	Y BBR(FT) L.E. SWEEP	REF LIFT	SF(LSQ.FT)	Avg 1/C			
TOTAL WING—	AREA(SQ.FT)	0.0	72.50	101.12	0.0	2.05	
TOTAL WING—	AREA(SQ.FT)	EFF. AR	Avg 1/C	UN(FT)	LIFT	P	
WING TANK—	1.02	1.02	2.65	163.35	6.0	0.315	0.369
TOTAL TANK—	0.0	0.0	0.0	4482.83	2763.53		
TAIL —	LENGTH(FT)	S. MEL(SQ.FT)	SWN(FT)	SW(SQ.FT)	SW(SQ.FT)		
TAIL —	27.00	7876.0	9.47	13.22	137.36		
WHEELS —	WHEEL	SWL(SQ.FT)	SWB(CU.FT)				
WHEELS —	2.00	11.50	9177.00	20000.00			
WHEELS —	10.50	914.00	23.50	400.00	406.00	25.00	
WHEELS —	7.00	7.00	0.03	3955.73	4.0	0.0	

## MISSION SUMMARY

INTERNATIONAL MISSION SITE DAY • 14.4 F

SEGMENT	INITIAL ALTITUDE (FT)	INITIAL MACH NO.	INITIAL FUEL (LB)	INITIAL WEIGHT (LB)	STOCH TOTAL DIST (IN MIL) (IN MI)	STOCH TOTAL TIME (MIN)	STOCH TOTAL TIME (MIN)	STORE TAB ID	ENGINE TAB ID	EXTERN TAB ID	Avg L/D	Avg SPC RATIO	Avg (FF/T)	MAX OVER PRES	
<u>TAKEOFF</u>															
POWER 1	6.0	0.0	750000.	3569.	0.	0.	10.0	0.	-97101.	0.	0.0	0.571	0.0		
POWER 2	0.0	0.500	7464.51.	0.036.	4615.	0.	0.5	10.5	0.	97201.	0.	5.18	1.308	0.0	
CLIMB	0.0	0.500	7463.55.	7162.	1e177.	4.	4.	1.1	11.5	0.	97201.	0.	7.45	1.446	0.0
CRUISE	5000.	0.413	7332.23.	4299.	21676.	0.	4.	15.5	0.	-97101.	0.	6.24	0.727	0.0	
ACCEL	5000.	0.413	7334.24.	1771.	22847.	1.	0.	0.3	15.5	0.	97201.	0.	9.96	1.472	0.0
CLIMB	5000.	0.531	7271.53.	2500.	45355.	36.	42.	4.7	20.5	0.	97201.	0.	11.25	1.508	0.0
CLIMB	34000.	0.494	7145.44.	49355.	44690.	255.	297.	1e-3	34.6	0.	97201.	0.	8.32	1.533	0.0
CLIMB	0.0	0.03	655510.	6.	40690.	0.	297.	0.0	34.8	0.	97201.	0.	8.73	1.563	0.0
CRUISE	60000.	2.62	655310.	224611.	314501.	3693.	3990.	144.7	179.5	0.	-97201.	0.	6.61	1.498	0.0
DECEL	73000.	2.062	436449.	96.	314396.	22.	4013.	0.4	160.4	0.	97501.	0.	6.42	-0.769	0.0
DESCENT	73000.	2.0309	436605.	1201.	320676.	154.	4166.	13.1	193.5	0.	97501.	0.	9.15	-0.386	0.0
DESCT 1	5000.	0.0	424322.	0.	320676.	0.	4166.	0.0	193.5	0.	0.	0.	0.0	0.0	0.0
CRUISE	5000.	0.413	424542.	4643.	323321.	0.	4166.	5.0	196.2	0.	-97101.	0.	11.17	0.829	0.0
DESCT 2	0.	0.0	426679.	0.	323321.	0.	4166.	0.0	198.5	0.	0.	0.	0.0	0.0	0.0
DESCT 3	0.	0.0	426679.	0.	323321.	-4166.	0.	*****	0.0	0.	0.	0.	0.0	0.0	0.0
RESERVE	0.	0.0	424674.	22332.	345455.	0.	0.	0.0	0.0	0.	0.	0.0	0.0	0.0	0.0
CLIMB	0.	0.466	444047.	2751.	348764.	2.	2.	0.4	0.4	0.	97201.	0.	9.71	1.444	0.0
CLIMB	1500.	0.50	401245.	132704.	362624.	22.	23.	3.0	3.4	0.	97201.	0.	9.85	1.504	0.0
CRUISE	43000.	0.466	317476.	16402.	372426.	167.	190.	19.0	22.4	0.	-97101.	0.	10.93	0.937	0.0
DESCT 1	43600.	0.966	377573.	774.	373200.	56.	246.	7.9	30.3	0.	97501.	0.	9.89	-0.491	0.0
CRUISE	43000.	0.466	376166.	756.	373457.	12.	260.	1.4	31.7	0.	-97101.	0.	10.92	0.938	0.0
DESCT 2	1500.	0.50	276144.	15416.	387668.	0.	260.	30.0	61.7	0.	-97101.	0.	11.29	0.851	0.0
Total k= 750000.0 Fuel k= 367667.6 Full k= 367667.6															

17-57

ORIGINAL PAGE IS  
OF POOR QUALITY

PRODUCTION

		1	2	3	4	5	YEARS	6	7	8	9	10	TOTAL
AIRFRAME		1724.50	1141.42	1267.29	1341.02	1512.00	1402.42	1325.60	1266.62	1219.90	1181.15	12945.97	
LASHES		4.560.	376.0	2982.	4231.	4472.	4053.	3760.	3538.	3362.	3217.	38746.	
HOURS		6.17	6.17	6.17	6.17	6.17	b.17	b.17	b.17	b.17	6.17		
LABOUR HIRE		9.42	9.42	9.42	9.42	9.42	9.42	9.42	9.42	9.42	9.42		
OVERHEAD HIRE		65.32	65.32	69.16	73.50	77.68	70.40	65.31	61.46	57.40	55.86	673.01	
TOTAL													
LASHING		524.2.	431.5.	4116.	567.7.	5367.	4464.	4512.	4246.	4034.	3860.	46495.	
HOURS		6.04	6.04	6.04	6.04	6.04	6.04	6.09	6.09	6.09	6.09		
LABOUR HIRE		12.36	12.36	12.36	12.36	12.36	12.36	12.36	12.36	12.36	12.36		
OVERHEAD HIRE		13.31	13.31	13.31	13.31	13.31	13.31	13.31	13.31	13.31	13.31	1857.83	
TOTAL													
MANUFACTURING		4366.4.	3762.6.	29817.	42312.	44716.	40530.	37596.	35382.	33620.	32171.	38746.	
HOURS		5.12	5.12	5.12	5.12	5.12	5.12	5.12	5.12	5.12	5.12		
LABOUR HIRE		10.72	10.72	10.72	10.72	10.72	10.72	10.72	10.72	10.72	10.72		
OVERHEAD HIRE		630.76	630.76	630.76	630.76	630.76	630.76	630.76	630.76	630.76	630.76	6137.33	
TOTAL													
QUALITY CONTROL		8757.	7524.	7933.	8412.	8944.	6106.	7520.	7076.	6724.	6434.	77492.	
HOURS		6.29	6.29	6.29	6.29	6.29	6.29	6.29	6.29	6.29	6.29		
LABOUR HIRE		10.72	10.72	10.72	10.72	10.72	10.72	10.72	10.72	10.72	10.72		
OVERHEAD HIRE		122.01	122.01	122.01	122.01	122.01	122.01	122.01	122.01	122.01	122.01	1318.13	
TOTAL													
MATERIAL		65.51	65.51	111.51	124.29	156.52	153.03	150.41	148.53	146.60	145.12	1299.96	
RAW AND PURCHASED		165.72	207.06	249.40	290.50	264.20	279.34	275.47	272.25	269.51	264.21		
PURCHASED EQUIPMENT		211.59	211.59	263.69	447.20	427.23	425.76	425.76	425.80	416.63	3714.17		
TOTAL													
MISCELLANEOUS		1747.	156.	156.	162.	1762.	1621.	1504.	1415.	1345.	1287.	15498.	
CHAMPS		5.12	5.12	5.12	5.12	5.12	5.12	5.12	5.12	5.12	5.12		
LABOUR HIRE		10.72	10.72	10.72	10.72	10.72	10.72	10.72	10.72	10.72	10.72		
OVERHEAD HIRE		21.44	21.44	25.23	26.61	26.33	25.68	23.82	22.42	21.30	20.38	245.49	
TOTAL													
ENGINES		210.72	210.72	204.65	352.70	395.71	360.64	367.40	357.01	348.50	341.33	3322.48	
AVIATION		4.00	4.00	12.00	15.00	18.00	18.00	18.00	18.00	18.00	18.00	150.00	
PROPL		172.04	172.04	190.09	206.77	226.90	210.44	196.84	196.02	182.98	177.17	1941.90	
INSURANCE		122.04	114.84	126.75	139.16	151.27	146.29	132.56	126.68	121.99	118.12	1294.60	
MARKETING		21.47	57.47	63.56	69.55	75.63	70.15	66.26	63.34	60.99	59.06	647.30	
TOTAL FLYAWAY		1826.92	1756.67	1964.12	2177.14	2382.19	2222.44	2106.68	2021.87	1952.37	1900.64	20308.05	

## COST SUMMARY

ITEM	TOTAL*	INVESTMENT		PER PLNG A/C/P*	DIRECT OPERATIONAL COST (DOCC)
		TOTAL*	PER PLNG A/C/P*		
PRODUCTION AIRCRAFT	4,644	PRODUCTION AIRCRAFT	203,605	6,7693.44	FLIGHT CREW 0.08896 4.64209
DESIGN ENGINEERING	652.10	PRODUCTION ENGINEERING	0.0	0.0	FUEL AND OIL 0.57925 30.21986
DEVELOPMENT TEST ARTICLES	416.00				INSURANCE 6.16551 9.57358
FLIGHT TEST	114.00				DEPRECIATION 0.59043 30.80304
ENGINE DEVELOPMENT COSTS	556.01				MAINTENANCE 6.47462 24.76144
ENGINE DEVELOPMENT LIFO	0.0				TOTAL DUE 1.91679 100.000
AIRCRAFT DEVELOPMENT	0.0				
Maintenance training utvts	0.0	Maintenance Training	0.0	0.0	DIRECT OPERATIONAL COST (DOCC)
OPERATOR MAINTENANCE	0.0	operator training	0.0	0.0	L/SHARE PERCENT
DEVELOPMENT TRAINING	0.0	PRODUCTION TRAINING	422.32	1441.08	0.00361 0.42359
SPECIAL SURVEY EQUIPMENT	16.00	SPECIAL SURVEY EQUIPMENT	32.03	2775.43	LUGAL 0.19186 21.30754
DEVELOPMENT SPARES	1.700	PRODUCTION SPARES	2963.04	9945.46	AIRCRAFT CONTROL 0.00517 0.57414
TECHNICAL DATA	41.00	TECHNICAL DATA	122.76	409.26	CABIN ATTENDANT 0.00652 7.60923
TOTAL KLT	4246.00	INITIAL INVESTMENT	24679.41	82264.64	FUGU AND BEVERAGE 0.02366 2.62962
MKT. DATA		RETURN ON INVESTMENT (ROI)			PASSENGER HANDLING 0.13766 15.28798
FARE (1st. MILLE)	4744.00	1ST. REVENUE PER YEAR *	466.11		CARGO HANDLING 0.00856 0.95030
BLK. SPRT. (MTH)	1.347.00	1ST. EXPENSE PER YEAR *	443.71		OTHER PASSENGER EXPENSE 0.33550 37.25967
FARE (2)	240.00	2ND. INVESTMENT *	1346.46		OTHER CARGO EXPENSE 0.00278 0.30849
FARE SIZE	12.00	2ND. EXPENSE PER YEAR *	3.34		GENERAL + ADMINISTR. 0.12290 13.64942
PRODUCTION COSTS		REV. AFTER TAXES	1.74		TOTAL LOC 0.90044 100.000
REV. PASSENGERS (MILLION YR.)	1.01				
AVG. LAKSH. PER FLIGHT	2000.00				*
FARE PER A/C PER YEAR	1011.54				** - MILLIONS OF DOLLARS
					*** - 1000 OF DOLLARS PER PRODUCTION A/C
					**** - CENTS PER SEAT MILE

17-59

ORIGINAL PAGE IS  
OF POOR QUALITY

## RESEARCH, DEVELOPMENT, TEST AND EVALUATION (ROUTE)

	DEVELOPMENT AND TEST	CONTRACT TEST AND EVALUATION	DEVELOPMENT AIRCRAFT	TOTAL ROT AND E
AIRCRAFT	156,653	462,19	630,07	2597.90
ENGINES	4,216			
MURKS	106,272	8.17	8.17	8.17
LABOR RATE	9.20	9.20	9.20	9.20
OVERHEAD RATE	174.17		54.04	1006.56
TOTAL				
INDULING				
MURKS	36,440	2592.	5165.	43617.
LABOR RATE	1.04	6.09	6.09	6.09
OVERHEAD RATE	12.36	12.36	12.36	12.36
TOTAL	747.02	474.83	95.66	670.77
MANUFACTURING				
MURKS	19370.	20740.	20740.	31109.
LABOR RATE	5.12	5.12	5.12	5.12
OVERHEAD RATE	10.72	10.72	10.72	10.72
TOTAL	164.26		326.51	492.77
QUALITY CONTROL				
MURKS	2079.	4149.	4149.	6222.
LABOR RATE	6.29	6.29	6.29	6.29
OVERHEAD RATE	10.72	35.21	70.56	10.72
TOTAL				105.83
MATERIAL				
KAN AND PRACTICAL	11.93	23.66	23.66	35.79
PURCHASED EQUIP	22.15	54.00	44.31	66.16
TOTAL				66.46
MISCELLANEOUS				
MURKS	415.	830.	830.	1244.
LABOR RATE	5.12	5.12	5.12	5.12
OVERHEAD RATE	10.72	10.72	10.72	10.72
TOTAL	5.57	13.14	13.14	19.71
ENGINES				
AIRUNIC	45.39	2.00	2.00	2.00
PROUTIAIRKAM	64.223	94.51	94.51	389.48
INJURIAIRKAM		63.01	63.01	63.01
MAKKANI		31.50	31.50	31.50
SUBTOTAL	531.52	966.48	966.48	4119.49
GREN ITEMS				177.31
TOTAL				4296.80

ORIGINAL PAGE IS  
OF POOR QUALITY

SUMMARY & NOTES 165

卷之三

אוגוסט 1934 גז עז

RIGHT 1-C-07000  
SLS STAGE 1-C-70000  
NUMBER OF ENGINES = 4  
RIGHT QUARTER CIRCLE STEP = 68-63 DEG  
RIGHT TAPIC FAILO = 0.0



SECTION 18

DESIGN

BY

C.W. LINDBLOM



## TABLE OF CONTENTS

<u>Section</u>	<u>Page</u>
INTRODUCTION	18-1
DESIGN APPROACH	18-3
Joining Methods	18-3
Design Ground Rules and Constraints	18-6
STRUCTURAL DESIGN — TASK I	18-9
Chordwise Stiffened Wing Design — Fasteners	18-9
Spanwise Stiffened Wing Design — Fasteners	18-17
Monocoque Wing Design — Fasteners	18-22
Monocoque Wing Design — Welded	18-30
Composite Reinforced Wing Design — Fasteners	18-35
Skin-Stringer and Frame Fuselage Design — Fasteners	18-35
Sandwich Shell Design — Welded	18-40
Design Problem Areas	18-43
DETAILED DESIGN — TASK II	18-45
Design Objectives	18-45
Scope of Design Studies	18-45
Wing Structure Design	18-46
Fuselage Structure Design	18-59
Potential Problems Not Resolved During Study — Design and Manufacture	18-60
Components for Further Evaluation and Test	18-61
REFERENCES	18-67



## LIST OF FIGURES

<u>Figure</u>		<u>Page</u>
18-1	Chordwise Stiffened Wing Design - Fasteners	18-11
18-2	Installation Space Requirements for Various Fasteners	18-15
18-3	Spanwise Stiffened Wing Design - Fasteners	18-19
18-4	Monocoque Wing Design - Fasteners	18-23
18-5	Monocoque Wing Design - Welded	18-31
18-6	Typical Module for Welded Sandwich Wing Structure	18-33
18-7	Composite Reinforced Wing Design - Fasteners	18-37
18-8	Sandwich Shell Design - Welded	18-41
18-9	Structural Design Concept - M2.7 Arrow-Wing Supersonic Transport Configuration (Near-Term)	18-47
18-10	Structural Design Concepts - Surface Panels and Substructure	18-49
18-11	Attachment of Truss Spar to Low Pressure Diffusion Bonded Surface	18-52
18-12	Structural Design Concepts - Truss Spar and Surface Panel at Transition Structure	18-53
18-13	Structural Design Concepts - Tank Sealing Concept and Rib Details	18-57

*PRECEDING PAGE BLANK NOT FILMED*



LIST OF TABLES

<u>Table</u>		<u>Page</u>
18-1	Vendor Contacts Made for Arrow-Wing Structures Study	18-2
18-2	Evaluation of Structural Approaches - Task I	18-4
18-3	Potential Problem Not Resolved - Wing Surface Panel Concept - Convex Beaded	18-61
18-4	Potential Problems Not Resolved - Wing Span Concept - Composite Reinforced Titanium Alloy Caps	18-62
18-5	Potential Problems Not Resolved - Wing Surface Panel Concept - Honeycomb Sandwich	18-62
18-6	Potential Problem Not Resolved - Fuselage Shell Concept - Skin and Stringer	18-63
18-7	Potential Problems Not Resolved - Tank Sealing Concept	18-63
18-8	Test Objectives	18-65
18-9	Fabrication Process Tests	18-65
18-10	Structural Element and Component Tests	18-66

PRECEDING PAGE BLANK NOT FILMED



## SECTION 18

### DESIGN

#### INTRODUCTION

An important facet of the structural design concepts study is the establishment of a firm design technology base that will permit the best possible judgement to be exercised in the selection of structural concepts and materials for the next generation supersonic transport. This design technology base was determined with the full consideration of:

- the practically obtainable benefits of applicable advanced technology
- the internal structural response to the complex interactions among inertial, aerodynamics and thermal loadings
- the effects of various structural arrangements, concepts and materials on these interactions

An underlying objective was the achievement of the minimum possible structural mass fraction since the economic effectiveness of the supersonic cruise aircraft is critically sensitive to inert mass as well as aerodynamic and propulsive efficiencies.

In approaching this task the following were identified as encompassing the potential for structural mass reduction:

- Improved titanium alloys (beta alloys)
- Improved fatigue quality through minimizing fasteners by the use of welding, bonding, brazing, weld bonding, weld brazing and rivet bonding
- Large scale fabrication to minimize the number of joints
- Minimizing or eliminating tank sealing by the use of large scale application of welding, bonding and brazing
- Selective reinforcing of metal structure with organic and metal matrix composites

- Determining the structural arrangements most efficient in coping with the interactive loading of a large, flexible arrow-wing
- Determining the most efficient structural concepts within these structural arrangements

The initial design effort was devoted to the establishment of the baseline configuration concepts and the subsequent development of internal details to provide inputs to mass distribution and other studies included in the structural study effort. The various drawings developed are presented in Section 2, Baseline Configuration Concept. The development of these drawings made full use of the information of Reference 1.

In developing the structural arrangement drawings for the various wing and fuselage design approaches, an extensive background of design data was available from the design and manufacturing studies of advanced structural designs having potential application in a Mach 2.7 arrow-wing configuration transport. These studies included numerous consultations with vendors (Table 18-1) and other contractors, extensive literature surveys and close collaboration with producibility personnel. This background data was fully utilized in the structural arrangement drawings discussed in the subsequent sections as well as in the determination of the design parameters (Section 8).

TABLE 18-1. VENDOR CONTACTS MADE FOR ARROW WING STRUCTURES STUDY

<u>Vendor</u>	<u>Subject Discussed</u>
Aeronca Mfg.	Aluminum Brazed Honeycomb Sandwich
Rohr Aircraft	Liquid Interface Diffusion (LID) Diffusion Braze Process
Northrop Aircraft	Nor-Ti-Bond Diffusion Braze Process
TRW Systems	Weld Bond
Advanced Structures and Technology Co.	STRESSKIN
Sciaky Brothers, Inc.	Welding
Avco	Metal Matrix Composites
Holosonics	NDT Inspection Methods

## DESIGN APPROACH

The various approaches in the arrangement of surface panel concepts and structure for primary structure design are presented in Section 1, Structural Design Concepts. The evaluation rationale of the structural approaches was also presented (Table 18-2). Each step of the procedure was outlined from:

- (1) Establishing the material system
- (2) Defining the fabrication and/or assembly method for the candidate concepts
- (3) Conducting the design analysis according to the guidelines defined
- (4) Establishing mass and cost data, and
- (5) Evaluating the results and selecting the most promising arrangement for further detailed study.

## Joining Methods

A vital part of the study matrix (Table 18-2) is the evaluation of the joining methods. These are important parameters because of their influence on such factors as:

- Fatigue quality and damage tolerance
- Manufacturing cost, facilities and techniques
- Serviceability and maintainability
- Fuel tank sealing
- Thermal stresses, residual stresses, and mass

Based on the comprehensive investigation into the various joining methods and their applicability to the candidate structural design concepts, two methods were selected as identified in the Fabrication and/or Assembly column of Table 18-2.

TABLE 18-2. EVALUATION OF STRUCTURAL APPROACHES – TASK I

MACH 2.7 - NEAR TERM START OF DESIGN

MATERIALS	STRUCTURAL ARRANGEMENTS	FABRICATION AND/OR ASSEMBLY	FABRICATION AND STRUCTURAL ARRANGEMENT TRADE-OFF	DESIGN GUIDELINE AND EVALUATION DATA		EVALUATION AND SELECTION
				IMPORTANCE OF:	EVALUATION OF:	
	<ul style="list-style-type: none"> <li>STRUCTURAL CONCEPTS           <ul style="list-style-type: none"> <li>• SPARS</li> <li>• RIBS</li> <li>• COVERS</li> <li>• FRAMES</li> </ul> </li>   <li>• BI-AXIALLY STIFFENED</li>   <li>• SPANWISE STIFFENED</li>   <li>• CHORDWISE STIFFENED</li> </ul>	<ul style="list-style-type: none"> <li>WELDED</li> <li>FASTENERS</li> <li>FASTENERS</li> <li>FASTENERS</li> </ul>	<ul style="list-style-type: none"> <li>WELDING VS FASTENERS</li> <li>AL BRAZED Ti HONEY COMB.</li> <li>FATIGUE QUALITY</li> <li>TANK SEALING (FASTENERS) VS WELDED</li> <li>BI-AXIAL VS SPANWISE VS CHORDWISE STIFFENING</li> <li>ALL METAL VS COMPOSITE REINFORCED METAL</li> <li>FASTENERS</li> <li>CHORDWISE STIFFENED</li> <li>CHORDWISE STIFFENED, SELECTIVE COMPOSITE REINFORCED</li> <li>FUSELAGE SKIN, STRINGER FRAME</li> </ul>	<ul style="list-style-type: none"> <li>• FATIGUE QUALITY</li> <li>• TANK SEALING</li> <li>• DAMAGE TOLERANCE</li> <li>• STRUCTURAL APPROACH</li> <li>• ARRANGEMENT</li> <li>• COVER, RIB, SPAR AND FRAME CONCEPTS</li> <li>• WING-BODY INTERFACE</li> <li>• THERMAL STRESSES</li> <li>• CONTROL SYSTEM</li> <li>• FLUTTER</li> <li>• STATIC AERO-Elasticity</li> <li>• FUEL VOLUME REQD</li> <li>• MATERIAL SELECTION</li> <li>• METALS</li> <li>• COMPOSITES</li> </ul>	<ul style="list-style-type: none"> <li>• IDENTIFY STRUCTURAL APPROACHES BEST SUITED FOR WING AND FUSELAGE</li> <li>• MATERIALS MERITING FURTHER DETAILED DESIGN &amp; ANALYSIS</li> <li>• EASE OF FABRICATION AND ASSEMBLY</li> <li>• MATERIAL AND FABRICATION COST</li> <li>• MAINTAINABILITY AND SERVICEABILITY</li> </ul>	

- The "fastener" joining method is taken as a baseline case and is investigated for all wing and fuselage structural arrangements.
- The two joining methods (welding and fasteners) are considered for the monocoque wing arrangements.

The logic behind this reduced matrix is that the study of the two methods noted above will yield sufficient data concerning the merits of each fabrication and/or assembly method to permit valid projections to be made concerning the effects of joining methods on the spanwise and chordwise stiffened wing arrangements without the need for a design development effort for each individual joining method. Titanium alloy Ti 6Al-4V is taken as the baseline metal for the design study even though Beta C and other titanium alloys were investigated.

As a matter of clarification, the joining methods described herein are concerned with methods used to assemble major components (wing surface assemblies, spar assemblies, etc.) to their next assembly. It does not imply that all attachments within these major components use the same joining method. For example:

- A wing structure design using honeycomb sandwich surface panels attached to substructure by fasteners is included in the "fastener" assembly concept even though the surface panels themselves might be fabricated as aluminum brazed, bonded or welded honeycomb sandwiches.
- A fuselage structure design with skin panel assemblies joined together by fasteners also is classified under the "fastener" concept even though stringers, frame segments and other detail parts of skin panel assemblies are attached by weld bonding, brazing or other means.

## Manufacturing/Subcontracting/Facilities Guidelines

The focus on the method of joining major components reflects the complexity required in manufacturing equipment, facilities and techniques. For example, the "fastener" concept permits conventional manufacturing approaches to be utilized. In contrast, the "welding" designation indicates that complex and expensive facilities and equipment may be required for manufacturing and maintenance. These factors relate to a number of items, including the feasibility of a particular "design go-ahead" date.

The interpretations above permit subassemblies to utilize advanced assembly processes, such as weld bonding, weld brazing and others, consistent with the assumed "design go-ahead" and the fabrication and transportation size limits established.

Guidelines in reference to manufacturing, subcontracting and facilities were established considering the above to aid in the design process. The guidelines, discussed in Section 7, Materials and Producibility and Section 8, Basic Design Parameters, are summarized below:

- The entire fuselage, except for the flight station, is designed for subcontracting (and transportation limitations).
- All wing segments, and the complete wing, to be assembled in a new facility assumed to be constructed in Palmdale. Wing components, such as spars and ribs, to be suitable for subcontracting.
- The new Palmdale facility is postulated to have autoclave and fusion and spot welding equipment suitable for fabricating large components.
- Fuselage segment joints need not coincide with wing segment joints.

## Design Ground Rules and Constraints

The ground rules enumerated below were established at the beginning of the study and are presented to define the basis for the design effort. Some of these rules might be modified by new developments or as a result of further study. Specific guidelines for manufacturing are presented in Section 7, Materials and Producibility.

- Minimum mass is the primary design objective.
- Design work is initially based on all-metal structure reflecting the technology level for a design go-ahead at the end of 1975. This technology level is expanded to include selective reinforcing of the metal structure with composites considering a design go-ahead in 1981.
- Bonding, weld bonding, rivet bonding, weld brazing and the aluminum braze (Aeronca) processes are postulated to be developed adequately and available for use.
- TIG, plasma arc and EB welding acceptable but laser welding not yet qualified.
- Component size limits, as dictated by fabricating processes, to be:
  - Hot vacuum forming - 15 feet wide by 35 feet long
  - Aluminum brazed sandwich - 68 inch wide by 40 feet long
  - Weld bonded and rivet bonded panels - 15 feet wide by 50 feet long
- Component size limits, as dictated by transportation method, defined in Section 7, Materials and Producibility.
- Structure to have an economic service life of 15 years, a service life of 50,000 flight hours, a design fatigue life of twice the service life and damage-tolerant structural concepts where possible.
- Structure design to be based on Mach 2.7 cruise speed.
- Fuel tank access to be provided by a minimum of 2 doors for each fuel tank or isolated portion thereof. Access opening size to be approximately 13 x 18 inches for vertical entry and 20 x 31 inches for horizontal entry.
- Minimum skin gauges (inch) to be:
  - 0.020 for exterior skins on the wing lower surface
  - 0.015 for exterior skin on the wing upper surface
  - 0.010 for the interior face of a sandwich

- All fasteners in exterior surface to be flush.
- External splice strap acceptable at all longitudinal panel splices in the fuselage and at BL 470 joint in the wing.
- At countersunk fasteners, the face sheet thickness shall be at least 0.010 inches greater than the countersink depth to avoid "feather edges" and degraded quality. This rule might be waived in joints where the reduced allowables and degraded quality resulting from feather edges are acceptable.
- Frame locations different from spar locations are considered acceptable but will be used only where an overall advantage is indicated after evaluation of any extra material required to redistribute and/or account for loadings encountered at BL 62.41 rib.
- For welded/corrugated web spars and ribs, it is assumed that the cap strips should be normal to the plane of the web. (Note: subsequent meetings with Sciaky welding specialists indicate the feasibility of welding caps to webs at angles varying as much as 15-degrees from normal to the web).
- Manually upset Ti rivets (B-120 and Beta C) limited to 0.156 inch diameter maximum.
- All Ti Hi-Tigue fasteners to have studs of Ti-6Al-4V in the STA condition.
- Shear (shallow) head flush fasteners acceptable in the outer skin.
- Single row of fasteners unacceptable at skin panel joint if the joint must be fuel tight.
- For welded joints:
  - Manual welding limited to an absolute minimum
  - Skin splice welds planished
  - All welds to be the butt type
  - All welds shaved on all surfaces unless impossible
  - Welds are designed for stress relieving where feasible. However, welded spars and ribs will not be stress relieved. Note that welded joints in members which are later hot formed are stress-relieved automatically.

- In the primary structure, access doors are to be the "clamped" type where feasible to avoid fastener holes in primary structure.
- From the manufacturing standpoint, blind fasteners are preferred over access doors.

Further study and development may indicate the need for amplification and/or modification of the above rules.

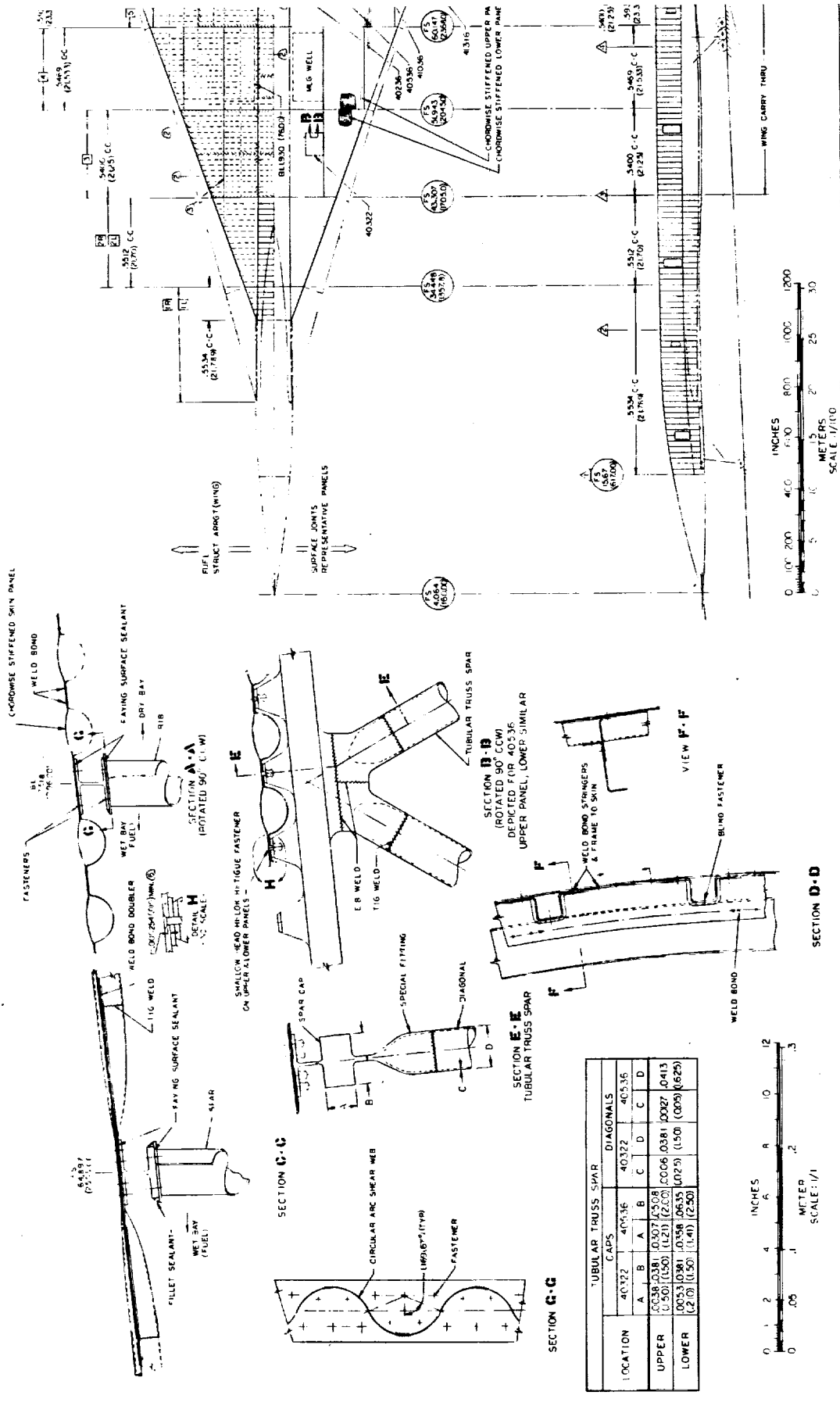
#### STRUCTURAL DESIGN — TASK I

##### Chordwise Stiffened Wing Design — Fasteners

The structural arrangement drawing in the chordwise stiffened wing design is presented in Figure 18-1. The arrangement of the substructure, fuel tanks and surface panel joints for the representative panels are indicated on the airplane planform. The highly efficient convex beaded surface panel design is shown with discrete submerged spar caps used to transmit the wing spanwise bending loads. Representative spar cap and truss-web geometry are indicated for selected point design regions identified on the wing planform. General features for this design are enumerated below:

- Double-skin wing surfaces in which both the inner and outer skins contain a series of chordwise-oriented stiffening beads.
- Numerous spanwise spars which are of truss design except where a spar serves as a fuel tank wall or a fuel surge pressure spar. Where spar depth or loading so dictates, the truss spar design may be replaced by a stiffened web or other arrangement.
- At fuel tank wall and fuel baffle locations, the spars have welded corrugated webs and I-section caps.
- Relatively few chordwise ribs are used. These also are of the truss type design except where the rib serves as a tank wall or baffle. In such applications, welded corrugated webs and I-section caps are used.
- Spars are spaced relatively close in the main wing box behind the main landing gear (MLG) well.





---

PRECEDING PAGE BLANK NOT FILMED

FINAL PAGE IS  
OF POOR QUALITY

FOLDOUT FRAME



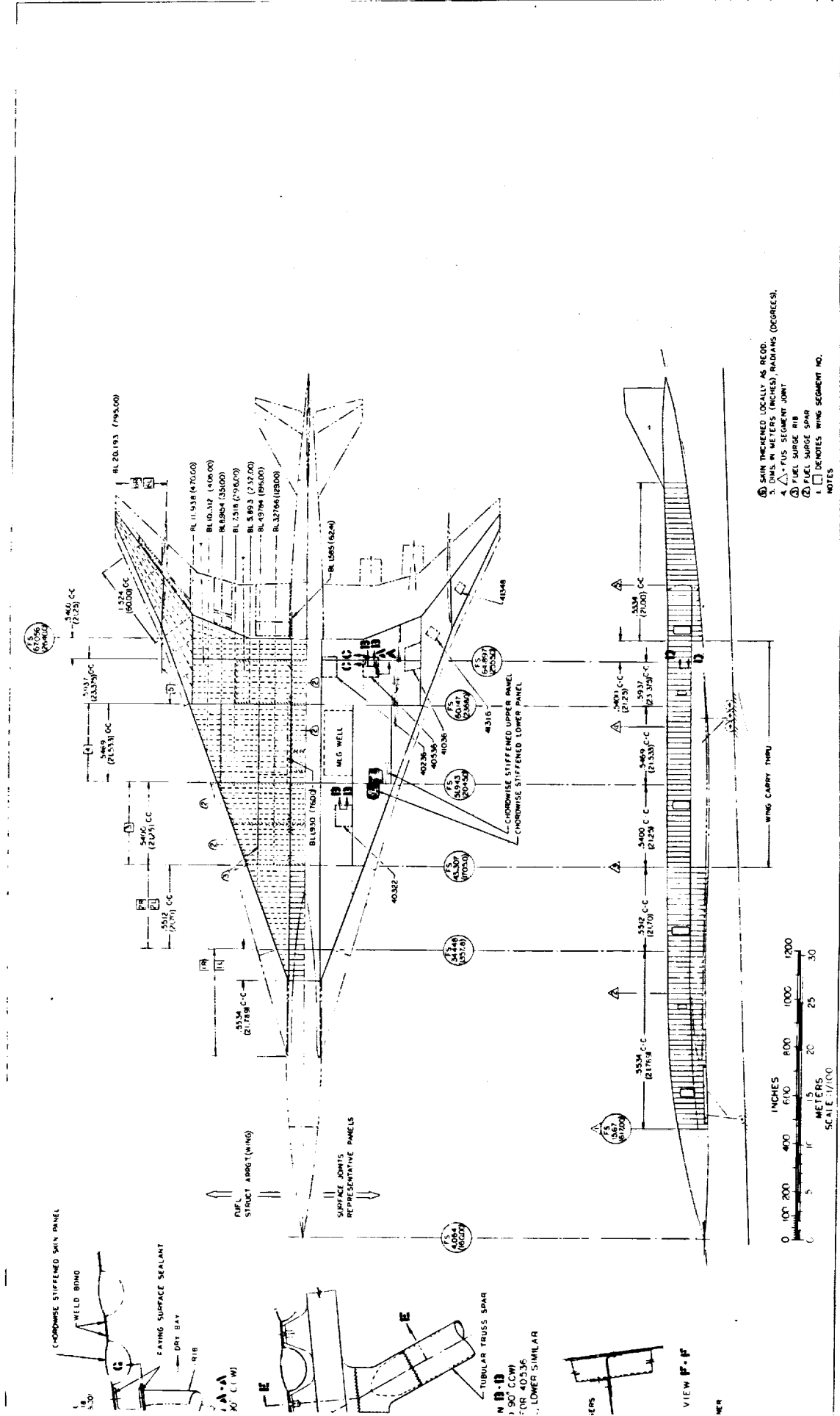


Figure 18-1. Chordwise Stiffened Wing

18-11

FOLDOUT FRAME 2



- Large surface panel assemblies are used.
- The "fastener" joining method is used throughout the entire wing in accordance with the matrix of Table 18-2. As discussed in the Design Approach section, this indicates that major components are joined together with fasteners in order to permit conventional assembly of major components to obtain the aircraft structure. Welding, weld bonding and other joining methods are used, where advantageous, in fabricating individual components such as spars, surfaces and other subassemblies.

The arrangement of the structure is based on the results of the analytical studies (Section 12, Structural Concepts Analysis) and is used to establish the mass estimates reported in Section 15, Mass.

The chordwise-beaded surfaces used in the structure of Figure 18-1 are similar in some respects to those used in the L-2000-7A and the YF-12/SR-71. However, the latter two aircraft used the bead design noted as "corrugation" rather than the circular arc-convex configuration shown in Figure 18-1. The latter bead design has been used because of its structural efficiency and the reduced eccentricity encountered at the terminations of the beads. It is recognized that the circular arc-convex beaded design may result in an increased drag penalty as well as increased danger of damage during aircraft maintenance, hail storms and from foreign object damage (FOD). However, the analytical results of the chordwise stiffened panel designs reported in Section 12, Structural Concepts Analysis, indicated the minimum mass potential for the design shown. The design is directed towards alleviating thermal stresses while still utilizing both skins in resisting shear. Also, heat transfer to the fuel heat sink is reduced, relative to a single skin design, because the fuel does not contact the outer skin in the areas covered by the beads in the inner skin. The cavities enclosed by the beads are vented to ambient atmosphere by means of a hole in the outer skin at each end of a cavity. With the beaded inner and outer skins the surfaces do not participate in resisting wing bending and all bending material is concentrated in the spar caps. This uncoupling of bending and torsional material permits either the bending or torsional stiffness to be varied independently of the other.

PRECEDING PAGE BLANK NOT FILMED

A major manufacturing joint, and a change in direction of the spars, occur at BL 470. This is the location of the outer rib for the outboard engine as well as the joint between the inner wing and the highly swept outer wing and tip.

The "fastener" concept used for assembly major components in the chordwise stiffened wing structure means that fasteners are used for the surface/substructure attachments. Problems arising in this area are much more severe if flush surface/substructure attachments are required.

Sources of attachment problems include those listed below:

- The thin outer skin thickness anticipated over much of the wing makes it difficult to avoid the "feather edges" encountered if a countersink extends through a sheet. It was strongly desired to avoid this condition even though feather edges were accepted on the L-2000-7A and the YF-12/SR-71 aircraft.
- Ti, CRES and similar rivets are difficult to drive and require relatively massive bucking bars and sizable access space. The submerged spar caps shown in Section B-B and the "I" cap spar shown in Section C-C of Figure 18-1 illustrates the restricted access for installing surface attachments.
- Since individual spars are not of fail-safe design, the failure of a spar results in sizable loads transmitted from the surface to adjacent spars and require numerous attachments for load redistribution.
- Upset type fasteners, particularly with thin skin, can result in deformation of the skin and damage or destruction of the bond between the inner and outer skins.

For preliminary design, minimum exterior skin gauges were assumed to be 0.020 inch for the lower surface and 0.015 inch for the upper surface. The minimum gauge of the inner skin was 0.010. Shear type (shallow head) flush head fasteners were considered acceptable in the outer skin.

Studies of access requirements for fastener installation yielded the results shown in Figure 18-2. As shown, blind fasteners require the minimum space. The space requirement for Hi-Tigue fasteners is based on the use of the special tool described

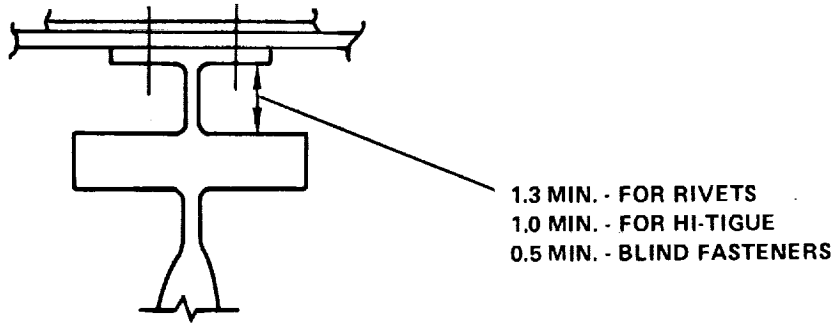


Figure 18-2. Installation Space Requirements for Various Fasteners

in Reference (3). Fastener studies also revealed an interesting new fastener, the "Cherrybuck." This is a one-piece bimetal fastener which has a Commercially Pure (CP) or ductile Ti tail on the end of a Ti-6Al-4V shank. This fastener, used on the B-1 and the F-5E, offers a high strength (95 ksi shear), lower weight than 2 or 3 piece fasteners, and a ductile Ti tail which upsets to 1.5 D without special tools. Investigation also was made of the LS 9714 rivet, a 100-degree miniature head solid rivet designed during the L-2000-7A program. The LS 9714 rivet was developed in two materials: A-286 CRES (95,000 psi min shear) and C.P. titanium (65,000 psi min shear). Comparison shows that the Cherrybuck rivet (all Ti) provides the same shear strength as the LS 9714 A-286 CRES rivet at a lower weight. These limited investigations indicate that:

- Cherrybuck rivets appear useful where an upset flush rivet is acceptable and where the 95 ksi shear strength is advantageous
- LS 9714 CP Ti rivets appear usable when an upset type of flush rivet is satisfactory and the higher shear strength (and probable higher cost) of a Cherrybuck rivet are not required.

As stated previously, concern is felt that upset type fasteners can result in deformation of thin skin and damage or destruction of the bond between the inner and outer skin. Suitable tests are recommended for resolving this question. Where this is found to be a problem, Hi-Lok or Hi-Tigue fasteners are applicable. Hi-Tigue fasteners are indicated where fatigue considerations are significant.

To avoid the feather edge problem in thin skin areas, several approaches have been considered. The two most interesting possibilities are discussed below:

- In one approach, thickened strips would be incorporated in the outer skin sheet in the areas directly above spar (and rib) caps. These strips would be welded in place as part of the process of welding sheets together to obtain the large outer skin weldment required for the large surface panel assemblies used. The thickness of these strips would be at least 0.010 ins. more than the depth of countersinks for flush fasteners. These strips would be machined so that the increased thickness area at fasteners would fair back into the basic skin thickness at a slope of 15/1 or more. This design would result in more welding in the outer skin than would otherwise be required and the thickened areas also would lead to a higher skin weight. Also, surface smoothness may be degraded somewhat.
- In another approach, the outer skins would be chemically milled from sheets whose initial thickness would be at least 0.010 ins. more than the depth of countersinks for flush fasteners. The chem milling would reduce the skin thickness as required in the non-fastened areas while maintaining the thickened areas around fasteners. Machining would be required to smoothly blend out the sharp edges obtained at the edges of chem milled areas. This approach has some merit, but available data indicates that chem milling etches welded areas about 10-percent faster than basic sheet. This is of some concern since the outer skin is a large weldment. However, this problem might be overcome in various ways, one of which is to chem mill individual skin segments before these segments are welded together to obtain the large final external skin required.

In approaching the thin skin/feather edge problem, it appears desirable to consider the steps outlined below.

- Identify those areas where the degraded structural quality associated with feather edges is permissible and accept the feather edge condition in those areas.
- Where possible, investigate smaller and more numerous fasteners as a potential method for avoiding the feather edge problem.

- Where warranted, the "chem milled skin" design outlined above appears feasible and the most practical choice at the present.

#### Spanwise Stiffened Wing Design - Fasteners

The structural arrangement drawing for the spanwise stiffened wing design is presented in Figure 18-3. The planform view of the airplane shows the arrangement of substructure, fuel tanks and surface panel joints.

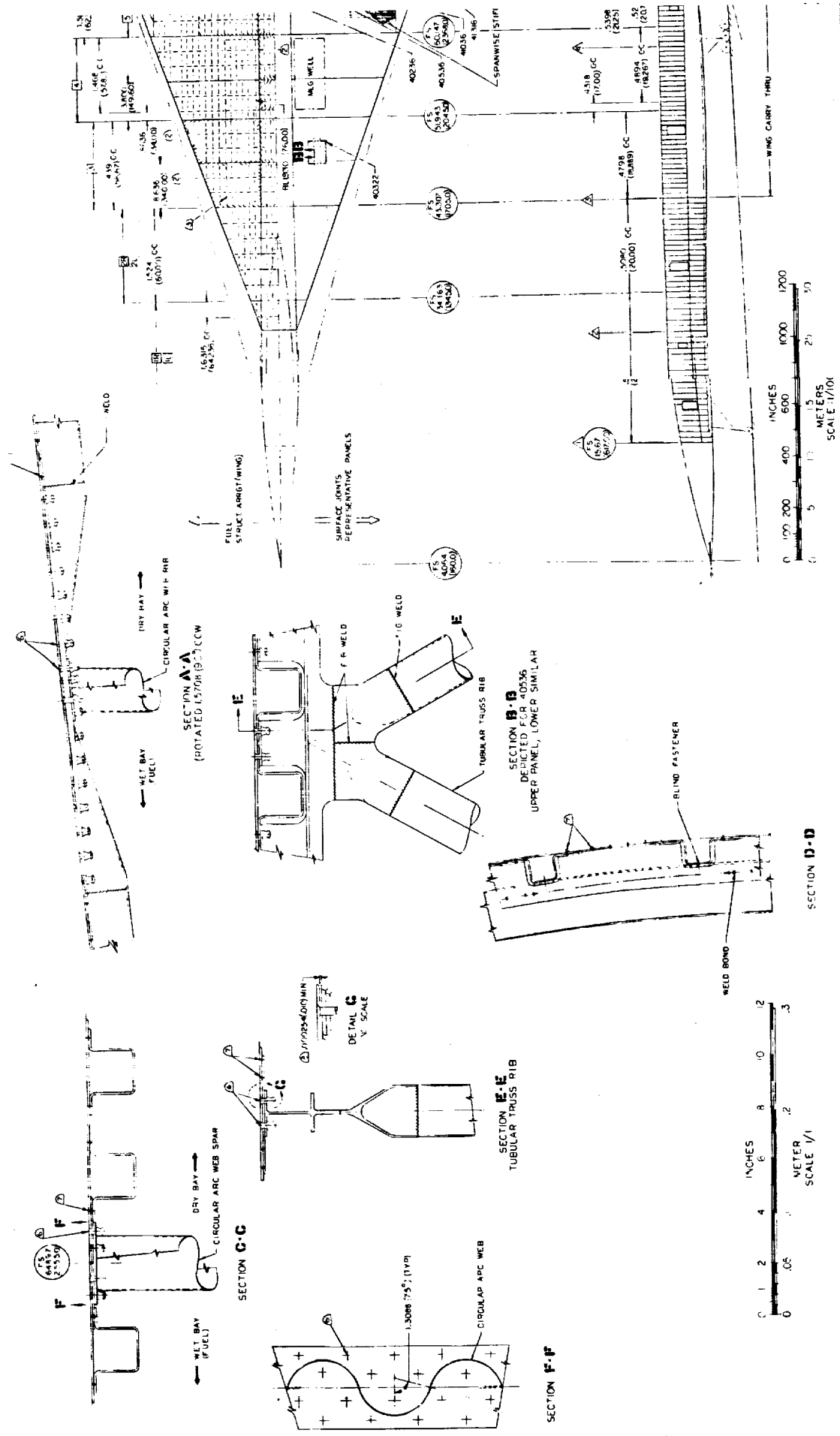
General features of the spanwise stiffened structures in Figure 18-3 include those listed below:

- Relatively widely spaced spars with closely spaced ribs.
- Spars and ribs are of truss design except where they serve as fuel tank walls or fuel tank baffles.
- At fuel tank wall and fuel baffle locations, spars and ribs have welded corrugated webs topped by I-section caps mechanically attached to the welded corrugated webs.
- Large surface panel assemblies are used.
- The "fastener" joining method is used throughout the entire wing in accordance with the matrix of Table 18-1. As discussed earlier, this means that major components are joined together with fasteners in order to permit conventional assembly of major components of the aircraft structure. As with all "fastener" designs, welding, weld bonding and other joining methods are used where advantageous in fabricating individual components such as spars and other subassemblies.

The spanwise stiffened wing structures of Figure 18-3 are configured on the basis of the factors noted below:

- Ribs are spaced relatively closely. As shown in the planview of Figure 18-3, the spacing is approximately 20 inches. Major ribs include two per engine, two per MLG strut and a rib at each side of the fuselage. As shown on the figure, major ribs are extended fore and aft, in some cases, to facilitate load distributions, assist in damage tolerance or serve as fuel baffles.





---

**PRECEDING PAGE BLANK NOT FILMED**

ORIGINAL PAGE IS  
POOR QUALITY  
WILDLIFE FRAME



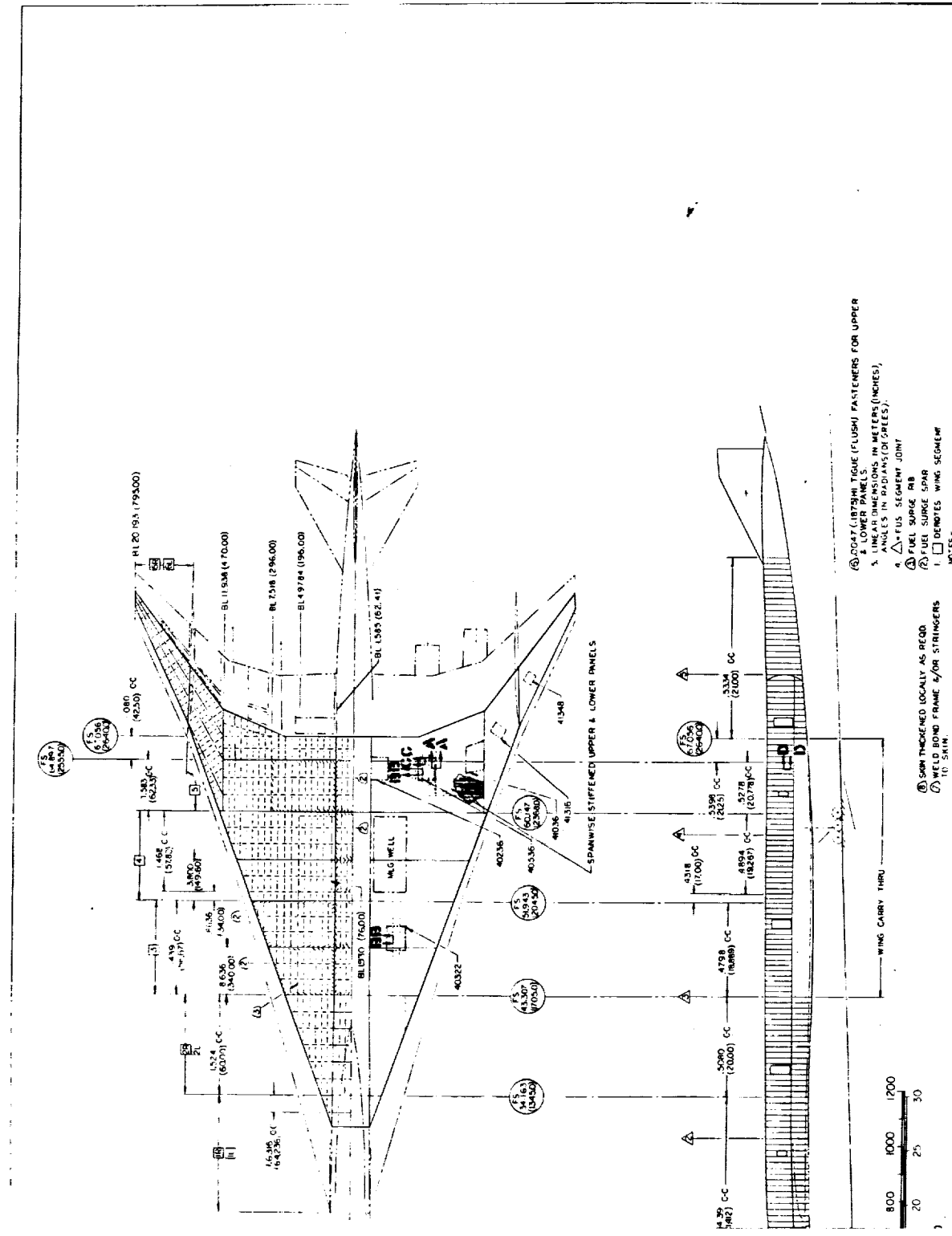


Figure 18-3. Spanwise Stiffened Wing

### 3-3. Spanwise Stiffened Wing Design - Fasteners

FOLDOUT FRAME 18-19



- A dry bay completely surrounds the MLG well so that no MLG support structure attaches directly to structure serving as a fuel tank wall. This reduces the possibility of damage to the fuel tanks in the event of a hard landing or similar occurrence.
- Forward of FS 1705, the forward end of center section fuel spars do not extend through the fuselage and the wing is supported from the side of the fuselage.
- The wing is built in segments which, except for the aft main box segment, include all wing structure from one leading edge to the opposite leading edge. The aft main wing box extends from the MLG cutout to the rear beam and from one fixed fin to the opposite fixed fin (a span of 100 ft.). This manufacturing breakdown is developed from the structural arrangement and is based on minimizing the number of segments while avoiding excessive size and difficult assembly and handling of the various segments.

The sheet metal hat stiffened surface panel design resulting from the analytical design study is shown. The surface assembly, which consists of the outer skin and hat stiffeners, is attached to the rib assembly comprised of the rib chords and diagonals fabricated as one weldment. See Section B-B of Figure 18-3.

With the hat-stiffened surface (closed section stiffeners), it is noted that heat transfer from the slipstream to the fuel heat sink is reduced in value when compared to the single skin-open section concepts, since more of the outside skin is in contact with the fuel.

Weld bonding has been selected for the stringer/skin attachment after consideration of several alternate methods. Surface panel sizes are shown on the planform view of Figure 18-3. For forming and fabricating individual panels, a size limit of 15 by 35 feet has been used. This limit is discussed in Reference (3). Where a joining operation involves bonding only, the panel length limit has been extended to 50 feet. This special length limit has been exploited wherever possible.

In the aft main wing box area the surface length extends from BL 62.41L to BL 470L and from BL 62.41R to BL 470R. A splice of the hat stiffeners, is integrated into the design (Section A-A of Figure 18-3) to accommodate a fuel rib at BL 296L and R.

PRECEDING PAGE BLANK NOT FILMED

This surface configuration eliminates a chordwise joint at BL 296L and R, however, results in a "fastened" (rather than "fastened/bonded") surface splice at BL 62.41L and R.

In fuel stowage areas, access is required to the interior of the tanks. For this purpose, two access doors in the surface are provided for each individual tank or isolated portion thereof. The design intent is to minimize the access doors in the outer surface by exploiting the openings between diagonals in truss type ribs and spars was emphasized. Access door cutouts in the surface result in more weight penalty in the spanwise than chordwise stiffened design since the surfaces contain bending as well as shear material.

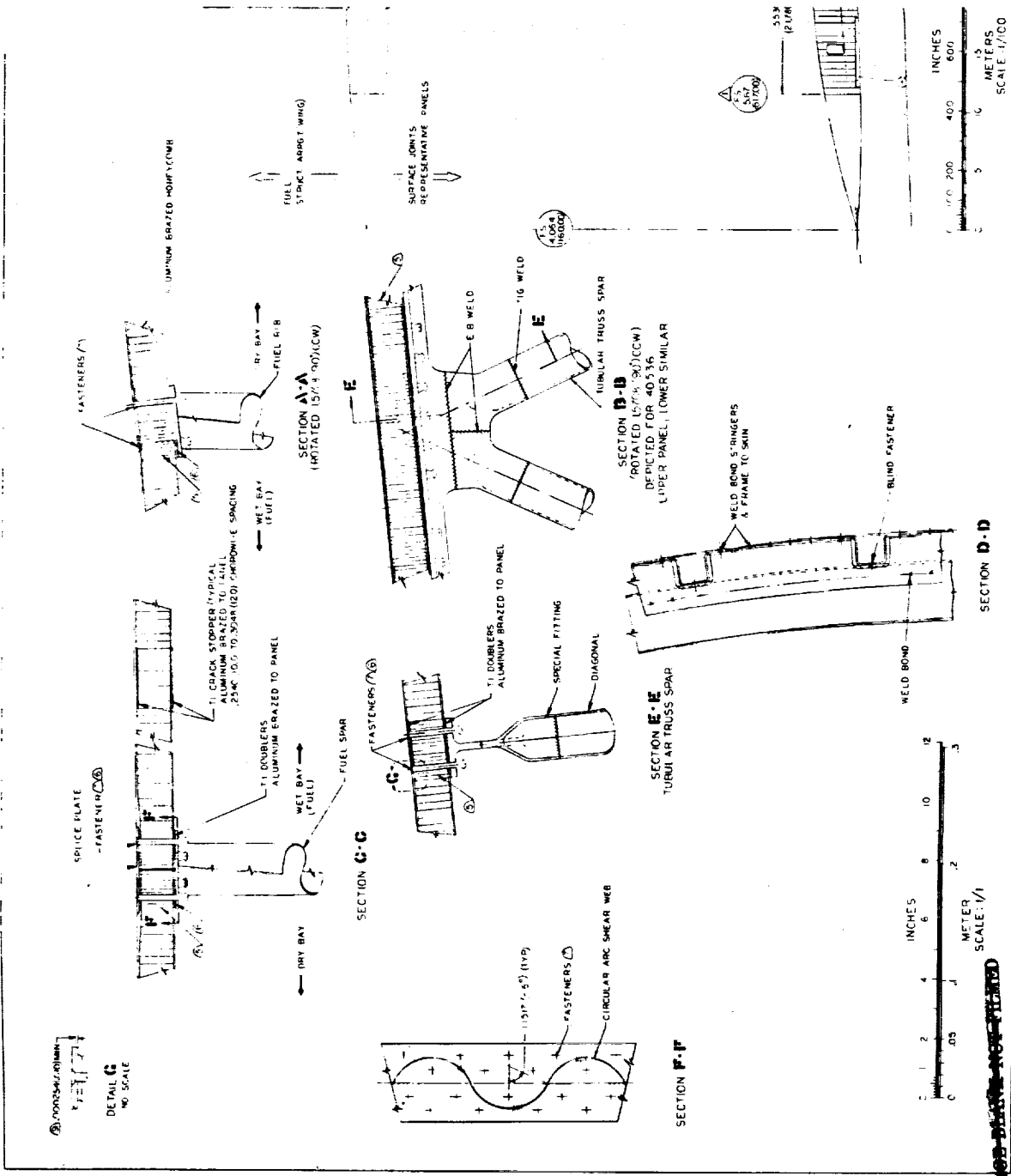
Additional provisions for fail-safe and damage tolerance were not required for the spanwise stiffened design as indicated in Section 13, Fatigue and Fail-Safe.

The "Fastener" concept used for assembling major components in the spanwise stiffened wing structures of Figure 18-3 means that fasteners are used for the surface/sub-structure attachments.

A major manufacturing joint and change in direction of the spars and surface panels occur at BL 470. This is the location of the outer rib for the outboard engine as well as the joint between the inner and outer wing.

#### Monocoque Wing Design - Fastener

The structural arrangement drawing of the monocoque wing design is presented in Figure 18-4. The surface panels consist of aluminum brazed honeycomb core sandwich panels with densified core for the "fastener" approach. The arrangement of the sub-structure, fuel tanks and surface panel joints is indicated on the wing planform.



ORIGINAL PAGE IS  
OF POOR QUALITY

ROLLDOWN FRAME /

ROLLDOWN FRAME



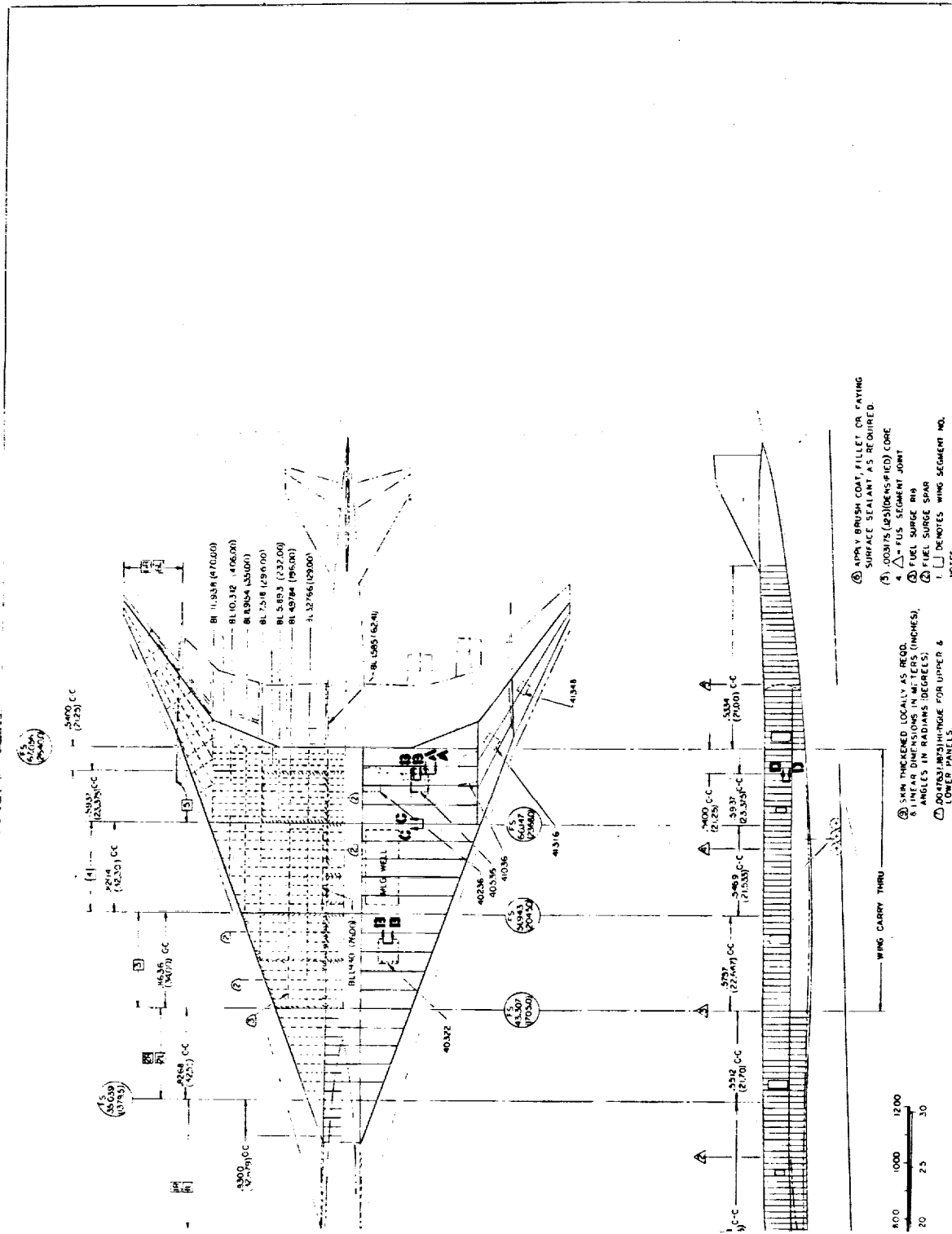


Figure 18-4. Monocoque Wing Design - Fasteners  
**FOLDOUT FRAME S** 18-23



The panel concept selection was based on the results of the analytical design of both the honeycomb and truss core sandwich designs discussed in Section 1, Structural Design Concepts. These panel concept designs were selected after a comprehensive review of numerous candidates and their applicability to a near-term arrow-wing configuration supersonic transport. The types of surface panel studied include:

- Aluminum brazed honeycomb sandwich surfaces made by the "Aeronca" process.
- Adhesive bonded honeycomb sandwich surfaces.
- Welded honeycomb sandwich (STRESSKIN) surfaces.
- Trusscore sandwich surfaces, a design using a unidirectionally corrugated core sheet between the sandwich face skins.

In addition to the above, both the Rohr Liquid Interface Diffusion (LID) and Northrop Nor-Ti-Bond processes were considered and evaluated for the fabrication of brazed sandwich surface panels. In the Nor-Ti-Bond process, copper is electroplated on the edges of the honeycomb cell walls before the core is brazed to the face sheets. The brazing step results in a diffusion brazed joint between the core and face sheets. The Rohr LID process is similar except that several elements, rather than copper alone, are electroplated on the edges of the honeycomb core cells. Both processes provide good mechanical properties as well as operating temperature capabilities. However, both have demanding tolerance requirements. For example, the core/face sheet gap must not exceed 0.005 ins. In contrast, the "Aeronca" process aluminum braze process can tolerate a core/face sheet gap up to 0.002 ins. Because of the manufacturing difficulties foreseen in applying the LID and Nor-Ti-Bond processes to the large wing surfaces for the near-term airplane, detail drawings were not made.

The waffle type of monocoque surface was not included for application to the large wing surface panels under consideration because of the difficulties and costs foreseen in fabricating and forming such panels.

The surface panels selected for design application use the "Aeronca" aluminum brazing process originally developed by Aeronca for the Boeing SST. In this process, a thin aluminum foil sheet (3003 alloy) is placed between the core and face sheet, or

**PRECEDING PAGE BLANK NOT FILMED**

other surfaces to be joined, and the brazing step conducted at a temperature of 1240 F. A detailed discussion of the Aeronca development work of this fabrication method is described in Reference 2.

The Aeronca process results in a thin coating of aluminum over the entire interior surface of the sandwich. This includes the inner surfaces of the face sheets as well as the walls of the honeycomb cells. As can be seen, this indicates that a significant amount of parasitic weight of unnecessary aluminum braze alloy is incorporated in the final brazed sandwich. This aluminum coating also results in a relatively high heat transfer to the fuel and substructure. When non-perforated core is used, each cell is hermetically sealed after brazing. This feature prevents fuel or other material from entering adjacent cells if the fuel or other liquid should somehow enter the cell(s) in a particular area.

The Aeronca aluminum braze process, which is fully discussed in Reference (4), has a number of advantageous features relative to design. These features include:

- The core depth can be varied, or tapered, within a given brazed panel.
- Separate doublers (or fail safe straps) can be incorporated within a brazed panel.
- An appreciable gap can be tolerated between the core and face sheets. Successful brazing has been accomplished with localized gaps up to 0.020 inches, which indicates a realistic process for application to large panels (such as wing surfaces).
- The core density and cell size can be varied within a brazed panel if required.
- Hermetic sealing of each cell, obtained with non-perforated core, means that fuel (or other liquid) which penetrates one cell is not automatically free to enter all other cells in the sandwich.
- No confining restraints apply relative to the thicknesses of the face sheets, the core and inserts. The thickness variation among these elements can be very large and is not restricted as is the case when, for example, the core is spotwelded to the face sheet.

- Considerable development effort has been expended on this type of structure and an appreciable amount of data is available. Boeing has received considerable DOT funding for development and tests of this structural concept.

The Aeronca process does, however, have a few disadvantages. Some examples include:

- A fairly significant weight penalty is incurred by the fact that 3003 aluminum braze alloy coats the entire interior of the sandwich. "Stop-off" and other techniques to alleviate this situation are discussed in Reference (4).
- The aluminum coating on the interior surfaces of the sandwich results in relatively high heat transfer to the fuel and substructure.
- The fact that the braze alloy melts and flows causes difficulties in brazing joints which have a significant slope ( $\geq$ about 20-degrees) relative to the basic plane of the panel. Aeronca has claimed development of proprietary techniques for alleviating this condition.
- Repair techniques need further development. Some work has been done using bonding techniques which appear promising. Welded repairs are not feasible in close proximity to aluminum brazed joints.
- Fabrication of large panels, postulated as feasible for this study, will require careful control of brazing temperature, dimensional changes and other factors.

For this study, a maximum brazed panel size of 68 inches by 40 feet has been postulated. This size limit, based on discussions with Aeronca personnel, contrasts with a size of approximately 3 feet x 25 feet for the largest panel brazed to date. At the beginning of this study, no data was available to confirm the fabricability of thick panels with heavy skins. However, data from Reference 2 indicates the feasibility of sandwich thicknesses to 1.60 inches and face sheets to 0.156 inches.

The general features of the monocoque design are enumerated below:

- Numerous spanwise spars which are of truss design except where a spar serves as a fuel tank wall or fuel surge pressure spar.

- At fuel tank wall locations, spars have welded circular arc webs.
- Relatively few chordwise ribs are used. These also are of the truss type except where the rib serves as a tank wall. In such applications, welded corrugated web ribs are used.
- The "fastener" joining method is used throughout the wing in accordance with the matrix of Table 18-2. As discussed in the Design Approach section, this indicates that major components are joined together with fasteners in order to permit conventional assembly of major components. Welding and other joining methods are used, where advantageous, in fabricating individual components such as spars and other subassemblies.
- Surface panels are long and narrow, consistent with the postulated size limit of 68 inches by 40 feet. With the spar spacing used, surface splices are located per Figure 18-4.

Two types of wing surface joints are utilized in the inner wing. A "balanced" (double shear) joint is proposed for heavily loaded areas (Section C-C of Figure 18-4) and where advantageous in structural mass. Section C-C illustrates such a joint at a flush surface splice. In general, all flush fasteners are envisioned as having shallow ("shear") heads to permit minimum countersink depths. The splice plate thickness is then made at least 0.010 inches greater than the fastener head height to avoid "feather edges" and the resulting degradation in structural quality. Note that Section C-C specifies densified (1/8 inch cell) core at the fasteners. In tests conducted by Aeronca, the 1/8 inch cell proved adequate in strength to permit full torquing of a 1/4 inch diameter fastener (to 175 in.-lb. torque) as well as the elimination of separate panel closure. A locally thickened pad machined integral with the skin is shown for load transfer from the face sheet to the splice plate. This approach requires the use of a suitably thick sheet or plate. An alternate approach is welding thicker strips into the face sheet at panel edges and other locations requiring additional thickness.

In the wing apex and other lightly-loaded areas, the "single-edge" panel splice is used with a zee-closure at the edge of the panel.

As previously noted, core cell size can be varied within a brazed panel. However, to date this has been done by poke welding (resistance welding) individual cell walls together at the interface joint between the different cell sizes. This poke welding, done with very small electrodes, is laborious and expensive. Development is needed for a procedure involving a brazed joint at the interface joint between the two different core cell size areas. Another potential solution is the use of alternate core cell shapes. This is an attempt to reduce the core cell joint areas and weights and to lower the heat transfer rate through a brazed panel.

The aluminum brazed panel design is adaptable to the incorporation of fail-safe straps. As shown a certain proportion of the face sheet material is shown segregated and incorporated in failsafe straps brazed to the face sheet during panel fabrication. It is assumed that these brazed straps will be effective as crack-stoppers. However, tests are required to verify that these integrally brazed straps will be effective crack stoppers.

The substructure in the inboard wing is similar to that used in the chordwise and spanwise stiffened wing designs discussed previously. This indicates that:

- Spars and ribs are of welded truss design except where used as tank walls or fuel baffles. This approach is used to provide good internal access for manufacturing and structural inspection purposes.
- At tank walls, spars and ribs have welded circular arc webs. The web cap directly contacts the surface sandwich as shown in Section A-A of Figure 18-4. At rib/spar joints, a splice plate is used between the web cap and the surface for load transfer. As previously noted, Sciaky has verified the practicality of welding the caps to the circular arc webs at angles as much as 15-degrees from normal to the web.

Hi-Lok or Hi-Tigue fasteners are envisioned for surface/substructure attachments in tank areas.

Feather edges at countersinks, and the associated degraded structural quality, are avoided wherever undesirable by local thickening of the outer skin. Thickness variation in the outer skins is envisioned as obtained by chemical milling/machining.

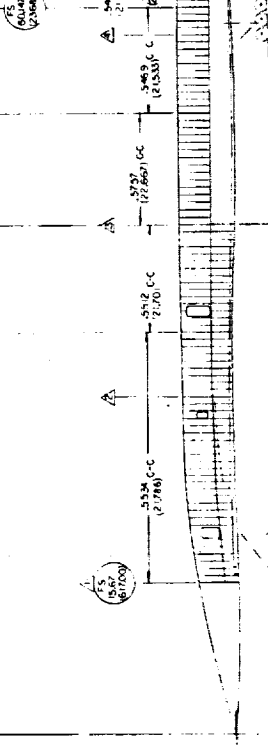
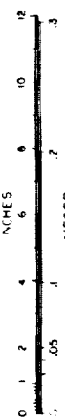
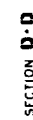
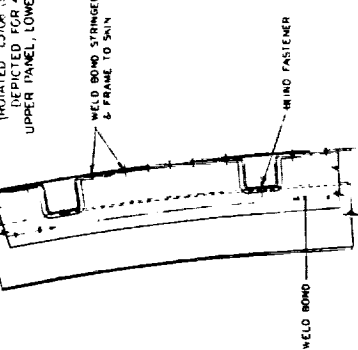
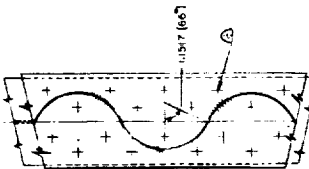
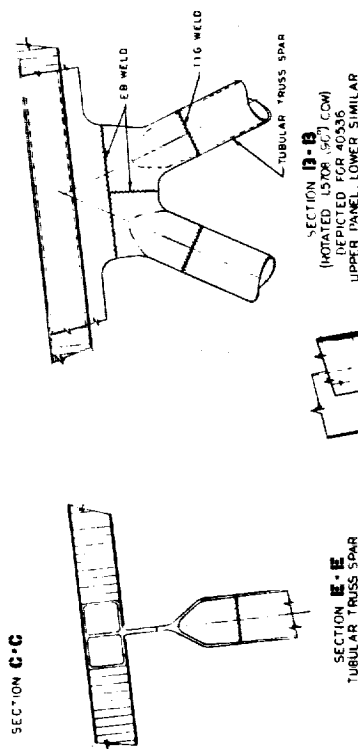
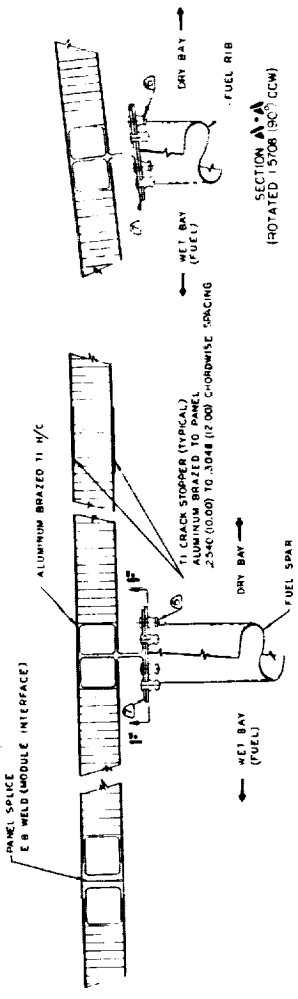
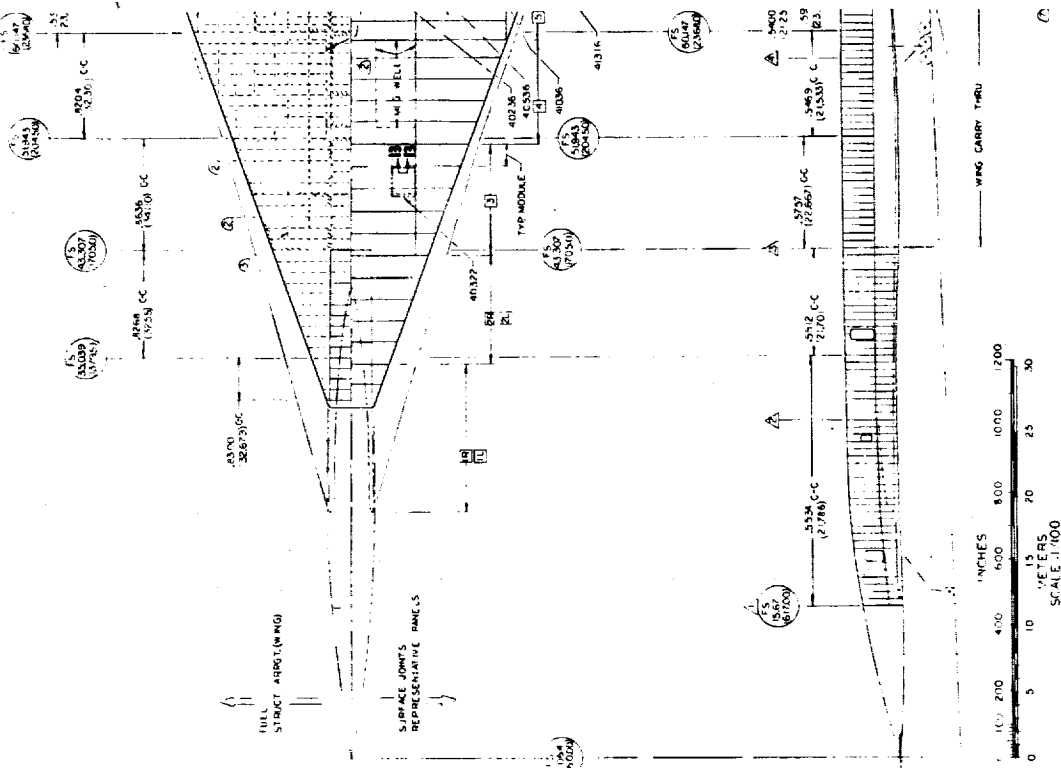
The upper and lower surfaces of the outer wing and wing tip are composed of separate brazed panels which are fastened to substructure. All or some panels of the upper surface are attached with screws and are removable for inspection and maintenance purposes.

The above approach is based on the desire to avoid numerous access door cutouts in the surfaces and the need for blind fasteners.

#### Monocoque Wing Design - Welded

The structural arrangement drawing of the monocoque wing design - "welded" approach is shown on Figure 18-5. The surface panels consist of aluminum brazed honeycomb core sandwich panels with tubular inserts to facilitate welding. The fuel and sub-cone arrangements are presented on the wing planform along with the surface panel joints of the representative panels.

The welded structure concept described in this section has many similarities to the fastened structure covered previously. This discussion is primarily intended to define differences in the structural design arising from the use of the welding concept.



1

ENID OUTRAM 2

卷之三

ORIGINAL PAGE



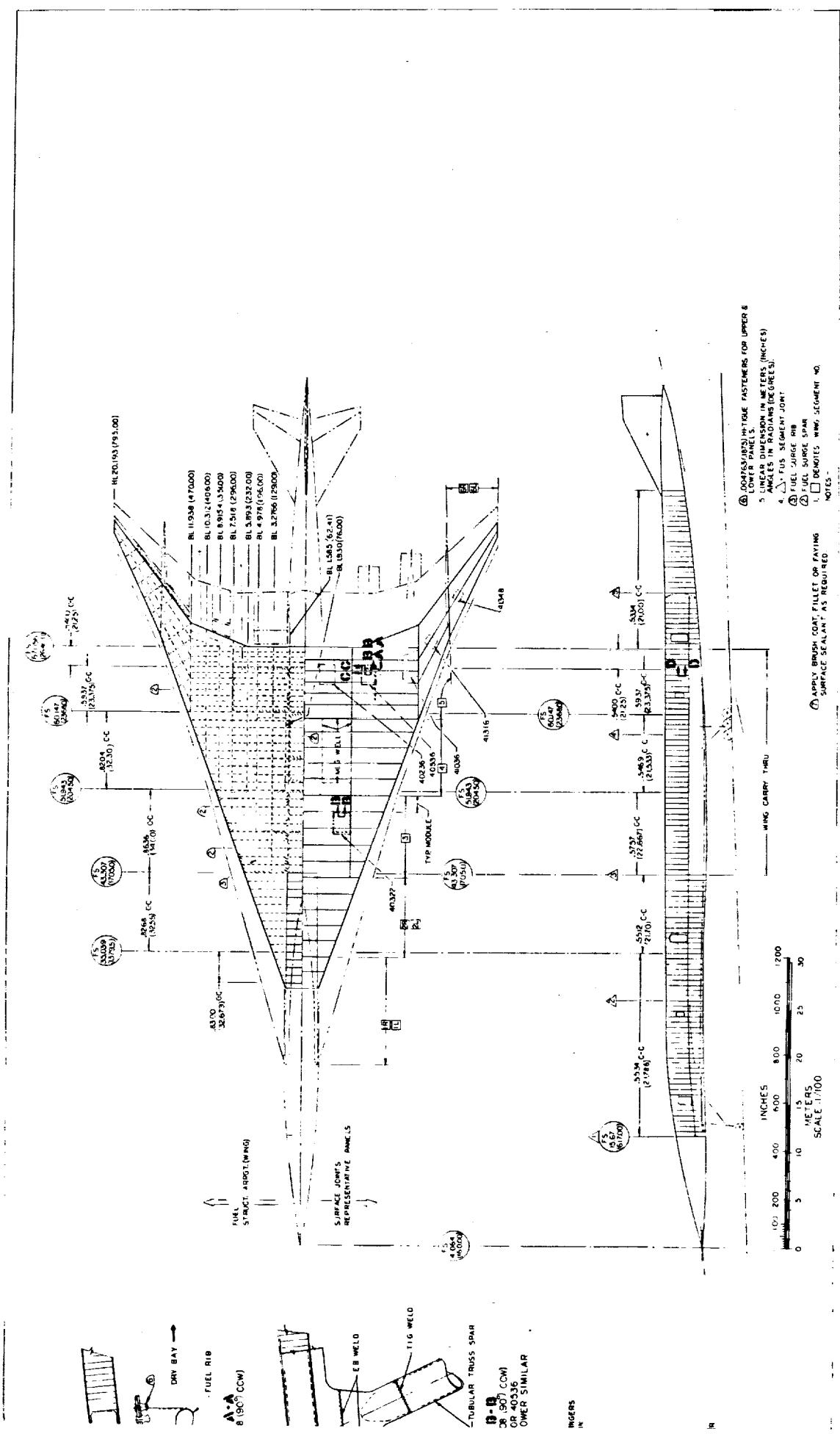


Figure 18-5. Monocoque Wing Design - Welded

FOLDOUT FRAME 2



The design objective in this investigation was development of a completely, or nearly completely, welded structure in an attempt to obtain such anticipated advantages as:

- The elimination of numerous fasteners and the minimization of the number of joints.
- A much simpler problem in sealing fuel tanks. In addition to easier tank sealing, the welding concept permits the avoidance of a significant weight increment associated with tank sealing compounds.

Figure 18-5 depicts the welded structure design developed for the area inboard of BL 470. It employs a unique "module" concept which is illustrated in the sketch of Figure 18-6. As shown therein, a module consists of two adjacent spars, rib segments and an upper and lower surface. The surface panels, twice as wide as the spar spacing, are joined to the adjacent module by spanwise EB welds assembling modules into wing segments. The location of segment joints is shown in Figure 18-5.

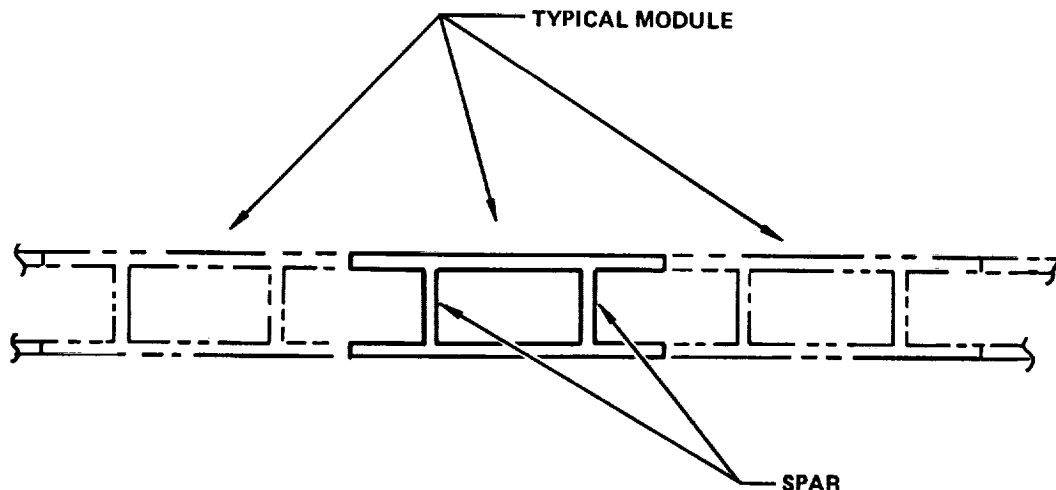


Figure 18-6. Typical Module for Welded Sandwich Wing Structure

Design guidelines used in developing the welded structure concept include:

- All welding is designed for automation wherever possible.
- EB welding is used wherever feasible, and not for surface joints alone, because of good mechanical properties, a minimum heat-affected zone and a high welding speed.
- All welds are dressed on all surfaces unless impossible.
- Wherever possible, welds are inspectable visually.
- The maximum possible joining of parts is accomplished during the panel brazing process. This is an attempt to minimize assembly labor.

In line with the latter point, spar caps, rib caps, panel closures and other elements are incorporated within the panel brazement. This is illustrated in the sectional views shown in Figure 18-5. This approach provides increased structural depth for spars and ribs. Some panel inserts are extended to the external surface so to provide the capability of extended visual inspection.

In fabrication, the spar and rib caps and panel edge members in a given panel are first EB welded together in a grid. The honeycomb core is poke welded to the inserts and the sandwich skins are then brazed to the insert grid and core to obtain a completed panel brazement. The inserts are shaped to facilitate poke welding to the core. Note that the brazing, performed at approximately 1240 F, stress relieves the welded grid assembly. Since very close tolerances are required for the EB welded joints between modules, the inserts at the module interfaces are made heavier to allow machining on assembly. This is shown in Section C-C of Figure 18-5.

Spars and ribs are of truss design, as with other structural designs in this report, except where they serve as tank walls or fuel baffles. A tank wall spar is shown in Section A-A on Figure 18-5.

Surface panel joints are the balanced, or double edge, type for good structural efficiency and are located midway between spars to allow access for welding equipment and to permit dressing of welds after the joining of modules. Surface panel size is assumed limited to 68 inches in width and 40 feet in length.

Welded joints must be configured and located carefully to ensure that the welding does not damage the brazed joints. The weld/braze clearances shown are preliminary estimates and would require verification tests before finalization.

In the cabin floor area, seat tracks are incorporated in the brazed panels to provide increased structural depth and to facilitate a longer span between supports.

The planview of Figure 18-5 shows that both the upper and lower surfaces of the outer wing and wing tip are composed of separate brazed panels. All or some panels of the upper surface are attached with screws and are removable for inspection and maintenance purposes. The major difference from the "Fastened" approach of Figure 18-4 is that the fasteners attaching the lower spar caps to the lower surface have been eliminated in the welded structures of Figure 18-5. This large reduction in the number of fasteners through the lower surface in the welded structure design has been accomplished by incorporating the lower spar caps in the lower surface.

#### Composite Reinforced Wing Design — Fasteners

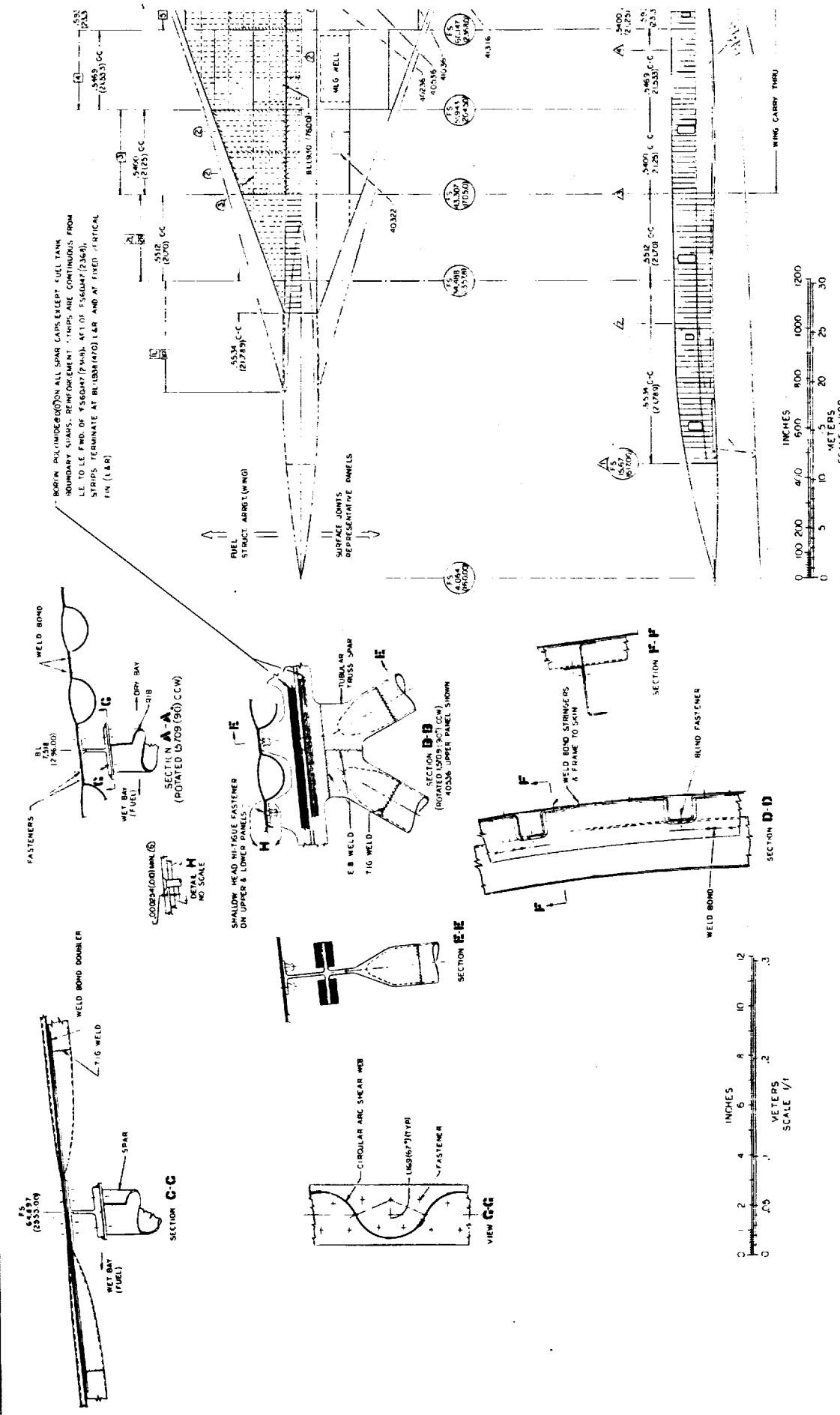
The structural arrangement of the composite reinforced wing design is presented in Figure 18-7. The basic arrangement of the structure and design features are identical to the chordwise stiffened wing design of Figure 18-1 and discussed in detail in the chordwise stiffened wing design section.

The structurally efficient circular arc-convex beaded surface panels of titanium alloy (Ti-6Al-4V annealed) are used. The titanium alloy spar caps are reinforced with boron/polyimide (B/PI) as shown in Section E-E of Figure 18-7. The reinforcement strips are continuous from leading edge to leading edge forward of F.S 2368. Aft of F.S. 2368 the reinforcing is continuous from BL 470L to BL 470R.

#### Skin-Stringer and Frame Fuselage Design — Fasteners

The fuselage structural arrangement shown with the various wing concept designs in Figures 18-1, 18-3, 18-4, 18-5 and 18-7 is a skin-stringer and frame construction. The closed hat stiffener configuration is used in the major portion of the fuselage with the zee stiffener used in the more lightly loaded but pressure critical forebody. The frames are zee-sections with continuous shear clips as indicated on the





PRECEDING PAGE BLANK NOT FILMED

ORIGINAL PAGE IS  
IF POOR QUALITY  
FOLDOUT FRAME /



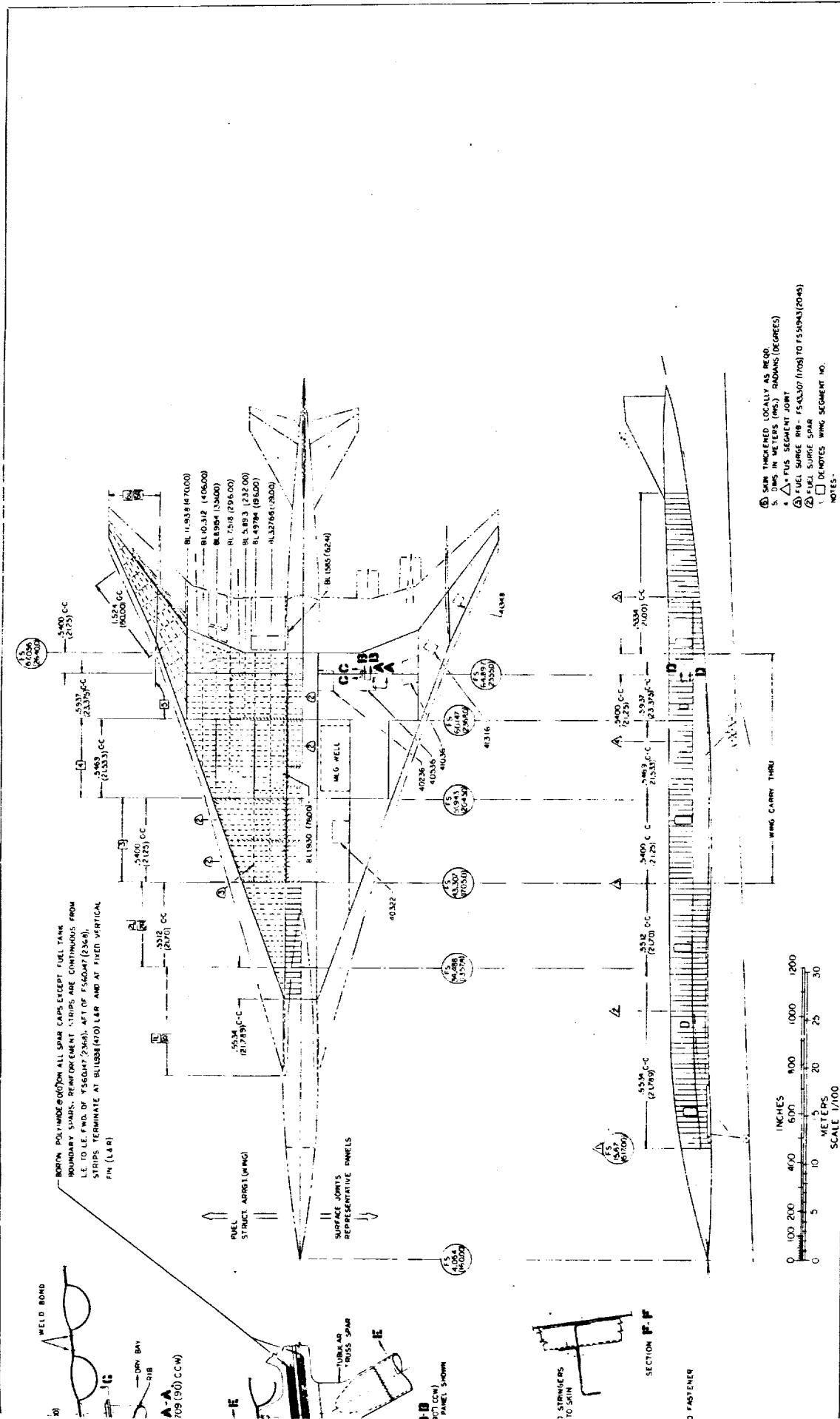


Figure 18-7. Composite Reinforced Wing Design - Fasteners



figures. The analytical studies reported in Section 12, Structural Concepts Analysis, resulted in a frame spacing of approximately 20 inches to yield minimum mass. Thus, for the chordwise stiffened wing design (including the composite reinforced spar caps design), the frames are located coincident with the spars. For the spanwise stiffened and monocoque wing designs, frames are located at various multiples of the spar spacing and are attached thereto; intermediate frames do not attach directly to the spars.

Weld bonding has been selected for the stringer/skin and frame/skin attachments. In this process, the basic spotweld attachment is made first and is followed by the infiltration of adhesive around the spotwelds. This enhances the fatigue properties of the joint in relation to a spotwelded joint and requires that individual fuselage panels be processed in curing ovens after being spotwelded together. Weld brazing is a backup for weld bonding if the weld bonding should prove unacceptable or impractical.

Since weld bonding is basically a spotwelding process, the panel size limits were established as a maximum of 15 feet in width. This width has been exploited in achieving a major advantage in that only one longitudinal skin panel splice, at the top centerline, is used in the cabin in the wing area. In the L-2000-7A design, spotwelding alone was used for skin/stringer and frame/stringer attachments in conjunction with skin panel splices at the 3 o'clock and 9 o'clock positions. At the top centerline and other panel splices, an external splice strip is used to provide a double shear joint with enhanced characteristics in fatigue. The top centerline splice in the cabin area is located at a plane of symmetry and minimizes the changes in skin thickness taking place at the splice since it means that thickness changes occur in the fore and aft direction only.

The fuselage segments are very close to 50 feet in length. This value is based on transportation considerations as well as the assumption of 50 feet long ovens for curing the adhesive used in the weld bonding and rivet bonding utilized extensively in fuselage fabrications. Furthermore, the fuselage is not broken at each wing segment. Instead, the fuselage is broken into approximately 50 foot long segments as discussed above. An important factor in the fuselage design is the fact that most, or all, of the fuselage is designed to permit subcontracting.

**PRECEDING PAGE BLANK NOT FILMED**

### Sandwich Shell Design - Welded

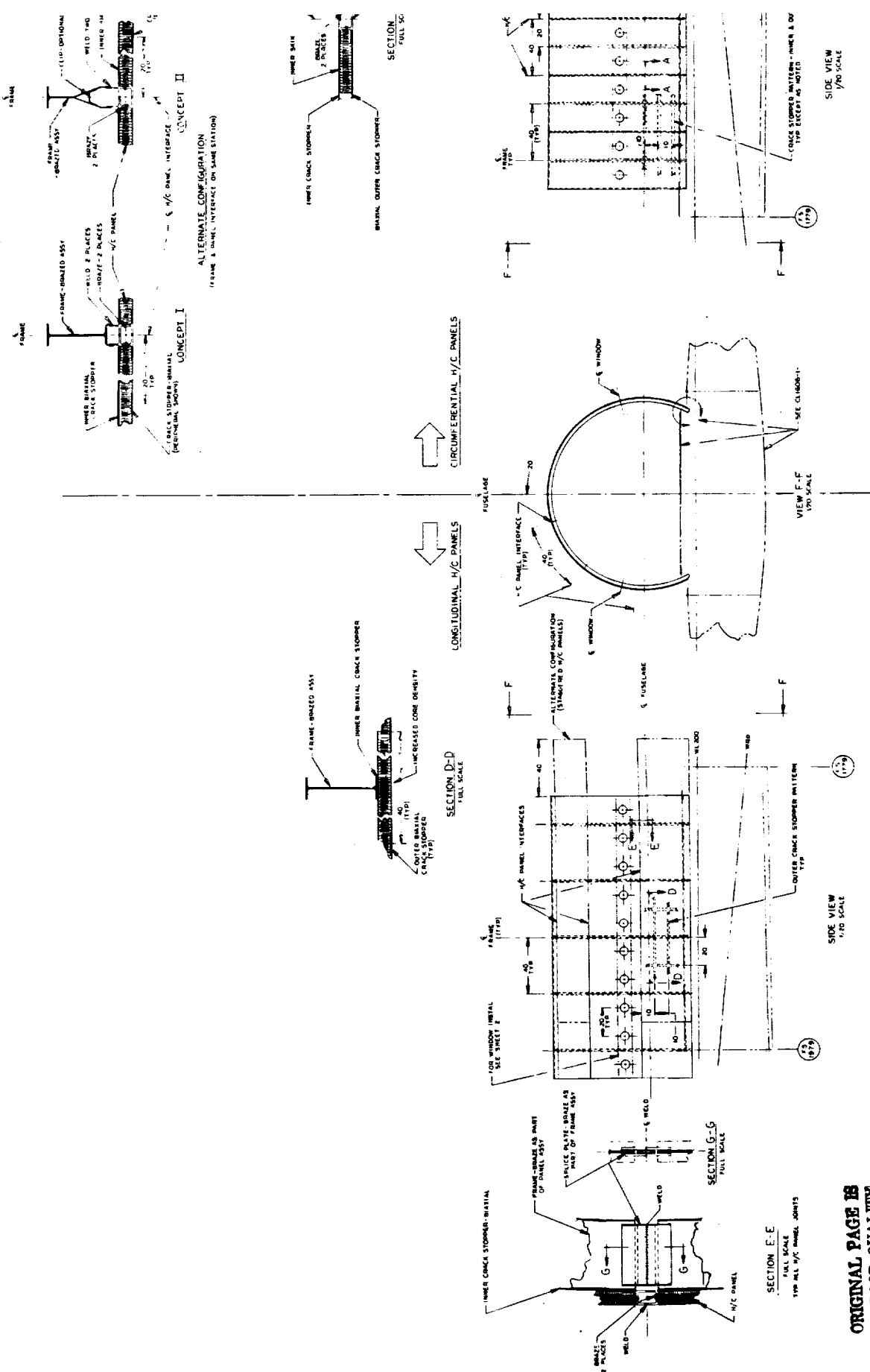
Various approaches for minimum mass fuselage designs were investigated. These studies were exploratory in nature but did identify the applicability of the concepts to a near-term start-of-design supersonic cruise aircraft.

Figure 18-8 presents one of the exploratory design studies made of sandwich fuselage structure. This particular study was based on the use of an aluminum brazed honeycomb sandwich shell ("Aeronca process") in conjunction with the welding joining method. It was recognized that the brazed sandwich results in a significant amount of parasitic weight of aluminum braze alloy, and thus increasing the difficulty of achieving a weight saving. However, the brazing process was assumed in this particular study because it offered the potential for structural integrity and reasonable adaptability to the welding joining method.

Two approaches are shown in Figure 18-8. The right side of the figure shows a design using circumferential panels which are continuous between floor/shell intersections. The design attempts to incorporate as many elements as possible within panel brazements to reduce assembly labor and joints. Panel brazements are EB welded together between frames and contain crack stoppers brazed to both skins. As shown, various frame designs and frame/shell joint designs were considered.

The left side of Figure 18-8 illustrates an approach using longitudinal panel brazements welded together with fore and aft EB welds. A panel width of 40 inches was assumed to minimize the contour deviation from a flat plane within each panel to reduce the problem with the braze alloy's tendency to run to the low point of the panel. Two variations of this design are shown. In one, circumferential panel joints are in a common fuselage station plane. In the other, circumferential panel joints are offset and not in a common fuselage station plane. This complicates the welding procedure but avoids a continuous welded joint in a single plane.

Although the studies showed the need for further development in several areas, the longitudinal panel design appears to be feasible and have some attractive features. Welded joints must be located carefully to avoid heat damage to the panels. The latter problem would be even more critical with an adhesive bonded/welded construction. An adhesive bonded circumferential panel design could, however, use



ORIGINAL PAGE IS  
POOR QUALITY



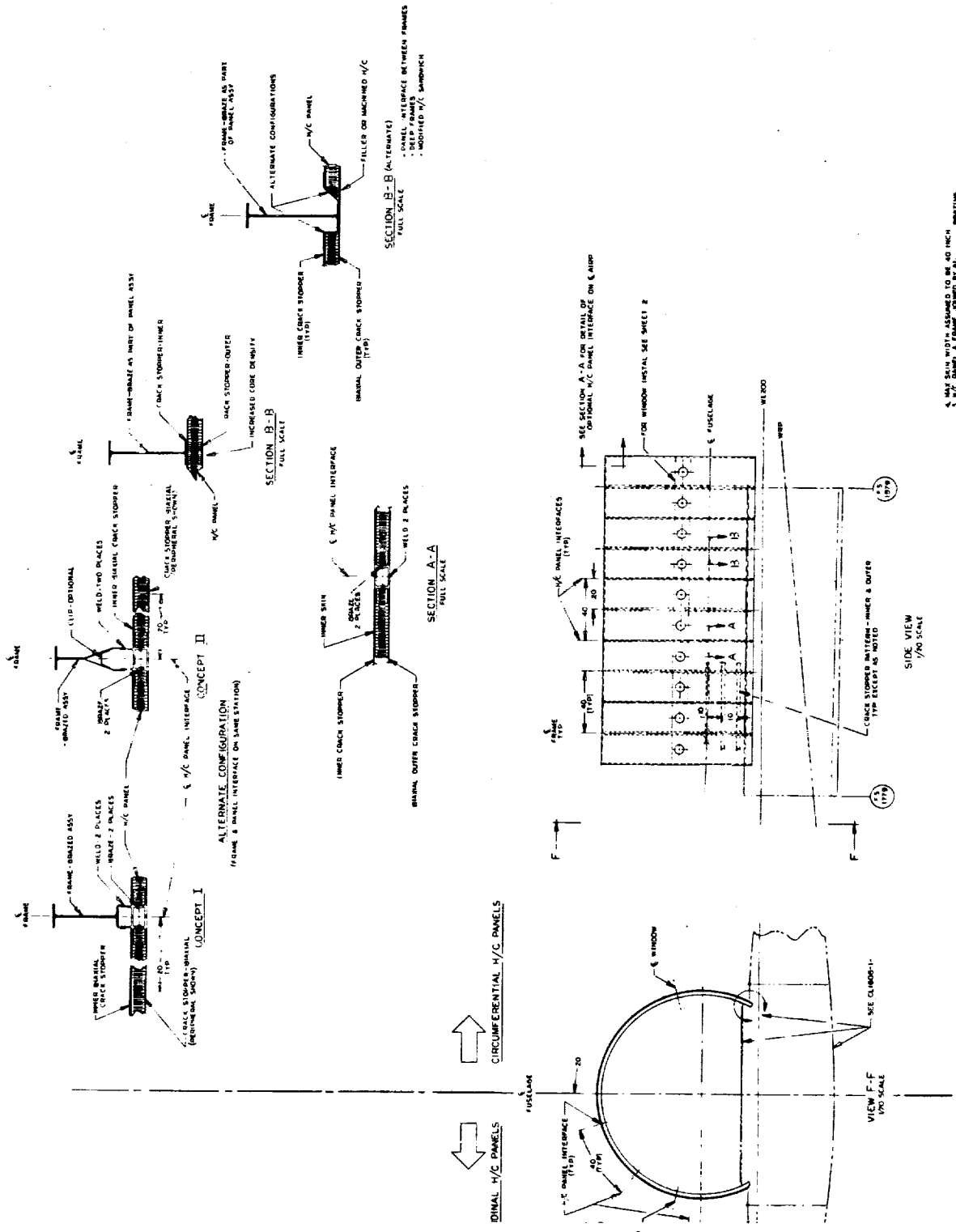


**Figure 18-8.** Sandwich Shell Design - Welded  
BRAZED T-JOINT FRAMES & M/C PANELS

NOTE: BRAZED TIPS ARE SHIPPED IN QUANTITIES OF 100 PER BOX.

Welded  
16-47

REVIEW ARTICLE



considerably larger panels than those shown in Figure 18-8 for the brazed design. The preliminary studies of sandwich fuselage structure indicated considerable risk in conjunction with a limited weight saving potential relative to semi-monocoque design.

#### Design Problem Areas

A wide variety of structural designs were developed for evaluation and potential application in the wing and fuselage of the arrow-wing configuration supersonic cruise aircraft. Further design studies were conducted to evaluate the three wing structural arrangement and variations thereof. Candidate fuselage arrangements were also evaluated. These studies together with related design and manufacturing data, the manufacturing plan and the numerous drawings were developed to represent the major output of the design task.

One of the goals of this study is the identification of problem areas. Problem areas associated with design are briefly noted below for the various types of structure:

- Chordwise Stiffened
  - a. With beaded outer skin, especially convex beads, thermal gradients and thermal cycling may cause disbonding at outer/inner skin weld bonded attachments. Loss of the bond would degrade fatigue and sealing properties. Therefore, verification tests are recommended.
  - b. Convex beads in the outer skin, with thin gauges, cause concern relative to damage from hail, maintenance operations, FOD and other causes.
  - c. Venting of inner/outer skin cavities at beads may present problems, particularly on the upper surface. One plan is to drill a 0.125 inch diameter hole in the outer skin at each end of a bead cavity. This might permit entry and accumulation of dirt and liquids over a long period and may require periodic cleaning of these cavities.

**PRECEDING PAGE BLANK NOT FILMED**

- d. Some concern is felt that the installation of fasteners-especially upset types-may cause disbonding even though a preliminary test indicates this may not be a problem.
  - e. Fretting of fastened joints is a concern.
  - f. The drag/fuel penalty associated with external beads in the outer skin has not been fully assessed.
  - g. When local thickening of the outer skin is used to avoid feather edges at countersinks in the outer skin, penalties in flushness/smoothness may result along with a significant cost increase.
  - h. Blind fasteners may be indicated in some areas as a result of a desire to minimize access doors.
  - i. The shape and size of submerged spar caps make it difficult to install surface/spar fasteners and constrain the type of fasteners.
  - j. Not all surfaces of all welds can be dressed and visually inspected. An example is a truss diagonal-to-end-fitting weld.
  - k. It is not feasible to stress relieve all weldments.
  - l. Fail-safe design of spar caps is difficult with this concept because of the monolithic nature and the large loads concentrated in spar caps. However, preliminary analyses indicate that the problem is soluble (without excessive mass penalty or complex measures) by exploiting load redistribution principles. Also, there may be a potential application for laminated structure for fail-safe metallic design.
- Spanwise Stiffened - See items d, e, g, h, j, k under the "Chordwise Stiffened" heading:
    - a. As noted in (a) of the Chordwise Stiffened discussion above, thermal gradients and thermal cycling may cause disbonding at the outer/inner skin weld bonded attachments. If suitable tests show weld bonding is not acceptable, weld brazing is a possible backup approach.

- Aluminum Brazed Honeycomb Sandwich (Monocoque)
  - a. This type of surface includes a significant parasitic weight of aluminum braze alloy. This also increases heat conduction through the sandwich. Development of "stop-off" or other fabrication techniques to minimize these problems is desirable.
  - b. Achievement of reliable faying surface brazed joints may present problems, particularly if the width of the brazed joint is significant.
  - c. Data are needed relative to the effectiveness of welded joints in crack-arresting applications.
  - d. The prevention of excessive creep at brazed joints under long-term/high temperature conditions results in allowables much lower than the static strength.

#### DETAILED DESIGN - TASK II

##### Design Objectives

The detailed design studies were directed towards the final definition of the structural design for the wing and fuselage of the Mach 2.7 arrow-wing supersonic cruise aircraft. Other goals of this effort are the identification of:

- Problems not resolved during the study
- Components warranting further evaluation by fabrication and test.

##### Scope of Design Studies

The Task I results reported in Section 17, Concept Evaluation and Selection identified the least mass and cost wing structure design to be the composite reinforced approach. The evaluation data also indicated the importance of minimum mass designs. Thus, a hybrid wing design was adopted for the detailed design studies effort. The hybrid design was developed by making full use of the minimum mass arrangement defined for the forward wing box, the aft wing box and the wing tip structure. The resulting minimum mass structural arrangement uses sandwich

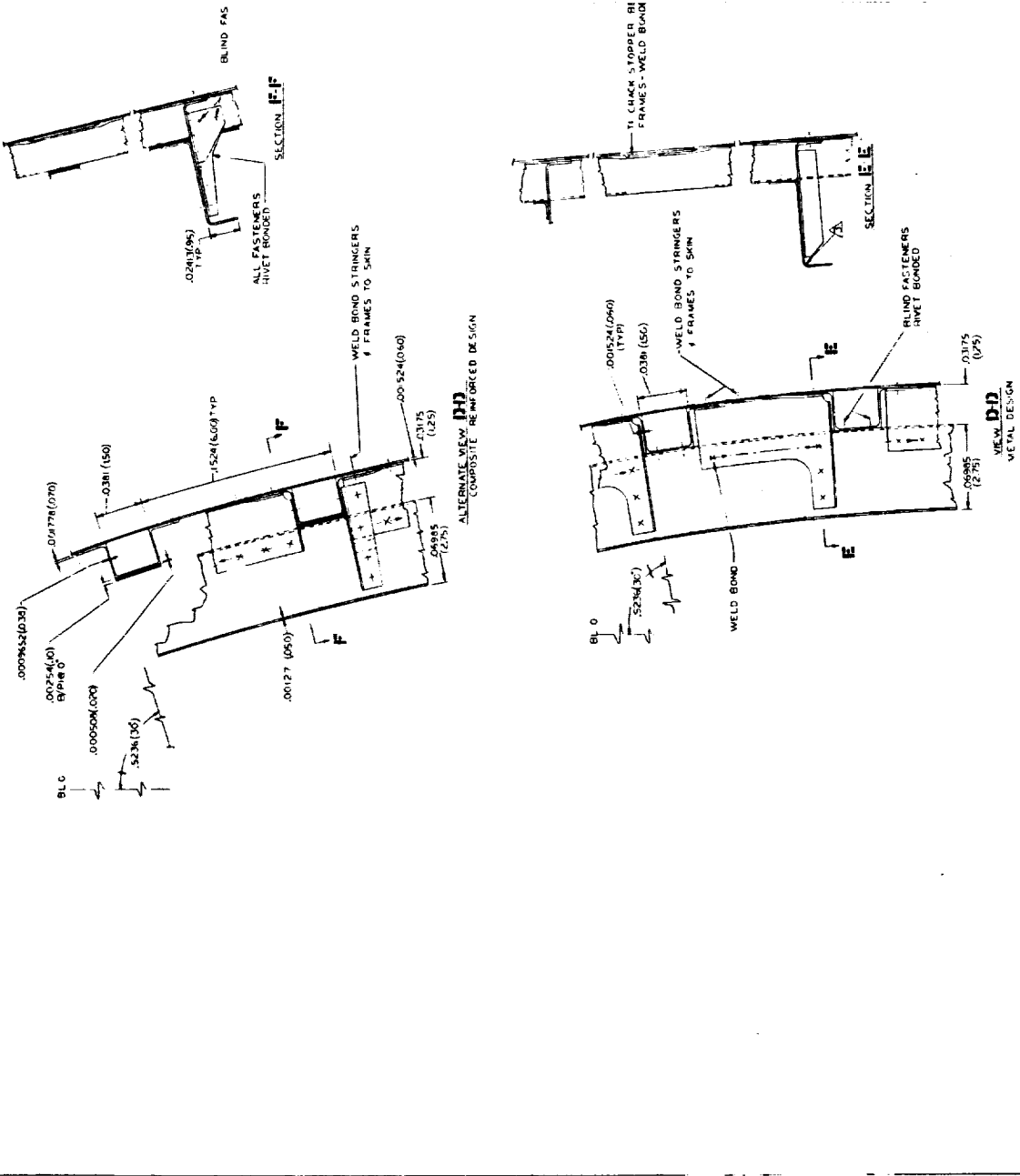
surfaces in the wing tip box and chordwise-stiffened surfaces with composite reinforced spar caps in the remainder of the wing box. The preliminary design drawings presented herein define the salient features listed below as applicable to both types of wing surface construction and the joint area between them:

- The overall structural arrangement for both the wing box and fuselage
- Surface and spar construction, as well as damage tolerance features, in the chordwise and monocoque and transition areas
- Fuselage structure design details for the skin/stringer/frame structural arrangement
- Composite reinforcement applications in the wing box and fuselage
- Manufacturing breakdown for the wing box and fuselage
- Fuel sealing provisions at tank wall spars and ribs and at intersections of composite reinforced spar caps with tank wall ribs

#### Wing Structure Design

The structural arrangement, manufacturing breakdown and the locations of representative panels and surface panel joints are presented in Figure 18-9 for the final design airplane. A hybrid structure consisting of the least mass chordwise stiffened - composite reinforced wing design and the monocoque wing design adopted for the final design are defined below:

Wing Structure - Inboard of BL 470L/R - The design details for a specific chordwise-stiffened surface panel and substructure are shown at the right of Figure 18-10. With this beaded skin design, wing bending material is concentrated in the spar caps and the surfaces primarily transmit the chordwise and shear inplane loads. The uncoupling of bending and torsional material permits either the bending or torsional stiffness to be varied independently of the other. Also, this surface design alleviates thermal stresses and reduces heat transfer to the fuel, relative to a flat skin, since only a portion of the fuel is in direct contact with the wing external skin.



ORIGINAL PAGE IS  
OF POOR QUALITY

FOLDOUT FRAME 1

FOLDOUT FRAME 2



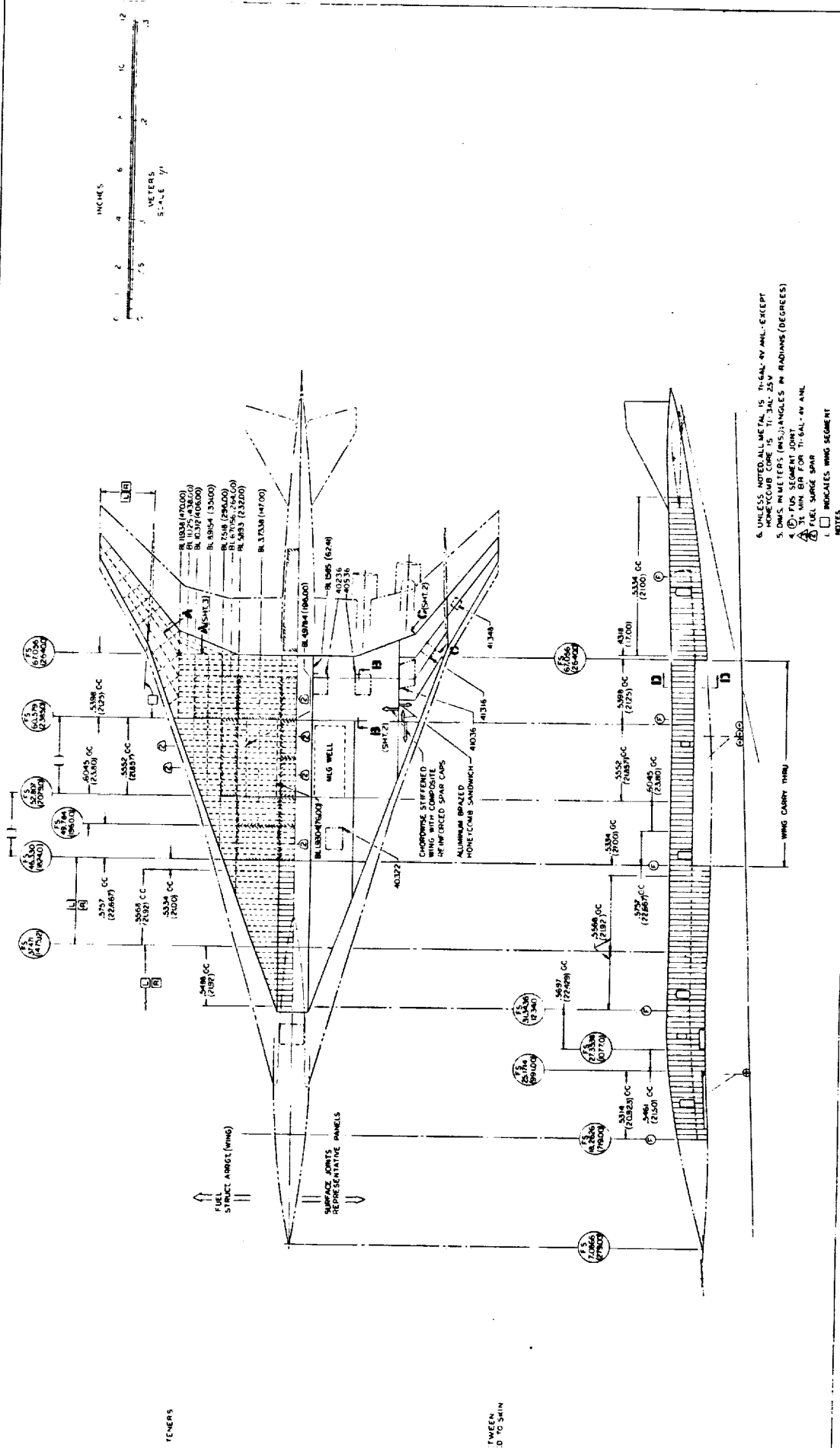


Figure 18-9. Structural Design Concepts - Surface Panels and Substructure



Weld bonding is the basic choice for joining the inner and outer skins of the surface assembly. Surface panel size has been held to 15 feet by 35 feet. The length limit is based on tooling considerations for hot vacuum forming of the skins while the width limit is based on the postulated size of spotwelding equipment.

Concern over potential damage from hail, FOD and maintenance operations has resulted in establishment of the following minimum gages:

- 0.020 in. for exterior skins on the wing lower surface
- 0.015 ins. for exterior skins on the wing upper surface
- 0.010 in. for inner skins of chordwise or biaxially stiffened surfaces

In locating wing spars in the chordwise-stiffened wing area, a minimum spacing of 21 inches has been maintained between constraints such as fuel tank boundaries. This spacing, at or slightly above the optimum determined in Task I, is based on providing a minimum of 19 inches clear passage between spars. This passage width, with sufficient depth, allows internal movement of personnel for installing surface attachment fasteners and performing inspection and maintenance operations. This spacing approach has been taken to avoid blind fasteners and minimize access doors.

The relatively thin external skin in the weld bonded surfaces, in conjunction with flush fasteners, result in feather edges at countersinks in some areas. Where this is unacceptable, thickened pads are incorporated in the skin. Section I-I of Figure 18-10 depicts an example of such a spar/surface attachment. As shown, diffusion bonding is specified as an alternate method for joining the inner and outer skins. Low pressure diffusion bonding is a very attractive process which, when adequately developed, would avoid or minimize the need for thickened pads in the outer skin and would thereby permit reductions in mass and surface roughness. If attachment clips are included in such a diffusion bonded surface assembly, the assembly could be fastened to a welded truss spar as sketched in Figure 18-11. By reducing fasteners through the surface, this approach would facilitate fuel sealing also.

**PRECEDING PAGE BLANK NOT FILMED**

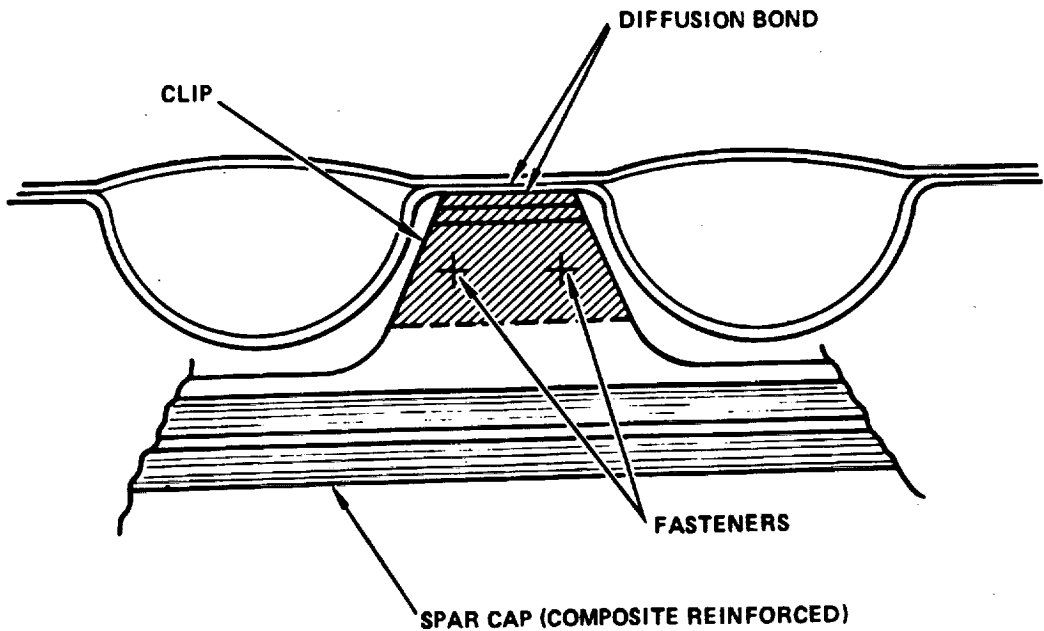
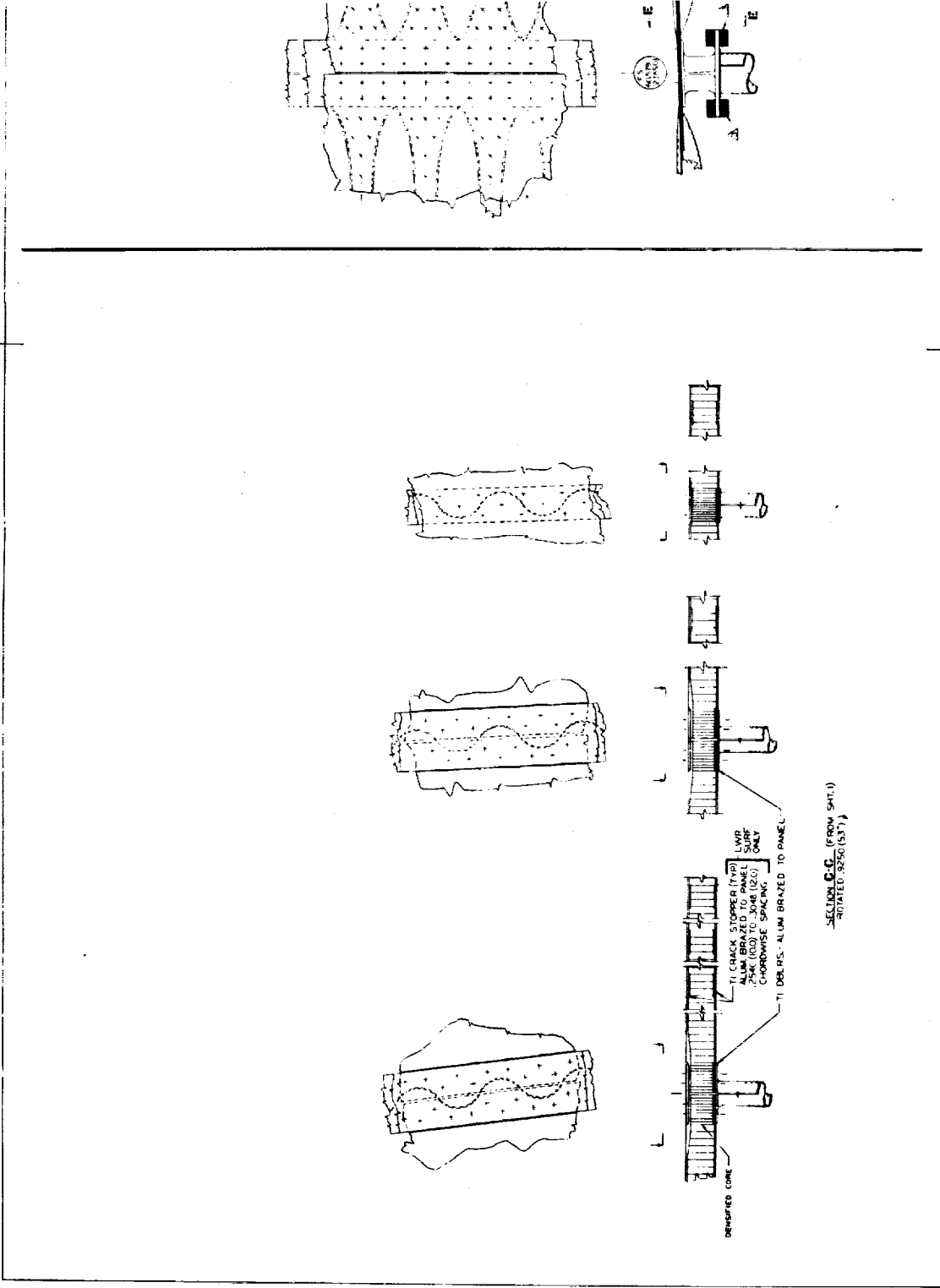


Figure 18-11. Attachment of Truss Spar to Low Pressure Diffusion Bonded Surface

Wing rib spacing is a nominal 60 inches but is modified as required to suit design constraints. In the chordwise-stiffened and transition areas, welded truss spars are used except where a spar serves as a fuel tank wall. At such locations, spars have welded circular arc webs with stiffened "I" caps. To facilitate fuel sealing, no surface beads extend across tank boundaries. Inner wing spars in the aft wing box are fabricated initially as continuous subassemblies between BL 470L and R. At the latter locations, as shown in Figure 18-12 spars are subsequently welded together to form continuous spars from one vertical fin to the opposite. An 85-foot long vacuum chamber has been postulated for electron beam welding of spar subassemblies. Whenever possible, all welds are designed for automation as well as stress relieving, dressing on all surfaces and visual inspection after welding.

Effective use is made of composite reinforcement with the major application involving unidirectional reinforcement of spar caps. At all welded truss spars, the composite reinforcement is continuous between BL 470L and R. Figure 18-12 details the outboard termination of the spar cap reinforcements. The continuity of these reinforcements is very desirable even though they penetrate fuel tank wall ribs. The design developed for fuel sealing at intersections of composite reinforced welded truss spars with



FOLDOUT FRAME 1

PRECEDING PAGE BLANK NOT FILMED  
ORIGINAL PAGE IS  
OF POOR QUALITY

...arm frame 2



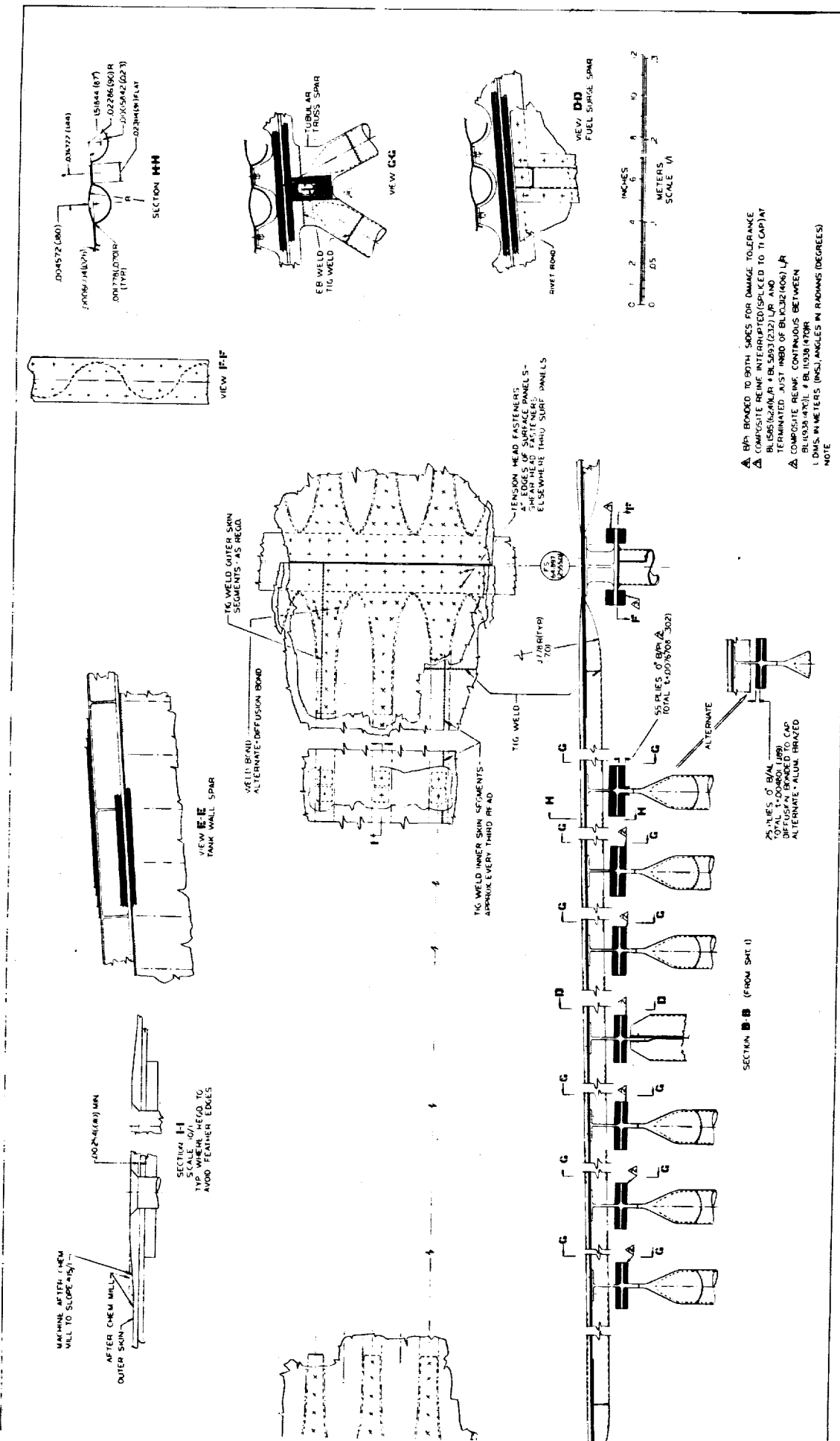
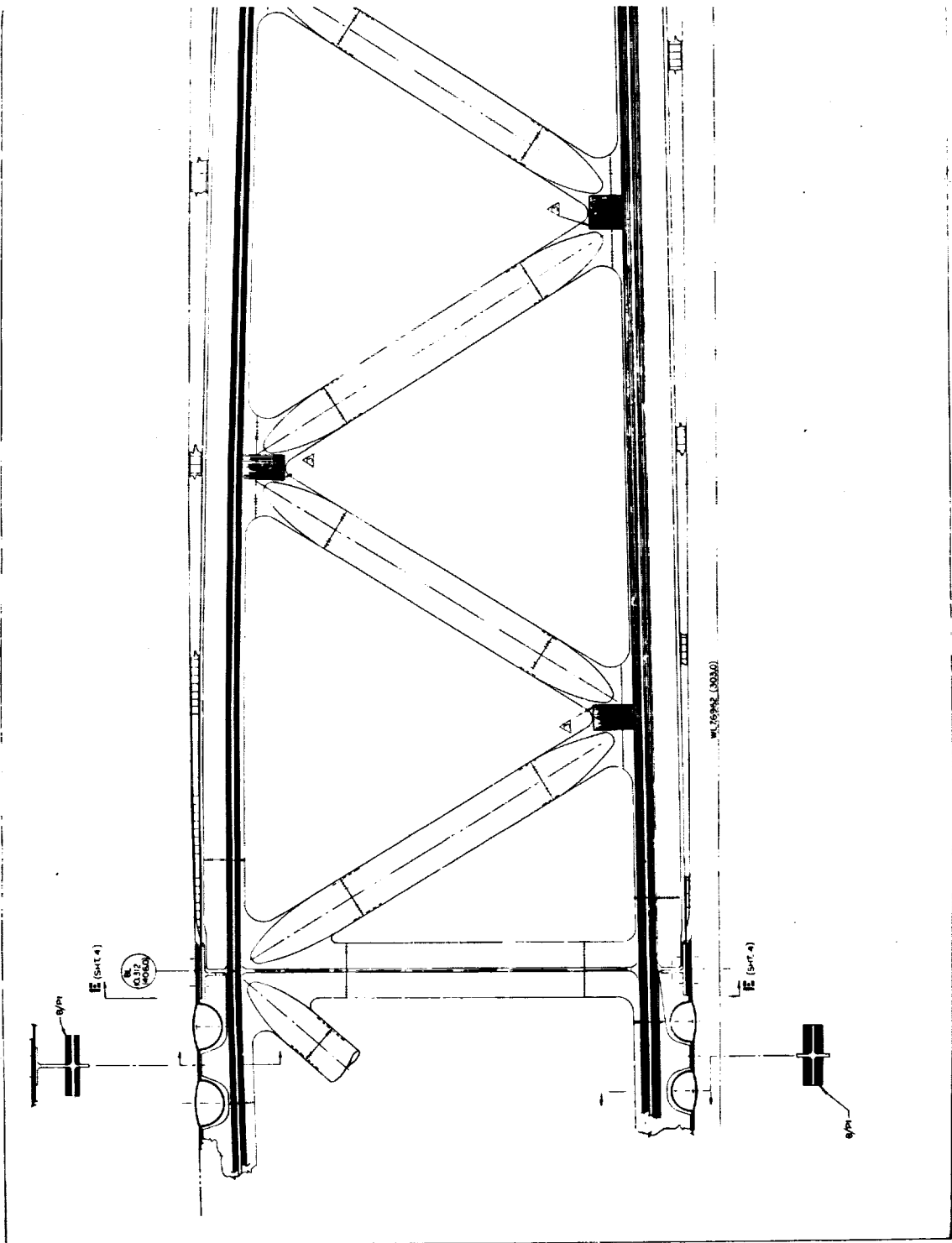


**Figure 18-10.** Structural Design Concepts—Truss Spar and Surface Panel at Transition Structure



FOLDOUT FRAME 2



FOLDOUT FRAME 1



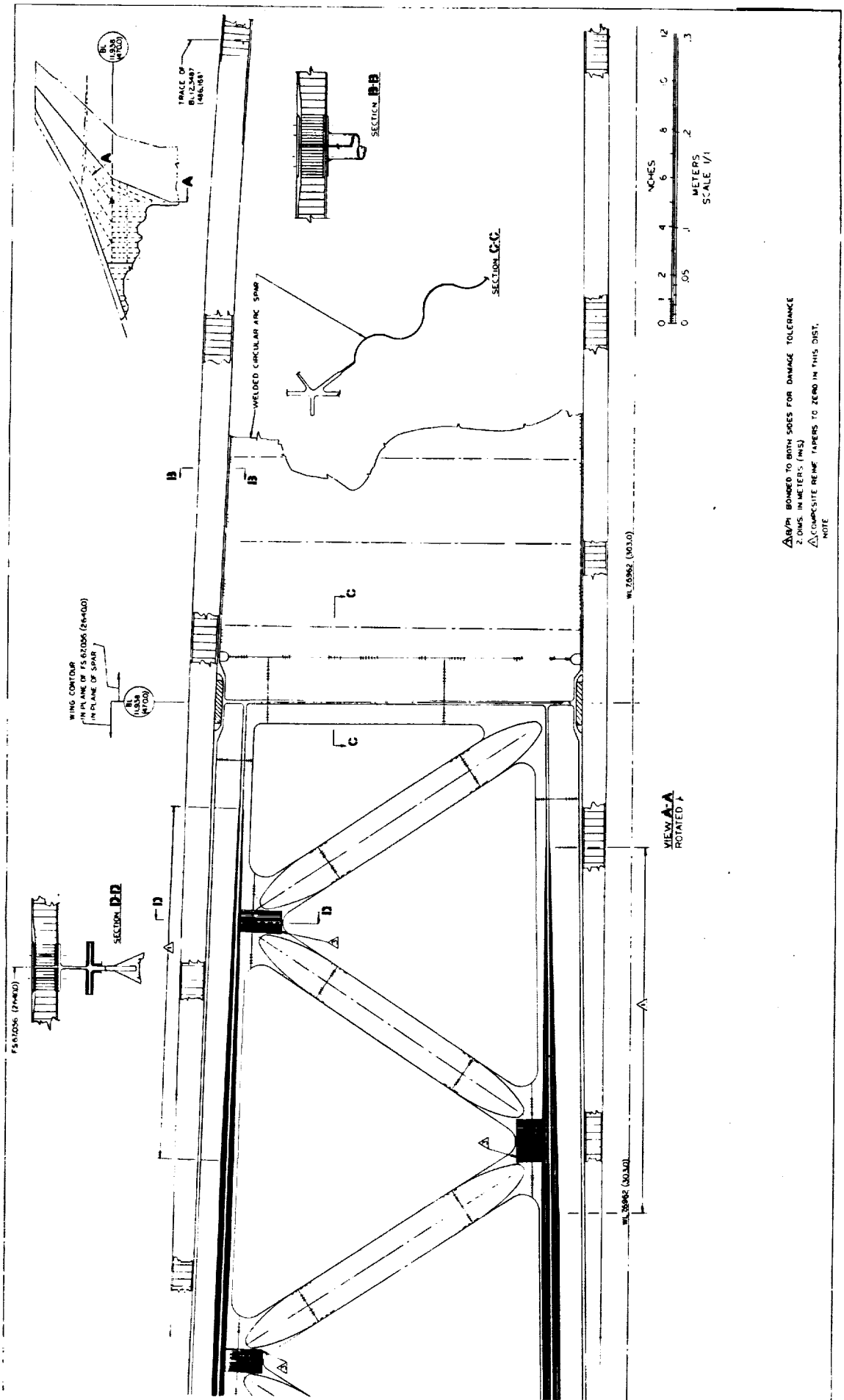


Figure 18-12. Structural Design Concepts  
Tank Sealing Concept and  
Rib Details  
**FOLDOUT FRAME**

18-53  
WING FRAME FOR A MR. 7



tank wall ribs is shown at the left of Figure 18-13. Machined aluminum fittings, which are not attached through the composite, fit tightly around the reinforced spar caps to provide both fuel sealing and spar cap support. The right side of Figure 18-13 shows the intersection of a composite reinforced truss spar with BL 406 tank wall rib aft of the area where fuel sealing is required. At tank wall spars, as shown in Figure 18-10, the composite reinforcement consists of separate reinforcement strips between adjacent tank wall ribs. This interruption is used so that a special metal fitting, made an integral part of the spar cap, can be designed to provide an efficient structural joint between tank wall ribs and tank wall spars while also permitting a clean tank corner amenable to fuel sealing.

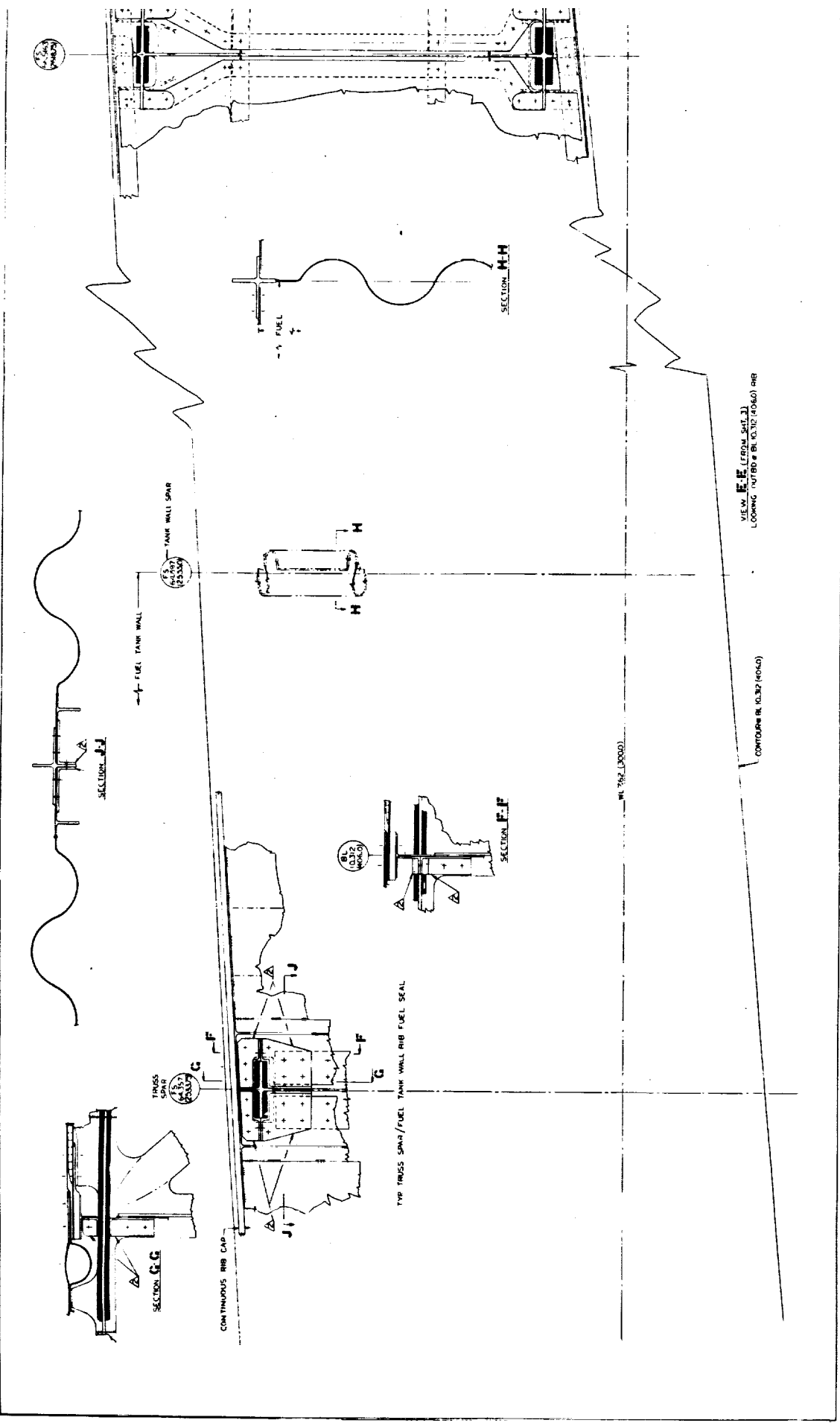
Boron/polyimide (B/PI) is specified as the basic composite material for spar cap reinforcement because of its lower cost and structural efficiency. The multiple element form of the B/PI spar cap reinforcement results in damage tolerance capability. Boron/aluminum (B/Al) diffusion bonded to spar caps is an alternate approach and one which has been used by Ameron. An additional alternate is the use of Borsic/aluminum reinforcements', which are aluminum brazed to the caps. In another extensive application, composite reinforcement is bonded to both sides of the welded diagonal-to-cap joints in all welded truss spars to serve as a crack stopper. This is depicted in View G-G of Figure 18-10 and Figure 18-12.

A tentative plan for venting the closed cavities at inner/outer skin beads is the use of a small diameter hole in the outer skin at each end of a bead cavity. For the upper surface in particular, this requires further review since this might permit entry and accumulation of dirt and liquids over a period of time.

Problem areas identified for the wing structural design are discussed in a later section.

Wing Structure - Outboard of BL 470L/R - Design details for the monocoque surfaces and the substructure in the wing tip box are defined at the left of Figure 18-9. The sandwich surfaces are brazed together using 3003 aluminum alloy as the brazing material (the "Aeronca" process). Outboard of BL 470, welded circular-arc spars and ribs are used since the minimum or zero need for web penetrations allows the realization of their inherent light weight and simplicity. Composite reinforcement is not used in the brazed surfaces or the welded circular arc spars and ribs.





PRECEDING PAGE BLANK NOT FILMED

FOLDOUT FRAME J

FOLDOUT FRAME



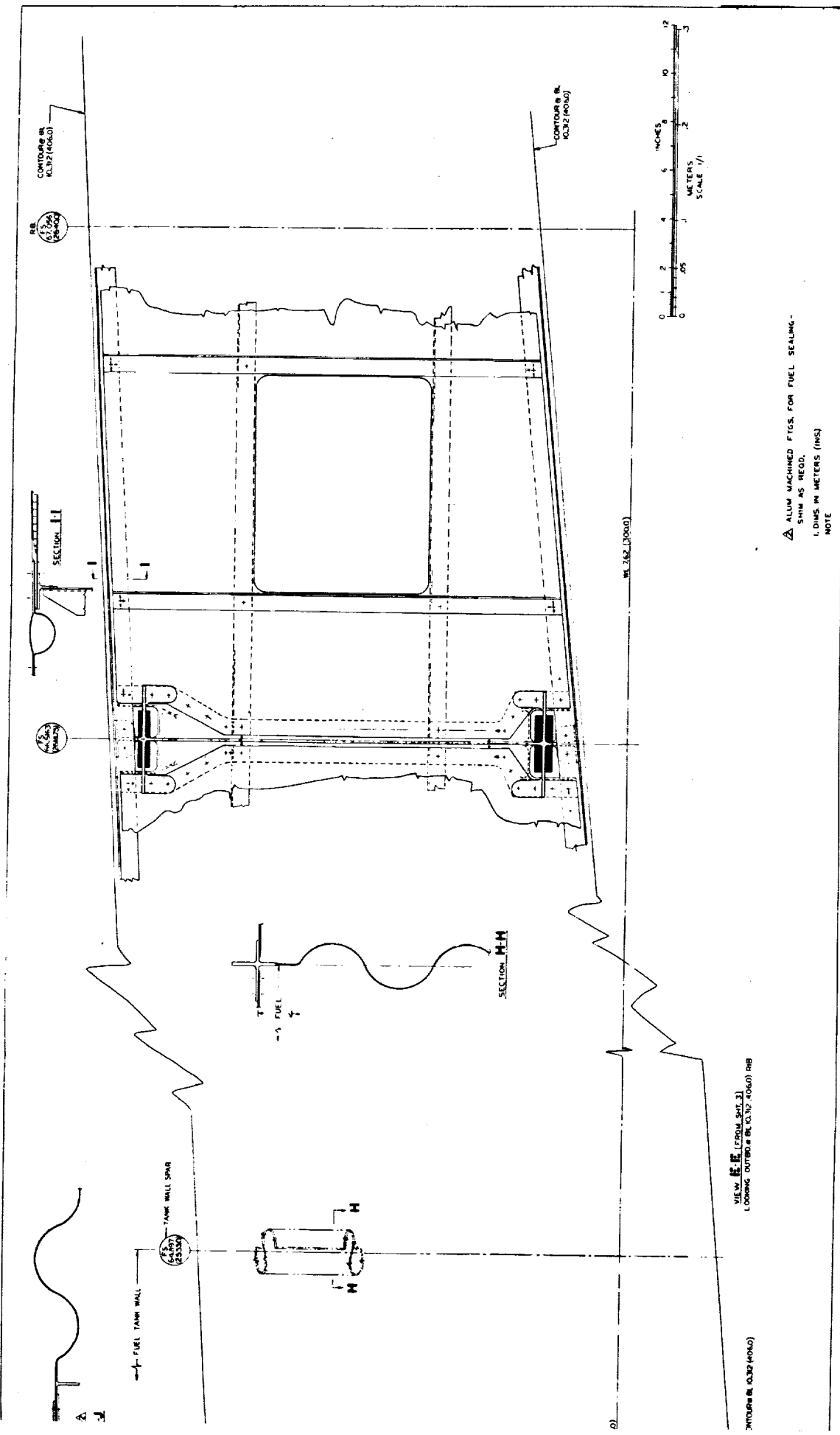


Figure 18-13. Structural Design Concept -  
M2.7 Arrow-Wing Supersonic  
Transport Configuration  
(Near-Term)

18-57



A size limit of 68 inches by 40 feet for brazed surfaces was postulated as a guide after consultation with Aeronca. The actual panel configurations defined in Figure 18-9 approximate this size and are based on the design philosophy that all or some panels of the upper surface are attached with screws and are removable for inspection and maintenance purposes.

The flexibility of the aluminum braze process is exploited by incorporating crack stoppers and panel edge doublers in the surface panel brazements. Also, the capability of tapering the panel thickness is utilized in the joint between the chordwise and monocoque surface areas. In the joint area, as shown in Figure 18-12, the outboard sandwich surfaces are extended inboard across BL 470 so that spanwise components of the outboard surface loads due to wing bending loads are transferred directly to the chordwise stiffened structure at the BL 406 rib.

Spanwise hat section stiffeners are aluminum brazed to the tapered wing surface panels in the joint area to provide the needed surface stiffening. Surface panel splice plates are sufficiently thick to avoid feather edges at countersunk fasteners.

#### Fuselage Structure Design

The fuselage structural arrangement and design details of a specific fuselage area for both all titanium and composite reinforced metal structure are shown in Figure 18-9. As shown, both designs include machined extrusion stringers, crack stoppers between frames and floating zee frames with shear clips. Closed hat section extruded stringers which provide structural efficiency, are machined to provide for crack stoppers and to vary stringer thickness. Extruded stringers also are well suited to effective installation of composite reinforcement. The floating zee frames with shear clips are considered preferable, from a fatigue standpoint, to full depth frames having notches for stringers. Also, zee frames avoid the offset shear center associated with channel section frames.

Weld bonding is used for attaching frames, stringers and crack stoppers to the skin because of economy, minimum mass, good fatigue characteristics and the avoidance of sealing problems. Satisfactory weld bonding of three thicknesses, as encountered at some locations, may require development. Weld brazing is a possible backup to weld bonding. Where fasteners are used at shear clips and frame/stringer

attachments, fastener bonding is utilized in lieu of fasteners alone to obtain enhanced fatigue properties. The size of fuselage skin panel assemblies has been limited to 15 ft by 50 ft; the former is based on the postulated size of spot-welding equipment, the latter on the postulated length of the adhesive curing ovens.

Longitudinal skin panel splices are located only at the top and bottom centerlines of the fuselage and at the floor/shell intersections fore and aft of the wing carry-through area. These longitudinal splices utilize external and internal splice plates in conjunction with fastener bonding to achieve a double shear splice having damage tolerance capabilities and good fatigue properties. Suitable combinations of fastener size and external splice plate thickness are utilized to avoid feather edges at countersinks for flush fasteners. At circumferential panel splices, and other locations as required, feather edges are avoided by incorporating thickened pads in the external skin in a manner similar to that for wing skins. Chemical milling is used to vary fuselage skin thickness in accordance with load requirements.

#### Potential Problems Not Resolved During Study Design and Manufacture

Preliminary design studies of a wide variety of structural design concepts were made to assess the relative merits of various concepts and materials suitable for an advanced supersonic cruise aircraft (Mach 2.7). Construction details were provided for wing and fuselage primary structure to enable mass and cost estimates to be made. In the process of preparation of the preliminary engineering drawings potential problems were uncovered and resolved (on the drawing) by applying good engineering judgement, related subscale experimental work and decisions made in consultation with Structures, Advanced Design, Materials and Producibility specialists.

The critical problems in the fabrication technology were joining, forming, sealing and related equipment requirements. These disciplines were further affected by the materials constraints. Some industry research and development programs have been initiated in these technologies, however, specific application to a supersonic cruise aircraft (Mach 2.7) with an arrow-wing design configuration presents many new prob-

lems to be resolved. The size effect of hardware components, for example, presents some of the critical fabrication problems.

A summary of the potential problem areas for design and manufacture of wing and fuselage primary structure are identified in Tables 18-3 through 18-7. These problem areas require further detailed study to develop the fabrication processes, tooling methods, and definition of the facilities to verify the manufacturing capability to produce hardware components that meet the engineering requirements.

TABLE 18-3. POTENTIAL PROBLEMS NOT RESOLVED - WING SURFACE PANEL CONCEPT - CONVEX BEADED

Wing Surface Panel Concept - Convex Beaded

- Welding of thin gage sheet to fabricate large panels (15 ft. x 35 ft.)
- Vacuum forming skin panels to final compound contour
- Continuous progressive rolling of inner skins
- Assembly of skin panels
  - Weld bonding
  - Weld brazing
  - Isothermal brazing
  - Diffusion bonding (low pressure)
- Fastening minimum gage skin panels to substructure
  - Disbonding at fasteners through weld bonded surfaces
  - Rivet types and installation clearance requirements
- Disbonding resulting from thermal gradients and cycling
- Venting of beaded skins
- Fail-safe characteristics and fatigue quality

TABLE 18-4. POTENTIAL PROBLEMS NOT RESOLVED DURING STUDY - WING SPAR CONCEPT - COMPOSITE REINFORCED TITANIUM ALLOY CAPS

Wing Spar Concept - Composite Reinforced Titanium Alloy Caps

- Boron/polyimide reinforcement
  - Autoclave and heat expanding rubber oven curing methods
  - Tooling methods
  - Process procedures
  - NDT methods
- Borsic/aluminum reinforcement
  - Aluminum brazing methods
- Boron/aluminum reinforcement
  - Diffusion bonding methods
- Boron/aluminum truss tubes
  - Diffusion bonding methods
  - Brazing methods
- Fail-safe characteristics

TABLE 18-5. POTENTIAL PROBLEMS NOT RESOLVED DURING STUDY - WING SURFACE PANEL CONCEPT - HONEYCOMB SANDWICH

Wing Surface Panel Concept - Honeycomb Sandwich

- Aluminum brazing large panels to compound contour
- Brazing doublers and fail-safe straps
- Core stop-off material and processes to prevent vertical cell wall braze flow during brazing cycle
- Braze panel structural repair methods
  - Potting compounds (organic plus ceramic materials)
  - Mechanical fastened patch plates
  - Tooling/equipment requirements
  - NDT techniques
- Fail-safe characteristics

TABLE 18-6. POTENTIAL PROBLEMS NOT RESOLVED  
DURING STUDY - FUSELAGE SHELL CONCEPT -  
SKIN AND STRINGER

Fuselage Shell Concept - Skin-Stringer

- Weld bonded panel assemblies (15 ft. x 50 ft.)
  - Skin and stringers
  - Frames
  - Fail-safe straps
  - Shear clips
- Rivet bond panel section splice
  - Longitudinal (50 ft. length)
  - Circumferential (204 in. length)
  - Equipment/processing techniques required
- Precision extruded titanium alloy sections
  - Hat section stringers
  - Variable wall thicknesses

TABLE 18-7. POTENTIAL PROBLEMS NOT RESOLVED DURING STUDY  
- TANK SEALING CONCEPT

Tank Sealing Concept

- Requirements
  - Fuel tank thermal environment
  - Application techniques
  - Curing methods
- Faying surface
  - Interstices between structural members
  - Corner gaps
  - Overlapping surfaces
  - Coating fastener, welds and pin hole openings
- Intersection of composite reinforced spar caps/tank rib caps
  - Sealing techniques
  - Metal fittings plus sealing material

### Components for Further Evaluation and Test

The development of structural concepts for supersonic cruise aircraft has been the subject of this reported analytical investigation.

This investigation has produced a number of promising concepts having good potential application for design of a supersonic airplane structure. However, experimental research is necessary to assess the validity of the structural concepts and to determine the combination of concepts best suited for design and fabrication of flight hardware for Mach 2.7 arrow-wing configuration transport.

The economic viability of a supersonic cruise aircraft is dependent upon achievement of a low structural mass fraction through lightweight and reliable structural design concepts. State-of-the-art structures and materials are inadequate to provide a viable commercial supersonic transport with a service life of 50,000 hours.

The principal objective of this planned research and development program was to assess the relative merits of various structural concepts and materials for a prescribed arrow-wing aerodynamic configuration; to determine the structural weight estimates based on in-depth structural design studies. The concepts were evaluated through design studies making use of the best available materials technology, design tools, design criteria and simplified cost benefit studies. The best concepts which merit experimental evaluation are identified.

As an integral part of the research and development program it is essential that an experimental program be initiated to verify the manufacturing capability to produce hardware components that meet the engineering requirements as shown in Table 18-8. Moreover, experimental data verifying fabrication processes (Table 18-9) from the element and component tests (Table 18-10) must be compared with predicted values of strength, deflections, temperature distributions, fatigue quality, fail-safe characteristics, and life to determine the degree to which concept performance can be predicted in a realistic structural application. The results of these tests should then be used to refine the methods of analyses and concept designs.

It is recommended that future studies be directed towards the design, fabrication, and testing (with appropriate attachment and restraint conditions) under simulated flight environment of larger structural assembly incorporating the refined concept designs. The outer wing and nacells of the NASA YF-12 aircraft could be effectively used as the baseline structural envelope for design and fabrication of such an assembly. After sufficient ground testing, actual flight experience at the high Mach ranges can be obtained.

TABLE 18-8. TEST OBJECTIVES

Conduct Sufficient Tests to Experimentally Validate the Structural Design Concepts:

- Manufacturing processes
- Strength and damage tolerance capability of the components for the load/temperature environment
- Correlate test results with the theoretical analysis
- Assess the impact upon the results of this design concept study

TABLE 18-9. FABRICATION PROCESS TESTS

Types of Test Recommended

- Fabrication processes
  - Tooling approach
  - Fabrication and assembly schedule
  - Joining methods
  - Chemical milling/shot peening
  - Metallurgical examination
  - Inspection/quality assurance methods

TABLE 18-10. STRUCTURAL ELEMENT AND COMPONENT TESTS

<u>Types of Test Recommended</u>
● Structural element and component
○ Room temperature
○ Elevated temperature
○ Cyclic
● Development tests
○ Crippling
○ Buckling
○ Column
○ Mechanical joints - fatigue quality, fretting
○ Chem mill/shot peen - fatigue properties
○ Crack growth/propagation
○ Crack stopper concept
○ Fail-safe and fatigue characteristics
○ Welded joints - fatigue and fracture properties

REFERENCES

1. Foss, R.L.: Studies of the Impact of Advanced Technologies Applied to Supersonic Transport Aircraft, LR 25827-3, Lockheed-California Company, January 1974
2. Elrod, S.D. and Lovel, D.T: Development of Aluminum Brazed Titanium Honeycomb Sandwich Structure, Boeing Aircraft Report D6-60203, July 1972 (Report No. FAA-SS-72-03).



SECTION 19

PROPULSION-AIRFRAME INTEGRATION

BY

S.J.SMYTH, D.M.URIE, T.A.SEDGWICK, I.F.SAKATA



## CONTENTS

<u>Section</u>	<u>Page</u>
INTRODUCTION	19-1
DESIGN INTEGRATION	19-1
Engine Forward Movement	19-7
Engine Spanwise Movement	19-11
Engine Size	19-11
Constraint Envelope	19-12
PROPULSION SYSTEM INTEGRATION	19-12
Boundary Layer Diverter	19-12
Inlet Mutual Interaction	19-12
AERODYNAMICS CHARACTERISTICS	19-17
Control Surface	19-17
Performance	19-20
STRUCTURAL CHARACTERISTICS	19-20
Flutter Characteristics	19-20
Sonic Fatigue	19-22
RESULTS	19-22
REFERENCES	

c. 4



## LIST OF FIGURES

<u>Figure</u>		<u>Page</u>
19-1	Baseline Powerplant Configuration	19-3
19-2	Duct Burning Turbofan Engine - Mach 2.7	19-5
19-3	Preliminary Nacelle	19-6
19-4	Flutter Speed Variation with Engine Placement	19-8
19-5	Overall Sound Pressure Level - Aft Mounted Engines	19-9
19-6	Overall Sound Pressure Level - Engine Forward	19-10
19-7	Constraint Envelope	19-13
19-8	Divertor Height Variation with Nacelle Longitudinal Position	19-14
19-9	Stable Operating Location of Aft Inlet	19-16
19-10	Incremental Lift Due to Inboard and Outboard Engine Spanwise Shift - Flaps at 20 Degrees	19-18
19-11	Incremental Lift Due to Outboard Engine Spanwise Shift - Flaps at 20 Degrees	19-18
19-12	Trimmed Lift as a Function of Outboard Engine Spanwise Location - Flaps at 20 Degrees	19-19
19-13	Effect of Outboard Engine Spanwise Location on Rolling Moment Due to Flaperons	19-19
19-14	Vertical Tail Required Due to Spanwise Shift of Outboard Engine	19-21
19-15	Effect of Mission Lift/Drag Ratio on Nacelle Forward Shift	19-21
19-16	Candidate Engine Location	19-23

**PRECEDING PAGE BLANK NOT FILMED**



LIST OF TABLES

<u>Table</u>		<u>Page</u>
19-1	Propulsion System Parameters	19-5
19-2	Propulsion-Airframe Integration Results	19-23

**PRECEDING PAGE BLANK NOT FILMED**



## SECTION 19

### PROPELLION - AIRFRAME INTEGRATION

#### INTRODUCTION

The study conducted to provide the proper integration of the engine and the airframe for meaningful completion of the detailed engineering design and analysis of Task II is reported in this section.

The orientation of the nacelles of the baseline configuration concept (Section 2) were derived from unpublished data of wind tunnel tests at the NASA Langley Research Center with their spanwise location determined from the NASA configuration data deck (identified as 733-336C Follow-on, April 1973). The engine characteristics for the selected duct-burning turbofan engine, designated BSTF 2.7-2, were obtained from Reference 1.

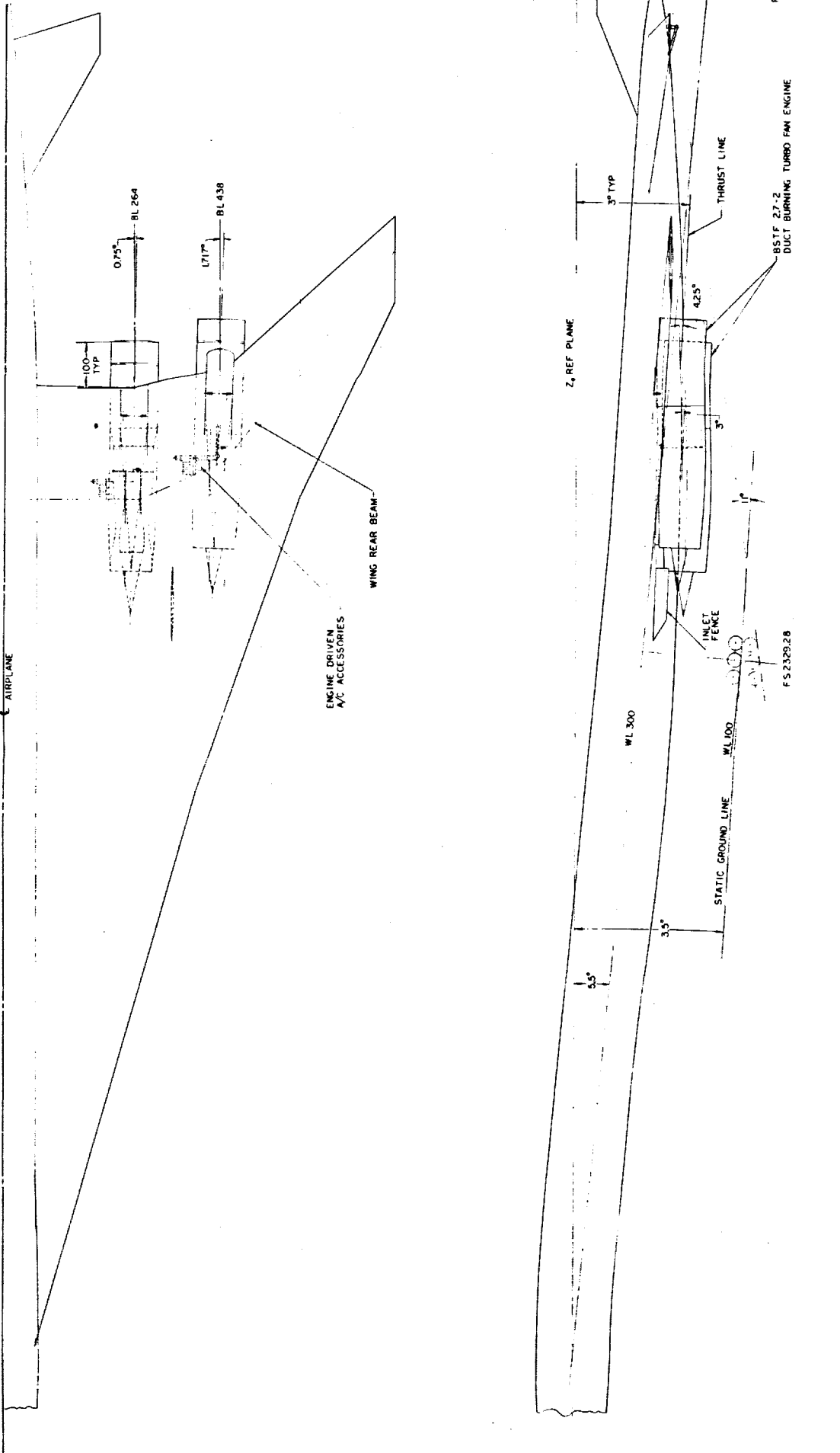
The aforementioned data were integrated into the baseline configuration concept to define the propulsion installation shown on Figure 19-1. Small longitudinal and spanwise movements from the baseline position were explored and sensitivities determined to aid in establishing the best aft mounted-underwing installation for the propulsion packages.

#### DESIGN INTEGRATION

The effect of engine location and size on the overall airplane structural, aerodynamic and performance characteristics were explored to establish a nacelle constraint envelope for the placement of four underwing nacelles on the arrow-wing configuration transport.

The duct-burning turbofan engine shown in Figure 19-2 was selected for the study. The engine, designated the BSTF 2.7-2, has a bypass ratio of 3.26 and a fan pressure ratio of 3.0. The scale-one engine has an uninstalled sea level static thrust of 78,000 pounds, a maximum diameter of 90 inches and an overall length of 255 inches. Other pertinent data are found in Engine Recommendations of Section 2. Table 19-1 gives the propulsion system parameters for the BSTF 2.7-2 engine.





PRECEDING PAGE BLANK NOT FILMED  
FOLDOUT FRAME 1  
ORIGINAL PAGE IS  
OF POOR QUALITY

FOLDOUT FRAME 2



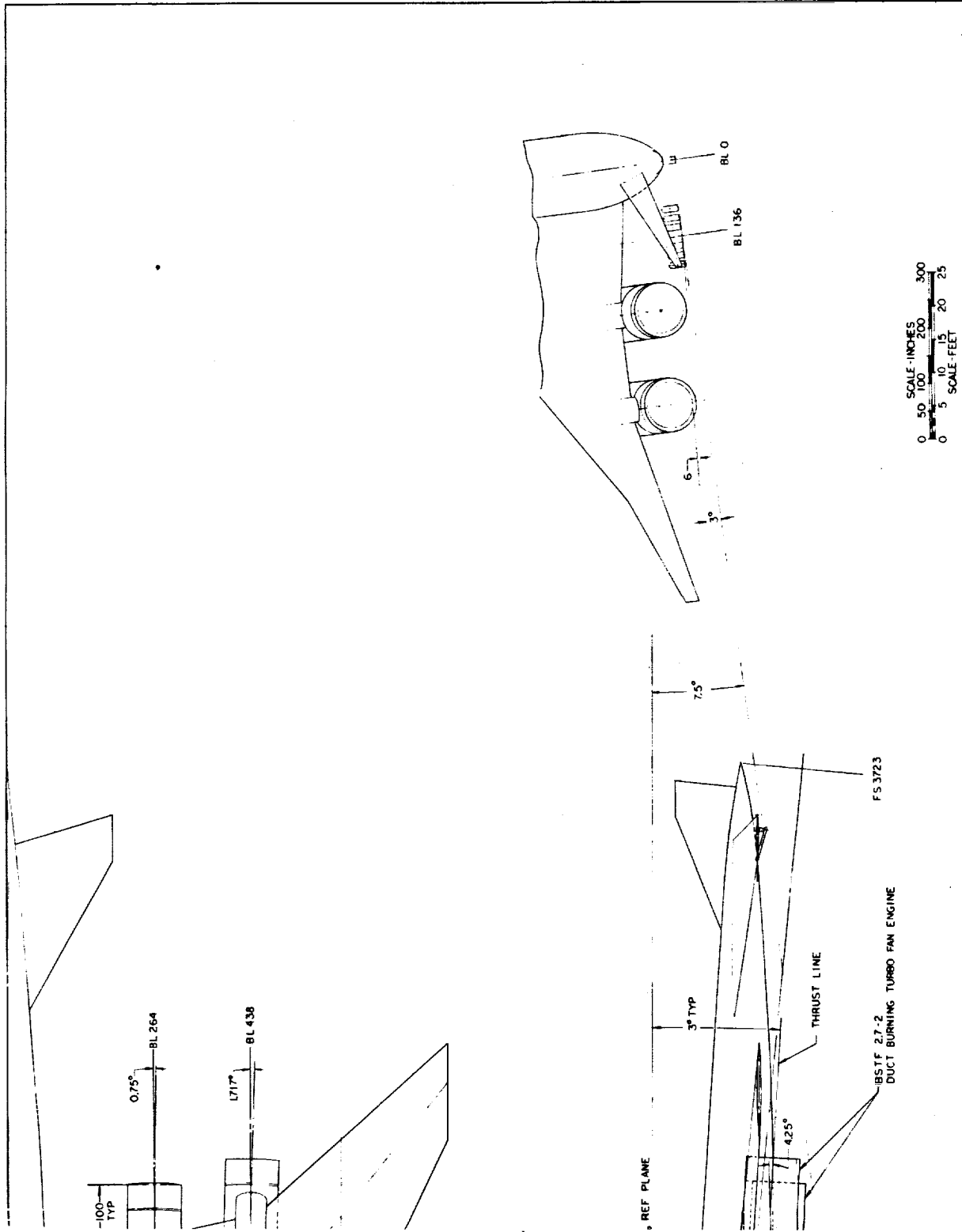


Figure 19-1. Power Plant Configuration -  
AST BSTTF2.7-2 Duct Burning Turbofan  
OLDOUT FRAME<sup>19-3</sup>



**CONCEPTUAL GAS PATH SCHEMATIC  
FAN PRESSURE RATIO = 3.0**

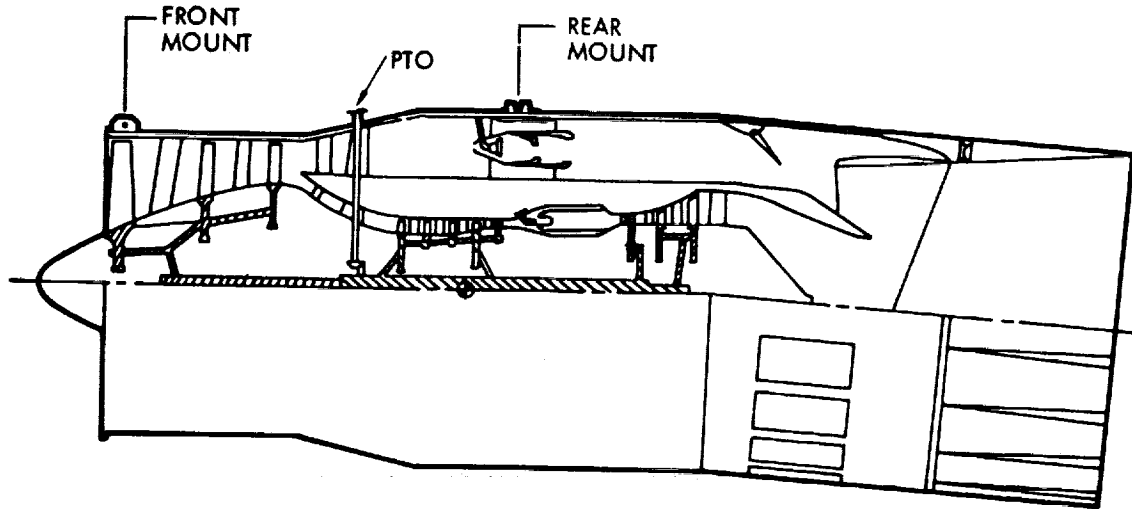


Figure 19-2. Duct Burning Turbofan Engine - Mach 2.7

TABLE 2-2. PROPULSION SYSTEM PARAMETERS

Engine:	BSTF 2.7-2 duct burning turbofan	
Number of engines:	4	
Noise suppression:	FAR 36-5	
Inlet/nozzle:	Axisymmetric/variable convergent-divergent	
Thrust/weight - (lift off):	0.36	
Lift of Speed:	Mach 0.30	
Scale Factor:	1.0 (Ref.)	1.147
Net thrust, lb. (A)	78,000	89,466
Engine weight, lb. (B)	11,143	12,781
ACAP, ft <sup>2</sup>	33.1	38.0
DMAX, in.	90	96.4
DCOMP, in.	79.4	85.0
DNOZ, in.	90	96.4
LENG, in.	255	267.5
LINLET, in.	189.3	203.9
Study Application	Task I	Task II

(A) SLS, Max. Power, uninstalled

(B) Includes reverser and suppressor

**PRECEDING PAGE BLANK NOT FILMED**

The layout of the preliminary nacelle with an axisymmetric mixed compression inlet and the BSTF 2.7-2 duct burning turbofan engine is shown in Figure 19-3. The inlet is as described in Boeing Report FA-SS-72-50, dated April 1972, scaled to account for the differences in engine face diameter and airflow. Supersonic diffuser lines are maintained as a function of Mach number and subsonic diffuse divergence is kept unchanged. The nozzle is rotated down 4-degrees 15-minutes relative to the engine center line to permit proper orientation of nacelles relative to the wing.

The propulsion installation of Figure 19-1 are toed in 0.75-degree and 1.717-degree for the inboard (BL 264) and outboard (BL 438) engines, respectively. The inlet is aligned with the underwing flow field and the nozzle tilted 3-degrees down relative to the  $Z_0$  reference line. The tilt prevents a loss in airplane lift/drag ratio as was determined in previous supersonic transport studies. The engine dimensional data used corresponds to the BSTF 2.7-2/(scale 1.147) duct-burning turbofan which has a maximum diameter of 96.4 inches. As shown in the figure, the rotation of the nozzle to prevent an L/D loss, the increased engine diameter, the nozzle clearance for a 3-degree roll at touch down requires an increase of 19 inches in the landing gear length from that shown for the Task I-Baseline Configuration concept. The engine mounts are located aft of the wing rear beam, and are supported from beams which extend aft (cantilevered) of the structural box. Engine accessories are arranged around the forward portion of the engine. The hydraulic pumps, constant speed driven generator, and engine power takeoff are located aft of the

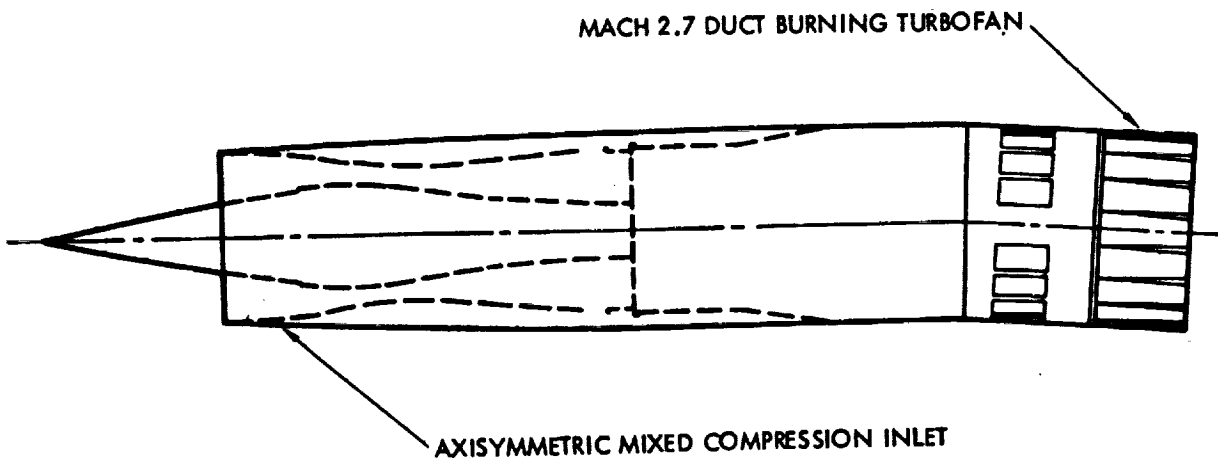


Figure 19-3. Preliminary Nacelle

wing box, as indicated on the figure. Further study indicates that these units should be moved forward of the rear beam, with an access panel located in the upper surface of the wing box. The area aft of the rear beam is congested with controls for the flaperons, flaps and spoilers. The engine driven compressor for the airplane environmental control system is located on the engine lower centerline and requires a faired bump in the lower nacelle (not shown on drawing). Inlet boundary layer diverter heights are 15 inches on the inboard nacelle and 8 inches on the outboard nacelle. The outboard inlet is aft of the inboard inlet and approximately one diameter away. Mutual interference will cause an unstart on the inboard inlet to unstart the outboard inlet. To prevent this an inlet fence is required between nacelles as shown.

#### Engine Forward Movement

Factors influencing longitudinal limits on nacelle placement include wing leading edge shock wave, flutter, sonic fatigue, thermal stresses, wave drag, airplane balance, airplane tail-down and roll angle, landing gear length, and inlet mutual interference.

The arrow-wing configuration in this study has a subsonic wing leading edge. This permits the underwing nacelles to be moved forward until the inlet lip is ahead of the wing leading edge and still remain in a favorable interference field. Practical limitations at the wing trailing edge reduced the potential for the forward movement of the nacelles to approximately 100 inches.

Engine longitudinal placement effect on flutter speed as presented in the Sensitivity Studies section (Vibration and Flutter, Section 9) indicated an increase in the bending and torsion mode flutter speed with a forward engine movement (Figure 19-4). This allows for a reduction in the mass to be added to the wing tip structure, and also a mass reduction resulting from shortening of the deflection critical engine rails.

As the engine is moved forward, the effect of nozzle exhaust increases sonic fatigue and thermal stresses on the trailing edge flaps, flaperons, and wing vertical fin. The increased sonic environment is visually displayed on Figures 19-5 and 19-6. The primary mass penalty, as indicated, is on the trailing edge structure.

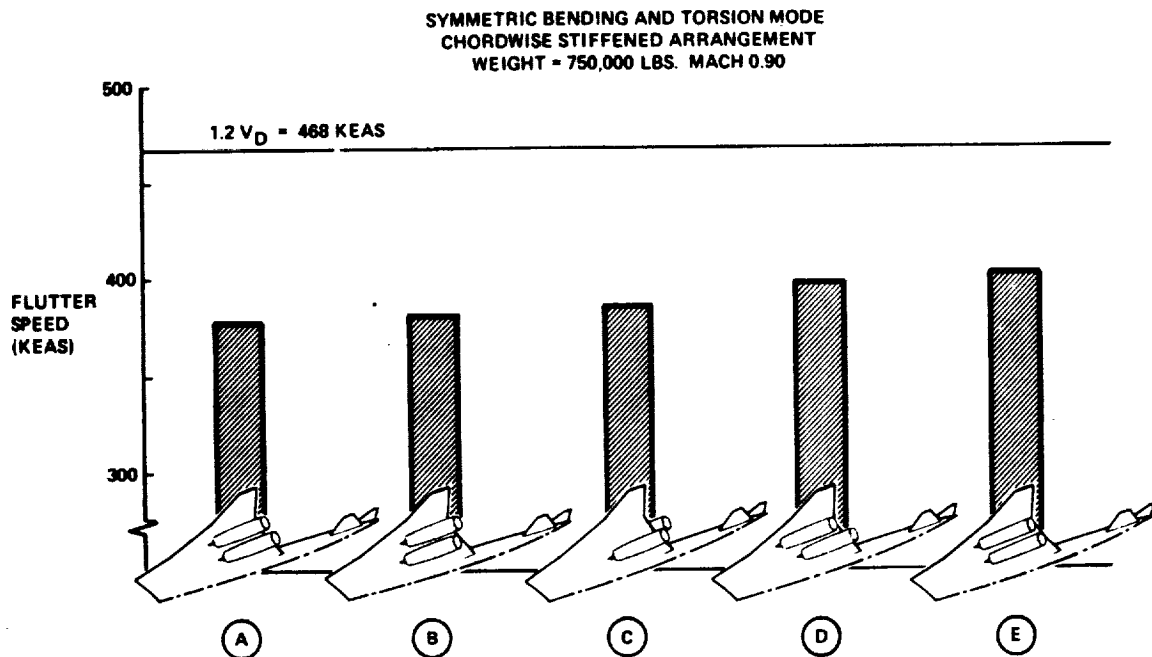
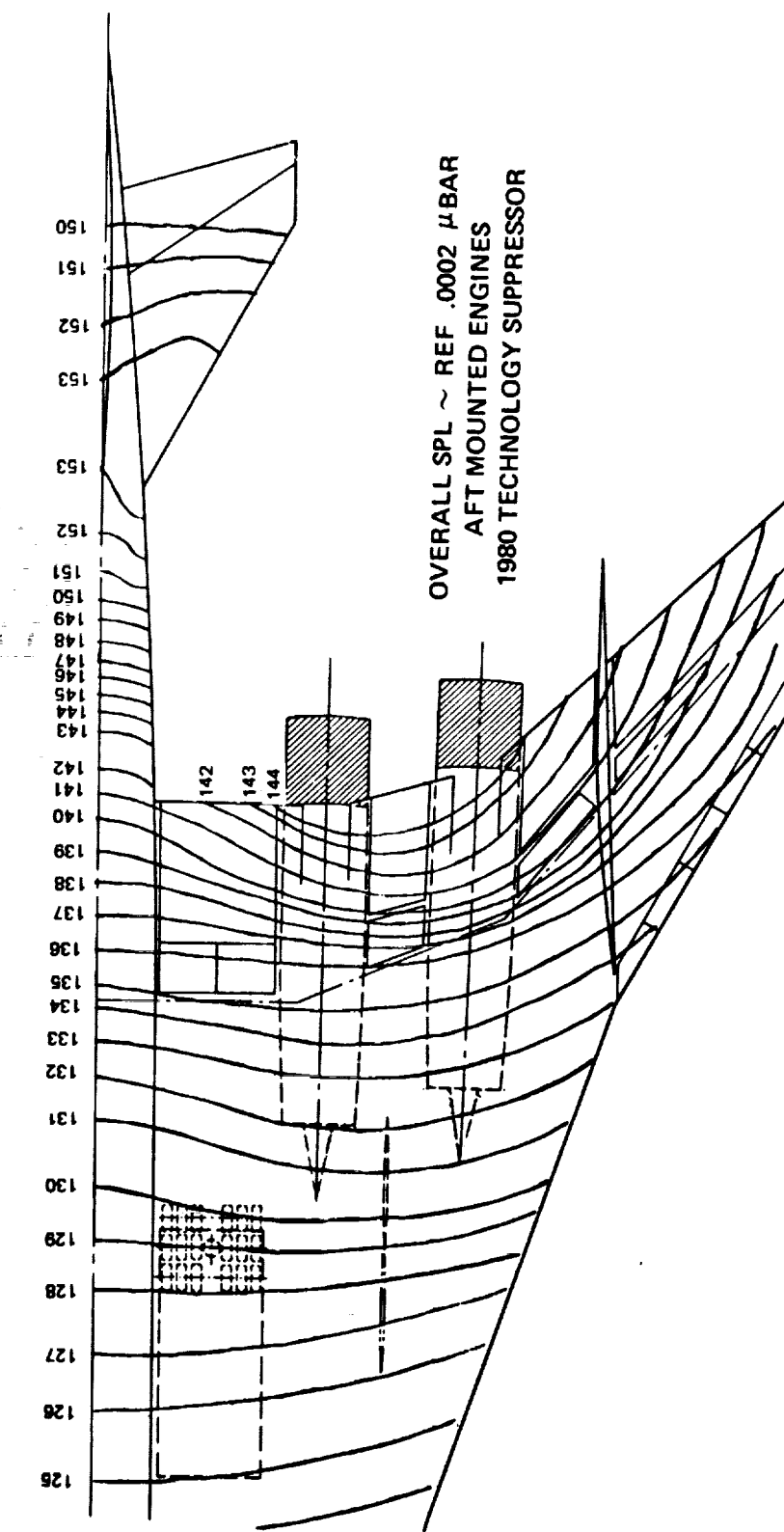


Figure 19-4. Flutter Speed Variation With Engine Placement

The forward movement of the nacelles however, permits a shorter landing gear for a given tail-down angle and roll-angle on landing. Fore and aft placement of the nacelles is further influenced by center of gravity restrictions in the balance of the airplane. Preliminary balance studies with the engine exhaust at the wing trailing edge indicates that the required balance can be achieved by shifting the fuselage relative to the wing and nacelles. The influence of an inboard inlet unstart disturbing or unstarting the outboard inlet is a function of longitudinal separation as well as spanwise and is discussed in the Propulsion System Integration section.

Figure 19-5. Overall Sound Pressure Level - Aft Mounted Engines



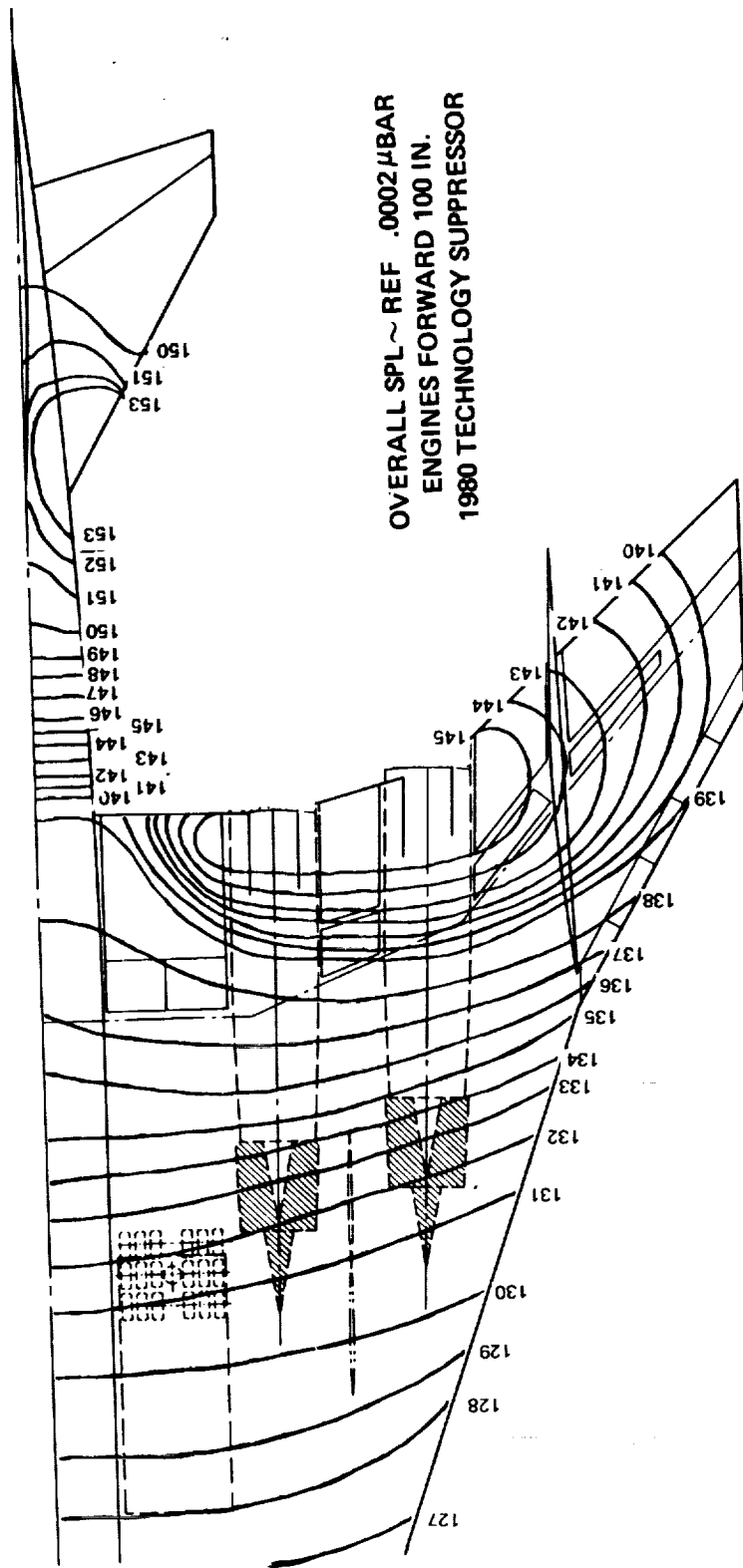


Figure 19-6. Overall Sound Pressure Level - Engines Forward

### Spanwise Engine Movement

The limits for spanwise location of the nacelles were influenced by wing trailing edge control surfaces, inlet mutual interference, flutter, and main landing gear location. Of these factors, the trailing edge control surfaces were the single most critical factor in spanwise location of nacelles. With the engine size shown on Figure 19-1, lift and roll control are adequate, but there is no margin for moving the inboard-nacelle inboard. Spanwise movement would require a larger wing area or change in aspect ratio and span. In addition, moving the engines inboard and forward must consider clearance with landing gear doors and the main landing gear strut. Moving the outboard engine outboard increases roll control and incremental lift from the flap, but increases the flutter problem and requires a larger all moving vertical tail. Since movement of the two nacelles away from each other was restricted by the above factors, it was not possible to separate the inlets by one and a half diameters and line them up fore and aft. Therefore, the inlet fence must be retained to prevent an inboard inlet unstart from upsetting the outboard inlet.

### Engine Size

The effects of engine size on the overall airplane performance were evaluated by arbitrarily increasing the size and weight of the BSTF 2.7-2/1.147 duct-burning turbofan engine. This increase was based on the assumption that the engine design was over-optimistic. The engine maximum diameter was increased from 96.4 inches to 107 inches, while the length remained unchanged. The engine T/W ratio was arbitrarily reduced from 7.0 to 6.0 for an increase in engine weight of 2,130 pounds per engine. The increased engine and structure weight resulted in a loss of over 200 nautical miles. The most difficult problem faced by this increased engine diameter on the arrow-wing configuration was in the wing trailing edge control surfaces. As discussed earlier, they are just adequate for the 96.4 inch diameter engine, but would be reduced to the point of insufficient lift and roll control for takeoff and landing with the larger engines. The only solution to this problem is a larger wing or increased span with resultant increased gross weight. The importance of controlling engine size, especially diameter and weight, was made very apparent in the development of the smallest, most efficient supersonic aircraft.

### Constraint Envelope

The placement of four underwing engines on the arrow-wing configuration was extremely limited. As noted earlier, there was no improvement from moving the nacelles spanwise, and therefore the constraint envelope, shown in Figure 19-7, maintains the same spanwise location as the NASA card deck. Longitudinal limits were not so restrictive, and as the constraint envelope indicates, the nacelles may move from the exhaust 100 inches aft of the wing trailing edge to the exhaust at the trailing edge. Movement farther forward was possible, but increases the sonic fatigue problem. Because of the lack of benefits identified in moving the engines spanwise, the primary effort was in the determination of the best longitudinal position for the nacelles.

### PROPULSION SYSTEM INTEGRATION

#### Boundary Layer Diverter

Boundary layer diverter height variation with nacelle longitudinal position (relative to the wing leading edge) was determined to aid in the design layout. The results shown in Figure 19-8 are independent of spanwise position and were derived from unpublished data of wind tunnel tests conducted at the NASA Langley Research Center. The diverter heights for the baseline configuration of the arrow-wing supersonic cruise aircraft are indicated on the figure.

#### Inlet Mutual Interaction

An important aspect of airframe/propulsion system integration is the minimization of inlet-to-inlet interaction effects. These mutual interaction effects can be particularly severe for underwing engine installations. Specifically, the disturbance associated with an inlet unstart may propagate through shock-boundary layer interaction effects to an adjacent inlet. If the disturbance is sufficiently strong the adjacent inlet will unstart. In order to prevent excessive aircraft pitch, yaw, and rolling moments, an adjacent inlet unstart should be prevented.

An analysis of experimental data (Reference 2) for inlet mutual interaction effects at an inlet Mach number of 2.6 indicates that a boundary layer fence

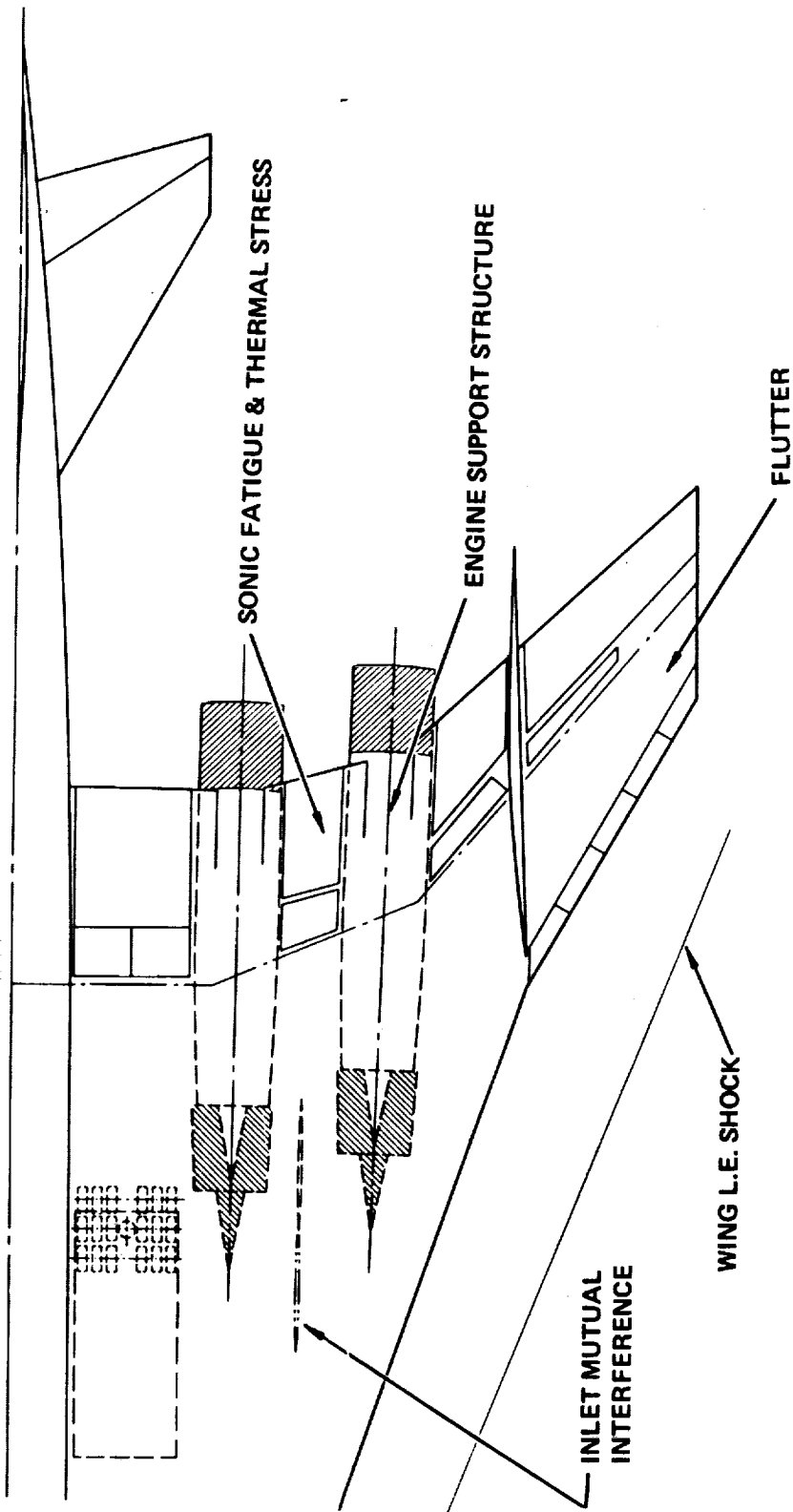


Figure 19-7. Constraint Envelope

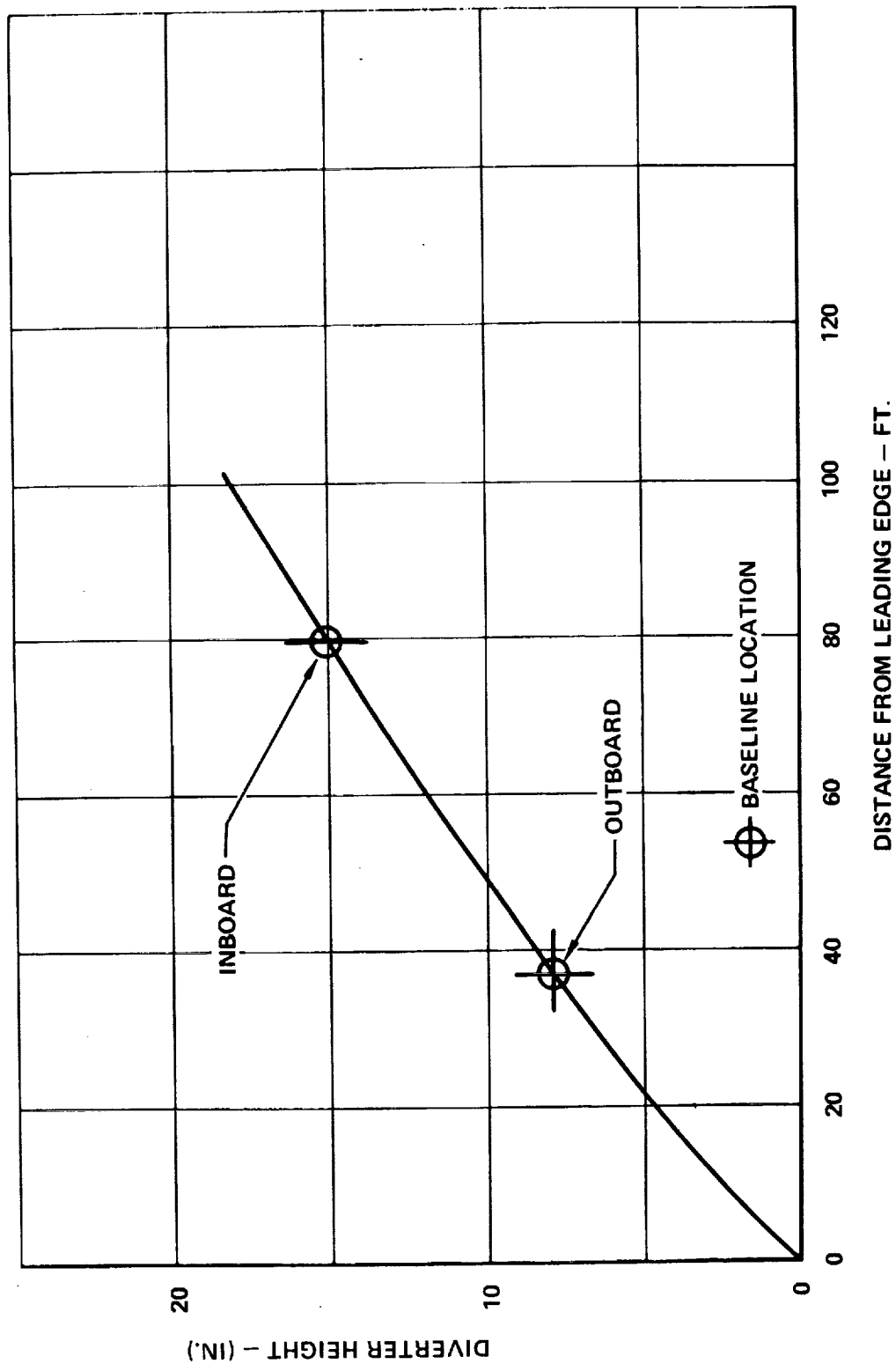


Figure 19-8. Divertor Height Variation With Nacelle Longitudinal Position

will be required to prevent an unstart of the downstream outboard inlet due to an unstart of the inboard inlet of the baseline study vehicle. Figure 19-9 shows the stable and unstable regions for operation of the outboard inlet during unstart of the inboard inlet, based on experimental data for two inlets with no wing. The results, which show the present location to be only marginally satisfactory, do not reflect the effect of the interaction between the expelled inlet shock wave and the wing boundary layer. Since the expelled inlet shock wave will propagate further forward due to separation of the wing boundary layer, the outboard inlet will most likely unstart. A boundary layer fence, similar to the one employed on the Boeing SST, was incorporated on the baseline vehicle to prevent this unstart.

An outboard inlet unstart can also be prevented by relocation of the inlet. Based on the Mach 2.6 data of Reference 3, the inlets would have to be laterally aligned and separated approximately three and one-half inlet diameters (cowl lip to cowl lip) to completely eliminate mutual interaction effects. Depending on the sensitivity of the inlet and engine to the adjacent inlet unstart disturbance, the inlets could possibly be placed closer together. However, because of the complex interactions involved, the minimum inlet separation distance would have to be determined experimentally.

As discussed in Reference 4, a lateral separation distance of one and one-half equivalent inlet diameters was found to be acceptable for the Lockheed L-2000 SST. The equivalent inlet diameter is defined as the diameter of an axisymmetric inlet which has the same capture area as the L-2000 SST two-dimensional inlet. This result was determined by tests of a scale model inlet in the presence of a simulated wing boundary layer and a simulated adjacent inlet unstart disturbance. The unstart disturbance was simulated by air injection through slots into the wing boundary layer, controlled to yield the same wing pressure distribution as previously determined from small scale aircraft/inlet model tests. Since two-dimensional inlets were employed in the above tests, the inlet stability results may not be completely applicable to axisymmetric inlet installations since the shock wave boundary layer interactions differ from one to the other.

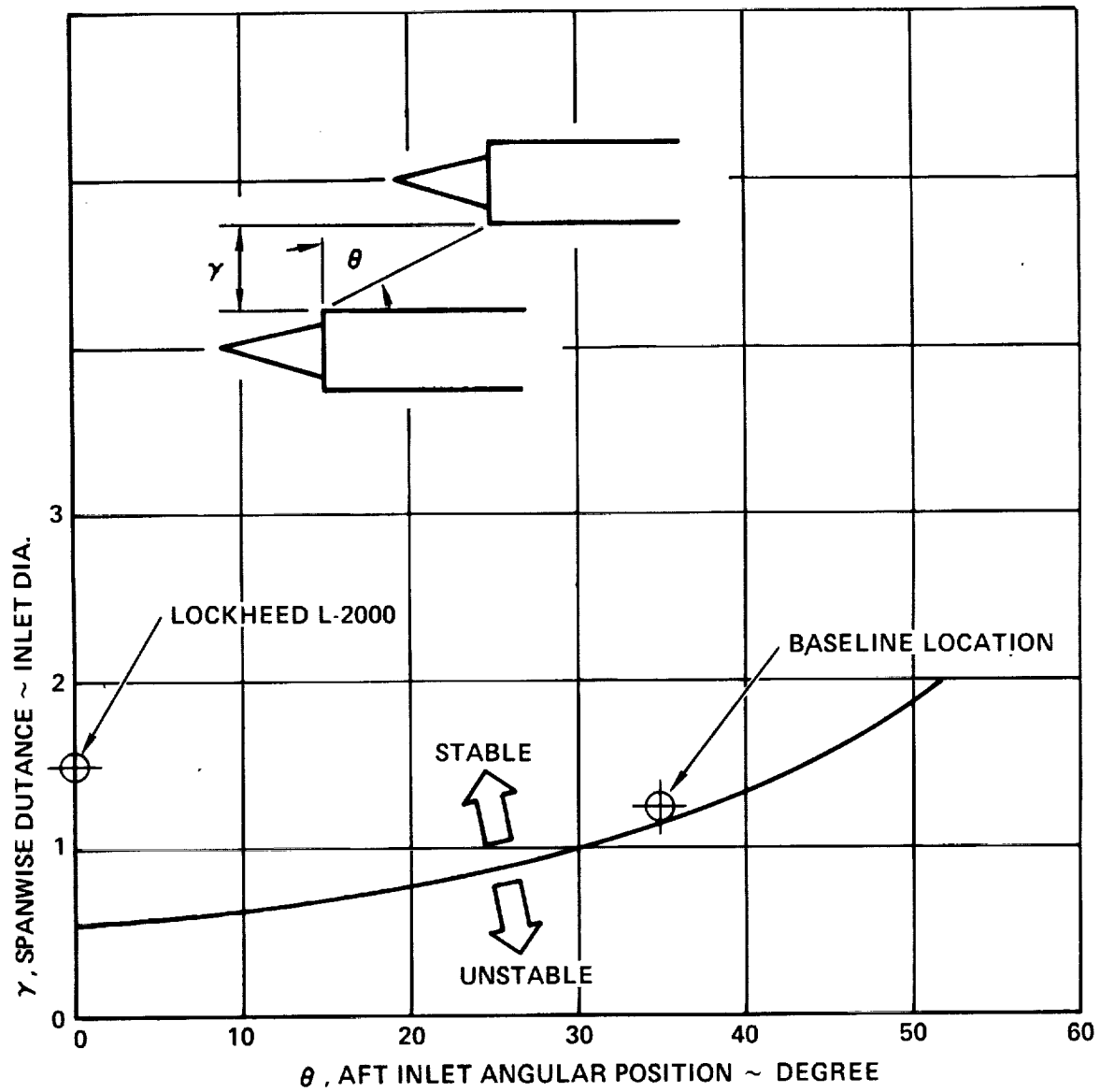


Figure 19-9. Stable Operating Location Of Aft Inlet

## AERODYNAMIC CHARACTERISTICS

The analyses to determine the aerodynamic effects of moving the engine nacelles from their baseline location (Figure 19-1) were performed. The range of potential locations was limited to spanwise positions along the lower surface of the wing trailing edge inboard of the wing vertical fin. Spanwise shifts of either nacelle cause changes in the size and location of the wing trailing edge flap panels. Also, the yawing moment due to the thrust of the outboard engine is changed.

### Control Surface

The panels affected by the spanwise shifts studied are  $F_1$ ,  $F_2$ , and  $F_3$  whose relative positions are shown in the sketch. Flap panel  $F_1$  is used only as a lift flap while  $F_2$  and  $F_3$  are flaperons providing both incremental lift and roll control. Figure 19-10 shows the incremental lift coefficient due to all three flap panels deflected 20-degrees. Both nacelles are shifted inboard and outboard from their baseline positions keeping the separation between them constant at the baseline value. This provides a trade off between panel  $F_1$  and panel  $F_3$ . Because the effectiveness of a flap is dependent in part on the area of wing in front of it, the addition of span to the inboard panel  $F_1$  at the expense of outboard  $F_3$ , increases the lift added by about ten percent. Similarly, a decrease of  $F_1$  and increase of  $F_3$  causes a net loss in flap lift effectiveness.

Figure 19-11 shows the effect of a trade between  $F_2$  and  $F_3$  while  $F_1$  was held constant. The airplane trimmed lift coefficient for conditions approximating second segment climb is shown as a function of outboard nacelle location in Figure 19-12.

Variation in the incremental lift potential of flaperon panels  $F_2$  and  $F_3$  coupled with the shift in panel center of pressure effects the roll control power available at Mach numbers up to 0.8. Rolling moment coefficient from  $F_2$  and  $F_3$  at full asymmetric deflection is shown in Figure 19-13. The individual contributions and their sum are shown as a function of outboard nacelle spanwise location.

A shift of the outboard engine inboard or outboard from the baseline position will change the yawing moment due to an inoperative engine. The all moving

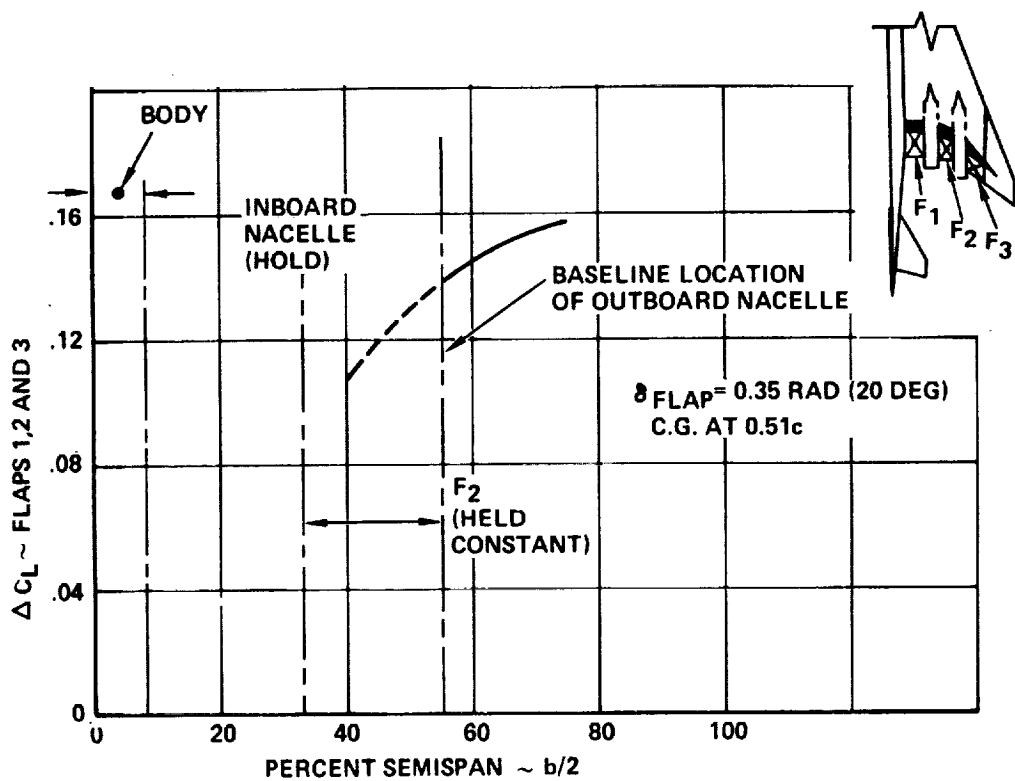


Figure 19-10. Incremental Lift Due To Inboard And Outboard Engine Spanwise Shift - Flaps at 20 Degrees

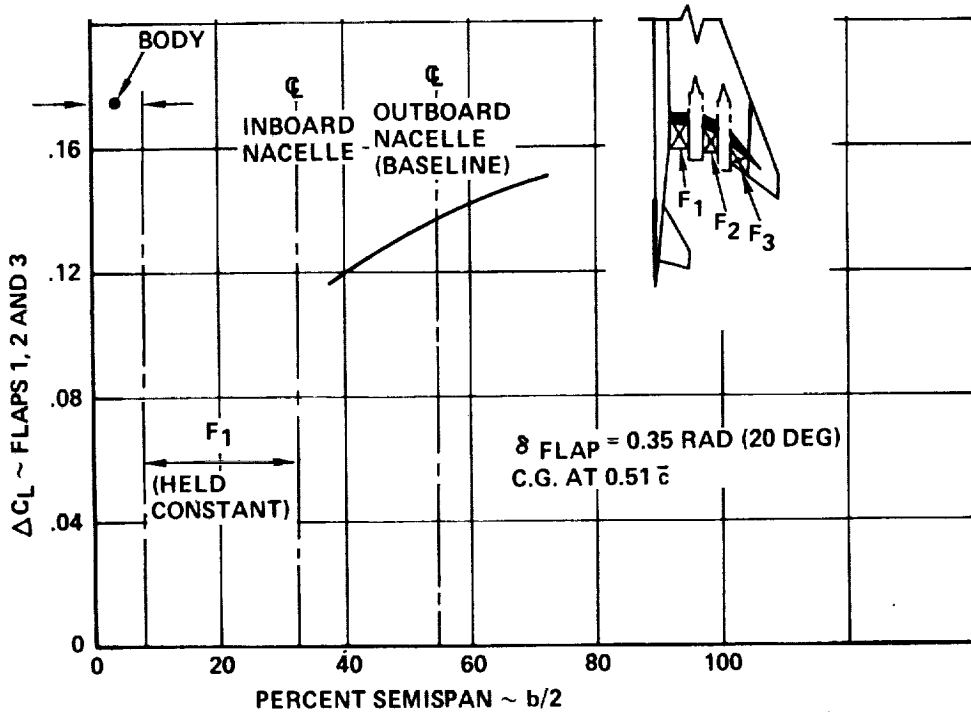


Figure 19-11. Incremental Lift Due To Outboard Engine Spanwise Shift - Flaps at 20 Degrees

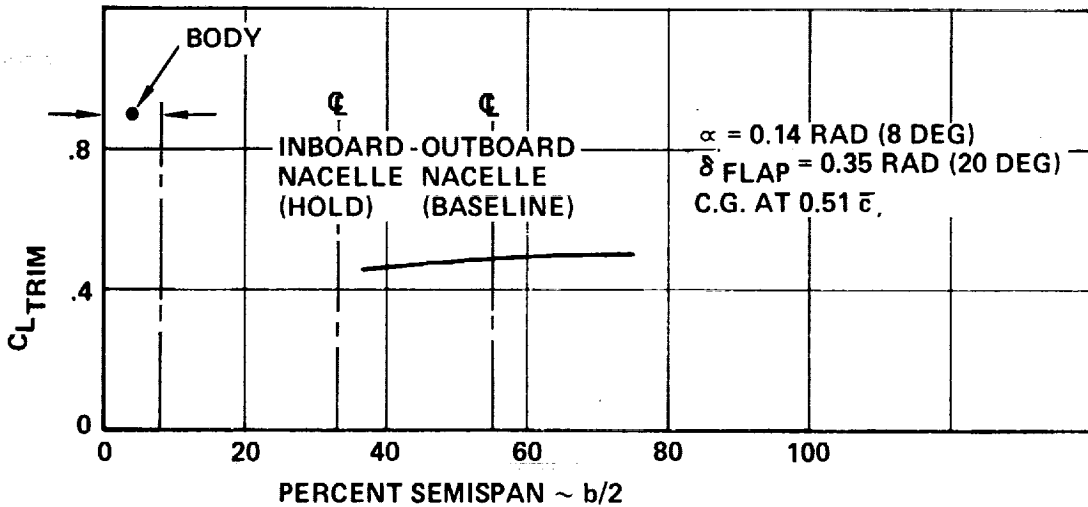


Figure 19-12. Trimmed Lift As A Function Of Outboard Engine Spanwise Location - Flaps At 20 Degrees

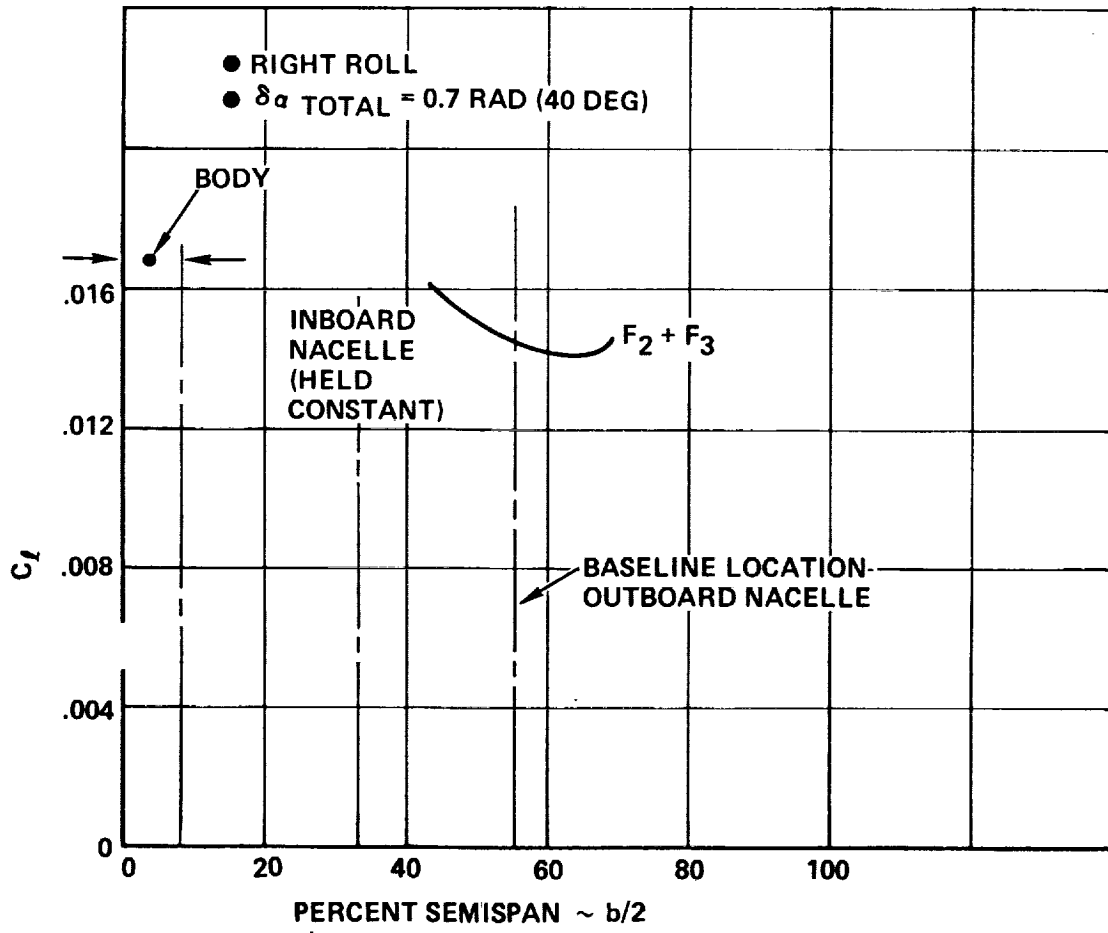


Figure 19-13. Effect Of Outboard Engine Spanwise Location on Rolling Moment Due to Flaperons

centerline vertical tail is sized to control this thrust asymmetry at low speed as required for acceptable performance. The dependence of this tail area on outboard engine position is shown for constant minimum control speed in Figure 19-14.

#### Performance

Fore and aft position of the engine nacelles does not modify relative flap size or vertical tail area and hence does not effect low speed aerodynamics. It does, however, effect wave drag at supersonic speeds. If both inboard and outboard nacelles are shifted 100 inches forward the wave drag is increased by approximately one count (0.0001) at cruise. One count of drag has the same effect on performance as adding 2500 pounds of empty weight or reducing range 31 nautical miles. The mission maximum lift to drag ratios for the baseline airplane and for the airplane with nacelles forward are shown in Figure 19-15.

#### STRUCTURAL CHARACTERISTICS

The structural effects of longitudinal and spanwise movements from the baseline position were identified with the change in flutter characteristics, sonic fatigue requirements, and mass and balance as discussed in the Design Integration section.

#### Flutter Characteristics

The flutter optimization results and engine placement investigation reported in Section 10, Vibration and Flutter, provided an insight into the structural mass trends with engine longitudinal position. The results of the study (Figure 19-4) indicates an increase in the flutter speed for the bending and torsion mode from 379 KEAS to 401 KEAS or an increase of 22 KEAS. This increase in flutter speed allows for a reduction of approximately 500 pounds of structure from the wing tip region. In addition, shortening of the engine support beams by 100 inches each permits a mass savings of approximately 450 pounds. Thus, the net potential savings is 950 pounds per aircraft.

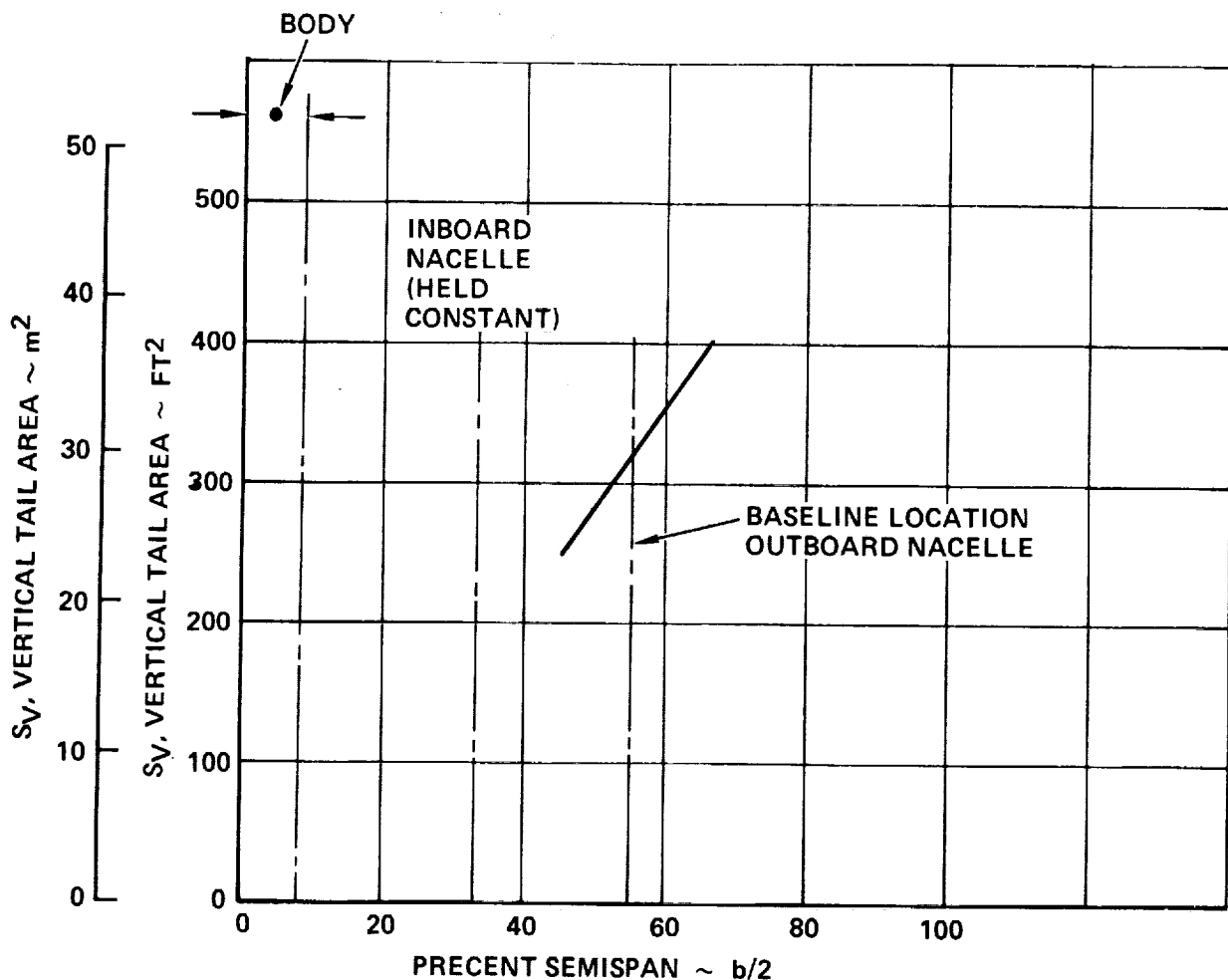


Figure 19-14. Vertical Tail Required Due To Spanwise Shift Of Outboard Engine

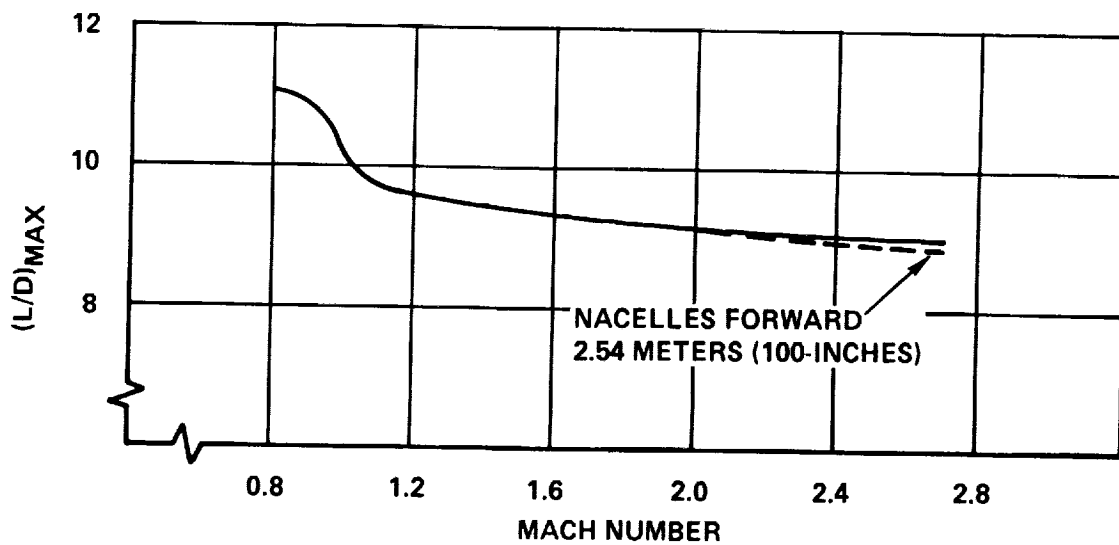


Figure 19-15. Effect Of Mission Lift/Drag Ratio On Nacelle Forward Shift

### Sonic Fatigue

The change in the acoustic environment on the trailing edge structure was assessed for a fixed geometry honeycomb core sandwich structure. The increase in thickness of titanium face sheet for the flap, flaperon and aileron resulted in a mass increment of 50 pounds.

### RESULTS

The propulsion-airframe integration study concentrated on the benefits of the exhaust being 100 inches aft of the wing trailing edge versus the exhaust at the trailing edge as shown in Figure 19-16. By moving the engines to the forward position, the mass added to the outer wing to prevent symmetric flutter was reduced by 500 pounds. The support structure for the engines (beams cantilevered off the rear beam) could also be reduced 450 pounds. The landing gear could be shortened 15 inches for a saving of 1100 pounds. The flaps, flaperons, and fixed vertical tails are designed for higher sonic fatigue levels, which would add 50 pounds. The net mass reduction would be approximately 2000 pounds for a 42 nautical mile increase in range as shown in Table 19-2. Against this is a reduction of 31 nautical miles in range due to an increase in wave drag when the nacelle moves forward. While the results appear inconclusive due to their closeness, it would appear that the engines should be maintained at the baseline location for the Task II design effort.

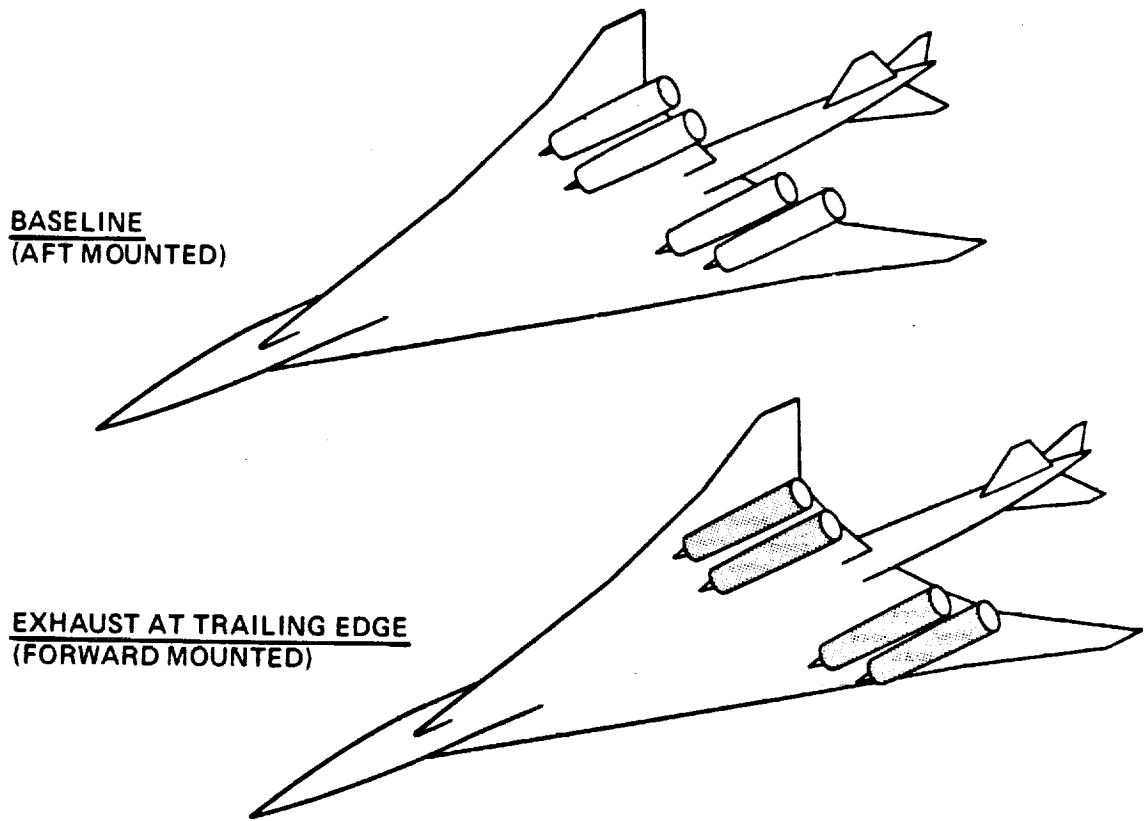


Figure 19-16. Candidate Engine Location

Table 19-2. Propulsion - Airframe Integration Results

WEIGHT CHANGE -

• FLUTTER _____	-500 LB
• ENGINE SUPPORT BEAMS _____	-450 LB
• LANDING GEAR LENGTH _____	-1,100 LB
• INCREASED SONIC FATIGUE _____	+50 LB
	<hr/>
	-2,000 LB

RESULTS -

• WEIGHT SAVING _____	+42 N.MI.
• WAVE DRAG PENALTY _____	-31 N.MI.
• NET _____	+11 N.MI.

CONCLUSION -

- MAINTAIN BASELINE ENGINE LOCATION



REFERENCES

1. R.L. Foss, "Summary Report - Task III Concept Refinement and Engine Coordination," Lockheed-California Company, LR 25827-3, 3 January 1974
2. Motycka, D.L., and Murphy, J.B., "Inlet to Inlet Shock Interference Tests," NASA CR-261, September 1965
3. Mitchell, G.A., and Johnson, D.F., "Investigation of a Nacelle Mounted Supersonic Inlet With a Wing Boundary Layer," NASA TM-X-2184, March 1971
4. Anon.: "Supersonic Transport Development Program - Phase III Proposal," Lockheed-California Company, FAA-SS-66-7, Vol. II-E Airframe Design, September 1966

~~PRECEDING PAGE BLANK NOT FILMED~~

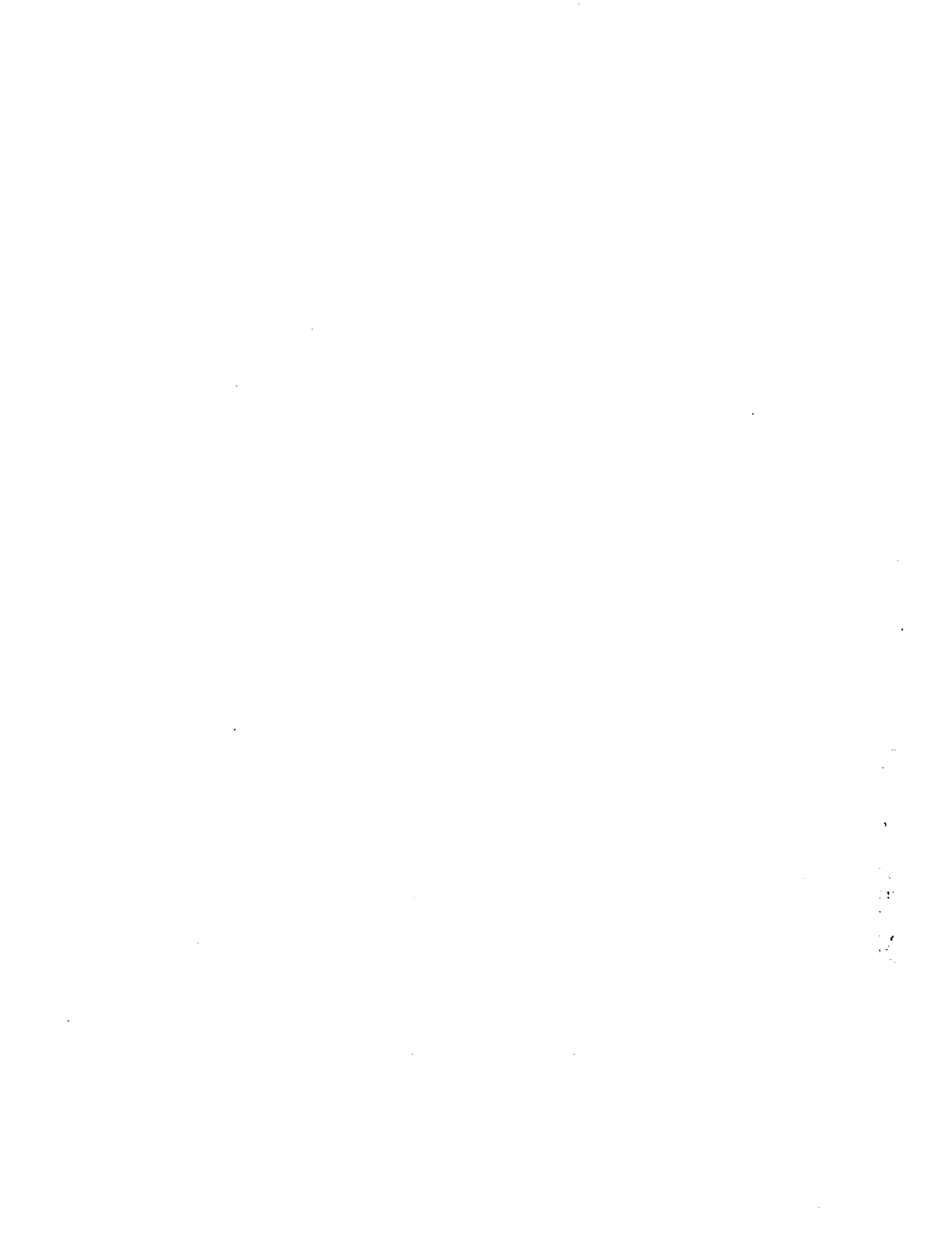


SECTION 20

ADVANCED TECHNOLOGY ASSESSMENT

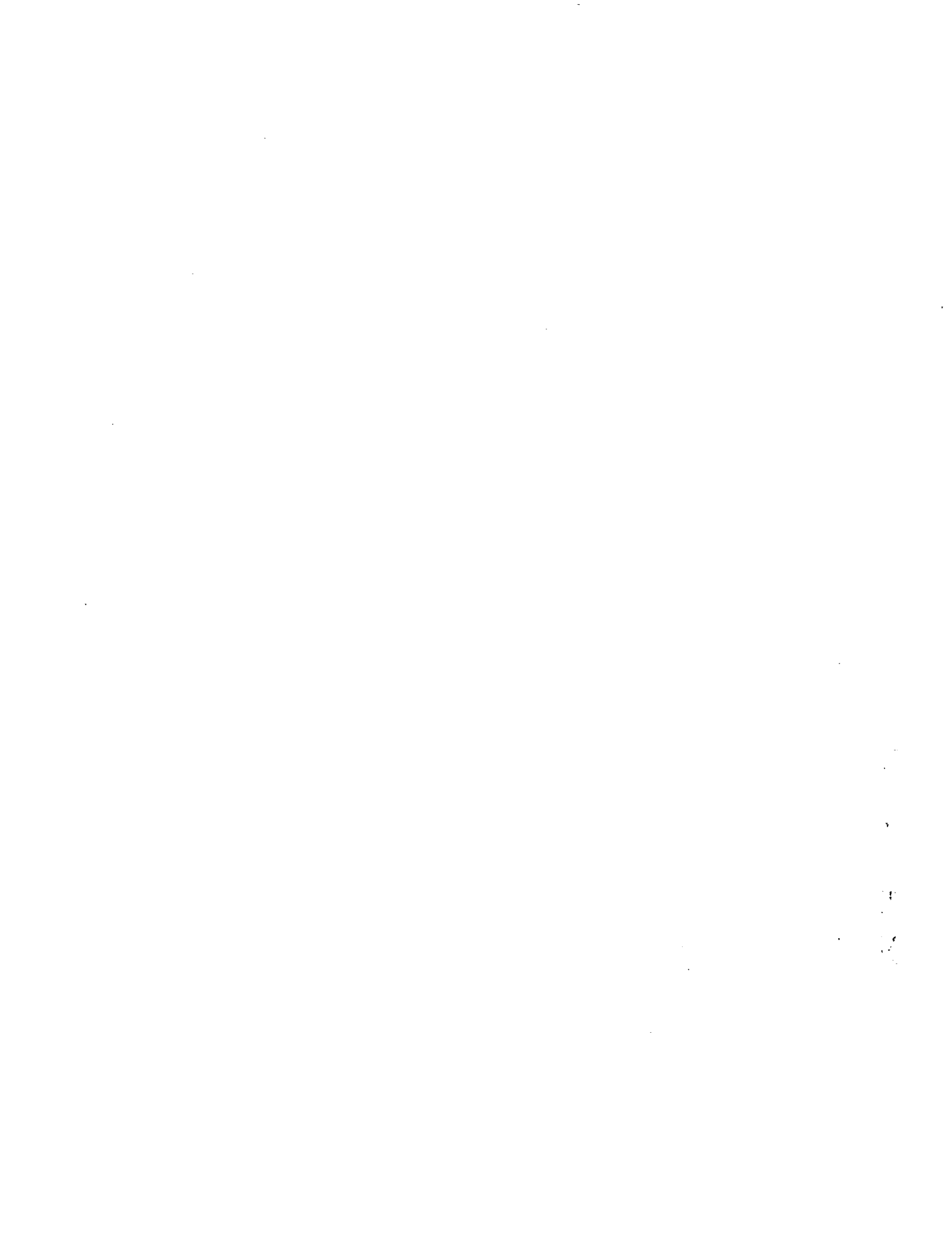
by

I. F. Sakata, R. N. Jensen and A. R. Holland



## CONTENTS

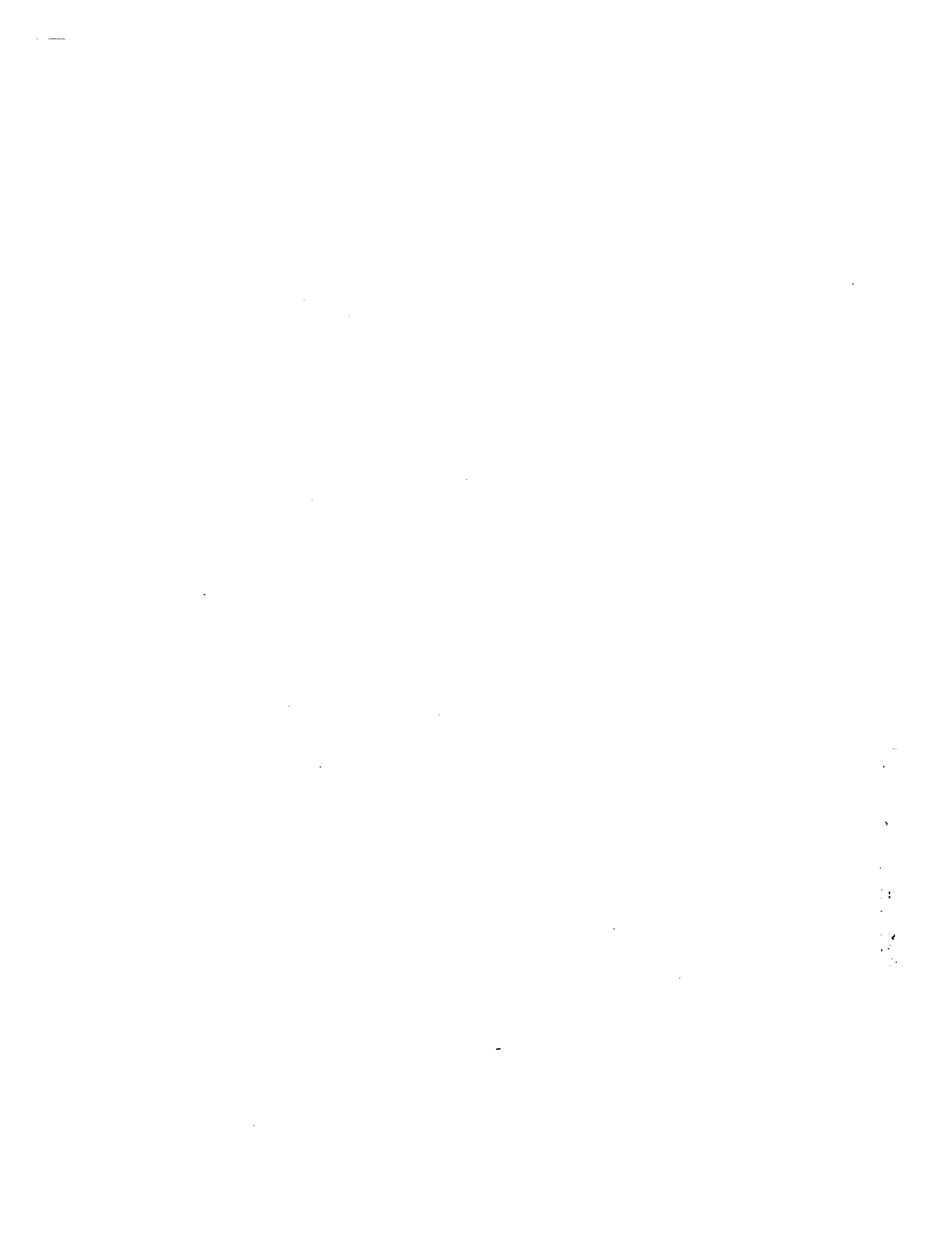
<u>Section</u>	<u>Page</u>
INTRODUCTION	20-1
ADVANCED TECHNOLOGY SELECTION	20-1
DESIGN APPROACH	20-3
Materials	20-4
Design Concepts	20-12
Point Design Regions	20-12
Wing Design Loads	20-16
Fuselage Design Loads	20-17
Results - Wing	20-17
Results - Fuselage	20-31
MANUFACTURING PLAN	20-46
MASS ESTIMATES	20-49
Wing Mass	20-51
Fuselage Mass	20-54
Secondary Structure Mass	20-54
FINAL DESIGN - ADVANCED TECHNOLOGY AIRCRAFT	20-57
REFERENCES	20-61



## LIST OF FIGURES

<u>Figure</u>		<u>Page</u>
20-1	Structure, Materials and Control Impact on SST Performance	20-3
20-2	Extensional and Shear Modulus for Boron/Epoxy and Boron/Polyimide	20-6
20-3	Extensional and Shear Modulus for Graphite/Epoxy and Graphite/Polyimide	20-7
20-4	Comparative Thermal Stress - Titanium vs Composite Materials	20-9
20-5	Comparative Buckling Efficiency and Specific Stiffness for Boron/Polyimide and Graphite/Polyimide	20-10
20-6	Surface Protection System for Composite Laminates	20-11
20-7	Composite Wing and Fuselage Design Concepts	20-11
20-8	Chordwise Stiffened Wing Design - All Composite Concepts	20-14
20-9	Definition of Wing Point Design Regions	20-15
20-10	Definition of Fuselage Point Design Regions	20-15
20-11	Fuselage Shear Diagram - Task I	20-20
20-12	Fuselage Bending Moment Diagram - Task I	20-20
20-13	Chordwise Stiffened All-Composite Design Concept	20-23
20-14	Monocoque All-Composite Design Concept	20-27
20-15	Composite Fuselage Laminate Directions	20-37
20-16	Idealized Cross-Section of Fuselage	20-37
20-17	Typical Frame-Stringer Intersection Schemes	20-43
20-18	Chordwise Stiffened Wing Panel Fabrication	20-48
20-19	Specific Stiffness Properties of Titanium and Composites	20-53
20-20	Advanced Hybrid Structural Approach - 1990 Start-of-Design (Far-Term)	20-58

***PRECEDING PAGE BLANK NOT FILMED***



LIST OF TABLES

<u>Table</u>		<u>Page</u>
20-1	Composite Design Properties for the 1980-1990 Time Period	20-5
20-2	Merits of Potential All-Composite Chordwise Stiffened Design Concepts	20-13
20-3	Critical Wing Loading Conditions	20-17
20-4	Design Loads for Chordwise Stiffened Arrangement - Ultimate	20-18
20-5	Design Loads for Monocoque Arrangement - Ultimate	20-19
20-6	Summary of Composite Chordwise Stiffened Wing Surface Panels	20-25
20-7	Graphite-Polyimide Substructure - Point Design 40322	20-26
20-8	Summary of Composite Monocoque Wing Surface Panels	20-29
20-9	Composite Truss Spar and Rib - Monocoque Design	20-30
20-10	Circular-Arc Corrugated Spar/Rib Webs - Reference Titanium Alloy	20-32
20-11	Composite Circular-Arc Corrugated Spar Web - Point Design 40322	20-33
20-12	Composite Circular-Arc Corrugated Web Weights	20-34
20-13	Wing Weight Comparison For Point Design Regions	20-35
20-14	Composite Tee-Stiffened Panel - FS 750	20-38
20-15	Composite Tee-Stiffened Panel - FS 2000 and FS 3000	20-39
20-16	Composite Hat Stiffened Panel - FS 2000 and FS 3000	20-40
20-17	Composite Tee-Stiffened Panel - FS 2500	20-41
20-18	Composite Hat-Stiffened Panel - FS 2500	20-42
20-19	Composite Fuselage Frames - FS 2000 and FS 3000	20-44
20-20	Composite Frame Weights	20-45
20-21	Composite Fuselage Weight Summary	20-47
20-22	Advanced Technology Aircraft Mass Comparison	20-50
20-23	All-Composite Wing Box Structure Mass Comparison	20-52
20-24	All-Composite Shell Structure Mass Comparison	20-55
20-25	Weight Reduction Factors for Advanced Technology Aircraft Secondary Components	20-56
20-26	Airplane Mass and Performance Comparison - Advanced Technology Aircraft	20-59

~~PRECEDING PAGE BLANK NOT FILMED~~



LIST OF SYMBOLS AND NOTATIONS

$E_1$	Young's modulus of laminae parallel to filament direction (lbs/in <sup>2</sup> )
$E_2$	Young's modulus of laminae transverse to filament direction (lbs/in <sup>2</sup> )
$E_{xx}$	Young's modulus of laminate along X reference axis (parallel to O direction) - (lbs/in <sup>2</sup> )
$E_{yy}$	Young's modulus of laminate along Y reference axis (parallel to 90° direction) - (lbs/in <sup>2</sup> )
$G_{12}$	Shear modulus of lamina in the lamina reference axis, parallel to filaments (lbs/in <sup>2</sup> )
$G_{xy}$	Shear modulus of laminate in the X-Y reference axis (lbs/in <sup>2</sup> )
$n_z$	Vertical inertia load factor - inertia force parallel to the airplane vertical reference axis divided by the weight (up is positive)
$N_x, N_y, N_{xy}$	Inplane stress resultants (lb/in) acting in the X- and Y- direction and the X-Y plane
$v_e$	Equivalent airspeed (keas)
$\alpha_1$	Linear coefficient of expansion in the filament direction (in/in/F)
$\alpha_2$	Linear coefficient of expansion transverse to the filament direction (in/in/F)
$\alpha_B$	Buckling coefficient (see text)
$\gamma_{12}$	Shear strain of the lamina in the lamina reference axis, parallel to filaments (in/in)
$\epsilon_1(T)$	Ultimate tensile strain allowable in the filament direction (in/in)
$\epsilon_2(T)$	Ultimate tensile strain allowable transverse to the filament direction (in/in)
$\epsilon_1(C)$	Ultimate compressive strain allowable in the filament direction (in/in)
$\epsilon_2(C)$	Ultimate Compressive strain allowable transverse to the filament direction (in/in)

**PRECEDING PAGE BLANK NOT FILMED**

$\nu_{12}$  Major Poisson's ratio of laminae relating contraction in the transverse direction due to extension in the filament direction.

$\nu_{21}$  Minor Poisson's ratio of laminate relating contraction in the filament direction due to extension in the transverse direction

$\rho$  density (lbs/in<sup>3</sup>)

## SECTION 20

### ADVANCED TECHNOLOGY ASSESSMENT

#### INTRODUCTION

The results of the Advanced Technology Assessment, which explored an aggressive application of composite materials and fabrication technology for wing and fuselage structure of a Mach 2.7 arrow-wing supersonic cruise aircraft, are presented in this section.

The analysis of selected wing and fuselage point design regions, considering the various structural arrangements, design concepts, and corresponding internal loads and flexibilities, were made by the Lockheed-Georgia Company. Weight reduction factors for secondary and other structural components were obtained from the results of the Advanced Technology Transport (ATT) studies of Reference 1 and were applied as appropriate to determine weights for an aircraft with a fixed takeoff weight of 750,000 pounds and an aircraft resized to provide a constant payload-range performance.

#### ADVANCED TECHNOLOGY SELECTION

Studies of advanced technology application to future transport performance and economics identified major technological advances that could reasonably be available during the 1980-1990 time period. The resulting trends indicated conclusively that the highest structural mass payoff was in the area of materials technology or more specifically, composite material system application. Furthermore, the most significant structural mass reduction resulted from resizing the airplane to reflect the lower structural weight achieved through advanced materials application.

Reference 1 presents the results of a study of the application of advanced technologies to long-range transport aircraft conducted by the Lockheed-Georgia Company. Trade studies were conducted to determine the effects of variation in technology advancements in the areas of (1) aerodynamics, (2) structures and materials, and (3) active controls systems. The most significant benefit was

obtained by the application of advanced materials as shown by marked improvements on airplane performance and economics. For example, for a 50-percent utilization of advanced materials, the takeoff gross weight was reduced by about 30-percent and the ROI is increased by about 35-percent. Above 50-percent utilization of advanced materials, however, the DOC increased and ROI decreased, because of the relatively inefficient application of advanced materials in this region.

Reference 2 presents the impact of advanced technologies on supersonic transport aircraft. Weight savings predictions based on the use of composites, new structural concepts and active controls were developed. The benefit of weight reduction was amplified by the growth factor for this class of aircraft (Reference Section 17); consequently, a pound saved in structure results in gross weight being approximately 6-pounds less for a supersonic transport maintaining the same payload-range capability. This reduction results from the smaller fuel requirement and the lighter structure associated with the reduced gross weight as follows:

Basic weight saving	1.0 lb.
Fuel reduction	2.8
Structural weight reduction	<u>2.2</u>
Total gross weight reduction	6.0 lb.

Although no attempt was made in the study of Reference 2 to single out individual structural improvements (i.e. materials, design concepts, active controls), a forecast was made of a 10-percent weight savings taking the improvements collectively. The impact of these technology improvements is illustrated in Figure 20-1.

Also shown on the figure are weight and performance trends resulting from the advanced technology assessment of this study (designated far-term) and the Task I results (designated near-term). The shaded band represents the potential improvements by application of advanced materials and concepts. The takeoff weight is approximately 100,000 pounds less, and the range increases 500 nautical miles.

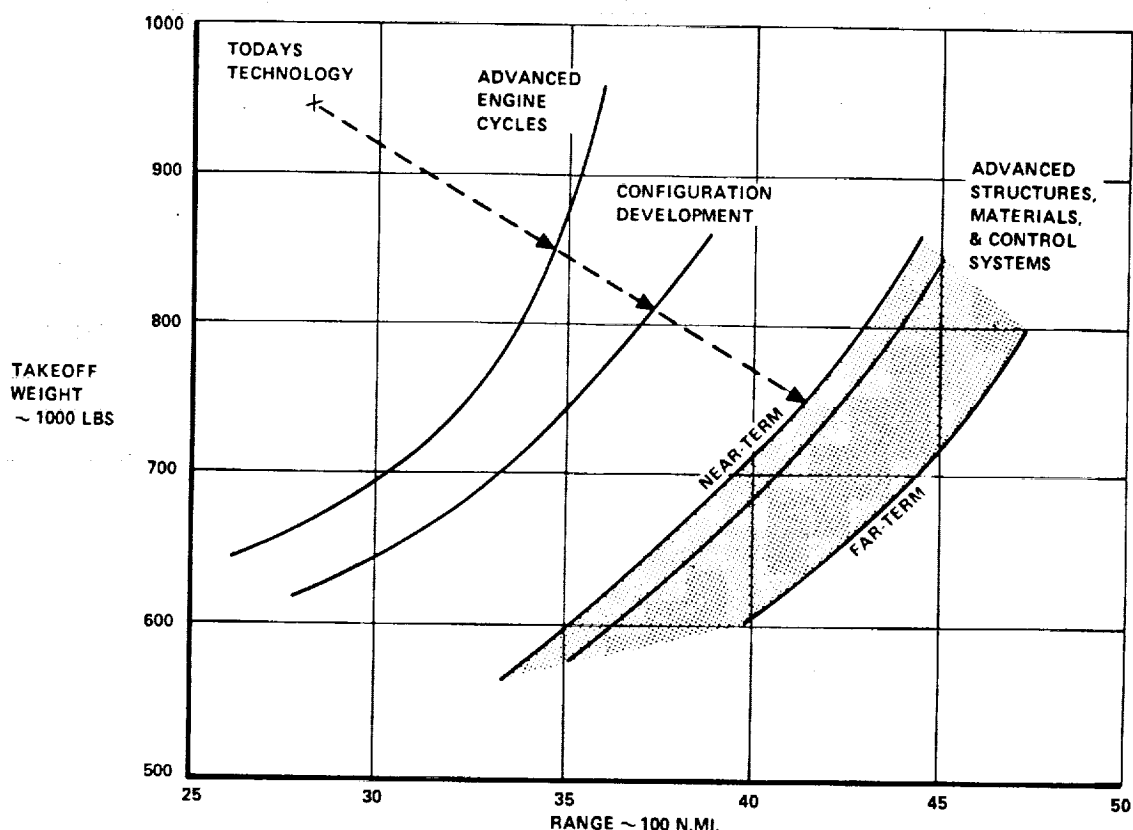


Figure 20-1. Structures, Materials, and Controls Impact

#### DESIGN APPROACH

Projected composite development trends predict the availability of improved stable high temperature resin systems such as thermoplastic polyimides or high temperature polyaromatics, large numerically controlled tape laying equipment, filament winding and pultrusion equipment, and larger autoclaves.

To arrive at projections for airframe structural mass for the advanced technology supersonic cruise aircraft, the results of the Task I Analytical Design Studies were used to size specific point design regions. The sizing data included the internal loads and stiffness requirements of the various airframe arrangements (i.e. chordwise stiffened, spanwise stiffened and monocoque designs). A comparison was then made with the minimum weight all-metal design to similar designs in graphite or boron composites.

Basic section weights were taken as the basis of comparison since nonoptimum factors resulting from advanced manufacturing techniques used for the near-term aircraft (e.g. welded design) assembly are offset by a bonded composite structure having approximately equal utilization of mechanical fasteners. Further, historical data for composite assemblies of the size and type considered are not available.

The use of composite materials to the extent considered in this study is dependent upon two restrictions related to the materials themselves. First, it was assumed that high service temperature capability polyimides would be available and that the material system could be processed with far less difficulty than 1974 polyimide resin systems. Processing of currently available high temperature systems would increase the complexity of assembly fabrication greatly. Second, it was premised that for the sake of economy, assembly sections were large and automatically produced. However, the time required for lamination, handling of such a large volume of material (by machine or otherwise), and the molding of part or assemblies of the sizes required offer problems which have never before been faced.

#### Materials

Design Properties - Considering the 1980-1990 time period, adjustments were made in the material properties to reflect improvements anticipated for these materials. In making the adjustments, no great revelations have been forecasted. Rather, it has been assumed that as a minimum, current inconsistencies in the material properties would diminish through refined processing. As a general guide, the 1980-1990 design values were obtained by assuming these values equal to the 1972-1973 mean property values. The resulting values for boron/polyimide and graphite/polyimide are compared to current values in Table 20-1. The data reported in Reference 3 provided the basis for the design values of both time periods.

No distinction has been made for room temperature and elevated temperature properties since, for the elevated temperatures of interest to this study, any variation in significant properties is within the accuracy of forecasted values.

Figures 20-2 and 20-3 presents comparative extensional modulus ( $E_{xx}$ ) and shear modulus ( $G_{xy}$ ) data for boron-epoxy, boron-polyimide, graphite-epoxy and graphite-polyimide. The data are room temperature properties for various percentage

TABLE 20-1. COMPOSITE DESIGN PROPERTIES FOR THE 1980-1990 TIME PERIOD

MATERIAL SYSTEM		BORON/PI		GRAPHITE/PI	
TIME PERIOD		1975	1985	1975	1985
<u>PROPERTY</u>					
$E_1$	$10^6$ psi	32.2	32.2	22.8	22.8
$E_2$	$10^6$ psi	2.0	2.0	1.98	1.98
$G_{12}$	$10^6$ psi	0.80	0.8	0.71	0.71
$\nu_{12}$		0.31	0.31	0.33	0.33
$\nu_{21}$		0.019	0.019	0.029	0.029
$\alpha_1$	$10^{-6}$ in./in./F	2.8	2.8	-0.17	-0.17
$\alpha_2$	$10^{-6}$ in./in./F	15.0	15.0	9.45	9.45
<u>ULTIMATE STRAINS</u>					
$\epsilon_1(T)$	$10^{-6}$ in./in.	6,340	7,500	7,100	8,250
$\epsilon_2(T)$	$10^{-6}$ in./in.	2,560	3,000	4,400	4,950
$\epsilon_1(C)$	$10^{-6}$ in./in.	7,100	9,750	6,700	8,250
$\epsilon_2(C)$	$10^{-6}$ in./in.	4,700	9,750	8,250	8,250
$\gamma_{12}$	$10^{-6}$ in./in.	15,000	15,000	15,000	15,000
$\rho$	lb/cu in.	0.072		0.056	
PLY THICKNESS (in.)		0.0055		0.007	

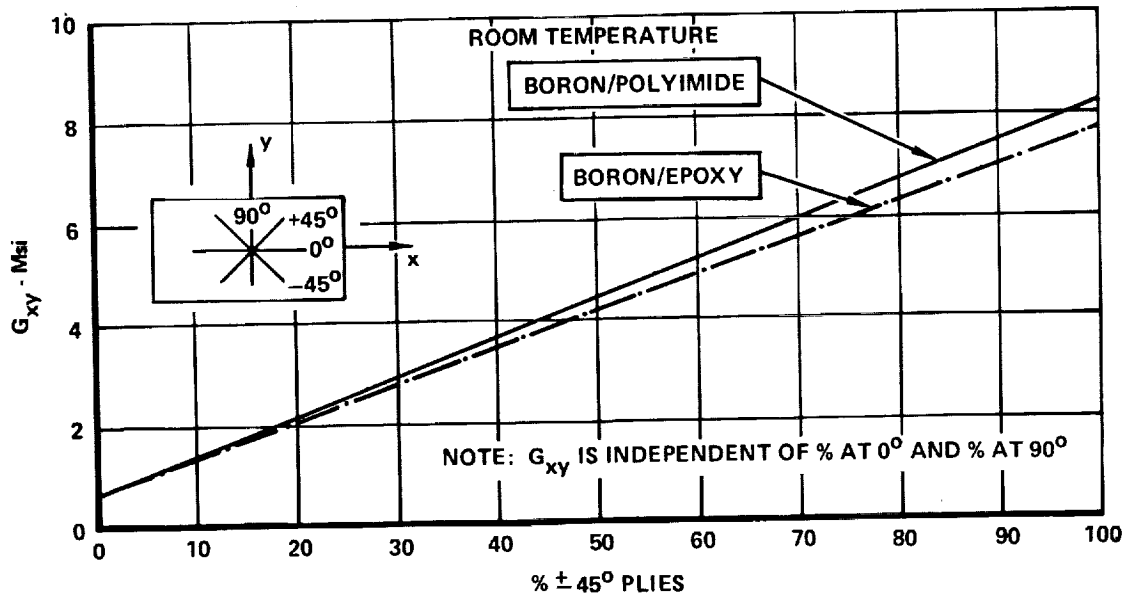
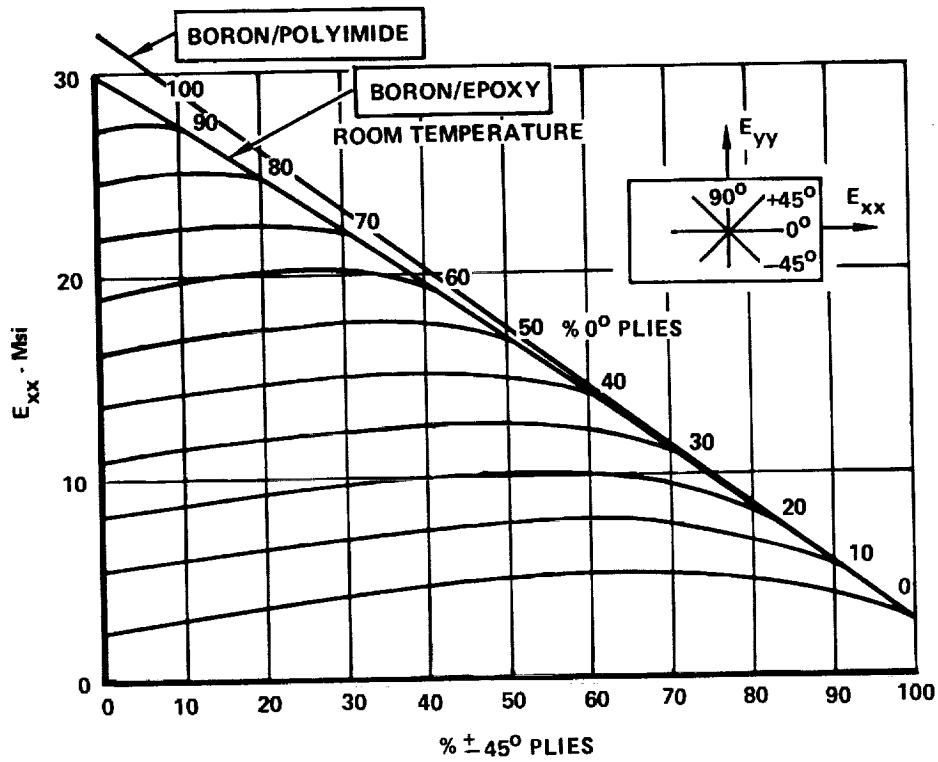


Figure 20-2. Extensional and Shear Modulus for Boron/Epoxy and Boron/Polyimide

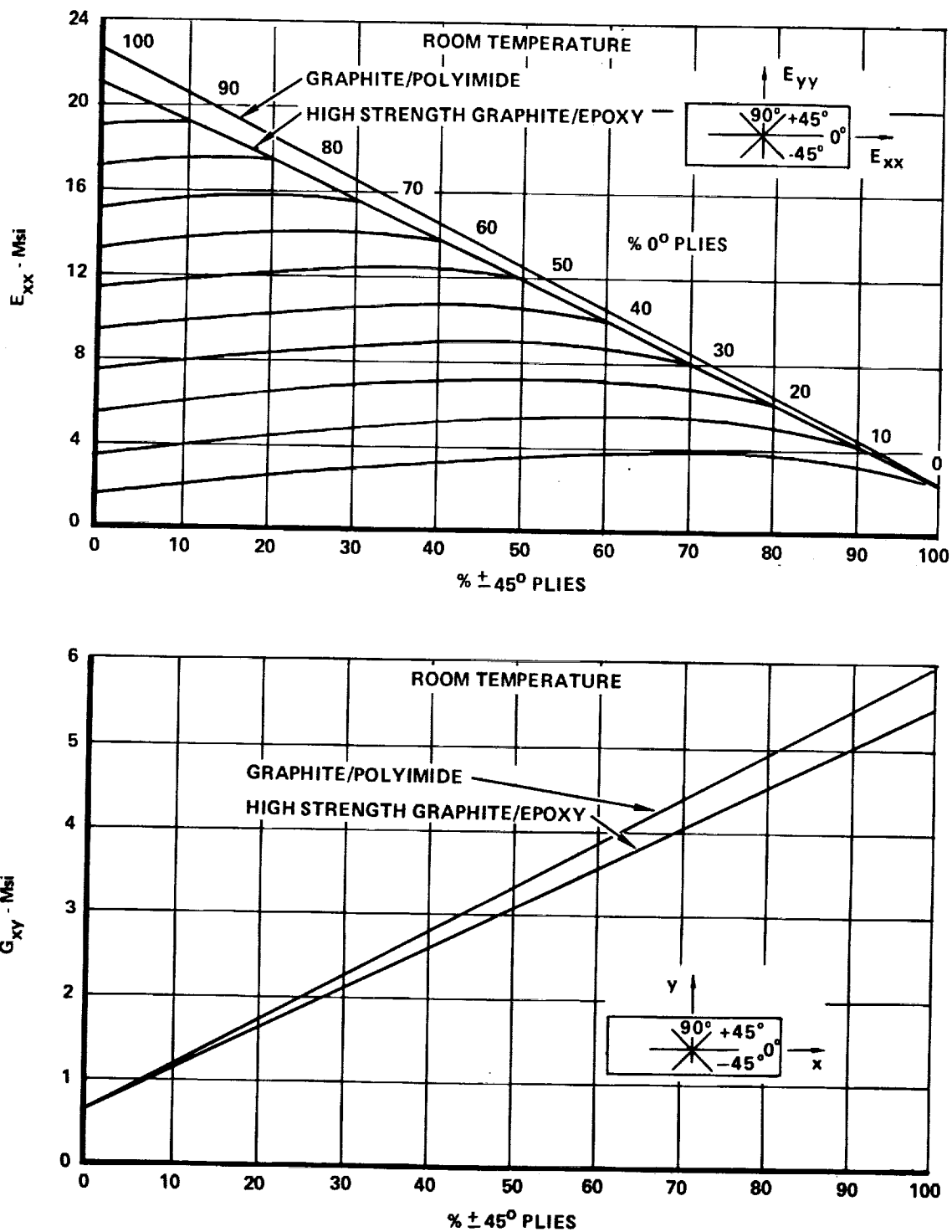


Figure 20-3. Extensional and Shear Modulus for Graphite/Epoxy and Graphite/Polyimide

of  $\pm 45$ -degree layup or combination of  $\pm 45$ -degree and 0-degree plies. Improvement in the polyimide material system properties are shown by the trends presented.

The thermal stress potential as measured by the product of the modulus of elasticity and coefficient of expansion is presented in Figure 20-4 versus percent of  $\pm 45$ -degree plies for the boron-polyimide and graphite-polyimide material systems. The potential for very small thermal stresses are noted by the near-zero  $E\alpha_x$  for the graphite-polyimide system. For comparison purposes, the  $E\alpha$  for titanium alloy 6Al-4V is also indicated. This figure does not reflect the thermal stresses that exist in an unrestrained cross-plied composite material due to change in temperature and due to different coefficient of expansion, which does not occur in titanium.

Figure 20-5 presents specific stiffness data for both the B/PI and Gr/PI as compared to the reference titanium system. Four-fold improvement in properties are indicated for both composite material system with the most significant improvement offered by the boron-polyimide material system. For buckling critical design, similar trends are indicated because of the improved modulus to density ratio.

Protective System - It is recognized that composite materials require provisions for protection beyond that of all-metal counterparts. In particular it is desirable to protect against degradation by aggressive environments such as electrical hazards, erosion, impact, and weathering. The basic external protective system arrangement assumed for this study is illustrated in Figure 20-6.

For lightning and static electricity problems the optimum protection, weight, and producibility is offered by the aluminum wire mesh. Two wire-mesh configurations have been provided. All exterior surfaces are to be covered with 200 x 200 mesh except the edge sections where 120 x 120 mesh is to be applied. The 120 x 120 mesh was selected for the leading edge to improve heat dissipation for this area. Additional composite protection is provided by an electrical insulating barrier consisting of one ply of 120 glass laminated between the laminate and the aluminum wire mesh. The 120 glass barrier ply and the aluminum wire mesh are cocured with the resin from the 120 glass, bonding the mesh to the composite. The wire mesh is connected to metallic substructure to provide a path for electrical discharge.

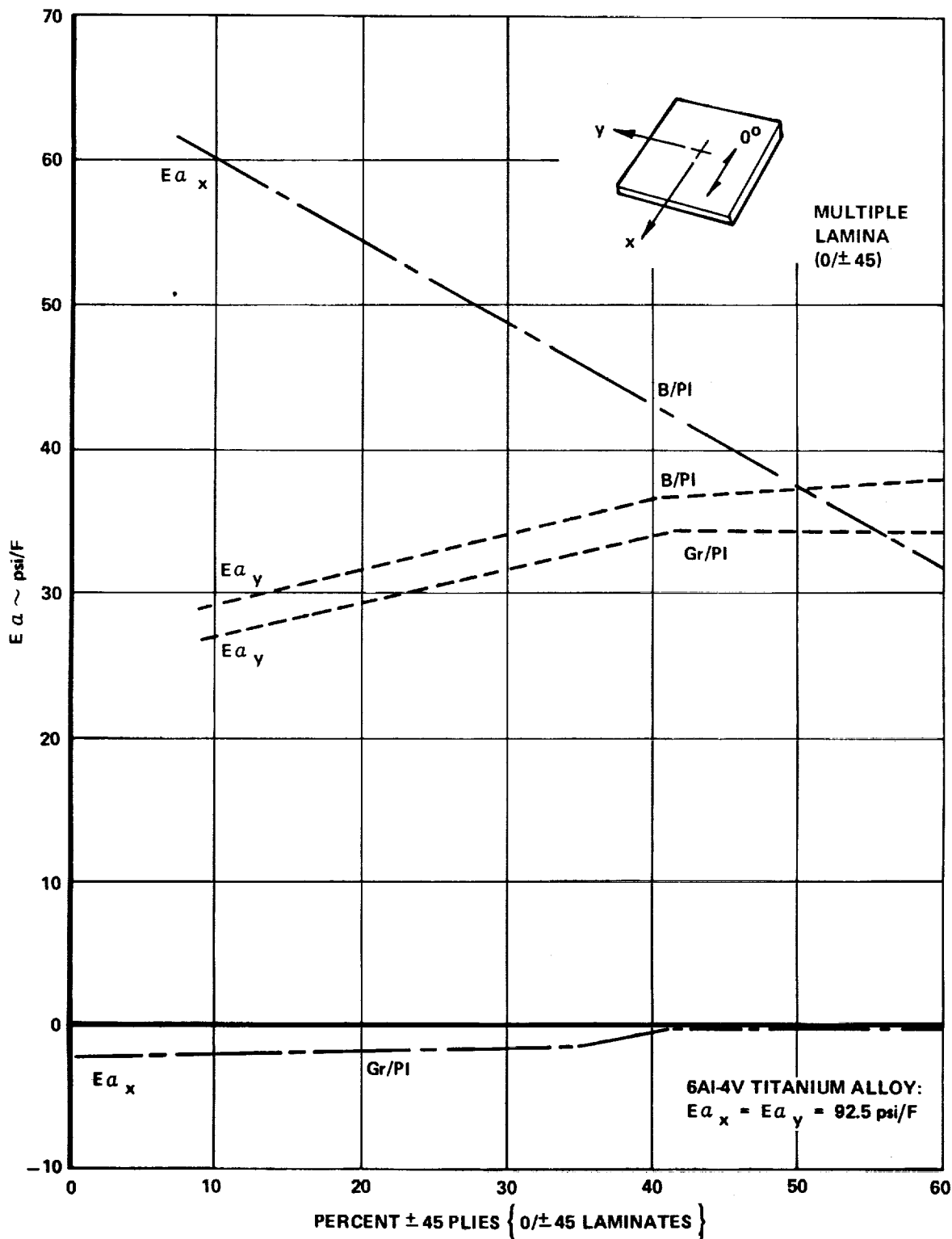


Figure 20-4. Comparative Thermal Stress - Titanium vs Composite Materials

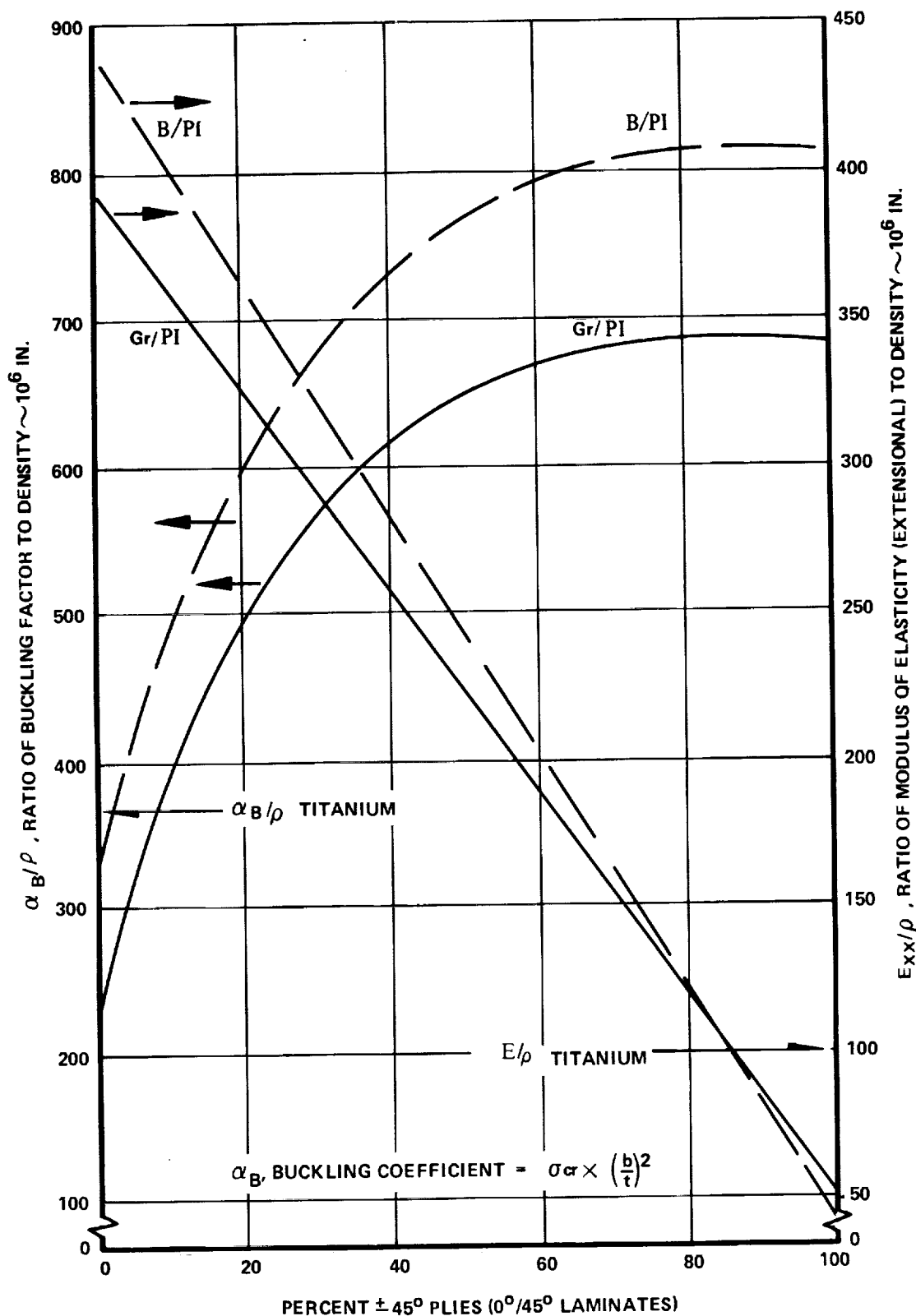


Figure 20-5. Comparative Buckling Efficiency and Specific Stiffness for Boron/Polyimide and Graphite/Polyimide

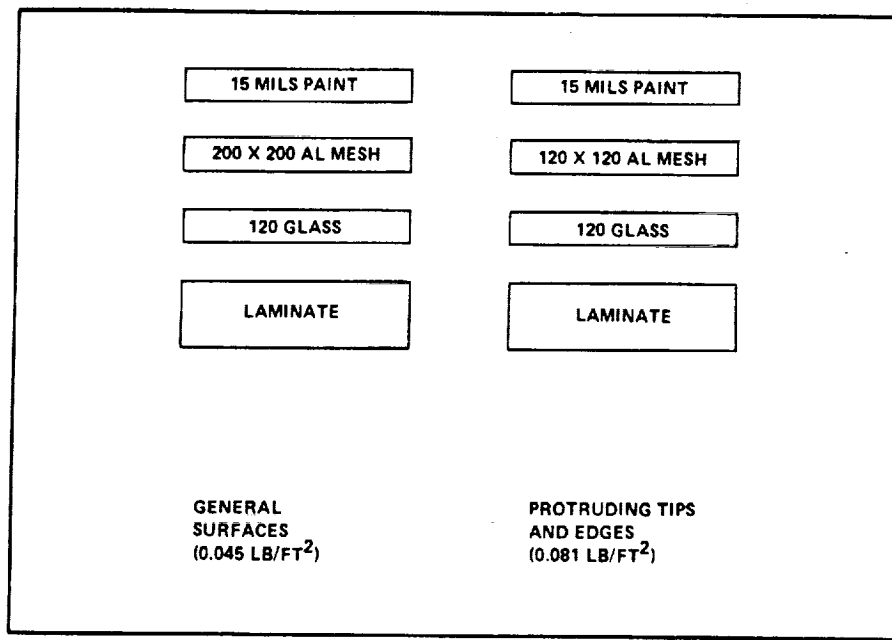


Figure 20-6. Surface Protection System for Composite Laminates

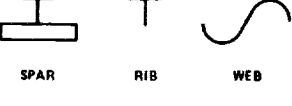
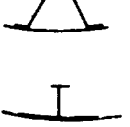
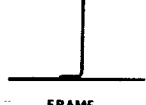
STRUCTURAL ARRANGEMENTS	BASIC CONCEPTS	
	SURFACE PANEL	SUBSTRUCTURE
WING CHORDWISE STIFFENED		 SPAR                    RIB                    WEB
WING MONOCOQUE		 TRUSS                    WEB
FUSELAGE SKIN/STRINGER AND FRAME		 FRAME

Figure 20-7. Composite Wing and Fuselage Design Concepts

Other protective measures include coating all surfaces with a polyurethane system (more desirable, higher service temperature systems are anticipated by 1985) sealing all cut edges, and wet installation of fasteners. The amount of protection required varies with the component location, with the greatest care required for leading-edge structure. Maximum protection, therefore, is assumed for these areas.

#### Design Concepts

The primary load carrying composite concepts for the far-term supersonic cruise aircraft design explored both biaxially and uniaxially stiffened surface panels. The concepts examined were variations of those evaluated in Task I, thus, the internal loads calculated for the Analytical Design Studies were directly applicable to this technology assessment study.

Figure 20-7 presents the basic design concepts evaluated for both wing and fuselage designs. All wing surface panel concepts are smooth skin designs and exploit the low coefficient of expansion characteristics, especially inherent in the graphite-polyimide system. For the fuselage, the more conventional skin-stringer and frame designs are evaluated. Further amplification of design variations are discussed in Table 20-2 and pictorially displayed in Figure 20-8.

#### Point Design Regions

Representative structure was specified at selective wing and fuselage regions. Analysis of the selected regions are performed to establish unit weights which are employed to establish total airplane weights.

Wing Point Design Regions - The location of wing point design regions are shown in Figure 20-9 and include the 3 regions which are displayed on the wing planform of the structural model. Point design regions are identified by the corresponding NASTRAN panel element numbers. Representative structure is specified at each of these locations and include a definition of the upper and lower surface panels, typical rib and spar structure, and the associated non-optimum factors. These regions were selected as representative of wing critical design regions. A description of these regions is as follows:

TABLE 20-2. MERITS OF POTENTIAL ALL-COMPOSITE CHORDWISE STIFFENED DESIGN CONCEPTS

CONCEPT A – CORRUGATED HAT STIFFENER

PROVIDES GOOD COMPRESSION EFFICIENCY, ESPECIALLY WITH EXTRA UNIDIRECTIONAL MATERIAL APPLIED IN HAT CROWN ELEMENT. CLOSED STIFFENER PROVIDES EXCELLENT TORSIONAL RIGIDITY AND LATERAL STABILITY PROPERTIES.

CONCEPT B – POINTED HAT STIFFENER

ALLOWS EFFICIENT PLACEMENT OF COMPRESSIVE MATERIAL, BUT REPRESENTS A REDUCTION IN LATERAL STABILITY FOR A CLOSED SECTION STIFFENER. SPAR CAP INTERFACE REPRESENTS WEIGHT PENALTY.

CONCEPT C – ROUND HAT STIFFENER

ALTHOUGH A ROUNDED SECTION REPRESENTS ADDED BUCKLING STRENGTH, THE INCREASE IS THOUGHT TO BE LESS FOR A LAMINATED COMPOSITE ELEMENT RELATIVE TO A CIRCULAR METAL STIFFENER. MANUFACTURING DIFFICULTIES AND SPAR CAP INTERFACE REPRESENTS ADDITIONAL PROBLEM AREAS.

CONCEPT D – HONEYCOMB STABILIZED HAT STIFFENER

THE RIGIDITY OF THE HONEYCOMB PRESENTS TOLERANCE PROBLEMS IN BOND AND CURE OF THE PANEL. THE CORE/SKIN INTERFACE UNDER THE HAT REPRESENTS A "HARD SPOT" RESTRAINING SMOOTH EXPANSION AND CONTRACTION, ESPECIALLY FOR BORON-POLYIMIDE MATERIAL.

CONCEPT E – TEE STIFFENER

FOR LIGHT WEIGHT COMPOSITE PANELS, TEE STIFFENERS OF MULTIDIRECTIONAL LAYERS REPRESENT A VERY WEAK TORSIONAL STABILITY CAPABILITY. TOTAL SKIN THICKNESS INCREASED RELATIVE TO A CLOSED STIFFENER LAYOUT.

CONCEPT F – BULB STIFFENER

ALTHOUGH COMPRESSION EFFICIENCY IS ENHANCED BY THE JUDICIOUS PLACEMENT OF A BUNDLE OF UNIDIRECTIONAL FIBERS, HERE AGAIN TORSIONAL RIGIDITY AND LATERAL STABILITY SUFFERS. ALSO, SPAR CAP INTERFACE WEIGHT PENALTIES WILL RESULT.

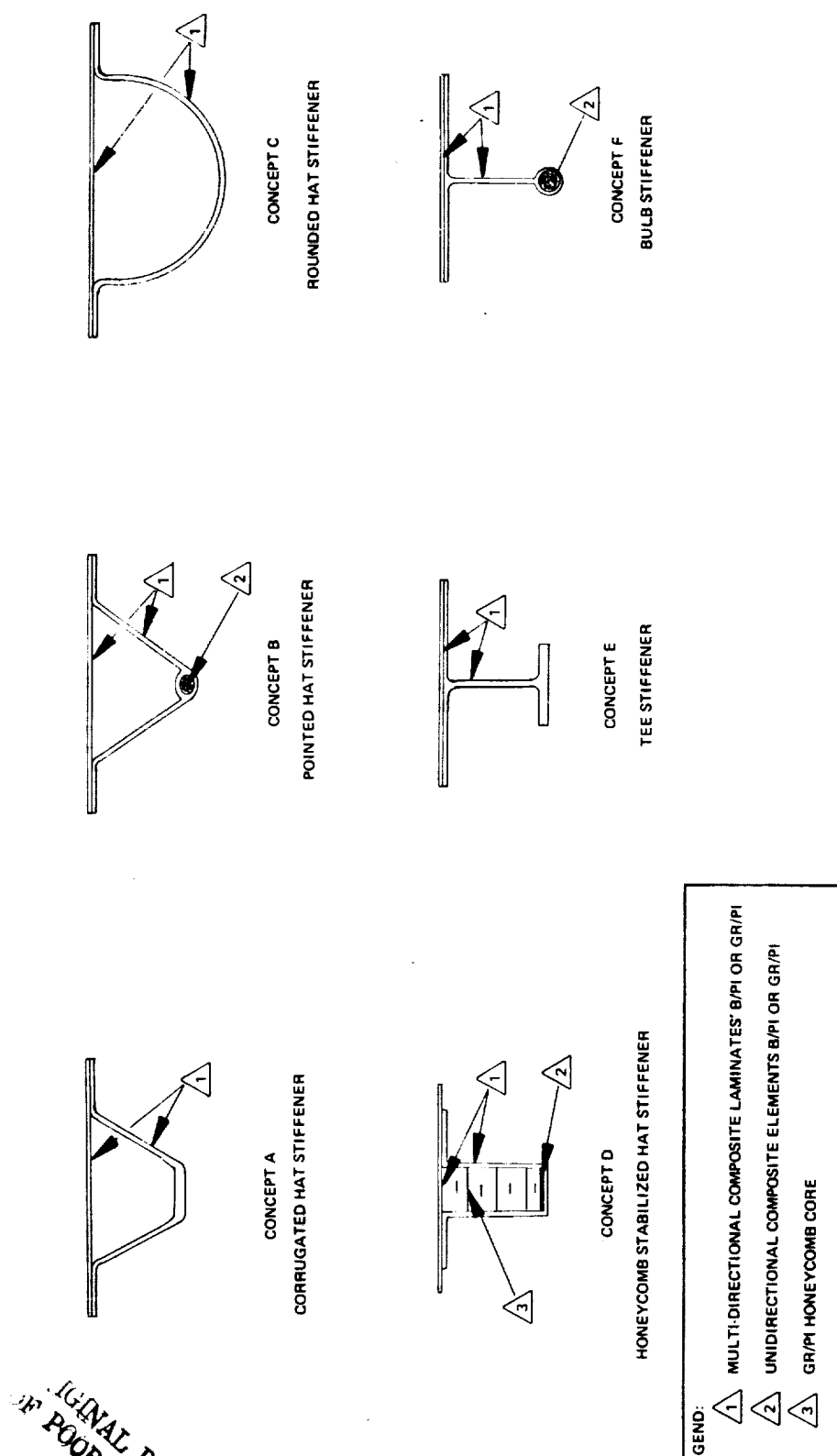


Figure 20-8. Chordwise Stiffened Wing Design - All Composite Concepts

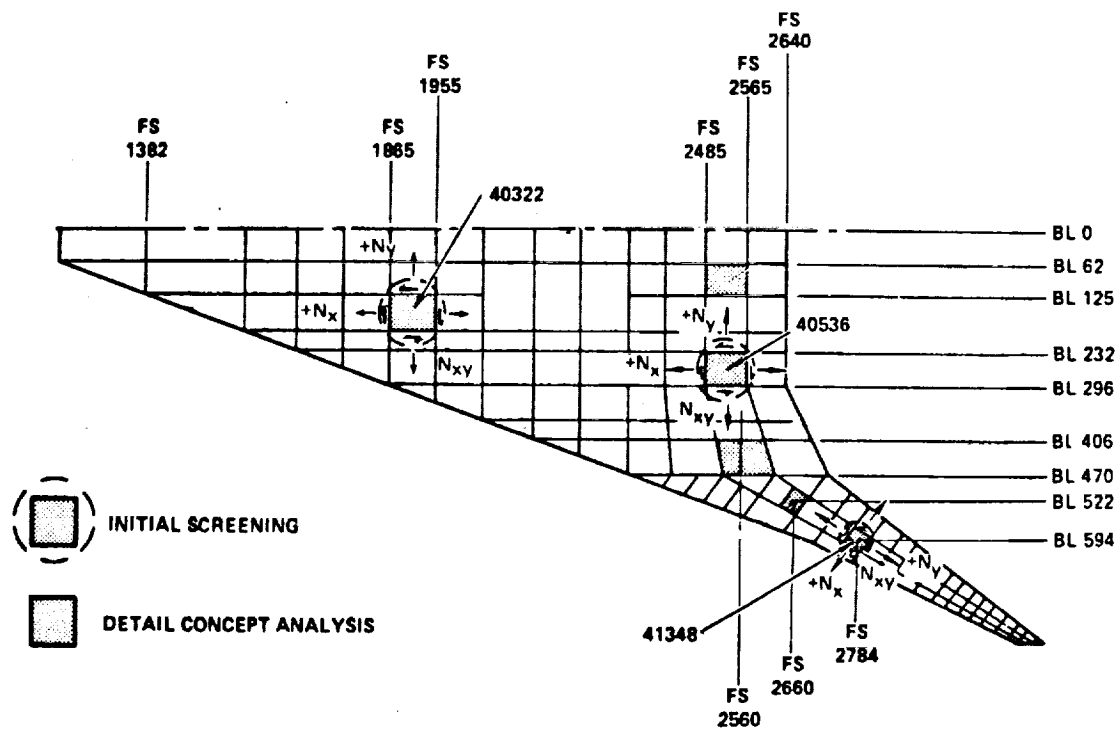


Figure 20-9. Definition of Wing Point Design Regions

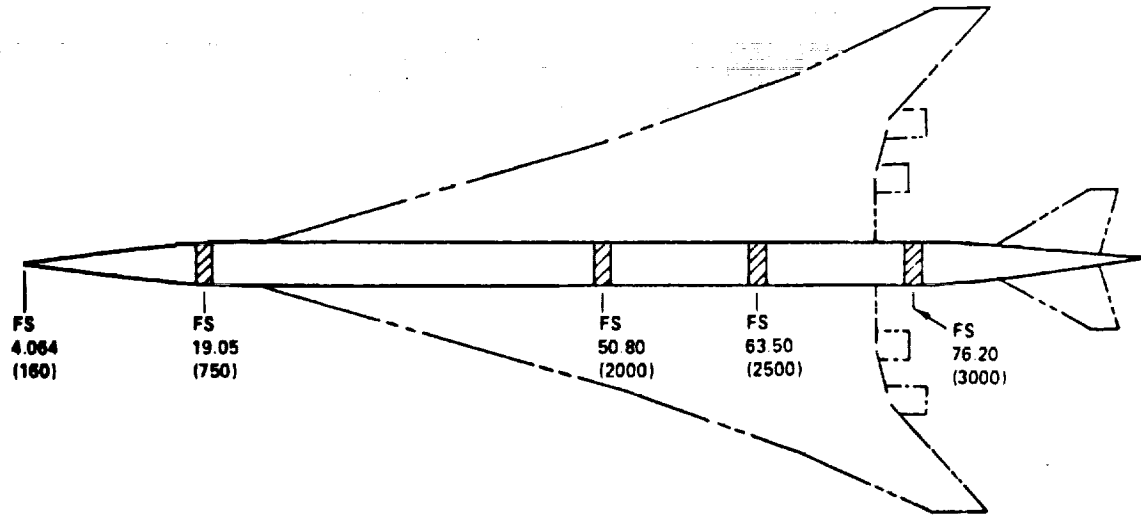


Figure 20-10. Definition of Fuselage Point Design Regions

- Forward wing box - Point design region 40322 is located forward of the main landing gear in a fuel tank region. This area is characterized as basically transmitting pressure loads with low load intensities with respect to wing bending loads.
- Aft box region - Point design region 40536, is located in the wing aft box in fuel tank region. In general, this area represents regions of high spanwise load intensities and variable chordwise load intensities due to wing bending.
- Wing tip region - Dry bay region 41348 is located approximately mid-span of the wing tip. High load intensities are indicative of the aeroelastic effect on this flexible region.

Fuselage Point Design Regions - Four point design regions were selected as representative of the actual fuselage design. These regions are shown in Figure 20-10 and are located at fuselage stations 750, 2000, 2500, and 3000. These regions were selected as typical of the critical design regions on the fuselage and, in general, classified as follows:

- Fuselage Forebody FS 750 - Generally characterized as fatigue design structure with low load intensities due to fuselage bending.
- Fuselage Centerbody (FS 2000 and 2500) - Wing/fuselage regions subjected to maximum body bending and wing spanwise loads.
- Fuselage Aftbody (FS 3000) - High body bending and torsion loads with regions subjected to a high acoustic environment.

Fuselage point design regions located at FS 2000 and FS 2500 are coincidental with the wing forward box and aft box point design regions.

#### Wing Design Loads

The Task I internal loads and surface pressures were scanned to identify the potentially critical conditions for wing and fuselage design. Table 20-3 presents the flight parameters associated with the selected design condition.

ORIGINAL PAGE IS  
OF POOR QUALITY

TABLE 20-3. CRITICAL WING LOADING CONDITIONS

LOAD CONDITION	WEIGHT (LB)	$V_e$ (KEAS)	MACH NO.	ALTITUDE ( $10^3$ FT.)	$n_z$
13	700,00	325	.90	30	2.5
20 $\Delta$	660,000	460	2.70	61.5	2.5
22 $\Delta$	550,000	433.6	2.70	64	2.5
31	690,000	265	1.25	52.4	2.5

$\Delta$  Start-of-Cruises     $\Delta$  Mid-Cruise

The surface load intensities and corresponding pressures are shown in Table 20-4 and 20-5 for the chordwise stiffened and monocoque designs, respectively. Load reduction based on reduced airframe weight potential of advanced composites application was not included.

#### Fuselage Design Loads

The fuselage design loads used for the composites design evaluation are in accordance with the data of Figure 20-11 and 20-12. The shears and bending moments were used to size panels and frames at the specified point design regions. In addition, the stiffness of the composite shell was maintained at least equivalent to the titanium shell design.

#### Results-Wing

Chordwise Stiffened Design Concept - Screening of the potential all-composite design concepts of Table 20-2 and Figure 20-8 were performed both on a qualitative and quantitative basis. The results of this assessment identified the Corrugated Hat Stiffener (Concept A) and the Tee Stiffener (Concept E) as the leading candidate for the all-composite design. The former provides good compression efficiency and the closed section offers excellent torsional rigidity. For the more lightly loaded, pressure critical, forward wing box structure the tee-stiffener concept was also evaluated. Although a torsionally-weak section, proper detail design often provides adequate structural integrity with minimum weight.

TABLE 20-4. DESIGN LOADS FOR CHORDWISE STIFFENED ARRANGEMENT - ULTIMATE

	LOAD CONDITION	POINT DESIGN REGION				
		40322	40536	41348	LOWER*	
13	$N_x$ $N_y$ $N_{xy}$ P	(lb/in.) (lb/in.) (lb/in.) (psi)	.531 -1,115 -.236 -E.14	271 -9,777 -778 -6.98	-633 -8,007 1,896 -3.86	
20	$N_x$ $N_y$ $N_{xy}$ P	(lb/in.) (lb/in.) (lb/in.) (psi)	-131 -866 -97 -7.67	-527 -8,740 -1,187 -7.47	-265 -7,415 855 -1.29	
22	$N_x$ $N_y$ $N_{xy}$ P	(lb/in.) (lb/in.) (lb/in.) (psi)	396 -775 -49 -6.65	-152 -7,355 -1,016 -5.80	-225 -6,670 745 -1.06	
31	$N_x$ $N_y$ $N_{xy}$ P	(lb/in.) (lb/in.) (lb/in.) (psi)	488 -1,063 -.120 -8.33	-1,305 -14,379 -2,354 -8.94	-1,402 -12,979 3,144 -5.87	
					0.96	

\*REVERSE SIGN OF UPPER SURFACE EXCEPT AS NOTED.

TABLE 20-5. DESIGN LOADS FOR MONOCOQUE ARRANGEMENT - ULTIMATE

		POINT DESIGN REGION					
		40322		40536		41348	
LOAD CONDITION		UPPER	LOWER*	UPPER	LOWER*	UPPER	LOWER*
13	$N_x$ (lb/in.)	-452		-1,218		-804	
	$N_y$ (lb/in.)	-671		-7,953		-5,908	
	$N_{xy}$ (lb/in.)	-218		-1,903		2,657	
	$p$ (psi)	-8.14	-9.26	-6.98	-8.40	-3.86	-0.3
20	$N_x$ (lb/in.)	-213		-1,945		-342	
	$N_y$ (lb/in.)	-463		-7,257		-6,037	
	$N_{xy}$ (lb/in.)	-135		-2,588		1,499	
	$p$ (psi)	-7.67	-9.47	-7.47	-7.47	-1.29	1.04
22	$N_x$ (lb/in.)	69		-1,381		-290	
	$N_y$ (lb/in.)	-378		-6,081		5,381	
	$N_{xy}$ (lb/in.)	-109		-2,196		1,305	
	$p$ (psi)	-6.65	-7.16	-5.8	-5.0	-1.06	0.86
31	$N_x$ (lb/in.)	51		-3,272		-1,678	
	$N_y$ (lb/in.)	-529		-11,787		-9,586	
	$N_{xy}$ (lb/in.)	-191		-4,795		4,225	
	$p$ (psi)	-8.33	-8.94	-6.94	-8.29	-5.07	0.96

\*REVERSE SIGN OF UPPER SURFACE EXCEPT AS NOTED.

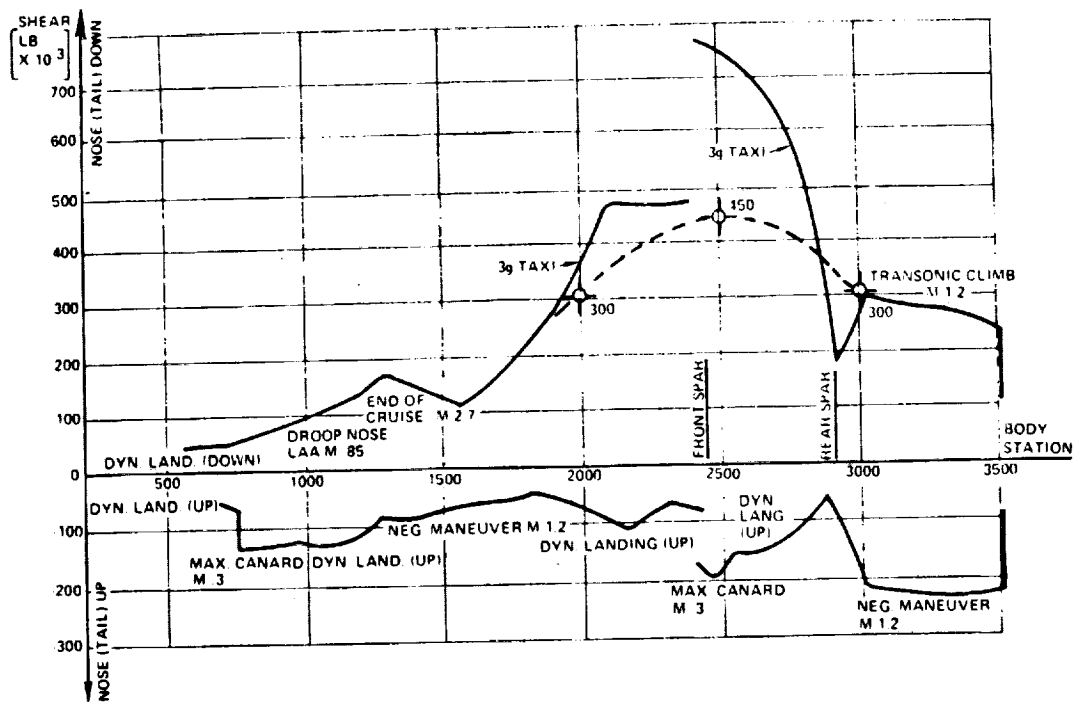


Figure 20-11. Fuselage Shear Diagram - Task I

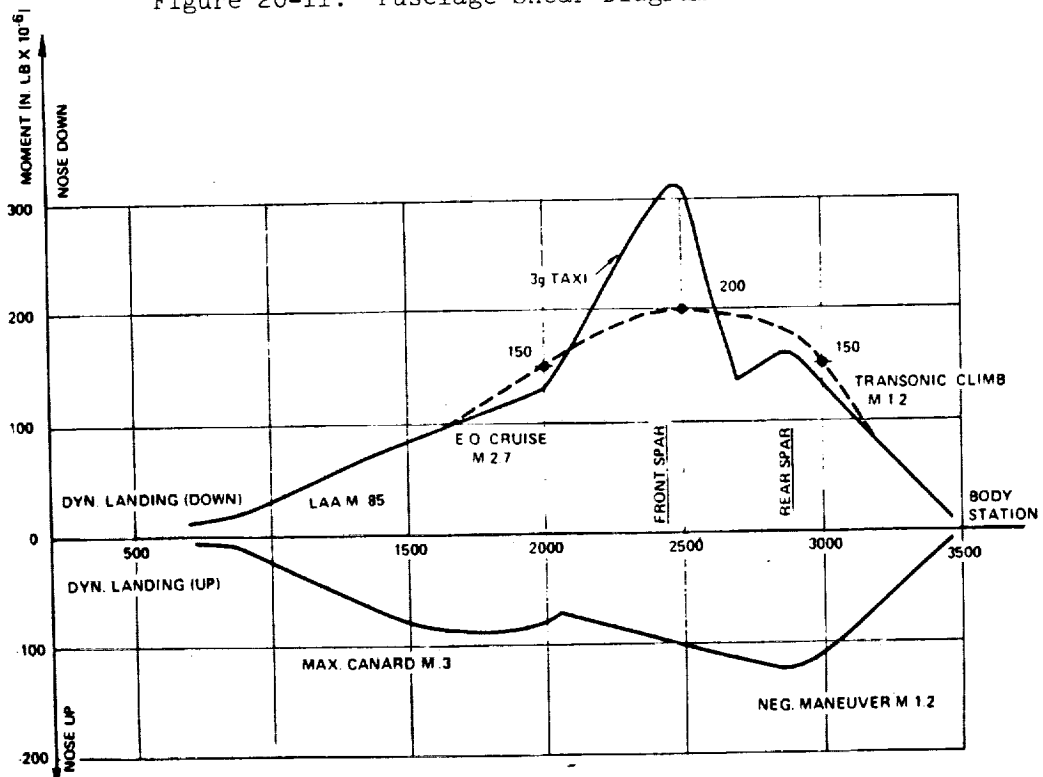


Figure 20-12. Fuselage Bending Moment Diagram - Task I

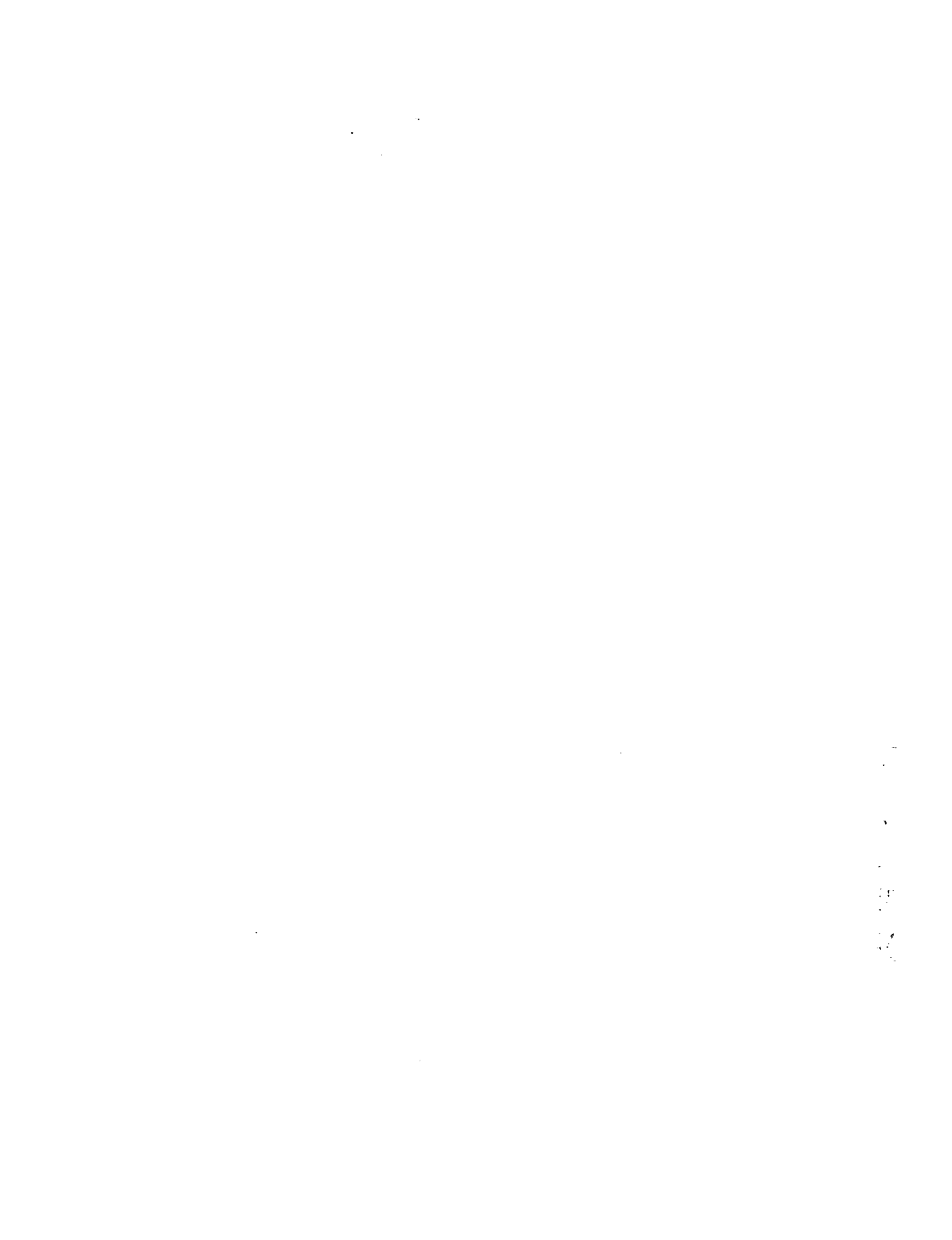
Figure 20-13 presents a layout of a typical section of the wing for the chordwise stiffened design. Representative truss and bulkhead spars are indicated. Both a honeycomb and corrugated bulkhead-type spar/rib web are conceptually shown. A summary of the composite wing surface panel designs are shown in Table 20-6. The geometry and layup for the hat-stiffener for point design region 40322 and 40536 are presented. For both the boron-polyimide and the graphite-polyimide material system, the same geometry is used for a given region. The ply thickness and density of the graphite and boron material varies thus resulting in slight variations in equivalent panel thickness and panel unit weight. The detail geometry for the tee-stiffener design indicates the reduced efficiency and thus higher unit weight by approximately 40-percent.

The substructure sizing results are displayed in Table 20-7 for the graphite-polyimide material system at point design region 40322. The details of representative substructure components (i.e. spar caps, rib caps, spar and rib webs) are tabulated. The geometry and layup orientation employed in the design are also shown. Proportionate unit weights were developed for the boron-polyimide substructure at the various point design regions.

Monocoque Design Concept - For the monocoque design only the honeycomb sandwich was evaluated. The design of the sandwich panel was based on laminated face skins of boron-polyimide and graphite-polyimide composites with a titanium alloy core. Condition 13 was critical for point design 40322 and condition 31 critical for both the aft box and tip box structure regions.

Figure 20-14 presents a layout of a typical wing section employing the honeycomb surface panel design. Although a total honeycomb system is pictorially displayed, the substructure weights are for representative truss spar/rib and corrugated spar/web designs. The details for the wing surface panels are shown in Table 20-8 for the B/PI and Gr/PI designs. The resulting panel unit weights include a protective system weight of .045-lb per square foot.

For the truss spar and rib design, a cruciform configuration was adopted in lieu of the tubular section used for the metallic design. The composite cruciform member was sized to yield a greater cross-section "EI" at the same column length as its titanium counterpart. Comparative data is shown in Table 20-9 for the titanium truss tubes and the composite section. A weight saving of approximately



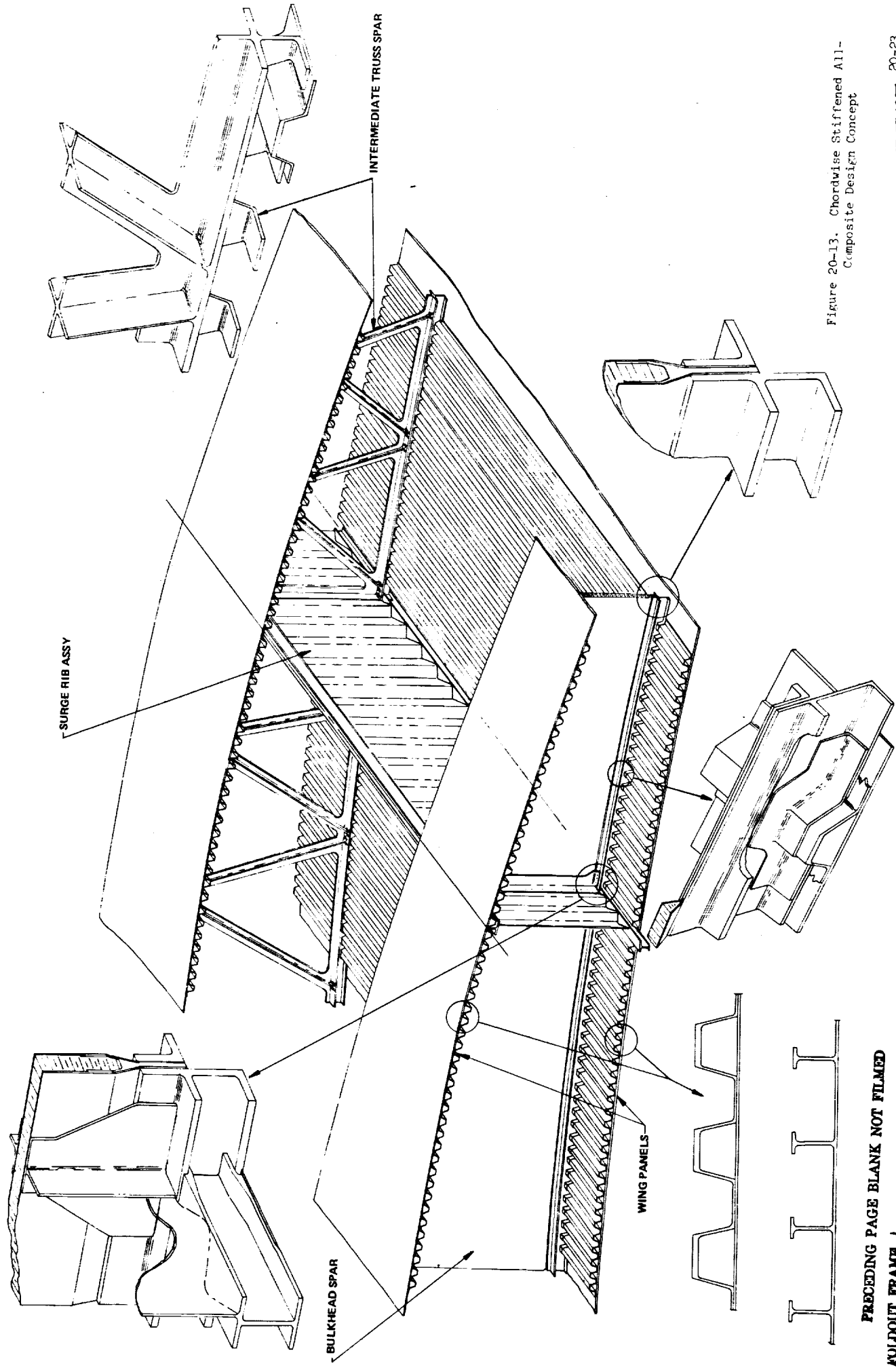


Figure 20-13. Chordwise Stiffened All-Composite Design Concept



ELEMENT CODES					
REGION		40322		40536	
MATERIAL	B/PI	Gr/PI	B/PI	Gr/PI	B/PI
ELEMENT					
1	LENGTH (in.)	3.0	2.5	2.5	2.5
	ORIENTATION	33% 0° - 67% ±45°	20% 0° - 80% ±45°	20% 0° - 80% ±45°	20% 0° - 80% ±45°
	PLIES	6	10	10	10
2	LENGTH (in.)	0.5	0.5	1.2	1.2
	ORIENTATION	33% 0° - 67% ±45°	50% 0° - 50% ±45°	20% 0° - 80% ±45°	20% 0° - 80% ±45°
	PLIES	6	8	10	10
3	LENGTH (in.)	1.0	1.0	1.2	1.2
	ORIENTATION	33% 0° - 67% ±45°	50% 0° - 50% ±45°	55% 0° - 45% ±45°	55% 0° - 45% ±45°
	PLIES	6	8	18	18
4	LENGTH (in.)	1.0	1.0		
	ORIENTATION	71% 0° - 29% ±45°	65% 0° - 35% ±45°		
	PLIES	14	23		
	SPACING (in.)	3.0	2.5	2.5	2.5
	PANEL t (in.)	0.092	0.117	0.159	0.202
	WEIGHT(A), p̄ (lb/ft <sup>2</sup> )	0.998	0.988	1.694	1.674
				1.384	1.370

(A) INCLUDES PROTECTIVE FINISH.

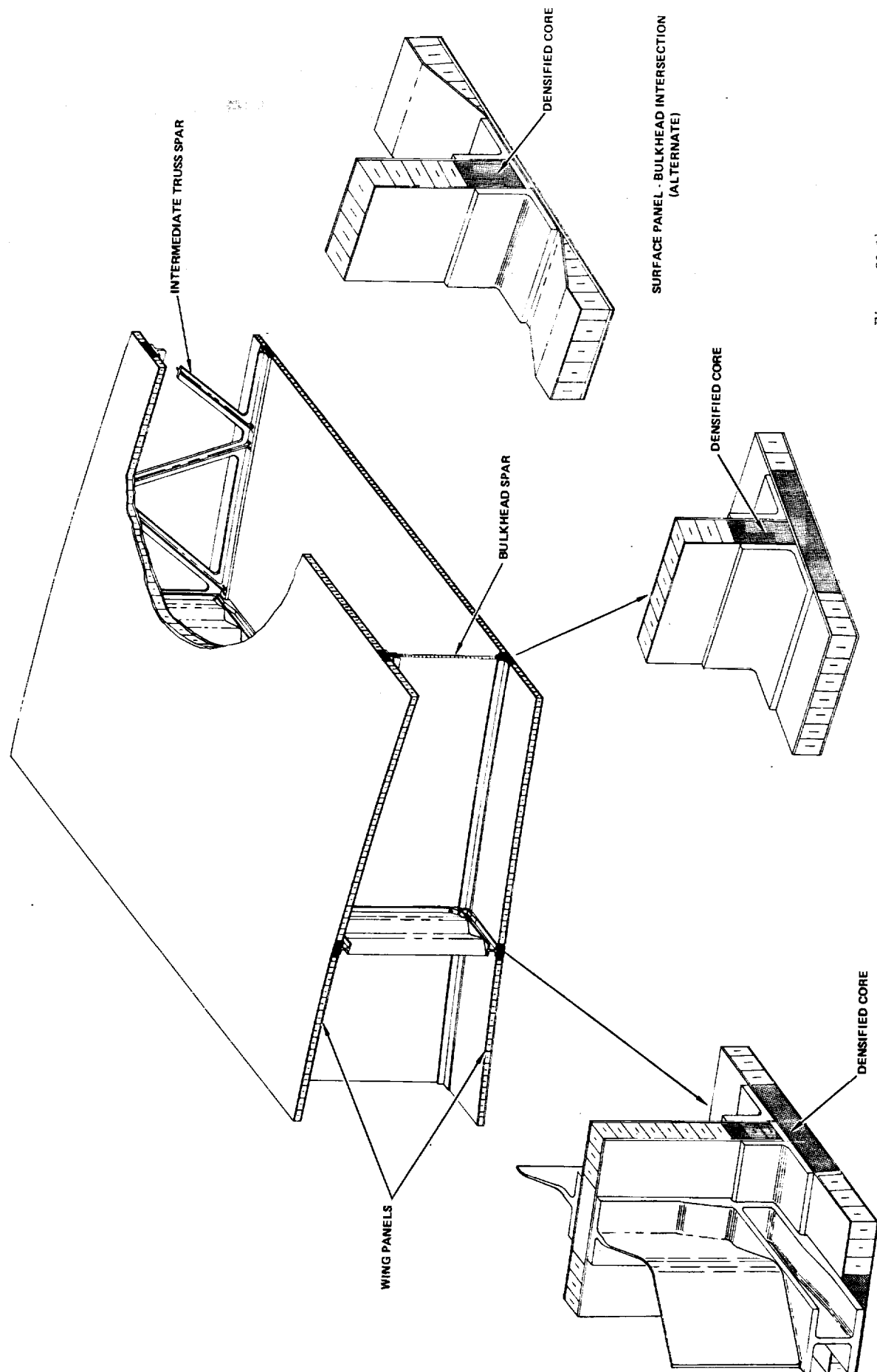
PRECEDING PAGE BLANK NOT FILMED

TABLE 20-6. SUMMARY OF COMPOSITE CHORDWISE STIFFENED WING SURFACE PANELS

TABLE 20-7. GRAPHITE-POLYIMIDE SUBSTRUCTURE - POINT DESIGN 40322

SUBSTRUCTURE COMPONENT	GEOMETRY	ORIENTATION	SURFACE OR ELEMENT	t	PLIES	AREA	$\rho A$	$\omega$
				(in.)	(n)	(in <sup>2</sup> )	(lb/in.)	(lb/ft <sup>2</sup> )
SPAR CAPS		0.32/-45/32 0.52/-45/52	UPPER	0.32	64	0.48	0.0264	0.127
			LOWER	0.52	104	0.78	0.0429	0.207
		$\Sigma$		0.84	168	1.26	0.0693	0.334
RIB CAPS		0.12/-45/8 0.4/-45/8	1	0.140	20	0.280	0.0157	0.038
			2	0.084	12	0.084	0.0047	0.011
		$\Sigma \times 2$		0.448	64	0.728	0.0408	0.098
SPAR AND RIB WEBS		0.1/-45/4 0.6	1	0.035	5	0.130	0.0073	0.411(A)
			2	0.042	6	0.042	0.0024	0.135(A)
		$\Sigma$		0.077	11	0.172	0.0097	0.546(A)

(A) UNIT WEIGHT OF WEB NOT COMPENSATED FOR DEPTH OF WEB OR SPACING. MULTIPLY BY 0.98 FOR UNIT SPAR WEIGHT;  
BY 1.06 FOR UNIT RIB WEIGHT.



SURFACE PANEL - BULKHEAD INTERSECTION

DENSIFIED CORE

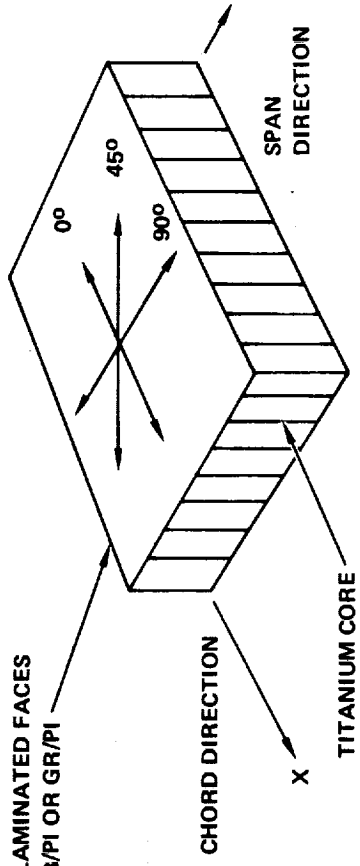
FOLDOUT FRAME /

Figure 20-1*b*. Monocoque All-Composite Design Concept



TABLE 20-8. SUMMARY OF COMPOSITE MONOCOQUE WING SURFACE PANELS

POINT DESIGN REGION		40322				40536				41348			
FACE MATERIAL		B/PI		GR/PI		B/PI		GR/PI		B/PI		GR/PI	
NO. PLIES/FACE		6	6	6	6	17	17	17	17	15	15	15	15
SURFACE		UPPER	LOWER	UPPER	LOWER	UPPER	LOWER	UPPER	LOWER	UPPER	LOWER	UPPER	LOWER
ORIENTATION		$0_2/\pm 45_2/90_2$				$0_3/\pm 45_3/90_6$				$0_2/\pm 45_2/90_5$			
SKIN	lb/ft <sup>2</sup>	0.729	0.771	0.722	0.764	1.993	2.595	1.964	2.556	1.745	1.894	1.738	1.886
CORE	lb/ft <sup>2</sup>	0.315	0.186	0.315	0.186	0.262	0.028	0.262	0.028	0.380	0.099	0.380	0.099
$\Sigma$	PANEL (A) lb/ft <sup>2</sup>	1.044	0.957	1.037	0.950	2.255	2.623	2.226	2.584	2.125	1.993	2.118	1.985



(A) INCLUDES 0.045 lb/ft<sup>2</sup>  
PROTECTIVE FINISH WEIGHT

(B) SPAR SPACING = 30 INCHES  
RIB SPACING = 60 INCHES

TABLE 20-9. COMPOSITE TRUSS SPAR AND RIB - MONOCOQUE DESIGN

POINT DESIGN REGION	TITANIUM TRUSS TUBES						COMPOSITE CRUCIFORM TRUSS					
	SPAC (in.)	A (in. <sup>2</sup> )	$\rho A$	$EI \times 10^6$ (lb/in. <sup>2</sup> )	w	H	t	A	$\rho A$	$EI \times 10^6$ (lb/in. <sup>2</sup> )	$w B/PI$ (lb/ft <sup>2</sup> )	$w Gr/PI$ (lb/ft <sup>2</sup> )
<u>40322</u>												
SPAR TRUSS	30	.093	.0149	0.40	0.284	2.0	0.044	.194	.0139	0.70	0.265	0.267
RIB TRUSS	30	.329	.0526	1.92	0.387	2.0	0.154	.678	.0488	2.50	0.359	0.362
<u>40536</u>												
SPAR TRUSS	20	.271	.0434	0.96	0.586	2.0	0.121	.532	.0383	1.94	0.517	0.523
RIB TRUSS	20	.709	.1134	5.02	0.406	2.0	0.308	1.256	.0976	5.06	0.349	0.354

6-percent is realized over the titanium alloy design. Note the unidirectional rod used in the center of the cruciform for achieving a high EA product.

The corrugated composite spar and rib webs were sized to provide a greater  $E_t$  or  $G_t$  than the titanium alloy design. This approach offered reasonable pressure (bending) and shear capability, respectively. The overall corrugation dimensions were retained for the composite webs. Table 20-10 presents the geometry data developed for the circular-arc corrugated spar/rib webs for the reference titanium alloy. The appropriate geometry for the 3 point design regions are shown. The results of the composite spar web design at point design region 40322 is shown in Table 20-11. The results indicate a weight saving of approximately 25-percent when composite designs are employed. Since the cross section properties for the spar and rib webs in regions 40322, 40536 and 41348 are of the same magnitude, the region 40322 spar web weight saving factor was used to calculate the composite web weights in all three point design regions as shown in Table 20-12.

Table 20-13 presents a comparison of unit wing weights for the 3 point design regions for the chordwise stiffened hat section design and the monocoque honeycomb sandwich design. The unit weights for the surface panels and individual sub-structure components are shown. The minimum weight design for each point design region is identified by the cross-hatching. Trends similar to the metallic design are noted, with the chordwise stiffened being least weight for the lightly loaded forward box region (40322) and the honeycomb design being least weight for the highly loaded aft box and stiffness critical tip box structure. These unit weights are applied to establish the total wing weights for the advanced technology aircraft.

#### Results - Fuselage

The assessment of the potential payoff for composite technology application to the primary shell structure was made observing practical constraints for passenger accomodation. The two major factors included: (1) the need for passenger windows and (2) the requirement for ingress and emergency egress.

It is foreseeable to arrive at a "windowless" aircraft with an aesthetic mural for the interior design for an advanced technology supersonic transport. This would provide further opportunities to exploit fully the sandwich shell design or shell

TABLE 20-10. CIRCULAR-ARC CORRUGATED SPAR/RIB WEBS - REFERENCE TITANIUM ALLOY

POINT DESIGN REGION	SPAC.	$t$	R	$\theta$	S	A	$\rho t$	$Et$	$Gt$	w	GEOMETRY
	(in.)	(in.)	(in.)	(deg)	(in.)	(in. <sup>2</sup> )	(lb/in. <sup>2</sup> )	(10 <sup>6</sup> lb/in.)	(10 <sup>6</sup> lb/in.)	(lb/ft <sup>2</sup> )	
<u>40322</u>											
SPAR WEB	30	.022	1.30	80	2.56	.080	.0050	.50	.14	1.031	
RIB WEB	60	.025	1.50	77	2.92	.101	.0055	.55	.16	0.570	
<u>40536</u>											
SPAR WEB	20	.025	1.40	66	2.56	.081	.0051	.51	.16	0.980	
RIB WEB	60	.036	1.40	70	2.63	.123	.0058	.58	.22	0.486	
<u>41348</u>											
SPAR WEB	30	.027	1.00	60	1.732	.056	.0052	.52	.17	0.300	
RIB WEB	60	.018	1.00	60	1.732	.038	.0029	.29	.11	0.100	
TYPICAL WEB CROSS-SECTION											

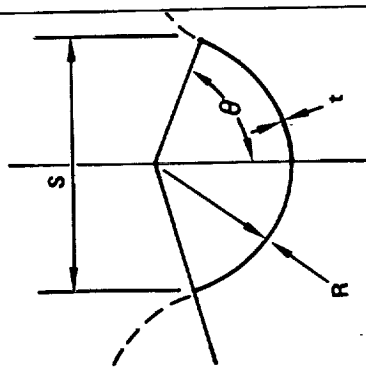


TABLE 20-11. COMPOSITE CIRCULAR-ARC CORRUGATED SPAR WEB - POINT DESIGN 40322

POINT DESIGN REGION	REFERENCE ( $T_1$ )			BORON/POLYIMIDE (B/PI)				GRAPHITE/POLYIMIDE (GR/PI)					
	$E_t \times 10^6$ (lb/in <sup>2</sup> )	$G_t \times 10^6$ (lb/in <sup>2</sup> )	$wT_1$ (lb/ft <sup>2</sup> )	$\bar{t}$ (in.)	$\rho\bar{t}$ (lb/in <sup>2</sup> )	$E_t \times 10^6$ (lb/in <sup>2</sup> )	$G_t \times 10^6$ (lb/in <sup>2</sup> )	$w_B/PI$ (lb/ft <sup>2</sup> )	$\bar{t}$ (in.)	$\rho\bar{t}$ (lb/in <sup>2</sup> )	$E_t \times 10^6$ (lb/in <sup>2</sup> )	$G \cdot \bar{t} \times 10^6$ (lb/in <sup>2</sup> )	$w_{Gr}/PI$ (lb/ft <sup>2</sup> )
<u>40322</u>													
SPAR WEB	0.50	0.14	1.031	.053	.00379	0.80	0.19	0.773	.067	.00376	0.74	0.17	0.763

TABLE 20-12. COMPOSITE CIRCULAR-ARC CORRUGATED WEB WEIGHTS

GEOMETRY	POINT DESIGN REGION	CIRCULAR-ARC CORRUGATION	REFERENCE Ti - 6A1 - 4V (lb/ft <sup>2</sup> )	BORON-POLYIMIDE (lb/ft <sup>2</sup> )	GRAPHITE-POLYIMIDE (lb/ft <sup>2</sup> )
40322	SPAR WEB RIB WEB	1.031	0.773	0.763	
		0.570	0.428	0.422	
40536	SPAR WEB RIB WEB	0.980	0.735	0.725	
		0.486	0.365	0.360	
41348	SPAR WEB RIB WEB	0.300	0.227	0.226	
		0.100	0.076	0.075	

$S = 2R \cos(90 - \theta)$   
 $A_1 = 2R\theta t_1; A_2 = 1.0t_2$   
 $\bar{t} = \sum A_i / S$

TABLE 20-13. WING WEIGHT COMPARISON FOR POINT DESIGN REGIONS

POINT DESIGN REGION	40322				40536				41348			
STR. ARRANGEMENT	CHORDWISE		MONOCOQUE		CHORDWISE		MONOCOQUE		CHORDWISE		MONOCOQUE	
SPAR SPACING (in.)	30	30	30	30	30	30	30	30	30	30	30	30
COMPOSITE MATERIAL	B/P1	GR/P1										
PANEL CONCEPT												
UPPER SURFACE	0.998	0.888	1.044	1.037	1.694	1.674	2.255	2.226	1.457	1.443	2.125	2.118
LOWER SURFACE	0.998	0.988	0.957	0.950	1.412	1.394	2.623	2.584	1.003	0.993	1.993	1.985
TRUSS SPAR	0.336	0.338	0.265	0.267	0.656	0.663	0.517	0.523	—	—	—	—
CORRUGA. SPAR	0.540	0.535	0.773	0.763	0.716	0.711	0.735	0.725	0.545	0.541	0.227	0.228
TRUSS RIB	0.102	0.095	0.359	0.362	0.099	0.100	0.349	0.354	—	—	—	—
CORRUGA. RIB	0.584	0.578	0.428	0.422	0.798	0.792	0.365	0.360	0.402	0.399	0.076	0.075
SPAR CAP	0.337	0.334	0.178	0.177	3.795	3.761	0.252	0.249	3.584	3.552	0.181	0.179
RIB CAP	0.099	0.098	0.138	0.137	0.118	0.117	0.130	0.129	0.118	0.117	0.131	0.130
$\Sigma$ TOTAL (lb/ft <sup>2</sup> )	3.994	3.955	4.142	4.115	9.288	9.212	7.226	7.150	7.109	7.045	4.733	4.713

NOTE: SPAR SPACING = 30 inch  
RIB SPACING = 60 inch

structure optimization without a frame spacing constraint. However, to obtain the design trends for this study, constraints for frame spacing of 20-inches and frame height of 3.0-inches were observed. Furthermore, the aforementioned constraints are consistent with the titanium skin-stringer and frame design evaluated in Task I and a direct comparison can be made to relate more directly the impact of composite utilization on the primary shell structure design.

The fuselage of the supersonic cruise aircraft is bending critical over most of its length as depicted in Figure 20-12, with internal pressure dictating requirements for the shell structure design forward of FS 1000. The basic concepts employed to satisfy the design requirements are shown in Figure 20-7. The tee-stringer design was adopted for the lightly loaded pressure critical forebody structure. For the bending critical regions both the tee-stringer and hat-stringer designs were evaluated.

For analysis, the fuselage shell was idealized as a circular shell as shown in Figure 20-15. The figure further reveals the skin-stringer and frame lamina directions identified in the subsequent tables. The analysis results of the fuselage cross section are identified by the notation of Figure 20-16; location 7 being representative of the lower centerline of the fuselage.

Tables 20-14 through 20-18 presents the sizing results of the design concepts employing boron-polyimide and graphite-polyimide composites. For comparison, the reference titanium shell properties are also indicated. In all cases the  $\bar{E}_t$  is greater for the composite material systems.

For fuselage frame design both the I-section and channel section frames were investigated. Typical frame-stringer intersections are shown in Figure 20-17. The figures indicate full depth frames with skin-flange continuity provided by integral clips. Table 20-19 indicates the proposed channel frames and the idealized frame employed for analysis. For composite application, a 10- to 20-percent increase in stiffness is indicated at FS 2000 and FS 3000 with a corresponding reduction in frame unit weights of approximately 20-percent, as shown in Table 20-20. To determine the frame weights at FS 2500 the above weight trend was applied and results tabulated.

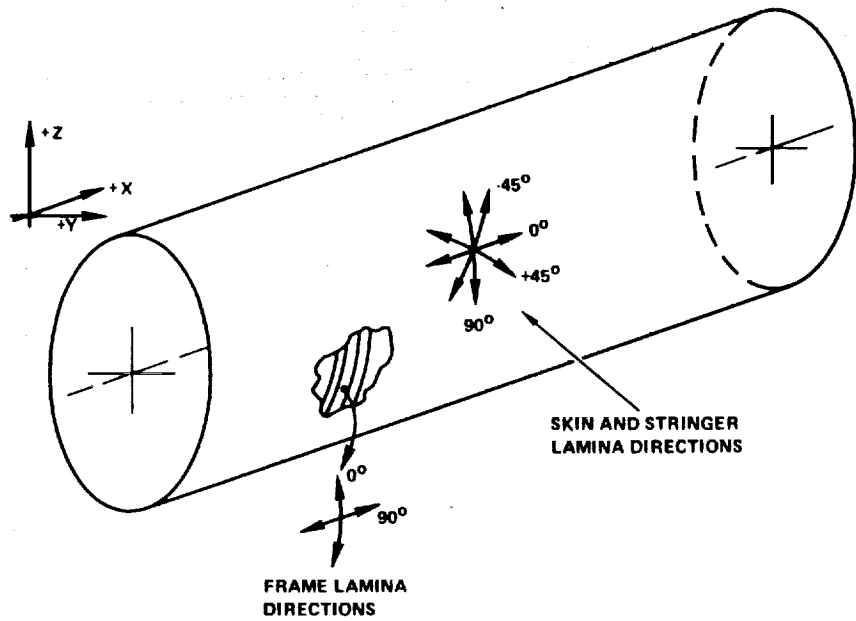


Figure 20-15. Composite Fuselage Laminate Directions

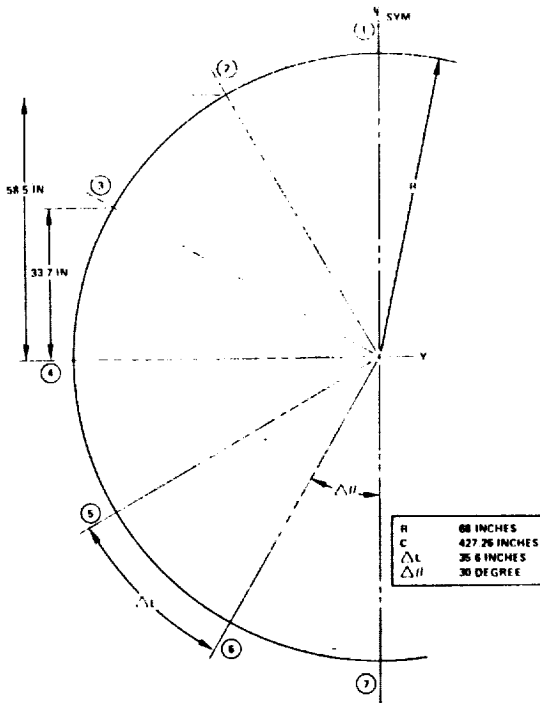
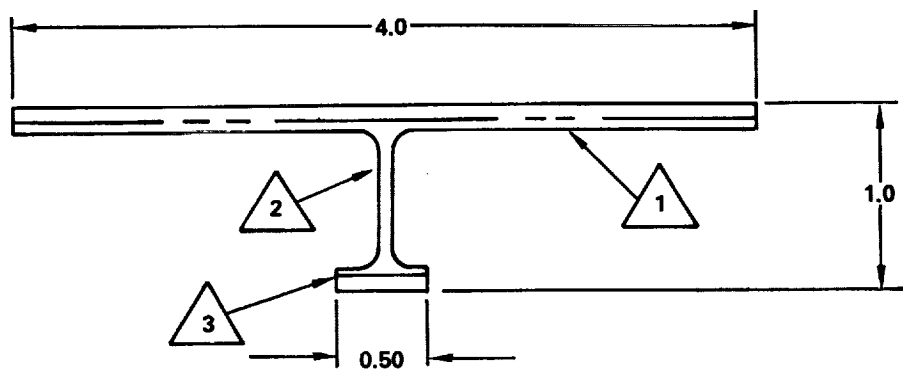


Figure 20-16. Idealized Cross-Section of Fuselage

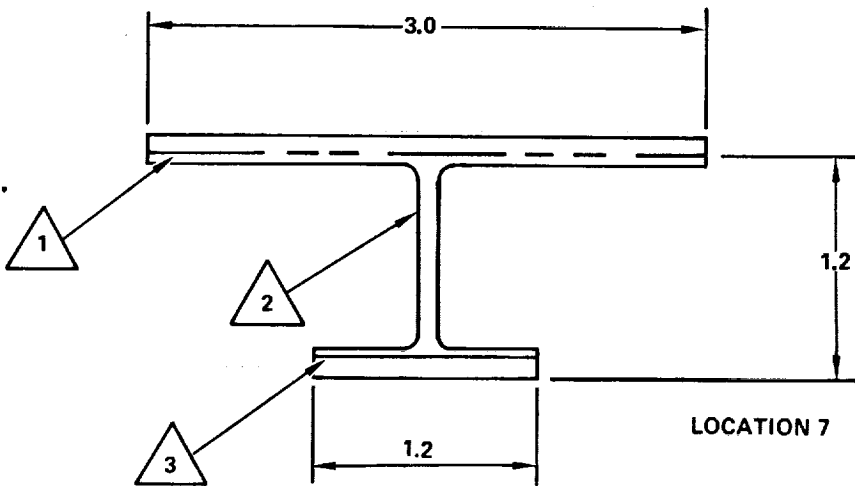
TABLE 20-14. COMPOSITE TEE-STIFFENED PANEL - FS 750



BORON-POLYIMIDE				GRAPHITE-POLYIMIDE			
NO.	ORIENTATION	b(in)	t(in)	NO.	ORIENTATION	b(in)	t(in)
1	$0_8/\pm 45_4/90_4$	-	0.088	1	$0_8/\pm 45_4/90_4$	-	0.112
2	$\pm 45_4$	0.90	0.022	2	$\pm 45_4$	0.90	0.028
3	$0_{12}/\pm 45_4$	0.25	0.088	3	$0_{12}/\pm 45_4$	0.25	0.112
$E_t \times 10^6$ (lb/in)		2.10		1.92			
$\rho t$ (lb/in <sup>2</sup> )		.00756		.00745			

REFERENCE TITANIUM:  $E_t = 0.92 \times 10^6$  lb/in;  $\rho t = .009$  lb/in<sup>2</sup>

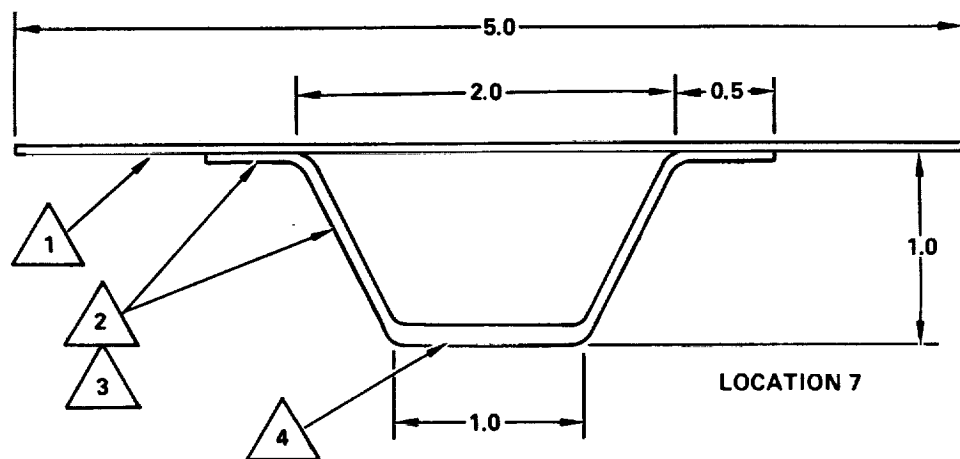
TABLE 20-15. COMPOSITE TEE-STIFFENED PANEL - FS 2000 AND FS 3000



BORON-POLYIMIDE				GRAPHITE-POLYMIDE			
NO.	ORIENTATION	b(in)	t(in)	NO.	ORIENTATION	b(in)	t(in)
1	$0_{12}/\pm45_{12}/90_4$	-	0.154	1	$0_{12}/\pm45_{12}/90_4$	-	0.196
2	$0_2/\pm45_{12}$	1.20	0.077	2	$0_2/\pm45_{12}$	1.20	0.098
3	$0_{16}/\pm45_{12}$	0.60	0.154	3	$0_{16}/\pm45_{12}$	0.60	0.196
$E\bar{t} \times 10^6$ (lb/in)		3.95		3.64			
$\rho\bar{t}$ (lb/in <sup>2</sup> )		.0176		.0175			

REFERENCE TITANIUM:  $E\bar{t} = 2.58 \times 10^6$  lb/in;  $\rho\bar{t} = .0254$  lb/in<sup>2</sup>

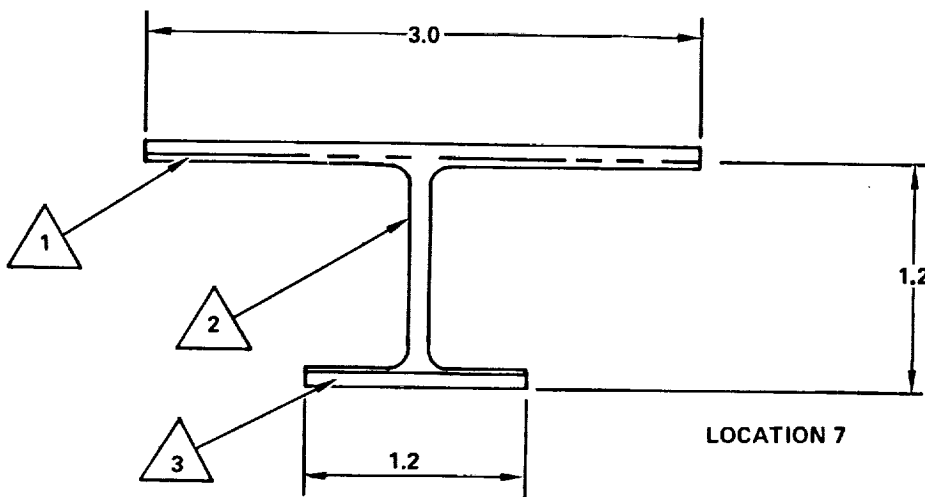
TABLE 20-16. COMPOSITE HAT STIFFENED PANEL - FS 2000 AND FS 3000



BORON-POLYIMIDE				GRAPHITE-POLYIMIDE			
NO.	ORIENTATION	b(in)	t(in)	NO.	ORIENTATION	b(in)	t(in)
1	$0_{12}/\pm 45_{12}/90_4$	—	0.154	1	$0_{12}/\pm 45_{12}/90_4$	—	0.196
2	$\pm 45_{12}$	1.15	0.066	2	$\pm 45_{12}$	1.15	0.084
3	$\pm 45_{12}$	1.15	0.066	3	$\pm 45_{12}$	1.15	0.084
4	$0_{12}/\pm 45_{12}$	1.00	0.132	4	$0_{12}/\pm 45_{12}$	1.00	0.168
$E_t \times 10^6$ (lb/in)		3.14		2.91			
$\rho_t$ (lb/in <sup>2</sup> )		.0161		.0160			

REFERENCE TITANIUM:  $E_t = 2.58 \times 10^6$  lb/in;  $\rho_t = .0254$  lb/in<sup>2</sup>

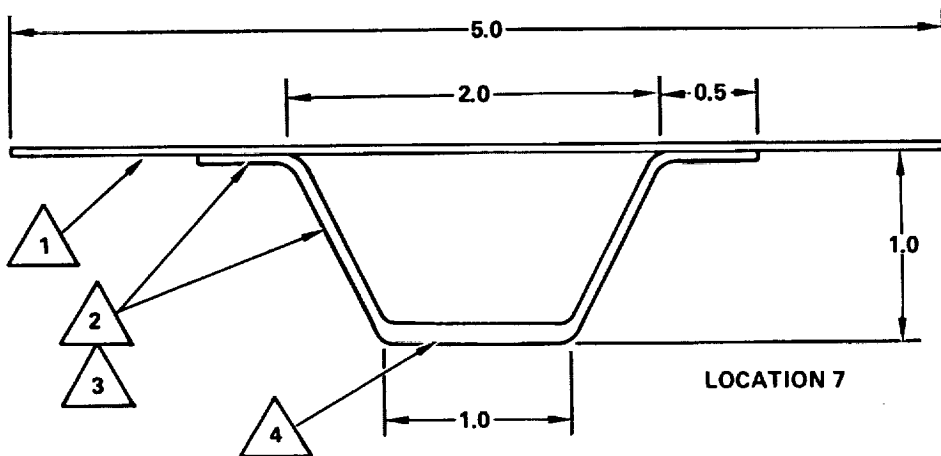
TABLE 20-17. COMPOSITE TEE-STIFFENED PANEL - FS 2500



BORON-POLYMIDE				GRAPHITE-POLYMIDE			
NO.	ORIENTATION	b(in)	t(in)	NO.	ORIENTATION	b(in)	t(in)
1	$0_{16}/\pm45_{12}/90_4$	-	0.176	1	$0_{16}/\pm45_{12}/90_4$	-	0.224
2	$0_2/\pm45_{12}$	1.20	0.077	2	$0_2/\pm45_{12}$	1.20	0.098
3	$0_{20}/\pm45_{12}$	0.60	0.176	3	$0_{20}/\pm45_{12}$	0.60	0.224
$E\bar{t} \times 10^6$ (lb/in)		4.94		4.53			
$\rho\bar{t}$ (lb/in <sup>2</sup> )		.0200		.0202			

REFERENCE TITANIUM:  $E\bar{t} = 3.06 \times 10^6$  lb/in;  $\rho\bar{t} = .0302$  lb/in<sup>2</sup>

TABLE 20-18. COMPOSITE HAT-STIFFENED PANEL - FS 2500



BORON-POLYIMIDE				GRAPHITE-POLYIMIDE			
NO.	ORIENTATION	b(in.)	t(in.)	NO.	ORIENTATION	b(in.)	t(in.)
1	$0_{16}/\pm45_{12}/90_4$	—	0.176	1	$0_{16}/\pm45_{12}/90_4$	—	0.224
2	$\pm45_{16}$	1.15	0.088	2	$\pm45_{16}$	1.15	0.112
3	$\pm45_{16}$	1.15	0.088	3	$\pm45_{16}$	1.15	0.112
4	$0_{16}/\pm45_{16}$	1.00	0.176	4	$0_{16}/\pm45_{16}$	1.00	0.224
$E\bar{t} \times 10^6$ (lb/in.)		4.04		3.73			
$\rho\bar{t}$ (lb/in. <sup>2</sup> )		0.0194		0.0192			

REFERENCE TITANIUM:  $E_t = 3.06 \times 10^6$  lb/in.;  $\rho\bar{t} = 0.0302$  lb/in.<sup>2</sup>

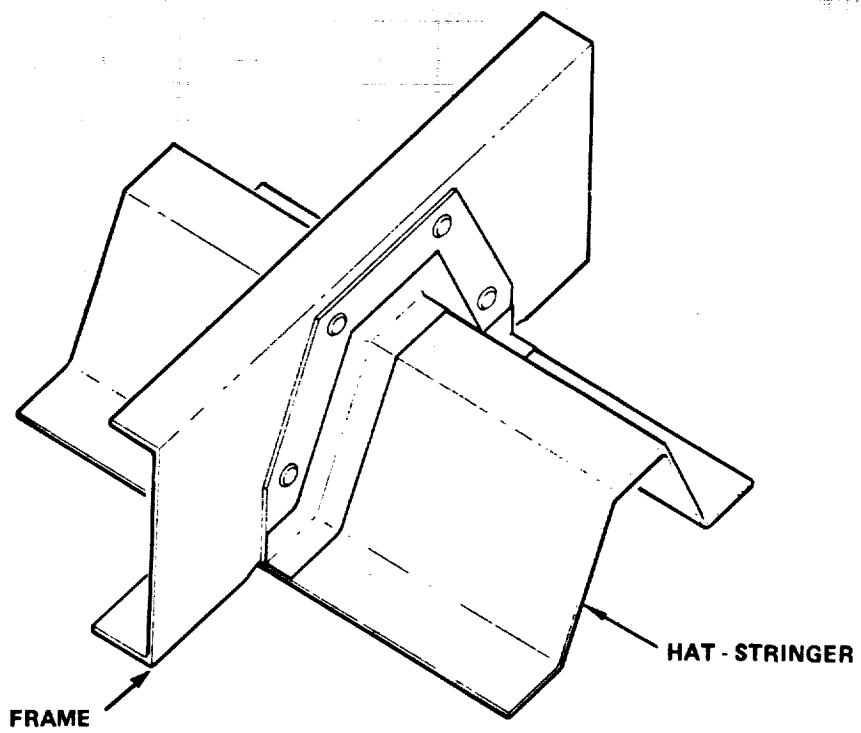
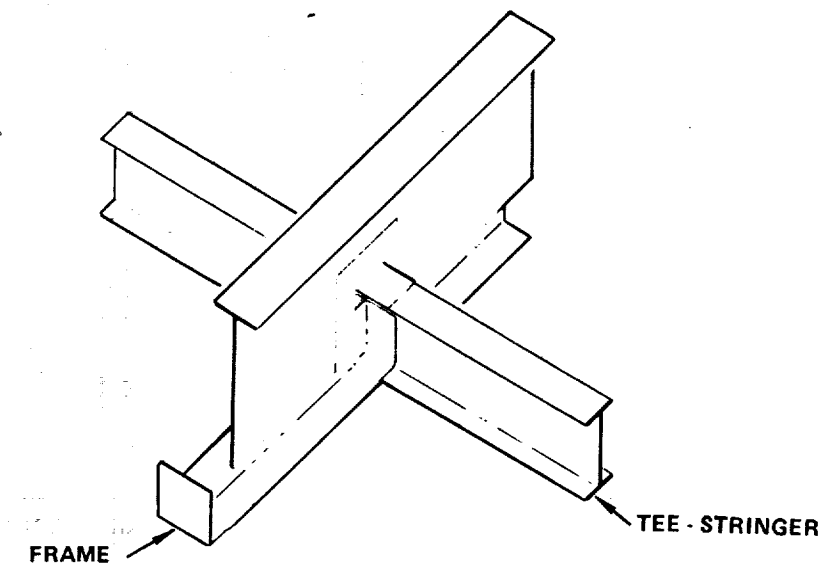
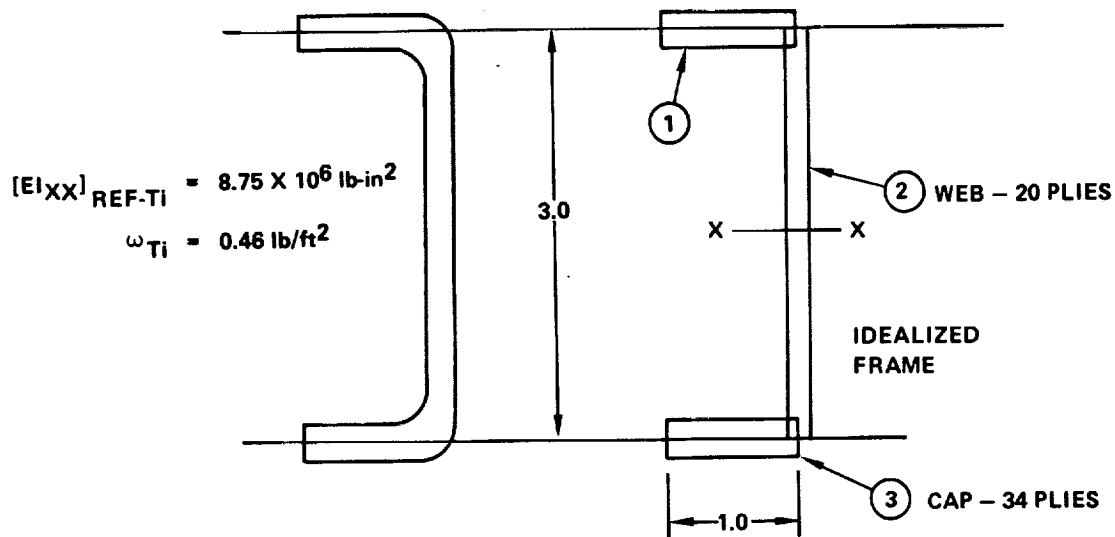


Figure 20-17. Typical Frame-Stringer Intersection Schemes

TABLE 20-19. COMPOSITE FUSELAGE FRAMES - FS 2000 AND FS 3000



BORON-POLYIMIDE.

ELEMENT		AREA	ORIENTATION	$E \times 10^6$	$EA \times 10^6$			
1	$1.0 \times 34 \times 0.0055$	0.187	$0_{18}/\pm 45_{16}$	10.88	2.034			
2	$3.0 \times 20 \times 0.0055$	0.330	$0_4/\pm 45_{16}$	6.36	2.099			
3	$1.0 \times 34 \times 0.0055$	0.187	$0_{18}/\pm 45_{16}$	10.88	2.034			
$\Sigma$		0.704			6.167			
$EI_{xx} = [(10.88 \times 10^6)(2)(0.187)(1.5)^2 + (6.36 \times 10^6)(0.110)(3)^3/12] = 10.73 \times 10^6 \text{ lb-in.}^2$								
$\rho \bar{t} = (0.072)(0.704/20) = 0.00253 \text{ lb/in.}^2$								

GRAPHITE-POLYIMIDE.

ELEMENT		AREA	ORIENTATION	$E \times 10^6$	$EA \times 10^6$			
1	$1.0 \times 34 \times 0.0070$	0.238	$0_{18}/\pm 45_{16}$	7.60	1.809			
2	$3.0 \times 20 \times 0.0070$	0.420	$0_4/\pm 45_{16}$	4.74	1.991			
3	$1.0 \times 34 \times 0.0070$	0.238	$0_{18}/\pm 45_{16}$	7.60	1.809			
$\Sigma$		0.896			5.609			
$EI_{xx} = [(7.60 \times 10^6)(2)(0.238)(1.5)^2 + (4.74 \times 10^6)(0.140)(3)^3/12] = 9.63 \times 10^6 \text{ lb-in.}^2$								
$\rho \bar{t} = (0.056)(0.896/20) = 0.00251 \text{ lb/in.}$								

TABLE 20-20. COMPOSITE FRAME WEIGHTS

## F.S. 2000 AND F.S. 3000

FRAME MATERIAL	$EI_{xx}$ ( $10^6$ lb-in. $^2$ )	$EI_{xx}$ INCREASE (PERCENT)	$\frac{\rho t}{10^3}$ (lb/in. $^2$ )	w (lb/ $ft^2$ )	WEIGHT SAVINGS (PERCENT)
TITANIUM	8.75	—	3.20	0.46	—
BORON-POLYIMIDE	10.73	22.6	2.53	0.365	20.6
GRAPHITE-POLYIMIDE	9.63	10.1	2.51	0.362	21.3

## F.S. 2500

FRAME MATERIAL	$EI_{xx}$ ( $10^6$ lb-in. $^2$ )	$EI_{xx}$ INCREASE (PERCENT)	ASSUMED WT SAVINGS (PERCENT)	w (lb/ $ft^2$ )
TITANIUM	10.94	—	—	0.576
BORON-POLYIMIDE	13.40	22.5	20.6	0.457
GRAPHITE-POLYIMIDE	12.05	10.1	21.3	0.452

The results of the fuselage skin panel and frame analysis are summarized on Table 20-21. The resulting weight trends for both boron-polyimide and graphite-polyimide composites are displayed for the panel concepts analyzed. Similar trends as observed for the metallic design are indicated with the tee-stiffener being least weight in the forebody and the hat stiffener design being least weight in the centerbody and aftbody structure. The data includes an estimate for the protection system weight of 0.045 lbs. per square foot. Also shown on the table is a summary of frame weight for the point design regions. The frame weights at FS 750 were conservatively taken as being equal to the requirements at FS 2000.

#### MANUFACTURING PLAN

The principal assumption for producing the 1980-1990 advanced technology aircraft is that polyimide resin systems will have developed to a point such that processing can be accomplished with ease. Thus, the low cost manufacturing method now being developed for epoxy processing were taken as feasible for polyimides. Restrictions on such factors as laminated thickness, bond pressure, etc. were neglected for this study.

Fabrication of ribs and spar caps as well as truss webs is accomplished by closed mold processing with elastomeric tooling as a pressure generator (Reference 5). Single stage molding and attachment of caps to truss or corrugated webs would be performed by similar techniques.

Wing skin panels, honeycomb or hat stiffened, would be produced with large sheets of material laminated by automated machines. Unit panels having dimension 10 ft. x 20 ft. were assumed. Since, for the most part, the wing skin gages are small, it assumed that the hat stiffener would first be produced as trapezoidal corrugation molded from a flat sheet. The hats would then be cocured to the skins using removable expansion mandrels. Because of contour complexity, flexible elastomeric tooling would be used extensively. The manufacturing sequence is pictorially displayed on Figure 20-18.

TABLE 20-21. COMPOSITE FUSELAGE WEIGHT SUMMARY

FUSELAGE SKIN PANELS					
MATERIAL SYSTEM	REFERENCE TITANIUM	BORON-POLYIMIDE	GRAPHITE-POLYIMIDE	BORON-POLYIMIDE	GRAPHITE-POLYIMIDE
w, UNIT WEIGHT	lb/ft <sup>2</sup>	lb/ft <sup>2</sup>	lb/ft <sup>2</sup>	lb/ft <sup>2</sup>	lb/ft <sup>2</sup>
F.S. 750	1.29	—	—	<u>1.134</u>	<u>1.118</u>
F.S. 2000	2.74	<u>2.363</u>	<u>2.349</u>	2.579	2.565
F.S. 2500	3.02	<u>2.839</u>	<u>2.810</u>	2.925	2.954
F.S. 3000	2.90	<u>2.363</u>	<u>2.349</u>	2.579	2.565

$$w_n = [(\rho \bar{t} \times 144) + (0.045)]$$

FRAMES			
MATERIAL SYSTEM	REFERENCE TITANIUM	BORON-POLYIMIDE	GRAPHITE-POLYIMIDE
w, UNIT WT.	lb/ft <sup>2</sup>	lb/ft <sup>2</sup>	lb/ft <sup>2</sup>
F.S. 750	0.25	0.365	0.362
F.S. 2000	0.53	0.365	0.362
F.S. 2500	0.576	0.457	0.452
F.S. 3000	0.53	0.365	0.362

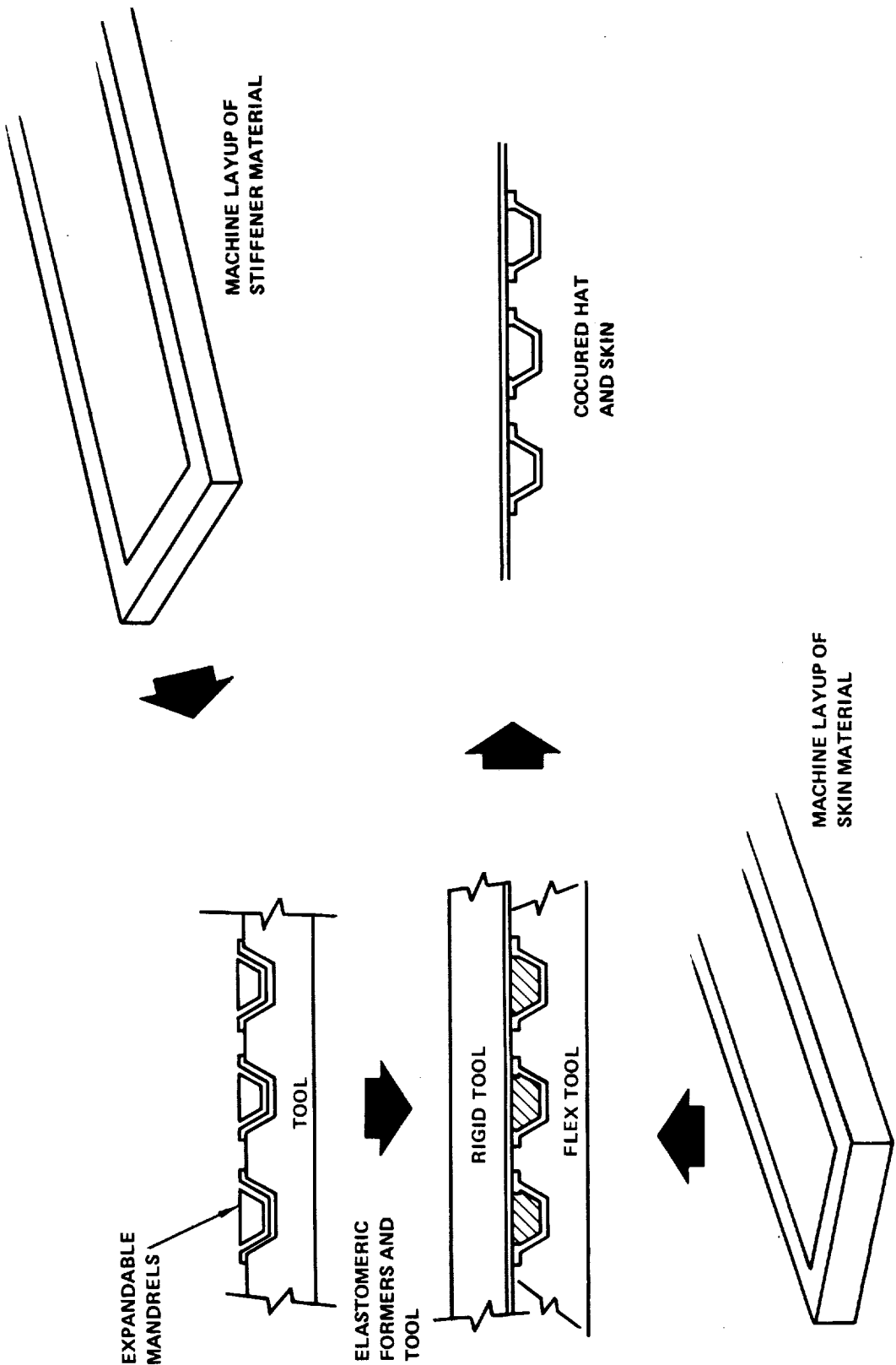


Figure 20-18. Chordwise Stiffened Wing Panel Fabrication

## MASS ESTIMATES

The advanced technology assessment exploited an aggressive application of composite materials to the airframe of a far-term supersonic transport. The weight advantages gained through the use of boron-polyimide (B/PI) and graphite-polyimide (Gr/PI) composites in the wing box and fuselage primary shell were determined through analysis of selected point design regions. The results of the advanced technology transport (ATT) studies (Reference 1) were used to establish weight trends for the other items. The comparison of weight trends for the far-term advanced technology supersonic transport and the near-term aircraft defined through indepth studies are summarized in Table 20-22.

A significant improvement in the fuel fraction for the fixed-size and weight airplane is shown for an all-composite and a hybrid far-term design. The range is increased from 4183 nautical miles to an excess of 4600 nautical miles, holding the payload constant at 49,000 pounds. When this aircraft carries a space-limit payload of 61,800 pounds (234 passengers x 200 + 1500 x 10) the range is approximately 4400 nautical miles. It is noted, however, that the fuel quantity indicated on the table exceeds the design capacity of 399,000 pounds. Thus, modification to the tank arrangement and capacity are required before a viable aircraft with the aforementioned performance potential can be achieved.

Another approach to exploit the weight advantages of composite application to the far-term design is resizing as shown in Table 20-22. The all-composite and hybrid design airplanes are resized to maintain a range of 4200 nautical miles with a payload of 49,000 pounds. The wing loading, takeoff thrust-to-weight ratio and fuel fraction are essentially held constant. For these cases, the taxi mass is 645,000 pounds and 641,500 pounds, for the all-composite and hybrid designs, respectively. The wing area has been reduced to approximately 9300 square feet. As indicated on the table, the Manufacturer's Empty Weight (MEW) has been reduced from 301,513 pounds to 246,762 pounds for the resized aircraft. This reduction of approximately 18-percent would result in a commensurate reduction in flyaway cost.

It is interesting to note that the reduction in structural mass between the near-term all-metal design and the far-term hybrid design is 21-percent. This result is consistent with the data of Reference 1 for the factors derived for the

TABLE 20-22. ADVANCED TECHNOLOGY AIRCRAFT MASS COMPARISON (LB)

ITEM	NEAR-TERM		FAR-TERM			
	TASK I INITIAL	TASK I HYBRID	ALL-COMPOSITE		HYBRID	
			FIXED SIZE	RESIZED	FIXED SIZE	RESIZED
WING	109,600	88,620	78,320	68,740	77,455	67,577
STRUCTURAL BOX "FIXED" WT. (L.E., T.E. ETC.)		[47,268] [41,352]	[45,279] [33,041]	[40,320] [28,420]	[44,414] [33,041]	[39,316] [28,261]
TAIL	11,340	11,340	8,845	8,170	8,845	8,127
FUSELAGE	41,000	42,688	36,721	36,721	36,721	36,721
SHELL "FIXED" WT. (FLT. STA., FAIRING, ETC.)		[23,148] [19,540]	[19,981] [16,740]			
LANDING GEAR	30,400	30,400	27,360	24,250	27,360	24,118
AIR INDUCTION	17,800	20,755	18,036	15,220	18,036	15,137
NACELLES	4,900	5,616	4,880	4,200	4,880	4,174
ENGINES	44,600	51,124	51,124	43,950	51,124	43,728
PROPULSION SYSTEMS	7,000	7,310	7,310	7,022	7,310	6,984
SURFACE CONTROLS	8,500	8,500	6,800	5,982	6,800	5,950
INSTRUMENTS	1,230	1,230	1,230	1,230	1,230	1,230
HYDRAULICS	5,700	5,700	5,700	4,900	5,700	4,875
ELECTRICAL	4,550	4,550	4,550	4,485	4,550	4,461
AVIONICS	1,900	1,900	1,900	1,900	1,900	1,900
FURNISHINGS AND EQUIPMENT	11,500	11,500	11,500	11,500	11,500	11,500
ECS	8,300	8,300	8,300	8,300	8,300	8,300
TOLERANCE AND OPTIONS	1,980	1,980	1,980	1,980	1,980	1,980
MEW	310,300	301,513	274,556	248,550	273,691	246,762
STD. AND OPER. EQ.	10,700	10,809	11,054	10,300	11,062	10,284
DEW	321,000	312,322	285,610	253,850	284,753	257,046
PAYOUT	49,000	49,000	49,000	49,000	49,000	49,000
ZFW	370,000	361,322	334,610	307,850	333,753	306,046
FUEL	380,000	388,678	415,390	337,150	416,247	335,454
TAXI MASS	750,000	750,000	750,000	645,000	750,000	641,500
RANGE, n. mi.	4,025	4,183	4,630	4,200	4,644	4,200
WING AREA, ft <sup>2</sup>	10,822	10,882	10,882	9,307	10,822	9,257
BODY LENGTH, ft	297	297	297	297	297	297
W/S, lb/ft <sup>2</sup>	69.3	69.3	69.3	69.3	69.3	69.3
W <sub>FUEL</sub> /W <sub>TO</sub>	0.507	0.518	0.554	0.523	0.555	0.523

40-percent advanced materials and applying the factors to the Task I weights shown. When comparing similar data to the hybrid design (i.e. composite reinforced) the reduction is 14-percent.

#### Wing Mass

The general expression used to evaluate the relative weights of the wing box structure is based on the three wing point design regions discussed earlier. The equation, which includes appropriate factors that produce consistent results with the Detailed Concept Analysis of Task I, is as follows:

$$W_{Box} = \frac{S_{Box}}{K_{Box}} (4.5308 w_{40322} + 2.0000 w_{40536} + 1.0540 w_{41348})(NOF)$$

where,  $S_{Box}$ , box planform area = 7165 ft<sup>2</sup>

$$K_{Box} = 7.5532$$

$$w_n, \text{ point design region unit weight (lb/ft}^2\text{)}$$

$$NOF, \text{ non-optimum factor} = 1.26$$

The total box weight (variable) is presented in Table 20-23 for the individual boxes (i.e. forward aft, tip). For comparative purpose the results of the hybrid design, Section 17, Concept Evaluation and Selection, is also shown.

Evaluation of the wing box weights for the near-term and far-term designs indicate the weight advantage of the minimum gage titanium alloy beaded panels of the forward box as compared to an equivalent stiffness composite design of either boron-polyimide or graphite-polyimide. For the stiffness critical tip structure, however, the application of composites afford a significant weight saving. The flutter penalty for the composite design is determined by providing equivalent added torsional stiffness based on the specific stiffness ( $G/\rho$ ) parameter for the respective material systems as shown in Figure 20-19.

TABLE 20-23. ALL-COMPOSITE WING BOX STRUCTURE MASS COMPARISON

ITEM	TASK II HYBRID (A)	ADVANCED TECHNOLOGY	
		B/PI	Gr/PI
START-OF-DESIGN	NEAR-TERM	FAR-TERM	
<u>POINT DESIGN REGION</u>			
40322 (lb/ft <sup>2</sup> )	3.80 <sup>(B)</sup>	3.99	3.96
40536 (lb/ft <sup>2</sup> )	7.27	7.23	7.15
41348 (lb/ft <sup>2</sup> )	5.50	4.73	4.71
<u>WING BOX</u>			
FORWARD (lb)	20,580 <sup>(B)</sup>	21,607	21,445
AFT (lb)	17,384	17,283	17,092
TIP (lb)	6,964	6,016	5,962
FLUTTER INCR (lb)	2,340 <sup>(C)</sup>	809 <sup>(C)</sup>	780 <sup>(C)</sup>
Σ TOTAL (lb)	47,268	45,715	45,279

NOTES: (A) COMPOSITE REINFORCED SPAR CAPS; BEADED PANELS EXCEPT H/C SANDWICH TIP BOX.  
 (B) SIGNIFICANT ADVANTAGE OF METAL SURFACE PANELS AND COMPOSITE REINFORCED SPAR CAPS.  
 (C) SIGNIFICANT ADVANTAGE OF COMPOSITE SANDWICH APPLICATION TO THE TIP STRUCTURE; FLUTTER INCREMENT BASED ON G/ρ RELATIONSHIP ASSUMING ±45° LAYUP.

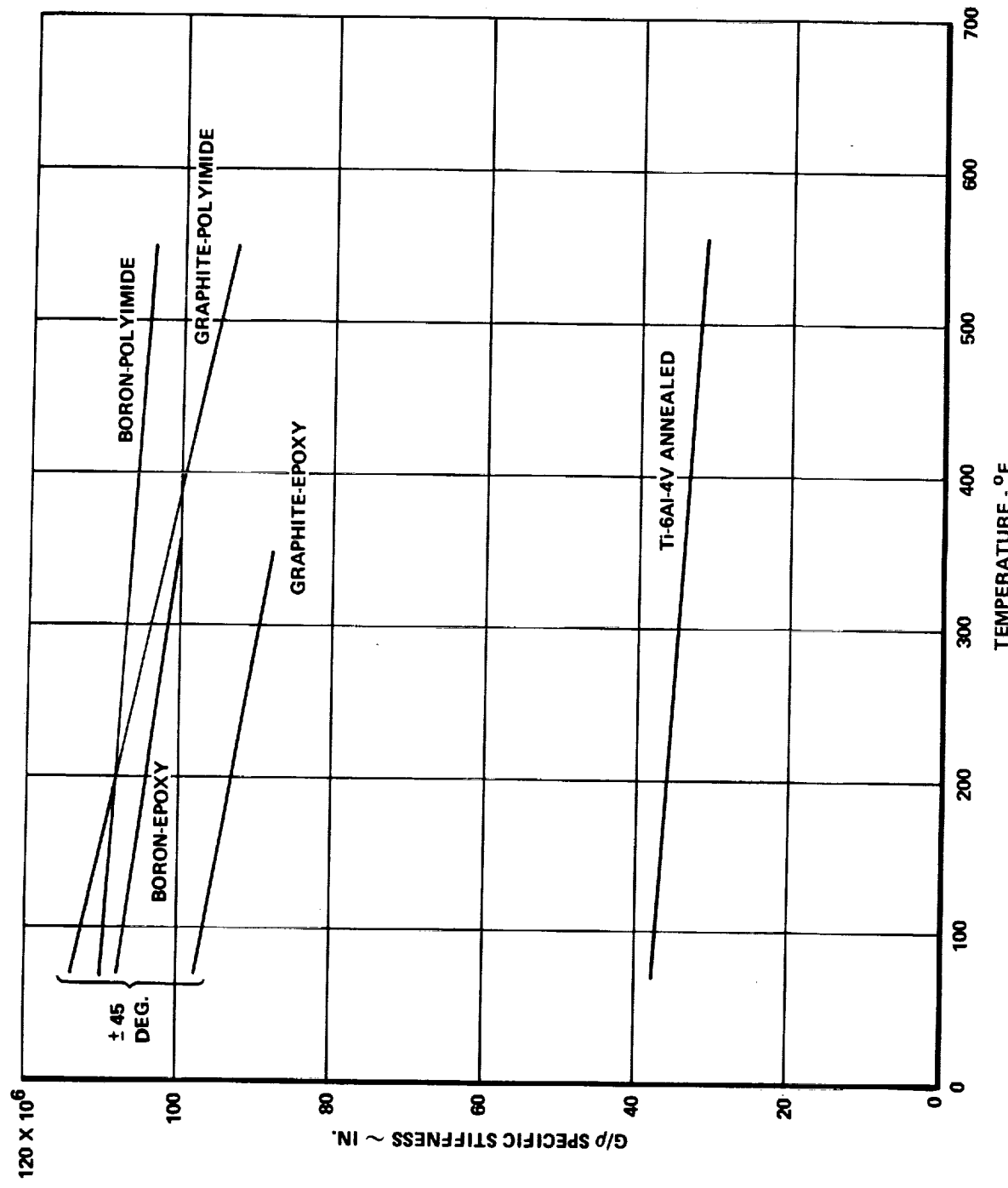


Figure 20-19. Specific Stiffness Properties of Titanium and Composites

### Fuselage Mass

The general expression used to evaluate relative weights of the shell structure is based on the four point design region defined at F.S. 750, F.S. 2000, F.S. 2500 and F.S. 3000. The equation, which contains parameters defined in Section 15, is as follows:

$$w_{\text{shell}} = \frac{S_{\text{shell}}}{K_{\text{shell}}} (w_{750} + w_{2000} + w_{2500} + w_{3000})(\text{NOF})$$

where,  $S_{\text{shell}}$ , shell wetted area = 7167 ft<sup>2</sup>

$$K_{\text{shell}} = 4.1544$$

$w_n$ , shell unit weight at each point design region (lb/ft<sup>2</sup>)

NOF, non-optimum factor = 1.14

Table 20-24 presents the shell unit weights for each point design region and resulting total shell weight. Both boron/polyimide and graphite-polyimide material system data are shown along with corresponding weights for the all-titanium shell. A decrease in shell unit weight is reflected at all point design regions; the magnitude varies from a 4-percent to a 21-percent weight saving potential. A weight savings for the total shell when employing advanced composites is 14-percent.

### Secondary Component Mass

The weight reduction factors for the secondary components were obtained from the results of the Advanced Technology Transport (ATT) studies conducted by the Lockheed-Georgia Company are reported in Reference 1. The appropriate reduction factors were applied to each component of the near-term design to arrive at the values used for the far-term aircraft as shown in Table 20-25. For the fixed weight items for the wing and fuselage, the overall reduction factor is 0.799 and 0.857, respectively.

The secondary components for the wing and fuselage total in excess of 60,000 pounds. The application of the respective reduction factors to the design results in a

MATERIAL SYSTEM:		NEAR-TERM	FAR-TERM		PERCENT CHANGE OVER NEAR-TERM
POINT DESIGN REGION	UNITS	TITANIUM 6A1-4V	BORON POLYIMIDE	GRAPHITE POLYIMIDE	
F.S. 750	lb. $\text{ft}^{-2}$	1.54	1.50	1.48	-3.9
F.S. 2000	lb. $\text{ft}^{-2}$	3.27	2.73	2.71	-17.1
F.S. 2500	lb. $\text{ft}^{-2}$	3.53	3.30	3.26	-7.6
F.S. 3000	lb. $\text{ft}^{-2}$	3.43	2.73	2.71	-21.0
$W_{\text{SHELL}}$	lb	23,148	20,178	19,981	-13.7

TABLE 20-24. ALL-COMPOSITE SHELL STRUCTURE MASS COMPARISON

TABLE 20-25. WEIGHT REDUCTION FACTORS FOR ADVANCED TECHNOLOGY AIRCRAFT  
SECONDARY COMPONENTS

ITEM	REDUCTION FACTOR <sup>(A)</sup>	NEAR-TERM	FAR-TERM
<b>WING-FIXED WEIGHT</b>			
LEADING EDGE	0.70	5,235	3,664
TRAILING EDGE	0.70	4,888	3,422
WING/BODY FAIRING	0.70	1,600	1,120
LEADING EDGE FLAPS	0.75	1,130	848
T.E. FLAPS	0.70	5,890	4,123
AILERONS	0.75	1,250	938
SPOILERS	0.75	1,360	1,020
MLG DOORS	0.75	2,904	2,178
SUPPORT STRUCTURE	1.00	3,750	3,750
B.L. 62 RIBS	0.86	1,430	1,230
FIN ATTACHMENT PROVISIONS	0.86	435	374
B.L. 470	0.86	700	602
REAR SPAR	0.86	3,400	2,924
ENGINE SUPPORT STRUCTURE	1.00	3,580	3,580
FUEL BULKHEADS	0.86	3,800	3,268
(SUBTOTAL)	0.799	41,352 lb	33,041 lb
<b>FUSELAGE-FIXED WEIGHT</b>			
NOSE AND FLIGHT STATION	0.93	2,500	2,325
NLG WELL	0.93	900	837
WINDSHIELD AND WINDOWS	1.00	1,680	1,680
FLOORING AND SUPPORTS	0.75	3,820	2,865
DOORS AND MECHANISM	0.80	4,170	3,336
UNDERWING FAIRING	0.70	1,870	1,309
CARGO COMP'T. PROV.	0.80	1,060	848
WING-TO-BODY FRAMES/FTGS.	1.00	1,500	1,500
TAIL-TO-BODY FRAMES/FTGS.	1.00	600	600
PROV. FOR SYSTEMS	1.00	740	740
FINISH AND SEALANT	1.00	700	700
(SUBTOTAL)	0.857	19,540 lb	16,740 lb

(A) REFERENCE 1

potential structural mass savings of approximately 10,000 pounds. These items alone offer significant weight payoff and improve aircraft performance for the supersonic cruise aircraft design.

#### FINAL DESIGN-ADVANCED TECHNOLOGY AIRCRAFT

The final design resulting from this advanced technology assessment is a hybrid structural approach as shown in Figure 20-20. The design makes extensive use of graphite/polyimide material system with a protective system of aluminum wire fabric and 120 glass. The chordwise stiffened structural arrangement-convex beaded surface panel concept of titanium alloy 6Al-4V resulted in minimum weight for the lightly loaded forward wing box structure. For the strength-stiffness critical wing aft box and tip structure, the honeycomb core sandwich using graphite/polyimide faces was found to be least weight. The fuselage structural arrangement is a skin-stringer-frame approach employing closed-trapezoidal hat stiffeners in the center body and aftbody with tee-section stiffeners used in the pressure critical forebody design.

The manufacturing plan postulated the applicability of low cost methods now being developed for epoxy processing. Fabrication of ribs and spar caps as well as truss webs would be accomplished by closed-mold processing with elastomeric tooling as the pressure generator. Single stage molding and attachment of caps to truss or corrugated webs would be performed by similar techniques. Wing skin panels would be produced with large sheets of material laminated by automated machines. Unit panels having dimensions of 10-feet x 20 feet are assumed. Because of contour complexity, flexible elastomeric tooling is extensively used.

The technology evaluation data presented in Table 20-26 compares the advanced technology aircraft with the near-term technology all-titanium and composite reinforced designs. The cascading effect of resizing of the advanced technology aircraft for a constant payload-range (49000-lb x 4200 n.mi) is shown. An 8.2-percent reduction in zero fuel weight considering a fixed airplane taxi weight is realized by the use of composites. This weight reduction is equated to a performance (range) increase of 500 nautical miles. Considering the growth factor

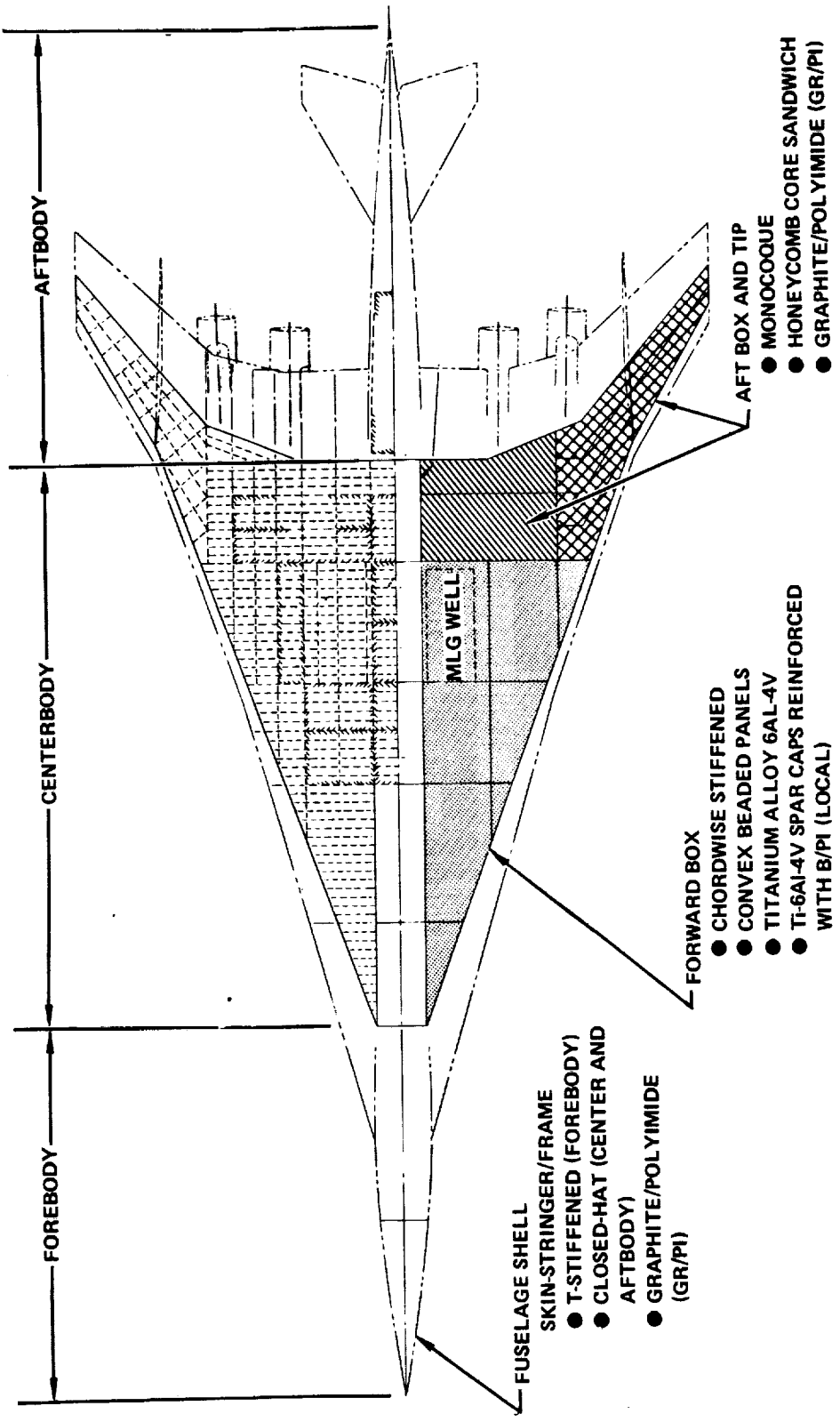


Figure 20-20. Advanced Hybrid Structural Approach - 1990 Start-of-Design (Far-Term)

TABLE 20-26. AIRPLANE MASS AND PERFORMANCE COMPARISON - ADVANCED TECHNOLOGY AIRCRAFT

TECHNOLOGY EVALUATION DATA		ADVANCED TECHNOLOGY	ADVANCED TECHNOLOGY	ADVANCED TECHNOLOGY	STRUCTURAL APPROACH	NEAR-TERM TECHNOLOGY
START-OF-DESIGN		FIXED TAKE OFF WEIGHT	RESIZED CONSTANT RANGE -PAYLOAD	RESIZED CONSTANT RANGE -PAYLOAD	TASK II ENGR. DESIGN STUDIES	FIXED TAKE OFF WEIGHT
<b>FAR TERM (1990)</b>						<b>NEAR-TERM (1980)</b>
<b>PRIMARY MATERIAL SYSTEM</b>						
<b>WING</b>	<b>STRUCTURAL ARRANGEMENT</b>	<b>GRAPHITE/ POLYIMIDE</b>	<b>GRAPHITE/ POLYIMIDE</b>	<b>Ti-6Al-4V B/P/I REINF. GRAPHITE/ POLYIMIDE</b>	<b>Ti-6Al-4V B/P/I REINF.</b>	<b>Ti-6Al-4V</b>
	<b>SURFACE PANEL CONCEPT</b>	<b>HYBRID: CHORDWISE STIFFENED &amp; MONOCOQUE</b>		<b>CONVEX BEADED &amp; H/C SANDWICH</b>	<b>H/C CORE SANDWICH</b>	<b>MONOCOQUE</b>
<b>STRUCTURAL BOX WEIGHT (lb) "FIXED" WT. (I.E., T.E., ETC.) (lb)</b>	45,279 33,041	40,320 28,420	28,216 28,251	47,268 41,352	50,978 41,352	
<b>TOTAL WEIGHT (lb)</b>	78,320	68,740	67,657	88,620	92,330	
<b>STRUCTURAL ARRANGEMENT</b>						
<b>FUSELAGE</b>	<b>SURFACE PANEL CONCEPT</b>	<b>TRAPEZOIDAL HAT STIFFENED</b>		<b>CLOSED HAT STIFFENED</b>		
	<b>SHELL WEIGHT (lb) "FIXED" WT. (FLT. STA., FAIRING, ETC.)</b>	19,981 16,740	19,981 16,740	18,981 16,740	23,148 19,540	23,148 19,540
<b>TOTAL WEIGHT (lb)</b>	36,721	36,721	36,721	42,688	42,688	
<b>ZFW, ZERO FUEL WEIGHT (lb)</b>	334,610	307,850	304,146	361,322	364,982	
<b>GTW, GROSS TAXI WEIGHT (lb)</b>	750,000	645,000	641,306	750,000	750,000	
<b>AIRPLANE RANGE (n.mi.)</b>	4,630	4,200	4,200	4,183	4,123	

ORIGINAL PAGE IS  
OF POOR QUALITY

for this class of aircraft which consists of approximately 50-percent fuel, resizing of the airplane was accomplished. The airplane taxi weight was reduced by approximately 100,000 pounds.

The results of this assessment has identified the potential benefits of the composite materials and fabrication technology for application to a 1990-plus start-of-design Mach 2.7 supersonic cruise transport. The impact on the airplane size and weight are significant but require further in-depth analytical and experimental studies for validation. This includes, not only, the primary structural components, but also, secondary components including the leading edge, trailing edge, flight station, fairings, etc. which contribute significantly to the potential savings.

## REFERENCES

1. R.H. Lange, et. al "Study of the Application of Advanced Technologies to Wing-Range Transport Aircraft," NASA CR 112088, Lockheed-Georgia Company, dated April 1971.
2. R.L. Foss, "Studies of the Impact of Advanced Technologies Applied to Supersonic Transport Aircraft," LR 26089, Lockheed-California Company, dated January 1974.
3. E.B. Birchfield, F. Kollsmanberger, "Develop Fabrication/Processing Techniques for High Temperature Advanced Composites For Use in Aircraft Structures," AFMC-TR-72-91, McDonnell Aircraft Company, July 1972.
4. T.M. Hsu, "Attainable Stress of Composite Panels Reinforced by Hat-Section Stiffeners," SMN 313, Lockheed-Georgia Company, January 1972.
5. W. Cremens, "Manufacturing Methods for Thermal Expansion Molding of Advanced Composite Aircraft Structures," First Quarterly Report, Contract F-33615-74-C-5150, Lockheed-Georgia Company, July 1974.



SECTION 21

DESIGN METHODOLOGY

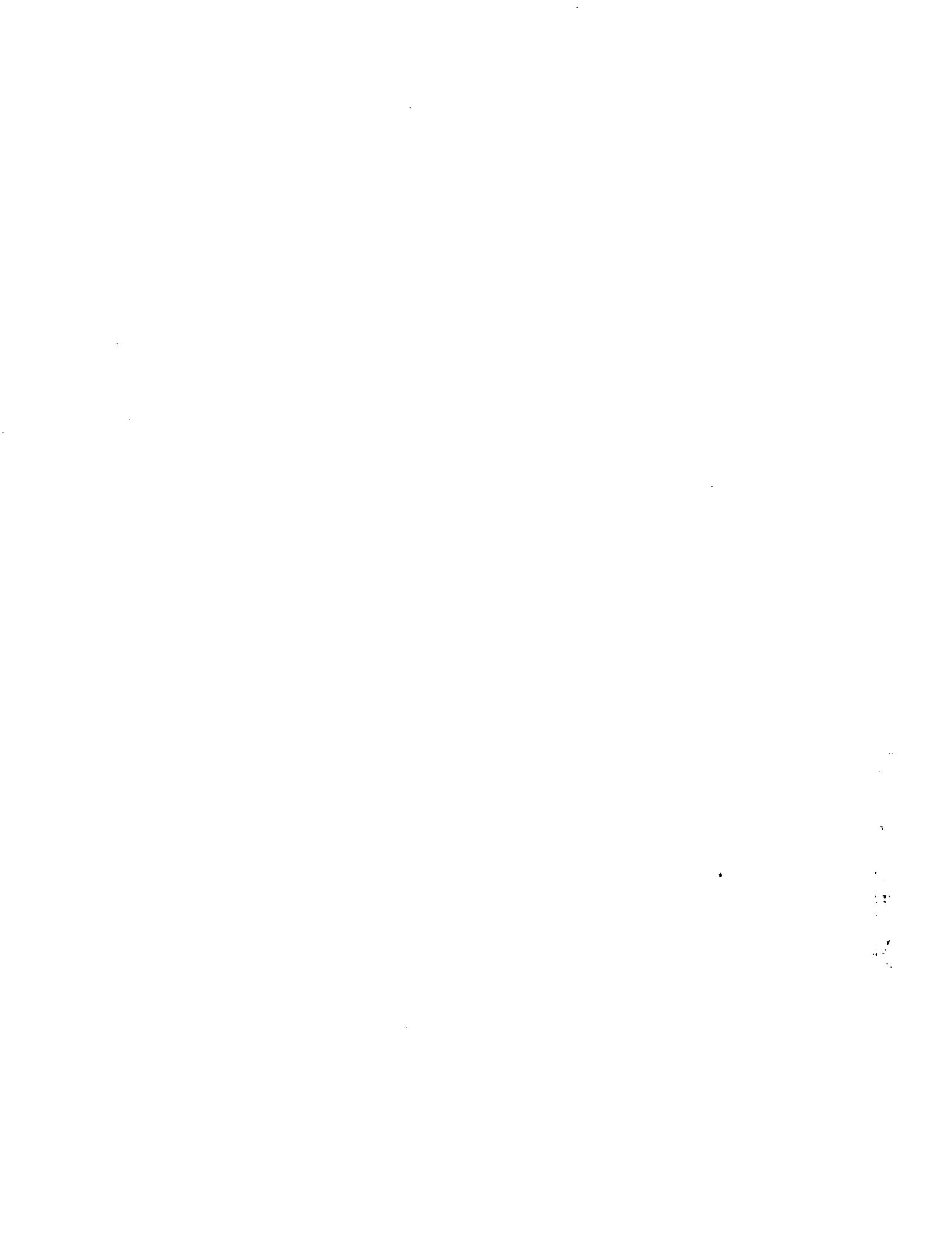
By

D. A. Brogan, G. W. Davis, G. A. Galins, E. A. Goforth, B. C. Wollner



## CONTENTS

<u>Section</u>	<u>Page</u>
INTRODUCTION	21-1
STRUCTURAL TEMPERATURE ANALYSIS	21-1
Math Models	21-3
Airframe Structural Temperatures	21-4
FINITE-ELEMENT STRUCTURAL ANALYSIS	21-7
Structural Models	21-7
Structural Influence Coefficients	21-12
Internal Loads Runs	21-12
AEROELASTIC LOADS ANALYSIS	21-14
Critical Flight Conditions	21-16
Theoretical Aerodynamics	21-16
Grid Transform	21-19
Mass Distribution	21-21
Jig-Shape Definition	21-22
Net Aeroelastic Loads	21-23
VIBRATION AND FLUTTER ANALYSIS	21-23
Structural Model	21-24
Vibration Analysis	21-24
Aerodynamic Formulation	21-26
Flutter Analysis	21-28
Flutter Optimization	21-31
REFERENCES	21-37



## LIST OF FIGURES

<u>Figure</u>		<u>Page</u>
21-1	Analytical Design Cycle	21-2
21-2	Lockheed's Integrated Structural Design Analysis System	21-2
21-3	Evaluation Procedure for Structural Temperatures	21-3
21-4	Wing Box Thermal Analyzer Network	21-5
21-5	Network Node Definition, Type-2 Wing Panels	21-5
21-6	Network Node Definition, Fuselage Panel and Frame	21-6
21-7	Airframe Structural Temperatures	21-6
21-8	Finite Element Structural Analysis Procedure	21-9
21-9	Structural Model Usage	21-9
21-10	Comparison of Wing Rear Beam Structural Influence Lines	21-11
21-11	Comparison of Fuselage Structural Influence Lines	21-11
21-12	Aeroelastic Loads Evaluation Procedure	21-15
21-13	Subsonic Aerodynamic Grid	21-17
21-14	Supersonic Aerodynamic Grid	21-17
21-15	Design Load Conditions - Strength/Stiffness	21-18
21-16	Net Integrated Wing Shears - Theoretical vs Measured	21-20
21-17	Span Loading Distribution - Mach 2.7	21-20
21-18	Wing Lift Coefficients - Mach 2.7	21-20
21-19	Load Panel Grid	21-22
21-20	Vibration and Flutter Analysis	21-24
21-21	Symmetric Degrees of Freedom for Vibration Analysis	21-25
21-22	Theoretical Aerodynamic Distribution	21-27
21-23	Normalized $C_L$ Versus Reduced Frequency	21-27

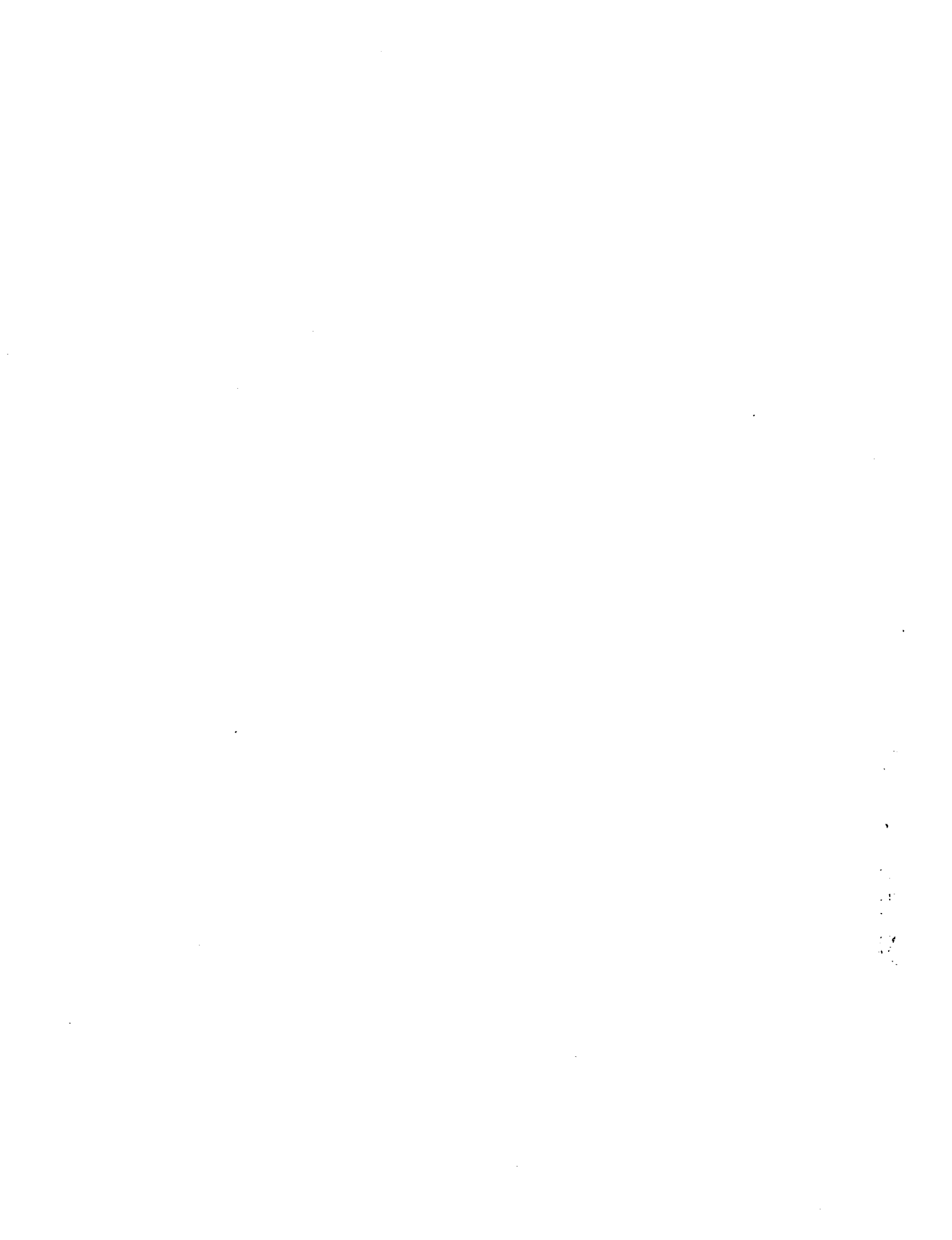
LIST OF FIGURES (Cont)

<u>Figure</u>		<u>Page</u>
21-24	The Effects of Number of Modes on the Flutter Solution	21-29
21-25	Flutter Speed Variation With Number of Modes	21-29
21-26	Flutter Analysis Results	21-30
21-27	Participation Coefficients - Mach 0.9 - FFFF-Mode 8	21-30
21-28	Symmetric Flutter Analysis - Mach 0.9 - FFFF	21-32
21-29	Design Regions for Flutter Optimization - Task I	21-34
21-30	Design Regions for Flutter Optimization - Task II	21-34
21-31	Nonlinearities in the Incremented Stiffness Matrix Elements, Arrow Wing	21-36

## LIST OF TABLES

<u>Table</u>		<u>Page</u>
21-1	Comparison of Wing Surface Load Intensities - All Models, Mach 0.90 Load Condition	21-13
21-2	Effect of Jig-Shape on Wing Upper Surface Load Intensities, Task IIB Hybrid Model	21-13
21-3	Critical Loading Conditions	21-15
21-4	Summary of Adjusted Aerodynamic Coefficient Matrices - Task I ( $k=0$ )	21-21
21-5	Analytical Methods for Vibration Analysis	21-25
21-6	Lower Frequency Symmetric Vibration Modes - Chordwise Stiffened	21-32

c.5



## LIST OF SYMBOLS

$b_o$	Reference length
$c$	Local chord
$C_l$	Local lift curve slope
$C_{L\alpha}$	Lift curve slope
$\bar{C}$	Area/span
$CC_l / \bar{C} C_{l\alpha}$	Normalized lift distribution
$[D_Z], [D_\theta]$	Deflection and slope transformation matrices
$[D_Z]^T, [D_\theta]^T$	Transpose of the deflection and slope transformation matrices
$h$	Height
$[K]$	Stiffness matrix
$[K_0]$	Base stiffness matrix
$k$	Reduced frequency, $\omega b_o / v$
$M$	Mach number
$[M]$	Mass matrix
$M_X, M_Y$	Bending moment about the x- and y-axis, respectively.
$N_X, N_Y, N_{XY}$	Normal and shearing forces per unit distance in the middle surface of plate
$n$	Number of values
$n_z$	Vertical inertia load factor
$P_z$	Force in the vertical direction
$p$	Non-dimensional time derivative operator, $\left(\frac{b_o}{v}\right) \left(\frac{d}{dt}\right)$
$[Q]$	Matrix of aerodynamic forces
$t$	Time; thickness
$v$	True airspeed
$w$	Weight
$X, Y, Z$	Cartesian coordinates
$\alpha$	Angle of attack
$\beta$	Design variable
$\Delta$	Incremental value(s)

LIST OF SYMBOLS (Cont'd)

$\ddot{\theta}$	Pitching acceleration
$\ddot{\phi}$	Rolling acceleration
$\omega$	Angular frequency in radians/second

SECTION 21  
DESIGN METHODOLOGY

INTRODUCTION

To achieve the objectives established for this program, a systematic multidisciplinary analysis was conducted to assess the effects of the complete environment on the structural integrity of the aircraft. This analysis involved the complex interactions between static aeroelasticity, thermodynamics, flutter, static and dynamic loads, and strength. The flow diagram of the design cycle from initial definition of the airplane configuration to the establishment of the Final Design is presented in Figure 21-1. Due to the complex nature of this design cycle, extensive use of computer programs and their associated math models were required. These calculations were accomplished using Lockheed's Structural Design Analysis System, Figure 21-2, which is an integrated system with the combined program capabilities of the NASTRAN and the Lockheed FAMAS Systems.

The Lockheed FAMAS System contains a very extensive matrix algebra and manipulation system, and a large family of functional modules for aerodynamic loads, structural response and flutter analysis. In addition, this system has completely compatible matrix input/output capability within all its programs. NASTRAN provides finite element capabilities in statics, dynamics, and structural stability analyses for this system. These two systems are integrated with an interface module which permits transit from one system to the other. In this fashion all the design load analysis capabilities of the FAMAS system are joined with the finite element analysis capabilities of the NASTRAN System. Similarly, NASTRAN stiffness or structural flexibility matrices, vibration mode vectors, etc., can be used in direct link with the flutter analysis system in FAMAS, as well as the aeroelastic loads calculations.

This section describes the methodology involved with the disciplines of the analytical design cycle: Structural Temperature Analysis, Finite-Element Structural Analysis, Aeroelastic Loads Analysis, and the Vibration and Flutter Analysis. The methodology employed in the other disciplines are described in previous sections of this report.

STRUCTURAL TEMPERATURE ANALYSIS

A series of mathematical models was employed to describe the heat flow paths within the primary structure and for determination of transient temperature histories for the structural components. The principles of the procedure for prediction of aerodynamic heating and resulting structural temperatures for input to the structural design and analysis are displayed in Figure 21-3.

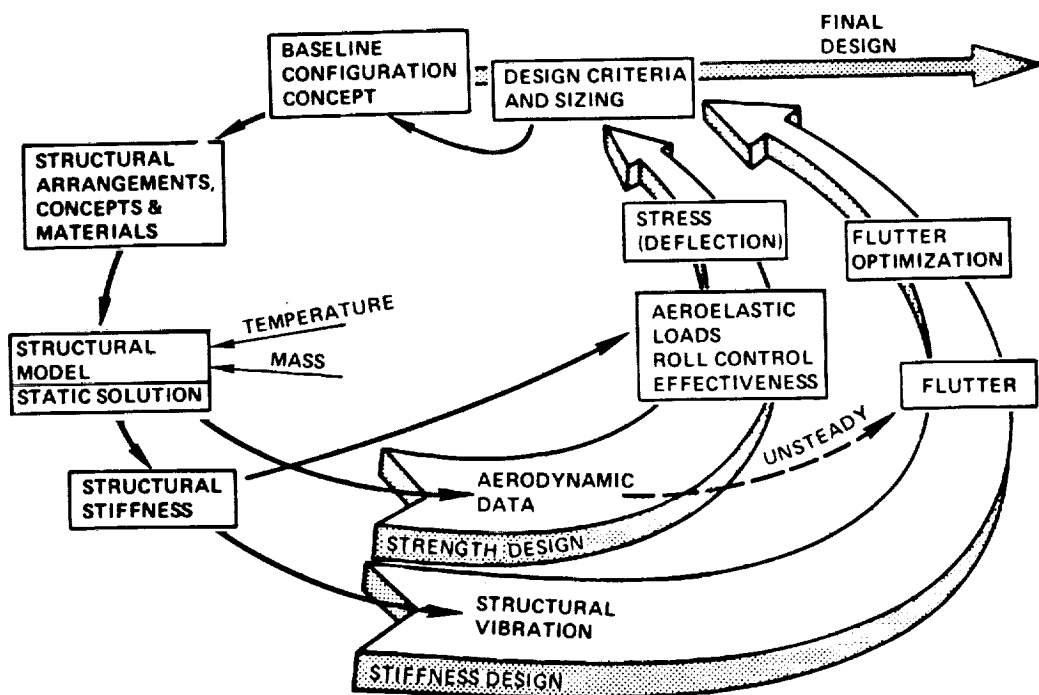


Figure 21-1. Analytical Design Cycle

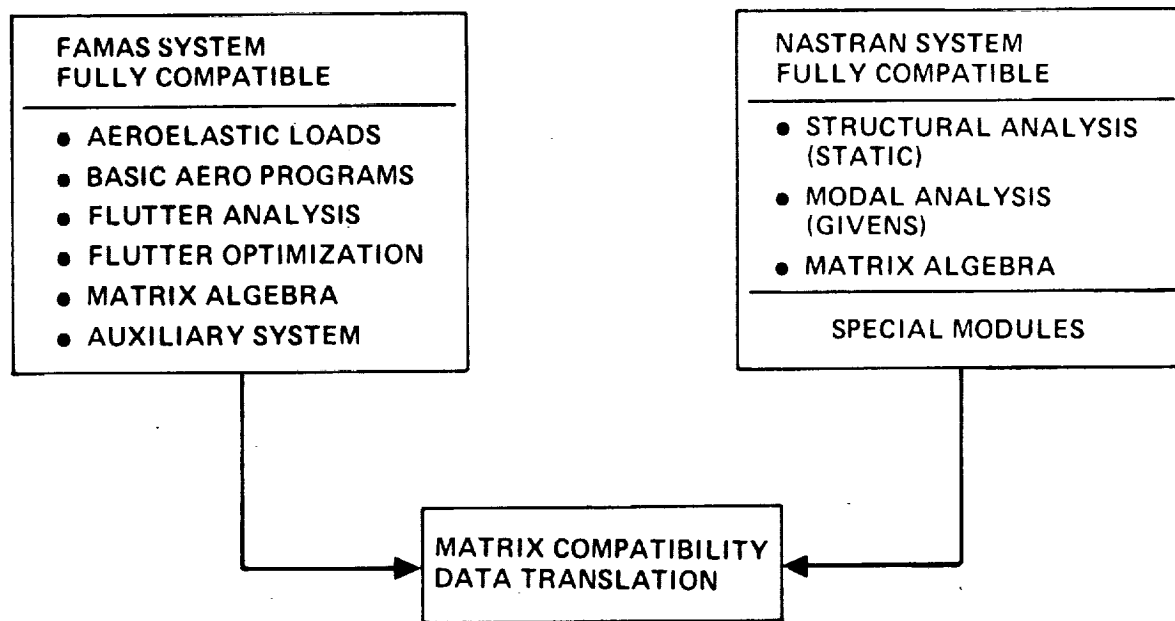


Figure 21-2. Lockheed's Integrated Structural Design Analysis System

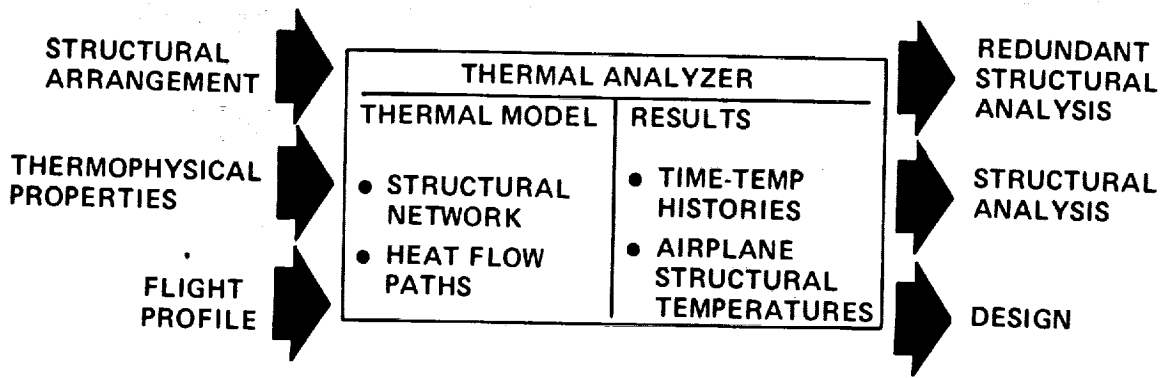


Figure 21-3. Evaluation Procedure for Structural Temperatures

#### Math Models

The mathematical models consist of networks of structural nodes interconnected by heat flow paths and set up for solution using Lockheed's Thermal Analyzer computer program (Reference 1). The solution method is analogous to the solution of voltage distribution in an electrical resistor-capacitor network: current (heat) flows through electrical (thermal) resistors as a function of the voltage (temperature) potential between connected points, and is stored as electrical (thermal) energy in components called capacitors (structural mass) at a rate that is a function of the electrical (heat) capacity of that component. Lockheed's Thermal Analyzer is a completely general and versatile computer program, permitting specification of any type of temperature- or time-dependent heat flow including conduction, convection, radiation, and variable heat storage. An additional capability allows reconnection of network elements during run time, permitting solution of complex problems such as exposure of fuel tank structure to interior radiation as fuel was drained from the tank.

The thermal networks were generalized to accept arbitrary dimensional data for applicability to similarly shaped structures. Detail dimensions were supplied as standard input data and the actual resistor and capacitor values calculated automatically for each case. This technique eliminated the need for minor network revisions each time a dimension was changed, and saved significant programming time.

All Thermal Analyzer networks were set up to compute in a transient mode. The flight profile for a "hot day" (standard plus 8K) international mission was used to determine aerodynamic heating and altitude effects. Cases were run from takeoff roll, to climb, through cruise, and descent to loiter before landing.

Heat transfer in the interior of the wing was determined by setting up a wing box network. The network (Figure 21-4) includes sets of nodes for the upper and lower panels, plus one node each for the four vertical webs (to form a rectangular box). The shape of the box was determined by panel size (spanwise by chordwise dimensions) and by wing depth obtained from wing contour drawings. All node areas were normalized with reference to one square foot of panel surface area to facilitate resistor and capacitor calculations. Heat transfer within the wing box includes radiation exchange, convection to boundary layer air when leakage was a factor, and for fuel tank areas, convection to fuel and fuel vapor.

Two sets of nodal representations for the surface panels were derived for inclusion in the wing box network. The first set was for the corrugation or hat-section stiffened panel concepts, and the second set was for the honeycomb panels. An example of the node definitions for the honeycomb panels are shown in Figure 21-5. Nodes 2 and 3 are defined as the outer and inner halves of the core, respectively. Nodes 1 and 4 include thermal capacity of the braze material. Heat transfer within the panel includes conduction (nodes 1-2, 2-3, and 3-4) and radiation (nodes 1-2, 1-3, 1-4, 2-3, 2-4, and 3-4). To reduce network complexity and computer running time, all braze material was assumed to remain in contact with the face sheets.

Node definitions for the fuselage frame network are shown in Figure 21-6. This network was set up to determine the variation in average skin panel and frame temperatures around the circumference of the fuselage. The hat-section stiffened skin concept is shown, and skin-panel heat transfer is identical to that for type-1 wing panels. Heat transfer to the frame was by conduction and radiation from the skin panels, and by conduction from the surrounding insulation. Conduction through the insulation to the inner skin was also included. Boundary conditions on the inner surface of the fuselage wall included a low convection rate to cabin air and radiation to cabin interior. The network at the fuselage forebody station was adjusted to simulate zee-section stiffeners with the hat-section model.

Heat flow paths were defined by thermal resistors connected between nodes representing structure or between nodes and given boundary condition temperatures. Heat flows directly into a node were also defined explicitly. The Thermal Analyzer network included the following types of heat flow paths: external and internal convection, conduction, external and internal radiation, and thermal capacity.

#### Airframe Structural Temperatures

Structural temperatures were calculated to define the thermal environment at selected wing and fuselage locations for the detail stress analysis and on the overall configuration for input into the structural models, Figure 21-7. These temperatures were developed by using the thermal analysis networks and structural data of the arrow-wing configuration and performing the airplane over a nominal Mach 2.7 cruise flight profile.

Time-temperature histories were developed using the Thermal Analyzer computer program at 14 wing and 10 fuselage locations. These locations were selected to include those point design regions used for the detail stress

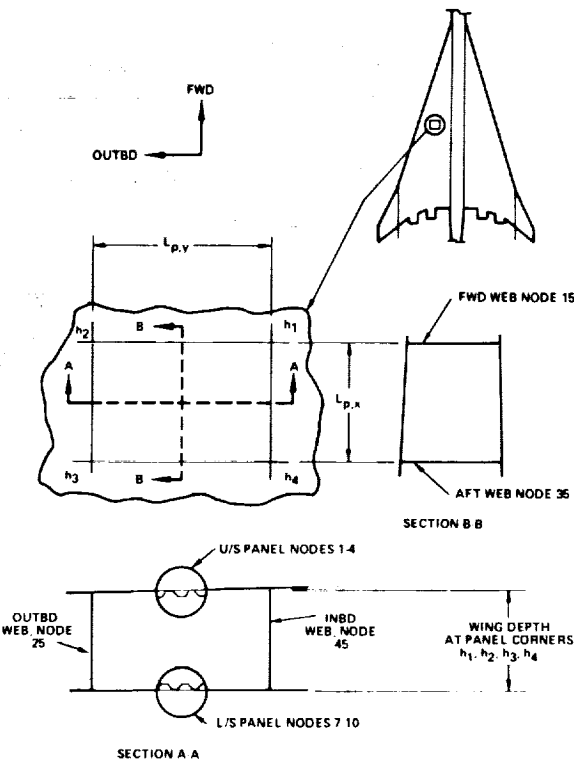


Figure 21-4. Wing Box Thermal Analyzer Network

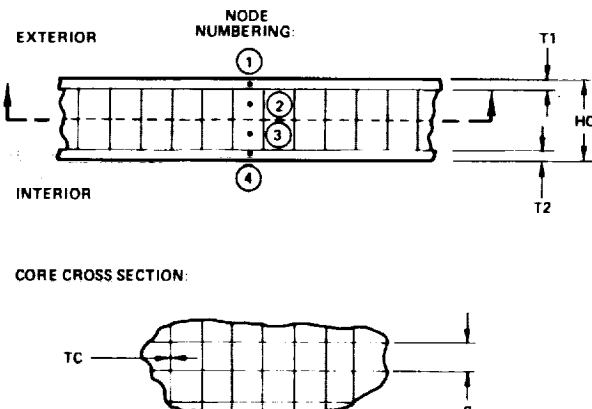


Figure 21-5. Network Node Definition, Type-2 Wing Panels

ORIGINAL PAGE IS  
OF POOR QUALITY

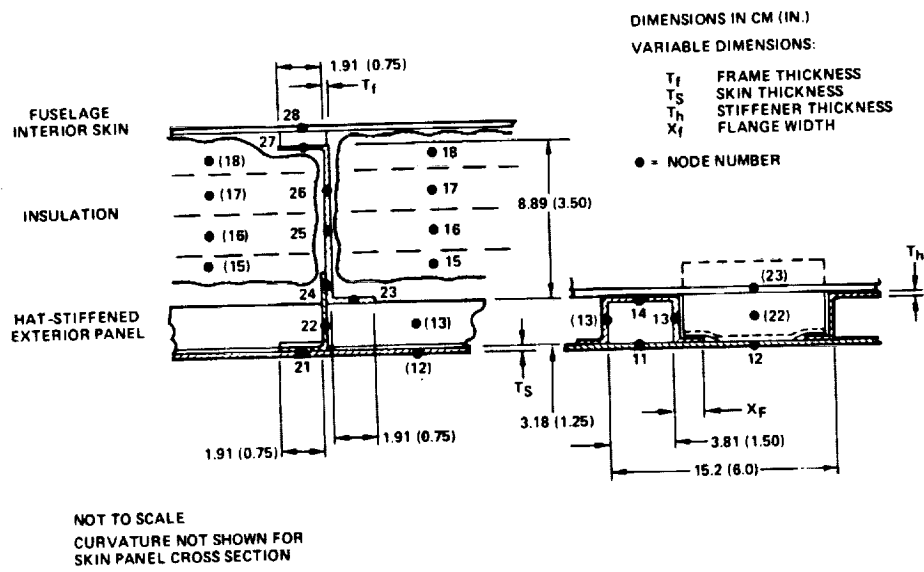


Figure 21-6. Network Node Definition, Fuselage Panel and Frame

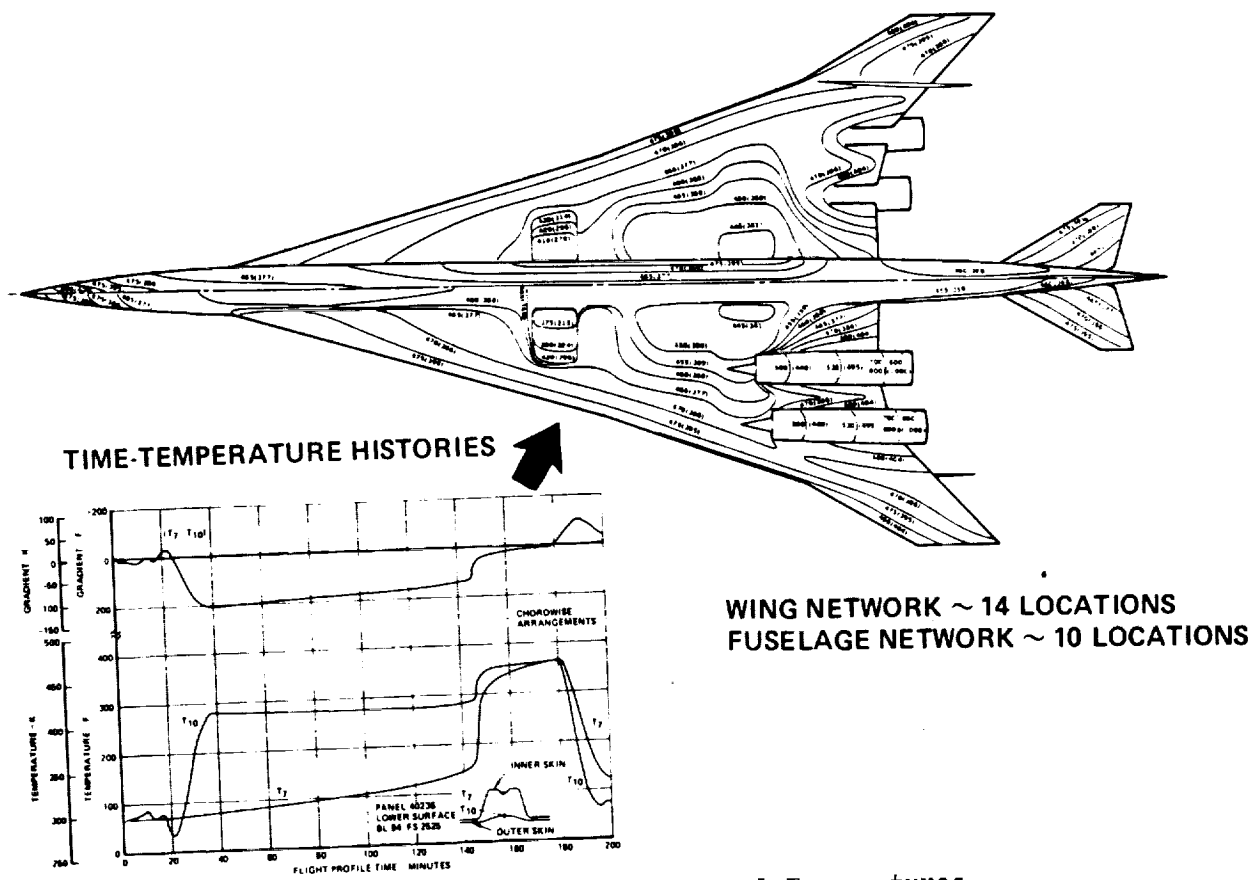


Figure 21-7. Airframe Structural Temperatures

analysis and provided the necessary temperature data to define the point design environment for these regions.

Temperatures were developed for the entire wing and fuselage based on the extrapolation of the time-temperature histories calculated at the selected wing and fuselage locations. In addition, grid point and element temperatures were developed from these overall wing and fuselage temperatures for inclusion in the finite-element structural model.

### FINITE-ELEMENT STRUCTURAL ANALYSIS

A series of finite element (F.E.) structural analysis models were used for the evaluation of structural design concepts. These models were coded for NASTRAN, and Lockheed's Structural Design Analysis System was used to provide internal loads and displacements for stress analyses, to calculate structural deflection influence coefficients for aeroelastic load analyses, and to determine reduced stiffness and mass matrices and compute vibration modes for flutter analyses. The principles of this analytical procedure are shown in Figure 21-8, and generally consisted of the following steps:

- (1) F.E. structural models were established using the basic airplane configuration and the flexibilities commensurate with the structural-material concept being studied. Plot routines and internal check runs were conducted to validate each model.
- (2) NASTRAN redundant-structure analysis solutions were obtained using the F.E. models formulated in step (1). Plot routines were used to verify the continuity of the resulting displacement structural influence coefficients (SIC). Upon verification of the SIC, both SIC and stiffness matrices were released for the aeroelastic loads and vibration analyses, respectively. The vibration analysis initiated the vibration and flutter evaluation with no further interaction with the F.E. structural analysis until the next design iteration was attempted. The SIC matrix, in association with the basic aerodynamics, mass matrices, and the flight parameters was used to calculate the static aeroelastic loads.
- (3) A NASTRAN internal loads run was conducted using the aeroelastic loads matrix derived in Step (2), with the resulting displacements and internal loads (stresses) subsequently used for the point design stress analysis.

#### Structural Models

The F.E. structural models used for the structural investigation are summarized on the flow schematic in Figure 21-9. These models are characterized by their basic modeling technique and their wing primary load-carrying structural arrangement. The three general types of structure and combination thereof evaluated were: chordwise-stiffened, spanwise-stiffened, biaxially-stiffened (monocoque), and the hybrid-stiffened arrangements. The two different modeling

techniques employed in the formulation of these structural models were: the pseudo 2-Dimensional (2-D) method and the conventional 3-Dimensional (3-D) method. A statistical comparison of the two modeling techniques is as follows:

MODEL	GRID POINTS	ELEMENTS	DEGREES OF FREEDOM	CPU TIME* (HR)
2-D	530	1300	1050	0.37
3-D	715	2450	2200	0.72

\* COMPUTER TIME TO GENERATE SYM. AND A/S SIC'S

In addition, the computer time required to formulate the symmetric and anti-symmetric structural influence coefficients (SIC) are included and indicate the cost effectiveness of the pseudo 2-D model, i.e., the 2-D model is half as costly (computer run time) as the more detailed 3-D model.

The simplified pseudo 2-D model technique was formulated for the initial studies as a rapid, cost effective method for evaluating the effects of the primary wing loads ( $P_z$ ,  $M_x$  and  $M_y$ ). A representative description of the modeling technique used on the 2-D models is included in Figure 21-9. This model represents the actual wing upper surface planform with a simplified wing cross-section and the fuselage was idealized as a simple beam. For the wing, a horizontal midplane (X-Y plane) of structural symmetry was assumed, which permits the size of the model to be substantially smaller since only the upper half of the wing needs to be specified in the model. The wing cross-section of the model was symmetrical about the X-Y plane. The Z coordinates (measured from the X-Y plane) defined the upper wing surface and were equal to one-half of the total wing depth of the model. Section properties were equal to the average stiffness of the wing upper and lower surfaces.

For the wing vertical fin model, a two-dimensional (X-Z plane) grid system with NASTRAN bar and shear panel elements was used to represent the equivalent bending and torsion stiffness of the fin. Fin loads are introduced into the wing by means of NASTRAN multipoint constraint (MPC) equations which were applied at the interface of the fin with the wing box.

Engine support beams were represented in the model by NASTRAN bar elements with the capability to transmit axial, torsional, and vertical and lateral bending loads from the engines into the wing box. The beams were located at the constrained wing midplane and were connected by MPC equations to the X-Y rigid body motions of the wing for the vibration analyses.

The 2-D models represent the fuselage as a simple beam and used NASTRAN bar elements with torsional, and vertical and lateral bending stiffness. The fuselage beam was connected to the wing model by MPC equations and scalar springs (NASTRAN CELAS elements) representing an approximation of the fuselage frame flexibility.

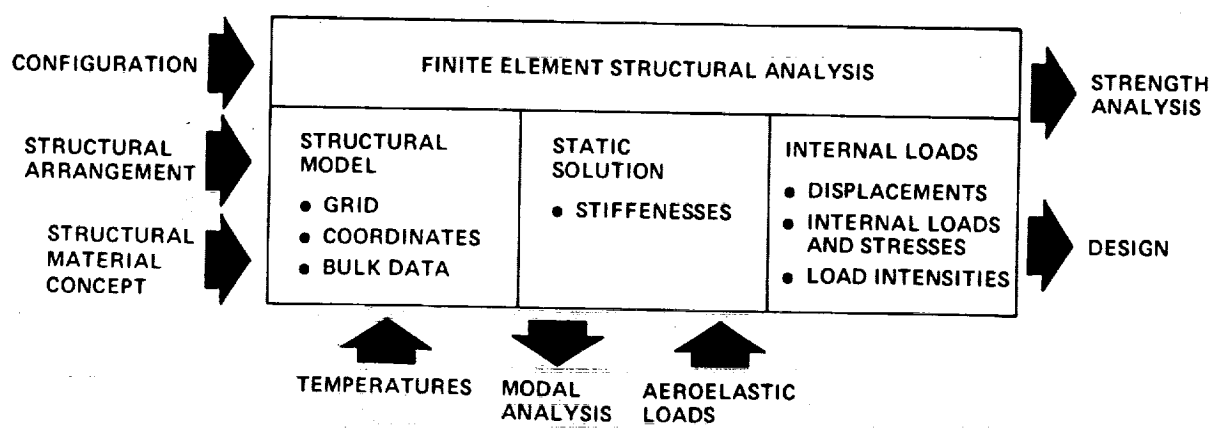


Figure 21-8. Finite Element Structural Analysis Procedure

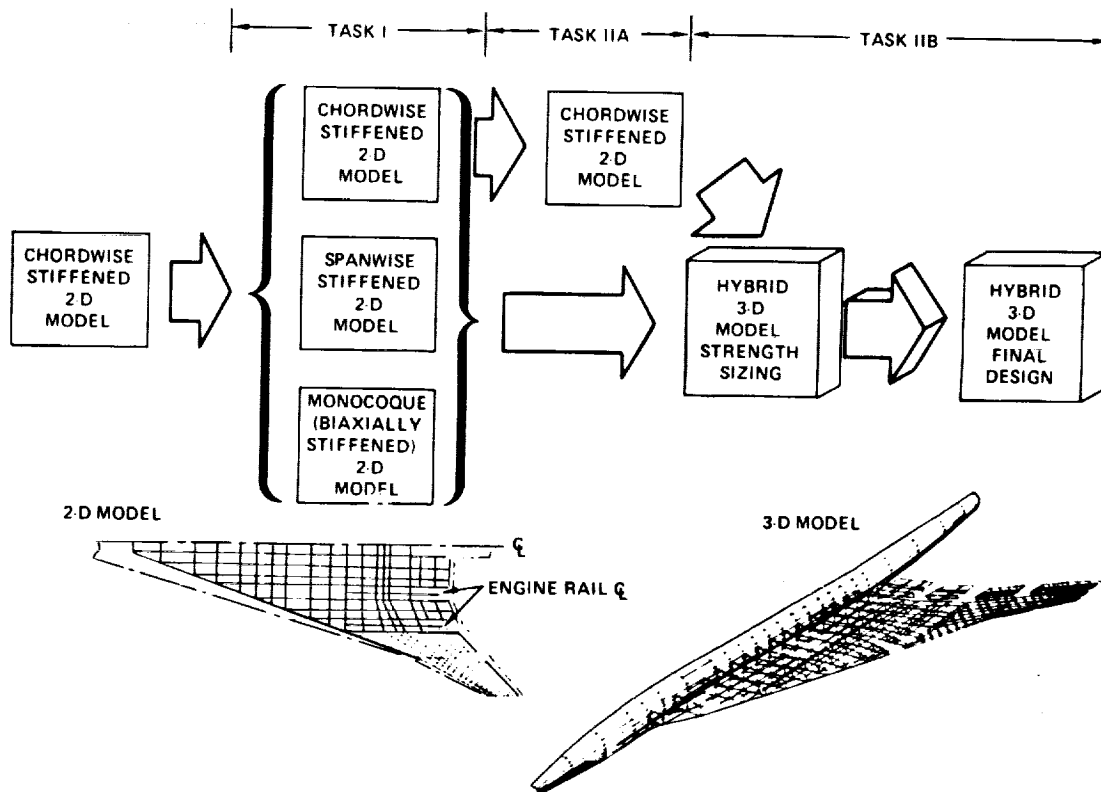


Figure 21-9. Structural Model Usage

For the Task II analyses, a more detailed, 3-D model was used to describe the airframe. An isometric view of this model is also included in Figure 21-9.

The wing planform grid for the 3-D model was approximately equal to the 2-D model grid. However, for the 3-D model both upper and lower wing surfaces were represented, including camber and twist of the actual airfoil. Flexible control surface actuators were represented using NASTRAN CELAS elements and MPC equations. The elimination of the X-Y wing midplane of structural symmetry (and load antisymmetry) used on the 2-D models required a redefinition of the location for the wing interfaces with the vertical fin, main landing gear and engines.

The 3-D model fuselage was idealized using 25 frame stations with approximately 10 nodes describing the fuselage half-circumference. NASTRAN bar elements are used to represent fuselage frames with rod elements and quadrilateral shear panels used to represent the fuselage shell.

For both modeling techniques, a network of unit loads, were used on the models to calculate SIC's and to introduce design loads into the model structure. Effective unit load locations are, in general, identical for both models with the exception of the unit loads applied to the 3-D model fuselage which differ from those used on the 2-D models in their application as distributed loads at each frame station. The corresponding structural influence coefficients on the 3-D fuselage model represent an average deflection of the frame node points to which the unit load was distributed.

To assess the results of the structural model techniques and provide insight for future research studies, an investigation was conducted to compare the accuracy (2-D versus 3-D) of the two modeling techniques. This investigation was conducted by up-dating the Task II-A chordwise structural model (2-D), completing a NASTRAN static solution, and comparing these results with those of the Final Design airplane which employed a 3-D structural model. Commensurate with model technique, the input data for the 2-D model reflected the identical coordinate and flexibility data used in the 3-D structural model.

Examples of the results of the 2-D NASTRAN static solution are presented in Figures 21-10 and 21-11 with the corresponding data from the 3-D model included for comparison purposes. These figures show the normalized structural influence coefficients for the wing rear beam and fuselage.

With reference to Figure 21-10, both 2-D and 3-D structural influence coefficients were normalized to the maximum wing tip displacement of the 2-D structural model. This data indicates approximately equal stiffnesses for both models in the basic wing region, inboard of BL 470, with the 2-D model having a more flexible wing tip, e.g., for equal loads applied at the wing tips, the wing tip displacement for the 2-D model would be approximately 10-percent greater than the corresponding displacement of the 3-D model.

**ORIGINAL PAGE IS  
OF POOR QUALITY**

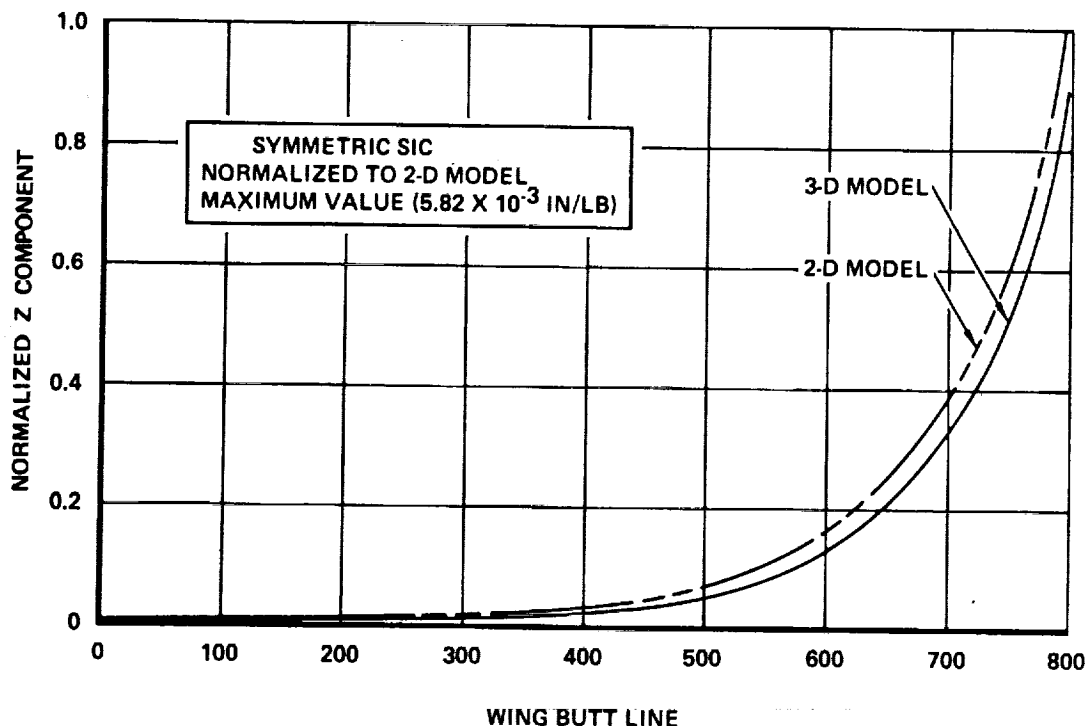


Figure 21-10. Comparison of Wing Rear Beam Structural Influence Lines

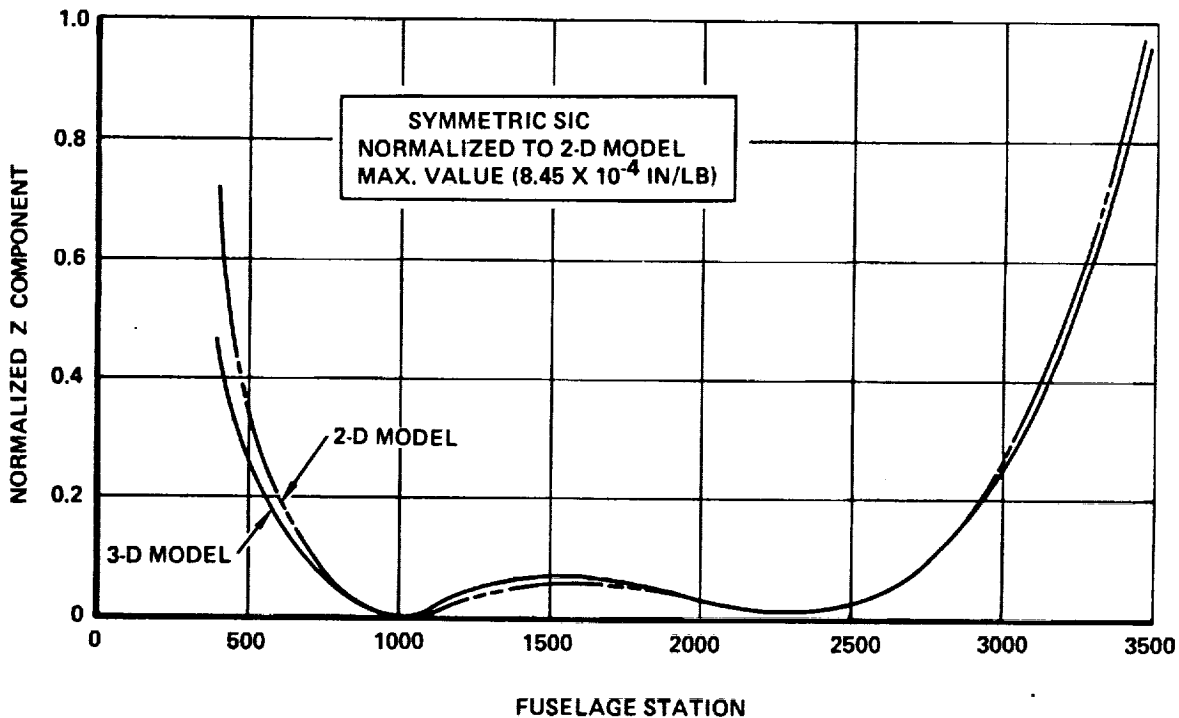


Figure 21-11. Comparison of Fuselage Structural Influence Lines

Similar to the wing results, Figure 21-11 indicates the 2-D model contains a more flexible fuselage forebody region than the 3-D model with a maximum difference in influence coefficients of approximately 50-percent occurring at the nose. Relatively good agreement between the influence lines are noted for the remaining centerbody and aftbody regions.

These results indicate only the relative trends in stiffness associated with each modeling technique; for a complete assessment of the accuracy, additional analyses are required including the overall effects of static aeroelasticity, vibration and flutter, and strength.

#### Structural Influence Coefficients

A total of 274 generalized coordinates were defined on the structural model for calculating the structural influence coefficients (SIC) matrix and the stiffness matrix. The SIC matrix was used to calculate the aeroelastic loads; whereas, the stiffness matrix after a reduction to approximately 180 degrees-of-freedom was used for the vibration and flutter analyses.

For both the symmetric and antisymmetric boundary conditions, the 274 generalized coordinates were primarily associated with the Z-displacement (vertical) degrees-of-freedom. The exception being the antisymmetric coordinates at the fuselage centerline which were related to the y-displacement (lateral) degrees-of-freedom. In addition, for both boundary conditions, rotational and y-displacement degrees-of-freedom were defined for the wing leading edge and wing vertical, respectively.

Because of the importance of the structural influence coefficients (SIC), an auxiliary plot routine was used to assist in the review of the NASTRAN generated SIC's. In general, this computer program (FAMAS plot routine) extracts the diagonal elements from the NASTRAN SIC matrix for selected sets of wing and fuselage points, normalizes these values to the largest absolute value of each set, and plots these as a function of location (fuselage station, butt line, or water line). These plots display the continuity or discontinuity of the influence lines and were an aid in assessing the validity of the flexibility data input to the structural model.

#### Internal Loads Runs

NASTRAN internal load runs were conducted on each Task I and Task II model using the aeroelastic loads commensurate with the model stiffness. In addition, the aeroelastic loads for the final design included jig-shape effects which are described in more detail in the following Aeroelastic Loads Analysis section.

The results of the NASTRAN solutions identified the displacements and internal forces (stresses) associated with the elements of each structural model. For the point design stress analysis, the internal loads and stresses from the NASTRAN solution were converted into running loads by an auxiliary FAMAS program.

A comparison of the wing upper surface load intensities (lb/in.) are shown in Table 21-1 for all structural models. These loads were based on the results

TABLE 21-1. COMPARISON OF WING SURFACE LOAD INTENSITIES - ALL MODELS, MACH 0.90 LOAD CONDITION

PANEL IDENTIFICATION		*LOAD INTENSITY (ULTIMATE), LBS/IN.						
		DIRECTION	TASK I			IIA	TASK II B	
REGION	NUMBER		CHORDWISE	SPANWISE	MONOCOQUE	CHORDWISE	HYBRID (STRENGTH)	HYBRID (FINAL)
WING FORWARD	40322	Nx Ny Nxy	10 1145 201	148 1155 275	199 595 211	819 1120 143	122 1109 112	219 1049 75
WING AFT BOX	40236	Nx Ny Nxy	188 10646 418	122 12181 1181	825 8102 858	377 11474 436	179 12779 271	15 14311 272
	40536	Nx Ny Nxy	85 10680 1118	132 12318 2288	1483 8763 2521	471 11207 1409	458 12680 1068	315 14410 1159
	41036	Nx Ny Nxy	274 6570 1369	36 6876 2027	1094 4544 1949	567 7040 1581	1052 3522 1583	1562 4725 1773
WING TIP	41316	Nx Ny Nxy	701 11655 3492	298 12546 3240	932 8268 2528	592 12145 3773	1226 9504 3686	1478 10106 3730
	41348	Nx Ny Nxy	719 6293 1535	574 5886 1797	605 4731 2132	1068 6402 1990	877 5148 2290	856 6598 2608

\* LOAD CONDITIONS:

TASK I CONDITION 12: MACH 0.90, n<sub>Z</sub> = 2.5, W = 700,000 LB, V<sub>e</sub> = 325 KEAS

TASK IIA CONDITION 9: MACH 0.90, n<sub>Z</sub> = 2.5, W = 700,000 LB, V<sub>e</sub> = 325 KEAS

TASK II B CONDITION 8: MACH 0.90, n<sub>Z</sub> = 2.5, W = 700,000 LB, V<sub>e</sub> = 325 KEAS

TABLE 21-2. EFFECT OF JIG-SHAPE ON WING UPPER SURFACE LOAD INTENSITIES, TASK II B HYBRID MODEL

PANEL IDENTIFICATION		* LOAD INTENSITY (ULTIMATE), LBS/IN.				PERCENTAGE DIFFERENCE (%)
		DIRECTION	ASSUMED JIG SHAPE			
REGION	NUMBER		MID-CRUISE	ZERO LOAD		
WING - FORWARD	40322	NX NY NXY	151 1106 130	166 1083 124		+10 -2 -5
WING - AFT BOX	40236	NX NY NXY	67 14650 453	133 15596 499		+98 +7 +10
	40536	NX NY NXY	1073 14303 1495	1182 15315 1750		+10 +7 +17
	41036	NX NY NXY	1812 4220 2106	2096 4612 2471		+16 +9 +17
WING - TIP	41316	NX NY NXY	1638 12407 4009	1700 14280 4262		+4 +14 +5
	41348	NX NY NXY	1207 6897 2284	1187 8192 2560		-9 +19 +12

\* LOAD CONDITIONS:

TASK II B CONDITION 12: MACH 1.25, n<sub>Z</sub> = 2.5, W = 690,000 LB, V<sub>e</sub> = 294 KEAS

ORIGINAL PAGE IS  
OF POOR QUALITY

of the NASTRAN static solution as defined at the six point-design regions used for the structural analysis. The direction of the inplane loads corresponds to the basic airplane axes with the exception of the wing tip regions (panels 41316 and 41318). For these panels the y-direction (spanwise) was parallel to the rear beam of the wingtip structure and the x-direction (chordwise) perpendicular to the rear beam. Conventional sign notation was used; positive signs denote tensile forces and conversely, negative signs denote compression.

A study of the effect of jig-shape on internal loads was conducted using the Task IIB strength-sized model. The structural deflections were determined for one-g flight condition during mid-cruise flight, these deflections were applied negatively to numerically define the jig-shape (i.e., local slope and deformation of the wing grid points). Having established these values the aeroelastic loads were calculated for the 2.5-g symmetric maneuver condition at Mach 1.25. A summary of these results, variation of the point design load intensities with and without the jig-shape effect, is shown in Table 21-2 with the percentage differences indicated.

All load intensities increased when the jig-shape effect was included in the aeroelastic loads calculations; the exception being the spanwise ( $N_y$ ) and shear ( $N_{xy}$ ) loads at point design region 40322 which were reduced by 2-percent and 5-percent respectively. As expected, the largest load intensity variations occurred on the more flexible regions of the wing (e.g., a 19-percent increase in spanwise load intensity for region 41348) which is approximately center span of the wing tip.

Because of the large variation in load intensity attributed to the jig-shape effect, the results of this study were incorporated into the element properties for the Final Design F.E. model. In addition, the final aeroelastic loads included the jig-shape effect.

#### AEROELASTIC LOADS ANALYSIS

Net aeroelastic loads were determined for the aerodynamic shape defined for the baseline configuration at selected conditions on the design flight profile. These loads were calculated using Lockheed's static aeroelastic loads program for inclusion in the NASTRAN internal loads solution, and reflected the specific airframe flexibility of each of the general-types of structural arrangements.

The general logic flow diagram of the aeroelastic loads analysis is presented in Figure 21-12. A more detailed description of the principal tasks involved are as follows:

- (1) Determination of the critical flight conditions and their related flight parameters (speed, altitude, acceleration, and gross weight).
- (2) Establishment of the basic aerodynamic grid system and local airfoil geometry for calculating the theoretical airloads distributions.
- (3) Calculation of the theoretical airloads distribution based on the applicable aerodynamic theory for the flight conditions under investigation. Condense and transfer these theoretical panel point loads

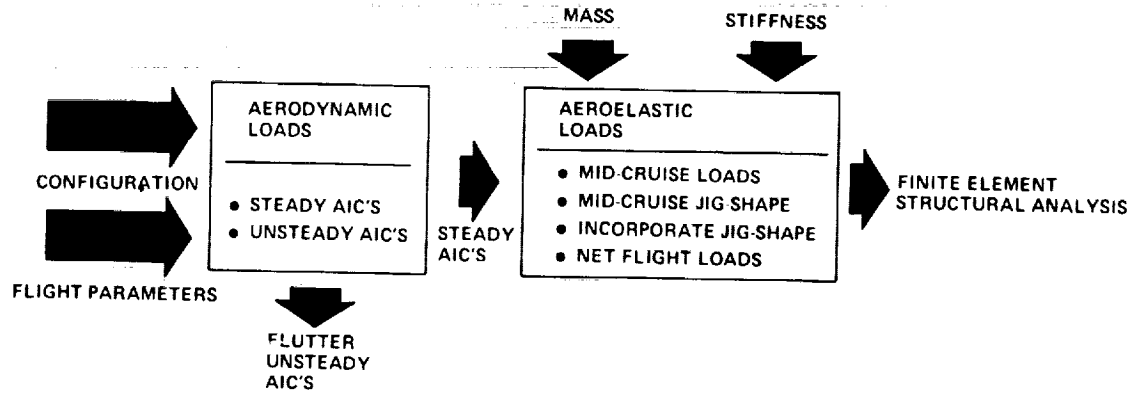


Figure 21-12. Aeroelastic Loads Evaluation Procedure

TABLE 21-3. CRITICAL LOADING CONDITIONS

	CONDITION	MACH NO.	$n_Z$	SCAT-15F	L-2000-7	969-336C	ARROW WING
Flight	Symmetric	0.30	2.0	-	-	✓	✓
		0.60	2.5	✓	✓	-	✓
		0.90	2.5	✓	✓	-	✓
		1.25	2.5	-	✓	✓	✓
		2.00	2.5	-	-	-	✓
		2.70	2.5	✓	-	✓	✓
		2.90	2.5	-	-	-	✓
	Asymmetric	0.30	0 & 1.67	-	-	-	✓
		0.90		-	-	-	✓
		1.25		-	✓	-	✓
Ground	Taxi Rotation Landing	-	2.0	-	-	✓	✓
		-	-	-	✓	-	✓
		-	-	-	-	-	✓

to the structural influence coefficient grid system of the finite-element model and adjust values to reflect any measured steady state lift coefficients and aerodynamic center data when required.

- (4) Determination of the net aeroelastic flight loads using the theoretical air load calculated in step (3), the mass matrices, and the airframe stiffness (SIC'S) as defined by the NASTRAN static solution. These data were combined with the aid of matrix algebra to formulate distributed grid point loads on the airplane consistent with the solution of the equations of motions for the prescribed maneuvers.

#### Critical Flight Conditions

Previous supersonic transport design studies were reviewed to identify potentially critical conditions for the baseline configuration concept. Design conditions for the SCAT-15F, Boeing 969-336C, and Lockheed L-2000-7 supersonic transport are summarized on Table 21-3. Loading conditions evaluated for this study are also included on the table to indicate the scope of potentially critical loading conditions investigated. For the baseline configuration, load conditions were evaluated at both maximum positive and maximum negative load factor and include all conditions where peak values or rapid change in aerodynamic coefficients exist. During the course of this study, all conditions identified on Table 21-3 were investigated sufficiently to assure that critical design loads are included for structural analysis. Supplemental conditions were developed to ascertain the design loads for specific regions of the wing and fuselage.

The loading conditions for the final design cycle included 8 subsonic speed symmetric maneuvers (steady and transient); 7 low supersonic cases, including negative normal acceleration conditions, steady and transient maneuvers at heavy and light gross weights; 4 Mach 2.7 conditions, including mid-cruise level flight and maneuver, and steady and transient maneuvers at start-of-cruise; 2 dynamic gust (pseudo) conditions at Mach 0.90 (positive and negative); and 4 dynamic landing conditions. These load cases are further identified on the design airspeed envelope of Figure 21-15. The gust and landing cases were supplemental conditions developed for the Final Design effort and were selected as critical for fuselage design. The asymmetric accelerated roll condition was not included for the final loads run. The roll case resulted in maximum inplane loads in local regions of the strength-designed wing tip structure. However, with the added stiffness requirements in this region to suppress flutter, the condition was deleted from the list of potentially critical conditions.

#### Theoretical Aerodynamics

Subsonic and supersonic airloads distribution were determined using the Discrete Load Line Element (DLLE) and Mach Box computer programs, respectively. The DLLE method is theoretically the same as the Doublet Lattice Method of Reference 2; the Mach Box method is described in Reference 3. Typical aero-dynamic grids used for determination of subsonic and supersonic aerodynamics are displayed in Figures 21-13 and 21-14.

ORIGINAL PAGE IS  
OF POOR QUALITY

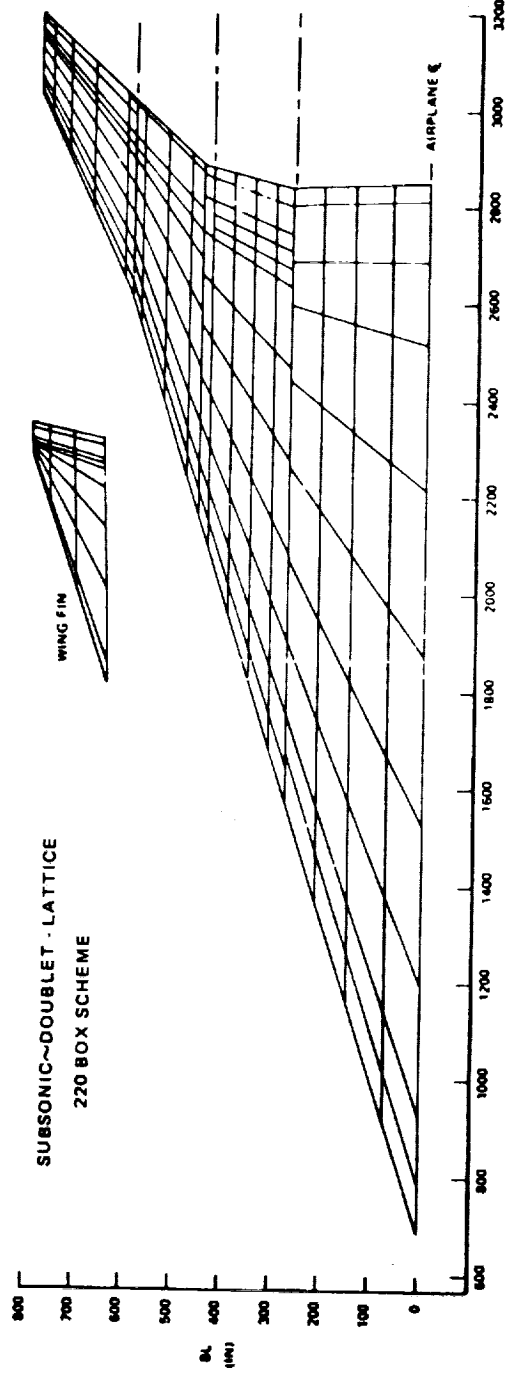


Figure 21-13. Subsonic Aerodynamic Grid

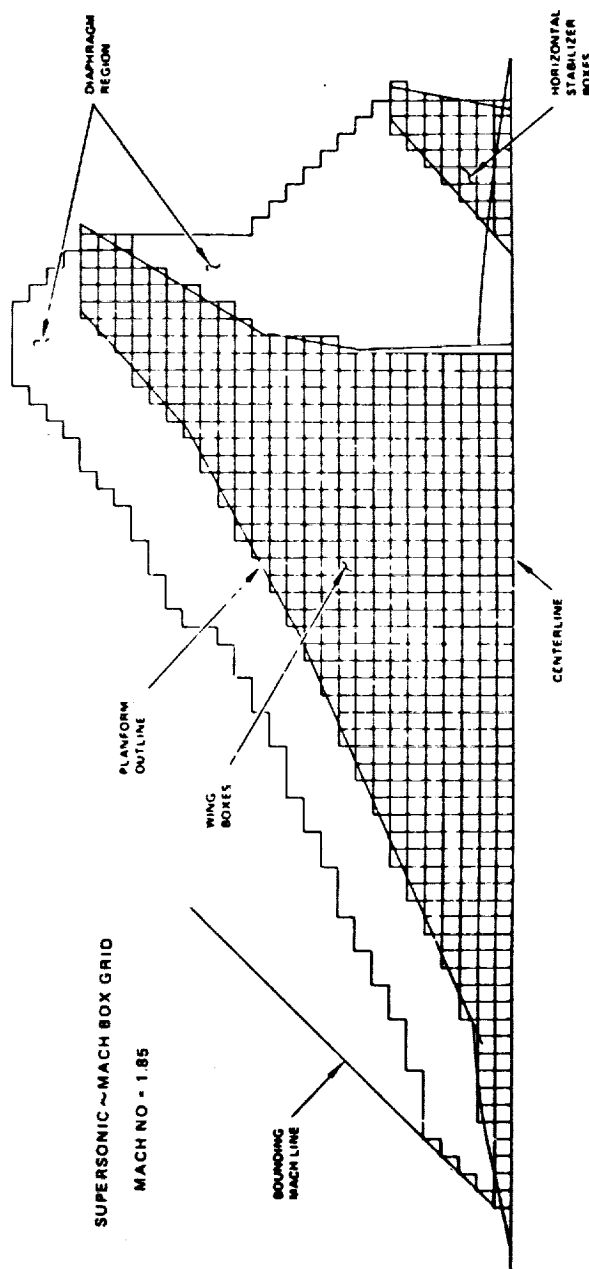


Figure 21-14. Supersonic Aerodynamic Grid

ORIGINAL PAGE IS  
OF POOR QUALITY

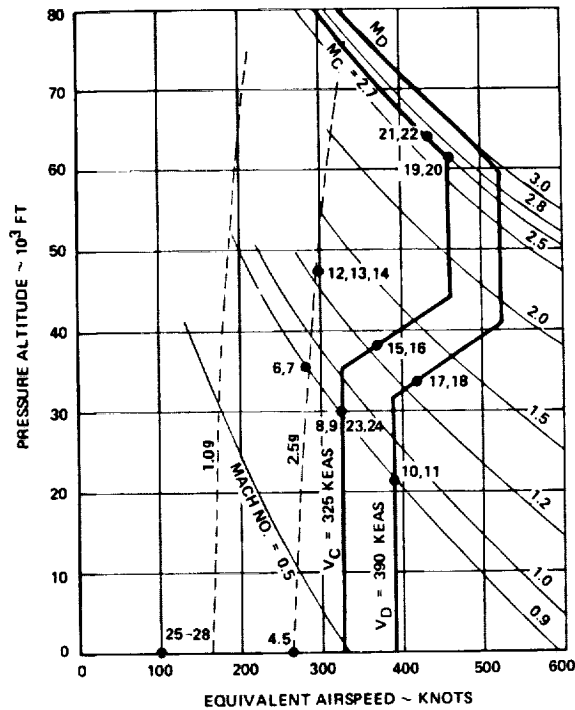


Figure 21-15. Design Load Conditions - Strength/Stiffness

The above theoretical subsonic and supersonic airload distributions were reviewed for correlation with data developed from the results of NASA wind tunnel tests of the Arrow-Wing configuration.

To assess the net loads effect, static aeroelastic loads were generated for a Mach 2.7 symmetrical maneuver condition using both the wind tunnel measured pressures and the theoretical airload distribution based on Mach box theory. For the airloads based on the wind tunnel data, the pressures on the wing grid system were obtained by interpolation of the corrected data and factored to obtain the lift on each grid element area. These distributions at each angle of attack were combined into a matrix format for application to the net loads program. The data in these matrices were used to define all the airloads on the airplane due to angle of attack. Redistribution of airloads due to flexibility was computed from theoretical aerodynamic influence coefficients.

A comparison of the net integrated wing shears derived by the Mach box method and by the application of the measured pressure data is shown in Figure 21-16. In addition to the wing shears, reduced values of bending moment and torsion at all wing span stations and reduced shears at all fuselage stations were noted for the loads generated using the pressure data. These results occur primarily from the large reduction in tip loading by the measured data causing a significant inboard shift of the spanwise center of pressure.

Reductions in net torsion were less pronounced in the vicinity of the fuselage due to the more forward location of the chordwise center of pressure from measured data at these inboard locations.

Figure 21-17 presents the results of another investigation which was conducted to evaluate the spanwise loading distributions over a wide range of angles of attack at Mach 2.7. Loading distributions were developed using both wind tunnel force and pressure data and a theoretical method using the Mach Box Program.

Span loading distributions from these methods are shown at two airplane angles of attack. The lower angle of attack is within the linear range of wing lift coefficient as a function of angle of attack. For the higher angles, the wind tunnel measured data indicates a significant unloading of outboard wing stations with a high section loading near the fuselage. The Mach Box data represents a wing lift equal to that from integrated pressure data although with a more outboard center-of-pressure location. Available force data indicate a higher wing lift but with the same slope.

Differences between the span loading distributions beyond the linear  $C_L$  versus  $\alpha$  range are more pronounced with the relationships between the several distributions as previously described. Both force data and integrated pressure data displayed on Figure 21-18 confirm the non-linear trend of wing lift coefficient at higher angles of attack. The Mach Box method is linear and does not display this tendency.

Results of the loading investigations, which were based on limited amount of wind tunnel measured pressure data at Mach 2.7, were inconclusive concerning the choice between using the theoretical aerodynamics or the wind tunnel test data for generating the panel point loads. Even though correlation was not obtained, some geometric similarities were noted between the curves generated using the theoretical aerodynamics and the measured data. For example, approximately equal wing lift slopes were noted for the Mach 2.7 condition using the Mach Box and force data, with higher wing lift values noted for the force data.

Since correlation was not obtained, the design loads for both subsonic and supersonic aerodynamics were based on the applicable theoretical aerodynamics (DLLE and Mach Box) and adjusted to reflect the measured steady state lift coefficients and aerodynamic centers derived from the wind tunnel force data. Table 21-4 presents a summary of the Task I aerodynamic coefficient matrices with their respective wing lift and aerodynamic centers data.

#### Grid Transform

Grid transforms were required for transferring aerodynamic loadings from the aerodynamic influence coefficient (load point) model to a system compatible with

ORIGINAL PAGE IS  
OF POOR QUALITY

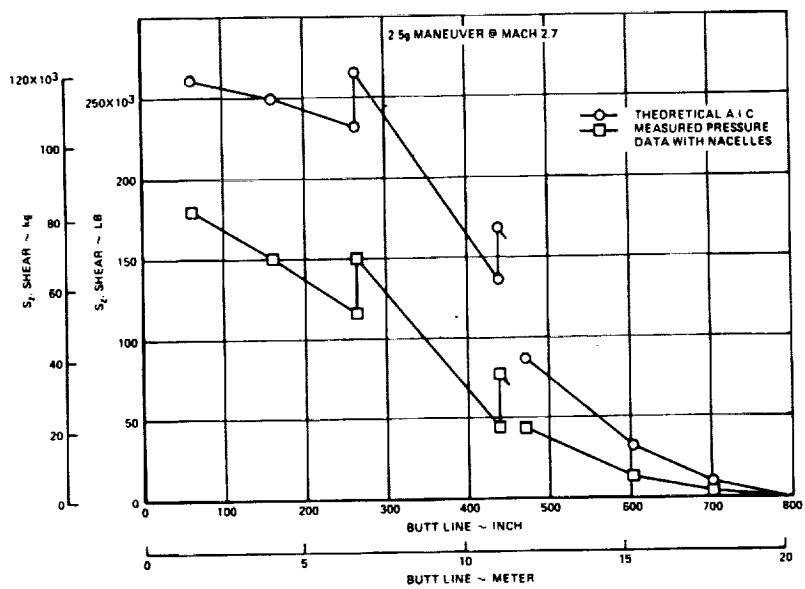


Figure 21-16. Net Integrated Wing Shears - Theoretical vs Measured

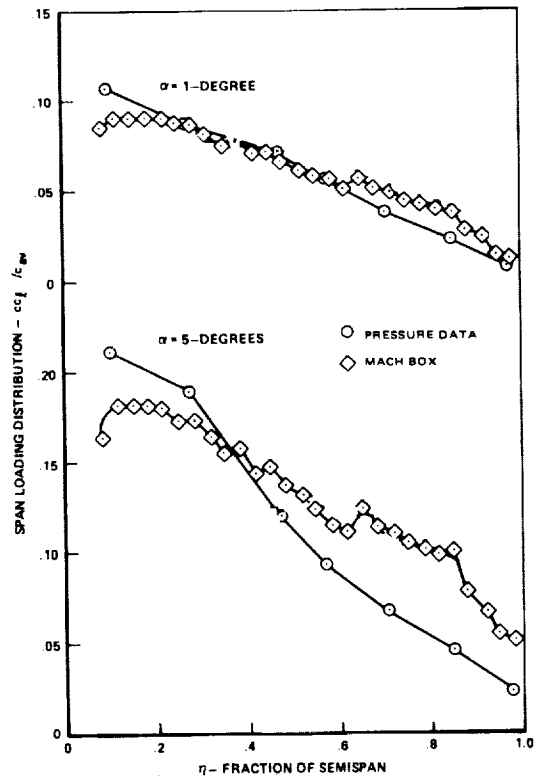


Figure 21-17. Span Loading Distribution - Mach 2.7

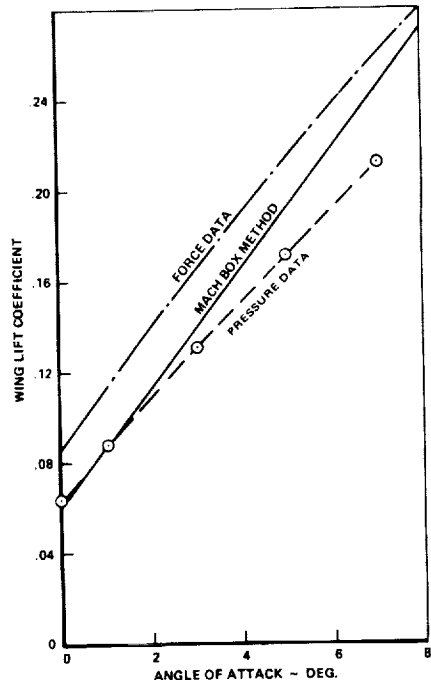


Figure 21-18. Wing Lift Coefficients - Mach 2.7

TABLE 21-4. SUMMARY OF ADJUSTED AERODYNAMIC COEFFICIENT MATRICES - TASK I ( $k=0$ )

MACH NUMBER	BOUNDARY CONDITION	MATRIX SIZE	TOTAL EFFECTIVE $C_L$	LOCATION OF A. C.
0.60	Symmetric	274 x 325	2.42	FS 2324
	Antisymmetric	274 x 233		
0.90	Symmetric	274 x 325	2.58	FS 2324
	Antisymmetric	274 x 233		
1.25	Symmetric	274 x 536	2.52	FS 2391
	Antisymmetric	274 x 487		
2.0	Symmetric	274 x 621	1.92	FS 2356
2.70	Symmetric	274 x 621	1.55	FS 2324

the structural influence coefficient (stress and weight) grid. The transformation matrices  $[D_z]$  and  $[D_\theta]$  express deflection,  $z$ , and chordwise slope,  $\theta$ , respectively, at the AIC points in terms of the deflection,  $z$ , at the SIC "given" points. An equivalent set of forces at the structural grid is obtained when the column of lumped aerodynamic forces and pitching moments were pre-multiplied by the matrices  $[D_z]^T$  and  $[D_\theta]^T$ .

The  $[Q]$  matrix, obtained from the aerodynamic influence coefficient program, relates the loading at load points (SIC points) to deflection at control points. Since load points correspond to SIC points on the structural model, a unit  $[D_z]$  matrix was used. Determination of angular deflections requires that the deflection at SIC points due to load at control points be defined. One set of control points was used in determining subsonic A.I.C.'s; however, each supersonic speed condition requires a set of control points since their number and location were a function of Mach number.

#### Mass Distribution

Inertia data were based on the mass distribution commensurate with each of the design stages. These masses were distributed as panel point loads concentrated at the load panel grid, Figure 21-19. This grid system is identical to the Structural Influence Coefficient (SIC) grid system of the structural model. Mass distributions were derived for the operating weight empty condition, and for the payload and fuel, respectively. Using these distributions, which represent one-half airplane values, and the pertinent flight data ( $n_z$ ,  $\theta$ , and  $\phi$ ) the inertia loadings at the S.I.C. grid points were determined for the flight conditions investigated. These inertia loading were stored in matrix format for the net loads program.

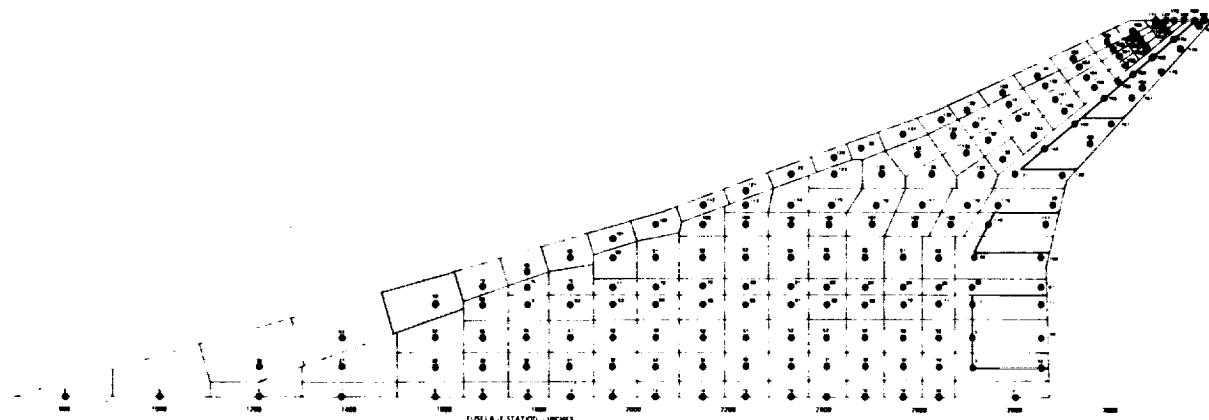


Figure 21-19. Load Panel Grid

#### Jig Shape Definition

The aerodynamic shape of the aircraft changes during flight due to aero-thermoelastic and inertial effects. This is a result of inflight variations in dynamic pressure, Mach number, gross weight, and weight distribution; the latter two result from fuel consumption.

The governing aerodynamic shape serving as the analytical starting point, was the shape providing the optimum performance characteristics in one-g mid-cruise flight. The initial shape of the aircraft was defined at the design cruise lift coefficient by a computer card deck supplied by NASA. This external shape reflected the NASA 15F airplane without a canard or inboard leading edge devices. During the course of this study additional modifications, mainly in the fuselage and wing tip areas, were adopted and incorporated into the configuration as defined by the data deck. Section 2 of this report contains a description of these configuration requirements.

The zero-load shape was designed into the aircraft so that when it was subjected to one-g level-flight loads and to temperatures occurring in the mid-cruise environment, the airframe elastic deformations resulted in an aircraft that had the desired optimum aerodynamic shape. The manufacture of the aircraft was then made in accordance to this zero-load shape in the jig, where the weight was supported in a manner that precludes elastic deformations.

The procedure to establish the jig shape was as follows:

- (1) The analytical starting point was the description (camber and twist) of the mid-cruise shape.

$$[\alpha_{C \& T, \text{mid-cr}}]$$

- (2) Analysis was performed to calculate structural deflections due to flight loads occurring during mid-cruise flight. Where the deflection matrix  $[\Delta\delta_z]$  is defined by the product of the structural influence

coefficients [E] and the rigid airplane l-g loads for the mid-cruise condition.

$$[\Delta\delta_z] = [E] [P_{z_{l-g \text{ mid-cr.rigid}}}]$$

Using these calculated deflections and the transform matrix  $[D_\theta]$ , the incremental changes in chordwise slope and deflection were defined.

$$[\Delta\alpha] = [D_\theta] [\Delta\delta_z]$$

- (3) The deflections were applied, negatively, to the mid-cruise shape to establish the jig shape.

$$[\alpha_{\text{jig shape}}] = [\alpha_{\text{C&T, mid-cr}}] - [\Delta\alpha]$$

The airplane shape used for analytical reference and loft purposes was thereby defined.

Using the Task II strength sized structural model, a test case was computed at Mach 1.25 ( $V_A$ ) using the jig-shape in lieu of the mid-cruise shape to quantitatively assess the effect of jig-shape on the net external loads and corresponding internal loads. The results of the net loads study indicated a 3-percent increase in bending moment ( $M_x$ ) at BL. 0 and approximately 10-percent increase at BL. 470. For the internal loads assessment, a matrix of panel point loads was formed and applied to the structural model for conducting an internal loads run. As expected, these results, which are documented in the Finite-Element Structural Analysis section of this section, reflect the same trends as indicated by the integrated loads used to form the net external loads. Based on these results, the aeroelastic loads calculations for the final design (Task IIB) incorporated the above defined jig shape, rather than the mid-cruise shape, for the analytical starting point.

#### Net Aeroelastic Loads

Net loads for the baseline configuration were formed using Lockheed Static Aeroelastic Loads Program - PSRL F-72. This program permits the aerodynamic influence coefficients to contain moment points and load points in direction other than vertical. Inertia loads were combined with aerodynamic loads to form aeroelastically balanced net loads using the stiffness matrices for each structural arrangement.

Panel point loads were formed into a stacked matrix containing the symmetric and anti-symmetric load components for each flight condition.

#### VIBRATION AND FLUTTER ANALYSIS

The logic flow schematic depicting the principles of the analytical procedure applied to flutter analysis and optimization of the baseline configurations is presented in Figure 21-20 and is discussed in more detail in the following text.

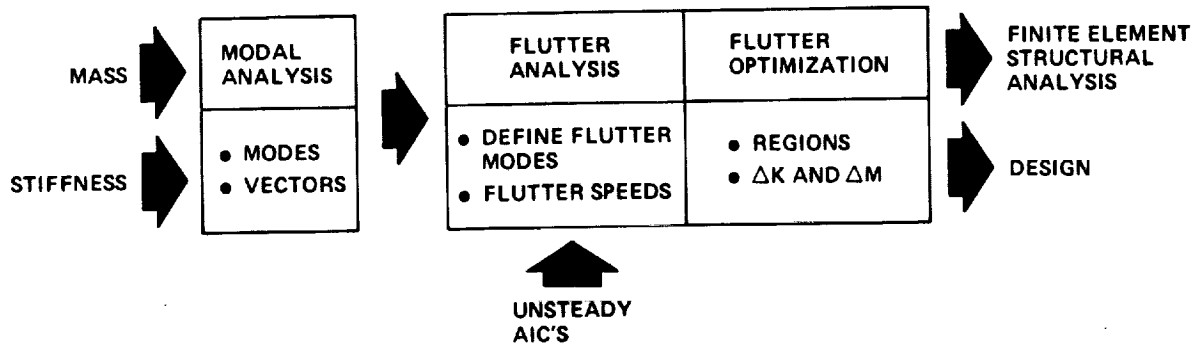


Figure 21-20. Vibration and Flutter Analysis

#### Structural Model

The vibration and flutter investigation used the Finite-Element Structural Model as the basis for formulating the analytical math model for each structural arrangement. Thus, these math models reflect the modeling technique, airframe stiffness, and mass associated with each of the structural models. A detail discussion of the structural models is contained in the previous section entitled "Finite-Element Structural Analysis".

The math models used in the vibration analyses employed a coordinate system and associated degrees-of-freedoms that related directly to the structural model structural influence coefficients grid. These degrees of freedom are of the 188th order symmetrically, Figure 21-21, and 178th order antisymmetrically. For both boundary conditions, the degrees of freedom are mainly associated with the Z-Axis displacements but includes Y-Axis displacements for the wing vertical fin. For the antisymmetric boundary, the fuselage degrees of freedom are related to Y-Axis displacements.

The stiffness matrices were obtained by condensing (Guyan Reduction) the large-order stiffness matrices generated by the NASTRAN static solutions to a size that is conformal with the symmetrical and antisymmetrical degrees of freedom.

The choice of the number of symmetric degrees of freedom was based on the constraint that a 188th order vibration problem was the maximum size that could be run in the Lockheed FAMAS computer system. It is felt though that a 188th order problem retains adequate structural definition and still gives good visibility for model trouble shooting and verification.

#### Vibration Analysis

Vibration modes were calculated using several different approaches and results compared to select the analytical method for application to the design concepts study, Table 21-5. The three methods investigated were: Inverse Power (INV) and Givens (GIV) method available in NASTRAN and the FAMAS QR method.

The first eigenvalue routine executed was the Inverse Power (INV). The approach was to take advantage of the sparseness of the stiffness and inertia matrices in the F-set (858th order) and solve for a limited number of modes. Computer time for the INV method was 80.5 seconds of CPU time per mode.

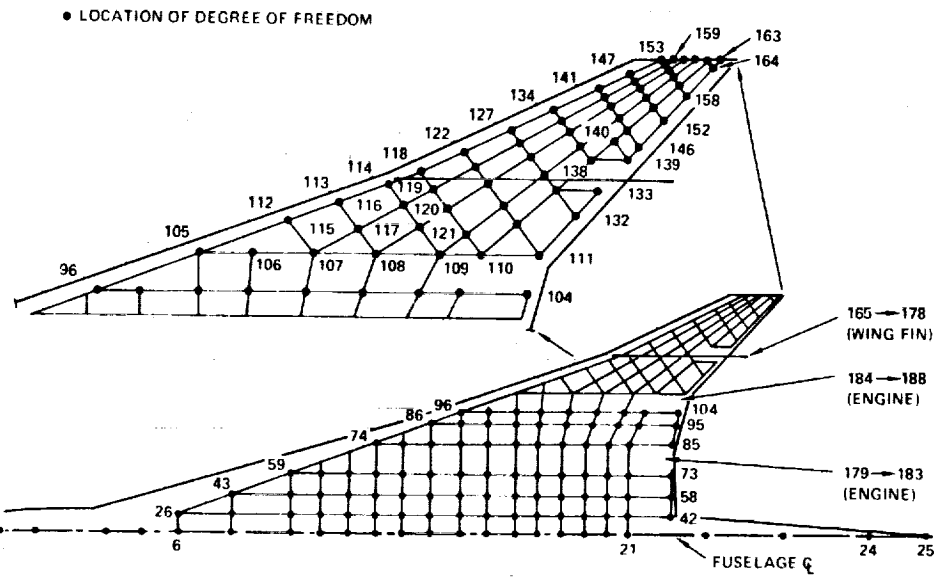


Figure 21-21. Symmetric Degrees of Freedom for Vibration Analysis

Because of the very high computer times, the problem was reduced to the 188th order. This matrix reduction required 89 seconds. The INV method was again executed and resulted in 60.5 seconds of CPU time per mode; whereas, the Givens method for the same reduced order problem resulted in 2.3 seconds of CPU time per mode.

The reduction to 188th order eliminated only a few inertial degrees of freedom (approximately 10-percent) and resulted in a problem size small enough so that the FAMAS QR method could also be exercised. The QR method resulted in 3.6 seconds of CPU time per mode.

The Givens and QR methods not only result in a marked reduction in computer time but also solve for all 188 roots, a definite advantage over the INV.

TABLE 21-5. ANALYTICAL METHODS FOR VIBRATION ANALYSIS

METHOD	MATRIX SIZE	NUMBER ROOTS	CPU TIME (SEC)		FREQUENCY (2) (HZ)	
			TOTAL	PER MODE (1)	MODE 1	MODE 2
INVERSE POWER	858	20	1610	80.5	1.470223	2.049600
INVERSE POWER	188	2	121	60.5	1.471204	2.055224
GIVENS	188	188 (40 VECTORS)	83	2.1	1.471203	2.055210
GIVENS	188	188 (40 VECTORS)	93	2.3	0.9275528	1.007738
QR	188	188 (40 VECTORS)	145	3.6	0.9275518	1.007738

(1) BASED ON NUMBER OF EIGEN VECTORS FOUND  
(2) FREQUENCIES 1 AND 2 ARE NOT NECESSARILY THE LOWEST FREQUENCIES. ALSO THE LAST TWO CASES (GIVEN AND QR) USED A DIFFERENT MASS MATRIX THAN THE FIRST THREE CASES

method where it is possible to miss a mode. No significant differences in accuracy was noted between the three methods.

Based on the results presented the Givens Method is superior to the other methods and was selected as the vibration analysis method for the study.

The stiffness matrices of each structural arrangement, as derived from the structural models, were combined with the appropriate inertia matrices to compute the symmetric and anti-symmetric eigenvectors and eigenvalues of the free-free airplane. The inertia matrices were formed for two airplane weight conditions namely: the operating weight empty (OWE), and the full fuel and full payload (FFFP). These weight conditions represent the extremes of minimum and maximum weight. No intermediate weight conditions were examined. In general, 50 vibration modes were extracted from each vibration solution for use in the flutter analysis and flutter optimization.

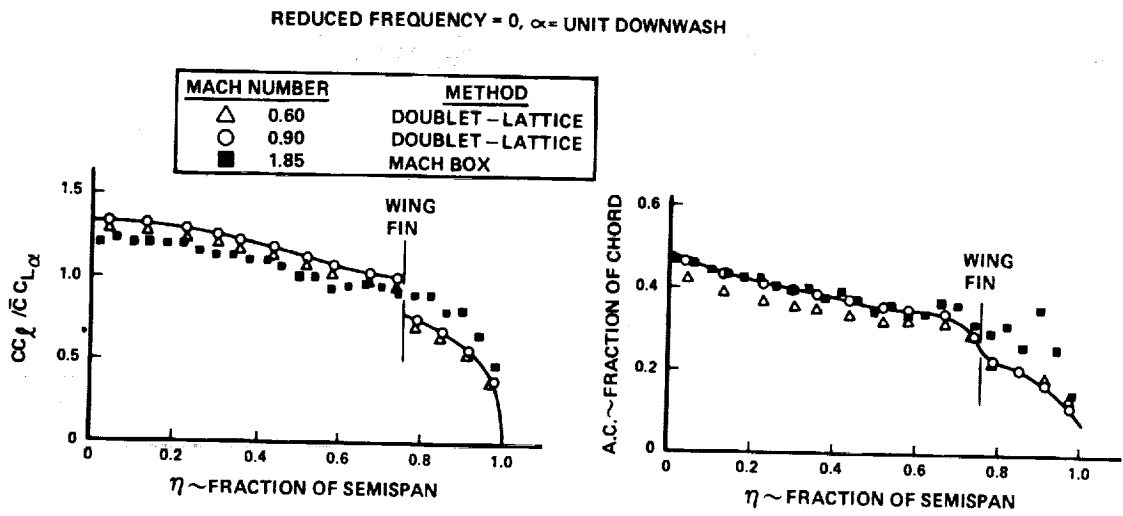
#### Aerodynamic Formulation

The steady and unsteady aerodynamic influence coefficients (AIC) were computed for Mach 0.60, 0.90, 1.25 and 1.85. The flutter analyses conducted on the Task II final design airplane included an analysis of these Mach numbers with the exception of the Mach 1.25 condition; whereas, the Task I analytical design studies encompassed only the first three Mach numbers. The Mach 0.60 and 0.90 AIC's were computed by the Doublet-Lattice method of Reference 2, while the Mach 1.25 and 1.85 AIC's were computed by the Mach Box method of Reference 3. The AIC's were computed for the wing, the wing fin, and the empennage surfaces, and were adjusted, when required, to reflect measured wind tunnel force data steady state lift coefficients and aerodynamic centers. The Mach 0.60 and 0.90 AIC calculations account for the interference between the wing and the wing fin; whereas, the Mach 1.25 and 1.85 AIC's do not include this effect.

The significance of the aerodynamic interference between the wing and wing fin is shown by Figure 21-22, which presents  $CC\ell/CC_{L\alpha}$  and aerodynamic center (a.c.) versus fraction of the semispan. The data visually relates the wing fin interference effect on the distribution for the applicable Mach numbers. For the Mach 0.60 and 0.90 conditions, which include the interference effect, an increase in the  $CC\ell/CC_{L\alpha}$  distribution inboard of the wing fin and a decrease in the  $CC\ell/CC_{L\alpha}$  distribution outboard of the wing fin is noted in contrast to the clean-wing aerodynamics calculated for Mach 1.85.

The normalized  $C_{L\alpha}$  versus reduced frequency is presented in Figure 21-23. The normalized  $C_{L\alpha}$  is  $C_{L\alpha}$  at a finite reduced frequency divided by  $C_{L\alpha}$  for a reduced frequency of zero. The figure presents the real and imaginary parts of the normalized  $C_{L\alpha}$  for Mach 0.90 and 1.85 and thus shows the variation in amplitude/phase as a function of Mach number and reduced frequency. As can be seen the Mach 1.85 aerodynamics is composed primarily of the real part. This differs from the Mach 0.90 aerodynamics which exhibits a mix of the real and the imaginary parts.

ORIGINAL PAGE IS  
OF POOR QUALITY



NOTE: THE WING/WING FIN AERODYNAMIC INTERFERENCE EFFECT:  
 • INCLUDED IN THE MACH 0.60 AND 0.90 AERODYNAMICS  
 • NOT INCLUDED IN THE MACH 1.85 AERODYNAMICS

Figure 21-22. Theoretical Aerodynamic Distribution

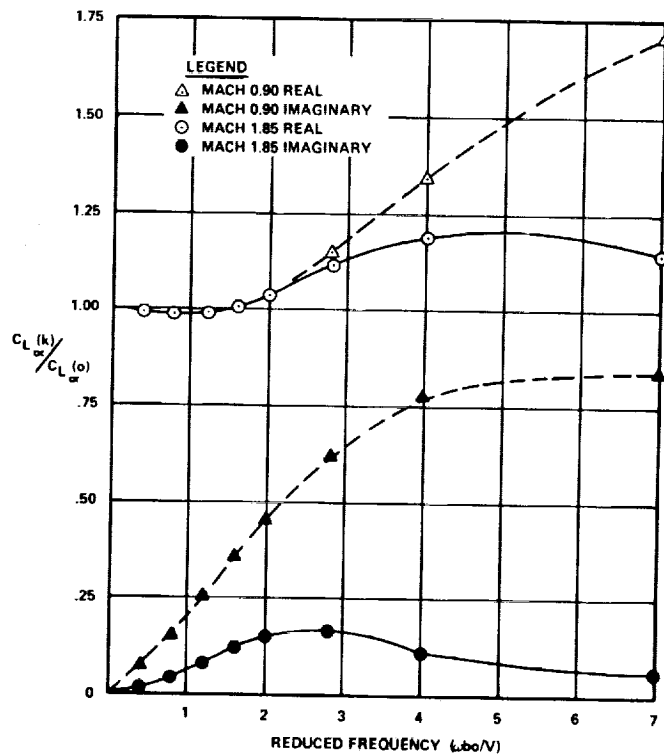


Figure 21-23. Normalized  $C_L$  Versus Reduced Frequency

## Flutter Analysis

The flutter analyses of each of the structural arrangements investigated for application to the arrow-wing configuration was conducted using the method of solution described in Reference 4 as the p-k method. This method is contained in the FAMAS library and results in a solution which defines rate of decay and frequency for preselected values of speed and gives matched altitude, Mach number, and reduced frequency (k) for each mode at each preselected velocity.

All matrices involved in this solution are real and uniquely defined, except for the aerodynamic influence coefficient matrix which is complex and must be given for a sufficient number of k values. For the p-k method, the flutter equation is solved at several values of airspeed and air density, or combinations thereof, for complex roots p associated with the modes of interest. These modes of interest were determined from a review of the vibration analysis and/or from previous flutter analysis. In addition, all analyses assume a structural damping of 2-percent.

Two fundamental questions arose during the flutter analysis, namely:

- (1) How many vibration modes are required to arrive at the converged flutter solution?
- (2) How many AIC matrices, as a function of reduced frequency (k), are required to arrive at a converged flutter solution?

Both of these questions were investigated during the course of the flutter studies.

In response to the first question, velocity versus damping for the 10, 15 and 20 vibration mode flutter analyses are shown in Figure 21-24. It can be seen that the character of the flutter modes can be significantly changed by going from 20 to 10 vibration modes. Figure 21-25 shows the flutter velocity of the bending and torsion flutter mode as a function of the number of vibration modes used in the flutter analysis. This figure shows that the flutter velocity changes only 1-percent when the number of vibration modes vary from 20 to 50. As a consequence of this study, 20 or more vibration modes were used in all subsequent flutter analyses.

The number of AIC matrices required to arrive at a converged flutter solution was investigated by running a flutter analysis with AIC matrices corresponding to 17 k values and then repeating this analysis with every other AIC matrix eliminated (9 k values). Within the reading accuracy of the flutter plots the results from these analyses were identical. As a consequence of this study, AIC matrices corresponding to at least 9 k values were used in all subsequent flutter analyses.

Symmetric and antisymmetric flutter solutions were conducted at sufficient Mach numbers to assess the structural dynamic characteristics of the various structural arrangements. And in general, these solutions were conducted for both operating weight empty (OWE) and full fuel and full payload (FFFP) airplane weight conditions. As an example of these solutions, the symmetric flutter solution for the OWE Final Design airplane at Mach 0.90 is shown in Figure 21-26. For this condition, the critical flutter mode was the wing bending and torsion mode. The figure also presents a trace of the critical flutter speed for this mode on

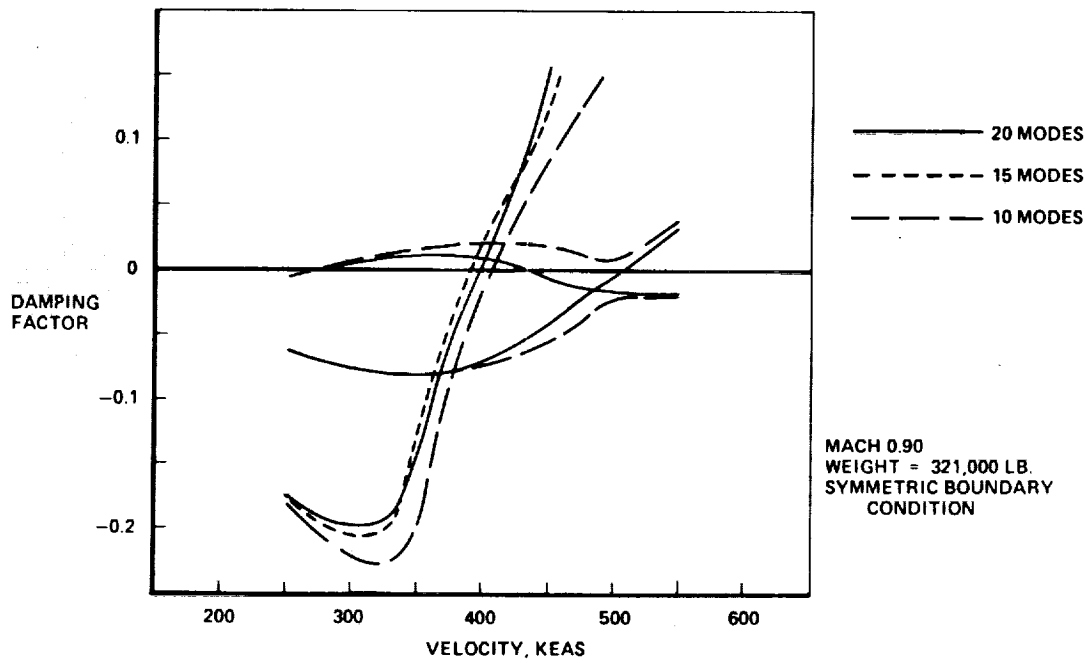


Figure 21-24. The Effects of Number of Modes on the Flutter Solution

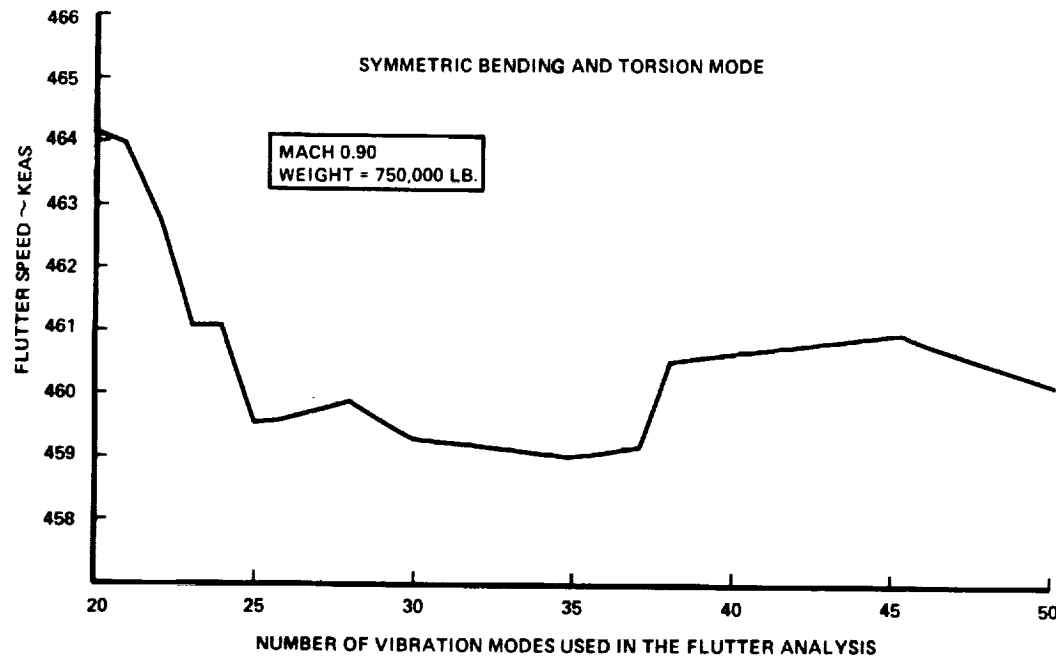


Figure 21-25. Flutter Speed Variation With Number of Modes

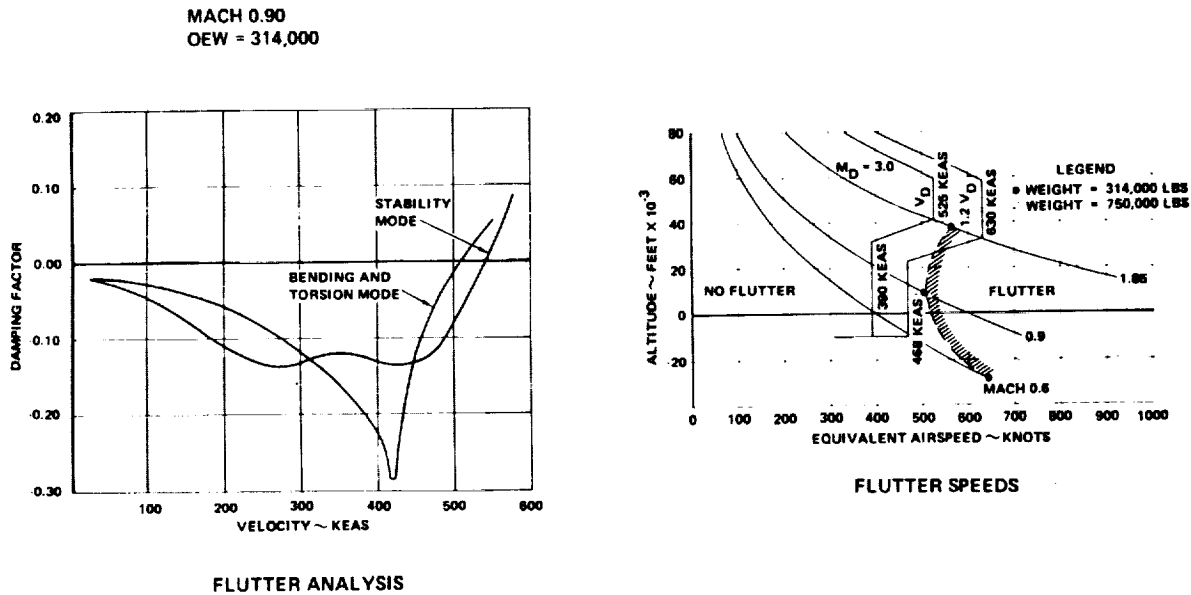


Figure 21-26. Flutter Analysis Results

SYMMETRIC FLUTTER ANALYSIS - CHORDWISE STIFFENED ARRANGEMENT  
MACH NO. = 0.90 WEIGHT = 750,000 LBS.  
PARTICIPATION COEFFICIENTS - FLUTTER MODE 8 - BENDING AND TORSION MODE

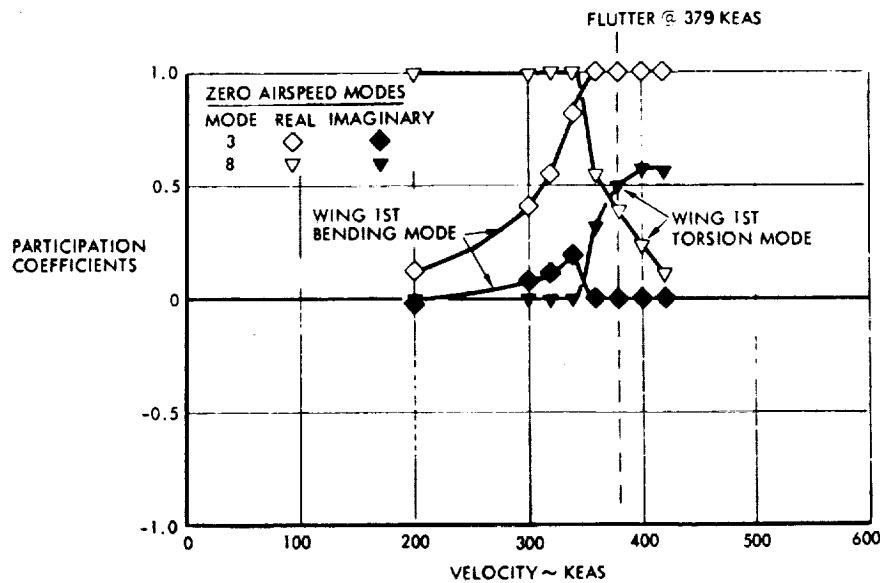


Figure 21-27. Participation Coefficients - Mach 0.9 - FFFP-Mode 8

the design flutter envelope. Similar critical speed traces were constructed for each flutter mode to completely define the flutter boundary.

In general, three distinct flutter mechanisms were noted throughout this investigation; they were: the bending and torsion mode, the hump mode, and the stability mode. Considerable insight into the modal composition of these flutter mechanisms was provided by reviewing the participation coefficients. Participation coefficients are the complex eigenvectors associated with the roots of a flutter solution.

As an example of this technique, the participation coefficients for the bending and torsion flutter mode (mode 8 of Figure 21-28) reveal that at flutter, this mode is principally composed of the zero airspeed Modes 3 and 8 (Table 21-6). Participation coefficients resulting from the symmetric flutter analysis at Mach 0.90 for the full fuel and full payload (FFFP) is shown in Figure 21-27. As indicated on this figure, the zero airspeed wing 1st bending mode rapidly transitions through the adjacent higher frequency modes and couples at flutter with the zero airspeed wing 1st torsion mode. This conclusion is not obvious by reference to the frequency velocity diagram of Figure 21-28.

To understand the flutter mechanisms of the arrow-wing configuration more thoroughly, a flutter analysis was conducted with the wing rigid inboard of BL 470, i.e., flexible wing tip. This investigation was conducted for the Mach 0.90 condition using the Task I chordwise-stiffened structural model for the 750,000-lb aircraft, (FFFP). The symmetric flutter analysis of this configuration showed that for Mach 0.90, the wing 1st bending mode rapidly increases in frequency with increasing velocity and coalesces with the wing 1st torsion mode to flutter at 418 keas. This flutter mechanism was identical to the flutter mechanism for the flexible aircraft. For the unrigidized or flexible aircraft the bending and torsion mode flutter velocity was 379 keas.

#### Flutter Optimization

An interactive computer graphics program was utilized in the optimization of the arrow-wing configuration. An abbreviated description of the equations, method of solution, and optimization procedure are presented in Reference 5. The general steps of the overall procedure are listed below, followed by a more detailed description of the flutter optimization process.

- Define the critical flight condition and associated flutter modes from a review of the basic vibration and flutter analyses.
- Establish the basic design regions and corresponding design variables for application to the flutter optimization process.
- Calculate a sufficient number of incremental stiffness matrices  $[\Delta K]$  and associated mass matrices  $[\Delta M]$  to cover the expected range of investigation.
- Operate the flutter optimization program to define the added mass (weight penalty) associated with attaining the design flutter speed.

SYMMETRIC FLUTTER ANALYSIS - CHORDWISE STIFFENED ARRANGEMENT  
MACH NO. = 0.9  
WEIGHT = 750,000 LBS

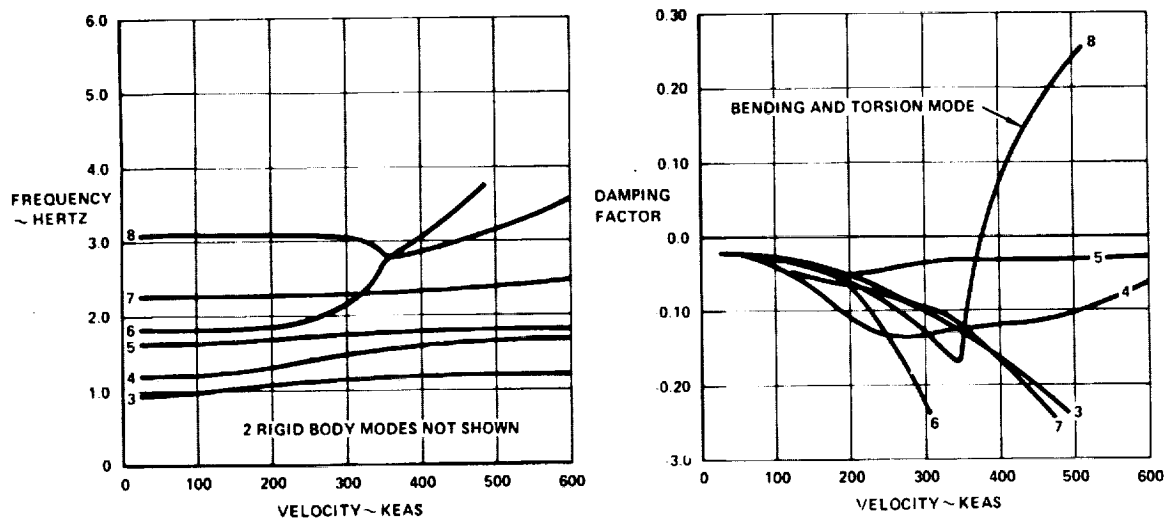


Figure 21-28. Symmetric Flutter Analysis - Mach 0.9 - FFFP

TABLE 21-6. LOWER FREQUENCY SYMMETRIC VIBRATION MODES - CHORDWISE STIFFENED

MODE NUMBER	MODE DESCRIPTION	MODE FREQUENCY ~ HERTZ	
		OWE	FFF
1	RIGID BODY	0.000	0.000
2	RIGID BODY	0.001	0.001
3	WING 1ST BENDING	1.009	0.933
4	FUSELAGE 1ST BENDING	1.381	1.206
5	ENGINE PITCH IN PHASE	1.641	1.627
6	ENGINE PITCH OUT OF PHASE	1.817	1.815
7	FUSELAGE 2ND BENDING	2.784	2.261
8	WING 1ST TORSION	3.288	3.104

OWE ~ WEIGHT = 321,000 LBS  
FFF ~ WEIGHT = 750,000 LBS

Basic Design Regions.- For the initial optimization studies conducted in Task I, the selection of design regions was of an exploratory nature to provide a general assessment of the effectiveness and optimum distribution of material for the overall wing planform. Thus, the wing planform was divided into 10 general regions (Figure 21-29), which included the two engine support beam locations. Natural boundaries were retained in the establishment of these regions as indicated by their location with respect to the landing gear well, major chordwise ribs, wing vertical, etc.

The application of the coarse-grid modeling philosophy to the optimization procedure provided the necessary insight for the investigator to eliminate the regions which least affected the critical flutter mechanism under investigation. Thus, a more detailed grid system, with fewer overall regions, can be concentrated at the most efficient wing location. As an example, the solution for the Task I monocoque design, which used the coarse grid system shown in Figure 21-29, indicated the wing tip structure to be the most effective region for adding stiffness and mass to achieve the desired flutter speed. It was also shown that the bending and torsion mode flutter mechanism was controlled by the wing inertial and flexibility characteristics outboard of BL 470. Thus, for the more detailed evaluation of the stiffness requirements for the Final Design airplane the optimization effort focused on the wing tip structure. Five design regions were defined for the wing tip structure planform (in lieu of 2 for Task I) as indicated on Figure 21-30. The establishment of the design region boundaries considered the location of the wing vertical and appropriate ribs and spars as may be required. However, the primary influence in the selection was the natural boundaries defined by the structural model.

Design Variables.- The flutter optimization procedure uses incremental stiffness and mass parameters as a set of structural design variables. Using these parameters, the expressions for mass and stiffness take the following form:

$$[M] = [M_0] + \sum_{i=1}^n \beta_i [M_i]$$

$$[K] = [K_0] + \sum_{i=1}^n \beta_i [K_i]$$

where  $[M]$ ,  $[K]$  are the matrices of total mass and stiffness;  $[M_0]$ ,  $[K_0]$  are matrices of the fixed mass and stiffness;  $[M_i]$  and  $[K_i]$  are mass and stiffness matrices associated with a unit of the design variable  $\beta$ . The design variable  $\beta$  can be a unit of area or thickness as related to their respective axial element or shear panel element defined in the structural model.

For the flutter calculations, a reduction in the size of stiffness matrix is required over the large-order stiffness matrix obtained from the structural model. As a result of this coordinate reduction, the relationship between the design variable  $\beta$  and its associated stiffness  $K$  are nonlinear and require additional computer runs to define this relationship with sufficient accuracy. Data points to define this nonlinear relationship are derived by formulating a

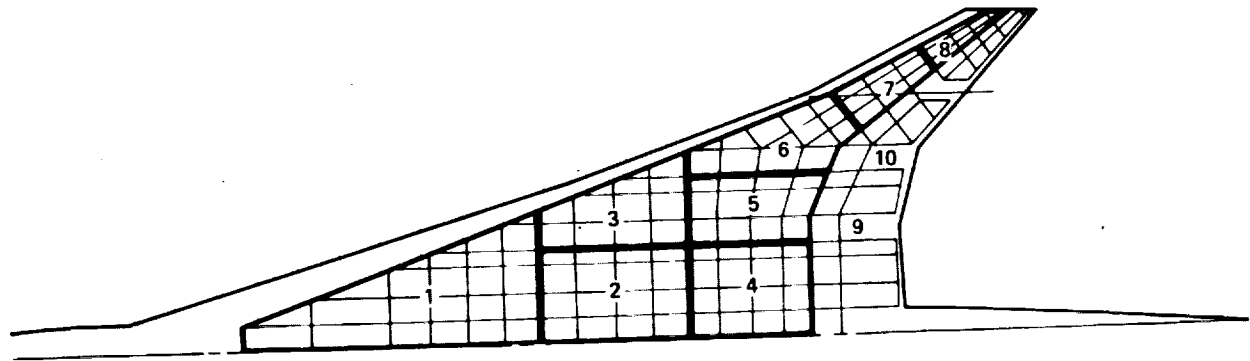


Figure 21-29. Design Regions for Flutter Optimization - Task I

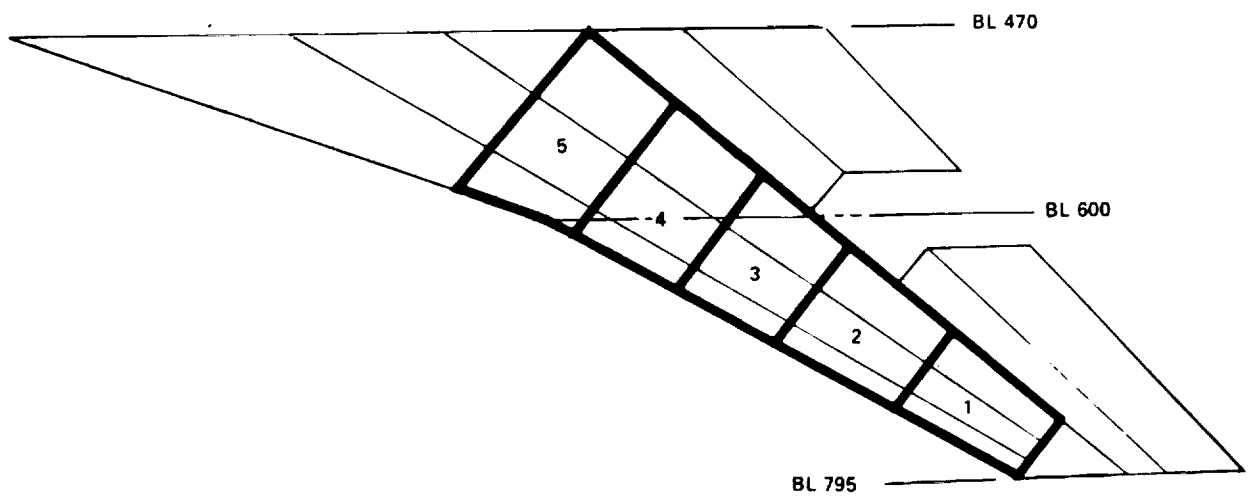


Figure 21-30. Design Regions for Flutter Optimization - Task II

separate NASTRAN bulk data deck for each of the basic design regions. These decks contain the element property cards with the incremental changes in geometry. Using these decks, the stiffness matrices are obtained from the NASTRAN static solution and condensed to the desired size for the flutter optimization process.

An example of this effect is shown in Figure 21-31, which shows the increments in four elements of the Arrow Wing stiffness matrix as a function of increments in cover sheet thickness of the appropriate design variable. The stiffness matrices from which these results were obtained are from the Task I chordwise-stiffened arrangement.

Optimization Procedure.- Once the basic design regions were established the optimization process was initiated. This involved the following steps:

- (1) The baseline stiffness,  $[K_0]$ , and mass matrices,  $[M_0]$ , were formed using NASTRAN in a large order system.  $[M_0]$  was input as a matrix in the NASTRAN Bulk Data Deck.
- (2) These matrices were condensed to 188th order using the Guyan Reduction so that a vibration case could be more readily obtained.
- (3) The vibration calculation which was then performed produced 50 normal mode shapes. These can be used to reduce the problem size to 50th order by a pre- and post-multiplication of the baseline 188th order  $[K_0]$  and  $[M_0]$ .
- (4) A flutter solution was then obtained using these matrices. This yielded the flutter speed for the baseline configuration.
- (5) NASTRAN was used to generate  $[\Delta K]$  and  $[\Delta M]$  matrices. Only the increment in element sizing for a particular  $[\Delta K]$  was input for the structural model. The base stiffness,  $[K_0]$ , was then added to  $[\Delta K]$  in the large order system, and the resulting  $[K_0 + \Delta K]$  was condensed by the Guyan Reduction to 188th order. The NASTRAN mass generator program was used to form  $[\Delta M]$  directly from the sizing increments ( $\Delta t$ ) on the element property cards in the NASTRAN Bulk Data Deck. This matrix was then reduced to 188th order by the same technique.  $[\Delta K]$  matrices in this system were formed by subtracting  $[K_0]$  from  $[K_0 + \Delta K]$ .
- (6) These  $[\Delta K]$  and  $[\Delta M]$  matrices were reduced to 50th order by modalizing with the normal mode shapes from the baseline vibration analysis.
- (7) All of these 50th order matrices were input into an interactive computer graphics flutter optimization program. This program allows the engineer to choose a flutter speed and then calculate  $\beta$ - "how much" of each  $[\Delta K]$ , taken one at a time, is necessary to satisfy this constraint. The engineer may update the structure to any combination of  $[\Delta K]$  and  $[\Delta M]$  matrices desired. In doing this, the  $\beta$  solutions are taken into account, and the structure is modified so that an optimum structure (minimum weight) results.

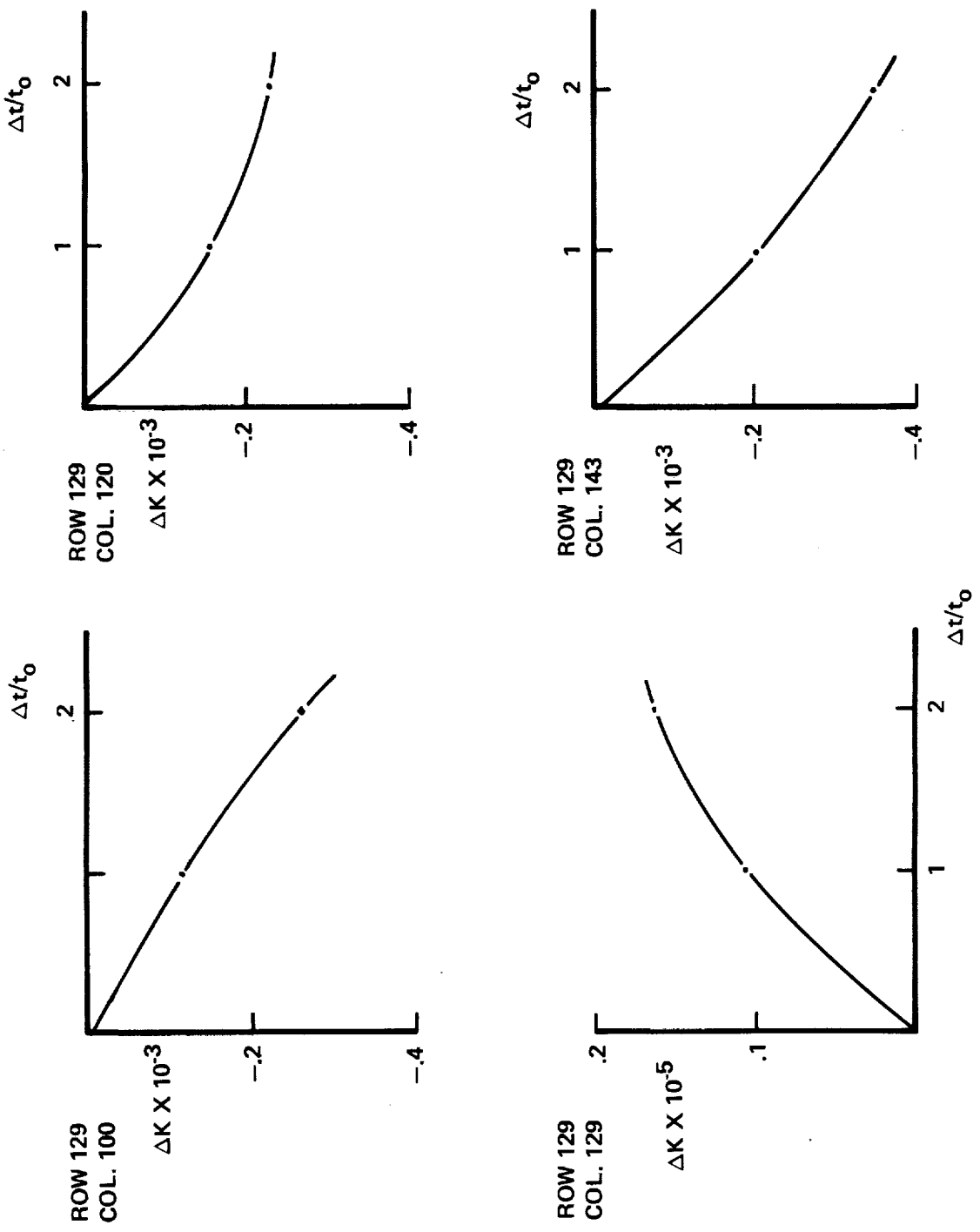


Figure 21-31. Nonlinearities in the Incremented Stiffness Matrix Elements, Arrow Wing

(8) Because the modifications made to the structure above were not reflected in the vibration modes used in the analysis, it was necessary to define a new baseline configuration. Thus the resulting structure from (7) was defined as a new baseline configuration and the process was repeated in an iterative manner until the distribution of  $\beta$ 's converged on a solution and gave the desired flutter speed. This was the optimum design for flutter.

#### REFERENCES

1. Schultz, H.D., "Thermal Analyzer Computer Program for the Solution of General Heat Transfer Problems", Lockheed-California Company Report LR 18902, 1965.
2. Albano, E. and Rodden, W.P., "A Doublet-Lattice Method for Calculating Lift Distributions on Oscillating Surfaces in Subsonic Flows," AIAA Journal, Volume 7, February 1969, pp 279-285, Errata AIAA Journal, Volume 7, November 1969, p 2192.
3. Pines, S., Dugundji, J., and Neuringer, J., "Aerodynamic Flutter Derivatives for a Flexible Wing with Supersonic and Subsonic Edges, J. Aeronaut. Sci. 22, pp 693-700 (1955).
4. Hassig, H.J., "An Approximate True Damping Solution of the Flutter Equation by Determinate Iteration," Journal of Aircraft, Volume 8, November 1971, pp 885-889.
5. Radovcich, N.A., "Structural Optimization with Flutter Speed and Minimum Gage Constraints," Lockheed-California Company Report LR 26405, April 15, 1974.

ORIGINAL PAGE IS  
OF POOR QUALITY

